

INFORMATION TO USERS

This manuscript has been reproduced from the microfilm master. UMI films the text directly from the original or copy submitted. Thus, some thesis and dissertation copies are in typewriter face, while others may be from any type of computer printer.

The quality of this reproduction is dependent upon the quality of the copy submitted. Broken or indistinct print, colored or poor quality illustrations and photographs, print bleedthrough, substandard margins, and improper alignment can adversely affect reproduction.

In the unlikely event that the author did not send UMI a complete manuscript and there are missing pages, these will be noted. Also, if unauthorized copyright material had to be removed, a note will indicate the deletion.

Oversize materials (e.g., maps, drawings, charts) are reproduced by sectioning the original, beginning at the upper left-hand corner and continuing from left to right in equal sections with small overlaps. Each original is also photographed in one exposure and is included in reduced form at the back of the book.

Photographs included in the original manuscript have been reproduced xerographically in this copy. Higher quality 6" x 9" black and white photographic prints are available for any photographs or illustrations appearing in this copy for an additional charge. Contact UMI directly to order.



University Microfilms International
A Bell & Howell Information Company
300 North Zeeb Road, Ann Arbor, MI 48106-1346 USA
313/761-4700 800/521-0600

Order Number 9307644

**Spectroscopic and photometric studies of main sequence M stars
and a search for late-type dwarfs in the solar vicinity**

Kirkpatrick, Joseph Davy, Ph.D.

The University of Arizona, 1992

U·M·I

300 N. Zeeb Rd.
Ann Arbor, MI 48106

SPECTROSCOPIC AND PHOTOMETRIC STUDIES OF
MAIN SEQUENCE M STARS
AND A SEARCH FOR LATE-TYPE DWARFS IN THE SOLAR VICINITY

by

Joseph Davy Kirkpatrick

A Dissertation Submitted to the Faculty of the
DEPARTMENT OF ASTRONOMY
In Partial Fulfillment of the Requirements
For the Degree of
DOCTOR OF PHILOSOPHY
In the Graduate College
THE UNIVERSITY OF ARIZONA

1 9 9 2

THE UNIVERSITY OF ARIZONA
GRADUATE COLLEGE

As members of the Final Examination Committee, we certify that we have
read the dissertation prepared by Joseph Davy Kirkpatrick

entitled SPECTROSCOPIC AND PHOTOMETRIC STUDIES OF MAIN SEQUENCE M
STARS AND A SEARCH FOR LATE-TYPE DWARFS IN THE SOLAR VICINITY

and recommend that it be accepted as fulfilling the dissertation
requirement for the Degree of Doctor of Philosophy

<u>Donald W. McCarthy, Jr.</u>	<u>9/9/92</u>
Donald W. McCarthy, Jr.	Date
<u>Conard C. Dahn</u>	<u>9/9/92</u>
Conard C. Dahn	Date
<u>James W. Liebert</u>	<u>9/9/92</u>
James W. Liebert	Date
<u>John T. McGraw</u>	<u>9/9/92</u>
John T. McGraw	Date
	Date

Final approval and acceptance of this dissertation is contingent upon
the candidate's submission of the final copy of the dissertation to the
Graduate College.

I hereby certify that I have read this dissertation prepared under my
direction and recommend that it be accepted as fulfilling the dissertation
requirement.

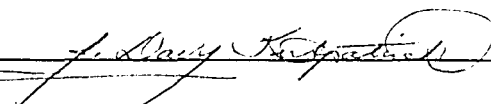
<u>Donald W. McCarthy, Jr.</u>	<u>9/9/92</u>
Dissertation Director Donald W. McCarthy, Jr.	Date

STATEMENT BY AUTHOR

This dissertation has been submitted in partial fulfillment of requirements for an advanced degree at The University of Arizona and is deposited in the University Library to be made available to borrowers under rules of the Library.

Brief quotations from this dissertation are allowable without special permission, provided that accurate acknowledgement of source is made. Requests for permission for extended quotation from or reproduction of this manuscript in whole or in part may be granted by the head of the major department or the Dean of the Graduate College when in his or her judgment the proposed use of the material is in the interests of scholarship. In all other instances, however, permission must be obtained from the author.

SIGNED: _____

A handwritten signature in cursive script, appearing to read "J. Larry Kuykendall", is written over a horizontal line.

DEDICATION

This thesis is dedicated to four individuals to whom I will always be indebted...

My ninth grade physical science teacher, Marilyn Morrison, said she saw something “special” in me and wanted to know if I had plans for my future. I told her that I wanted to become an astronomer, and she informed me that I would have to take a lot of physics and math and that I would most likely have to major in those subjects in college. The idea of taking a lot of physics classes didn’t appeal to me, but since Mrs. Morrison held an advanced degree and was also a teacher of physics and math at our local community college, I knew that her opinion was based on facts... and seven years later I finally held that degree in mathematics and physics/astronomy which enabled me to enter graduate school. Because of her, my education always had a clearly defined path, and I thank her especially for making me feel that *I* had special talents.

My aunt Mag was just like a best friend to me. We always had a great time cracking jokes around (and especially *about*) one another and finding joy in the simplicity of the Southern way of life. She taught me about compassion and about values. She, too, made me feel special, and she unwaveringly gave of herself. She was always supportive of my academic pursuits and made me feel that I would make something of myself. I only wish she could have lived long enough to see me get this degree. Mag, I’ll always think the world of you, and thanks for not trading me “for all the cows in Texas”!

Finally, there are my amazing parents. There’s my Dad who, on the one hand, would tell me that my pile of Vanderbilt homework would “take care of itself,” yet, on the other hand, would pull out on those rare occasions his poignant and *horrible* phrase “Let your conscience be your guide.” Dad, whenever I’m faced with a dilemma, I think of that saying. There’s my Mom who instilled in me the importance of reading and of acquiring a good education; she showed me that learning was fun, and besides it made you a better Jeopardy player and crossword puzzle worker! Mom, I’ll always regard you as one of the smartest people in the world. I don’t know how they did it — they never seemed to push me — but they saw me all the way through to the completion of this degree. Thanks for your undying support both emotionally and financially. I owe everything to you, and I love you both.

ACKNOWLEDGEMENTS

Those people listed below helped make this thesis possible, kept me sane during graduate school, or both. To all of you, I extend my sincerest thanks.

I would like to thank my advisor, Don McCarthy, for his frequent and useful insights, for financial assistance, and for being my weight-room partner over the past several years; Todd Henry for innumerable scientific discussions and for assistance with Chapters 3.1 and 3.3; Jim Liebert for financial assistance and for careful readings of Chapters 3.2, 3.3 and 4; Conard Dahn for invaluable help in acquiring and reducing (along with Hugh Harris) the calibration photometry of Chapter 4 and for his many useful suggestions regarding that chapter; John McGraw for conceiving of the CTI concept and for maintaining that the CTI data are of high quality; Doug Kelly for his 50% co-authorship of Chapter 3.2; George Rieke for financial assistance and for overseeing the development of Chapter 3.2; France Allard and Rainer Wehrse for providing unpublished theoretical spectra and for careful readings of Chapter 3.2; Betsy Green for useful discussions regarding the calibration in Chapter 4; Patricia Boeshaar for many unpublished spectral types tabulated in Chapter 5 and for her continued support of my scientific endeavors; and finally my sister Ann Kirkpatrick for (voluntarily!) assisting me in the cross-checking of columns 1 and 3 of Table 5.1.

There are a number of behind-the-scenes people I would also like to thank: Tom Hess, Charles Bridges, Brian Schmidt, Lisa LaFlame, Anne Lierman, and Lexi Moustakas for their assistance in CTI related matters; the crew at the MMT, particularly the telescope operators Janet Robertson, Carol Heller, Bill Kindred, and John McAfee, for surviving my acquisition of over 300 spectra; and Conard and Carol Dahn for providing me a room at their house during my two stints in Flagstaff over the summer of 1992.

With Joan (see you in Texas) Morrill, Diana (Mythica Q.) Johnson, and Sally ("pahl-EEZE!") Oey I have shared good times both during and outside of Astronomy Camp. I am grateful for my friendship with each of you. I am also grateful to those who have unselfishly given their time and talents to help me in my photographic pursuits, particularly Todd Henry, Michael ("I'm always 2nd") Merrill, Tom ("hey, buddy") Connor, and Jorden ("well, dog my cats") Woods.

As for Katy Moore and Kim Dow, they have always been willing to lend an ear when I needed consoling and have provided me with some very interesting diversions. Katy, thanks for listening to me gripe and moan, and maybe someday soon we'll do that joint art exhibition! Kim, I admire your compassion and your unbelievably high energy level. In fact, if the two of you didn't own cats, you'd be darn near perfect!

Lastly, I would like to tell Todd Henry how much I appreciate his friendship. Graduate school would have had a distinctly different flavor had I not met you, Todd. You've given me some of the most memorable and enjoyable experiences I've ever known — our trips to California, our crazy poolside chats, our movie rankings, our overanalyzing of almost any subject! Thanks for being there for me. Life wouldn't be the same without you...

TABLE OF CONTENTS

	Page
LIST OF ILLUSTRATIONS	9
LIST OF TABLES	12
ABSTRACT	15
CHAPTER 1: INTRODUCTION	17
1.1 The Missing Mass	20
1.2 A Companion to the Sun?	22
1.3 A Recent History of Searches for Very Low-mass Stars and Brown Dwarfs	24
1.4 Goals for this Thesis	26
CHAPTER 2: THE CCD/TRANSIT INSTRUMENT (CTI)	28
2.1 Telescope and Data Base	28
2.2 Scientific Programs	30
2.3 CTI's Role in this Thesis	32
CHAPTER 3: RED/INFRARED SPECTROSCOPY OF LOW-MASS OBJECTS	39
3.1 Spectral Library for K and M Stars from 6300 to 9000 Ångstroms	41
3.1.1 Object Lists	42
3.1.2 Observations and Data Reduction	44
3.1.3 Line Identifications	47
3.1.4 Spectral Classification	49

3.1.5 Extension of the Classification System beyond M6.5	54
3.1.6 Luminosity Classification	57
3.1.7 Classification of Other Spectroscopic Data	59
3.1.8 Spectral Class Versus Mass Relation	62
3.1.9 Summary	63
3.2 The Temperature Scale for M Dwarfs Derived Using Spectra from 0.6 to 1.5 Microns	113
3.2.1 Data Acquisition and Reduction	114
3.2.2 Combining the Red and Infrared Spectra	115
3.2.3 Spectral Features	118
3.2.4 Fits to Theoretical Spectra of M Dwarfs	119
3.2.5 Temperature Scale	125
3.2.6 Discussion	128
3.2.7 Summary	129
3.3 The Unique Spectrum of GD 165 B — A Brown Dwarf?	149
3.3.1 Observations and Data Reduction	151
3.3.2 Comparison to the Spectra of Other Low-luminosity Objects	154
3.3.3 Discussion	156
3.3.4 Summary	159
3.4 Spectra of Low-mass Companions	169
3.4.1 Data Acquisition and Reduction	170
3.4.2 Differential Spectroscopy of the Composite Systems	171
3.4.3 Results	183
3.4.4 Summary	184
3.5 Conclusions	200

CHAPTER 4: SYSTEMATIC SEARCH FOR OTHER LOW-MASS OBJECTS	201
4.1 The Search for Late-M Dwarfs in the CTI Strip	203
4.1.1 Object Selection	203
4.1.2 Spectra of CTI Objects	206
4.2 Determination of the Luminosity Function from CTI Data	208
4.2.1 Photometric Calibration	208
4.2.2 Completeness and Contamination in the Strip	212
4.2.3 Analysis of the Photometric Data	216
4.2.4 CTI Luminosity Function and Comparison to Others	221
4.3 Implications for the Mass Function	229
4.4 Summary	232
CHAPTER 5: GOALS FOR FUTURE STUDIES	280
5.1 Follow-up to Luyten's Work	281
5.1.1 Spectroscopic Identifications of LHS Objects	284
5.1.2 Late-type Stars in Binary and Multiple Systems	286
5.1.3 Spectroscopic Identifications for "The Stars of Low Luminosity"	288
5.2 A New Proper Motion Survey	289
5.3 A New Photometric Search for Late Dwarfs	293
CHAPTER 6: CONCLUSIONS	607
APPENDIX A: FINDER CHARTS FOR CTI SPECTROSCOPIC TARGETS	611
LIST OF REFERENCES	746

LIST OF ILLUSTRATIONS

	Page
2.1 CTI Path Through Galactic Coordinates	36
2.2 Typical CTI Field near the North Galactic Pole	37
2.3 Typical CTI Field in the Galactic Plane	38
3.1 Primary Dwarf Spectral Standards	90
3.2 Secondary Dwarf Spectral Standards	94
3.3 Giant and Higher Luminosity Spectra	98
3.4 Spectra of Miscellaneous Objects	100
3.5 Feature Identifications for a Range of Spectra	101
3.6 Color Ratios for use as Luminosity Discriminants	105
3.7 Ratios of Ratios for use as Luminosity Discriminants	106
3.8 Spectra of Additional Objects	107
3.9 Additional Luminosity-Discriminant Data	111
3.10 Spectral Class vs. Mass Relation for M Dwarfs	112
3.11 The 0.63-to-1.50 Micron M Dwarf Spectral Sequence	139
3.12 Feature Identifications from 0.63 to 1.50 Microns	140
3.13 Fits of Model Atmospheres to Observed Red Spectra	142
3.14 Model Fit for an M8 Dwarf	144
3.15 Fits of Models Atmospheres to Observed Infrared Spectra	145
3.16 The H-R Diagram with New M Dwarf Temperature Sequence	147
3.17 Spectra of GD 165 A and B	164
3.18 Spectra of the Four Latest Dwarfs Known	166

3.19 Absolute Magnitude vs. Temperature for M Dwarfs	167
3.20 Possible Positions of GD 165 B on the H-R Diagram	168
3.21 Differential Spectra for GL 234 B (Ross 614 B)	194
3.22 Differential Spectra for LHS 1047 B (GJ 1005 B)	195
3.23 Differential Spectra for GL 22 C (BD +66° 34 C)	196
3.24 Differential Spectra for GJ 1081 B (G 96-45 B)	197
3.25 Differential Spectra for G 250-29 B (LHS 221 B)	198
3.26 Revised Spectral Type vs. Mass Relation for M Dwarfs	199
4.1 $(V - I)_{CTI}$ vs. $(R - I)_{CTI}$ Diagram for Spectroscopic Targets	257
4.2 Luminosity Ratios for CTI Spectroscopic Targets	258
4.3 $(V - I)_{KC}$ and $(R - I)_{CTI}$ vs. Spectral Class for Photometric Calibration Targets	259
4.4 $(R - I)_{CTI}$ vs. $(V - I)_{KC}$ Calibration Plot	260
4.5 $M_{I_{KC}}$ vs. $(V - I)_{KC}$ Calibration Plot	261
4.6 ΔI vs. $(V - I)_{KC}$ Calibration Plot	262
4.7 Plots of $M_{I_{KC}}$ vs. $(V - I)_{KC}$ for Objects of Low, Intermediate, and High V Space Velocity	263
4.8 $M_{I_{KC}}$ vs. $(V - I)_{KC}$ Calibration Plot for Objects of Low V Space Velocity	264
4.9 Plot Showing Completeness Limit of R_{CTI}	265
4.10 $(V - I)_{CTI}$ vs. $(R - I)_{CTI}$ Diagram for Objects used in the CTI Luminosity Function	266
4.11 $(B - I)_{CTI}$ vs. $(R - I)_{CTI}$ Diagram for Objects used in the CTI Luminosity Function	267
4.12 $(B - I)_{CTI}$ vs. $(R - I)_{CTI}$ Diagram for Spectroscopic Targets	268
4.13 RA Distribution of CTI Objects used in Final Binning	269

4.14 Comparison of CTI Luminosity Function at I to Leggett & Hawkins' Luminosity Function at the South Galactic Pole	270
4.15 Comparison of CTI Luminosity Function at I using Two Different Calibrations	271
4.16 Comparison of CTI Luminosity Function at I (with and without Malmquist Correction) to Luminosity Function of Nearby Stars ...	272
4.17 Comparison of Luminosity Function derived Photometrically with that derived from the Nearby Star Census	273
4.18 Comparison of CTI Luminosity Function at V to Reid & Gilmore's Luminosity Function	274
4.19 Comparison of CTI Luminosity Function at V using Two Different Calibrations	275
4.20 Comparison of CTI Luminosity Function at V (with and without Malmquist Correction) to Luminosity Function of Stars Within 20 Parsecs	276
4.21 $M_{I_{KC}}$ vs. Mass Calibration Plot	277
4.22 Comparison of Resulting Mass Functions for M Dwarfs (I)	278
4.23 Comparison of Resulting Mass Functions for M Dwarfs (II)	279
5.1 Plot of $m_{pg} - m_R$ vs. Spectral Type for LHS 1-552	295
5.2 MMT Spectra of Red LHS Targets (Dwarfs)	296
5.3 MMT Spectra of Red LHS Targets (Subdwarfs)	297
5.4 MMT Spectra of LHS Dwarf Carbon Stars	298

LIST OF TABLES

	Page
2.1 Objects Discovered During a Preliminary Survey for Blue and Emission-line Objects	34
3.1 Primary Dwarf Spectral Standards	65
3.2 Secondary Dwarf Spectral Standards	68
3.3 Giant (and Higher Luminosity) Spectral Standards	70
3.4 Miscellaneous Objects	71
3.5 Features Found in Late K to Late M Spectra from 6300 to 9000 Angstroms	72
3.6 Comparison of Spectral Types for Very Late “Dwarfs”	79
3.7 Integration Limits for Color Ratios	79
3.8 Color Ratios Determined from the Spectra	80
3.9 Other Dwarf/Subdwarf Spectra	87
3.10 Stars with Observed Spectra and Known Masses	89
3.11 Log of 0.63 to 1.50 Micron Spectroscopy	131
3.12 Comparison of $I - J$ Values	132
3.13 Surface Gravities	133
3.14 Temperatures Derived from the Best Fit to Allard’s Model Spectra with $[M/H] = 0, \log g = 5$	133
3.15 Observed vs. Synthetic Colors	134
3.16 Comparison of Temperature Sequences	135
3.17 The Coolest “Dwarf” Spectra	160
3.18 Low-mass Companions for Which Spectra Do Not Exist	162

3.19 Colors, Absolute Magnitudes, and Temperatures for a Sequence of M Dwarfs	163
3.20 Spectra of Single M Dwarfs Obtained on 1991 Nov 13	186
3.21 Spectra of Composite Systems (M Dwarf + Low-mass Secondary) Obtained on 1991 Nov 13	187
3.22 Magnitude Differences for the Components of the Five Composite Systems	188
3.23 Colors of the Composite Systems	189
3.24 Absolute Magnitudes of the Composite Systems	190
3.25 Mean Colors vs. Spectral Type for M Dwarfs	191
3.26 Mean Absolute Magnitudes vs. Spectral Type for M Dwarfs	192
3.27 Results of the Differential Spectroscopy	193
4.1 USNO Photometry of CTI M Dwarfs	234
4.2 Bright, Contaminating Stars in (or near the Edge of) the CTI Strip	235
4.3 Stars from the NLTT Catalogue Which should be in the CTI Strip	236
4.4 Objects used in the Derivation of the CTI Luminosity Function	240
4.5 The CTI Luminosity Function at I	252
4.6 Redistribution of Objects in the First Three Bins of the CTI Luminosity Function When Calibration Equation 4.4 is used instead of Equation 4.2	253
4.7 Luminosity Function Data for Objects with $M_I \geq 7.0$, $\delta > -20^\circ$, and $d \leq 5.2$ Parsecs (White Dwarfs Excluded)	255
4.8 The CTI Luminosity Function at V	256
5.1 The Spectroscopic LHS Catalog	295
5.2 Cross-list: Gliese (GL/GJ) — LHS	503
5.3 Cross-list: Giclas (G) — LHS	514
5.4 Cross-list: Common Name — LHS	534

5.5 Cross-list: Bayer Designation — LHS	535
5.6 Cross-list: Flamsteed Designation — LHS	536
5.7 Cross-list: HR — LHS	537
5.8 Cross-list: BD — LHS	539
5.9 Cross-list: CD — LHS	549
5.10 Cross-list: CP — LHS	554
5.11 Cross-list: Wolf — LHS	558
5.12 Cross-list: Ross — LHS	560
5.13 Cross-list: Variable Star Designation — LHS	563
5.14 Cross-list: Miscellaneous Name — LHS	564
5.15 LHS Objects Between 1001 and 5413 with $m_{pg} - m_R \geq 2.5$	565
5.16 Spectroscopic Observations of Objects Listed in Table 5.15	567
5.17 List of Confirmed or Suspected Multiple Systems Given as Single LHS Entries	568
5.18 Possible Very Late Type Stars, Brown Dwarf Candidates, and Extreme Subdwarfs from <i>The Stars of Low Luminosity</i>	591
5.19 Objects with the Highest Proper Motions (as of 1992)	604
5.20 Objects with Proper Motions Exceeding $0.57''\text{yr}^{-1}$ Which are not listed in the LHS Catalogue	606

ABSTRACT

As any introductory astronomy student knows, M dwarfs are the most common stars in the Galaxy and are the faintest of the core hydrogen burners. A comprehensive study of these faint objects is crucial to our understanding of the stellar composition of the Galaxy and necessary for a more complete knowledge of the transition between main sequence M stars and their slightly less massive counterparts, the brown dwarfs, which never achieve hydrogen burning in their cores.

In this thesis, a spectroscopic catalog of 125 K and M dwarfs is first presented. This catalog covers the wavelength range from 6300 to 9000 Å, near where these objects emit most of their light. Eight of these spectra, covering classes M2 through M9, are combined with infrared spectra from 0.9 to 1.5 μm to create a second catalog. The two sets of spectra are used to search for temperature-sensitive atomic lines and molecular bands, which are then used in fitting the observed spectra to a sequence of theoretical models. As a result, a new temperature scale for M dwarfs is determined, and this scale is more accurate than previous determinations which have depended on blackbody energy distributions. The sequence of spectra is also used to compare the spectrum of the brown dwarf candidate GD 165 B to known M dwarfs. Furthermore, the spectral catalog is used in an attempt to separate the spectra of faint companions from their M dwarf primaries in systems where the two objects are too close for conventional spectroscopy to resolve the individual components.

A survey for faint M dwarfs is also launched using the data acquired through the CCD/Transit Instrument (CTI) on Kitt Peak, Arizona. Follow-up spec-

troscopy is presented for 133 of these objects, and several more very late M dwarfs are identified. This spectroscopy combined with photometric data from the CTI are used to construct a luminosity function for M dwarfs which is in excellent agreement with determinations from previous surveys.

Finally, possible avenues for future work are discussed. These include spectroscopic follow-up of the reddest of Luyten's proper motion objects — the first results from which have uncovered, in just twelve observations, two objects of type M7 and one of type M8, among the coolest objects yet recognized. Future searches, such as an all-sky survey for objects of extremely high proper motion, are also outlined.

CHAPTER 1

INTRODUCTION

Thou know'st 'tis common.

— William Shakespeare, Hamlet, Act I, scene ii, line 72 (1600)

This thesis is an in-depth study of the most common stars in the Galaxy — the so-called “M dwarfs” — and while this might ordinarily mean that the subject matter would be interesting only in an academic context, my reasons for studying this subject are deeply rooted in my early perceptions of a science in which I read frequently about the making of discoveries and the uncovering of new puzzles. The puzzle explored in these pages can be stated as follows: although M dwarfs are the commonest of stars in the Milky Way, and because one would guess *a priori* that the less massive M dwarfs would be even commoner still, very few of these lowest mass objects are currently recognized. Unless the presumptions about our own local galactic milieu are in error, these objects must exist in hordes. Yet, this myriad of low-mass stars awaits positive detection. Finding the answer to this problem provides the impetus behind this thesis...

I remember in particular a clear, moonless night from my childhood when, while riding on the hay wagon *en route* to one of our frequent “wienie roasts” in the Old Field, I asked my father, “Daddy, what’s the name of that star?” His response was, “I don’t know.” Undaunted, I found another and asked, “What’s

the name of *that* star?” His answer was the same. Nonetheless, this experience left me with a passion for wanting to find out what those stars were called. Lesson #1: I *had* to know.

Later, in the second grade, I was introduced to my elementary school’s library, and eventually I was able to locate the five or six books that comprised the library’s astronomy section. Unfortunately, some of the books were too advanced for me to read, but there were two, both by H. A. Rey, that were written at my level. As I flipped through them, I found, much to my delight, that the stars names were all listed! Lesson #2: Research pays off.

Then there was the summer afternoon as a teenager when my order from Dover Books arrived: a three volume set called *Burnham’s Celestial Handbook*. Noteworthy objects in every constellation were described in detail. I literally couldn’t put the books down. There were so many fascinating discoveries there — I could scarcely imagine what other exciting discoveries might lie hidden in the Universe just waiting to be uncovered by some probing astronomer. As I “rounded up” the cows that day for their afternoon milking, I took the first volume along with me. The cows were up at the pond, and I remember being somewhat annoyed at having to climb the steep hill which led there because I wasn’t able to walk and read simultaneously. It was then that I began to think seriously about making a career out of astronomy; besides, if I did things right, I wouldn’t have to sweat in the hot and humid tobacco fields of Middle Tennessee the rest of my life! Lesson #3: I was hooked...

And so with this thesis I begin an astronomical quest: a search for the intrinsically faintest stellar members of our Galaxy. It seems a paradox that we can identify countless quasi-stellar objects lying on the outskirts of the Universe,

yet are unable to find the vast numbers of low-luminosity stars and possibly substellar objects which undoubtedly lie within a few parsecs of our own Sun. In an interesting twist to my childhood conundrum, we now know the name of a certain class of “star” — those that never achieve hydrogen burning in their cores — but have no examples to serve as illustrations. If I were to ask my father today, “Dad, are any of those points of light up there brown dwarfs?”, he could honestly reply, “I don’t know... and neither does anybody else.”

1.1: THE MISSING MASS

Consider a population of kinematically well mixed stars. Using observational measurements, the density and velocity distribution of those stars as a function of distance from the galactic plane can be computed. The more total matter there is concentrated close to the plane, the stronger the gravitational potential will be and the more rapidly will the density of the “tracer” stars drop with increasing distance from the plane. Thus, based on the observations, the density of total matter in the plane of the Galaxy can be estimated.

Oort (1932, 1960) pioneered this kind of analysis, and his results showed that a substantial fraction of the derived total mass could not be accounted for by observed matter. That is, the data suggested a large amount of “missing mass” to reside in the solar neighborhood — mass which must be associated with an unseen, “dark” component of the disk. Using updated observations and better theoretical techniques, Bahcall (1987, and papers referenced therein) showed that half of the mass in the solar neighborhood must reside in the form of unobserved matter. The scale height of this material was computed to be less than 700 pc, and if the constituents are objects having masses under $0.1 M_{\odot}$, then the nearest one would be about 1 pc away and would have a proper motion exceeding 1 arcsecond per annum.

Recent results have begun to cast doubt upon the reality of this “missing mass,” however. Bienaymé, Robin, & Crézé (1987) use a technique based on star counts to obtain a local mass density of 0.09 to $0.12 M_{\odot}pc^{-3}$, consistent with the observed value of 0.10 to $0.11 M_{\odot}pc^{-3}$ (Bahcall 1984). Kuijken & Gilmore (1989a), using data on K dwarfs near the south galactic pole (SGP), conclude

that there is no missing mass in the solar vicinity, with the same result being found when a re-analysis of data on F dwarfs and K giants is used (Kuijken & Gilmore 1989b). Kuijken (1991) confirms these results using a nearby sample of K dwarfs in addition to the SGP sample.

In response to these claims, Bahcall, Flynn, & Gould (1992) use data on K giants at the SGP to produce a local mass estimate in which the systematic and random uncertainties are well understood. In a “one-experiment” run, they find that a model having no dark matter is inconsistent with the data at an 86% confidence level. These authors give a critical analysis of the Kuijken & Gilmore (1989a, b) mass determinations and conclude that a more robust analysis of the same data would imply a substantial fraction of missing matter. The inhomogeneity in the Bienaymé, Robin, & Crézé (1987) star count sample, as well as in the combined K dwarf sample of Kuijken (1991), should be treated, according to Bahcall, Flynn, & Gould (1992), with caution, as this may introduce unwanted systematic errors.

Clearly, the last has not been written on this subject. If there *is* missing mass, the best possibilities would appear to be very low luminosity degenerates, faint M dwarfs, or brown dwarfs. Liebert, Dahn, & Monet (1988) have shown, however, that the contribution to the local space density by low luminosity white dwarfs is negligible. This has led researchers to begin new surveys in an attempt to identify previously unrecognized M dwarfs and brown dwarfs of faint absolute magnitude.

1.2: A COMPANION TO THE SUN?

Inadequate knowledge about the low-luminosity membership of our own solar neighborhood was reflected in a recent study to come out of the field of marine palaeontology. Raup & Sepkoski (1984) studied marine fossil records throughout the Phanerozoic (the last 600 million years) and found, as they were expecting, evidence that mass extinctions have occurred many times, but to their surprise, the extinctions appeared to be cyclical with a period of 26 Myr, at least over the last 240 Myr (Lewin 1983). Two major, competing hypotheses were then born. The first, advocated by Rampino & Stothers (1984), introduced the idea that the oscillatory motion of the solar system about the plane of the Galaxy would allow for large clouds of gas and dust to perturb the Oort comet cloud. Such a scenario would send comets showering into the inner solar system, and some of these would strike the earth, eradicating many forms of life as global climactic conditions changed abruptly. A variation of this idea is put forth by Schwartz & James (1984), but they argue, based on the sun's current position, that the extinctions occur when the solar system is at its extreme points *away* from the plane, and here the extinction would be caused, perhaps, by biospheric alterations induced by larger doses of cosmic or X rays.

The second hypothesis invokes a companion to the sun as the perturber of the Oort cloud (Davis, Hut, & Muller 1984; Whitmire & Jackson 1984). According to Davis, Hut, & Muller (1984), this companion, which they dub "Nemesis," has a moderately eccentric orbit, a period of 26 Myr, and is currently near its aphelion distance of ~ 0.7 pc. As a brown dwarf, its presence in the solar vicinity could have gone unnoticed because of faint apparent magnitude. As an M9 dwarf, it

would have an apparent magnitude of $m_V = 13.5$, but negligibly small proper motion since it is at aphelion. Only its parallax of 1.4 arcseconds would reveal its true identity, leading Perlmutter et al. (1986) to begin a parallax survey of all faint red stars catalogued by the Dearborn Observatory.

As this sample serves to illustrate, our census of objects near the sun is admittedly incomplete — we are currently unable to rule out the existence of a possibly stellar companion which would lie even closer to the sun than Proxima Centauri! Furthermore, our knowledge of brown dwarfs is based on theoretical grounds only; we have only the crudest idea what the apparent magnitude of such a solar companion might be or what it might look like spectroscopically.

1.3: A RECENT HISTORY OF SEARCHES FOR VERY LOW-MASS STARS AND BROWN DWARFS

This renewed interest in the original Oort missing mass problem, as well as speculation about an undiscovered solar companion, has helped to spark new surveys, implementing new techniques and technologies, to search for brown dwarfs and the faintest M dwarfs. Imaging fields around nearby stars (Jameson, Sherrington, & Giles 1983; Skrutskie, Forrest, & Shure 1989) is being done to detect possible faint companions. Advances in infrared speckle imaging are enabling astronomers to search nearby M dwarfs for companions as close as 0.2 arcsecond to their primaries and fainter by up to 6 magnitudes at H and K (Henry & McCarthy 1990; Henry 1991; see also Mariotti & Perrier 1991); this technique is providing positive confirmation for some companions first detected during astrometric searches (see, e.g., Lippincott 1978). Obtaining photometry of white dwarfs is continuing in an attempt to detect possible infrared excesses which might indicate the presence of low-mass, very red companions (Probst & O'Connell 1982; Probst 1983a, b; Kumar 1985; Shipman 1986; Kumar 1987; Zuckerman & Becklin 1987a; Becklin & Zuckerman 1988; Zuckerman & Becklin 1992). Photometric studies aimed primarily at discovering young, hot brown dwarfs are focusing on young star clusters and star formation regions such as the Taurus Molecular Cloud (Forrest et al. 1989), the ρ Ophiuchi complex (Rieke, Ashok, & Boyle 1989; Rieke & Rieke 1990), the Pleiades (Stauffer et al. 1989; Jameson & Skillen 1989; Hambly, Hawkins, & Jameson 1991; Simons & Becklin 1992), and the α Persei cluster (Prosser 1992; Rebolo, Martín, & Magazzù 1992). Other studies have instead looked into nearby, older clusters such as the Hyades

(Leggett & Hawkins 1989; Bryja et al. 1992), since for older clusters it should be easier to distinguish on a color-magnitude diagram between brown dwarfs and stars settling toward the main sequence. Other photometric searches have used molecular clouds merely as backdrops to define a well-determined sample volume (Jarrett 1992). Photometric studies have begun in the field, often on much larger areas of sky (Reid & Gilmore 1982; Gilmore, Reid, & Hewett 1985; Boeshaar & Tyson 1985; Boeshaar, Tyson, & Seitzer 1986; Chester et al. 1986; Hawkins 1986; Hawkins & Bessell 1988; Tinney, Mould, & Reid 1992; this thesis). Proper motions are also being measured for faint stars in the Southern hemisphere (Ruiz et al. 1988), and very accurate radial velocity studies are being conducted for (mainly) nearby stars (Campbell, Walker, & Yang 1988; Marcy & Benitz 1989; Latham et al. 1989; Marcy & Butler 1992). Brown dwarfs and planets are now being reported as companions to neutron stars (Fruchter et al. 1990; Bailes, Lyne, & Shemar 1991 — but retracted by Lyne at the 1992 AAS Meeting in Atlanta; Wolszczan & Frail 1992), as possible maser-causing sources in red giants (Struck-Marcell 1988), and as the cause of purported gravitational micro-lensing effects (Irwin et al. 1989). In the past year, quasar searches have even begun to uncover faint, late-M dwarfs and brown dwarf suspects (Schneider et al. 1991; Irwin, McMahon, & Reid 1991).

Despite all of these efforts, however, only six objects (see §3.3) have been identified which are distinctly later in spectral type, and presumably lower in luminosity, than van Biesbroeck 10 discovered in 1944! Why haven't previous searches found these objects in great numbers?

1.4: GOALS FOR THIS THESIS

In the chapters which follow, I pursue three different approaches to the continuing search and study of these objects at the end of the main sequence. My original idea was to begin a new, large area survey of these stars using the data base provided by the CCD/Transit Instrument (CTI), described in Chapter 2. After some research into the literature on the subject, though, I found that no comprehensive compendium of late M dwarfs and brown dwarf candidates existed. Furthermore, no one had sought to observe each of these objects in a systematic way so that differences and similarities within the group could be studied. The most obvious tool for such a study is low-resolution spectroscopy. Unfortunately, this, too, presented a problem — standard spectral classification had always been done in the ordinary photographic region, but these objects emit most of their light in the red and infrared portions of the spectrum. Blueward of this, many are beyond the detection limit of even the largest telescopes.

Thus, the first approach became obvious — establishing a new spectral classification scheme for these objects at wavelengths where they were more easily observable. This work is presented in Chapter 3.1. With the development of this spectral sequence, other possibilities arose, such as extending the sequence into the infrared and comparing it to newly produced stellar atmospheric models (Chapter 3.2), obtaining a spectrum of the best brown dwarf candidate known to see if it differed from other spectra in the sequence (Chapter 3.3), and introducing new spectroscopic tools which make it possible for the spectrum of a faint component in a binary system to be studied (Chapter 3.4).

With the establishment of this spectral sequence, the second approach could

begin, and this uses both photometric *and* spectroscopic criteria to study faint, red objects found in the CTI data archives. With this information, a luminosity function (LF) for M dwarfs is produced. Comparisons to other determinations of the LF, as well as an examination of the stellar initial mass function, will help answer the question “Why haven’t more of the very lowest mass objects been found?” This work is presented in Chapter 4.

The third approach involves a detailed outline for future research in this area. Spectroscopic acquisition of very red objects already catalogued could reveal many more late dwarfs; a larger sample is badly needed if the gross properties characterizing the population are to be distinguished from the subtle differences existing from spectrum to spectrum. This proposed survey is highlighted in Chapter 5.1. In the context of obtaining a more detailed picture of the makeup of the solar neighborhood, the potential pay-offs of an all-sky survey for high proper motion objects is discussed in Chapter 5.2. The rewards of an all-sky photometric survey are also briefly addressed in Chapter 5.3

In Chapter 6, the major conclusions of this thesis are summarized.

CHAPTER 2

THE CCD/TRANSIT INSTRUMENT (CTI)

Astronomy compels the soul to look upwards
and leads us from this world to another.

— Plato, The Republic, book VII, 529 (c. 428 - c. 348 B.C.)

The photometric data base used in the determination of the luminosity function (Chapter 4) is the result of an on-going survey conducted by the CCD/Transit Instrument, otherwise known as CTI. Descriptions of this telescope, its data acquisition, and its archives are given in §2.1. Many astronomical investigations are possible with such a data base, as discussed in §2.2, and the results of the author's previous blue object/emission-line object survey are briefly highlighted as an example. In §2.3 the CTI's role in this thesis is outlined.

2.1: TELESCOPE AND DATA BASE

The CTI is a 1.8-m, f/2.2 meridian-pointing telescope located on Kitt Peak, Arizona. It has no moving parts, but utilizes two 320×512 RCA charge-coupled devices (CCDs) aligned with columns in the east-west direction and operated in a “time-delay and integrate” (TDI) mode at the apparent sidereal rate to form an image of the transitting sky (McGraw, Cawson, & Keane 1986). The strip is 8.25-arcminutes wide (north to south) and spans the full range of right ascension.

The telescope is pointed at a declination of $+28^\circ$, where it can monitor, for example, both the central portion of the Coma Berenices galaxy cluster and areas contained within the Taurus Molecular Cloud. Figure 2.1 shows the course of the CTI strip through galactic coordinates. Note that the strip passes nearly through the North Galactic Pole (NGP), crosses the plane of the galaxy twice, and probes as far south of the plane as $b \approx -35^\circ$. Figure 2.2 shows a typical field near the NGP. This can be compared to Figure 2.3, which shows a field near the galactic plane. In a year's time the CTI surveys about 45 square degrees.

Photometric precision is enhanced by utilization of the TDI technique which averages all spatial instrumental corrections into more stable linear functions. In the space of about 1 minute, an object will traverse 512 lines on the CCD, sampling the flat field vertically as it transits the detector. In such a system, only a flat-field *line* needs to be measured, and this averaging results in a flatter flat field. Bias acquisition is done similarly. Calibration of the CTI photometry will be discussed in Chapter 4.

One of the two CCDs in the focal plane always observes through a V filter while the other observes through B , R , or I depending upon the sky brightness. Because it is necessary to maintain a uniform optical path length through the filters so that the CTI will remain in focus regardless of filter choice, the CTI filter system is slightly different from the Johnson/Cousins $BVRI$ system, with each filter having a thickness of 3 mm (McGraw, Cawson, & Keene 1986). The nightly limiting magnitude is $V \approx 21$.

The pixel data are searched to find every detectable object, and photometric parameters are calculated for each. These parameters become part of a "Pool List" and a "Master List" which contain the best estimate for each parameter,

and a “History List” for each color which maintains a light curve for every detected object. (A step-by-step description of the CTI data reduction process can be found in Cawson, McGraw, & Keane 1986a). The “Pool List” contains information on every detection, sorted by right ascension. The “Master List” is a subset of the “Pool List” containing only those objects having a high likelihood of being real. The data listed for each object are variance-weighted mean parameters determined using all available, reduced nights of photometry. Each entry lists, among other parameters, the right ascension and declination (for the 1987.5 equinox) of the object, the average magnitude and magnitude error in each detected bandpass, the number of observations in each bandpass, the image area on the CCD, the ellipticity of the image, the image’s peak surface brightness, and pointer numbers referring to its entries in the various “History Lists.” There is a “History List” for each bandpass containing the object’s coordinates, the individual magnitudes and errors for each detection, and the dates for each individual magnitude determination. The software which is used to interrogate these data bases is described in Cawson, McGraw, & Keane (1986b).

2.2: SCIENTIFIC PROGRAMS

The number of scientific programs which can be pursued with the data base is almost limitless. A few examples are listed below.

Extragalactic Astronomy:

- **Galaxies** — The distribution of galaxies in the surveyed strip can be determined. The density function of Tyson & Jarvis (1979) predicts that 1000 galaxies

are detected per night down to $V = 18$ and that there are some 40,000 total in the strip down to a limiting magnitude of $V = 21$.

- Supernovae — Using the supernova production rate per average galaxy of Tammann (1977), it is predicted that one or more bright supernovae ($V < 16$) will be detected before maximum each year and that some 15 supernovae can be detected per year in galaxies brighter than $V = 18$. Using the data base, the light curves of these supernovae can be monitored and the supernova production rate can be measured.

- Quasars — Complete samples of quasars, based both on color and on variability, can be selected (McGraw *et al.* 1988). The density function of Schmidt & Green (1979) predicts that there are over 500 quasars with $V \leq 20$ in the CTI strip. With this sample the space density and luminosity function as functions of redshift can be determined, and the hypothesis that all quasars are luminosity variables can be studied (McGraw, Angel, & Sargent 1980).

Galactic Astronomy:

- Galactic structure — The structure of our galaxy can be studied to faint magnitudes by investigating the distribution of stars via multi-color star counts.

- Variable stars — The data bases can also be used to study many kinds of variables and specifically to identify and study novae and dwarf novae.

- White dwarfs — Large samples of white dwarfs can be obtained to study scale height and to determine the distribution of white dwarf spectral classes.

- Proper motion stars — By comparing the CTI positional data to a digitized version of the same area of sky taken from the 1950 Palomar Sky Survey (Humphreys, Pennington, & Zumach 1989), previously unknown nearby stars

of faint apparent magnitude can be discovered. In fact, as the CTI continues to collect data, its own timeline of positions can be searched to discover proper motion objects (Benedict *et al.* 1991).

- M dwarfs — See §2.3.

Between 1987 and 1989, the author undertook a survey of blue and emission-line objects in the CTI data base. Some of the more interesting objects uncovered by this investigation were white dwarfs, blue subdwarfs, quasars, a starburst galaxy, a Seyfert galaxy, a planetary nebula, and a dMe star. These objects are listed in Table 2.1 in order of right ascension. The first column gives the CTI positional designation using equinox 1987.5; columns 2 and 3 give the 1950 coordinates of the object; column 4 gives the V magnitude; and column 5 gives the object's spectral type. Spectra and finder charts for these objects are available from the author upon request. This preliminary survey illustrates the potential which exists for pure astronomical discovery in the CTI strip.

2.3: CTI'S ROLE IN THIS THESIS

In the present study, the CTI data base will be used to define a photometrically selected sample of M dwarfs to faint limiting magnitudes. Specifically, the $R - I$ color will be used as the selection criterion, with $V - I$ also being used when V magnitudes are available. Since in general only a single color is used for selection, contamination by background giants, which becomes more problematic near the galactic plane, cannot be estimated with the usual color-color diagrams. Instead, the percentage of contamination by giants is estimated by spectroscopically observing a subset of the photometrically selected objects. The

CTI data base is also used to check for the long-term, high-amplitude variability characteristic of all M giants of type M5 and later.

Dwarf stars of type M6 and later are very important to our understanding of the end of the main sequence, and CTI is a valuable tool for uncovering more of these objects. Spectroscopic follow-up is used to verify all CTI objects suspected through their $R - I$ colors to be of extremely late spectral type. To recognize these objects and to differentiate them from their higher luminosity counterparts, a series of standard spectra has first been obtained. These standard observations are reported in Chapter 3 along with some of the subsequent investigations which have arisen based upon the establishment of the standard spectral sequence. In Chapter 4 the photometrically selected CTI sample of M dwarfs is discussed, and the faint end of the stellar luminosity function is calculated.

TABLE 2.1
OBJECTS DISCOVERED DURING A PRELIMINARY SURVEY
FOR BLUE AND EMISSION-LINE OBJECTS

CTI Object No.	RA (1950)	Dec	V	Sp. Type
001249.6+280414	00:10:52.9	+27:51:43	19.3	Quasar ($z=2.34$)
004226.5+275906	00:40:26.4	+27:46:47	19.4	Quasar ($z=2.31$)
012903.9+280046	01:26:58.7	+27:49:09	18.6	DA
013255.2+280041	01:30:49.6	+27:49:09	18.8	DA
014501.4+275847	01:42:54.5	+27:47:31	18.6	DA wk
015332.9+280203	01:51:25.1	+27:51:00	19.5	DB
015809.8+280132	01:56:01.5	+27:50:36	18.7	DA
015836.1+280551	01:56:27.7	+27:54:56	19.2	DB
015844.7+275957	01:56:36.4	+27:49:02	18.9	Quasar ($z=0.75$)
020125.3+275914	01:59:16.7	+27:48:24	19.2	DA
021331.9+280443	02:11:22.1	+27:54:13	19.2	DA
035037.2+280044 ^a	03:48:19.5	+27:53:59	18.1	DA
045934.1+280335 ^a	04:57:13.1	+28:00:15	17.1	DA
054326.7+280448	05:41:04.8	+28:03:50	18.6	DA
054438.5+280224 ^a	05:42:16.6	+28:01:30	17.9	DA
062219.2+280323	06:19:57.3	+28:04:32	18.4	DA
102739.6+280341	10:25:33.7	+28:15:11	17.6	Quasar ($z=0.36$)
104847.9+275823 ^{a,b}	10:46:44.3	+28:10:28	15.3	DA
120403.9+275822 ^c	12:02:09.0	+28:10:54	15.5	Seyfert I galaxy ($z=0.165$)
125858.5+275856	12:57:09.9	+28:11:04	17.6	DC(?)
134910.5+275904 ^d	13:47:27.4	+28:10:13	16.3	sdB
134927.6+275849	13:47:44.5	+28:09:58	17.3	Quasar ($z=0.70$)
135700.6+280448 ^a	13:55:18.3	+28:15:45	17.0	DA
135755.3+280057	13:56:13.1	+28:11:53	16.8	dMe
142500.4+280449	14:23:20.9	+28:14:57	18.3	Quasar ($z=1.85$)
143808.4+275934 ^a	14:36:30.1	+28:09:15	17.8	DA
144827.0+280525	14:46:49.6	+28:14:44	17.8	Starburst galaxy($z=0.030$)
163440.3+280306 ^a	16:33:09.9	+28:07:42	17.0	DA
175353.4+280005 ^e	17:52:24.8	+28:00:27	12.6	Planetary nebula
184708.4+280127	18:45:39.2	+27:58:56	17.4	sdB
195027.4+275957 ^{a,f}	19:48:55.7	+27:54:11	18.5	DA

TABLE 2.1 — continued

Notes:

- ^a See Kirkpatrick & McGraw 1988.
- ^b Given as WD 1046+281 (Ton 547) in McCook & Sion 1987.
- ^c Given as QSO 1202+281 (GQ Com) in Hewitt & Burbidge 1980.
- ^d Shows a proper motion of ~ 0.25 arcsecond/yr; also known as G 150-43.
- ^e Given as PK 053+24.1 (Vy 1-2) in Perek & Kohoutek 1967.
- ^f Shows a proper motion of ~ 0.20 arcsecond/yr.

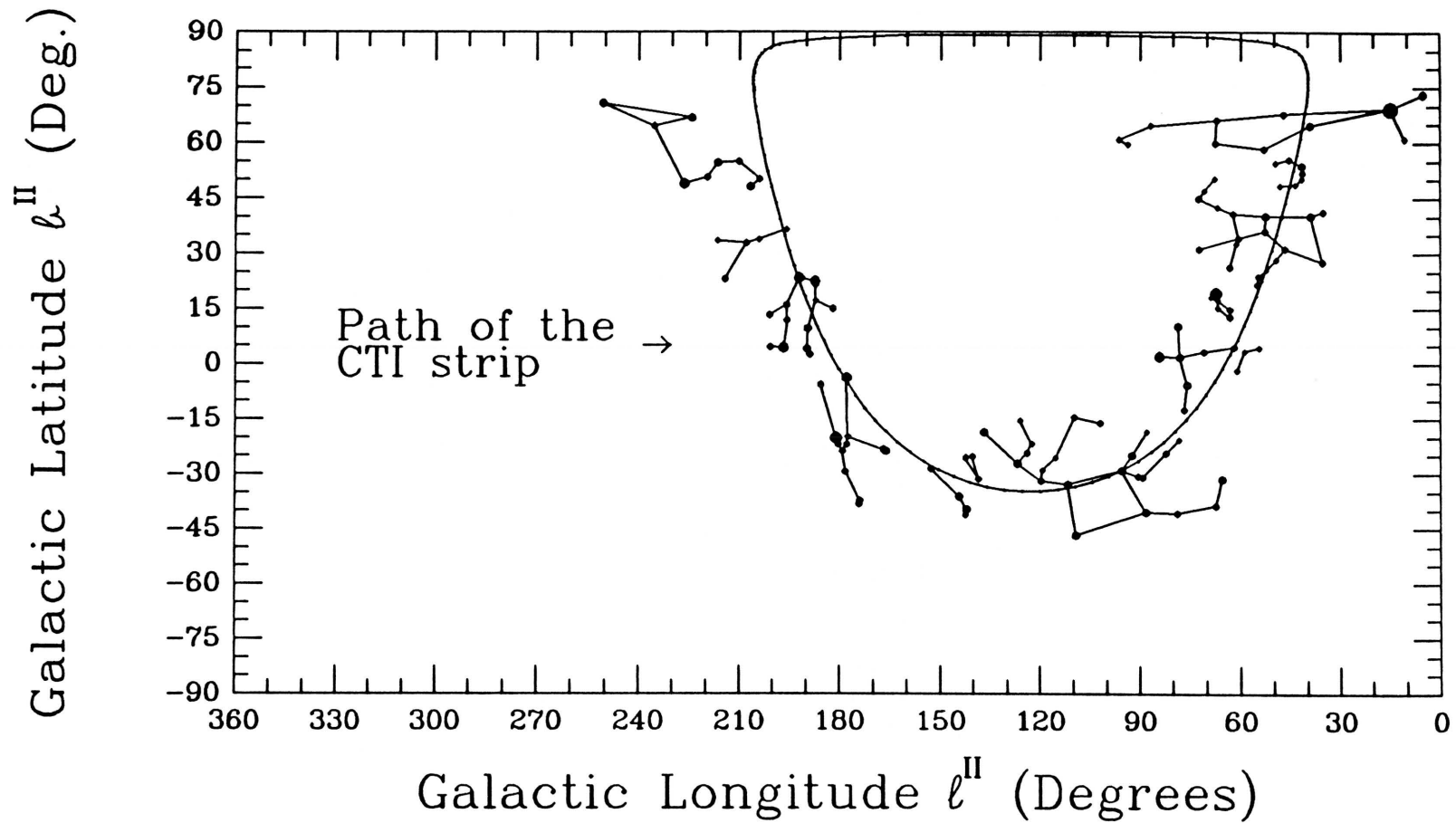


FIG. 2.1. — The path of the CTI survey in galactic coordinates. Familiar constellations are shown along its course. Note that the strip crosses nearly through the North Galactic Pole, crosses the plane of the Galaxy twice (in Cygnus and again in Gemini/Taurus), and probes as far south as $b \approx -35^\circ$. Note also that Pollux (β Geminorum) and Scheat (β Pegasi) fall in the strip, with Albireo (β Cygni) falling just outside.

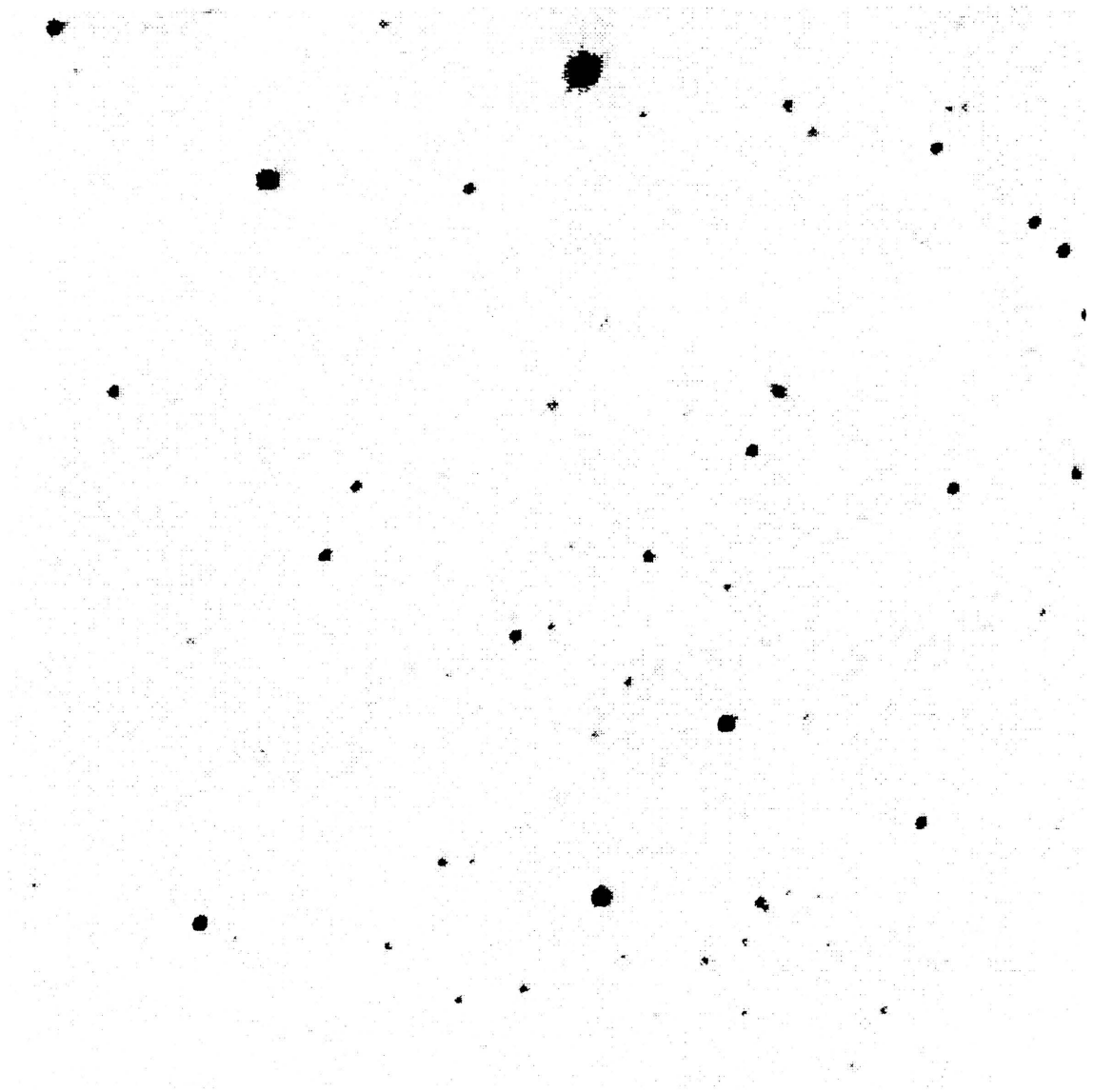


FIG. 2.2. — A typical 1-minute CTI exposure (8.25-arcminutes on a side) in Coma Berenices near the North Galactic Pole. This frame was taken with the “clear” filter and is centered at RA (1950) 12:21:51. North is up, with east to the left. Note the paucity of objects.

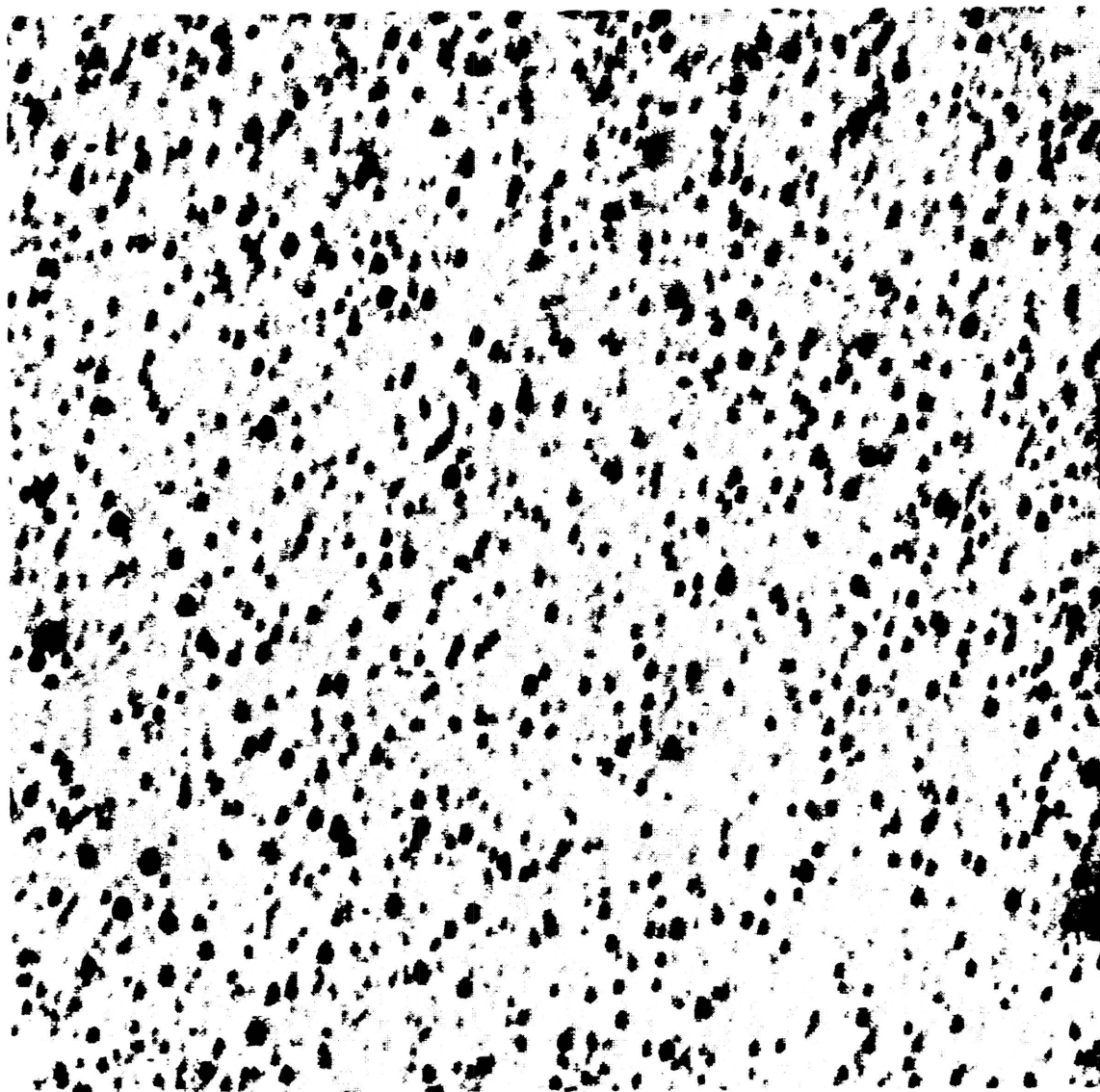


FIG. 2.3. — A typical 1-minute CTI exposure (8.25-arcminutes on a side) in the galactic plane in Cygnus. This frame was taken with the *I* filter and is centered at RA (1950) 19:43:47. Again, north is up, with east to the left. Note the plethora of objects.

CHAPTER 3

RED/INFRARED SPECTROSCOPY OF LOW-MASS OBJECTS

Ice is the silent language of the peak;
and fire the silent language of the star.

— Conrad Aiken, And in the Human Heart, Sonnet 10 (1940)

In this chapter, a better understanding of low-mass objects will be obtained by studying their language — that is, their spectra — in a variety of contexts: What spectral characteristics do these objects possess? Can they be differentiated from giants of the same temperature? How does the spectral signature change with decreasing temperature? What *are* the temperatures of these objects? Do there exist spectral characteristics which can discriminate between a low mass stellar object and an even lower mass brown dwarf? Can we establish an empirical relation between a dwarf's spectral class and its mass? If so, what is the smallest mass for which the empirical relation is known? How many objects are currently known which reside near the end of the main sequence?

Specifically, this chapter originated as a necessary first step in checking the photometric results from CTI. Obtaining spectra aids in the investigation of the kinds of objects found in the CTI data base and how well the colors are correlated with spectral type. Nearby, very cool dwarfs will be intrinsically faint, so a large telescope is needed for the acquisition of their spectra. Furthermore,

because these dwarfs are very red, only a small percentage of their total flux will be found at visible wavelengths, where traditional spectroscopy has been done. Obtaining spectra closer to the peak of the energy distribution will allow for shorter integration times and a wider sampling of objects. With current CCDs, adequate throughput is possible out to around 9000 to 10000 Å (0.9 to 1.0 μm). Recent advances in infrared spectroscopic instrumentation, though revolutionizing the field, still leave the fainter objects unobservable.

Unfortunately, a uniform set of spectral standards has never been acquired in the region longward of H α (6563 Å). So, to place the spectra of the CTI objects on a standard classification system means that a set of spectral standards will have to be observed over the same wavelength range. This standard sequence is presented in §3.1. Some scientific by-products from this spectral sequence are given in subsequent sections: In §3.2 spectra of some of the brighter objects are combined with near-infrared (0.9 to 1.5 μm) spectra and compared to recent theoretical models to establish temperatures for M dwarfs down to M9. In §3.3 the spectral sequence is used to verify that the spectrum of GD 165 B, the best current brown dwarf candidate, is unlike that of any M dwarf, although its temperature, estimated from the data in §3.2, and its luminosity place it near the end of the stellar main sequence on the H-R Diagram. In §3.4 very high signal-to-noise spectra are presented for some of the objects listed in §3.1, and differential spectroscopy is performed on five composites to obtain spectra of the lower mass secondaries. The results of this chapter are summarized in §3.5.

3.1: SPECTRAL LIBRARY FOR K AND M STARS FROM 6300 TO 9000 ÅNGSTROMS

A well-defined standard sequence for late-type stars in the red/near infrared is useful in many astrophysical applications including spectral classification, spectral definition of subdwarf objects, calibration of the temperatures of late-type stars, definition of the end of the main sequence, detection and deconvolution of close binary systems, and development of the stellar luminosity function for the reddest stars, which is currently not well determined.

An extensive spectral catalog from class K5 to M9 is provided here. There are 108 spectra of dwarfs alone, with an additional 17 spectra of objects from other luminosity classes. For classification purposes, obtaining as large a spectral range as possible was the main priority, so the region from 6300 to 9000 Å was chosen. This region encompasses a number of titanium oxide (TiO) bands, useful in classifying early M dwarfs, and a number of vanadium oxide (VO) bands, useful in classifying late M dwarfs (see, *e.g.*, Keenan and Schroeder 1952). The short-wavelength cutoff at 6300 Å provides overlap with the system of Boeshaar (1976), who used features out to 6800 Å and whose dwarf spectral classification system is used in this paper. The B-system band of the CaH molecule, useful as a discriminant between M dwarfs and M subdwarfs (Ake and Greenstein 1980), falls at 6385 Å, near the cutoff. The long-wavelength cutoff at 9000 Å occurs where telluric water absorption begins to dominate the spectrum. This spectral region corresponds more closely than do the bluer systems with the blackbody peaks of M dwarf stars, whose temperatures range from 4000 to 2400 °K (Berriman and Reid 1987; Liebert, Boroson, and Giampapa 1984; a revision of this temperature

scale in given in §3.2).

This large spectral range enables us to investigate whether there are any gross differences among the spectra of the latest M dwarfs which might help discriminate between two distinct groups — late-type stars and hot brown dwarfs. These spectra also provide an important link between optical and near infrared spectra, the latter of which are quickly approaching the resolution of broadband optical spectra used for spectral-typing purposes.

The kinds of objects chosen and the rationale behind their selection is discussed in §3.1.1. The observation and reduction procedures for all spectroscopic data are presented in §3.1.2. A detailed line identification list, including over 50 features useful in describing the spectra of late-type stars, is given in §3.1.3. The method for classifying the spectra, using a combination of spectral features and spectral slope, is outlined in §3.1.4, and a justification for the late-type (M6.5 and later) dwarf classification used here is provided in §3.1.5. The criteria used for luminosity classification are discussed in §3.1.6. Subsequent spectra, not listed as either primary or secondary standards, are presented and classified in §3.1.7. In §3.1.8, the relation between spectral class and mass for dwarf stars is presented, illustrating that mass estimates can be made for main-sequence stars based on an object's spectral class alone. The results are summarized in §3.1.9.

3.1.1: Object Lists

Primary dwarf spectral standards were taken from the lists of Boeshaar (1976), Keenan and McNeil (1976, 1989), Turnshek et al. (1985), Boeshaar and Tyson (1985), Giampapa and Liebert (1986), McCarthy et al. (1988), and

Henry and Kirkpatrick (1990). All of these references use the classification system of Boeshaar (1976). Because most of the standards from Boeshaar (1976) are unobservable in the summer months, spectra of a number of M dwarfs from Gliese (1969) and other sources including Luyten (1979) were obtained and reclassified against the primary standards to generate a list of secondary standards.

The primary reason for observing giants and supergiants was to verify that these higher luminosity stars could be reliably distinguished from the dwarfs at the resolution of our data. Standards were taken from the lists of Turnshek et al. (1985), Jacoby, Hunter, and Christian (1984), and Keenan and McNeil (1976, 1989). Classification of giants presents a problem in that giants later than M5 are spectrum variables and are thus unsuitable as spectral standards (Merrill, Deutsch, and Keenan 1962; Abt 1963); the same is true of the latest supergiants although attempts at classifying both have been made (*e.g.*, Solf 1978). No giant or supergiant stars later than M5 have been observed in this study.

M subdwarfs present a different problem. Part of the difficulty lies with the taxonomy itself, *i.e.*, the term "subdwarf" encompasses any number of characteristics including photometric, spectral, or kinematic properties, and a star, whether it fits only one or several of these characteristics, may still be dubbed a "subdwarf." Subdwarfs include stars which are underluminous with respect to the dwarf sequence (an effect which may be due to various line or molecular blanketing effects); stars which are metal poor, indicative of an old halo (population II) origin; and stars with velocities placing them in the halo population. For example, Barnard's Star (GL 699) is sometimes listed as a subdwarf (Veeder 1974), although its gross spectral characteristics, at least in the range covered by our data, do not distinguish it from a dwarf star. (See, however, discussions by

Mould (1976) and Mould and McElroy (1978) on the use of CaH to TiO band ratios as discriminants between old disk dwarfs and halo subdwarfs.) There is also a class of subdwarfs with very strong metallic hydride bands (Bessell 1982). Other stars in our survey which have been classified as subdwarfs in the past include GL 275.2 A (Eggen and Greenstein 1965), GL 213 (Joy and Abt 1974), GL 643 (Veeder 1974), and GJ 2155 (Gliese and Jahreiss 1979). In this paper, we will use the term subdwarf to refer only to those stars whose gross *spectral* characteristics distinguish them to be such. The spectrum of two such subdwarfs, LHS 515 and LHS 2067, are presented here.

3.1.2: Observations and Data Reduction

a) Dwarf Standards

Tables 3.1 and 3.2 summarize the observations of 77 dwarf spectral standards. All but three were observed with the Red Channel Spectrograph, equipped with a TI CCD, on the Multiple Mirror Telescope (MMT — effective aperture 4.5 m) on Mt. Hopkins, Arizona. A 270 line mm^{-1} grating with an LP-495 order blocking filter was used to cover the range from 6300 to 9000 Å at a resolution of 18 Å. The remaining three dwarfs were observed on 1989 July 24 at the Steward Observatory 2.3-meter telescope with the setup described in §3.1.2b. To assure placement of very faint objects in the aperture, we used a 2.0-arcsec wide slit. It was not deemed necessary to rotate the slit to counteract the effects of atmospheric refraction because even at an airmass of 2.00, the differential refraction between 6500 Å and 9000 Å is only 0.5 arcsecond (Filippenko 1982). Most of these spectra were taken at airmasses of less than 1.2, where the differential

refraction over this wavelength range is less than 0.2 arcsecond.

In the tables, GL (Gliese 1969) numbers are given in the first column and other names are listed in the second column. The third column gives each object's published spectral type, and the fourth gives the spectral type determined here. The date of observation and the length of integration are given in the final two columns.

Figures 3.1 and 3.2 show the spectra of all objects listed in Tables 3.1 and 3.2. Reduction of all spectroscopic data was done with the Image Reduction and Analysis Facility (IRAF) as follows. Each of our MMT observations was contained in a 200×800 pixel area on the CCD chip. To determine the bias to subtract from each row of data, we derived an estimate from 18 overscan pixels per row. The bias strip was first reduced to a one-dimensional image by medianing the pixels along rows; this value was then subtracted from the data frame, row by row. To eliminate the pixel-to-pixel variations in the dark current, a median of several dark frames was produced and then subtracted from all object, lamp, flux standard, and flat field frames. Next, to determine the pixel-to-pixel sensitivity variations over the chip, a median of the flat fields was taken and a two-dimensional surface (consisting of a low-order cubic spline along both the rows and the columns) fit to the resultant frame. This surface was then divided into the flat fields, and the resultant flat-field images were divided into each object, lamp, and standard frame.

The spectra of the program objects were not perfectly parallel to the rows of the chip. Therefore, for the sky subtraction, regions typically seven pixels wide just above and below each object spectrum on the chip were fit, along columns, to the background and then subtracted from each spectrum. Because the fit is

done along pixel *columns* (which are not perfectly orthogonal to the dispersion axis of the sky spectrum), these areas were chosen to be close to the object spectrum so that sky subtraction would not be adversely affected. In this way, only those night sky features which are in emission have been removed; removal of absorption features such as the atmospheric A-band has not been attempted.

Next, the spectra were aperture-summed to include all light from the object, and the corresponding lamps were summed over exactly the same area to preserve the wavelength information. Lines in each of the resulting one-dimensional lamp spectra (consisting of helium and argon lines) were then identified to provide a dispersion solution, which was applied to each object and standard star spectrum. Next, the spectra were extinction-corrected using the extinction coefficients for Kitt Peak, which are tabulated in IRAF, and a sensitivity function was derived for each standard spectrum. The standard stars used were from Filippenko and Greenstein (1984). Each spectrum was flux-calibrated in units of F_λ using this sensitivity function, and each was inspected for contamination by cosmic rays. Last, each spectrum was normalized to its flux at 7500 Å.

b) Giant and Higher Luminosity Standards

The giant and higher luminosity standards are given in Table 3.3; the description of the columns is the same as that for Tables 3.1 and 3.2, except that the first column gives the SAO number of the star. These higher luminosity standards (with the exception of SAO 82478, which was observed with the MMT setup described above), as well as the dwarf standards GL 83.1, GL 51, and GL 866 AB, were observed with the Boller and Chivens Spectrograph with TI CCD

on the Steward Observatory 2.3-m telescope on Kitt Peak, Arizona. A 400 line mm^{-1} grating was employed with a 2-59 order blocking filter to cover the spectral range from 6900 to 9000 Å. This is 600 Å less coverage than obtained at the MMT, but the resolution is improved to 8 Å. The slit width was 2.5 arcseconds.

Figure 3.3 shows the spectra of the 14 objects listed in Table 3.3; the reduction was the same as for the MMT data. The flux standards were from Massey et al. (1988), where an extension, via a blackbody fit to the data, was required for wavelengths longer than 8100 Å. Each spectrum was also normalized to 7500 Å. In Figure 3.3 (as well as for GL 83.1, GL 51, and GL 866 AB in Figure 1) the 2.3-meter data have been rebinned and smoothed to convert them to the same resolution as the MMT data. All subsequent analyses in this paper use these rebinned and smoothed 2.3-meter data.

c) Miscellaneous Objects

Table 3.4 gives the information on GL 756.2 and LHS 515. Both were taken with the MMT setup described above, and their spectra are shown in Figure 3.4. Details on these two objects are given in §3.1.3c.

3.1.3: Line Identifications

An extensive list of features identifiable in the spectra is given in Table 3.5. All obvious atomic and molecular features between 6300 and 9000 Å have been identified using sources dating back to the pioneering work of Öhman (1934). This compilation is presented here to serve as a general reference list for red/near infrared features in late K and M stars of all luminosity classes. The question of

whether each of the listed wavelengths is a laboratory value or a value measured on a spectrum was ignored because of the low resolution (18 \AA) employed here. The reader, if concerned about this question, should refer to the paper(s) cited.

Figure 3.5 shows detailed spectra of one supergiant, three giants, three dwarfs, and one subdwarf with line identifications marked. The most obvious lines in these late-type spectra are molecular bands of TiO (and VO for the latest types) and the atomic lines of Ca II, Na I, and K I. Also obvious are the telluric lines of H₂O and the telluric A-band and B-band of O₂. In the cooler stars, some of the H₂O absorption is due to the stellar atmosphere, but this is generally overwhelmed by the absorption due to the earth's atmosphere (Spinrad and Newburn 1965; Spinrad et al. 1966).

As can be seen by the spectra in Figure 3.5, supergiants are distinguished by prominent lines of the Ca II triplet and of Fe I and Ti I, as well as prominent bands of CN. In giants of the same spectral type, all of these features are weaker. Dwarfs of similar class have even weaker lines of the Ca II triplet but have much stronger lines of the K I and Na I doublets. The one subdwarf observed shows very strong CaH bands. In short, luminosity classification of the spectra is relatively straightforward except for class II, which is virtually indistinguishable from either class I or class III in this spectral range (Keenan 1957).

As for spectral class, it is clear that K dwarfs, unlike M dwarfs, have little absorption by TiO so that their spectra have much smoother continua. The latest M dwarfs (M7 and later) are distinguished by prominent absorption by VO. Bands of CaH, which are strong in K dwarfs, disappear around spectral class M0 as TiO becomes more prominent. At the resolution of these spectra, H α can be seen in absorption in K dwarfs and occasionally in emission in M

dwarfs. Lines of Fe I and Ca II, which are strong in K through mid-M dwarfs, vanish for late-M dwarfs as absorptions by TiO and VO gain prominence.

Giants, like dwarfs, have little TiO absorption in the K-types, in contrast to mid-M types. The latest M giants are dominated by VO absorption, although none of our giant spectra are late enough to show these VO bands (Keenan and Schroeder 1952). Quantitative criteria for these classifications are given in §3.1.6.

3.1.4: Spectral Classification

In this paper we present a different approach to spectral classification than has generally been used in the past. Instead of using only the strengths of the features to determine a spectral type, the slope of the spectrum is also used. This spectrophotometric approach is outlined in §3.1.4a(i) and is compared to the more widely used method in §3.1.4a(ii).

a) Primary Standards

i) Spectrophotometric Method

Each of the spectra in Figure 3.1 was run through a least-squares minimization program to determine an ordering for the primary spectra. The program compares one normalized spectrum with each of the other normalized spectra in the list of primary standards by taking the difference between the flux values of the two spectra at 3 Å intervals in wavelength. The sum of the squares of these differences is then obtained for each pair of spectra.

The spectra have been normalized to 7500 Å because there is little absorption

present at this wavelength. However, because there is some level of noise in each of the spectra, the relative normalization for any pair may not be optimal. Therefore, the normalization for each of the spectra in the library is multiplied by a number near 1 (typically between 0.95 and 1.05) until the minimum of the squared differences between it and the spectrum being matched is found.

The minimization program can compute this “least squares” value for any specified spectral region covered by the data. In particular, the program was used to produce least-squares matches based on the data set from 6950 to 8950 Å, on only the *short-wavelength* end of the data (6950 to 7500 Å), and on only the *long-wavelength* end of the data (8400 to 8950 Å). Wavelengths shortward of 6950 Å were not included so that the 2.3-meter data, which begin around 6900 Å, could be compared to the rest of the data.

The matches on the entire data set were useful in determining a rough ordering of the spectra from bluest to reddest, but to obtain the exact ordering in those cases where two or more spectra were very similar to one another, the matches on the ends of the spectra were used. For example, consider two nearly identical spectra. If the normalization for spectrum 1 had to be multiplied by a number *greater* than 1.0 to yield the best match to spectrum 2 at the short-wavelength end, but had to be multiplied by a number *less* than 1.0 to yield the best match to spectrum 2 at the long-wavelength end, then spectrum 1 is clearly redder than spectrum 2. In this way, we ordered the entire catalog of primary standards, from bluest to reddest, and this ordering is given in Table 3.1.

With this ordering, the consistency between the Boeshaar (1976) spectral types and those determined here could be checked. It was found that those spectral types needing revision were changed by only a half spectral subclass at

most. Of the twelve revisions, five were changed by half a subclass, and seven were changed by only a quarter subclass. The distinction between those with a Boeshaar designation of “+” or “-” and those without was not evident, so these designations were dropped from the newly adopted types. Since historically there has been little reason to introduce spectral classes K6, K8, and K9, these designations have also not been used here. In fact, it is found that in this wavelength region the differences between K5 and K7, as well as between K7 and M0, are very slight and do not warrant further subdivisions in spectral class.

For the giants, bright giants, and supergiants, the ordering technique did not result in any necessary changes in spectral class. They are listed from bluest to reddest in Table 3.3.

ii) *“Spectral Features” Method*

The more widely used approach to spectral classification is to use the information contained in the spectral features only and to disregard the overall slope of the spectrum. To do this, the continuum must first be divided out of the data. For the latest stars, there are at best only six points in this spectral range which can possibly be labelled as continuum points: 6530 Å, 7040 Å, 7560 Å, 8130 Å, 8840 Å, and 9040 Å. For each of the spectra in the list of primary standards, a second-order polynomial was fit to the fluxes at each of the six continuum points, and the fit was then divided out of the data to yield a flattened spectrum. The flattened spectra were then run through the least-squares minimization technique described above. In assigning an order and spectral classes to the spectra, this method and the spectrophotometric method are identical,

with three minor exceptions:

(1) The method using spectral features alone indicates the following ordering, from bluest to reddest, of the stars with spectral classes of M3.5 or M4: GL 725 B, GL 273, GL 402, GL 275.2 A, and GL 213. Boeshaar's original spectral classes for these are M3.5, M4, M4, M4+;, and M4+, respectively, showing no discrepancies in ordering. Our adopted spectral types for these stars are M3.5, M3.5, M4, M4, and M4, respectively, also showing no discrepancies in ordering.

(2) The "spectral features" method also indicates that G 208-45 and GL 65 A should be switched in the ordering of Table 3.1 so that the spectral class for G 208-45 is identical to or earlier than GL 65 A. However, in our adopted types, as well as in the literature, G 208-45 has a later spectral class than GL 65 A.

(3) This second method also indicates that LHS 523 and G 51-15 should be switched in the ordering of Table 3.1. This is of little consequence, however, because our classification, as well as that of Boeshaar, is M6.5 for both.

Therefore, the results of the two methods are almost identical. The spectrophotometric method requires that the flux calibrations for the data be relatively accurate so that any errors in the slope of the spectra remain small. The method based only on spectral features can be done without the introduction of flux calibration, but a fit to the continuum of each spectrum must be accomplished. Because the number of continuum points is small and because these are doubtless not true continuum points but rather opacity minima between certain bandheads of TiO, for example, this second method is probably more prone to error than the spectrophotometric method. Hence, the procedure outlined in §3.1.4a(i) will be used for spectral classification throughout the rest of this paper. It is not suggested that this method be used for more distant samples of stars

since for these groups interstellar reddening could affect their classifications. The stars discussed here, however, are all nearby and therefore do not suffer from this problem.

b) Secondary Standards

Each of the secondary standards was run through the least-squares minimization program to obtain its best match in the list of primary spectra. In this way, each was assigned a spectral type. The newly adopted spectral type was often considerably different from the spectral type quoted in the literature, sometimes by as much as three subclasses. In most cases, the inconsistencies just reflect the differences between the system of Boeshaar (1976) used here and the systems quoted for their spectral types in Gliese (1969). Boeshaar's Table 3 shows several cases of spectral types disagreeing by up to two subclasses between her system and the systems of Joy and Abt (1974) and Kuiper (1938, 1942). In other cases, slight differences may be due to the fact that the current spectra are observed at longer wavelengths than have been used for spectral classification purposes previously. If a faint, unresolved, red companion is present, this may change slightly the subclass of the primary.

By the technique described in §3.1.4a(i), the secondary standards were also ordered from bluest and reddest. The adopted spectral types and ordering are given in Table 3.2. Since the secondary standards have been rigorously typed against the primary standards, both sets serve equally well as spectral standards.

c) Miscellaneous Objects

GL 756.2 was matched via least-squares minimization to the set of giant standards in Table 3.3 (see §3.1.6). Its resulting spectral type is K7 III. LHS 515 was matched against the set of primary dwarf standards, but only over the region from 7050 to 8950 Å in order to exclude the CaH band from 6750 to 7050 Å. The spectrophotometric classification results in a spectral type of sdM2.5, which we have adopted in Table 3.4. When the “spectral features” technique is used over the same wavelength range, however, the resulting type is found to be sdM0.5, indicating that this object has weaker TiO bands, for example, than a dwarf of the same temperature.

3.1.5: Extension of the Classification System Beyond M6.5

In the original MKK system of spectral classification, the dwarfs were defined only out to M2 (Morgan, Keenan, and Kellman 1943). The subsequent list of standards, the MK system (Johnson and Morgan 1953), extended the dwarf sequence out to M5 by using Barnard’s Star (GL 699) as the reference standard, but this object is now sometimes classified as a subdwarf. The adoption of quantitative classification criteria for dwarfs out to M6.5 was not accomplished until the completion of Boeshaar’s (1976) thesis. Before that time, M dwarfs were classified on one of three systems: the Yerkes system of Morgan (1938) and Kuiper (1942), the Mt. Wilson system of Joy (1947) and Joy and Abt (1974), and various authors’ attempts at extensions of the MK system.

Unfortunately, astronomers are now presented with a similar problem for spectral classification beyond M6.5. The long-known red objects VB 8 (GL 644

C) and VB 10 (GL 752 B) were not classified by Boeshaar (1976), and subsequent discoveries of objects with even cooler spectra prompted another extension of the classification system. Liebert was the first to obtain spectra of many of these late objects, and Boeshaar was asked for her input in assigning their spectral types. These later types, which are presented in Boeshaar and Tyson (1985), have been used throughout this paper as the basis for the classification of the reddest objects.

In the meantime, Wing was continuing to develop a classification system based on narrow-band photometry of TiO bands. Between M0 and M6, Wing's spectral types are almost identical to those of Boeshaar (Wing and Yorka 1979), but later than this the two systems rapidly diverge. In his system, dwarfs and giants of the same spectral subclass have the same TiO band strengths (Wing 1979). Bessell (1991) has adopted Wing's system and assigns types as late as M10 for giants and as late as M7 for dwarfs. For the coolest dwarfs, he also uses the appearance of VO as an indicator of type, doubtless out of necessity because the TiO bands saturate. A comparison between the latest types used in this paper and those adopted by Bessell (1991) is shown in Table 3.6.

Our reasons for adopting the spectral type extension out to M9 are as follows:

(1) Morgan states that the standards of reference for the MK system "do not depend on values of any specific line intensities or ratio of intensities; they have come to be defined by the appearance of the totality of lines, blends, and bands in the ordinary photographic region" (Morgan and Keenan 1973). Bessell (1991) objects to the use of even the "yellow" portion of the spectrum for late M classification and endorses the use of temperature sensitive features in a region near the maximum flux — a valid point, which is the reason that his spectra

and those of this paper cover nearly the same spectral region. Using TiO band strengths as the sole indicator of spectral type, however, is undesirable because it disregards all of the other information present in the spectrum (the “totality” of which Morgan speaks). Furthermore, Bessell (1991) determines the TiO band strengths by fitting a blackbody curve through the highest “continuum” points. Allard (1990) has calculated M dwarf atmospheres before and after the addition of TiO, H₂O, and atomic lines. The depression of the entire spectrum after the addition of these atoms and molecules is striking. Thus, the highest points in an M dwarf spectrum are much below the location of the true continuum, making absolute band strengths unreliable. Ratios are better, and the use of many temperature sensitive ratios is the best.

(2) Note that all of the objects in Table 3.6 have the same Bessell type (M7) except for VB 8 (GL 644 C), which is half a spectral subclass earlier. For the same objects, the classifications in this paper range from M7 to M9. Adopting a system which extends to M9 satisfies the basic tenet which underlies any classification system in any science — things which appear different should be placed into separate categories. The subtle differences in spectral features which distinguish an M0 dwarf from an M1 dwarf may not be immediately apparent from the spectra of Figure 1, but the differences between M7 and M8, or between M8 and M9, are obvious. If spectra which look very similar (like M0 and M1) are segregated, then spectra like those of M7, M8, and M9 should not be placed into the same subclass.

(3) A very fundamental reason for having several subclasses for the coolest spectra, even if few of these objects are currently known, is to search for any peculiarities which could distinguish the spectrum of a brown dwarf from that of

a low-mass star. Above all else, it is these differences that should be noted.

3.1.6: Luminosity Classification

The least-squares minimization techniques described in §3.1.3 are very efficient at determining spectral class, but to distinguish between luminosity classes, other criteria are needed: line ratios, flux deficits, or colors. Both line ratios and flux deficits are unsatisfactory because both of these methods require a *continuum* to be drawn to the data — a rather subjective task since M stars exhibit no true continua. Measuring colors, on the other hand, depends only upon the zero-point offset and somewhat upon the resolution of the spectrum. The zero-point dependence is minimized if we take the ratio of two colors which are closely spaced. Therefore, the emphasis here will be placed on color *ratios*.

Examples of useful color ratios are shown in Figure 3.6. The regions over which the flux was summed were wide enough that, despite any shift due to the object's radial velocity, the features examined still fell in the flux regions. Several lines and bands given in Table 3.5 are useful luminosity discriminants: a) the CaH band around 6975 Å is strong in metallic hydride subdwarfs, weaker in dwarfs, and even weaker in giants, b) the Ti I line at 7358 Å is strongest in giants and supergiants, c) the Na I doublet at 8183 Å and 8195 Å is strongest for the dwarfs, and d) the lines of the Ca II triplet (notably the one at 8542 Å which is less contaminated by nearby lines) are strong for giants and supergiants and weak in dwarfs.

For each of the four features mentioned above, a relatively uncontaminated area in the spectrum close to the feature was found to serve as the “continuum”

against which to ratio the flux. In Figure 3.6(a), for example, the flux under the CaH band was integrated from 6960 to 6990 Å, and this was divided into the flux integrated in the nearby “continuum” area of the same width, from 7020 to 7050 Å. The integration limits for each of the color ratios is presented in Table 3.7 along with the features being measured.

All of the stars in Tables 3.1, 3.2, 3.3, and 3.4 are plotted in Figure 3.6 except for the three stars in Table 3.2 which have spectral types earlier than K5. Dwarfs are marked by filled circles, giants by open circles, the bright giant by an open square, and supergiants by crosses. The subdwarf LHS 515 is denoted by a filled square, and GL 756.2 is denoted by an open triangle. As an example, Figure 3.6(a) shows that the metallic hydride subdwarf has the strongest CaH band for its spectral type, followed by the dwarfs and then the higher luminosity stars. Clearly, this criterion separates the luminosity classes very well.

In the remaining graphs of Figure 3.6 — those involving the Ti I line, the Na I doublet, and the Ca II line — there is also a division between luminosity classes. Unfortunately, the dividing line between the dwarfs and the giants is not strong. Note, however, that for two of the graphs in Figure 3.6 the dwarfs fall above the giants in the diagram, and for the other two they fall below. This suggests that ratios of *these* ratios can be constructed to enhance the division between the luminosity classes. These are shown in Figure 3.7. Here, the separations between the dwarfs, giants, and supergiants are much more pronounced, especially in the ratios of the Ca II line at 8542 Å to the Na I doublet, shown in Figure 3.7(d). Any one of the ratios shown in Figure 3.7 would serve as an excellent luminosity discriminant. The values of the ratios used to generate the graphs in Figures 3.6 and 3.7 are listed in Table 3.8.

It should be noted that GL 756.2, marked with a triangle in the figures, shows strong evidence for being a giant star and not a dwarf as published in Gliese (1969) (see Table 3.4). The most convincing evidence for this is shown in Figure 3.7(d), where it is located well above the locus of dwarf stars but below the area occupied by the supergiants. Furthermore, its uncertain parallax is estimated spectroscopically, not trigonometrically, in the Gliese Catalog, and it has negligible proper motion. In addition, Leggett and Hawkins (1988) have noted that this star has red giant colors.

3.1.7: Classification of Other Spectroscopic Data

The previous spectra were obtained primarily as the result of a cloudy-night back-up program developed in conjunction with a clear-night program aimed at obtaining spectra of very faint, red CTI objects (Chapter 4). These observational programs concluded in September, 1991, well after the writing of the original paper (Kirkpatrick, Henry, & McCarthy 1991) which introduced the set of 93 spectral standards presented in Tables 3.1-3.4. Since additional cloudy weather was encountered, we had the opportunity to acquire more spectra of brighter objects. These are presented in Table 3.9 and Figure 3.8 and are classified using the techniques discussed in §3.1.3 and §3.1.6. Figure 3.9 plots the color ratios of these objects on the same scale as the plots of Figure 3.7. The values of the ratios used to generate these plots are also listed in Table 3.8. Clearly, most of these objects fall along the locus of dwarfs.

Three objects listed in Table 3.9 are worthy of special mention. The first is LHS 2067, whose companion, LHS 2068, has an earlier spectral type than K5

and is thus not plotted in Figure 3.9 or listed in Table 3.8. LHS 2067 itself is plotted with a filled square in Figure 3.9 and falls away from the area occupied by the dwarfs, much as LHS 515 does in Figure 3.7. For this reason, LHS 2067 is classified here as a subdwarf. A comparison of its spectrum (Figure 3.8) to the spectra just above and below it demonstrates that it has more prominent absorptions by CaH at 6382 - 6389 Å and at 6750 - 7050 Å and by K I at 7665 and 7699 Å. Bessell (1982) lists this star as a metallic hydride dwarf, but curiously mis-identifies it in Bessell (1991), where the spectrum is shown as an M10 giant. The reason for the confusion is that the wrong pair of stars is marked on the finder chart in Luyten & Albers (1979). The real LHS 2067 and 2068 are the two stars ~ 40 arcseconds to the northeast of the pair that is marked on the chart. Enough time has elapsed since the chart was taken in the 1950's (the Palomar Sky Survey) for current observations to reveal the true pair via its high proper motion, and hence its displacement, relative to the other stars in the field.

The second noteworthy object is Pleiad #2, a brown dwarf candidate detected in the Pleiades by Stauffer et al. (1989, see their table 1). Although classified here as an M5.5 V, this object could, in fact, be a young, hot brown dwarf with spectral characteristics much like that of a normal M dwarf. Pleiad #2 may have slightly enhanced bands of TiO, as compared to other objects of the same spectral class. Its position in the plots of Figure 3.9 is shown by a filled triangle, and it falls in the region occupied by dwarfs for all of the plots except Figure 3.9(b), but this could be spurious due to the fact that the spectrum itself is rather noisy. The spectrum of Ap 0325+4853 (shown in Rebolo, Martín, & Magazzù 1992), a brown dwarf candidate in the α Persei cluster, also appears much like that of an M dwarf. If these are substellar objects and not

stars, the spectral distinction is not obvious. The Li I doublet at 6708 Å has been proposed by Rebolo, Martín, & Magazzù (1992) as a discriminant which could possibly differentiate between brown dwarf and M dwarf spectra. Unfortunately, higher resolution and higher signal-to-noise are necessary before this discriminant can be tested.

The third noteworthy object is RG 0050-2722, which was discovered by Reid & Gilmore (1981). Based upon the strengths of the spectral features — particularly the appearance of VO — this object should be given a designation of M8 (Liebert & Ferguson 1982; Boeshaar 1992). However, the spectrum presented here is clearly redder than GL 752 B (vB 10), the standard M8 dwarf. A comparison of the $I - J$ color of RG 0050-2722 (Reid & Gilmore 1982) and the $I - J$ colors of other M dwarfs (see Table 3.2.5, which gives colors on the same system as that of Reid & Gilmore) shows that this object is redder than vB 10 but not as red as LHS 2924. A comparison of the $J - H$ and $J - K$ colors shows it to be redder than *both* vB 10 and LHS 2924. We hereby assign RG 0050-2722 a spectral class of M8: indicating the discrepancy between its feature strengths and its colors. A comparison of near-infrared spectroscopy of this object and of other late-M dwarfs should prove interesting.

Other objects in Table 3.9 (see §3.1.8) are used in an update of the spectral class versus mass relation originally presented in Kirkpatrick, Henry, & McCarthy (1991), and several of these are discussed in more detail in §3.4. The significance of objects with spectral types later than M6 — which includes four objects in Table 3.9, six objects in Table 3.1, and two objects in Table 3.2 — is discussed in §3.3.

3.1.8: Spectral Class versus Mass Relation

In an effort to provide a mass calibration for the dwarf spectral sequence established here, we have examined several M dwarfs in binary systems for which component masses have been determined dynamically (not photometrically). In practice, individual component spectra are difficult to obtain unless the two objects in the system are separated by greater than $2''$. Unfortunately, such systems necessarily have long orbital periods and hence poorly determined masses. Nevertheless, seven nearby M dwarfs have separations wide enough to allow the acquisition of component spectra and reasonably accurate masses: GL 65 A and B, GL 166 C, GL 725 A and B, and GL 860 A and B. To this special class of objects we have added eight pairs with separations less than $1''$. In six of these, the primary is much more luminous than the secondary so that its light dominates the spectrum: GL 22 AC, GL 234 AB, GL 508 AB, GL 623 AB, LHS 1047 AB, and G 208-44 AB. In addition, the close binaries GL 352 AB and GL 661 AB possess components of nearly equal masses, and presumably the spectral type of the composite is that of the individual stars.

Table 3.10 lists the masses and spectral types of the calibration M dwarfs. The masses are based on new infrared speckle imaging results and on new parallaxes, and the errors given are standard errors which were determined from the literature (Henry 1992). Shown in Figure 3.10 is the spectral class versus mass relation which allows mass estimates for dwarfs to be made based upon spectral class alone. Because only a few objects are available with known masses and spectra on this system, no corrections for age and metallicity effects on spectral types have been attempted.

As can be seen from Figure 3.10, the trend of spectral class with mass is quickly approaching the line which separates the lowest mass stars from the highest mass brown dwarfs ($0.08 M_{\odot}$). If the trend on this semilog plot is fit with a straight line, it is found that any object with a spectral class of approximately M7 or later can no longer be a star by virtue of its low mass. Interestingly, this is also the point in the spectral sequence where absorption by vanadium oxide becomes apparent (although at higher resolution, VO can be seen at class M5 (Boeshaar (1976))). However, there is no *a priori* reason to believe that the trend in Figure 3.10 is not, for example, asymptotic downward as the mass limit for hydrogen burning is approached. Unfortunately, we cannot presently probe any closer to the brown dwarf line because there are no reliable masses known for objects typed as M6.5 or later. All objects of extremely late spectral class are either single objects (*e.g.*, LHS 2924 and LHS 2065) or are in binaries with very long orbital periods ($P \approx 500$ years for the GL 569 AB system — Forrest, Skrutskie, and Shure 1988), making accurate mass determinations impossible (see §3.3 of this thesis).

3.1.9: Summary

Spectra of 125 late K to late M spectroscopic standards in the region from 6300 to 9000 Å have been presented. Spectral classification has been accomplished by using a spectrophotometric least-squares technique in which both the features and the slope of the spectrum are used. Luminosity classification has been accomplished by identifying luminosity-dependent features in the spectra and creating ratios of narrow-band colors centered on those features. An exten-

sive list of features (from 6300 Å to 9000 Å) identifiable at a resolution of 18 Å in K and M stars of all luminosity classes has been produced. Using dwarfs whose masses are well determined, we have found a tight correlation of mass with spectral class which illustrates that the later M dwarfs are very quickly approaching the brown dwarf limit of $0.08 M_{\odot}$. To examine the trend below $0.10 M_{\odot}$ requires accurate masses to be determined for stars of class M7 or later.

The spectral sequence will also be used to check against current models of cool-star atmospheres from Allard (1990). The spectra provided here represent a stepping stone between the optical spectral sequences developed in the past and the near infrared spectra which are rapidly approaching resolutions similar to that used for spectral classification. As shown in the next section, moderate resolution spectra of late-type stars from 0.63 to $1.5 \mu m$ permit definite temperature scales to be assigned to these very red objects. It is hoped that such a calibration will allow a better determination to be made of the location of the end of the main sequence.

TABLE 3.1
PRIMARY DWARF SPECTRAL STANDARDS

Gliese Number	Other Name	Boeshaar Spec. Type ^a	Adopted Spec. Type	Date Obs. (UT)	Integ. (sec)
820 A	61 Cyg A	K5 V ^{b,c}	K5 V	1989 Jul 14	2
820 B	61 Cyg B	K7 V ^{b,c}	K7 V	1989 Jul 14	2
380	HD 88230	K7 V	K7 V	1990 Jan 22	5
328	BD +2°2098	M0.5 V	M0 V	1990 Jan 22	120
270	BD +33°1505	M0 V	M0 V	1990 Jan 22	597
846	HD 209290	M0.5 V	M0.5 V	1989 Jul 14	5
229	HD 42581	M1 V	M1 V	1990 Jan 22	370
205	HD 36395	M1.5 V	M1.5 V	1990 Jan 22	60
411	HD 95735	M2 V	M2 V	1990 Jan 22	9
382	BD -3°2870	M2 V	M2 V	1990 Jan 22	45
250 B	BD -5°1844 B	M2.5 V	M2.5 V	1990 Jan 22	600
381	G 53-28	M3 V	M2.5 V	1990 Jan 22	95
352 AB	BD -12°2918 AB	M3+ V	M3 V	1990 Jan 21	8
436	BD +27°28217	M3 V	M3 V	1990 Jan 22	720
251	Wolf 294	M3.5 V	M3 V	1990 Jan 22	360
752 A	HD 180617	M3 V	M3 V	1989 Jul 10	17
725 A	HD 173739	M3 V ^c	M3 V	1989 Jul 14	5
273	BD +5°1668	M4 V	M3.5 V	1990 Jan 22	120
725 B	HD 173740	M3.5 V ^c	M3.5 V	1989 Jul 14	5
213	Ross 47	M4+ V	M4 V	1990 Jan 22	130

TABLE 3.1 (continued)

Gliese Number	Other Name	Boeshaar Spec. Type ^a	Adopted Spec. Type	Date Obs. (UT)	Integ. (sec)
275.2 A	G 107-69	M4+: V	M4 V	1990 Jan 22	1200
402	Wolf 358	M4 V	M4 V	1990 Jan 22	900
83.1	G 3-33	M4.5 V	M4.5 V	1989 Jul 24	660
268 AB	Ross 986 AB	M4.5 V	M4.5 V	1990 Jan 22	842
166 C	40 Eri C	M4.5 V	M4.5 V	1990 Jan 20	15
234 AB	Ross 614 AB	M4.5 V	M4.5 V	1990 Jan 22	1980
51	Wolf 47	M5 V	M5 V	1989 Jul 24	960
866 AB	G 156-31 AB	M5+ V	M5 V	1989 Jul 24	420
—	G 208-44 AB	M5+ V	M5.5 V	1989 Jul 13	75
65 A	G 272-61 A	M6— V ^d	M5.5 V	1990 Jan 20	25
—	G 208-45	M6 V ^e	M6 V	1989 Jul 13	225
65 B	UV Cet	M6— V ^d	M6 V	1990 Jan 20	25
406	Wolf 359	M6 V	M6 V	1990 Jan 20	80
—	LHS 523	M6.5 V ^f	M6.5 V	1989 Jul 13	600
—	G 51-15	M6.5 V	M6.5 V	1990 Jan 20	243
644 C	VB 8	M7 V ^{f,g}	M7 V	1989 Jul 10	1200
752 B	VB 10	M8 V ^{c,f,g}	M8 V	1989 Jul 10	1800
569 B	BD +16°2708 B	M8.5 ^h	M8.5	1989 Jul 14	2100
—	LHS 2924	M9 ^{f,g}	M9	1989 Jul 13	1980

TABLE 3.1 (continued)

- ^a Boeshaar 1976 unless otherwise noted.
- ^b Keenan and McNeil 1989.
- ^c Turnshek *et al.* 1985.
- ^d GL 65 A and GL 65 B typed as one spectrum by Boeshaar 1976.
- ^e McCarthy *et al.* 1988.
- ^f Giampapa and Liebert 1986.
- ^g Boeshaar and Tyson 1985.
- ^h Henry and Kirkpatrick 1990.

TABLE 3.2
SECONDARY DWARF SPECTRAL STANDARDS

Gliese Number	Other Name	Published Spec. Type ^a	Adopted Spec. Type	Date Obs. (UT)	Integ. (sec)
764.1 A	HD 184860	K2 V	< K5 V	1989 Jul 14	21
250 A	HD 50281	K6 V	< K5 V	1990 Jan 22	274
340.3	HD 80632	K8 V	< K5 V	1990 Jan 22	45
775	HD 190007	K4 V	K5 V	1989 Jul 14	3
764.1 B	BD -10°5130 B	K5 V	K7 V	1989 Jul 14	21
265 A	BD +27°1311 A	M0 V	K7 V	1990 Jan 22	300
786	HD 193202	M0 V	K7 V	1989 Jul 14	10
748.2 A	BD +1°3942 A	M0 V	K7 V	1989 Jul 14	80
430	BD +63°965	M0 V	K7 V	1990 Jan 22	210
338 B ^b	HD 79210	M0 V	K7 V	1990 Jan 22	10
734 A	HD 230017	M0 V	M0 V	1989 Jul 14	15
763	HD 184489	M1 V	M0 V	1989 Jul 14	17
338 A	HD 79211	M0 V	M0 V	1990 Jan 22	10
748.2 B	BD +1°3942 B	—	M0 V	1989 Jul 14	80
839	G 215-20	M2 V	M0.5 V	1989 Jul 14	17
—	GJ 2155	sdM ^c	M0.5 V	1989 Jul 14	25
761.2	BD +0°4241	M1 V	M0.5 V	1989 Jul 14	35
720 A	BD +45°2743	M2 V	M0.5 V	1989 Jul 14	20
767 A	BD +31°3767 A	M1 V	M0.5 V	1989 Jul 14	30
220	Ross 59	M2 V	M2 V	1990 Jan 22	120

TABLE 3.2 (continued)

Gliese Number	Other Name	Published Spec. Type ^a	Adopted Spec. Type	Date Obs. (UT)	Integ. (sec)
22 AC	BD +66°34 AC	M2.5 V	M2 V	1990 Jan 21	23
806	G 209-41	M3 V	M2 V	1989 Jul 14	30
767 B	BD +31°3767 B	M2 V	M2.5 V	1989 Jul 14	30
226	G 222-11	M3 V	M2.5 V	1990 Jan 22	320
22 B	BD +66°34 B	M4.5 V	M3 V	1990 Jan 21	23
569 A	BD +16°2708 A	M0 V	M3 V	1989 Jul 14	20
669 A	Ross 868	M4 V	M3.5 V	1989 Jul 10	210
748 AB	Wolf 1062 AB	M4 V	M3.5 V	1989 Jul 14	30
643	Wolf 629	M4 V	M3.5 V	1989 Jul 10	1920
734 B	BD +10°2734 B	—	M3.5 V	1989 Jul 14	60
699	Barnard's Star	M5 V	M4 V	1989 Jul 10	7
232	Ross 64	M6 V	M4 V	1990 Jan 22	900
791.2	G 24-16	M6 V	M4.5 V	1989 Jul 10	210
669 B	Ross 867	M5 V	M4.5 V	1989 Jul 10	510
—	LHS 3339	M5.5 V ^d	M5.5 V	1989 Jul 13	1200
—	LHS 5142	—	M6.5 V	1990 Jan 21	900
—	LHS 191	M7: V ^d	M6.5 V	1990 Jan 21	900
—	LHS 2065	—	M9	1990 Jan 21	1500

^a Gliese 1969 unless otherwise noted.

^b Earlier spectral type than its companion, GL 338 A.

^c Gliese and Jahreiss 1979.

^d Boeshaar 1992.

TABLE 3.3
GIANT (AND HIGHER LUMINOSITY) SPECTRAL STANDARDS

SAO Number	Other Name	Published Spec. Type ^a	Adopted Spec. Type	Date Obs. (UT)	Integ. (sec)
52516	BS 8726	K5 I ^{b,c}	K5 I	1989 Jul 24	1
22994	HD 13136	M2 I ^b	M2 I	1989 Jul 24	15
67559	δ^2 Lyr	M4 II ^d	M4 II	1989 Jul 24	2
30653	γ Dra	K5 III ^c	K5 III	1989 Jul 24	3
21753	BD +59°128	K7 III ^b	K7 III	1989 Jul 24	50
36509	BS 152	K7 III ^{d,e}	K7 III	1989 Jul 24	1
141052	δ Oph	M0.5 III ^d	M0.5 III	1989 Jul 24	4
127976	55 Peg	M1 III ^c	M1 III	1989 Jul 24	4
91792	χ Peg	M2 III ^f	M2 III	1989 Jul 24	4
28843	83 UMa	M2 III ^d	M2 III	1989 Jul 24	1
63349	BD +31°2450	M3 III ^b	M3 III	1989 Jul 24	320
82478	HD 110964	M4 III ^b	M4 III	1989 Jul 10	10
34651	BS 8621	M4 III ^g	M4 III	1989 Jul 24	3
141344	HD 151061	M5 III ^h	M5 III	1989 Jul 24	4

^a Turnshek *et al.* 1985 unless otherwise noted.

^b Jacoby, Hunter and Christian 1984.

^c Also from Keenan and McNeil 1989.

^d Keenan and McNeil 1976.

^e Listed as K6 III in Keenan and McNeil 1989.

^f Listed as M2+ III in Keenan and McNeil 1989.

^g Listed as M4+ III in Keenan and McNeil 1989.

^h Listed as M5 to M5.5 III in Keenan and McNeil 1989.

TABLE 3.4
MISCELLANEOUS OBJECTS

Gliese Number	Other Name	Published Spec. Type	Adopted Spec. Type	Date Obs. (UT)	Integ. (sec)
756.2	HD 182196	K5 V ^a	K7 III	1989 Jul 14	2
—	LHS 515	sdM0-2 ^b	sdM2.5	1989 Jul 13	1200

^a Gliese 1969.

^b Giampapa and Liebert 1986.

TABLE 3.5
FEATURES FOUND IN LATE K TO LATE M
SPECTRA FROM 6300 Å TO 9000 Å

λ (Å)	Identification	Notes	References
6322 6358 6448 6512	TiO	early to late M	1
6346	CaH	strongest in K dwarfs	1
6382 6389	CaH	seen in dwarfs — disappears by mid-M; strong	2, 3, 4
6415	CaOH	(not seen by us — it falls in the bad column on the chip)	1
6497	Ba II blended with Ti, Fe, Ca	seen in K and early-M stars	5, 6
6563	H α	in absorption in K stars; sometimes in emission in M stars	6
6569 6596 6629 6649	TiO	mid- to late-M stars	1
6651 6680 6713 6746 6814 6852	TiO	mid- to late-M stars	1
6708	Li I	seen in some K and M stars	7, 8

TABLE 3.5 (continued)

λ (Å)	Identification	Notes	References
6750	CaH	strongest in early M dwarfs; particularly strong in metallic hydride subdwarfs	3, 4, 6
6903			
6908			
6921			
6946			
7050			
6867	telluric O ₂ (B-band)	—	6, 7
7000			
6979	Fe I	K and early-M supergiants	6
7053	TiO	found in all; strongest in early- to mid-M	1, 6
7087			
7124			
7159			
7197			
7219			
7270			
7186	telluric H ₂ O	—	6
7273			
7334	VO	seen only in late-M stars	6, 9
7372			
7393			
7405			
7418			
7472			
7534			
7345	Ti I	obvious in K and early-M giants and supergiants	10
7358			
7364			

TABLE 3.5 (continued)

λ (Å)	Identification	Notes	References
7389	Fe I	obvious in K and early-M giants and supergiants	10
7411	Fe I	obvious in K and early-M giants and supergiants	10
7589 7628	TiO	found in all; lies in atmospheric A-band	11
7594 7685	telluric O ₂ (A-band)	—	6, 7
7665 7699	K I	obvious only in dwarfs and subdwarfs; blended with A-band and TiO	7
7666 7672 7705 7743 7752 7783 7820 7828 7861	TiO	prominent in M stars; strongest at mid-M	6, 12
7851 7865 7897 7900 7919 7929 7939 7961 7967 7973	VO	obvious in late-M dwarfs	6, 12

TABLE 3.5 (continued)

λ (Å)	Identification	Notes	References
7878	CN	obvious in supergiants, weaker in giants; not seen in dwarfs	11
7895			
7916			
7941			
7963			
8026			
8044			
8068			
8075	Fe I	seen in subdwarfs	13
8164	telluric H ₂ O	—	6
8177			
8183	Na I	found in all; strongest in dwarfs	6
8195			
8206	TiO	found in all; strongest at mid-M	6, 12
8251			
8289			
8303			
8335			
8373			
8386			
8420			
8457			
8472			
8506			
8513			
8558			
8569			
8227	telluric H ₂ O	—	6
8282	telluric H ₂ O	—	13

TABLE 3.5 (continued)

λ (Å)	Identification	Notes	References
8308	Ti I and Fe I	marginally visible in	11
8330	blends	giants and supergiants	
8327	Fe I	found in K dwarfs	12, 13
8388	Fe I	strongest in K to mid-M stars	12
8432	TiO	prominent in mid- to	12
8442		late-M stars	
8452			
8435	Ti I	obvious in giants and supergiants	12
8440	Fe I	obvious in K and early-M stars; dominated by TiO elsewhere	13
8468	Fe I, Ti I	most obvious in giants and supergiants and K dwarfs	12, 13
8498	Ca II	strongest in late-K through	12
8542		mid-M; strongest in supergiants	
8662		then giants; weaker in dwarfs	
8514	Fe I	most obvious in giants and supergiants	12
8518	Ti I	most obvious in giants and supergiants	12

TABLE 3.5 (continued)

λ (Å)	Identification	Notes	References
8521	VO	found only in late-M stars	9, 12
8538			
8574			
8597			
8605			
8624			
8649			
8668			
8582	Fe I	found in K and early- to mid-M stars	13
8593			
8599			
8611			
8616			
8622			
8689	Fe I	strongest in K dwarfs	7
8710	Fe I	strongest in K and early-M dwarfs and subdwarfs	13
8713			
8718	Mg I	strongest in mid-M dwarfs	13
8757	Fe I	strongest in giants and supergiants	13
8764			
8793	Fe I	found in giants and supergiants	13
8805			
8807	Mg I	found in all but late-M stars	13
8824	Fe I	most obvious in mid-M dwarfs and subdwarfs	13

TABLE 3.5 (continued)

λ (Å)	Identification	Notes	References
8838	Fe I	strongest in K giants	13
8859	TiO	most obvious in mid- to late-M stars	14, 15
8868			
8937			
8867	Fe I	blended with TiO	13
8912	Ca II, Mg I blend	weak in K giants	13
8924			
8927			
8952	telluric H ₂ O	—	13
8972			
8980	telluric H ₂ O	—	13
8992			

REFERENCES: (1) Faÿ, Stein, & Warren 1974; (2) Ake & Greenstein 1980; (3) Öhman 1934; (4) Öhman 1936; (5) Gahm 1970; (6) Turnshek et al. 1985; (7) Keenan 1957; (8) Keenan & McNeil 1976; (9) Keenan & Schroeder 1952; (10) Davis 1947; (11) Sharpless 1956; (12) Solf 1978; (13) Swensson et al. 1970; (14) Wing, Spinrad, & Kuhl 1967; (15) Phillips 1950.

TABLE 3.6
COMPARISON OF SPECTRAL TYPES FOR VERY LATE "DWARFS"

Name	Spectral Types	
	This paper	Bessell(1991)
GL 644 C (VB 8)	M7	M6.5
LHS3002 ^a	—	M7
GL 752 B (VB 10)	M8	M7
LHS 2397a	M8 ^b	M7
LHS 2065	M9	M7
LHS 2924	M9	M7

^a Classified as M7 by Boeshaar 1992.

^b See §3.1.7.

TABLE 3.7
INTEGRATION LIMITS FOR COLOR RATIOS

Ratio	Numerator	Denominator	Feature Measured
A	7020-7050 Å	6960-6990 Å	CaH 6975 Å
B	7375-7385 Å	7353-7363 Å	Ti I 7358 Å
C	8100-8130 Å	8174-8204 Å	Na I 8183,8195 Å
D	8567-8577 Å	8537-8547 Å	Ca II 8542 Å

TABLE 3.8
COLOR RATIOS DETERMINED FROM THE SPECTRA

Object Name	Spec. Type	A	B	C	D	B/A	B/C	D/A	D/C
Primary Dwarf Spectral Standards (see Table 3.1)									
GL 820 A	K5 V	1.02	1.02	1.13	1.19	1.00	0.90	1.17	1.05
GL 820 B	K7 V	1.02	1.01	1.12	1.20	0.99	0.90	1.18	1.07
GL 380	K7 V	1.06	1.04	1.16	1.18	0.98	0.90	1.11	1.02
GL 328	M0 V	1.08	1.05	1.15	1.17	0.97	0.91	1.08	1.02
GL 270	M0 V	1.08	1.04	1.14	1.14	0.96	0.91	1.06	1.00
GL 846	M0.5 V	1.11	1.03	1.17	1.20	0.93	0.88	1.08	1.03
GL 229	M1 V	1.13	1.05	1.17	1.13	0.93	0.90	1.00	0.97
GL 205	M1.5 V	1.15	1.06	1.19	1.14	0.92	0.89	0.99	0.96
GL 411	M2 V	1.17	1.05	1.13	1.12	0.90	0.93	0.96	0.99
GL 382	M2 V	1.17	1.06	1.18	1.13	0.91	0.90	0.97	0.96
GL 250 B	M2.5 V	1.20	1.06	1.15	1.11	0.88	0.92	0.93	0.97
GL 381	M2.5 V	1.22	1.05	1.18	1.11	0.86	0.89	0.91	0.94
GL 352 AB	M3 V	1.21	1.06	1.14	1.12	0.88	0.93	0.93	0.98
GL 436	M3 V	1.22	1.06	1.16	1.11	0.87	0.91	0.91	0.96
GL 251	M3 V	1.24	1.07	1.18	1.10	0.86	0.91	0.89	0.93
GL 752 A	M3 V	1.20	1.06	1.21	1.11	0.88	0.88	0.93	0.92
GL 725 A	M3 V	1.23	1.06	1.17	1.09	0.86	0.91	0.89	0.93

TABLE 3.8 (continued)

Object Name	Spec. Type	A	B	C	D	B/A	B/C	D/A	D/C
GL 273	M3.5 V	1.25	1.08	1.18	1.08	0.86	0.92	0.86	0.92
GL 725 B	M3.5 V	1.28	1.07	1.24	1.13	0.84	0.86	0.88	0.91
GL 213	M4 V	1.28	1.08	1.17	1.09	0.84	0.92	0.85	0.93
GL 275.2 A	M4 V	1.30	1.08	1.22	1.09	0.83	0.89	0.84	0.89
GL 402	M4 V	1.27	1.09	1.25	1.09	0.86	0.87	0.86	0.87
GL 83.1	M4.5 V	1.36	1.09	1.28	1.08	0.80	0.85	0.79	0.84
GL 268	M4.5 V	1.31	1.08	1.24	1.06	0.82	0.87	0.81	0.85
GL 166 C	M4.5 V	1.33	1.09	1.15	1.09	0.82	0.95	0.82	0.95
GL 234 AB	M4.5 V	1.37	1.08	1.26	1.07	0.79	0.86	0.78	0.85
GL 51	M5 V	1.38	1.11	1.28	1.07	0.80	0.87	0.78	0.84
GL 866 AB	M5 V	1.39	1.11	1.38	1.08	0.80	0.80	0.78	0.78
G 208-44 AB	M5.5 V	1.46	1.07	1.29	1.10	0.73	0.83	0.75	0.85
GL 65 A	M5.5 V	1.46	1.11	1.22	1.08	0.76	0.91	0.74	0.89
G 208-45	M6 V	1.53	1.09	1.31	1.08	0.71	0.83	0.71	0.82
GL 65 B	M6 V	1.43	1.09	1.22	1.09	0.76	0.89	0.76	0.89
GL 406	M6 V	1.42	1.11	1.24	1.08	0.78	0.90	0.76	0.87
LHS 523	M6.5 V	1.82	1.09	1.46	1.11	0.60	0.75	0.61	0.76
G 51-15	M6.5 V	1.53	1.11	1.24	1.11	0.73	0.90	0.73	0.90
GL 644 C	M7 V	1.67	1.10	1.41	1.14	0.66	0.78	0.68	0.81
GL 752 B	M8 V	1.31	1.08	1.22	1.15	0.82	0.89	0.88	0.94
GL 569 B	M8.5	1.34	1.03	1.15	1.14	0.77	0.90	0.85	0.99
LHS 2924	M9	1.28	1.02	1.05	1.04	0.80	0.97	0.81	0.99

TABLE 3.8 (continued)

Object Name	Spec. Type	A	B	C	D	B/A	B/C	D/A	D/C
Secondary Dwarf Spectral Standards (see Table 3.2)									
GL 775	K5 V	1.01	1.02	1.15	1.25	1.01	0.89	1.24	1.09
GL 764.1 B	K7 V	1.05	1.03	1.18	1.14	0.98	0.87	1.09	0.97
GL 265 A	K7 V	1.04	1.03	1.12	1.16	0.99	0.92	1.12	1.04
GL 786	K7 V	1.05	1.03	1.19	1.23	0.98	0.87	1.17	1.03
GL 748.2 A	K7 V	1.04	1.02	1.14	1.15	0.98	0.89	1.11	1.01
GL 430	K7 V	1.06	1.04	1.14	1.19	0.98	0.91	1.12	1.04
GL 338 B	K7 V	1.08	1.05	1.13	1.16	0.97	0.93	1.07	1.03
GL 734 A	M0 V	1.07	1.03	1.17	1.21	0.96	0.88	1.13	1.03
GL 763	M0 V	1.08	1.03	1.12	1.14	0.95	0.92	1.06	1.02
GL 338 A	M0 V	1.08	1.04	1.13	1.16	0.96	0.92	1.07	1.03
GL 748.2 B	M0 V	1.06	1.01	1.14	1.18	0.95	0.89	1.11	1.04
GL 839	M0.5 V	1.08	1.04	1.15	1.24	0.96	0.90	1.15	1.08
GJ 2155	M0.5 V	1.08	1.03	1.16	1.20	0.95	0.89	1.11	1.03
GL 761.2	M0.5 V	1.09	1.02	1.15	1.20	0.94	0.87	1.10	1.04
GL 720 A	M0.5 V	1.11	1.03	1.14	1.16	0.93	0.90	1.05	1.02
GL 767 A	M0.5 V	1.16	1.03	1.16	1.15	0.89	0.89	0.99	0.99
GL 220	M2 V	1.16	1.05	1.15	1.13	0.91	0.91	0.97	0.98
GL 22 AC	M2 V	1.19	1.05	1.11	1.13	0.88	0.95	0.95	1.02

TABLE 3.8 (continued)

Object Name	Spec. Type	A	B	C	D	B/A	B/C	D/A	D/C
GL 806	M2 V	1.19	1.03	1.17	1.16	0.87	0.88	0.97	0.99
GL 767 B	M2.5 V	1.21	1.04	1.18	1.15	0.86	0.88	0.95	0.97
GL 226	M2.5 V	1.20	1.06	1.15	1.10	0.88	0.92	0.92	0.96
GL 22 B	M3 V	1.29	1.05	1.17	1.15	0.81	0.90	0.89	0.98
GL 569 A	M3 V	1.22	1.05	1.19	1.12	0.86	0.88	0.92	0.94
GL 669 A	M3.5 V	1.27	1.06	1.25	1.12	0.83	0.85	0.88	0.90
GL 748 AB	M3.5 V	1.26	1.06	1.19	1.13	0.84	0.89	0.90	0.95
GL 643	M3.5 V	1.32	1.07	1.27	1.10	0.81	0.84	0.83	0.87
GL 734 B	M3.5 V	1.26	1.06	1.20	1.10	0.84	0.88	0.87	0.92
GL 699	M4 V	1.38	1.07	1.27	1.11	0.76	0.84	0.80	0.87
GL 232	M4 V	1.32	1.07	1.21	1.08	0.81	0.88	0.82	0.89
GL 791.2	M4.5 V	1.39	1.07	1.28	1.10	0.77	0.84	0.79	0.86
GL 669 B	M4.5 V	1.35	1.07	1.26	1.06	0.79	0.85	0.79	0.84
LHS 3339	M5.5 V	1.45	1.11	1.31	1.09	0.77	0.85	0.75	0.83
LHS 5142	M6 V	1.47	1.09	1.25	1.08	0.74	0.87	0.73	0.86
LHS 191	M6.5 V	1.63	1.10	1.32	1.10	0.67	0.83	0.67	0.83
LHS 2065	M9	1.25	1.08	1.04	1.08	0.86	1.04	0.86	1.04

TABLE 3.8 (continued)

Object Name	Spec. Type	A	B	C	D	B/A	B/C	D/A	D/C
Giant (and Higher Luminosity) Spectral Standards (see Table 3.3)									
SAO 52516	K5 I	1.01	1.08	1.06	1.36	1.07	1.02	1.35	1.28
SAO 22994	M2 I	1.04	1.10	1.03	1.36	1.06	1.07	1.31	1.32
SAO 67559	M4 II	1.09	1.13	1.06	1.28	1.04	1.07	1.17	1.21
SAO 30653	K5 III	0.99	1.07	1.05	1.29	1.08	1.02	1.30	1.23
SAO 21753	K7 III	1.03	1.10	1.06	1.28	1.07	1.04	1.24	1.21
SAO 36509	K7 III	0.99	1.06	1.05	1.26	1.07	1.01	1.27	1.20
SAO 141052	M0.5 III	1.00	1.09	1.11	1.28	1.09	0.98	1.28	1.15
SAO 127976	M1 III	1.01	1.08	1.09	1.30	1.07	0.99	1.29	1.19
SAO 91792	M2 III	1.02	1.09	1.07	1.26	1.07	1.02	1.24	1.18
SAO 28843	M2 III	1.01	1.09	1.10	1.31	1.08	0.99	1.30	1.19
SAO 63349	M3 III	1.03	1.10	1.10	1.26	1.07	1.00	1.22	1.15
SAO 82478	M4 III	1.13	1.12	1.07	1.18	0.99	1.05	1.04	1.10
SAO 34651	M4 III	1.08	1.12	1.06	1.28	1.04	1.06	1.19	1.21
SAO 141344	M5 III	1.12	1.18	1.05	1.25	1.05	1.12	1.12	1.19
Miscellaneous Objects (see Table 3.4)									
GL 756.2	K7 III	1.03	1.04	1.08	1.33	1.01	0.96	1.29	1.23
LHS 515	sdM2.5	1.56	1.01	1.21	1.21	0.65	0.83	0.78	1.00

TABLE 3.8 (continued)

Object Name	Spec. Type	A	B	C	D	B/A	B/C	D/A	D/C
Other Dwarf/Subdwarf Spectra (see Table 3.9)									
GL 301 AB	K7 V	1.07	1.01	1.09	1.14	0.94	0.93	1.07	1.05
GL 338.1 AB	K7 V	1.05	1.01	1.08	1.14	0.96	0.94	1.09	1.06
GL 677 AB	K7 V	1.01	1.03	1.13	1.17	1.02	0.91	1.16	1.04
GL 863.1ABC	K7 V	1.05	1.03	1.12	1.16	0.98	0.92	1.10	1.04
GL 809	M0 V	1.12	1.04	1.11	1.15	0.93	0.94	1.03	1.04
GL 649	M0.5 V	1.14	1.05	1.19	1.15	0.92	0.88	1.01	0.97
GL 508 AB	M1 V	1.13	1.03	1.11	1.13	0.91	0.93	1.00	1.02
GL 625	M1.5 V	1.23	1.04	1.20	1.16	0.85	0.87	0.94	0.97
GL 880	M1.5 V	1.14	1.05	1.14	1.16	0.92	0.92	1.02	1.02
GL 623 AB	M2.5 V	1.21	1.06	1.19	1.13	0.88	0.89	0.93	0.95
GL 661 AB	M3 V	1.20	1.06	1.15	1.08	0.88	0.92	0.90	0.94
GL 754.1 B	M3 V	1.26	1.07	1.22	1.11	0.85	0.88	0.88	0.91
GL 860 A	M3 V	1.26	1.08	1.22	1.06	0.86	0.89	0.84	0.87
GL 829	M3.5 V	1.27	1.06	1.16	1.10	0.83	0.91	0.87	0.95
GL 873	M3.5 V	1.33	1.08	1.18	1.09	0.81	0.92	0.82	0.92
G 117-B15 B	M3.5 V	1.31	1.07	1.19	1.07	0.82	0.90	0.82	0.90
GL 169.1 A	M4 V	1.24	1.06	1.19	1.05	0.85	0.89	0.85	0.88
GL 860 B	M4 V	1.37	1.08	1.27	1.06	0.79	0.85	0.77	0.83
LHS 1047AB	M4 V	1.32	1.06	1.19	1.09	0.80	0.89	0.83	0.92
GL 831	M4.5 V	1.29	1.07	1.22	1.07	0.83	0.88	0.83	0.88

TABLE 3.8 (continued)

Object Name	Spec. Type	A	B	C	D	B/A	B/C	D/A	D/C
G 77-31	M5 V	1.30	1.10	1.26	1.06	0.85	0.87	0.82	0.84
LHS 2067	sdM5	1.75	1.05	1.45	1.09	0.60	0.72	0.62	0.75
GL 473 AB	M5.5 V	1.43	1.09	1.29	1.06	0.76	0.84	0.74	0.82
GJ 1116 AB	M5.5 V	1.59	1.08	.28	1.08	0.70	0.84	0.68	0.84
Pleiad #2	M5.5 V	1.50	1.03	1.05	0.94	0.69	0.98	0.63	0.90
GL 283 B	M6 V	1.49	1.08	1.27	1.09	0.72	0.85	0.73	0.86
GL 316.1	M6 V	1.50	1.09	1.26	1.07	0.73	0.87	0.71	0.85
LHS 292	M6.5 V	1.62	1.07	1.31	1.10	0.66	0.82	0.68	0.84
LHS 2930	M6.5 V	1.71	1.08	1.38	1.10	0.63	0.78	0.64	0.80
LHS 2397a	M8	1.50	1.04	1.24	1.10	0.69	0.84	0.73	0.89
RG0050-2722	M8:	1.33	1.00	1.13	1.06	0.75	0.88	0.80	0.94

TABLE 3.9
OTHER DWARF/SUBDWARF SPECTRA

Gliese Number	Other Name	Published Spec. Type ^a	Adopted Spec. Type	Date Obs. (UT)	Integ. (sec)
—	LHS 2068 ^b	—	<K5 V	1991 May 07	600
301 AB	BD −13°2439 AB	M0	K7 V	1990 Nov 23	11
338.1 AB	BD +77°361 AB	K5	K7 V	1990 Nov 23	11
677 AB	BD +29°3029 AB	M0	K7 V	1990 Sep 14	21
863.1 ABC	BD +53°2911 ABC	M0	K7 V	1990 May 22	17
809	BD +61°2068	M2 V	M0 V	1990 Nov 23	10
649	BD +25°3173	M2	M0.5 V	1990 May 23	240
508 AB	BD +48°2108 AB	M2	M1 V	1990 Nov 23	40
625	G 202-48	M2	M1.5 V	1990 May 23	10
880	BD +15°4733	M2	M1.5 V	1990 Nov 22	90
623 AB	G 202-45 AB	M3	M2.5 V	1990 May 23	120
661 AB	BD +45°2505 AB	M3-3.5	M3 V	1990 May 04	4
754.1 B	—	M5	M3 V	1990 Sep 13	140
860 A	BD +56°2783 A	M3	M3 V	1990 Sep 13	5.6
829	Ross 775	M4	M3.5 V	1990 Nov 23	20
873	BD +43°4305	M4.5	M3.5 V	1990 Nov 22	180
—	G 117-B15 B	—	M3.5 V	1991 May 07	300
169.1 A	Stein 2051 A	M4	M4 V	1991 Mar 14	900
860 B	BD +56°2783 B	M4.5	M4 V	1990 Sep 13	5.6
—	LHS 1047 AB	M4 ^c	M4 V	1990 Nov 23	330
831	Wolf 922	M4.5	M4.5 V	1990 Nov 23	75

TABLE 3.9 (continued)
OTHER DWARF/SUBDWARF SPECTRA

Gliese Number	Other Name	Published Spec. Type ^a	Adopted Spec. Type	Date Obs. (UT)	Integ. (sec)
—	G 77-31	M5 V ^d	M5 V	1990 Sep 13	130
—	LHS 2067 ^b	sdM ^e	sdM5	1991 May 07	600
473 AB	Wolf 424 AB	M5.5	M5.5 V	1990 May 04	105
—	GJ 1116 AB	~M5? V ^f	M5.5 V	1990 Nov 23	130
—	Pleiad #2 ^g	—	M5.5 V	1990 Jan 20	3900
283 B	LHS 234	M6 V ^h	M6 V	1990 Nov 23	600
316.1	LHS 2034	M6 V ⁱ	M6 V	1990 Nov 23	600
—	LHS 292	M6.5 V ^h	M6.5 V	1990 Nov 23	360
—	LHS 2930	M6.5 V ⁱ	M6.5 V	1991 May 07	1200
—	LHS 2397a	M8 V ^j	M8	1990 Nov 22	1500
—	RG 0050-2722	M8 V ^h	M8:	1991 Sep 15	3600

^a Gliese 1969 unless otherwise noted.

^b Wrong star marked on finder chart in Luyten & Albers 1979.

^c Bidelman 1985.

^d Boeshaar 1976.

^e Bessell 1982; mis-identified by Bessell 1991.

^f Cowley & Hartwick 1982.

^g Star number 2 in Stauffer et al. 1989.

^h Boeshaar 1992.

ⁱ Bessell 1991.

^j Giampapa & Liebert 1986.

TABLE 3.10
STARS WITH OBSERVED SPECTRA AND KNOWN MASSES

Object Name	Spectral Type	Mass (M_{\odot}) ^a
GL 508 AB	M1 V	0.709 ± 0.178^b
GL 22 AC	M2 V	0.356 ± 0.046^b
GL 623 AB	M2.5 V	0.300 ± 0.032^b
GL 725 A	M3 V	0.370 ± 0.134
GL 661 AB	M3 V	0.262 ± 0.020^c
GL 860 A	M3 V	0.257 ± 0.029
GL 352 AB	M3 V	0.199 ± 0.062^c
GL 725 B	M3.5 V	0.316 ± 0.115
GL 860 B	M4 V	0.167 ± 0.019
LHS 1047 AB	M4 V	0.138 ± 0.184^b
GL 234 AB	M4.5 V	0.180 ± 0.061^b
GL 166 C	M4.5 V	0.155 ± 0.029
G 208-44 AB	M5.5 V	0.118 ± 0.018^b
GL 65 A	M5.5 V	0.097 ± 0.011
GL 65 B	M6 V	0.094 ± 0.011

^a Henry 1992.

^b Light of primary dominates spectrum; mass is that of the primary.

^c Components are nearly equal in magnitude; mass is the mean of the two.

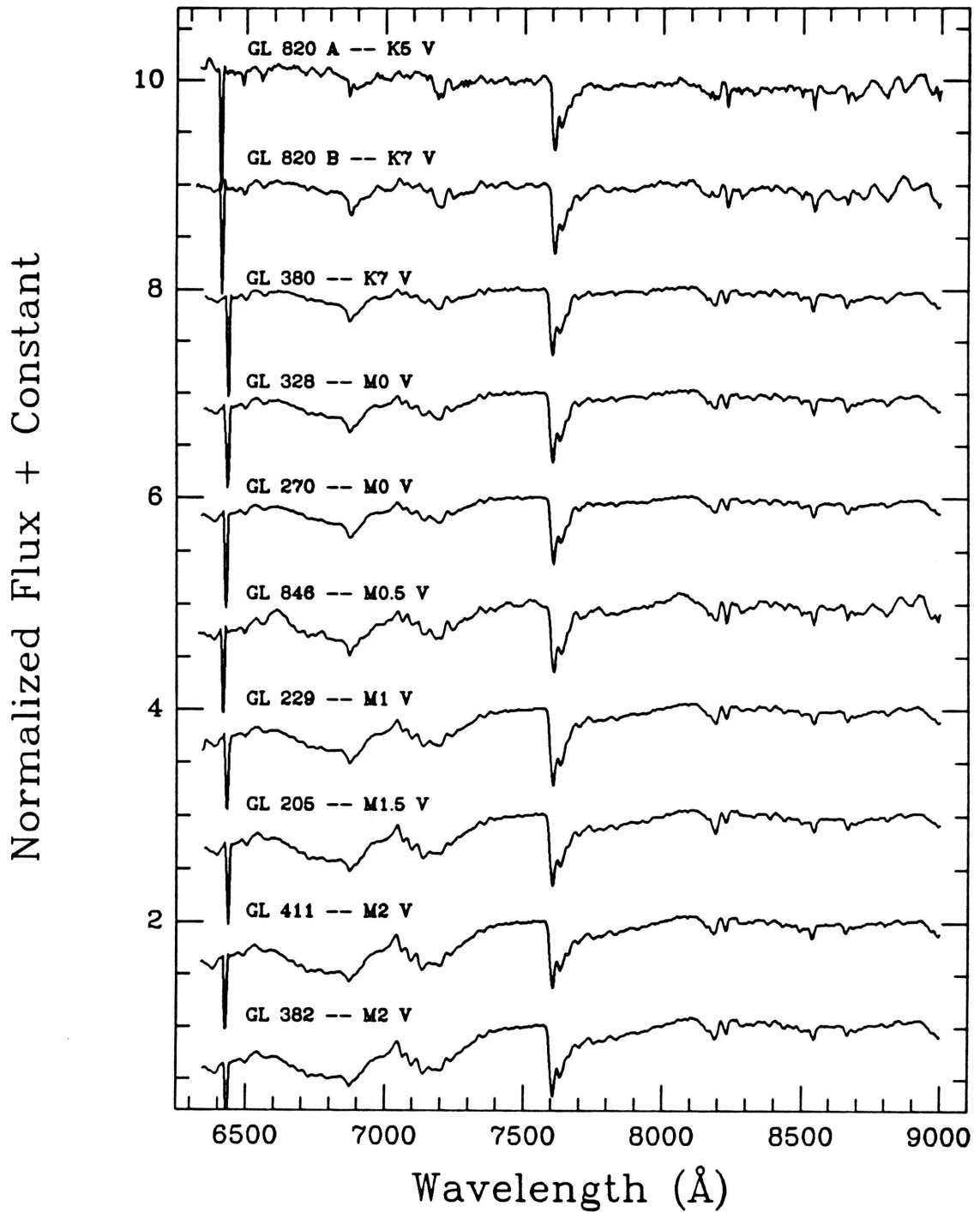


FIG. 3.1. — Spectra of the 39 primary dwarf standards in Table 3.1. All of these were observed at the MMT and have a resolution of 18 \AA except for GL 83.1, GL 51, and GL 866 AB which were observed at the Steward Observatory 2.3-meter telescope. These three spectra have been rebinned and smoothed \rightarrow

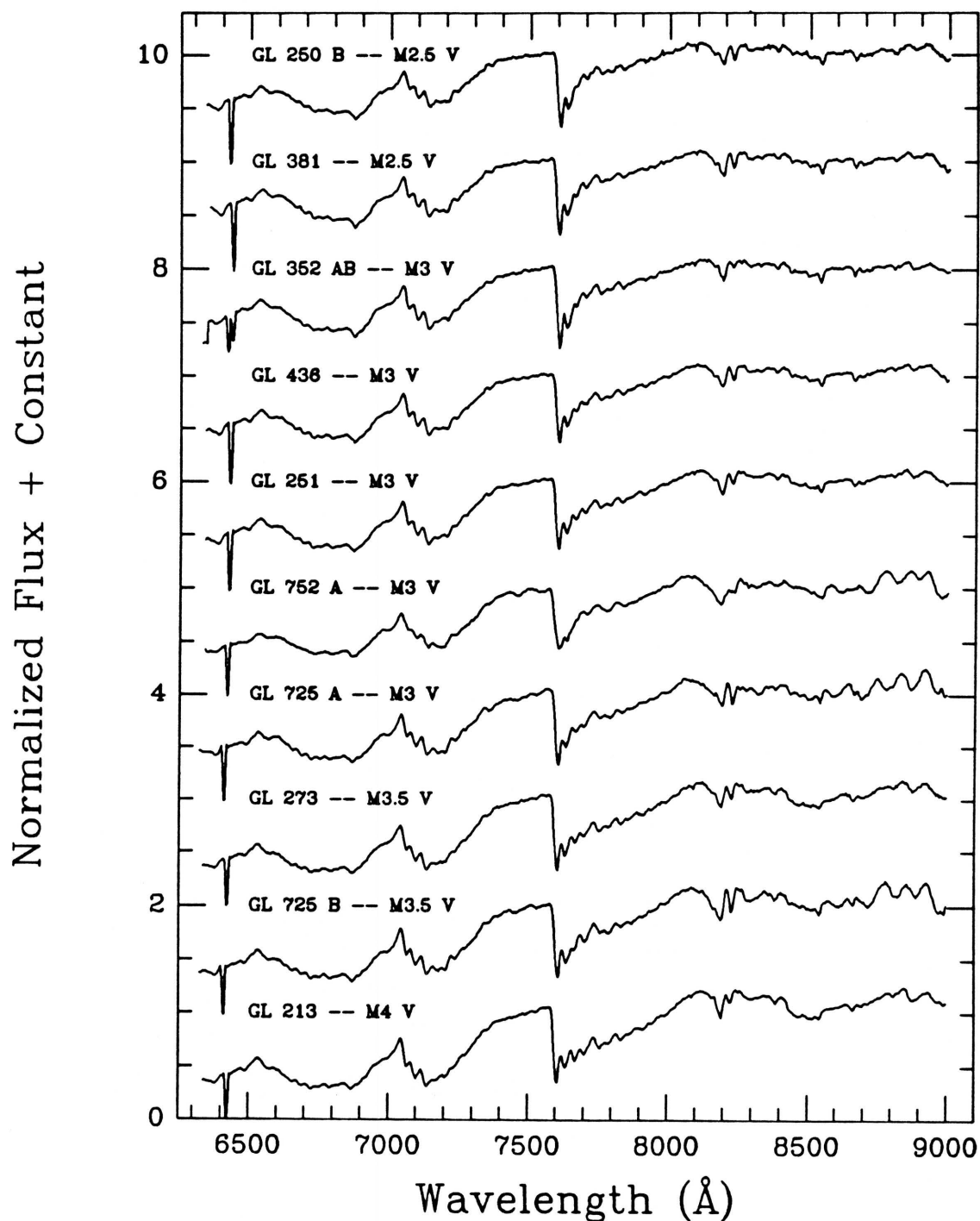


FIG. 3.1. (continued) — so that the resolution matches that of the MMT spectra. Each of the spectra has been normalized to its flux (in units of F_λ) at 7500 Å and an offset added to separate the spectra vertically. The zero level for each spectrum is its flux value at 7500 Å (which is always an integer) minus 1. For →

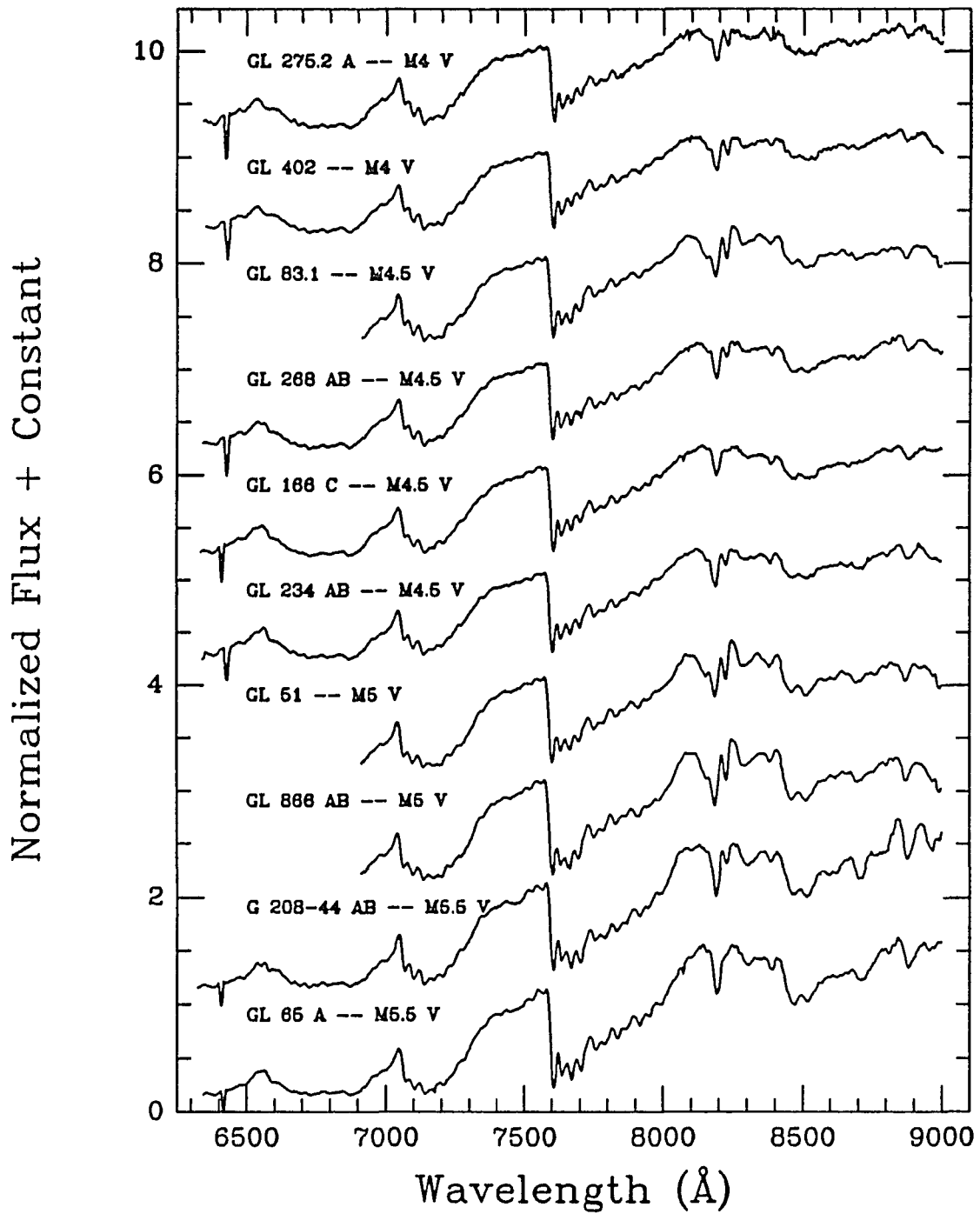


FIG. 3.1. (continued) — example, the zero level for the spectrum of GL 820 A is 9. The “absorption” feature at 6415 \AA is due to a dead column on the MMT CCD chip and has not been interpolated over because this is the exact location of a CaOH band. Absorption by telluric O_2 and H_2O →

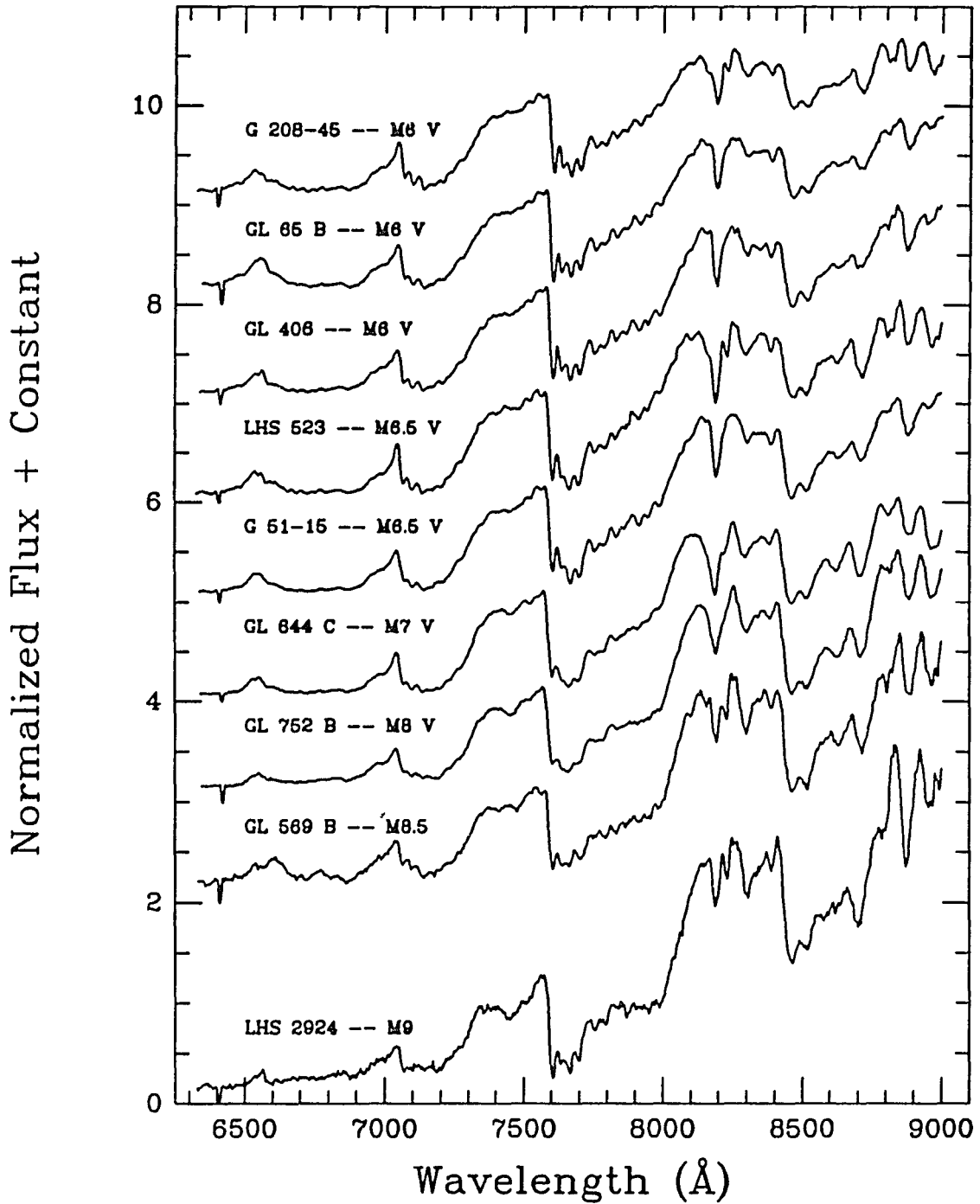


FIG. 3.1. (continued) — has not been removed. GL 569 B and LHS 2924 do not have luminosity classifications given because these objects may not be true stars; they could be brown dwarfs. The same uncertain nature is true of GL 644 C (VB 8) and GL 752 B (VB 10), except that we have retained their designations of luminosity class V for historical reasons.

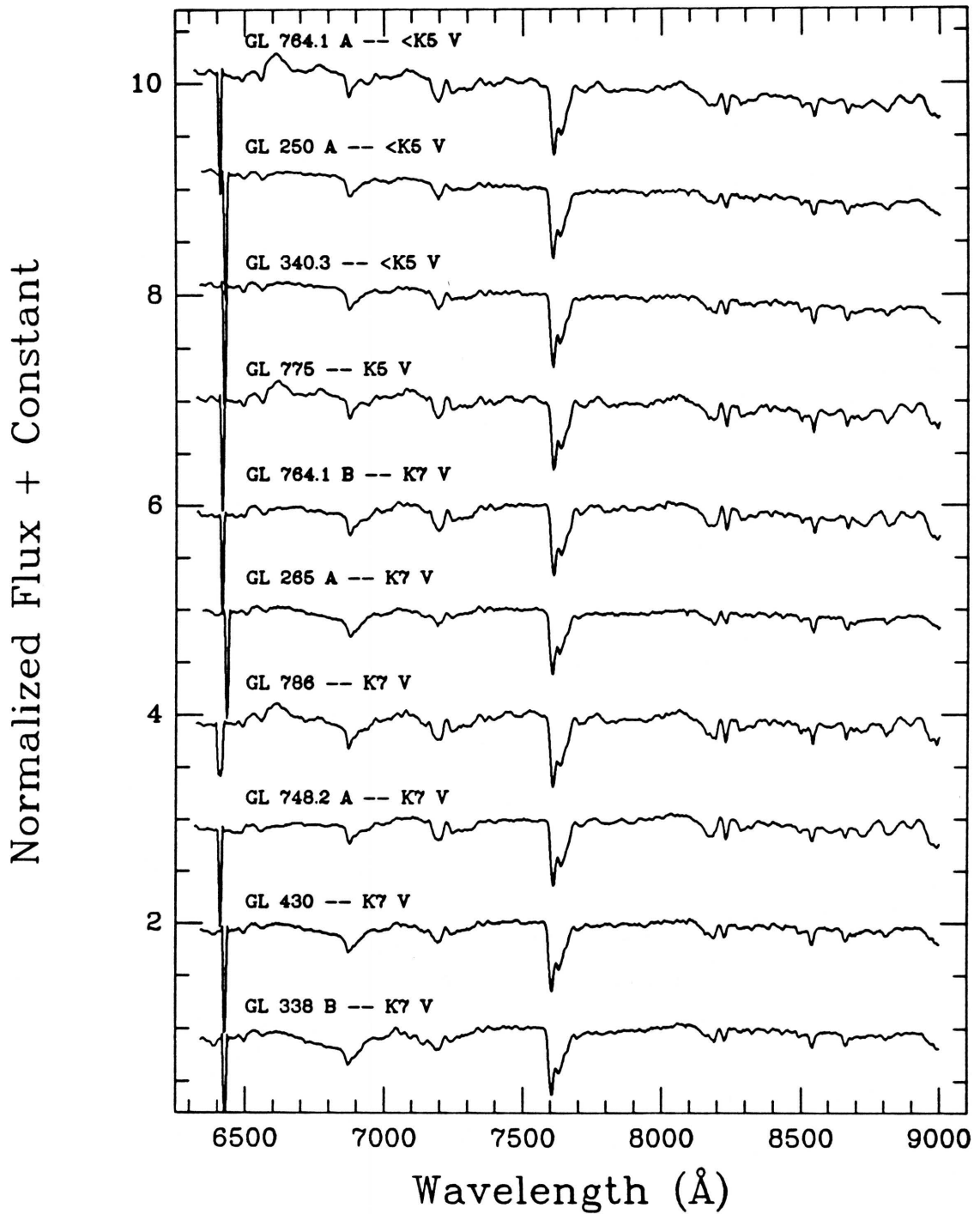


FIG. 3.2. — Spectra of the 38 secondary dwarf standards in Table 3.2. All of these were observed at the MMT and have a resolution of 18 Å. See the caption to Figure 3.1 for more details.

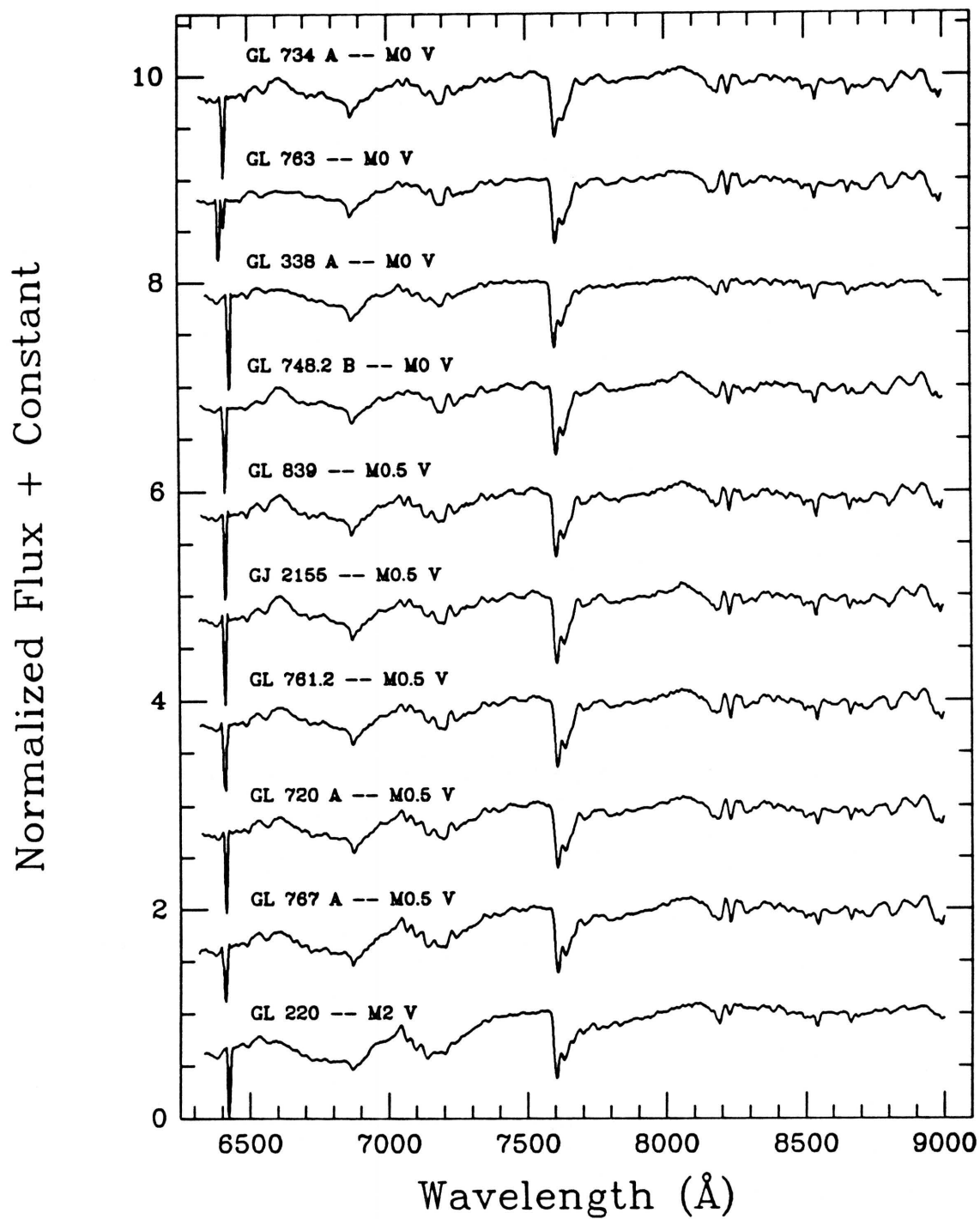


FIG. 3.2. (continued)

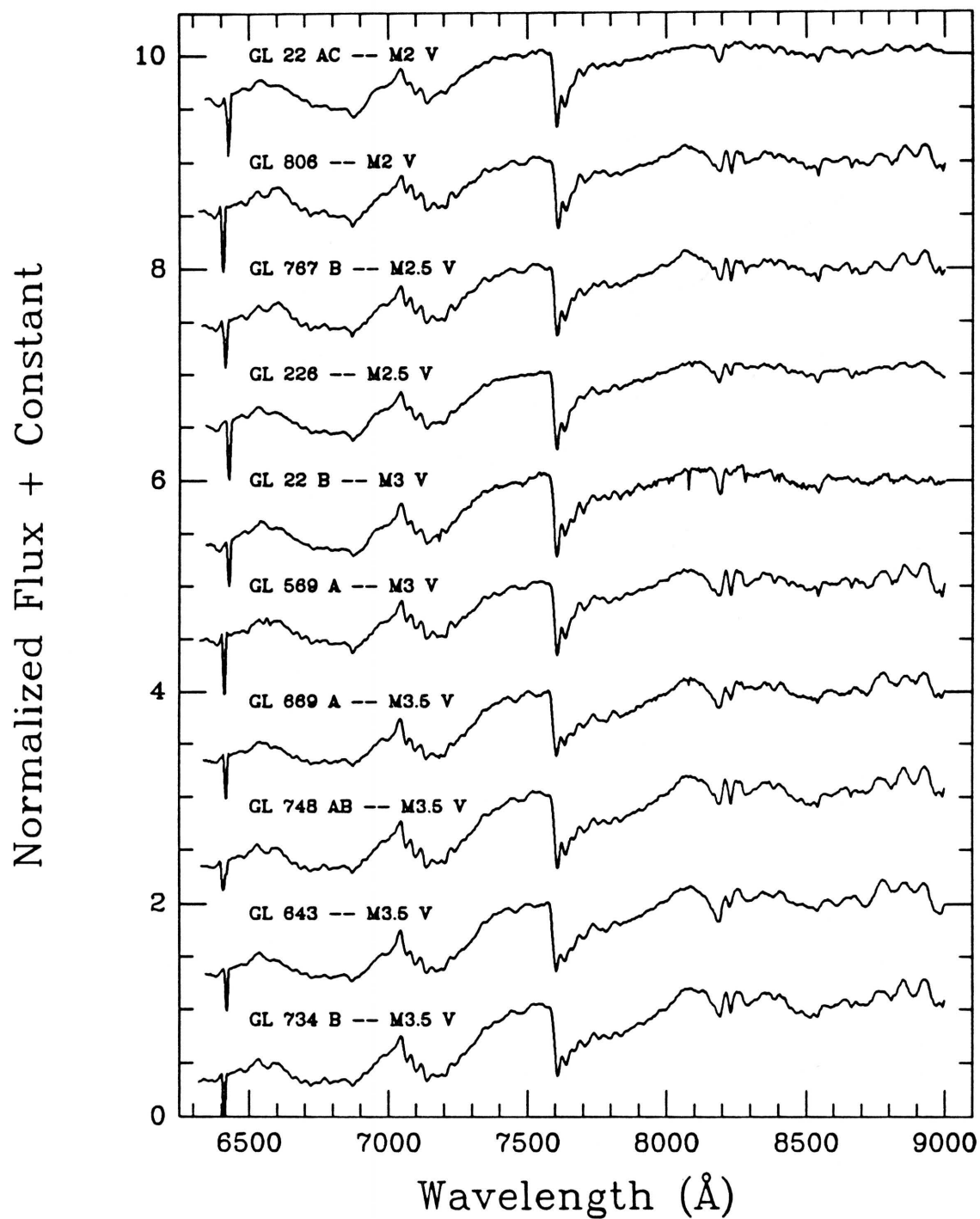


FIG. 3.2. (continued)

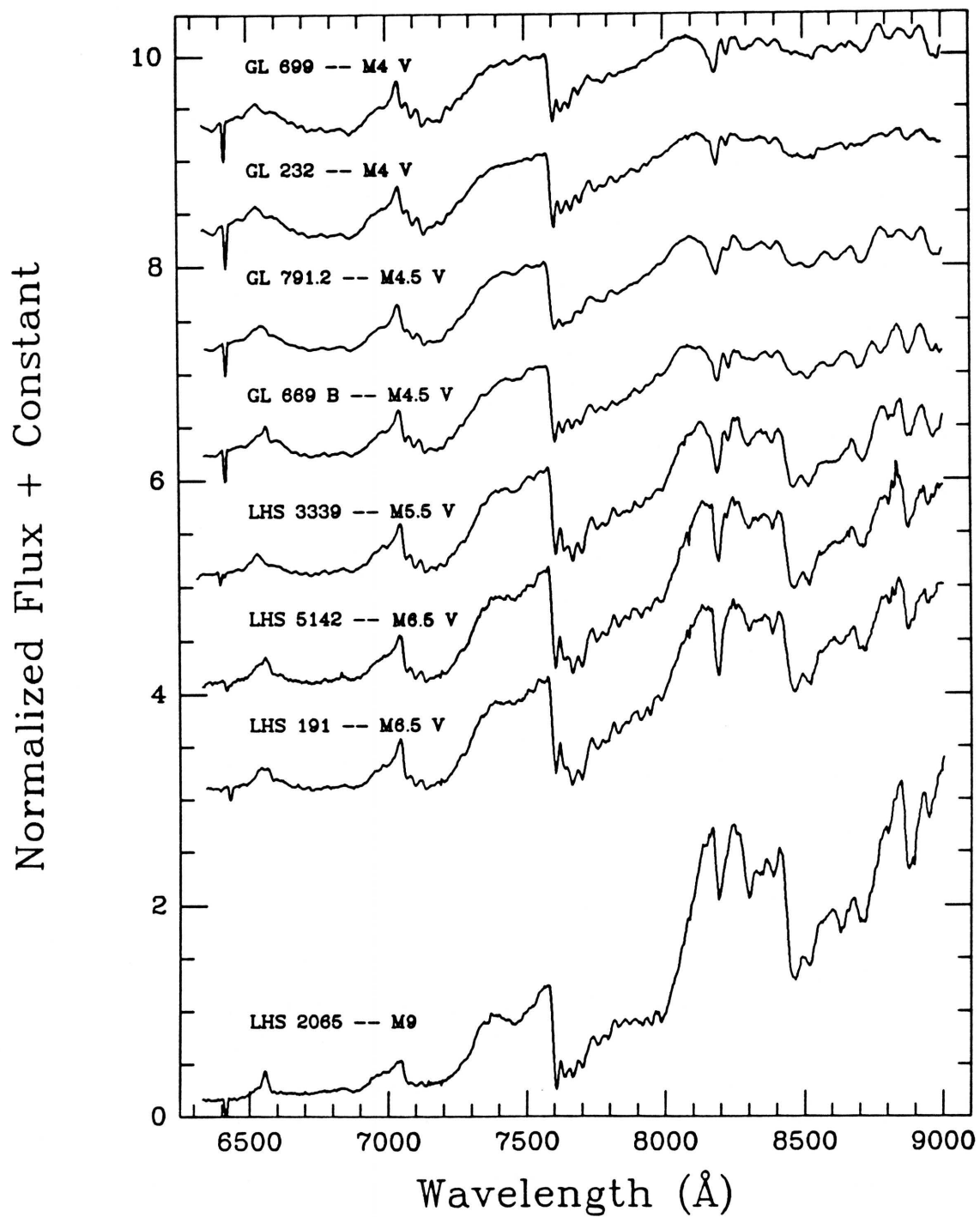


FIG. 3.2. (continued)

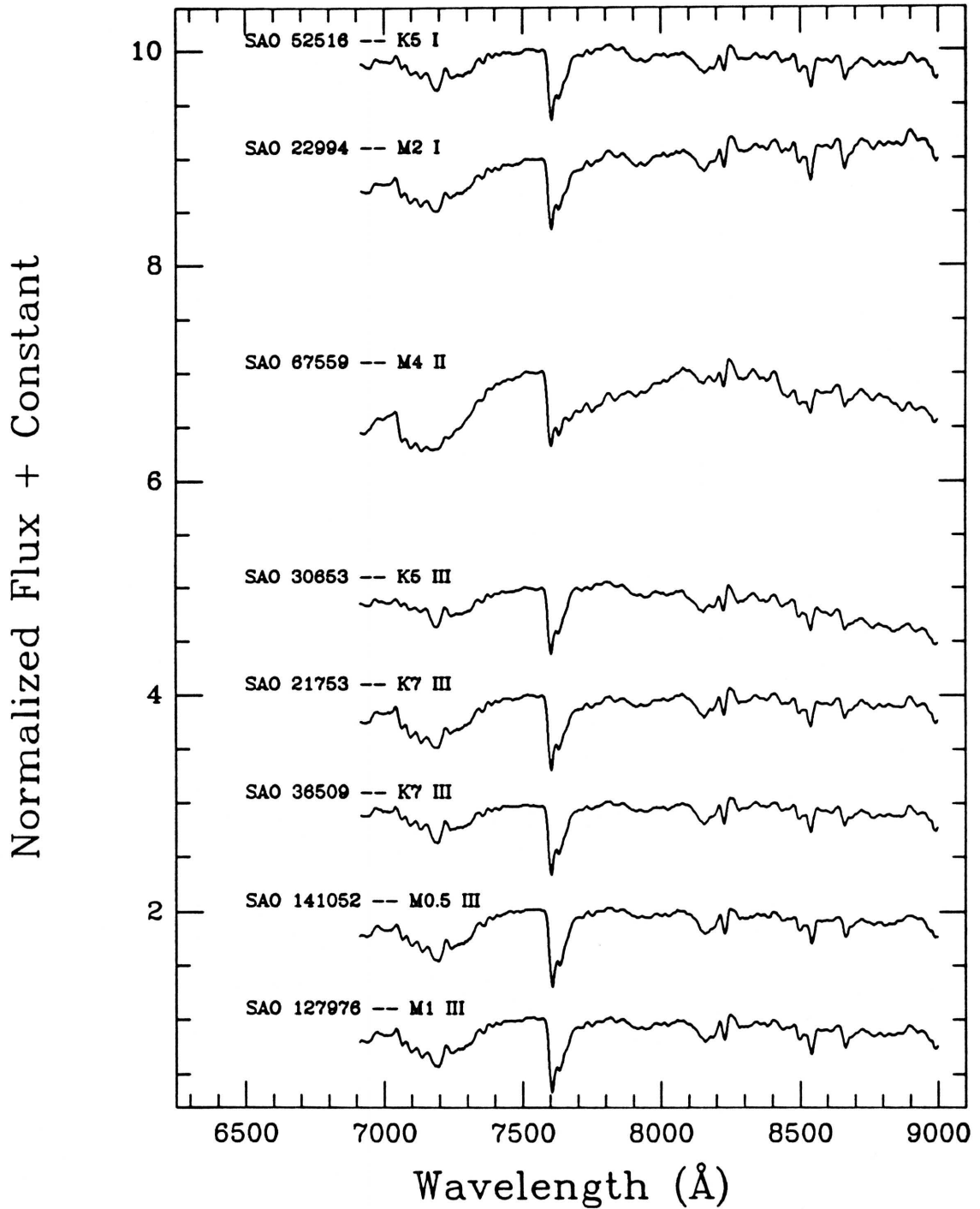


FIG. 3.3. — Spectra of the 14 giant and higher luminosity standards listed in Table 3.3. All but one of these (SAO 82478, taken at the MMT) were observed at the Steward Observatory 2.3-meter telescope, but all have been rebinned and smoothed to match the resolution of the MMT spectra. See the caption to Figure 3.1 for more details.

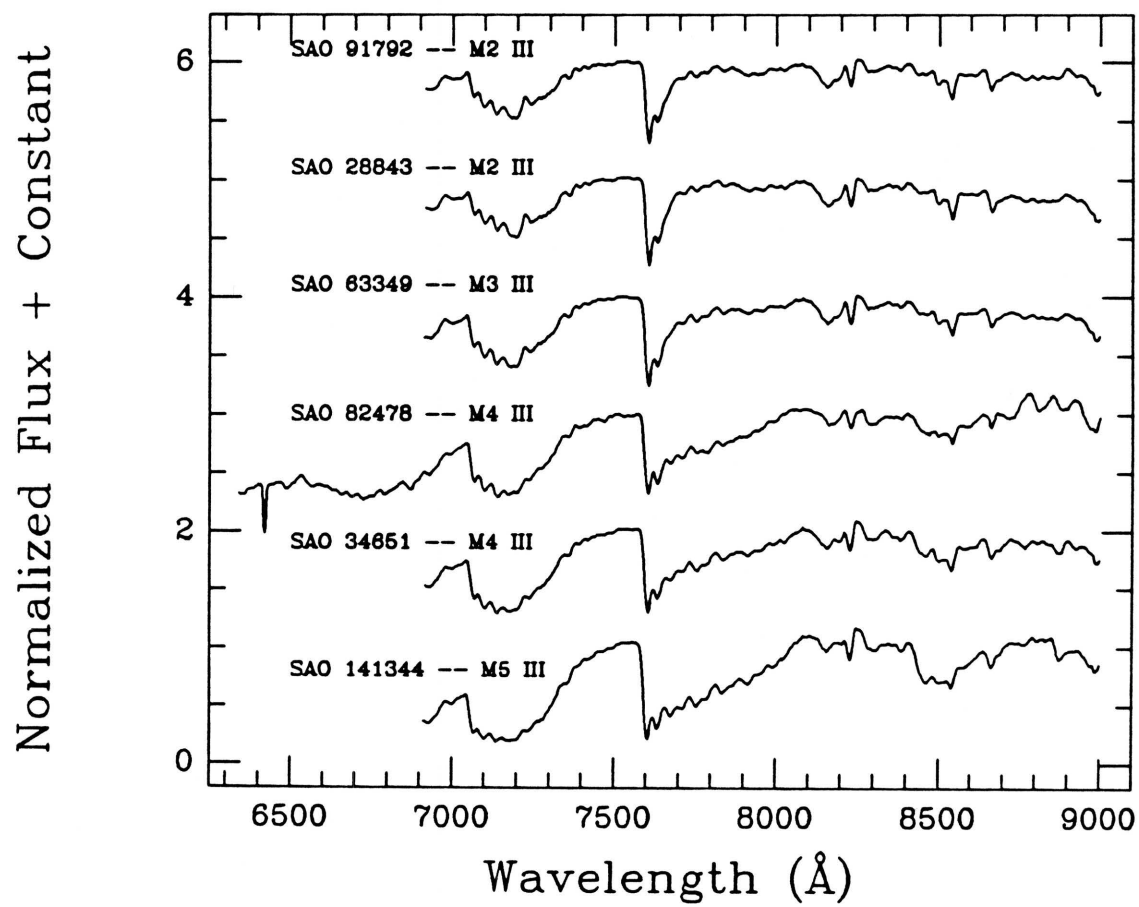


FIG. 3.3. (continued)

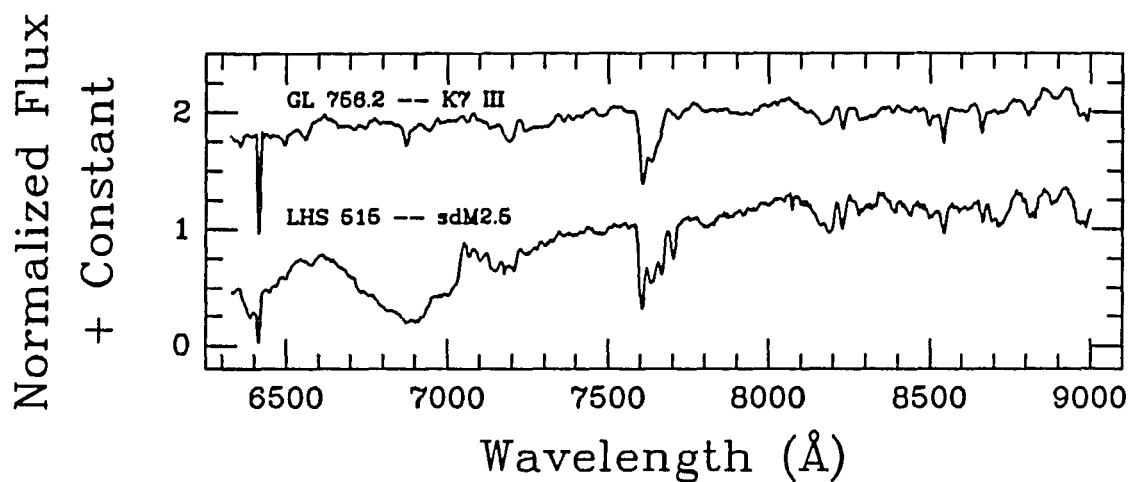


FIG. 3.4. — Spectra of the 2 objects listed in Table 3.4. Both were observed at the MMT and have a resolution of 18 Å. See the caption to Figure 3.1 for more details. Note the prominent absorption lines of the Ca II triplet (8498 Å, 8542 Å, and 8662 Å) in the spectrum of GL 756.2 and the striking absorption feature from 6750 to 7050 Å due to CaH in the spectrum of LHS 515.

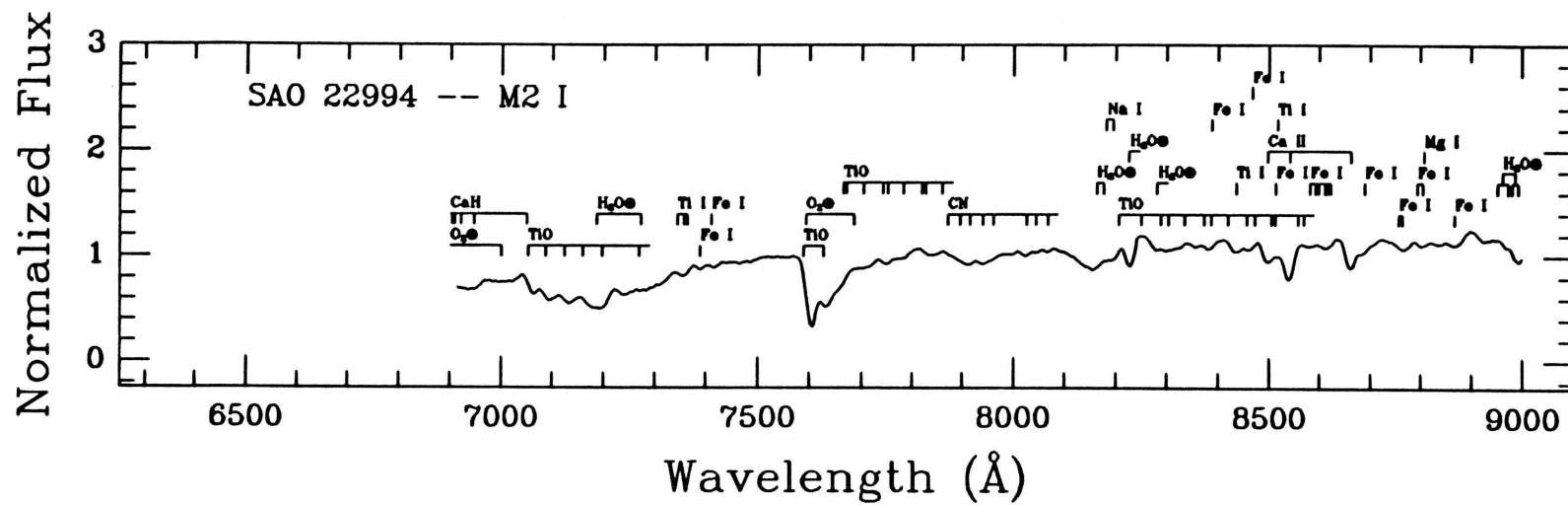


FIG. 3.5. — Detailed spectra of some of the objects in Figures 3.1 through 3.4 with line identifications from Table 3.5 marked. (a) A supergiant of class M2. →

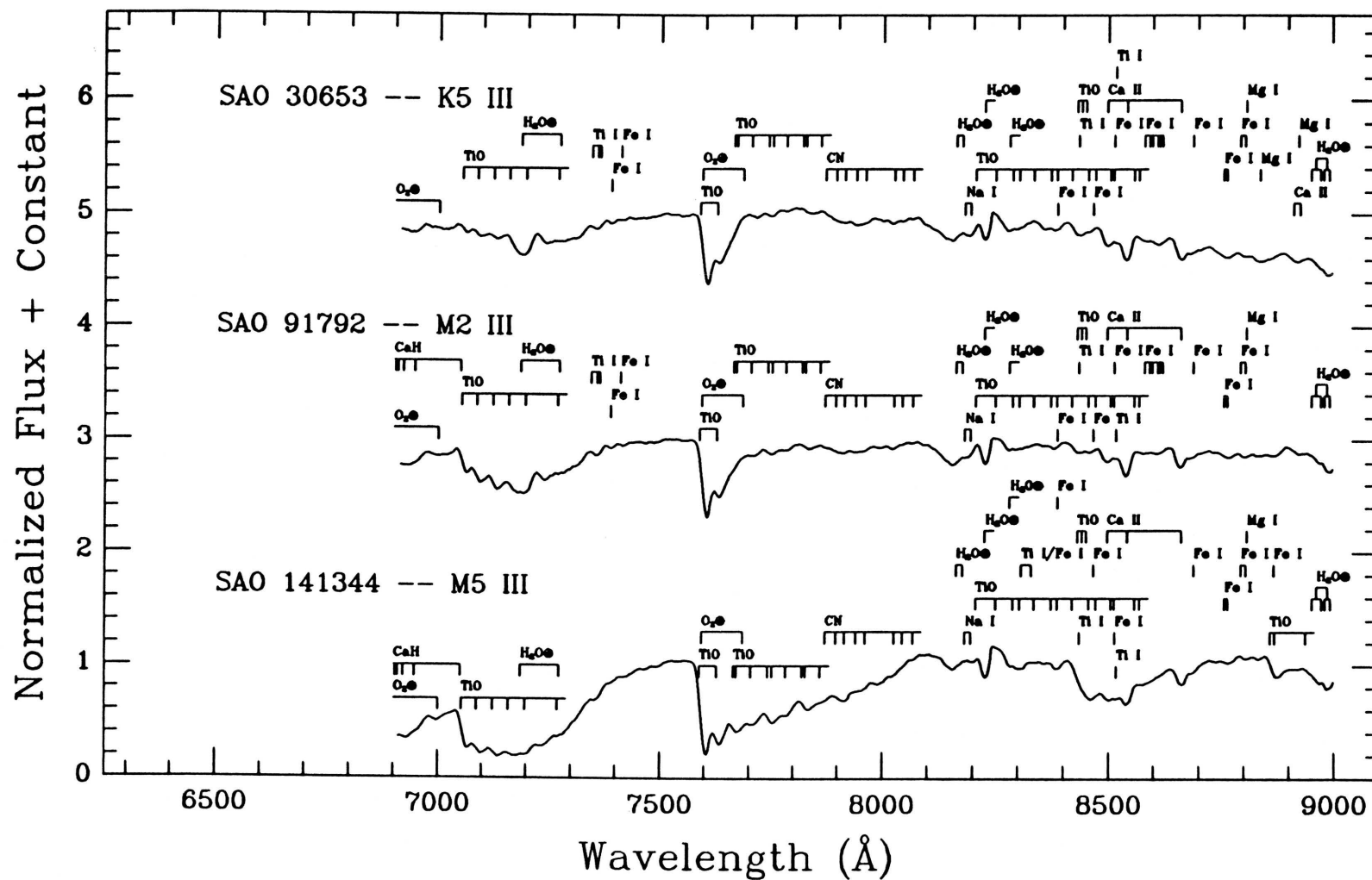


FIG. 3.5. (continued) — (b) Giants of class K5, M2, and M5. In the figure, offsets of two and four have been added to the spectra of SAO 91792 and SAO 30653, respectively, for clarity. →

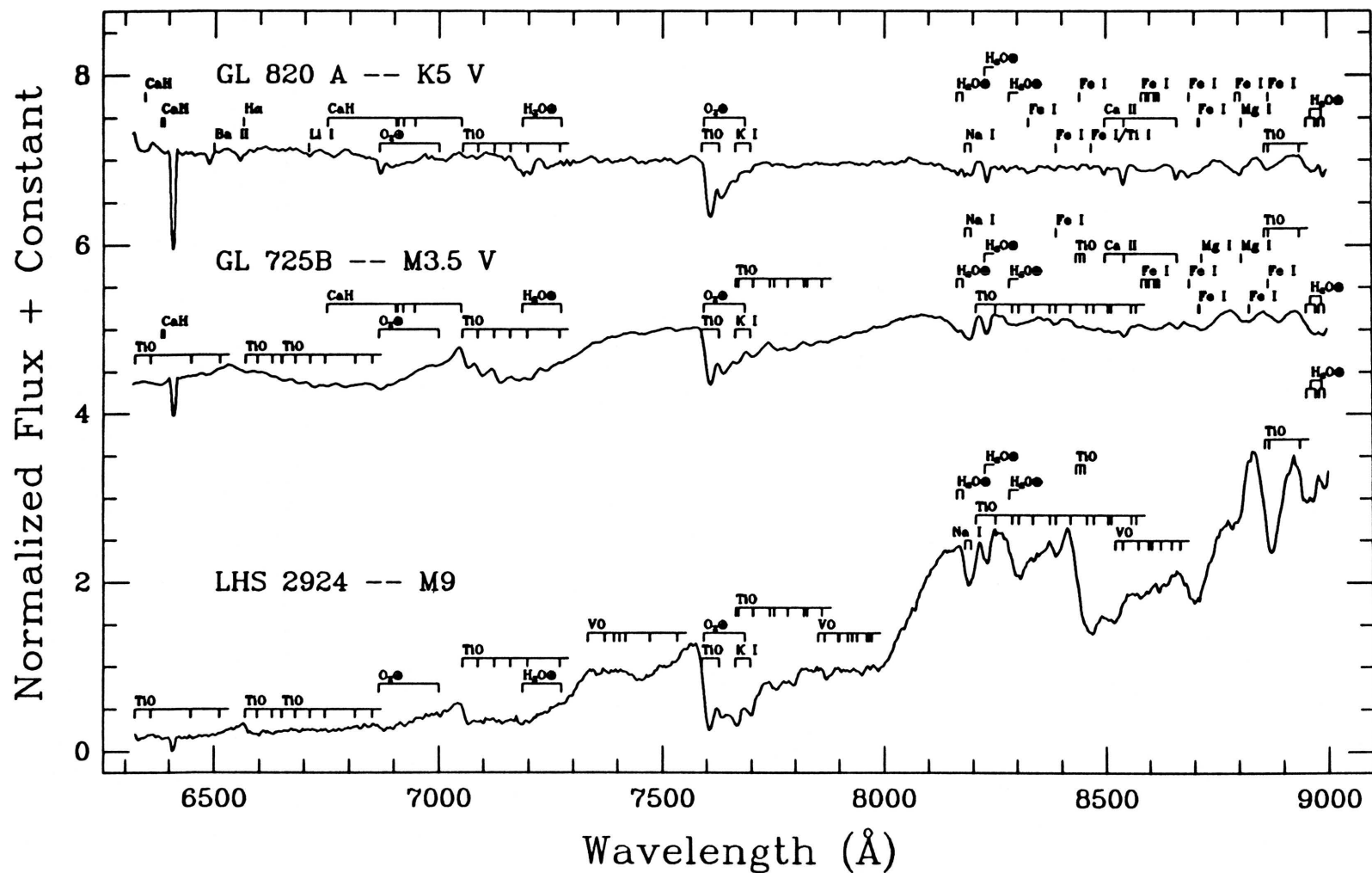


FIG. 3.5 (continued) — (c) Dwarfs of class K5, M3.5, and M9. Offsets of four and six have been added to the spectra of GL 725 B and GL 820 A, respectively, for clarity. →

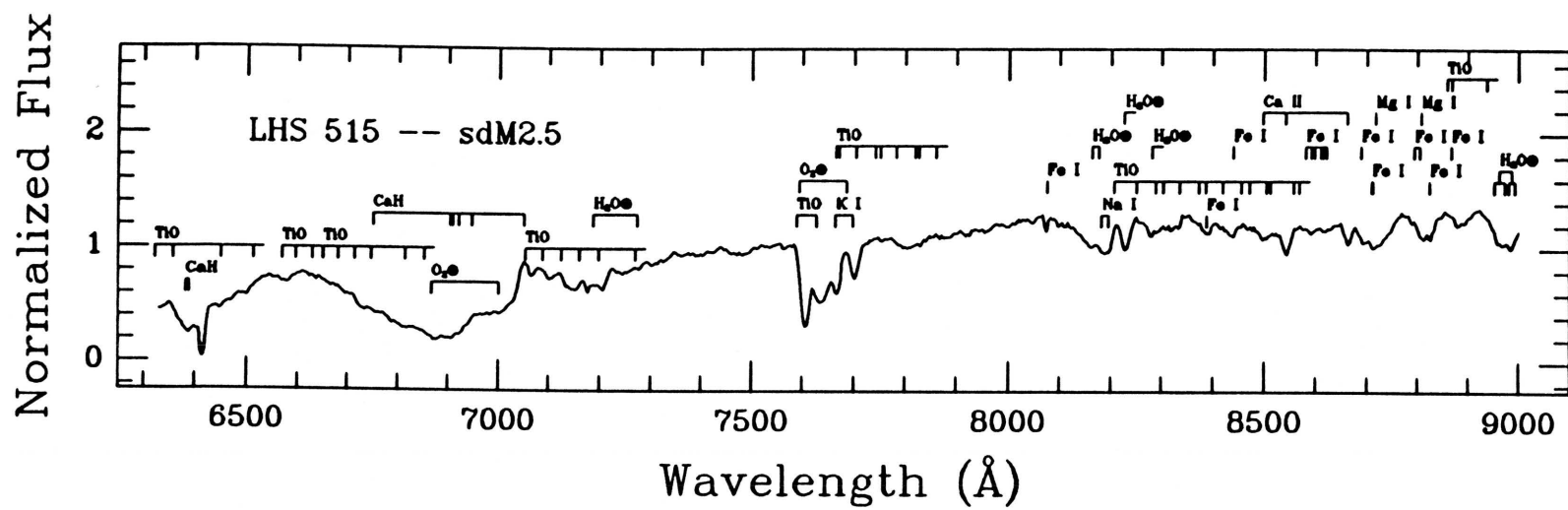


FIG. 3.5. (continued) — (d) A metallic hydride subdwarf of class M2.5.

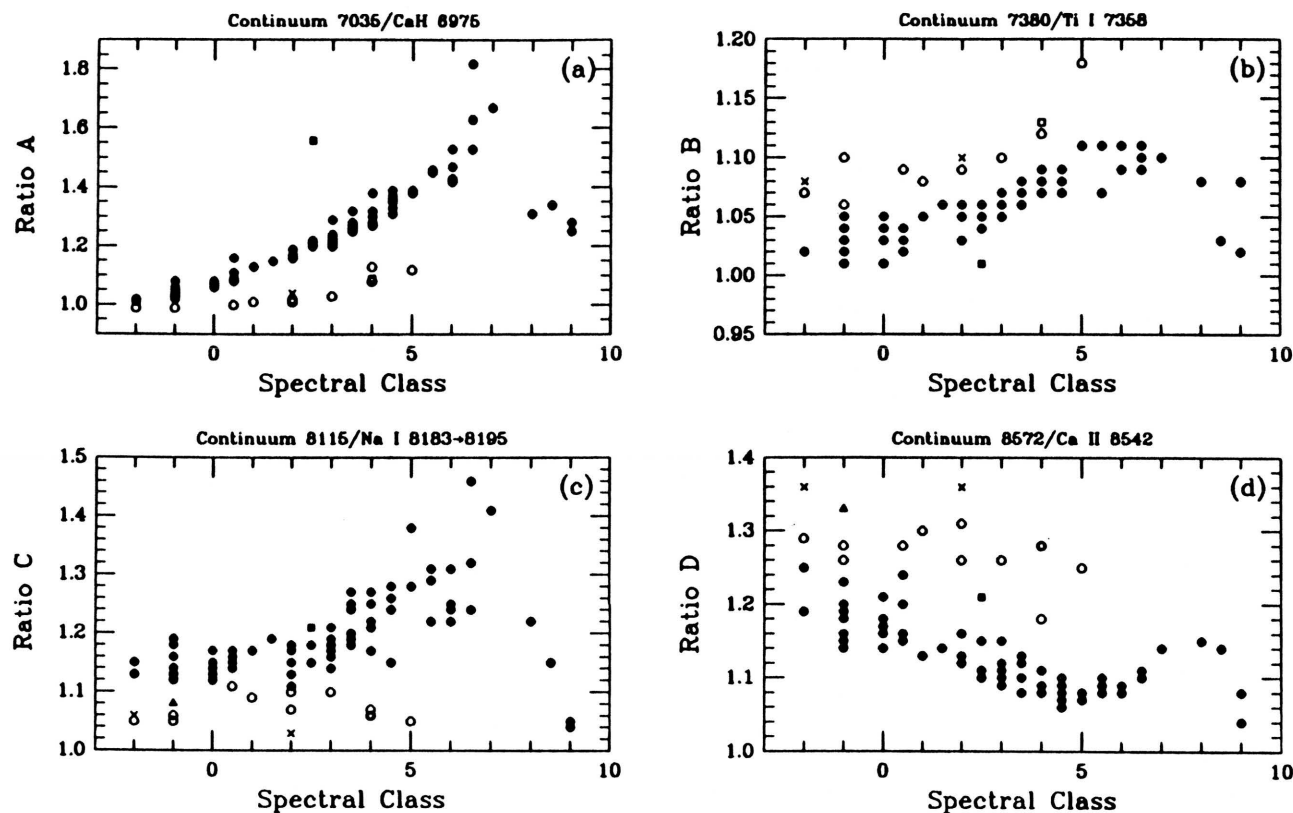


FIG. 3.6. — Color ratios useful as luminosity discriminants. Descriptions of the ratios are given in Table 3.7. Supergiants are marked by crosses, the bright giant by an open square, giants by open circles, and dwarfs by filled circles. The giant GL 756.2 is denoted by an open triangle, and the subdwarf LHS 515 is denoted by a filled square. Along the horizontal axis negative numbers represent K spectral types. K5 is located at the “-2” mark, and K7 is located at the “-1” mark. Positive numbers represent M spectral types; “0” stands for M0, “4.5” for M4.5, etc. The figure shows ratios of four different luminosity dependent lines or bands to nearby “continuum” areas, regions where there is little contaminating absorption.

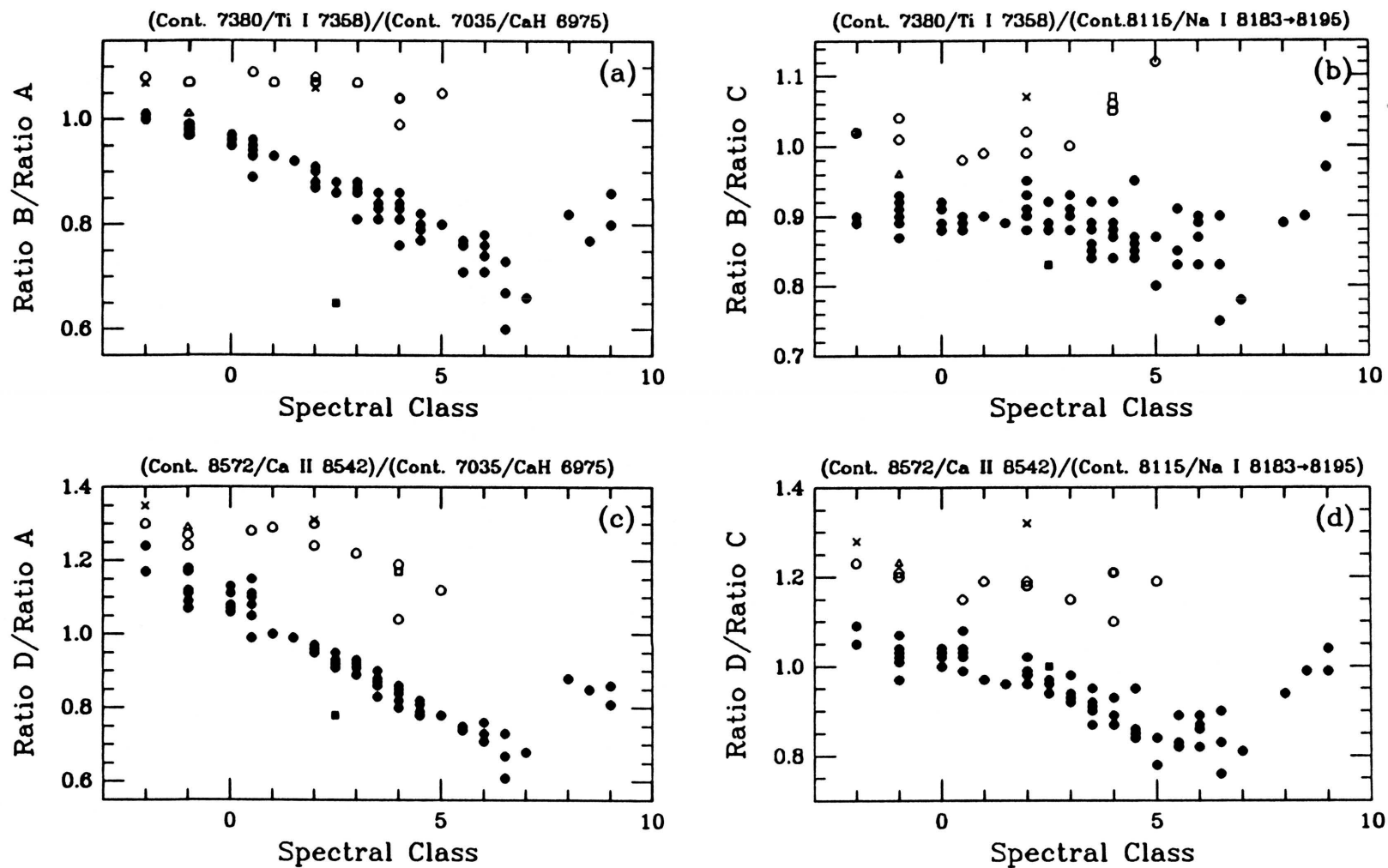


FIG. 3.7. — The same as Figure 3.6, except that the ratios shown are based on the ratios given in Figure 3.6. See text for details.

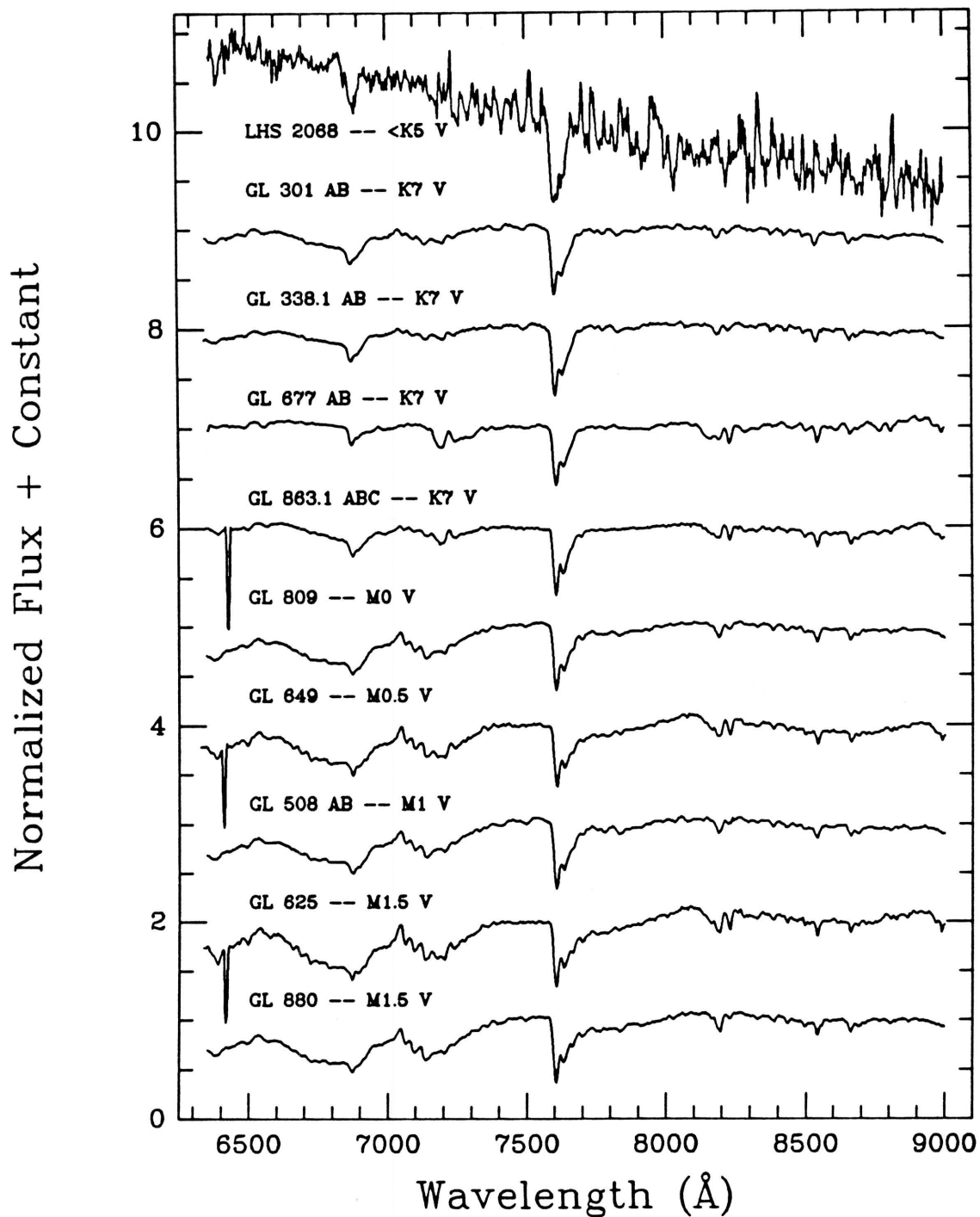


FIG. 3.8. — Spectra of 32 additional objects listed in Table 3.9. All of these were observed at the MMT and have a resolution of 18 \AA . See the caption to Figure 3.1 for more details.

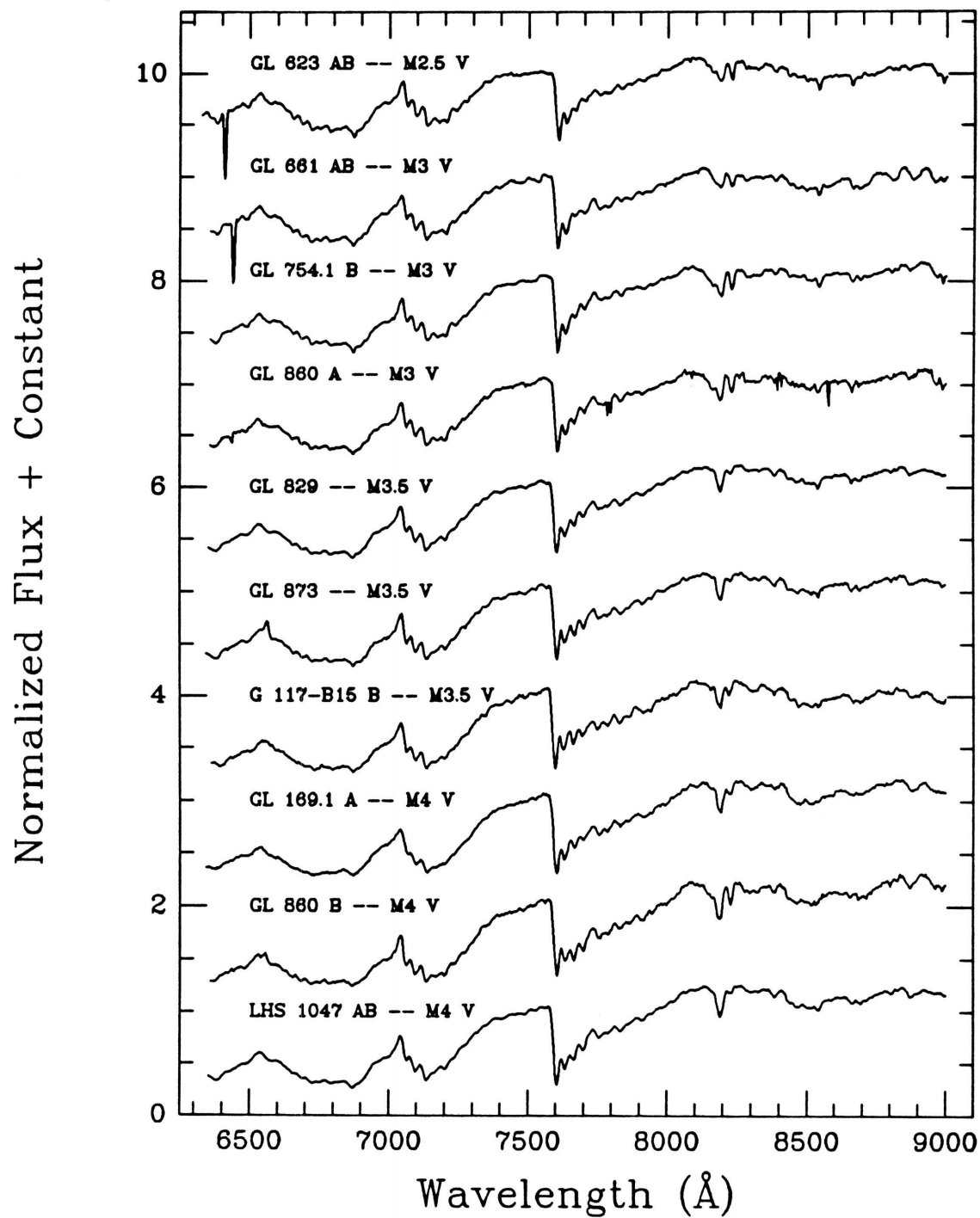


FIG. 3.8. (continued)

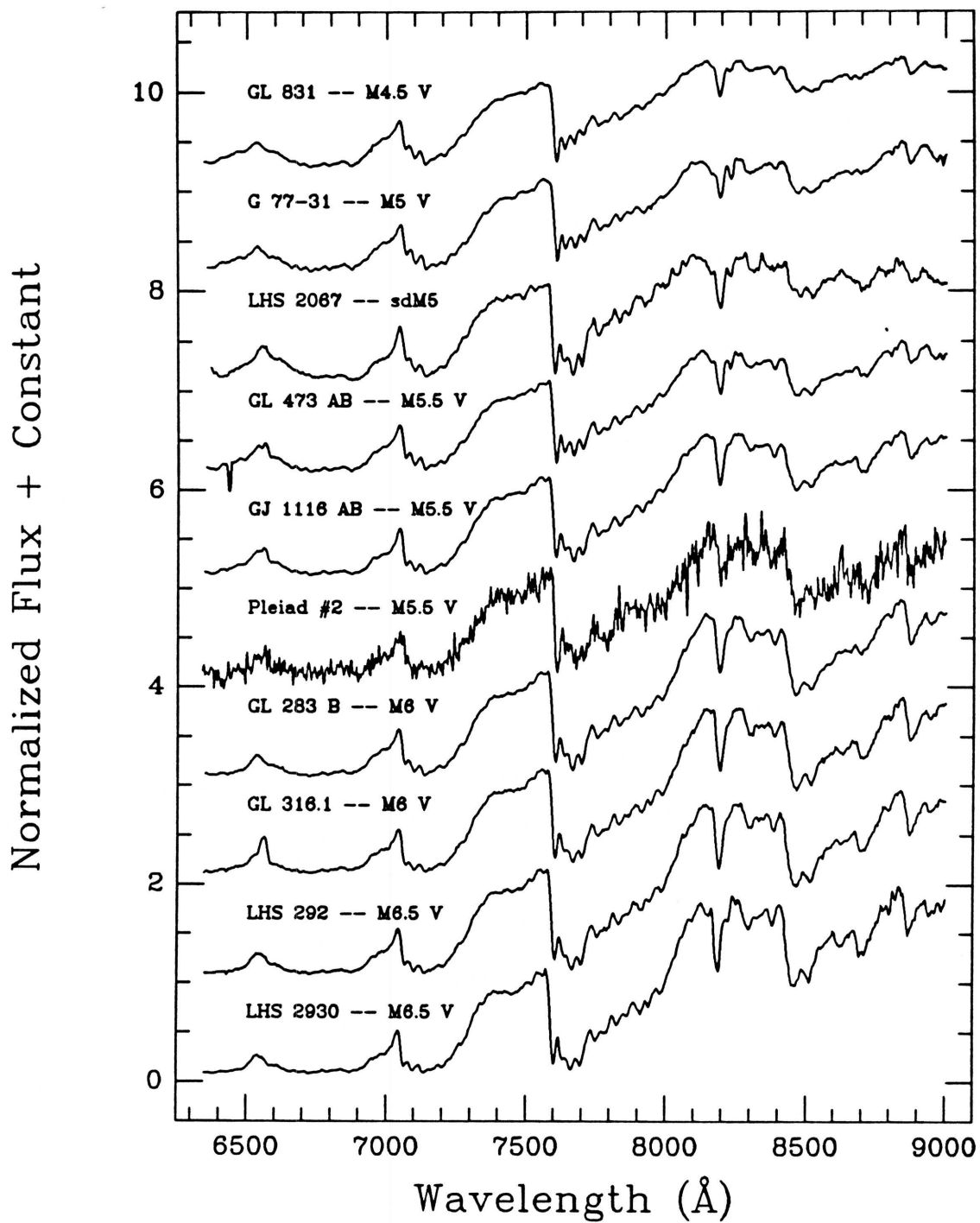


FIG. 3.8. (continued)

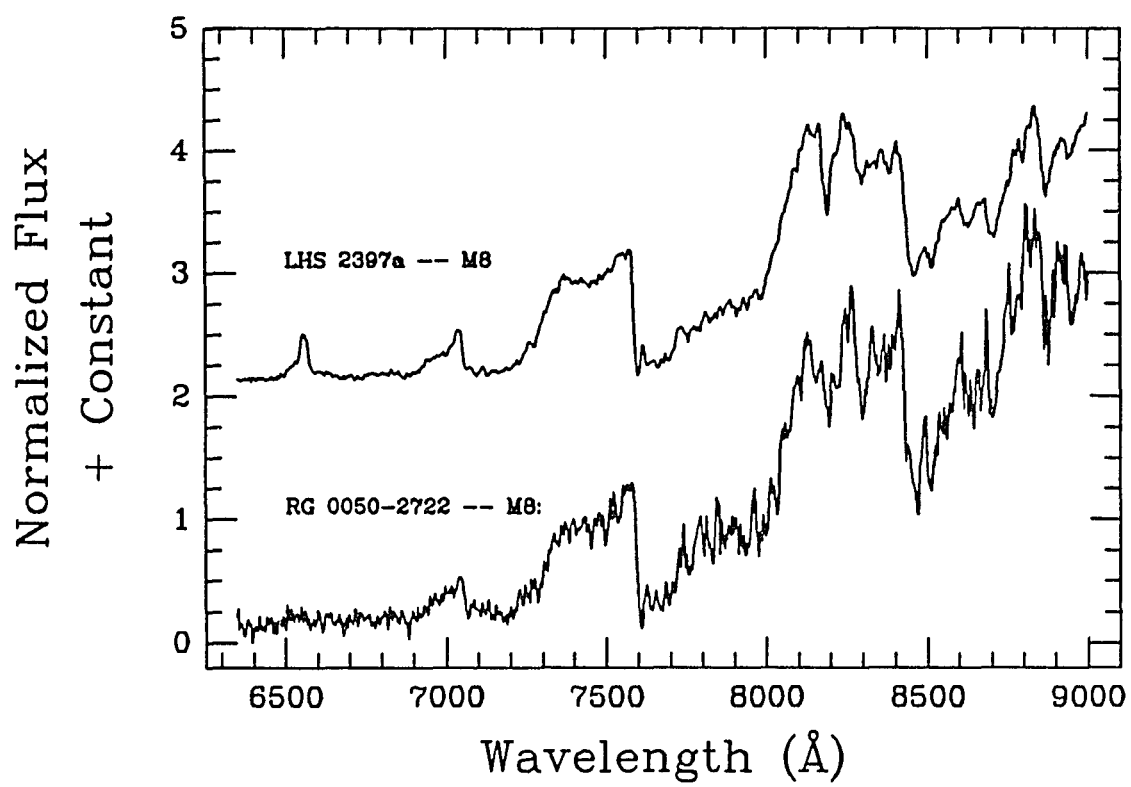


FIG. 3.8. (continued)

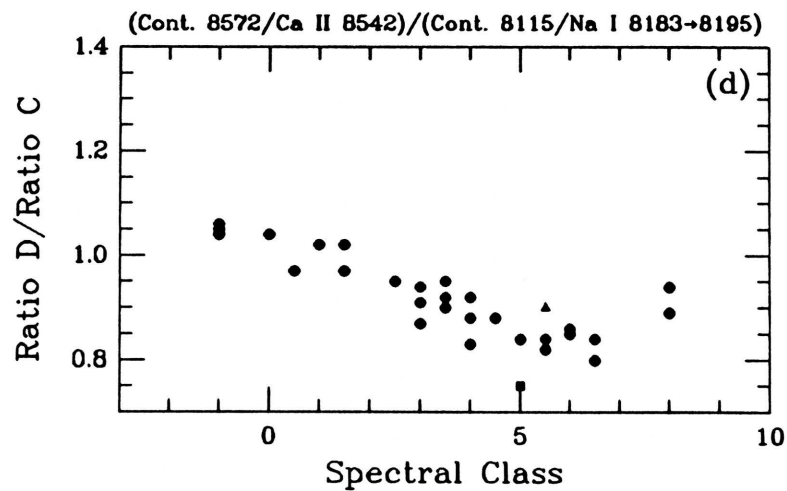
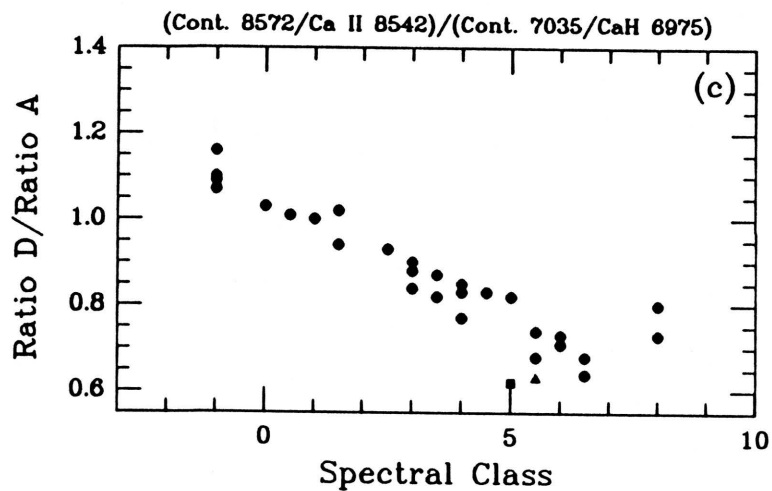
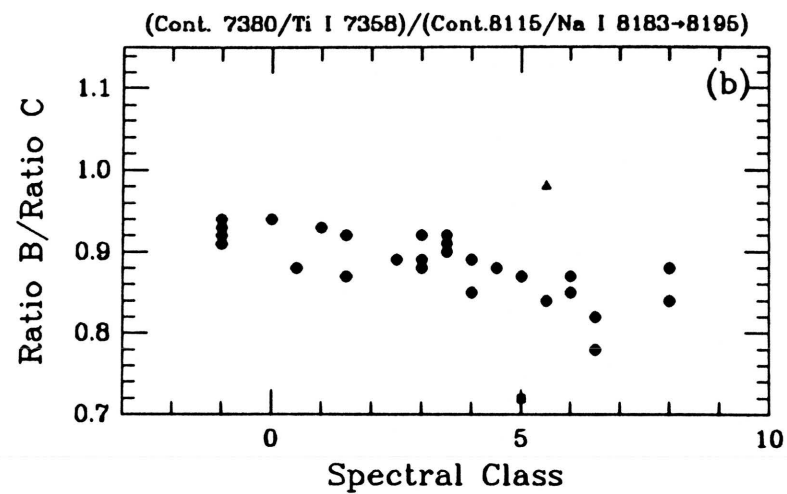
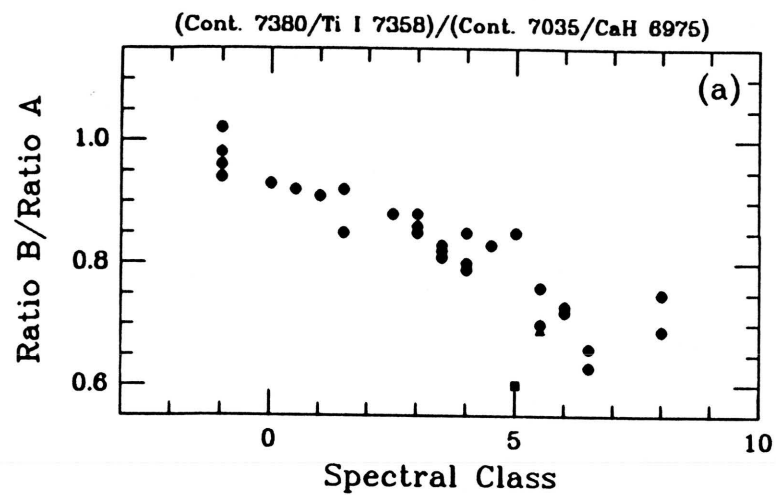


FIG. 3.9. — The same as Figure 3.7, except that the data plotted here are for the stars listed in Table 3.9.

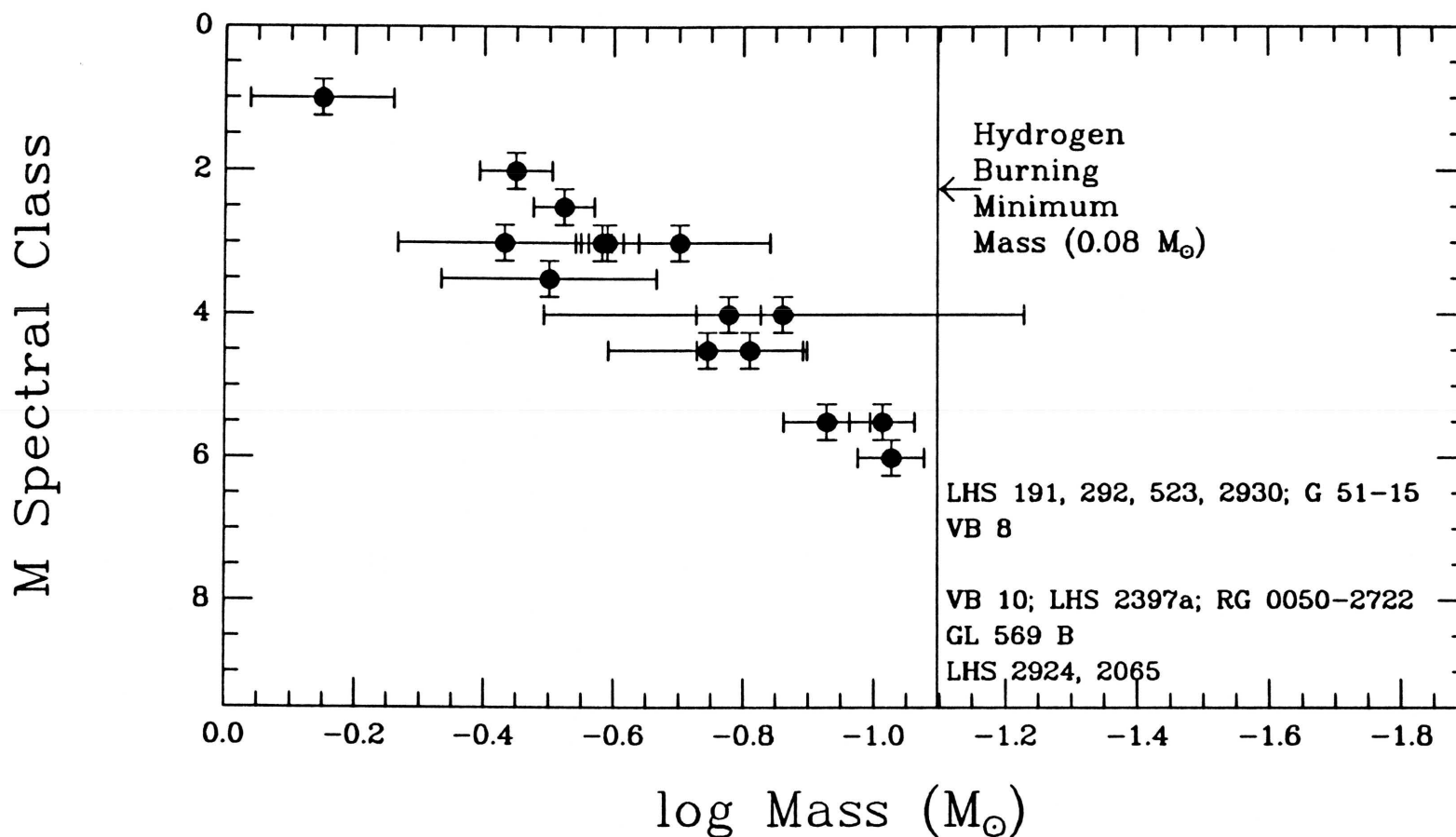


FIG. 3.10. — M spectral class versus the logarithm of the mass for those dwarfs listed in Table 3.10. The vertical line at $0.08 M_{\odot}$ represents the minimum mass for core hydrogen burning; objects to the right of the line would be brown dwarfs. The point of highest mass here, representing GL 508 AB, may be spurious; a third member of this system may be present as suggested through radial velocity variations on the order of 10 km/sec (Wilson 1967).

3.2: THE TEMPERATURE SCALE FOR M DWARFS DERIVED USING SPECTRA FROM 0.6 TO 1.5 MICRONS

M dwarfs are the most common stars in the Galaxy and could be responsible in part for its missing mass; however, these objects are poorly understood physically. Although spectral data provide a wealth of information on such parameters as surface gravities, temperatures, and chemical compositions, it has proven challenging to extract this information because of the difficulty in relating existing data to theoretical models. Traditionally, spectra have been obtained in the visual, but for the coolest stars this has become an obstacle both because they are very faint and because the visual region lies on the Wien side of their blackbody emission, where modelling uncertainties can be very large. As a result, spectral atlases rarely contained data for stars later than M5. Recently, however, high quality spectra of M dwarfs have been obtained in the red and near-infrared, where these objects are emitting their peak fluxes. Spectral sequences are now available for the entire range of M dwarfs, and a comparison between observational and theoretical data can provide more insight into these objects.

Unfortunately, modelling the atmospheres of M dwarfs has proven to be a very complicated problem due to the large number of opacity sources present in their spectra, the uncertainty with which many molecular constants and oscillator strengths are known, and the inability of current models to describe adequately the transition from the radiative layers to the convective ones. (Convection itself, which is the main mode of energy transport in these stars, is fortunately not a major problem, and the high densities force the real temperature gradient

to be very close to the adiabatic one.) The first attempt at modelling these atmospheres was the work of Mould (1976), which included only the early M stars. Two recent PhD theses — Allard (1990) and Ruan (1991) — have attempted to refine these models and to extend them to the temperatures of the coolest dwarfs. The energy distributions from both model grids are quite similar since the majority of subroutines employed was identical.

In this paper we present an M-dwarf spectral sequence against which to check the success of these new models. We have obtained spectra from 0.6 to 1.5 μm of well-studied, nearby stars with accurate trigonometric parallaxes. The observations and reductions are presented in §3.2.1. The method for combining the red and the infrared data is given in §3.2.2. Features which serve well as temperature discriminants are discussed in §3.2.3. Model spectra from Allard (1990) are fit to the empirical data and discussed in §3.2.4. The resulting temperature sequence and H-R Diagram for M dwarfs are given in §3.2.5, and the shortcomings of the present models are discussed in §3.2.6. The conclusions are highlighted in §3.2.7.

3.2.1: Data Acquisition and Reduction

The objects observed for this project are listed in Table 3.11. Spectral classifications are from §3.1. All of the red spectra were observed at the Multiple Mirror Telescope (MMT) and have a resolution of 18 Å. Spectral coverage, observation date, and integration time are given in columns (4) - (6). Observing setups and reduction procedures can be found in §3.1. Since many of these observations were taken through spotty cloud cover, corrections for atmospheric

absorption were considered unreliable and thus not attempted. Features such as the A- and B-band of telluric O₂ are still present.

The infrared spectra were taken at the Steward Observatory 2.3-m telescope using a spectrometer that employs a 2×32 array of germanium photodiode detectors. The spectrometer was used with a pair of round, 6-arcsecond apertures separated by 1 arcminute. The 150 line/mm grating provides sampling every 30 Å, and the observational linewidth is 48 Å. Each grating setting covers about $0.1 \mu m$, so many settings were needed to cover the spectral range. Each setting had a central wavelength displaced by $0.05 \mu m$ from the previous one to insure overlap between adjacent spectral pieces. These adjacent pieces were connected by renormalizing one of the two pieces by the median flux ratio in the region of overlap. Dwarf stars of type F and G were observed for flatfielding and flux calibration. Telluric absorption was removed during the flatfielding procedure. However, Paschen absorption features in the spectra of the F and G dwarfs introduced small residual “emission lines” into the spectra of several of the program objects. For a more detailed discussion of the observing procedure and data reduction, see Rix et al. (1990). Spectral coverage, observation date, and total integration time for each object are given in columns (7) - (9) of Table 3.11.

3.2.2: Combining the Red and Infrared Spectra

To fit the two parts of the spectrum together, the infrared data for each object were renormalized relative to the red data by using a least-squares minimization technique (described in §3.1) on the overlap region. This procedure takes the difference between the flux values of the two spectra at 3 Å intervals

in wavelength. The sum of the squares of these differences is computed over the overlap region. The infrared spectrum is then shifted vertically up or down relative to the red spectrum, and a new sum is calculated. In this way the shift giving the smallest residual is found. (Because absorption by unremoved telluric H₂O is present, the red spectra were truncated shortward of 0.905 μm . For each object, the remaining amount of overlap between the red and infrared spectra can be determined from column (7) of Table 3.11.) Once the shift was found, the spectra were renormalized and then connected by averaging the flux values in the overlap region at intervals equivalent to the pixel size for the red data (~ 3.5 Å). The resulting spectra are shown in Figure 3.11. Each spectrum is normalized to one (in units of F_λ) at its peak flux. Since the two pieces of spectra for LHS 2924 do not overlap, their relative normalizations relied solely upon the photometric data discussed below.

The fitted spectra include the regions investigated by broadband I and J filters, so it is possible to extract an $I - J$ color for each spectrum to evaluate the effectiveness of our fitting technique. These extracted $I - J$ colors were compared to values listed in Berriman & Reid (1987, hereafter BR) and Leggett & Hawkins (1988, hereafter LH). The I photometry from both sources is on the Kron-Cousins system. However, BR give J photometry on the AAO system, whereas LH give their J (and K) data on the CIT (or CTIO) system. The data sets can be placed on the same system by converting the J_{CIT} values into J_{AAO} values via the equation

$$J_{AAO} = 1.115J_{CIT} - 0.115K_{CIT} + 0.004, \quad (3.1)$$

which can be derived from Elias et al. (1983). The resulting $I_{KC} - J_{AAO}$ colors for the program objects are listed in columns (2) and (3) of Table 3.12. Two of

our objects — GL 411 and GL 406 — had photometry listed in both sources. Column (5) of Table 3.12 gives the difference between the LH and BR colors for these two stars. This comparison demonstrates that the colors agree to within ± 0.1 mag.

Photometry on the $I_{KC} - J_{AAO}$ system was then extracted from the spectra of Figure 3.11. The values for $(F_\lambda)_{I_{KC}}$ and $(F_\lambda)_{J_{AAO}}$ were determined over a rectangular bandpass whose cut-on and cut-off wavelengths correspond to the wavelengths at half maximum of the filter. Half power for the I_C ($\sim I_{KC}$) filter occurs at 0.725 and 0.875 μm (Bessell 1979), which gives a central wavelength for the rectangular bandpass of 0.80 μm . For J_{AAO} , half power occurs at 1.08 and 1.38 μm (Allen & Cragg 1983), giving a central wavelength of 1.23 μm . The colors measured from the spectra were therefore computed using the formula

$$\begin{aligned} I_{KC} - J_{AAO} &= 2.5 \left\{ \log \left[\left(\frac{(F_\lambda)_{J_{AAO}}}{(F_\lambda)_{I_{KC}}} \right) \left(\frac{\lambda_{J_{AAO}}}{\lambda_{I_{KC}}} \right)^2 \left(\frac{(F_{\nu_0})_{I_{KC}}}{(F_{\nu_0})_{J_{AAO}}} \right) \right] \right\} \\ &= 2.5 \left\{ \log \left[\left(\frac{(F_\lambda)_{J_{AAO}}}{(F_\lambda)_{I_{KC}}} \right) \left(\frac{1.23 \mu\text{m}}{0.80 \mu\text{m}} \right)^2 \left(\frac{2550 \text{ Jy}}{1640 \text{ Jy}} \right) \right] \right\}. \end{aligned} \quad (3.2)$$

The zero-magnitude fluxes are taken from Berriman & Reid (1987) and Allen & Cragg (1983). The derived colors are shown in column (4) of Table 3.12. Column (6) shows the differences between our photometry and that of LH. The average difference of ~ 0.08 mag, which is similar to the disagreement found between the BR and LH color data, is small enough that we consider our technique of combining the spectra to be reliable.

Since the red and infrared spectra of LHS 2924 do not overlap, the photometry from LH was used to find the relative normalizations of the two pieces. Since the $I - J$ values derived from the spectra are systematically ~ 0.1 mag bluer than

the LH values, a value of $I - J = 3.3$ was assumed for the normalization, and, of course, no independent measurement of the color was possible.

For M dwarfs, the purest temperature index of all the red/infrared colors (according to LH) is $I - J$. Table 3.12 shows that $I - J$ increases with increasing spectral type through the M stars, with the possible exception of the G 208-44/45 system. According to our photometry, G 208-44 AB, whose red spectrum is classified as an M5.5 V, is 0.07 mag *redder* in $I - J$ than its sister star G 208-45, whose red spectrum is classified as an M6 V. Although this difference is within the errors determined above, the composite spectrum of G 208-44 AB may be too bright at J for its type due to the contribution from its very red, low-mass secondary, G 208-44 B. The same color effect is found in the photometry presented in McCarthy et al. (1988).

3.2.3: Spectral Features

The spectra of Figure 3.11 show many changes in spectral shape and feature strengths along the sequence of M stars. The peak flux (in units of F_λ) for an M2 star occurs in the red portion of the spectrum, around $0.80 \mu m$. By M8 and M9, the flux in the infrared portion around 1.1 to $1.2 \mu m$ greatly dominates. If these peaks corresponded to blackbody maxima, temperatures ranging from 3600 to 2400 K would be derived. Clearly, though, these spectra are far different from those of blackbodies, so a temperature determination based on model fitting and calibration of temperature-sensitive features would be better.

There are several temperature-sensitive atomic lines and molecular bands that are easily visible in this spectral range. Figure 3.12 shows identifications

for an M2 and an M8 spectrum. Most obvious perhaps are the red TiO bands, which gain prominence through the early- and mid-M stars, saturating beyond spectral type M6. At our resolution, VO absorption begins to appear after M6 and is a good indicator of temperature for the latest objects. FeH at $0.99\ \mu\text{m}$ begins to appear after M4 and increases with decreasing temperature throughout the sequence. The most obvious temperature-dependent feature in the infrared portion is the H₂O absorption at $1.35\ \mu\text{m}$ — by M9 it is the most striking feature in the entire spectrum. Other prominent features are H₂O at $1.14\ \mu\text{m}$, OH at $1.20\ \mu\text{m}$, and a number of sharp absorption features at 1.169 , 1.177 , 1.243 , and $1.252\ \mu\text{m}$ that are likely due to K I. These last four positions are the only features in the $1.1 - 1.5\ \mu\text{m}$ solar spectrum which are identified by Livingston & Wallace (1991) as K I, and all four correspond very closely to prominent features found in the spectra of our coolest objects. The $1.177\text{-}\mu\text{m}$ line was first identified in the spectrum of R Leo by Spinrad and Wing (1969), who note that the neutral potassium lines are favored at lower temperatures. A more detailed identification of features in the far red portion of the spectrum can be found in §3.1.3.

3.2.4: Fits to Theoretical Spectra of M Dwarfs

The spectra of Figure 3.12 can be compared to the theoretical models of Allard (1990). (Additional discussion of Allard's models can be found in Leinert et al. 1990.) Her models cover a grid of metallicities ($[M/H] = 0, -1, -2, -3, -4$), surface gravities ($\log g = 4, 5, 6$), and temperatures (3500, 3250, 3000, 2750, 2500, 2250, 2000 K). Surface gravities for some of the stars in this paper can be determined using radii derived in Lacy (1977) and masses derived from M_K

values, and the M_K vs. mass relation, presented in Henry and McCarthy (1990). Independent determinations can be made using the radii and masses given in Caillault and Patterson (1990). The results, which are shown in Table 3.13, indicate that an integral value of $\log g = 5$ best describes the stars from type M2 to M6. (The surface gravities of GL 752 B and LHS 2924 are not known since masses have not been determined for either.) Therefore, only the models with $\log g = 5$ have been considered further. As for metallicity, the models with $[M/H] = -1$ have a very striking CaH absorption feature at $0.675 \mu m$, which is typical of extreme subdwarfs such as LHS 515 (see §3.1.4) and LHS 2045 (see §5.3). Since none of the spectra presented here show this strong feature, only the models with $[M/H] = 0$ were used.

a) Fits in the Red Region

As with the observational data, each model spectrum was normalized to unity at its peak flux, in units of F_λ . By applying the least-squares minimization technique (see §3.1.4) on only the red portion ($0.70 - 0.90 \mu m$), each observed spectrum was compared to each of the model spectra, and the best match in temperature was found. In order to make a finer grid in temperature, a linear interpolation between Allard's spectra was used to produce models with $T = 3375, 3125, 2875, 2625, 2375, \text{ and } 2125 \text{ K}$, giving us a resolution of 125 K .

Figure 3.13 shows each of the red spectra overplotted with the model spectrum that provided the best match. In the case of GL 411, a model warmer than the one at 3500 K would clearly have provided a better match. Generally, the Na I feature at $0.82 \mu m$ is fit well by the models, as is the slope of the spectrum

between 0.77 and $0.81 \mu m$ and the relative opacity minimum from 0.69 to $0.72 \mu m$ that lies between consecutive TiO bands. The similar minimum between 0.64 and $0.67 \mu m$ is not fit well, nor is the one between 0.73 and $0.76 \mu m$. For the later spectra ($\geq M6$), the models predict less flux at $0.90 \mu m$ than is indicated in the observational data, and the overall appearance of the model spectra is in worse agreement with the true spectra. The temperatures of these fits in the red are given in column (2) of Table 3.14.

b) Fits in the Infrared Region

When the infrared portion of the spectrum is compared to the models, the discrepancy in the region around $1.00 \mu m$ is immediately apparent (see Figure 3.14). A small part of this discrepancy arises because Allard (1990) does not include FeH at $0.99 \mu m$ in her calculations. The models from Ruan (1991), which do include FeH, show substantial discrepancies in the $1.00 \mu m$ region as well. For example, in both the Allard and Ruan models the VO absorption around $1.05 \mu m$ is virtually absent. In general it appears that throughout this region there are important opacity sources not yet included in the models.

The general *shape* of the spectral “continuum,” however, is traced out well from ~ 1.08 to the steam feature at $1.35 \mu m$, even though the models do not include many of the sharp features such as the H_2O absorption at $1.14 \mu m$ and the OH absorption at $1.20 \mu m$. To obtain a second set of temperature estimates, the least-square minimization technique was again applied, this time over 1.08 to $1.35 \mu m$, to find the model providing the best match. Specifically, only the pseudo-continuum and the H_2O feature at $1.35 \mu m$, both of which are

temperature-dependent, were fit. Absorptions not reproduced in the models ($1.10 - 1.12 \mu m$, $1.13 - 1.145 \mu m$, $1.165 - 1.18 \mu m$, $1.19 - 1.215 \mu m$, and $1.235 - 1.28 \mu m$) were excluded from the fit. For the latter half of the spectral sequence, at least as late as M8, the models give a fair match to both the “continuum” and the $1.35 \mu m$ steam feature. The best fits are illustrated in Figure 3.15, and the resulting temperatures are listed in column (3) of Table 3.14. This comparison of the infrared spectra with theoretical models suggests, even for the coolest stars, a modeled continuum which is approximately correct but which has a number of missing absorption species.

As demonstrated in Figure 3.14 (see §3.2.4c), fits that simultaneously match the red and infrared data give poor results. Nonetheless, when taken *singly*, the red and infrared portions of the models provide, in many cases, reasonably good fits to the data. Specifically, good fits are obtained in the red region for stars earlier than about M6. However, the density of features in the spectra of cooler objects makes a continuum in the red difficult to identify, and the models are generally poor fits to the data. These later objects, on the other hand, are fit well by the infrared portions of the theoretical models, but these same models cannot be fit reliably to stars earlier than M6 because of the lack of strong temperature-sensitive features in the infrared. Therefore, the combination of red and infrared spectra promises to provide improved accuracy in relating the stars to a sequence of models of differing temperatures.

c) Synthetic Photometry

Figure 3.14 is plotted so that the best fit to the data in the 1.08 to 1.35 μm region is shown. Notice that the red portion (0.70 to 0.90 μm) of the model should be shifted downward to achieve a better match. Although the least-squares minimization technique found that the same model yielded the best fits in both the red and infrared portions of the spectrum, the normalization of the model in each region was different. This shift cannot be accounted for on observational grounds because, as discussed in §3.2.2, the combined red/infrared spectra successfully reproduce the observational $I - J$ colors. Clearly, the $I - J$ color of the model and that of the true data are in disagreement. To explore this effect further, synthetic IJK photometry was obtained from the best-fit models and was compared to observed colors. These values are listed in Table 3.15. The $J - H$ and $J - K$ colors were derived using, for H_{AAO} and K_{AAO} , respectively, central wavelengths of 1.64 and 2.19 μm and zero-magnitude fluxes of 1030 and 650 Jy (Allen & Cragg 1983). For each of the observed spectra, synthetic colors were derived from the model that fit best in the red for spectral types $< M6$ and from the model that fit best in the infrared for spectral types $\geq M6$.

For early M dwarfs, the disagreement between the observed and modelled $I - J$ is around 0.05 mag, which is within the uncertainty noted before. However, for later types, the disparity becomes increasingly large; for LHS 2924, the difference between the true $I - J$ and that of the model is 0.86 mag! Part of this discrepancy arises because the modelled I flux is too large due to an underestimate of the opacity around 0.74 μm . The true $J - H$ and $J - K$ colors increase for later

spectral types, whereas the $J - H$ and $J - K$ colors from the models *decrease* for later spectral types. Despite this backward trend, the $J - H$ color of the models is still in general only ~ 0.1 mag different from the true color. For the early M dwarfs, the same difference is seen in the $J - K$ colors, but for later types the discrepancy is ~ 0.4 mag.

Allard (1990) derives her own synthetic photometry of the models and notes the same effect presented above, i.e., that $J - H$ and $J - K$ get bluer for the cooler models. This effect can be attributed to gross incompleteness in the opacities, or specifically to the strong influence of water blanketing in the models. Nonetheless, these models are certainly closer to the actual spectra of M dwarfs than are blackbodies and should be used in preference to blackbody curves. The colors of these objects are distinctly unlike those of a blackbody and are likewise not well predicted by the models, especially beyond M5. The best match to the true data is, therefore, achieved by fitting theoretical models to observed *spectra*.

d) Comparison to Ruan's Models

Ruan (1991) overplots her model spectra with those of Allard (1990). From 0.70 to $0.90 \mu m$, these two sets of $\log g = 5$, $[M/H] = 0$ models are virtually identical, convincing us that a temperature scale derived from Ruan's models would give us the same results as Allard's for stars earlier than M6. Ruan's overplots in the infrared show nearly identical H_2O strengths and continuum slopes as well, reassuring us that the same temperature scale would also have been derived for objects of type M6 and later. The major difference between the Ruan and Allard models is the inclusion of $0.99\text{-}\mu m$ FeH in the Ruan set. A

temperature sequence could be derived, potentially, based on this feature alone, as the Ruan models show its strengthening with later type in accordance with observations. Unfortunately, these models do not include either of the obvious absorption species just redward and just blueward of the FeH band, making an accurate fit to the feature impossible. Like Allard, Ruan also notes a blueward trend of $J - H$ and $J - K$ in the models, i.e., that these colors become bluer for later spectral types. Based on this information, we are confident that a temperature scale derived from Ruan (1991) would not differ from that presented here.

3.2.5: Temperature Scale

As discussed in §3.2.4b, an accurate temperature sequence can be established for all M dwarfs by using temperatures from red fits for stars earlier than M6 and temperatures from infrared fits for objects of later spectral type. As Table 3.14 demonstrates, the temperatures of the best-fit models in the red and the best-fit models in the infrared are never different by more than 125 K. For objects earlier than type M6, the red and infrared fits assign identical temperatures. In fact, for five of the eight spectra, the same model provided the best fit in both regions. In light of such agreement, we are confident in adopting the temperature determined by the part of the spectrum giving the better fit. These assigned temperatures are listed in column (2) of Table 3.16, where the objects are presented in order of increasing M_V . Based on the agreement of the red and infrared fits to the data, we assign an uncertainty in our temperatures of ± 125 K.

The luminosities of these objects can be determined from their parallaxes

and from photometry. The parallaxes are listed in column (3) of Table 3.16 and were used to calculate the absolute magnitudes M_V , M_I , and M_J in columns (4) - (6). A linear interpolation of Bessell's (1991) M_I vs. BC_I relationship gave the values of BC_I (column 7) used to determine the bolometric magnitude in column (8). Notice that these assigned temperatures decrease monotonically with increasing M_V , M_I , M_J and M_{bol} . Finally, luminosities were determined (column 9) assuming that the Sun has $M_{bol} = 4.75$.

As a test of the accuracy of the bolometric corrections, we compared for GL 752 B the flux determined by integration of the 0.6-1.5 μm spectrum with the flux determined by trapezoidal integration under the broadband magnitudes. In spite of the strengths of the absorption features in the spectrum, the two techniques agreed to within roughly 5%. For earlier spectral types, the agreement should be much better. Compared to typical uncertainties in distances, the bolometric corrections given by Bessell seem to be fairly reliable. For later spectral types, however, it is clearly preferable to determine the bolometric flux from spectra rather than from broadband photometry.

Also listed in Table 3.16 are the temperature sequences assigned by BR and by Veeder (1974). To assure a set of data on a standard system, the luminosities of their stars and ours were calculated using parallaxes, photometry, and bolometric corrections from the same sources. Neither the BR or Veeder sequences exhibit the monotonic behavior that ours does, but perhaps this is not too surprising considering the number of data points present in those two sequences, the errors inherent in assigning temperatures from photometric data, and the uncertainties in the parallax. The temperatures assigned by Veeder are determined by fitting a blackbody (by eye) to the observed broad-band colors of each star. Short

wavelengths are assumed to have a certain amount of blocking, but the total flux under the blackbody curve and the total flux observed from the star are required to be equal. BR assumed that no significant backwarming or blanketing occurs at $2.2\ \mu m$. The temperature for each star was determined from the blackbody curve having (1) flux equal to the observed flux at $2.2\ \mu m$ and (2) the same total flux observed from the star. BR quote an uncertainty in their temperatures (which do not differ significantly from the revised temperatures presented in Berriman, Reid, & Leggett (1992)) of ± 110 K, whereas Veeder (1974) quotes one of ± 150 K.

The temperatures and luminosities from all three sequences are presented in the H-R Diagram of Figure 3.16. The temperatures assigned in this paper are generally *warmer* at a given absolute magnitude than the temperatures assigned by either BR or Veeder, particularly for the lowest-luminosity objects. For $\log(L/L_{\odot}) \leq -3.0$, the difference between our temperatures and those of the other authors is ~ 500 K. This is not surprising since the models show strong pressure and temperature dependences as well as radiative transfer effects. Figure 3.16(a) shows theoretical tracks of the lower main sequence by D'Antona & Mazzitelli (1985, hereafter DM) and by Burrows, Hubbard, & Lunine (1989, hereafter BHL). The DM curve is for the zero-age main sequence, and the BHL curves are for an age of 10 Gyr. (The BHL curves for an age of 1 Gyr are in very close agreement with those plotted here. Only at the low luminosity end do these tracks deviate noticeably from the 10 Gyr models. Specifically, these younger tracks bring the models *closer* to our plotted positions of GL 752 B and LHS 2924.) Figure 3.16(b) shows the theoretical tracks of Dorman, Nelson, & Chau (1989, hereafter DNC), with the DM curve plotted again for comparison.

The DNC models are also calculated for the zero-age main sequence. Using our temperature scale, the positions of M dwarfs on the H-R Diagram fall closer than previous determinations to theoretical tracks of the lower main sequence.

3.2.6: Discussion

This first attempt to fit a sequence of M dwarf spectra with model energy distributions demonstrates clearly that the general slope of the distributions and many of the features can be well reproduced by present-day models. As a result, it is possible to construct an improved temperature scale that is quite consistent with interior models. Shortcomings of the atmospheric models are, however, obvious. For example, the fluxes for wavelengths between major absorption bands are often too high, indicating that additional opacity sources are important but have not yet been included in the calculations (in most cases, due to the lack of laboratory data). It should also be noted that the electronic f -values for many bands are of very low accuracy (cf. Bessell & Scholz 1990).

These problems show up in the spectra more strongly when the gradient of the Planck function is steep, i.e., the uncertainties are highest for the coolest models (as can be seen in the comparison of observed and calculated spectra in Figure 3.15) and in a given model are strongest for the short-wavelength, or Wien, portion of the spectrum. This latter point implies that an analysis based on fluxes at wavelengths shorter than that of the maximum flux is rather unreliable (cf. the analogous discussion for limb-darkening by Scholz & Takeda 1987). Therefore, in this paper we draw our main conclusions from the energy distributions in the region of the peak flux.

The differences between the observed and the calculated colors are also largely due to these problems. In particular, the fact that the observed colors involving the I filter are much redder than the calculated ones can be traced back to high fluxes in the $0.74\text{-}\mu\text{m}$ region of the models. Additional reasons for the discrepancies could result from uncertainties in the filter functions and the color equations; however, these effects are considered to be small since the synthetic photometry obtained from the combined spectra agrees to within 0.1 mag of the observed colors (see §3.2.2). Furthermore, changes in our adopted filter transmissions do not adversely affect the calculated photometry. For example, when the half-power points of the J bandpass are shifted by $\pm 10\%$ of the filter width, the newly calculated $I - J$ colors of the 2750 K model are only ~ 0.02 mag different from the previously derived $I - J$ color. Since these differences are small compared to the differences noted between observed and theoretical photometry, it must be concluded that the biggest factor contributing to the color discrepancy is the absence or uncertain modelling of opacity sources in the models.

3.2.7: Summary

This paper presents the first set of $0.6 - 1.5\ \mu\text{m}$ spectra for a full sequence of M dwarfs. Strong, temperature-sensitive absorptions by H_2O , TiO , VO , OH , K , I , and FeH are present. The observed spectra show many more features than are currently included in the models. Identifications have been made of the strongest of these missing absorption species, and follow-up observations are planned at higher resolution.

Using these spectra, a new temperature sequence has been determined for

M dwarfs. Allard's (1990) models have been used for the temperature fits and yield the same results as Ruan's (1991) models. The models present a good fit to dwarfs earlier than type M6 in the region around the I bandpass but are far less successful in reproducing the observed spectra of later dwarfs. Dwarfs of type M6 and later have a significant steam feature at $1.35\ \mu m$ that increases with later spectral type, and the shape of the infrared "continuum" is also temperature-dependent. As a result, these later dwarfs were fit by the models in the region of the J bandpass. The sequence has been established, therefore, by fitting models to the red and infrared portions of the data independently.

Although the red and infrared fits assigned very similar temperatures to the same object, the colors deduced from the models are in sharp contrast with observed colors determined from broad-band photometry. The models predict consistently bluer $I - J$ colors than are observed. Also, the $J - H$ and $J - K$ colors from the models get bluer with later spectral type, in direct contrast to the observed trend. These trends illustrate that it is difficult to assign temperatures to M dwarfs based on colors. The preferred method is to fit models to temperature-sensitive features in the spectra.

The temperatures assigned here are warmer than those of Veeder (1974) and Berriman & Reid (1987), particularly at the lowest luminosities. When plotted on an H-R Diagram, our sequence is in better agreement with theoretical tracks of the lower main sequence.

TABLE 3.11
LOG OF 0.63 TO 1.50 MICRON SPECTROSCOPY

Gliese No.	Other Name	Spectral Type	Far Red			Infrared		
			Spectral Range (μm)	Date Obs. (UT)	Integ. (sec.)	Spectral Range (μm)	Date Obs. (UT)	Int. ^a (sec.)
411	HD 95735	M2 V	0.63-0.92	1990 Jan 22	9	0.90-1.50	1990 Jun 12	238
273	BD +5° 1668	M3.5 V	0.63-0.92	1990 Jan 22	120	0.90-1.60	1990 Nov 06	904
213	Ross 47	M4 V	0.63-0.92	1990 Jan 22	130	0.90-1.60	1990 Nov 05	2515
—	G 208-44 AB	M5.5 V	0.63-0.92	1989 Jul 13	75	0.85-1.60	1989 Sep 20	1860
—	G 208-45	M6 V	0.63-0.92	1989 Jul 13	225	0.85-1.60	1989 Sep 20	1800
406	Wolf 359	M6 V	0.63-0.92	1990 Jan 20	80	0.85-1.51	1990 Apr 11	1135
752 B	VB 10	M8 V	0.63-0.92	1989 Jul 10	1800	0.85-1.55	1989 Sep 17/20	2700
—	LHS 2924	M9	0.63-0.92	1989 Jul 13	1980	1.00-1.35	1990 Apr 14	2190

^a Total integration time for all of the spectral segments.

TABLE 3.12
COMPARISON OF $I - J$ VALUES

Name	$(I - J)$ Reference			$\Delta_{I_{KC} - J_{AAO}}$	
	LH ^a	BR ^b	us ^c	LH - BR	LH - us
GL 411	1.13	1.23	1.04	-0.10	+0.09
GL 273	1.40	—	1.32	—	+0.08
GL 213	1.47	—	1.39	—	+0.08
G 208-44 AB ^d	—	—	2.11	—	—
G 208 - 45 ^e	—	—	2.04	—	—
GL 406	2.31	2.27	2.24	+0.04	+0.07
GL 752 B	2.74	—	2.65	—	+0.09
LHS 2924 ^f	3.38	—	—	—	—

^a Data from Leggett & Hawkins 1988

^b Data from Berriman & Reid 1987

^c Data from this paper

^d $(I_{KC} - J_{Steward}) = 2.19$ from McCarthy et al. 1988.

^e $(I_{KC} - J_{Steward}) = 2.15$ from McCarthy et al. 1988.

^f Because there is no overlap between the far red and the infrared data, Leggett & Hawkins 1988 photometry was used to scale the two spectral pieces. Thus, no independent measurement of $I - J$ was possible.

TABLE 3.13
SURFACE GRAVITIES

Name	$\log g$	
	(1) ^a	(2) ^b
GL 411	4.59	—
GL 273	4.71	5.00
GL 213	—	5.11
GL 406	5.08	5.49

^a Based on data from Lacy 1977 and Henry & McCarthy 1990

^b Based on data from Caillault & Patterson 1990

TABLE 3.14
TEMPERATURES DERIVED FROM THE BEST FIT TO
ALLARD'S MODEL SPECTRA WITH $[M/H] = 0$, $\log g = 5$

Name	Far-red Portion (0.70 - 0.90 μm)	IR Portion (1.08 - 1.35 μm)
GL 411	>3500 K	>3500 K
GL 273	3500 K	3500 K
GL 213	3375 K	3375 K
G 208-44 AB	3125 K	3125 K
G 208-45	3000 K	3125 K
GL 406	2875 K	3000 K
GL 752 B	2875 K	2875 K
LHS 2924	2750 K	2625 K

TABLE 3.15
OBSERVED VS. SYNTHETIC COLORS^a

Name	Observed Colors			Colors from Best-fit Model		
	$I - J$	$J - H$	$J - K$	$I - J$	$J - H$	$J - K$
GL411 ^b	1.13	0.54	0.75	—	—	—
GL 273	1.40	0.52	0.77	1.35	0.63	0.84
GL 213	1.47	0.53	0.78	1.42	0.62	0.84
G 208-44 AB ^c	2.19	0.52	0.89	1.64	0.59	0.82
G 208-45 ^c	2.15	0.50	0.89	1.64	0.59	0.82
GL 406	2.31	0.62	0.98	1.78	0.56	0.80
GL 752 B	2.74	0.67	1.11	1.99	0.54	0.78
LHS 2924	3.38	0.65	1.12	2.52	0.48	0.72

^a Photometry is I_{KC} , J_{AAO} , H_{AAO} , and K_{AAO} from Leggett & Hawkins 1988, unless otherwise noted

^b None of the models is warm enough to fit this spectrum adequately

^c Observed colors are from McCarthy et al. 1988 and are not on a standard system

TABLE 3.16
COMPARISON OF TEMPERATURE SEQUENCES

Name	T(K)	$\pi('')$ ^a	M_V ^a	M_I ^b	M_J ^b	BC_I ^c	M_{bol}	$\log(L/L_\odot)$ ^d
This paper								
GL 411	>3500	0.397	10.49	8.32	7.10	0.50	8.82	-1.63
GL 273	3500	0.270	11.98	9.33	7.83	0.36	9.69	-1.98
GL 213	3375	0.168	12.73	9.86	8.30	0.30	10.16	-2.16
G 208-44 AB	3125	0.211	15.03	11.59 ^e	9.40 ^e	0.00	11.59	-2.74
G 208-45	3125	0.211	15.61	12.10 ^e	9.95 ^e	-0.12	11.98	-2.89
GL 406	3000	0.426	16.68	12.63	10.21	-0.36	12.27	-3.01
GL 752 B	2875	0.173	18.57	13.98	11.11	-0.95	13.03	-3.31
LHS 2924	2625	0.0908 ^f	19.37 ^g	15.09	11.57	-1.45	13.64	-3.56
Berriman & Reid (1987) ^h								
GL 884	3650	0.130	8.46	6.79	5.80	0.61	7.40	-1.06
GL 752 A	3200	0.173	10.31	7.99	6.69	0.55	8.54	-1.52
GL 411	3250	0.397	10.49	8.32	7.10	0.50	8.82	-1.63
GL 821	3500	0.093	10.5	8.67	7.50	0.45	9.12	-1.75
GL 643	3150	0.161	12.73	10.09	8.60	0.26	10.35	-2.24
GL 699	3100	0.552	13.25	10.50	9.04	0.19	10.69	-2.38
GL 447	3200	0.301	13.50	10.57	8.91	0.18	10.75	-2.40
GL 866 AB	2650	0.305	14.60	11.06	8.94	0.09	11.15	-2.56

TABLE 3.16 (continued)

Name	T(K)	$\pi(^{\prime\prime})^a$	M_V^a	M_I^b	M_J^b	BC_I^c	M_{bol}	$\log(L/L_{\odot})^d$
Berriman & Reid (1987) continued								
GL 406	2600	0.426	16.68	12.62	10.21	-0.35	12.27	-3.01
GJ 1111	2450	0.278	17.03	12.86	10.46	-0.45	12.41	-3.06
GL 644 C	2450	0.161	17.69	13.32	10.80	-0.65	12.67	-3.17
Veeder (1974)								
GL 278 C	3750	0.069	8.26	—	5.16	—	—	—
GL 820 B	3900	0.296	8.39	—	5.85	—	—	—
GL 717	4000	0.054	8.4	—	—	—	—	—
GL 205	3600	0.170	9.12	—	—	—	—	—
GL 239	3650	0.104	9.71	7.85	6.71	0.56	8.41	-1.46
GL 48	3400	0.114	10.34	—	—	—	—	—
GL 644 AB	3450	0.161	10.80	7.59	6.31	0.56	8.15	-1.36
GL 661 A	3450	0.155	10.91	—	—	—	—	—
GL 725 A	3450	0.282	11.15	—	7.45	—	—	—
GL 745 A	3500	0.119	11.15	8.92	7.69	0.41	9.33	-1.83
GL 669 A	3300	0.095	11.25	8.63	7.18	0.45	9.08	-1.73
GL 829	3300	0.153	11.27	8.63	7.23	0.45	9.08	-1.73
GL 860 A	3350	0.253	11.87	—	—	—	—	—
GL 725 B	3300	0.282	11.94	9.37	7.97	0.38	9.75	-2.00
GL 285	3100	0.165	12.29	9.30	7.69	0.37	9.67	-1.97

TABLE 3.16 (continued)

Name	T(K)	$\pi(^{\prime\prime})^a$	M_V^a	M_I^b	M_J^b	BC_I^c	M_{bol}	$\log(L/L_{\odot})^d$
Veeder (1974) continued								
GL 669 B	3100	0.095	12.81	—	—	—	—	—
GL 234 A	3050	0.252	13.08	—	—	—	—	—
GL 699	3250	0.552	13.25	10.50	9.04	0.19	10.69	-2.38
GL 15 B	3150	0.282	13.29	10.51	9.01	0.19	10.70	-2.38
GL 729	3000	0.345	13.3	10.34	8.89	0.22	10.56	-2.32
GL 299	3200	0.151	13.66	10.83	9.27	0.13	10.96	-2.48
GL 51	2950	0.107	13.81	—	—	—	—	—
G 69-47	2700	0.079	14.30	10.86	8.97	0.13	10.99	-2.50
GL 866 AB	2750	0.305	14.60	11.06	8.94	0.09	11.15	-2.56
GL 905	2800	0.318	14.80	11.41	9.39	0.03	11.44	-2.68
GL 473 AB	2800	0.231	15.09	10.80	8.79	0.14	10.94	-2.48
GL 65 A	2700	0.367	15.27	—	—	—	—	—
G 158-27	2700	0.214	15.39	11.84	9.96	-0.05	11.79	-2.82
GL 551	2700	0.761	15.45	—	—	—	—	—
GL 406	2500	0.426	16.68	12.63	10.21	-0.36	12.27	-3.01
G 51-15	2450	0.278	17.03	12.86	10.46	-0.45	12.41	-3.06

^a from Gliese 1969 or Gliese & Jahreiss 1979 unless otherwise noted

^b calculated using I_{KC} and J_{CTIO} values from Leggett & Hawkins 1988 unless otherwise noted

^c linearly interpolated from BC_I vs. M_I relation in Table 2 of Bessell 1991

^d assuming $(M_{bol})_{\odot} = 4.75$

TABLE 3.16 (continued)

^e on the Steward system of McCarthy et al. 1988

^f from Dahn, Probst, & Liebert (unpublished)

^g from Monet et al. 1992

^h temperatures do not differ significantly from the revised values presented in Berriman, Reid, & Leggett 1992

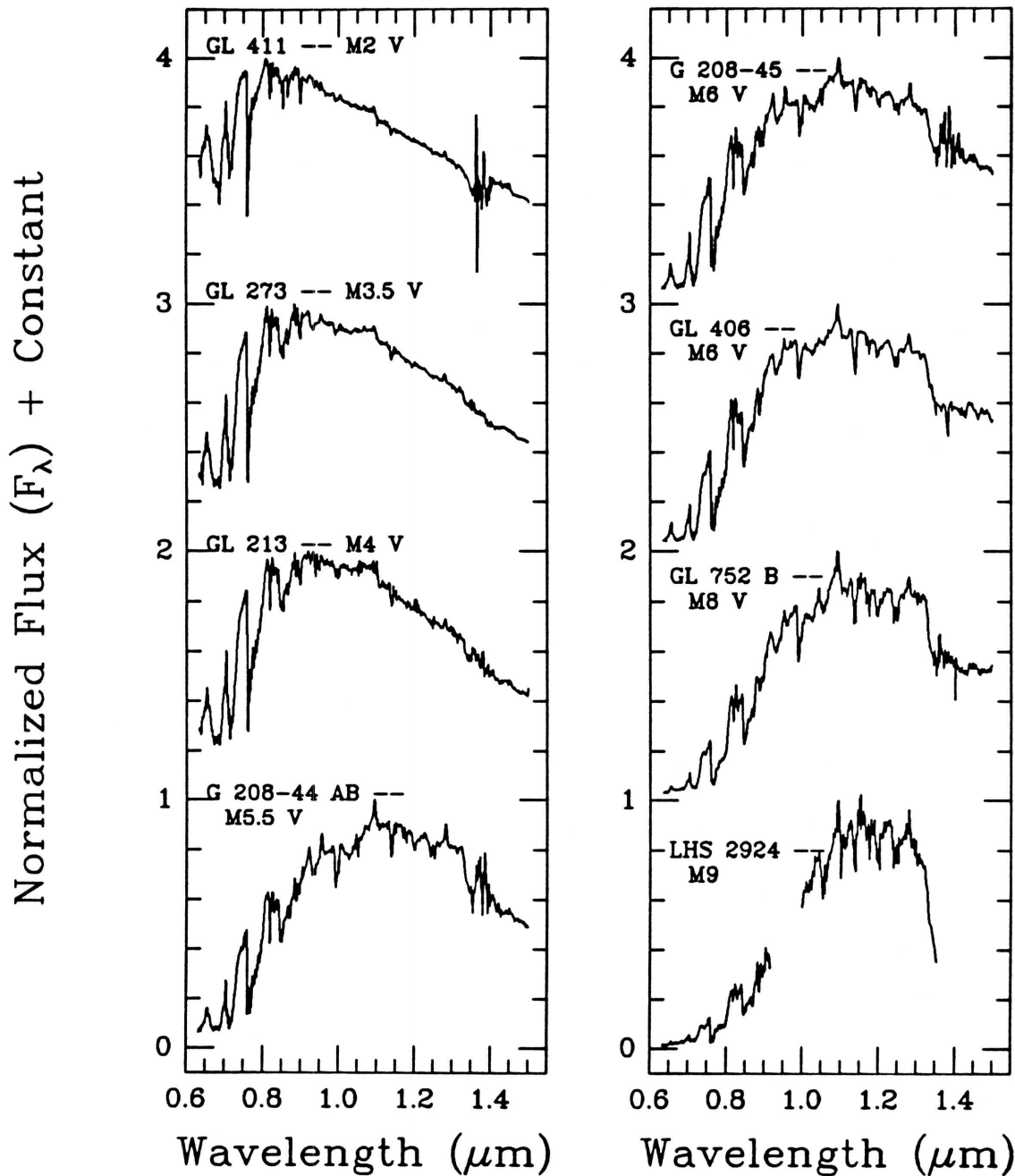


FIG. 3.11. — Spectra of the eight objects listed in Table 3.11. The red portion ($0.63 - 0.92 \mu\text{m}$) of the spectra has a resolution of 18 \AA , and the infrared portion ($0.92 - 1.50 \mu\text{m}$) has a resolution of 48 \AA . Each spectrum is normalized to unity at its peak flux (which is in units of F_λ), and integral offsets have been added to separate the spectra vertically. Note that for early M dwarfs, the infrared region is relatively featureless compared to the red region. For late M dwarfs, many absorption features are seen in the infrared, the most striking of which is the water vapor band at $1.35 \mu\text{m}$.

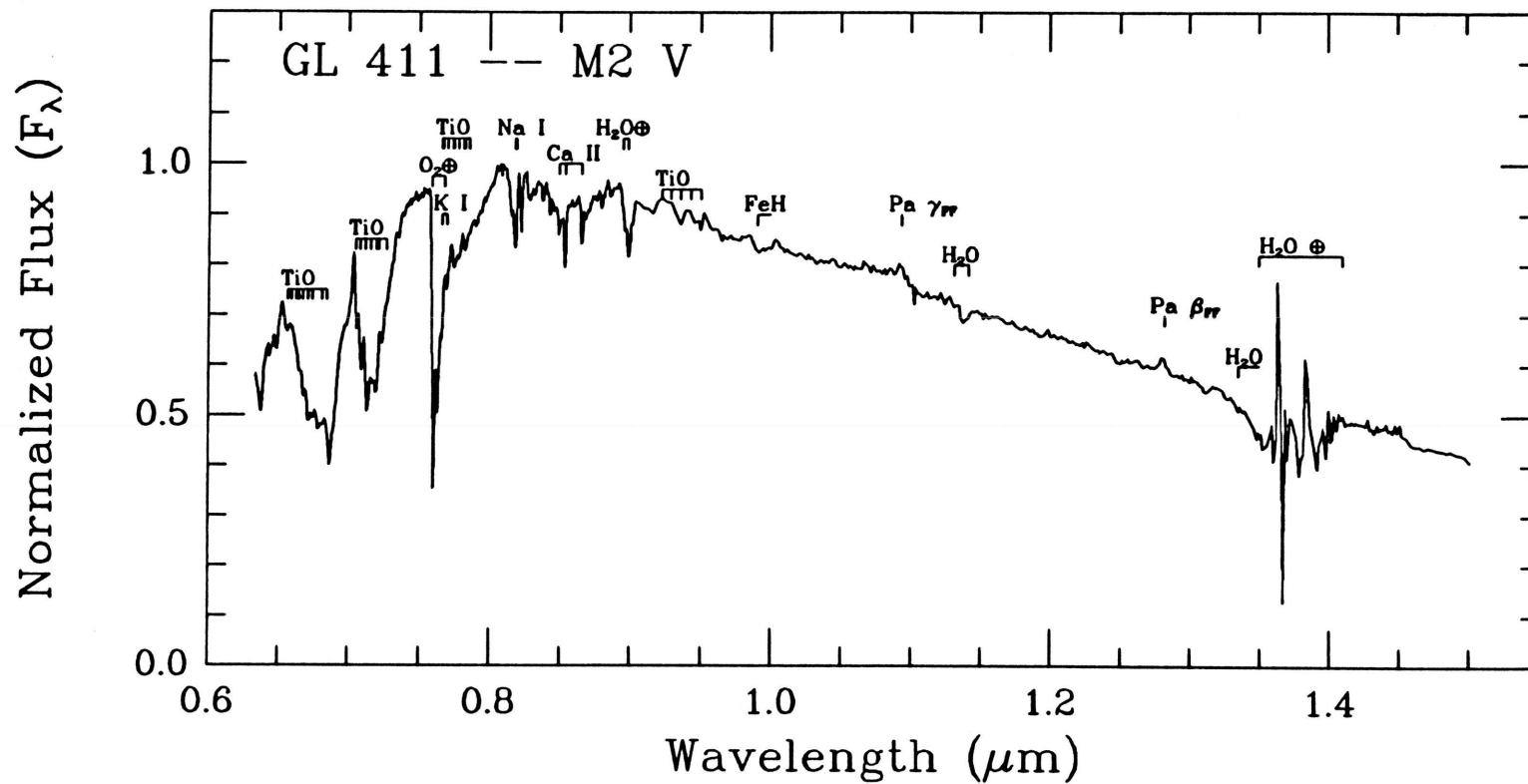


FIG. 3.12. — Identifications of the most prominent features in M dwarf spectra from 0.63 to 1.50 μm . (a) The spectrum of GL 411 — spectral type M2 V. →

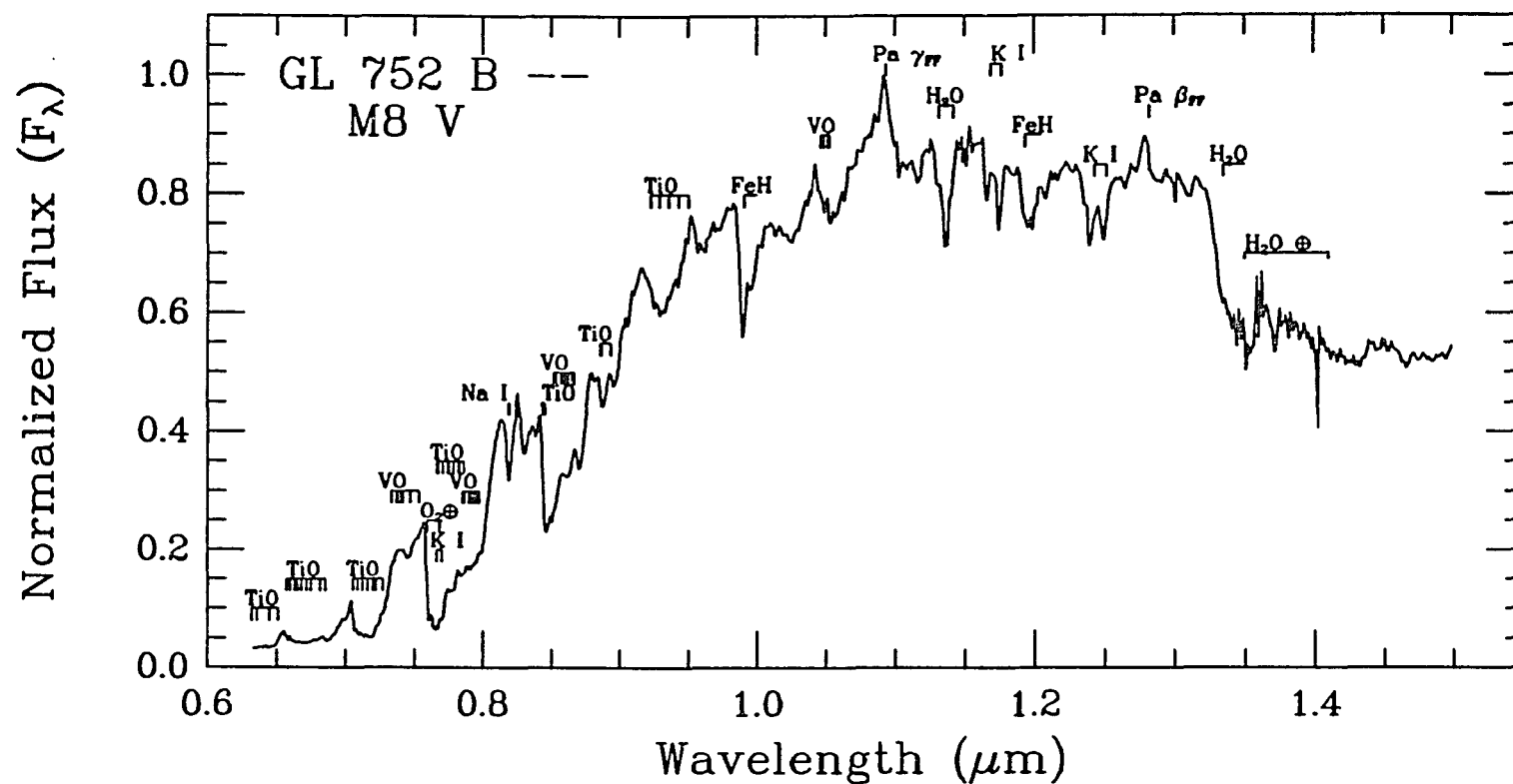


FIG. 3.12. (continued) — (b) The spectrum of GL 752 B (VB 10) – spectral type M8 V. Bands of VO, OH, FeH, and H₂O all serve well as temperature indicators. In both spectra, the subscript “FF” refers to residual Paschen lines, an artifact of flatfielding with F and G stars.

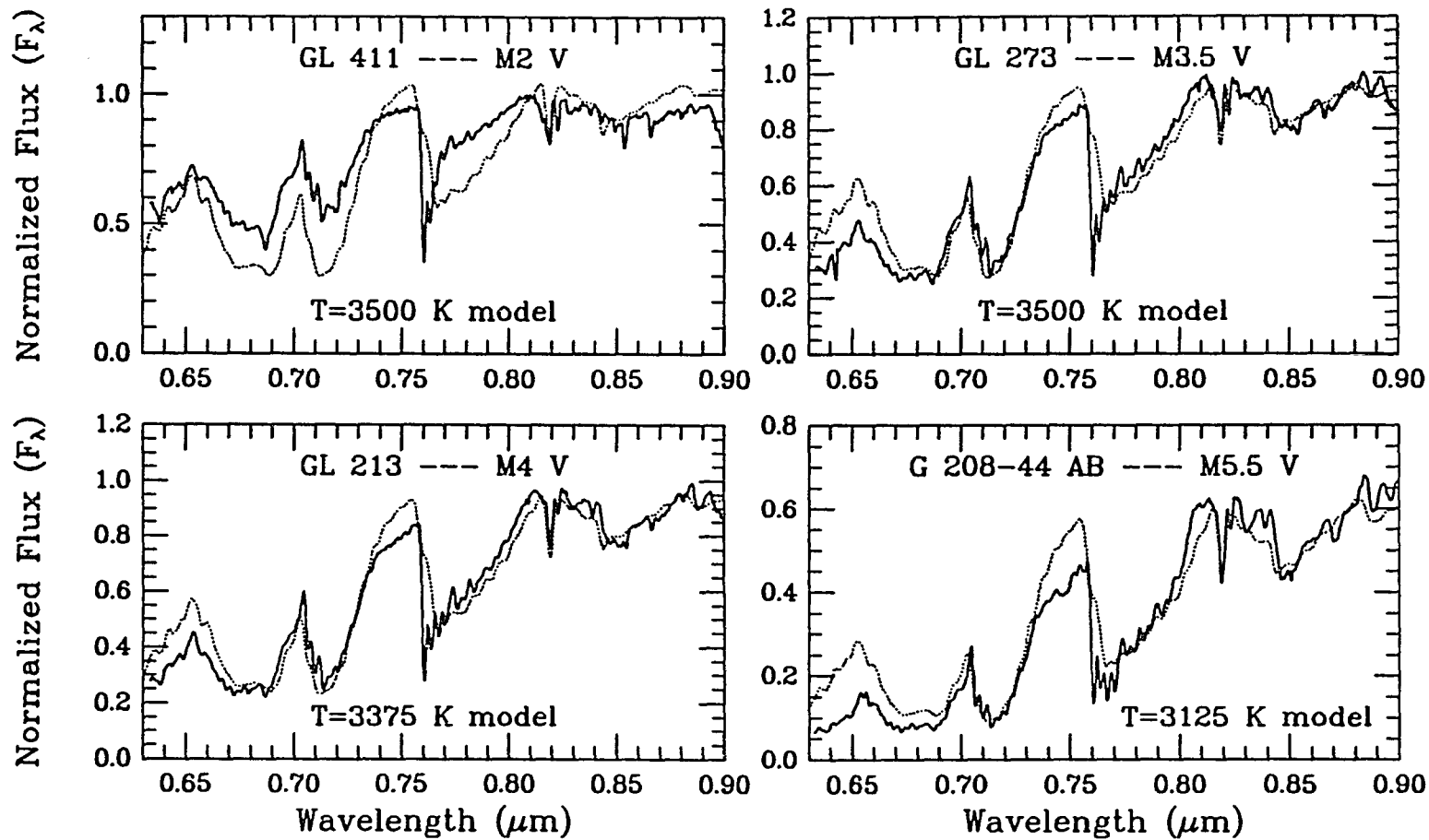


FIG. 3.13. — The best fits to the red spectra. The observational data are shown by the solid lines, and the model data by the dotted lines. The method for determining the best match is explained in the text. The spectrum of GL 411 could be better fit by a warmer model, but the Allard models →

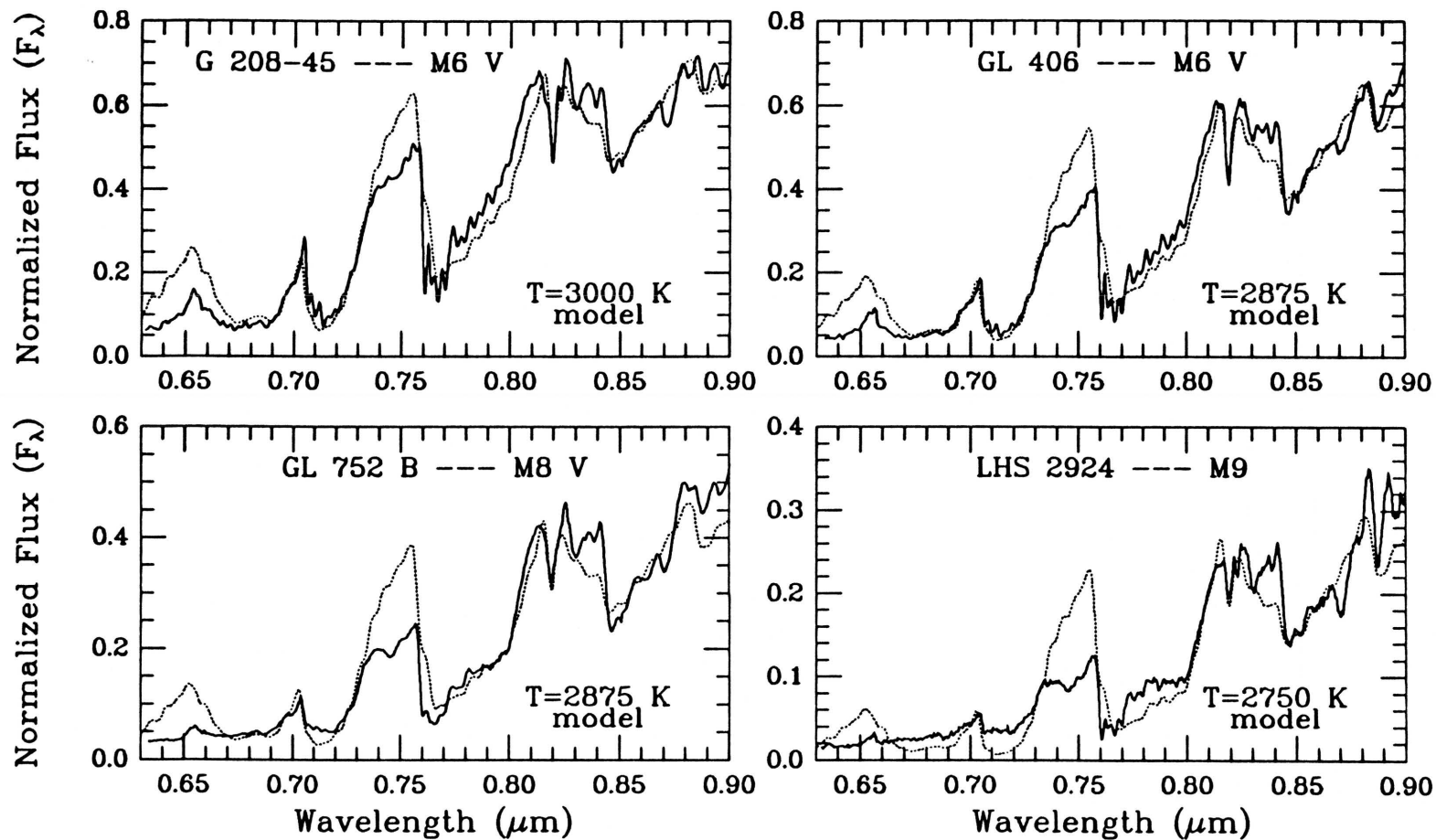


FIG. 3.13. (continued) — do not go hotter than 3500 K. The agreement is generally very good, although the flux near 0.65 and $0.75\text{ }\mu\text{m}$ is always overestimated. For cooler objects the disagreement between the true spectra and the predicted ones is much more pronounced.

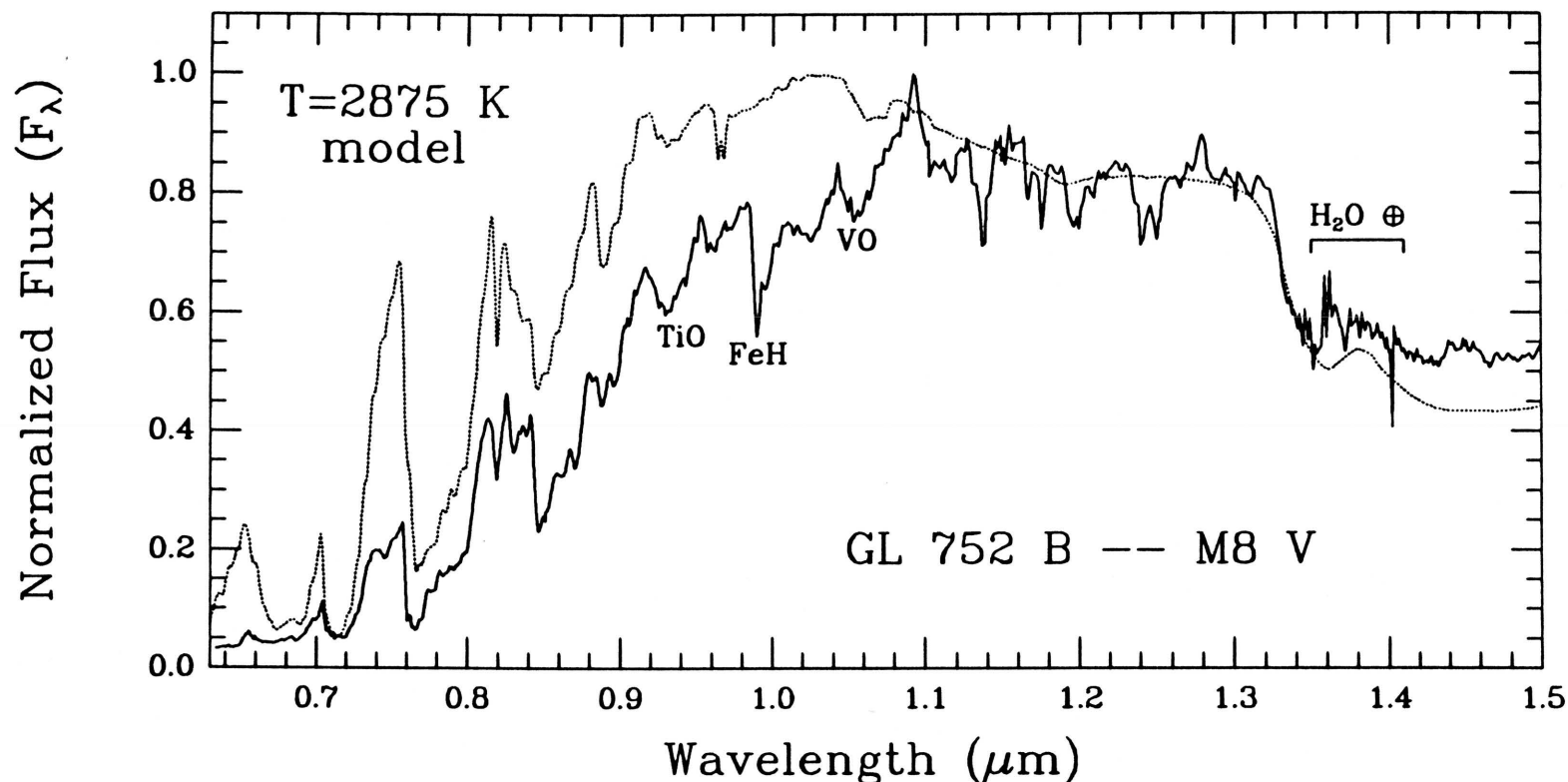


FIG. 3.14. — The spectrum of an M8 dwarf and the model that provides the best fit in the red. Unlike Figure 3.13, each spectrum here is normalized to unity at its peak flux. Note the failure of the model to predict the shape of the stellar “continuum” in the region from 0.9 - 1.1 μm . Notably absent from the models are FeH at 0.99 μm and VO at 1.3 μm . The strength of the TiO band at 0.93 μm is also underestimated. Coincidentally, the least-squares minimization technique finds the 1.08 - 1.35 μm fit plotted here to be the best, correctly normalized fit to the *J* region. This illustrates another point: although the fit at *J* looks adequate, the same model would have to be shifted downward in the 0.70 - 0.90 μm region to achieve a good fit. In other words, *I* - *J* colors for the observational and theoretical spectra do not agree. See text for more details.

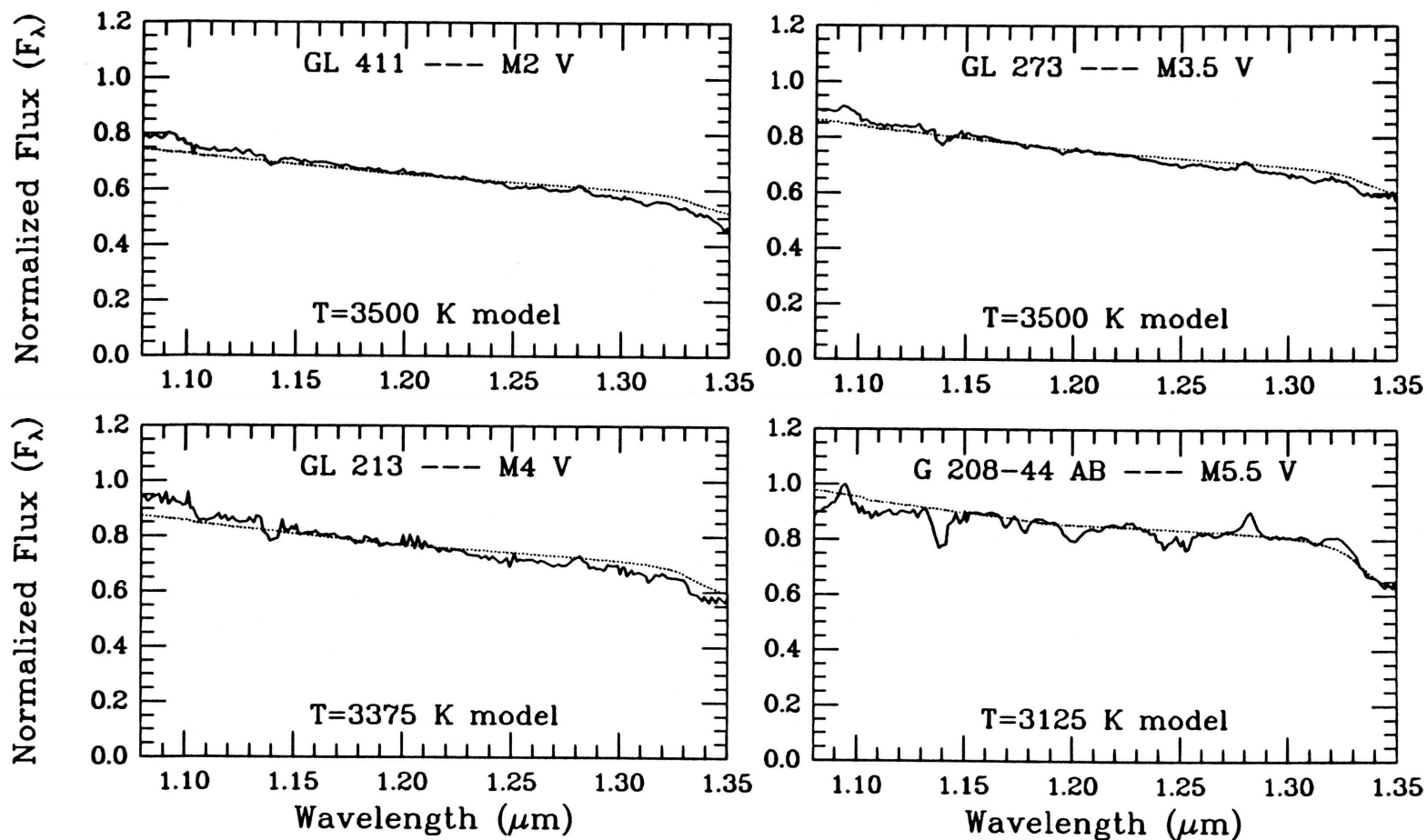


FIG. 3.15. — The best fits to the infrared spectra. The observational data are shown by the solid lines, and the model data by the dotted lines. The method for determining the best match is explained in the text. As in Figure 3.13, →

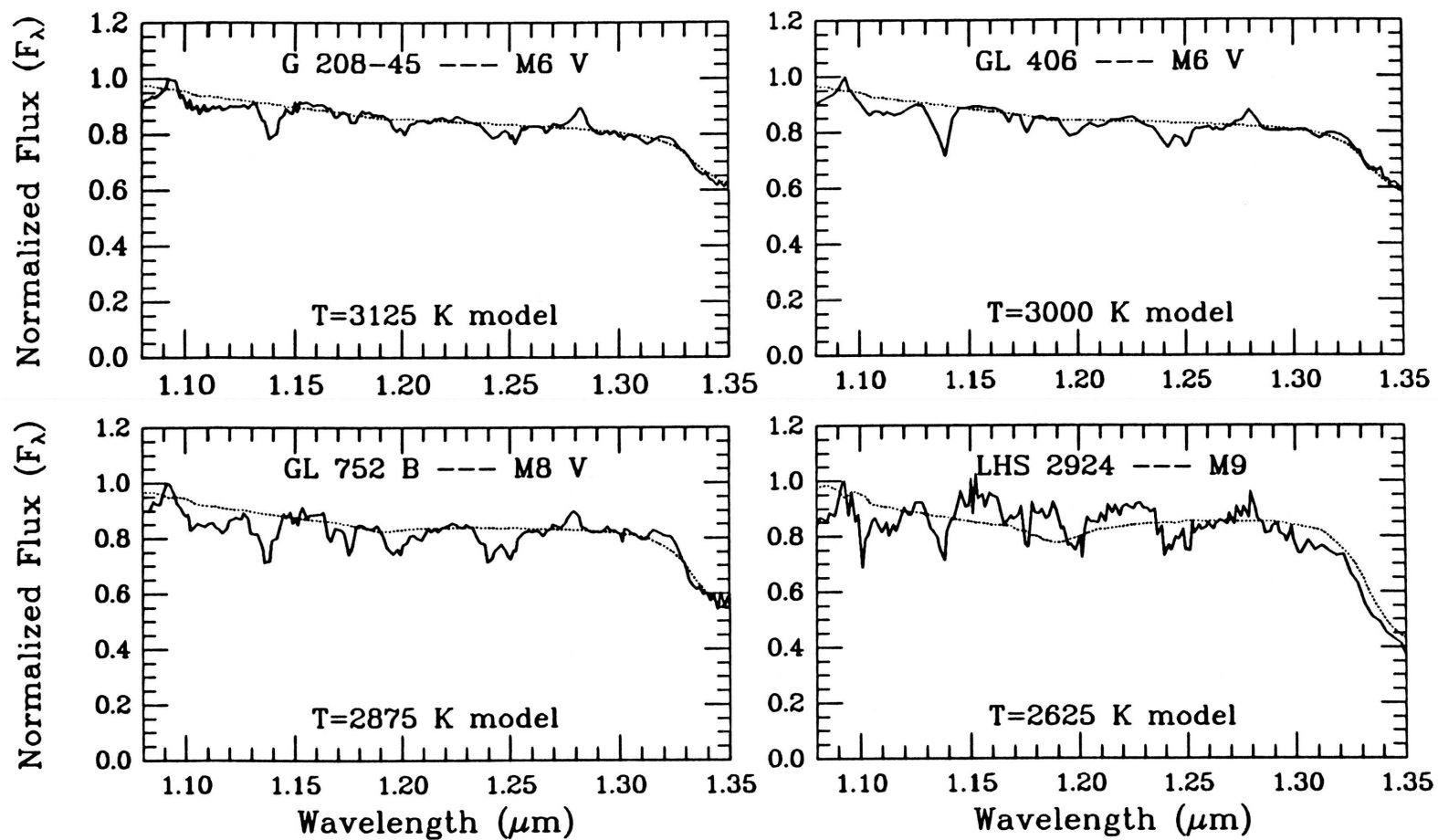


FIG. 3.15. (continued) — the spectrum of GL 411 could be better fit by a warmer model. In general, the steam feature at $1.35 \mu\text{m}$ and the pseudo-continuum are fit well.

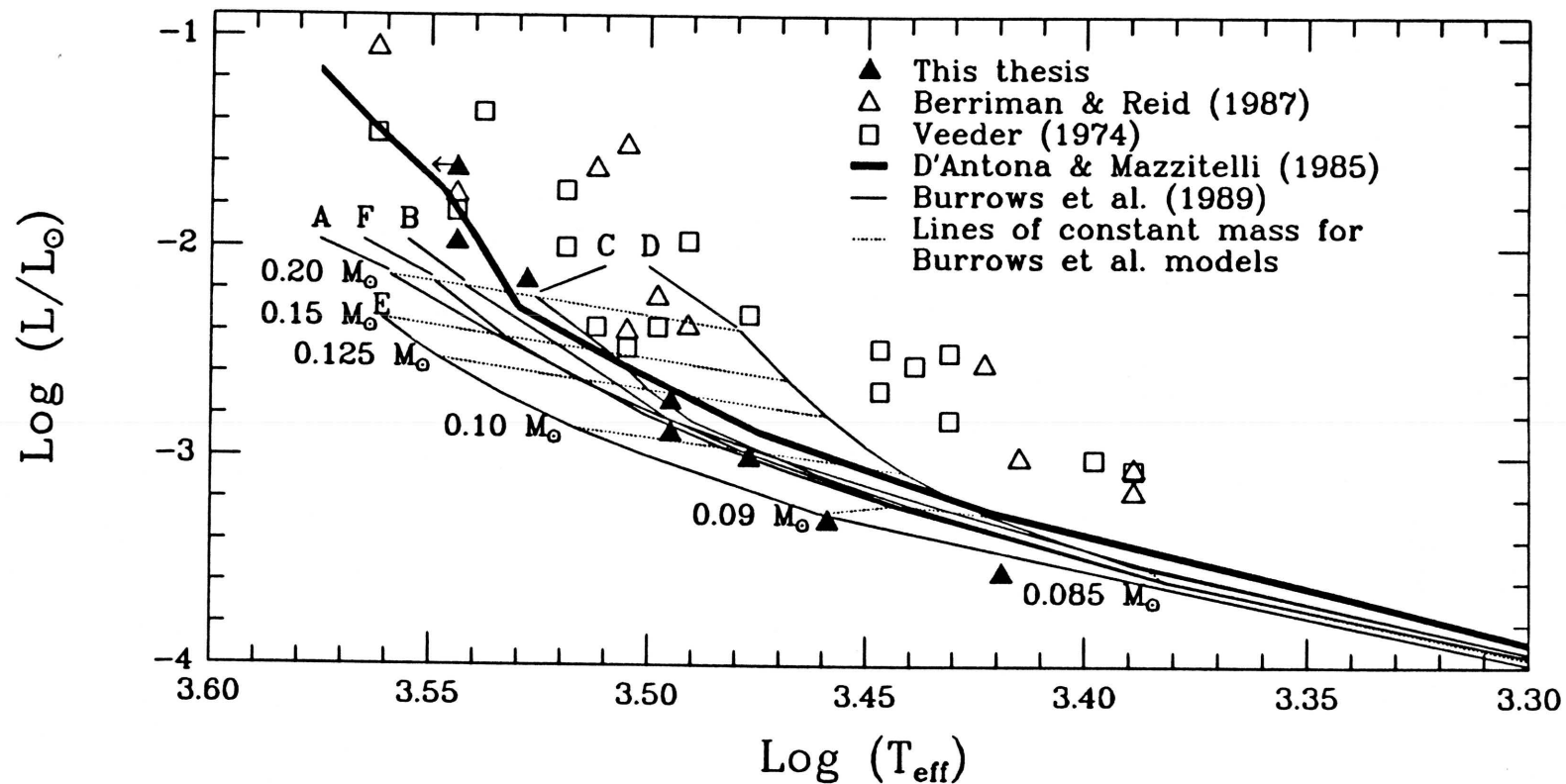


FIG. 3.16. — The H-R Diagram for M dwarfs. Data from this paper are represented by filled triangles, data from Berriman & Reid (1987) by open triangles, and data from Veeder (1974) by open squares. (The data point for GL 411 is indicated with an arrow since our derived temperature is a lower limit.) (a) The theoretical main sequence of D'Antona & Mazzitelli (1985 — heavy line) and the 10 Gyr tracks of models A, B, C, D, E, and F from Burrows, Hubbard, & Lunine (1989 — lighter lines) overplotted with the three temperature sequences. Lines of constant mass (dashes) are indicated on the Burrows et al. models. →

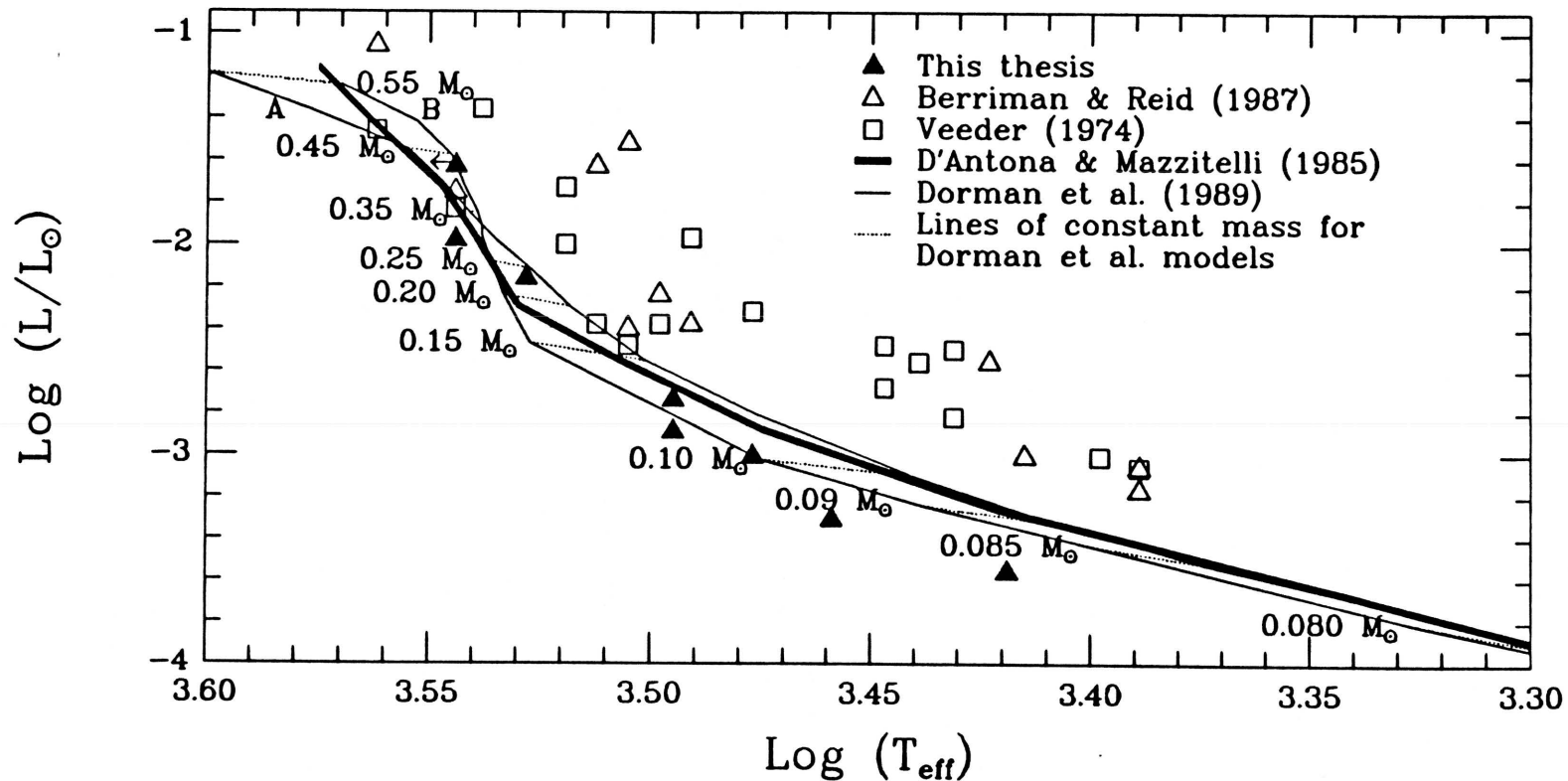


FIG. 3.16. (continued) — (b) The theoretical main-sequence tracks A and B of Dorman, Nelson, & Chau (1989 — lighter lines), with the track of D'Antona & Mazzitelli (1985 — heavy line) and the three temperature sequences shown again for comparison. Lines of constant mass (dashes) are also indicated on the Dorman et al. models. As both figures show, the temperature sequence presented here brings the observed M dwarf track into closer agreement with theoretical tracks. Note that the Burrows et al. and the Dorman et al. models (and also the Burrows et al. models for an age of 1 Gyr) predict all of the objects presented here, even LHS 2924 (M9), to be stellar since they lie within the locus of hydrogen-burning stars ($M \geq 0.08M_{\odot}$).

3.3: THE UNIQUE SPECTRUM OF GD 165 B — A BROWN DWARF?

After it was first reported that $\sim 30 - 60\%$ of the mass in the solar neighborhood was unaccounted for (Oort 1960; Bahcall 1985), some astronomers proposed that the presence of many faint, previously undetected M dwarfs might explain the discrepancy. If not, there might be a sufficient, additional number of brown dwarfs, first theorized by Kumar (1963), to comprise the remainder of the missing mass. Oddly, until the early 1980's, GL 752 B (VB 10) was still recognized as the lowest-luminosity star, having held that title since its discovery almost 40 years earlier (van Biesbroeck 1944). Three objects discovered during the course of Luyten's survey (see Luyten 1979), however, would later be recognized as objects of even later spectral type: LHS 2924 (Probst & Liebert 1983), LHS 2397a (Liebert, Boroson, & Giampapa 1984), and LHS 2065 (see Reid 1987; Bessell 1991).

Despite new claims that there is far less (or zero) missing mass than previously thought (Kuijken & Gilmore 1989; see alternate viewpoint in Bahcall, Flynn, & Gould 1992), various surveys implementing new techniques and technologies, especially at infrared wavelengths, have begun in the last decade to search for even fainter and redder objects. During a photometric search for low-luminosity objects orbiting white dwarfs, Becklin & Zuckerman (1988; hereafter, BZ) discovered excess infrared radiation from the DA4 (McCook & Sion 1987) white dwarf GD 165. Follow-up infrared imaging verified the presence of a faint companion, designated as GD 165 B, approximately 4 arcseconds distant. At the time of its discovery, there was some question as to whether or not the object were merely a background source falling along nearly the same line of sight as the white dwarf. Fortunately, the large proper motion of GD 165 A (0.25 arcsecond

yr^{-1} — Luyten 1961) has in just a few years lead to the confirmation of the two objects as a common proper motion pair (Zuckerman & Becklin 1992; hereafter, ZB). Because of its extremely red colors and low luminosity, GD 165 B is now generally regarded as the best brown dwarf candidate.

At present, a direct measurement of the mass is the only criterion which can distinguish between a brown dwarf and a star. Unfortunately, the 4-arcsecond separation of the components implies an orbital period on the order of 1600 years, so it will not soon be possible to calculate component B's dynamical mass. However, there may be other, more easily observable parameters which in principle could differentiate between stars and brown dwarfs, specifically red/near-infrared spectra, which have been obtained for many low-luminosity objects. In the case of the GD 165 system, the 4-arcsecond separation is, in another respect, advantageous: a spectrum of the secondary, uncontaminated by the light of the primary, can be acquired and can be compared to the spectra of other very red objects.

Table 3.17 lists all of those known dwarfs which have later spectral types than GL 65 A and B — the reddest dwarfs for which spectra have been acquired *and* for which dynamical masses have been determined (see Table 3.10 and Figure 3.10). GL 65 A and B, also known as L 726-8 and UV Ceti, respectively, have approximately equal masses of $0.095M_{\odot}$, tantalizingly close to the upper mass limit, $\sim 0.08M_{\odot}$, for brown dwarfs. (The purported substellar masses for Wolf 424 A and B have been discussed by Henry et al. 1992 and Davidge & Boeshaar 1991. It now appears that the components are most likely stellar.) All dwarfs redder than GL 65 A and B (1) are single, where a dynamical mass is impossible to determine, (2) are in binary or multiple systems with orbital periods of several hundreds to many thousands of years, or (3) have had masses determined from

the technique of infrared speckle imaging — masses which, when the errors are considered, could put them on either side of the M dwarf/brown dwarf dividing line. Several objects in this third class are known, but they are too close to their primaries to yield uncontaminated spectra. These are listed in Table 3.18. Tables 3.17 and 3.18 thus represent the most complete compilation of low-luminosity objects currently known.

This thesis presents spectra of many of the objects in Table 3.17. Since it is not known if the spectrum of a brown dwarf should be fundamentally different from that of a late-M star, it is conceivable that spectra of hot brown dwarfs already exist in the literature and have been labelled as M-star spectra. On the other hand, it is possible that differences exist which would distinguish between them; i.e., a brown dwarf at the same temperature as a low-mass star should differ in τ , $\log g$, and possibly Z — any of which will produce changes in the spectra. To address this issue, a spectrum was obtained of GD 165 B — the coolest, reddest entry in Table 3.17 and thus the most likely object to be a bona fide brown dwarf. The spectroscopic observations and the reduction of the data are detailed in §3.3.1. The spectrum of GD 165 B is compared to the spectra of other low-luminosity objects in §3.3.2. Possible interpretations of the data are discussed in §3.3.3, and conclusions are given in §3.3.4.

3.3.1: Observation and Data Reduction

The spectrum of GD 165 B was obtained on UT 1991 May 07 with the Red Channel Spectrograph of the Multiple Mirror Telescope (MMT — effective aperture 4.5 meters). The observing setup is the same as that described in §3.1.2.

Since the object is invisible on the MMT TV acquisition screen, the slit was first centered on the position of GD 165 A, and then the offsets given in BZ were used to move the slit to the position of GD 165 B. The revised values of the offsets given in ZB only differ from the previous values by 0.6 arcsecond in declination. Since the width of the slit employed was 2 arcseconds, this revision did not effect our ability to position the unseen secondary on the slit correctly.

All observations were obtained when the object was near the meridian, so differential refraction effects were negligible. As a result we were free to adjust the position of the slit on the sky to place the much brighter A component as far away from the slit as possible, while still allowing enough displacement along the direction of the slit to separate the spectrum of its spillover light cleanly from the spectrum of B on the CCD. For each exposure, the spectra were displaced on the CCD by 3.2 arcseconds, and component A was ~ 1 arcsecond away from the edge of the slit. In all, a sequence of three 40-minute integrations was made. Afterwards, GD 165 A was placed in the slit and a 5-minute integration was taken.

Because of excellent seeing and guiding, the 3.2-arcsecond displacement of spectra on the chip was sufficient to eliminate almost all spillover light from the white dwarf into the spectrum of GD 165 B. The spectra were reduced via the same procedures as those outlined in §3.1.2, except that special care was taken to trace and define the extraction apertures so that this contaminant light was minimized. Only at short wavelengths, where the flux from the white dwarf is highest, is contamination of the GD 165 B spectrum evident, and even here its effects are small. The 120-minute spectrum of GD 165 B and the 5-minute spectrum of GD 165 A are presented in Figure 3.17.

Because of excellent weather conditions on the night of observation, it is possible to extract I_C magnitudes from the spectra in Figure 3.17. Values for $(F_\lambda)_{I_C}$ were determined over a rectangular bandpass whose cut-on and cut-off wavelengths correspond to the wavelengths at half maximum of the I_C filter — 7250 and 8750 Å. These fluxes were then converted to magnitudes by using 2550 Jy as the zero-magnitude flux (Bessell 1979). For a more complete discussion of this procedure, see §3.2.2. The resulting magnitudes are found to be $I_C = 14.2$ and 20.7 for GD 165 A and B, respectively. The parallax of the system is 0.0278 ± 0.0034 arcsecond (ZB), which gives absolute magnitudes of $M_{I_C} = 11.4$ and 17.9 for GD 165 A and B, respectively.

A lower (brighter) limit for the R_C magnitude of GD 165 B can also be made if it is assumed that the mean flux level between 5700 Å (the filter cut-on) and 6350 Å is comparable to the flux level seen in our spectrum from 6350 Å to the filter cut-off at 7200 Å. As mentioned previously, nearly all of the flux seen in our spectrum from 6350 to 7200 Å is contaminant light from the primary, so the true flux of GD 165 B will be substantially less than what is found here. Using a zero-magnitude flux of 3080 Jy (Bessell 1979), it is found that the magnitude must be fainter than $R_C = 21.5$, corresponding to an absolute magnitude of $M_{R_C} > 18.7$. If this object is assumed to have an $R-I$ color comparable to the latest M dwarfs (Leggett 1992 gives $(R-I)_C = 2.4$ for vB 8), then this implies that the absolute magnitude of GD 165 B is $M_{R_C} \sim 20.3$. Photometric surveys like those of Reid & Gilmore (1982), Hawkins & Bessell (1988), Leggett & Hawkins (1988), and this thesis, which have relied mainly upon R and I measurements, would have detected objects like GD 165 B lying only within 9 pc for a limiting magnitude of $R \sim 20.0$ or within 6 pc for a limiting magnitude of $R \sim 19.0$. This illustrates

that objects like GD 165 B have not been missed because they are necessarily rare, but because they are exceedingly dim at these wavelengths.

3.3.2: Comparison to the Spectra of Other Low-Luminosity Objects

In Figure 3.18 are plotted the spectra of GD 165 B and three of the lowest luminosity, red objects known: PC 0025+0447, LHS 2065, and LHS 2924. Spectral features are identified for LHS 2924. Observation and reduction procedures for the spectra of LHS 2924 and LHS 2065 have been discussed elsewhere (§3.1.2). The spectrum of PC 0025+0447, an unusual object discovered by Schneider et al. (1991), was acquired on UT 1991 October 17 with the Red Channel Spectrograph at the MMT with the same setup described in §3.3.1 above. Like GD 165 B, this object was invisible on the MMT TV acquisition screen, but in this case the position given in the discovery paper quotes an error of 5 arcseconds. To improve our chances of finding this object, the slit was first centered on a nearby bright star, SAO 109220, then offsets were used to point to the position given in Schneider et al. (1991). A “quick” 5-minute integration on this position revealed no evidence on the CCD of an unseen object, so the slit was moved 2 arcseconds (the slit width) to the east, and another 5-minute integration taken. Again, no spectrum was seen. After several failed attempts to find the object to the west, a faint spectrum was finally revealed at a location 4 arcseconds east of the original position. Believing that the object was perhaps lying near the edge of the slit, the slit was moved another 1 arcsecond east. The spectrum recorded there was, in fact, brighter, so this position was retained for all subsequent exposures. In all, nine 20-minute integrations were made. The spectrum of PC 0025+0447

shown in Figure 3.18 is the addition of all three hours of integration.

PC 0025+0447 is unique in its own right. Based on the fact that its VO bands, most noticeably the one between 7851 and 7973 Å, are somewhat stronger than those of LHS 2924 and LHS 2065, we classify this object as an M9.5. Unlike LHS 2924, which has weak H α emission, and LHS 2065, which has H α emission similar in strength to other dMe's, PC 0025+0447 has an H α equivalent width ten times larger than any dwarf M star known (Schneider et al. 1991). Apart from the unusual emission feature, this object seems, nonetheless, to be a continuation of the spectral sequence to temperatures cooler than that of LHS 2924 and LHS 2065.

It is clear that the spectrum of GD 165 B, however, does not closely resemble the three other spectra in Figure 3.18 or, in fact, any of the spectra of low-mass stars presented in §3.1. (No statement can be made about the presence or absence of H α emission since no flux attributable to the B component is detected at this wavelength.) Notably absent are the TiO absorptions at 8432 Å and 8859 Å, which are quite strong for late M dwarfs. The close Na I doublet at 8183 and 8195 Å may be present, but this is an uncertain identification since there is also telluric water absorption between 8164 and 8177 Å. Absorptions by TiO may be marginally present at 8303 and 8510 Å, while the obvious absorption at 8624 Å may correspond to VO, although much stronger than the VO absorption seen in an M9 or M9.5. These features could, therefore, be caused by the same molecular species which dominate the spectra of late M dwarfs, only that the absorption profiles and strengths are different due to the lower temperature of this object. On the other hand, it is also possible that new sources of opacity not present in the spectrum of an M9 or an M9.5 are strongly affecting the spectrum

of GD 165 B from 8700 Å to our cutoff of 9000 Å. Before any of these features are adequately identified, a higher signal-to-noise spectrum at higher resolution is required.

Assuming that the object is a cooler version of LHS 2924, the extreme redness and unique appearance of its spectrum would suggest a classification later than M10, since we have classified PC 0025+0447 as an M9.5. Since there are few spectral features on which to base a true spectral classification and currently no other spectra to bridge the gap between the M9/M9.5 objects and GD 165 B, we are forced to delay classification until other such objects are discovered. Only when the spectral type can be *quantified* should a type be assigned.

3.3.3: Discussion

Table 3.19 gives observed colors and absolute magnitudes for GD 165 B and a sequence of M dwarfs. (BZ give $J = 15.75$ for GD 165 B, but this and the other J values in their table are on the CIT system, not the IRTF system (Zuckerman 1992). All infrared photometry listed in Table 3.19 has been transformed to the AAO system using the equations given in Leggett (1992).) These data clearly show that GD 165 B has extremely red colors and extremely low luminosity, indicative of a very cool temperature. Also given for the first eight objects in Table 3.19 are the temperatures determined in §3.2. The models do not currently predict a spectrum like that of Figure 3.17(b), but some idea of the temperature of this object can be estimated by extrapolating the trends of M_I and M_J with temperature to the absolute magnitudes calculated for GD 165 B. These extrapolations are shown in Figure 3.19. A linear least-squares fit is shown

for each graph, where the lower limit to the temperature for GL 411 has been ignored. The trend of M_I vs. temperature suggests $T \approx 2250$ K for GD 165 B, whereas the trend of M_J vs. temperature suggests $T \approx 2350$ K. As a result, the rounded value of $T = 2300 \pm 100$ K will be adopted as the temperature estimate of GD 165 B based on these fits. ZB derive an estimate of the temperature based on blackbody fits to the observed colors with additional allowance for the H_2O blanketing seen in the spectrum taken by Tokunaga et al. (1990 — the spectrum itself is unpublished). Their result is $T = 1800 \pm 200$ K, cooler by 500 K than the temperature derived here. This discrepancy is not unexpected, however. As noted in §3.2, when compared to temperatures derived from fits to the models, temperatures based on various blackbody fitting techniques, though in good agreement for early M dwarfs, are lower by up to 500 K for late M dwarfs such as GL 752 B (vB 10).

For some range of temperatures, the spectra of cool objects should begin to bridge the gap between the observed spectra of late M dwarfs (dominated in the red and infrared by molecules such as VO, TiO, H_2O , and CO) and the observed spectra of Jupiter and Saturn (which are dominated in this region by molecules such as CH_4 and NH_3). This transition is apparently not a simple one. Absorption by TiO cannot be distinguished in the spectrum of GD 165 B, although VO may still be present. Absorptions by CH_4 , which appear prominently in the spectra of Jupiter and Saturn, would be present in a broad band extending from 7600 to 8200 Å (Wolstencroft & Smith 1979), in another band extending from 8500 to 8750 Å with a minimum at ~ 8600 Å, and in another, more prominent band with a sharp cut-on near 8800 Å, a gradual cut-off near 9100 Å, and two minima at ~ 8825 and 8873 Å (Owen 1969). (For full coverage of this region, refer to

the laboratory spectra of methane in Dick & Fink (1977) and the observational spectra of Jupiter in Taylor (1965).) Although these wavelengths correspond to the same general regions where absorption occurs in the spectrum of GD 165 B, the shape of the bands and the locations of the minima do not match, indicating that methane is not the absorber. Moreover, as Lunine, Hubbard, & Marley (1986) state, the dominant carbon species should switch from CO to CH₄ only at temperatures around 1000 K — much cooler than that found for GD 165 B. Absorption by ammonia, though weaker than methane, is also found between 7500 and 9000 Å but is expected only at even lower temperatures. In other words, the molecules found in M dwarf spectra may no longer be prominent, and the molecules found in planetary spectra do not appear at temperatures as warm as GD 165 B. The features found in our spectrum are likely to be new, presently unidentified molecular absorptions.

Until a broader wavelength coverage is obtained for spectra in the infrared, the bolometric luminosity of this object will be difficult to estimate. Greenstein's (1990) best estimate, when updated to reflect the currently accepted distance of 36 parsecs, is $1.2 \times 10^{-4} L_{\odot}$, in excellent agreement with the estimate of $1 \times 10^{-4} L_{\odot}$ by ZB, who quote an uncertainty of $\sim 40\%$. Figure 3.20 shows the H-R Diagram for M dwarfs using data from §3.2. Also shown are the theoretical zero-age main sequence of D'Antona & Mazzitelli (1985) and the sequences, based on two different equations of state, of Dorman, Nelson, & Chau (1989). Two positions for GD 165 B are given in Figure 3.20. The first uses the temperature derived here and the second uses the temperature estimated in ZB; for both, the luminosity estimate of $1 \times 10^{-4} L_{\odot}$ is adopted. Both points fall near the region occupied, according to theory, by stellar objects marking the end of the

main sequence; however, considering the errors in the plotted quantities, both points are near enough to the stellar/substellar dividing line ($\sim 0.08 M_{\odot}$) to leave the true nature of GD 165 B ambiguous.

3.3.4: Summary

It has been shown that the 6300 - 9000 Å spectrum of GD 165 B is unlike that of any known M dwarf. Bands of VO, which appear only in the latest M dwarfs, may be present, though significantly stronger. The estimated temperature is low enough that new molecular absorptions, not found in warmer spectra like that of LHS 2924, may be appearing. The temperature is not cool enough, however, for this spectrum to begin to resemble the observed spectra of the Jovian planets. At present, the precise location of GD 165 B on the H-R Diagram is not known, due to large uncertainties in calculating both the temperature and the bolometric luminosity. The temperature will only be accurately known once theoretical energy distributions are able to reproduce spectra such as this one. This requires accurate identifications of possibly new molecular absorption species. Furthermore, the bolometric luminosity can only be determined once the spectrum is obtained at longer wavelengths, where the object emits most of its radiation. Both problems can be addressed by acquiring high quality spectra of GD 165 B throughout the infrared.

TABLE 3.17
THE COOLEST “DWARF” SPECTRA

Object Name	Spectral Type ^a	Ref.	Note
H 2118-4342	—	1	Single?
LHS 207	M6.5:	2	Single?
LHS 1317	M6.5:	2	Single?
LHS 523	M6.5	3,4	Single?
G 51-15 (LHS 248)	M6.5	3,4	Single? ^b
LHS 191	M6.5	3,4	Single?
LHS 292	M6.5	4	Single? ^c
GL 316.1 (LHS 2034)	M6.5	2	Single?
LHS 3332	M6.5	2	Single?
CTI 015607.7+280241	M6.5	4	Single?
CTI 092539.9+280018	M6.5	4	Single?
CTI 153915.6+280446	M6.5	4	Single?
CTI 174729.0+280322	M6.5	4	Single?
LHS 2351	—	5	Single?
LHS 2876	—	5	Single?
LHS 2930	M6.5	4,5	Single?
LHS 2980	M6.5	4	Single?
LHS 3003	—	5	Single?
LHS 5142	M6.5	4	Single?
GRH 2208-2007	—	6	Single?
VB 8 (LHS 429)	M7	3,4	Member of quadruple+ system ^d , P ~100000?? yr
LHS 3002	M7	5	Single?
LHS 2632	M7	4	Single?
LHS 2645	M7	4	Single?
ESO 207-61	—	7	Single?
HB 2124-4228	—	8	Single?
HB 2115-4518	—	8	Single?
BRI 0021-0214	—	9	Single?
CTI 115638.5+280002	M7	4	Single?

TABLE 3.17 (continued)

Object Name	Spectral Type ^a	Ref.	Note
VB 10 (LHS 474)	M8	3,4	Member of double system ^c , P ~20000? yr
LHS 2397a	M8	4	Single?
RG 0050-2722	M8	4,10	Single?
LHS 2243	M8	4	Single?
LH 0418+1339	—	11	Single?
GL 569 B	M8.5	4,12	Member of double system, P ~500 yr
CTI 012657.5+280202	M8.5	4	Single?
LHS 2065	M9	3,4	Single?
LHS 2924	M9	3,4	Single?
PC 0025+0447	M9.5	4,13	Single?
GD 165 B	<i>very late</i>	4	Member of double system, P ~1600 yr

^a Given on an extension of the Boeshaar 1976 system, as reported in Kirkpatrick, Henry, & McCarthy 1991 and this thesis.

^b No companions detected to $M_K = 11.3$ at separations of 1 to 10 AU via infrared speckle imaging (Henry 1991).

^c No companions detected to $M_K = 11.1$ at separations of 2 to 10 AU via infrared speckle imaging (Henry 1991).

^d This is the fourth, widely separated component (GL 644 C) in the system with GL 643 and GL 644 AB. No companions detected to $M_K = 11.8$ at separations of 2 to 10 AU via infrared speckle imaging (Henry 1991).

^e This is the low-luminosity, widely separated secondary of the GL 752 AB system. No companions detected to $M_K = 12.1$ at separations of 5 to 10 AU via infrared speckle imaging (Henry 1991).

REFERENCES TO SPECTRA IN THE LITERATURE. — (1) Hawkins 1986; (2) Boeshaar 1992; (3) Kirkpatrick, Henry, & McCarthy 1991; (4) This thesis; (5) Bessell 1991; (6) Gilmore, Reid, & Hewett 1985; (7) Ruiz, Takamiya, & Roth 1991; (8) Hawkins & Bessell 1988; (9) Irwin, McMahon, & Reid 1991; (10) Reid & Gilmore 1981; (11) Leggett & Hawkins 1989; (12) Henry & Kirkpatrick 1990; (13) Schneider et al. 1991.

TABLE 3.18
LOW-MASS COMPANIONS FOR WHICH SPECTRA DO NOT EXIST

Name	Mass (M_{\odot})	Note	Ref.
GL 623 B (LHS 417 B)	0.115 ± 0.040^a , 0.078 ± 0.008	P = 3.73 yr	1 2
Ross 614 B (GL 234 B)	0.080 ± 0.025	P = 16.60 yr	1
G 208-44 B (GJ 1245 C)	0.075 ± 0.015	P = 15.22 yr	1
LHS 1047 B (GJ 1005 B)	0.060 ., 0.055 ± 0.032	P = 4.63 yr	1 3
G 29-38 B	unknown	Dust?	4,5,6,7,8

^a Derived using speckle and astrometric data.

MASS REFERENCE. — (1) Henry & McCarthy 1992; (2) Marcy & Moore 1989; (3) Ianna, Rohde, & McCarthy 1988; (4) Zuckerman & Becklin 1987; (5) Greenstein 1988; (6) Tokunaga, Becklin, & Zuckerman 1990; (7) Graham et al. 1990; (8) Barnbaum, Misch, & Zuckerman 1992.

TABLE 3.19
COLORS, ABSOLUTE MAGNITUDES, AND TEMPERATURES FOR A SEQUENCE OF M DWARFS^a

Name	Sp.Type	$I - J$	$J - H$	$J - K$	M_I	M_J	Temp (K)
GL 411	M2 V	1.13	0.54	0.75	8.32	7.10	> 3500
GL 273	M3.5 V	1.40	0.52	0.77	9.33	7.83	3500
GL 213	M4 V	1.47	0.53	0.78	9.86	8.30	3375
G 208-44 AB ^b	M5.5 V	2.19	0.52	0.89	11.59	9.40	3125
G 208-45	M6 V	2.15	0.50	0.89	12.10	9.95	3125
GL 406	M6 V	2.31	0.62	0.98	12.63	10.21	3000
GL 752 B	M8 V	2.74	0.67	1.11	13.98	11.11	2875
LHS 2924	M9	3.38	0.65	1.12	15.09	11.57	2625
GD 165 B	<i>very late</i>	4.8	1.09	1.84	17.9	13.2	see text

^a For data on the first eight objects refer to §3.2; see text for data on GD 165 B. I magnitudes are given on the Kron-Cousins system; J , H , and K magnitudes have been transformed to the AAO system. (The J magnitudes listed in Table 1 of Becklin & Zuckerman 1988 are on the CIT system, not the IRTF system, despite what is implied by their second footnote (Zuckerman 1992).)

^b Composite spectrum, colors, and magnitudes assumed to be dominated by the A component.

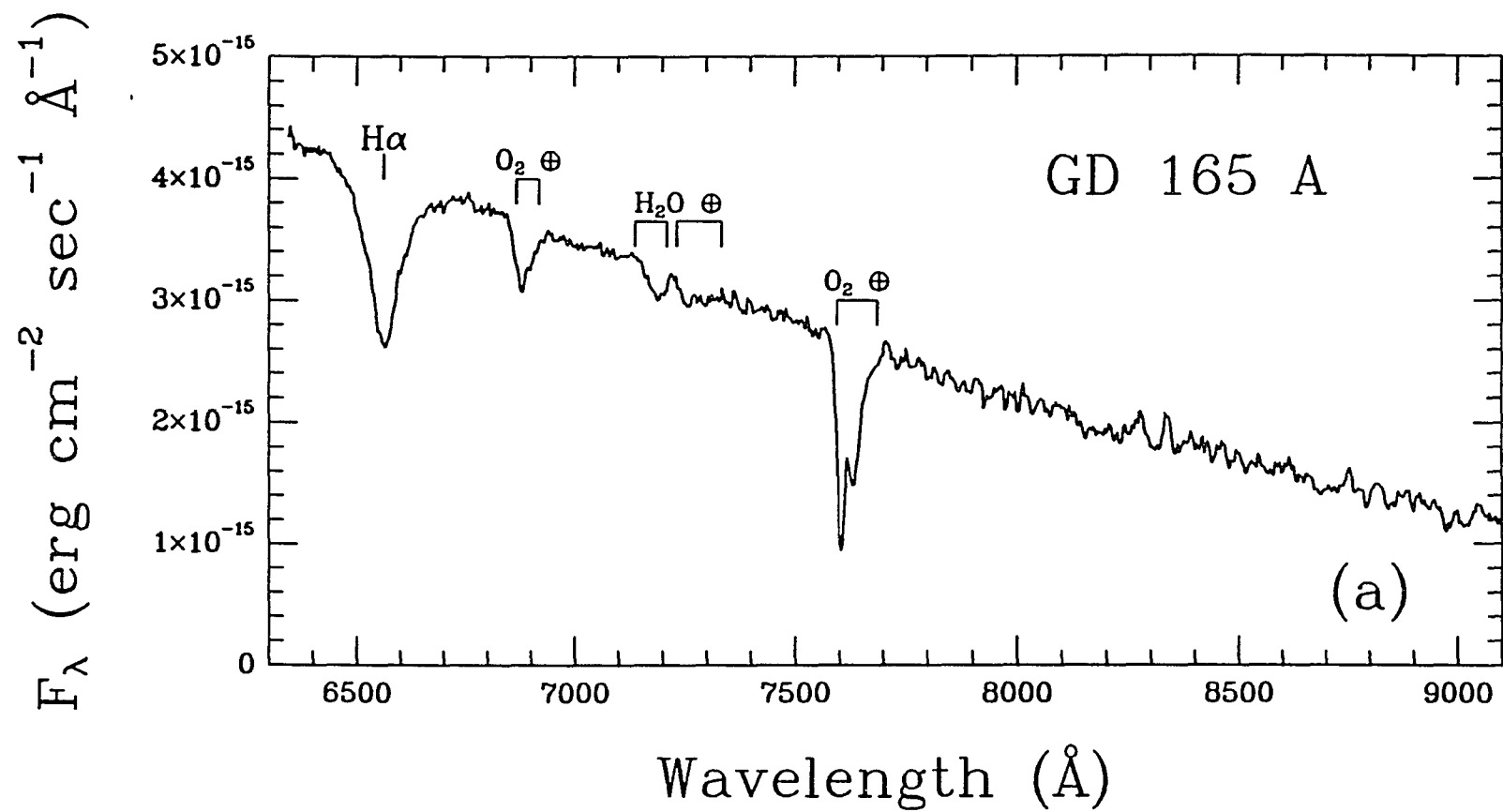


FIG. 3.17. — Spectra of the GD 165 system taken with the Red Channel Spectrograph of the Multiple Mirror Telescope. The resolution is 18 \AA . Telluric absorption features have not been removed. (a) The spectrum of the DA4 white dwarf GD 165 A. The broad $\text{H}\alpha$ absorption is labelled. →

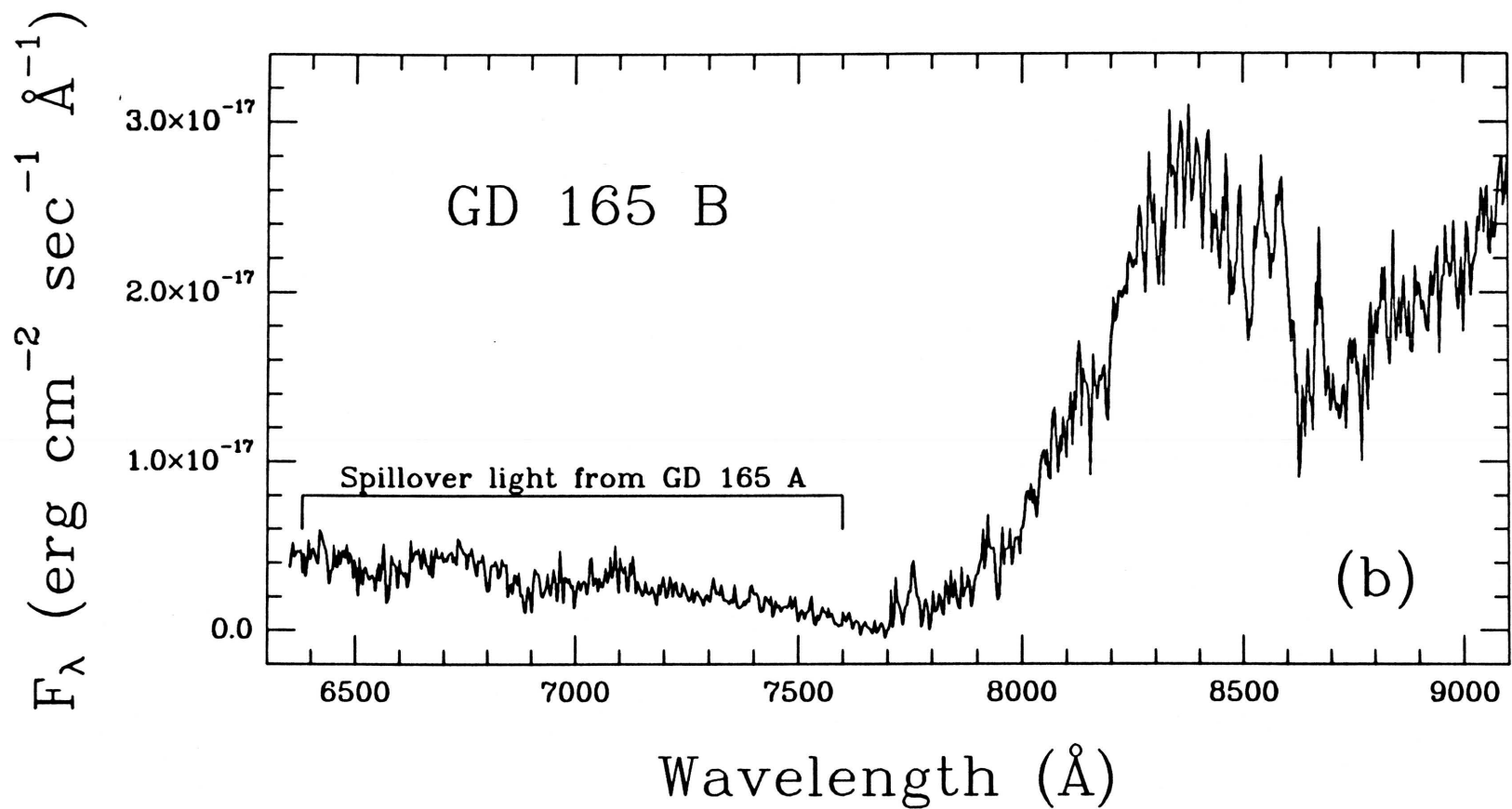


FIG. 3.17. (continued) — (b) The spectrum of the brown dwarf candidate GD 165 B. Spillover light from GD 165 A can be seen at the shortest wavelengths presented here. By 7500 \AA , this flux has dropped to almost zero, demonstrating that at longer wavelengths the spectrum of GD 165 B is uncontaminated by the light of the primary.

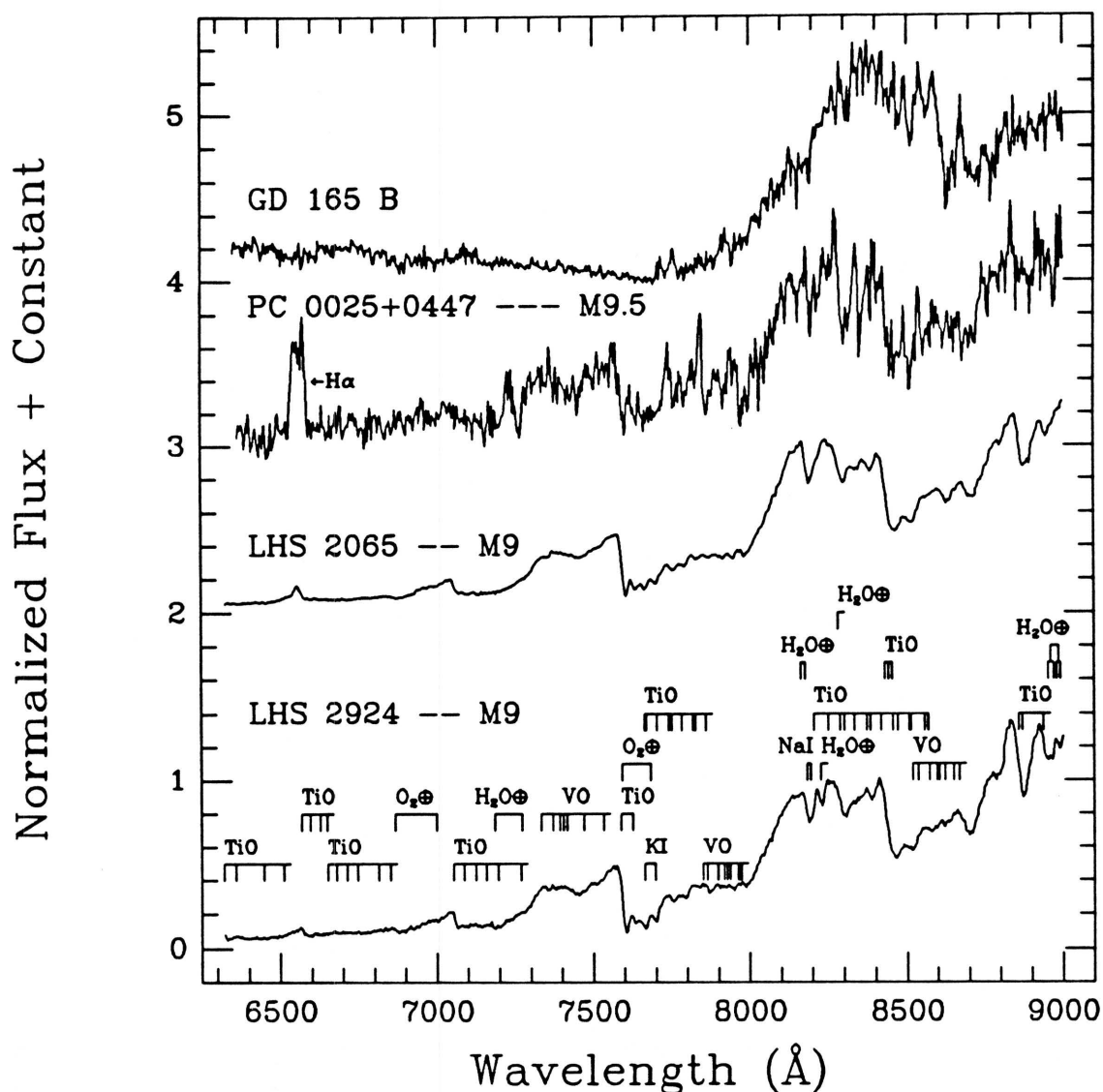


FIG. 3.18. — Spectra of the four latest “dwarfs” known. The spectra were taken at the Multiple Mirror Telescope and have a resolution of 18 Å. The flux (in units of F_{λ}) for each spectrum has been normalized to unity at 8250 Å (where there seems to be a common opacity minimum), and integral offsets have been added to separate the spectra vertically. Absorptions by telluric O₂ and H₂O have not been removed. Features listed in §3.1.3 are identified in the spectrum of LHS 2924. Note the continuation by PC 0025+0447 of the familiar M dwarf sequence to even cooler temperatures, as evidenced by increased absorption by VO. Also note the lack of similarity between the spectrum of GD 165 B and any of the other spectra presented here.

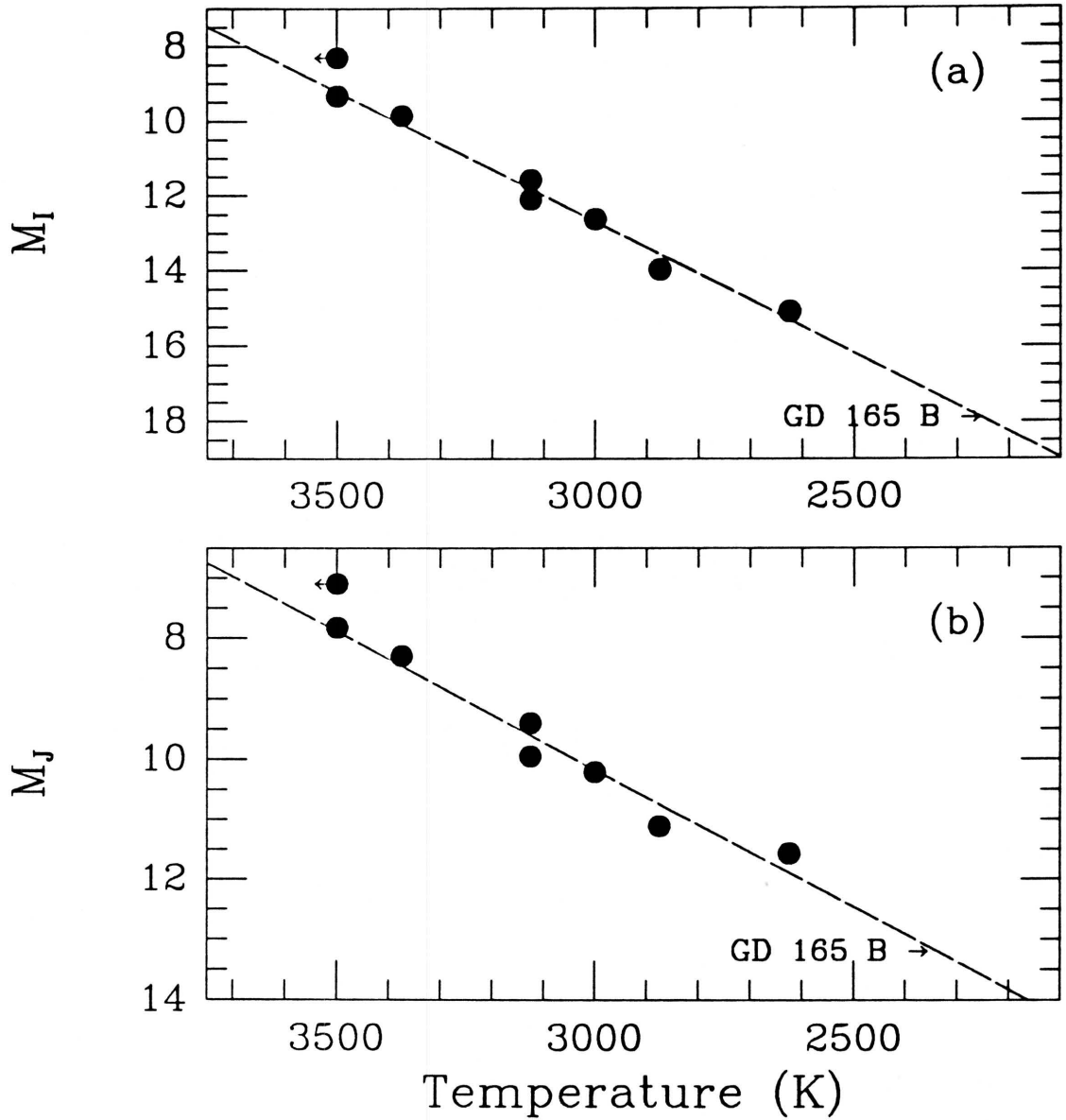


FIG. 3.19. — Absolute magnitude versus temperature for those dwarfs presented in Table 3.19. The dashed line represents a linear least-squares fit to the data, excluding the upper-limit point for GL 411. The absolute magnitude of GD 165 B is indicated with an arrow. (a) M_I vs. temperature. The extrapolation gives $T \approx 2250$ K for GD 165 B. (b) M_J vs. temperature. The extrapolation gives $T \approx 2350$ K for GD 165 B.

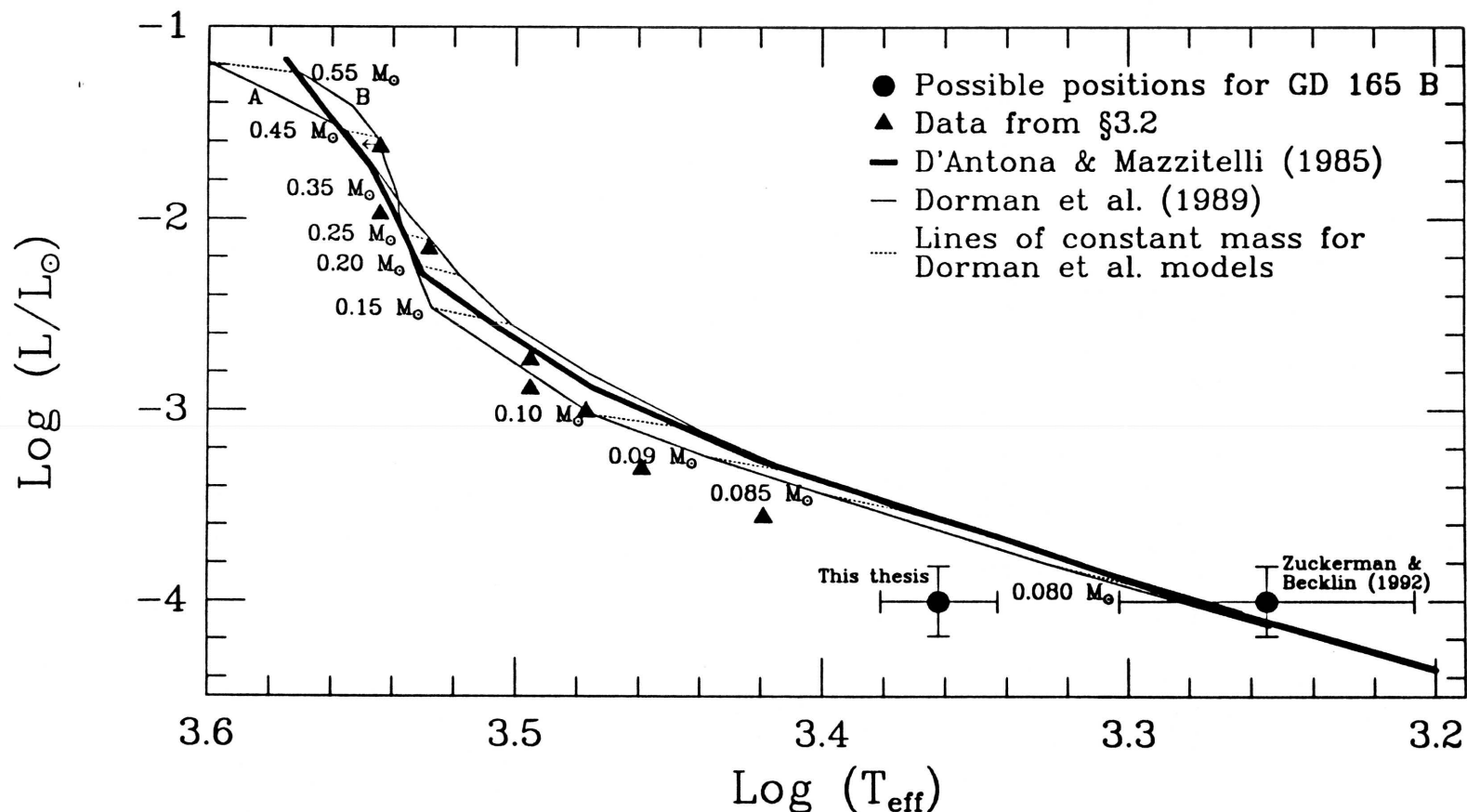


FIG. 3.20. — H-R Diagram for M dwarfs and GD 165 B. This figure is an adaptation of Figure 3.16. Indicated are the theoretical zero-age main sequences of DM (1985 — heavy line) and of DNC (1989, models A and B — lighter lines). Lines of constant mass are indicated by dashes on the DNC models. Triangles represent the first eight objects listed in Table 3.19, and the circles give two possible locations for GD 165 B. The circle at higher temperature uses the luminosity estimated in Greenstein (1990) and temperature derived from the fits in Figure 3.19. The circle at lower temperature uses data calculated in ZB. Both points place GD 165 B at the end of the main sequence at a mass of $\sim 0.08 M_{\odot}$, the dividing line between stars and brown dwarfs.

3.4: SPECTRA OF LOW-MASS COMPANIONS

The results of the last three sections have introduced several very interesting astrophysical questions: What are the masses of dwarfs which are typed as M7 and later? Do these masses fall in the stellar or substellar regime, or does the familiar M dwarf sequence, perhaps, correspond only to objects near the end of the main sequence, with brown dwarfs being characterized by qualitatively different spectra — like that of GD 165 B?

In an attempt to address these issues, high signal-to-noise spectra have been obtained of some of the composite systems in Table 3.18. Each of the composites consists of an M dwarf primary and an object whose dynamical mass places it near the brown dwarf limit of $0.08 M_{\odot}$. From data acquired through speckle imaging techniques, the percentage of flux attributable to each of the components is known. The spectral type of the primary star can also be deduced from the speckle data. Thus, the spectrum of the low-mass secondary can be “acquired” by subtracting (in the correct percentage from the composite) a spectrum of a single star having the same spectral type as the primary. The power of this technique lies with the facts that for each of the composite systems, (1) its status as a binary is well-established and (2) in a given bandpass the fraction of flux corresponding to the fainter secondary has been measured or can be estimated based on existing data.

The objects chosen for this analysis are listed in §3.4.1, where the acquisition and reduction of the spectroscopic data are also described. The composite systems are addressed individually in §3.4.2, and differential spectroscopy is performed on each. In §3.4.3 these results are discussed, and the conclusions are

given in §3.4.4.

3.4.1: Data Acquisition and Reduction

Five composite systems were targeted during this investigation: GL 234 AB, LHS 1047 AB, GL 22 AC, GJ 1081 AB, and G 250-29 AB. The composite spectra of these objects range in type from M2 V for GL 22 AC to M4.5 V for GL 234 AB, so spectra of single M dwarfs were obtained over the same range. In total, 6300-to-9000 Å spectra of two single stars at each half spectral subclass were obtained with the MMT Red Channel on 1991 November 13 using the same setup described in §3.1.2. These objects are listed in Table 3.20. Brighter objects were selected so that high signal-to-noise could be achieved, and as a result many short exposures were taken to avoid saturation effects on the CCD. The integration times listed in Table 3.20 are the sums of the short exposures. Individual spectral types are from §3.1. Because this set of spectra will be used to perform the differencing, it is essential that none of these objects is a binary itself; also included in the table are the references to the observations indicating that the stars are single. The data reduction techniques are identical to those outlined in §3.1.2.

Many short exposures were also taken of the composite systems, which are listed in Table 3.21. The slit width employed was 2 arcseconds — wide enough so that in all cases the spectrum acquired is a true composite of the two members in the system. The spectral types were taken from §3.1 for GL 22 AC, LHS 1047 AB, and GL 234 AB; for G 250-29 AB and GJ 1081 AB the types were assigned using the least-squares minimization technique. References to the duplicity of

each of these systems is given in the last column of Table 3.21. Each of these double systems is discussed in detail in the following section.

3.4.2: Differential Spectroscopy of the Composite Systems

a) GL 234 AB (Ross 614 AB)

The variable proper motion of this star was first recognized by Reuyl (1936), and the companion was confirmed photographically by Baade (Lippincott 1955). Probst (1977) remeasured 285 photographic plates taken between 1928 and 1975 and recomputed the masses of the components: $0.13 \pm 0.04 M_{\odot}$ for GL 234 A and $0.07 \pm 0.02 M_{\odot}$ for GL 234 B. The mass of the secondary falls very close to the hydrogen-burning limit of $0.08 M_{\odot}$, indicating that this object could be a brown dwarf. A recent reanalysis using infrared speckle observations results in a similar mass of $0.080 \pm 0.025 M_{\odot}$ for GL 234 B (Henry 1992).

Table 3.22 lists the magnitude differences between the components at V , R , I , J , H , and K . The values of ΔJ , ΔH , and ΔK were derived by Henry (1992) as a result of infrared speckle observations. Probst (1981), in an analysis of late-type dwarf stars and resolved binaries, determined mean magnitude-difference relations of $\Delta R/\Delta V = 0.83$, $\Delta I/\Delta V = 0.67$, $\Delta J/\Delta V = 0.56$, $\Delta H/\Delta V = 0.55$, and $\Delta K/\Delta V = 0.53$, which in this case have been used to generate ΔV , ΔR , and ΔI for GL 234 AB. Leggett (1992) has reported (Johnson-Cousins-CIT) $VRIJHK$ joint photometry of the pair, which is listed as colors in Table 3.23 and as absolute magnitudes, using the parallax of 0.2432 ± 0.0020 arcsecond determined by Probst (1977), in Table 3.24. The colors of the stars in Leggett's

(1992) compilation are the means of many different measurements from various researchers. She states that the mean error for colors involving V or R is typically 5%. For colors involving IJK , the error is $\sim 3\%$.

Since the magnitude differences, Δm_1 and Δm_2 , are known, it can be shown that the color $(m_1 - m_2)$ for star A is given by

$$(m_1 - m_2)_A = (m_1 - m_2)_{AB} + 2.5 \log \left(\frac{1 + 10^{\frac{-\Delta m_1}{2.5}}}{1 + 10^{\frac{-\Delta m_2}{2.5}}} \right), \quad (3.3)$$

where $(m_1 - m_2)_{AB}$ is the color of the composite system, which is also known. Then, the $(m_1 - m_2)$ color for the B component is simply

$$(m_1 - m_2)_B = (m_1 - m_2)_A + \Delta m_1 - \Delta m_2. \quad (3.4)$$

Colors of the individual components (GL 234 A and GL 234 B) have been determined and are listed beneath the composite colors in Table 3.23.

Likewise, the absolute magnitudes of star A and component B are

$$M_A = M_{AB} + 2.5 \log \left(1 + 10^{\frac{-\Delta m}{2.5}} \right); \quad (3.5)$$

$$M_B = M_A + \Delta m, \quad (3.6)$$

where the absolute magnitude of the composite, M_{AB} , is known. The absolute magnitudes of the individual components are given in Table 3.24.

To perform the differential spectroscopy, the correct spectrum of the primary needs to be subtracted from the composite spectrum. It is not known *a priori* what the spectrum of the primary is, but using the photometry given in Tables 3.23 and 3.24, an estimate of its spectral type can be made. To complement these two tables, Tables 3.25 and 3.26, which give mean colors and mean absolute magnitudes as a function of spectral type, are presented. Again, photometry is

kept on the standard system used in Leggett (1992), and spectral types are on the standard system presented in §3.1. In the last column of Table 3.25 is given a list of the objects whose photometry was used in computing the means for both tables; the values in parentheses after each averaged color or absolute magnitude represent the number of data points used in calculating that average. Only single objects were used to construct Tables 3.25 and 3.26. The standard deviation for the mean colors at each half spectral subclass in Table 3.25 is typically ~ 0.03 magnitude; the standard deviation for the mean absolute magnitudes in Table 3.26 ranges typically from 0.10 to 0.60 magnitude. This large dispersion is due primarily to the large effect that small uncertainties in the parallax have on the determination of the absolute magnitudes. The parallaxes used are those listed in Leggett (1992).

As can be seen from Table 3.25, the $R - I$ and $I - J$ colors increase monotonically with later spectral types and cover a large range of values. The $V - R$ color is also a good indicator of spectral type. A comparison to the colors of GL 234 A in Table 3.23 to the colors given in Table 3.25 clearly demonstrates that the values of $V - R$, $R - I$, and $I - J$ for GL 234 A are consistent with this object's having a spectral type around M4 or M4.5. A comparison of the absolute magnitudes in Table 3.26 to those values for GL 234 A in Table 3.24 suggests that the primary has a spectral type between M4 and M5, in agreement with the colors. However, considering the uncertainties in the absolute magnitudes, the colors should be considered more reliable and a better indicator of the spectral type. Therefore, it is concluded that the spectrum of GL 234 A falls roughly around spectral type M4 or M4.5.

There are two spectra in Table 3.20 with type M4 V and two with type

M4.5 V: GL 169.1 A, GL 213, GL 83.1, and GL 166 C. Leggett (1992) presents photometry of GL 213, GL 166 C, and GL 83.1, which can be compared directly to the values derived for GL 234 A in Table 3.23. This comparison demonstrates that GL 83.1 is ~ 0.10 magnitude redder than GL 234 A in both (V - R) and (R - I), with GL 213 being bluer in the same colors by 0.05 magnitude and GL 166 C bluer by only 0.03 magnitude. No photometry is given for GL 169.1 A, but it is presumed to be bluer by virtue of its M4 V classification. Because only the colors of GL 213 are significantly different from those of GL 234 A, three attempts can be made at extracting the spectrum of GL 234 B from the composite.

The spectra presented here span the range including the *I* bandpass, and since $\Delta I = 1.99$ for GL 234 AB, then the A component contributes $\sim 86\%$ (or a fraction $[1 + 10^{-\Delta I/2.5}]^{-1}$) of the total light of the composite spectrum at *I*. Each of the single M4 or M4.5 V spectra has been subtracted from the spectrum of GL 234 AB individually so that the flux in the *I* bandpass of the remainder is 14% of the *I* flux in the composite. These resulting spectra are plotted in Figure 3.21, below the observed spectrum of GL 234 AB. The differenced spectra in Figure 3.21b-d are the results of subtracting out the spectra of, from top to bottom, (b) GL 169.1, (c) GL 213, and (d) GL 166 C. The spectra of both Figure 3.21b and c resemble normal M dwarf spectra; that of Figure 3.21d is anomalous in that it appears to show VO absorption at 7450 Å (though nowhere else) like a late M dwarf, but the slope of the spectrum has the appearance of a much earlier object. The Na I doublet (~ 8190 Å) also appears much too strong. These features could result in differing metallicities between GL 166 C and GL 234 A. Furthermore, the appearance of H α changes wildly from spectrum to spectrum. GL 234 AB is listed as a dMe in Gliese (1969), as is GL 166 C. Sometimes, the H α emission

is of comparable strength and subtracts out well (Figure 3.21d), but since GL 169.1 A and GL 213 are not dMe stars, the $H\alpha$ emission remains in the difference (Figure 3.21b and c).

Each of the three differenced spectra was fit to the set of standards in §3.1 via the least-squares minimization technique over the wavelength range from 6950 to 8950 Å. The region shortward of 6950 Å was excluded from the fit (1) because low flux levels here make the subtraction process less certain and (2) because of the bad subtraction of the $H\alpha$ emission. Overplots of these best fits are shown as the dashed spectra in Figure 3.21b-d. The fit to Figure 3.21c is quite good, with the fits to Figure 3.21b and d being less so. As a result of these fits to the differential spectra, a spectral type of $\sim M5.5-6.5$ V is adopted for GL 234 B.

A comparison of the derived colors for GL 234 B (Table 3.23) with the averaged colors of Table 3.25 suggests a spectral type for GL 234 B of $M5.5-6$ V based on $V-R$, $R-I$, and $I-J$. A similar comparison of the absolute magnitudes of GL 234 B (Table 3.24) with the averages in Table 3.26 also supports a spectral type of $M5.5-6$ V. Both of these comparisons confirm the result obtained above.

b) LHS 1047 AB (GJ 1005 AB)

The astrometric perturbation of this system was first noted by Ianna (1979) and the companion was confirmed visually by Heintz (1987). Infrared speckle observations were reported by Ianna, Rohde, & McCarthy (1988), who made the first mass determination of the components — $0.17 \pm 0.12 M_{\odot}$ for LHS 1047 A and $0.055 \pm 0.032 M_{\odot}$ for LHS 1047 B. Again, because of the large error in the mass, the secondary could fall on either side of the stellar/substellar dividing

line.

Ianna, Rohde, & McCarthy (1988) determined that $\Delta K = 1.5$, and using the relations from Probst (1981), the magnitude differences in other bandpasses can be estimated. These results are shown in Table 3.22. Ianna, Rohde, & McCarthy (1988) also give *VRIJHK* photometry for the composite (on the same photometric system used in the last section) and list the parallax as 0.189 ± 0.005 arcsecond. Observed colors for LHS 1047 AB are listed in Table 3.23, and absolute magnitudes are given in Table 3.24. Using the formulae given above, colors and absolute magnitudes for LHS 1047 A and LHS 1047 B have also been computed and entered into the tables.

A comparison of the colors of LHS 1047 A to the color given in Table 3.25 show that the values of $V - R$ and $R - I$ are consistent with this object's having a spectral type of M3.5 V. The $I - J$ color is more consistent with a type of M3 V. Of the four single stars in Table 3.20 having a type of either M3 or M3.5 V, three have photometry in Leggett (1992). The $V - R$, $R - I$, and $I - J$ colors of GL 725 A (M3 V) are generally 0.12 magnitude bluer than those of LHS 1047 A, whereas the colors of the M3.5 V stars are in much closer agreement, with GL 873 having identical $V - R$ and $R - I$ colors to LHS 1047 A, although the $I - J$ value differs by 0.07 magnitude.

Since $\Delta I = 1.90$, the A component contributes $\sim 85\%$ of the total light of the composite at I. Using this information, two attempts can be made at extracting the spectrum of LHS 1047 B from the composite. The resulting differential spectra are plotted in the lower portion of Figure 3.22, below the observed spectrum of LHS 1047 AB. The residual “H α absorption” feature in Figure 3.22b results from the fact that the subtracted spectrum (GL 873) is a dMe while the com-

posite spectrum of LHS 1047 AB is not. The least-squares fits of the differential spectra to the set of standard stars is shown again by dashed lines in Figure 3.22b and c. The resulting spectral types are in very close agreement and suggest a spectral type of M4.5-M5 V for LHS 1047 B.

The derived colors for LHS 1047 B suggest a spectral type of M5.5 V, with the exception of the $I - J$ color which indicates a type around M4.5 V. A comparison of the absolute magnitudes for the B component with the averaged values suggests that LHS 1047 B is around type M5.5-6 V based on M_V , M_R , and M_I , and around type M6-6.5 V based on M_J , M_H , and M_K . These results indicate that the spectral type determined above could be as much as 1.5 spectral subclasses too early, but again the absolute magnitude information should be given low weight. Nonetheless, to satisfy all of the available data, a type of M4.5-6.5 V is assigned.

c) GL 22 AC (BD +66° 34 AC)

Parallax measurements of the primary star in the GL 22 A/GL 22 B system revealed the presence of a third member, GL 22 C (Alden 1947). Hershey (1973) published the first orbit for the unseen companion around GL 22 A, and using an infrared speckle camera, McCarthy et al. (1991) were the first to image it, determining masses of $0.36 \pm 0.05 M_\odot$ for GL 22 A, $0.18 \pm 0.02 M_\odot$ for GL 22 B, and $0.12 \pm 0.02 M_\odot$ for GL 22 C.

Magnitude differences between the A and C components of $\Delta H = 2.11$ and $\Delta K = 1.94$ were measured by McCarthy et al. (1991). The other magnitude differences in Table 3.22 were again estimated using the relations from Probst

(1981). No *VRI* photometry exists for this system (at least none could be found using SIMBAD), although McCarthy et al. (1991) present *JHK*. Unfortunately, the McCarthy data have rather large error bars (~ 0.13 magnitude for $H - K$, for example) so typical colors for an M2 V (Table 3.25) have been entered for GL 22 AC in Table 3.23. No determination of the absolute magnitudes of the composite is possible at present. As before, colors for GL 22 A and GL 22 C have been estimated and are also listed in Table 3.23.

A comparison of the colors of GL 22 A to the colors in Table 3.25 demonstrates that GL 22 A must fall around spectral type M1.5 or M2 V. The only single object of Table 3.20 having a spectral type in this range and photometry in Leggett (1992) is GL 806, which has $V - R = 0.99$, $R - I = 1.20$, $I - J = 1.19$, $J - H = 0.59$, and $H - K = 0.22$. Based on this evidence, this object appears to be of slightly later class than GL 22 A. The only other single object of M2 V in Table 3.20 (no M1.5 V spectra were acquired) is GL 220. Eggen (1989) gives $V - R$ and $R - I$ colors for this object, which can be transformed to the Johnson-Cousins system by comparing the Eggen (1979) photometry of GL 205 (M1.5 V) and GL 411 (M2 V) to the Leggett photometry. Because these stars are of nearly identical spectral type to GL 220, a simple linear transformation with no color term can be obtained to convert the Eggen colors to the Johnson-Cousins system. When this is done, values of $V - R = 0.95$ and $R - I = 1.13$ are acquired for GL 220. These colors are a good match to the colors of GL 22 A given in Table 3.23.

Since $\Delta I = 2.51$, GL 22 A contributes $\sim 91\%$ of the light of the composite spectrum at I . Figure 3.23b shows the result of differencing the GL 220 spectrum from the GL 22 AC spectrum. The composite itself is shown in Figure 3.23a. The

best least-squares match (dashed line) to the differential spectrum has spectral type M5.5 V. However, the differential spectrum has negative flux from 6350 to 7100 Å, indicating perhaps that too large a percentage of the spectrum of GL 220 was subtracted from the composite. If the assumption is made that GL 22 A contributes only 85% of the light at I (which would correspond to $\Delta I = 1.88$, significantly smaller than the measured value), then the result is a differential spectrum having mainly positive flux at the short wavelength end and having a somewhat earlier spectral type of M4.5 V. In this case, the match to the spectral standard is more convincing (see Figure 3.23c). Additionally, this exercise illustrates that a small error in the magnitude difference does not seriously affect the resulting spectral type of the secondary — the difference here being only one spectral class. It should be noted that subtracting off a spectrum with type earlier than M2 makes the problem of negative flux worse.

The derived colors for GL 22 C (Table 3.23), when compared to the values in Table 3.25, suggest a spectral type between M4 and M5.5 V. Based on this evidence, together with the evidence presented in Figure 3.23, a type of M4-5.5 V is adopted.

Curiously, the values of M_J , M_H , and M_K given in McCarthy et al. (1991) would suggest a spectral type of M3 V for GL 22 AC, which is a full spectral class later than that of the observed spectrum. Using these absolute magnitudes with the ΔJ , ΔH , and ΔK quoted above, it is found that GL 22 C would have $J - H = 0.74$ and $H - K = 0.48$, supporting a type of M8 or M9, which is in conflict with the above results. To understand this system better, VRI photometry should be acquired and the infrared magnitudes and magnitude differences should be measured, if possible, with higher precision.

d) GJ 1081 AB (G 96-45 AB)

Astrometric perturbations were first noted for GJ 1081 by Routly (1972) and Behall & Harrington (1976), and the latter authors determined masses of $0.27 M_{\odot}$ for GJ 1081 A and $0.10\text{-}0.16 M_{\odot}$ for GJ 1081 B. The companion was verified through infrared speckle imaging by McCarthy (1986).

The magnitude difference at K is rather uncertain, but is ~ 0.10 magnitude (McCarthy 1992). Using Probst's (1981) relations, the other magnitude differences in Table 3.22 can be estimated. Weis & Upgren (1982) present VRI photometry of this system, which can be transformed to the Johnson-Cousins system by utilizing the formulae presented in the appendix of Leggett (1992). The resulting colors are entered in Table 3.23. Using a parallax of 0.063 ± 0.003 (Behall & Harrington 1976), absolute Johnson-Cousins VRI magnitudes have likewise been computed (Table 3.24). Using the estimated magnitude differences, the colors and absolute magnitudes for GJ 1081 A and GJ 1081 B have also been computed and entered in Tables 3.23 and 3.24.

The $V - R$ and $R - I$ colors of GJ 1081 A are consistent with a spectral type of M3-3.5 V (Table 3.25). Of the M3 and M3.5 V single stars in Table 3.20, three have Leggett (1992) photometry: GL 725 A has $V - R = 1.07$ and $R - I = 1.39$, both of which are 0.08 magnitude bluer than the colors of GJ 1081 A; GL 725 B has $V - R = 1.12$ and $R - I = 1.43$, which are only 0.03-0.04 magnitude bluer than GJ 1081 A; and GL 873 has $V - R = 1.17$ and $R - I = 1.52$, making it later in type than GJ 1081 A. The fourth star, GL 22 B, is assumed to have similar colors to GL 725 A since both are spectral type M3 V. Therefore, based on this argument, the spectrum of GL 725 B would be the best

match to the primary's spectrum. Interestingly, though, the spectral type of GL 725 B (M3.5 V) is later than that of the GJ 1081 AB composite, which would lead to the secondary spectrum having a type earlier than the primary. This is clearly aphysical.

The photometry of the composite may not be accurate enough to use in this application. A comparison of these values of $V - R$ and $R - I$ with the colors in Table 3.25 would suggest that GJ 1081 AB has a type of M3.5 V. This is half a subclass later than the observed type. If the colors for an M3 V in Table 3.25 are chosen for GJ 1081 AB instead of the transformed Weis & Ugren values (a similar assumption was made for GL 22 AC above), then the colors (especially $R - I$) for GJ 1081 A are more consistent with an object like GL 226 or GL 767 B (M2.5 V).

Since $\Delta I = 1.26$, GJ 1081 A contributes $\sim 76\%$ of the flux to the composite spectrum at I . Use of this number results in the residual spectra shown in the lower panels of Figure 3.24, with the composite spectrum of GJ 1081 AB shown in the upper panel. The best least-squares matches to the standard spectra are shown by the dashed lines. In both cases, a spectral type of M5 is the best fit.

The colors of GJ 1081 B in Table 3.23 are consistent with a spectral type of M4.5-5 V. This agrees well with the determination above, so a type of M4.5-5 V is hereby adopted for GJ 1081 B.

e) G 250-29 AB (LHS 221 AB)

The binary nature of this system was first recognized by Borgman and subsequent observations led to the visual confirmation of the secondary (Heintz 1986).

The companion was also verified through infrared speckle imaging (McCarthy 1986), and a determination of $\Delta K = 1.0$ was made (McCarthy 1992). Refer to Table 3.22 for the estimated magnitude differences in other bandpasses. The orbit and masses for this system have not yet been calculated.

Leggett (1992) does not present photometry of this object, so the colors given in Table 3.23 are the averages for an M2.5 V listed in Table 3.25. The derived colors for G 250-29 A are consistent with a spectral type of M2-2.5 V. Dawson & Forbes (1989) present *VRI* photometry for G 250-29 AB which, together with the parallax of 0.091 ± 0.04 determined by Heintz (1986), can be used to calculate the absolute *VRI* magnitudes in Table 3.24. (The $V - R$ and $R - I$ colors adopted in Table 3.23 are 0.08 and 0.10 magnitude bluer, respectively, than the Dawson & Forbes $V - R$ and $R - I$ colors, which suggest an erroneous spectral type of M3-3.5 V for the composite. This difference is doubtless the result of a small but unknown offset between the Dawson & Forbes photometry and the Johnson-Cousins system. However, several tenths of a magnitude separate the absolute magnitudes for each half spectral subclass in Table 3.26, so the unknown offset is considered negligible when comparing the values for G 250-29 AB in Table 3.24 to the averaged values in Table 3.26.)

Leggett (1992) gives $V - R$ and $R - I$ colors for two of the four M2-2.5 V stars in Table 3.20. Both of the colors for GL 226 (M2.5 V) are somewhat redder (by 0.05-0.08 magnitude) than those in Table 3.23 for G 250-29 A, but the colors of GL 806 (M2 V) are only slightly bluer (by 0.02). Therefore, the spectra of the M2 V stars (GL 220 and GL 806) will be used to perform the differential spectroscopy.

Because $\Delta I = 1.26$, G 250-29 A contributes $\sim 76\%$ of the I flux to the composite spectrum. Using this value for both of the M2 V spectra results in the differenced spectra shown in Figure 3.25b-c, with the spectrum of the G 250-29 AB composite shown in Figure 3.25a. The best least-squares matches to the standard spectra indicate spectral types of M5 and M4.5 V for these differenced spectra.

The colors of G 250-29 B in Table 3.23 are consistent with a spectral type in the range M3.5-4.5 V. The absolute magnitudes given in Table 3.24 are consistent with a type of M4 V. Therefore, a spectral type in the range M3.5-5 V is adopted for G 250-29 B.

3.4.3: Results

Based on the lines of evidence presented in earlier sections of this chapter, one might have expected that the spectra of these low-mass secondaries, some of which are viable brown dwarf candidates, would resemble the spectra of very late objects like vB8, vB10, and LHS 2924 or perhaps even resemble that of GD 165 B, the best substellar candidate known. Astonishingly, the latest spectral type found for any of the secondaries is M5-6.5 V — for the low-mass object GL 234 B; LHS 1047 B, also having a very low mass, was similarly typed as an M4.5-6.5 V.

The results of the previous section are summarized in Table 3.27 and are plotted as open symbols on the spectral type vs. mass diagram of Figure 3.26. These new points confirm the trend noted in Figure 3.10. In fact, GL 234 B and LHS 1047 B, despite having masses which place them very near or just off the

end of the main sequence, have spectral types in the mid-M range — between M4.5 and M6.5 V. This indicates that objects of type M7 and later, because they would presumably have even *smaller* masses, are likely to be brown dwarfs.

If this supposition is correct, then it implies that the break between low-mass stars and brown dwarfs, according to Table 3.26, falls near $M_K \sim 9.7$, which is also the point at which the infrared (M_K) luminosity function of Henry & McCarthy (1990) is seen to plummet. Furthermore, it means that astronomers have already discovered 21 brown dwarfs (because the last 21 objects in Table 3.17 are all of type M7 or later). This hypothesis must, however, be tested — researchers must begin to scrutinize these 21 objects to see if any are members of short-period binary systems. Only then can dynamical masses be calculated for these objects, whose true nature remains unknown.

3.4.4: Summary

Differential spectroscopy has been performed on five composite systems containing an early- to mid-M type primary star and a low-mass secondary. In each case, information acquired through speckle imaging techniques was essential in determining the correct spectral type of the primary and in determining the percentage that its spectrum contributes to the composite.

The surprising result of this differencing is that all of the secondaries were found to have a spectral type of M6.5 or earlier. If any of these is a brown dwarf, which is a possibility for at least two of the secondaries, then its spectrum does not obviously differentiate it from the familiar M dwarf sequence. Furthermore, objects of later type ($\geq M7$) presumably have lower masses and are even more

likely to be brown dwarfs. Confirmation awaits the direct measurement of a dynamical mass for an object of type M7 V or later.

TABLE 3.20
SPECTRA OF SINGLE M DWARFS OBTAINED ON
1991 NOVEMBER 13

Object Name	Other Name	Spectral Type	Integ. (sec)	Single status suggested via speckle observations by...
GL 220 ^a	Ross 59	M2 V	570	—
GL 806	G 209-41	M2 V	990	1
GL 767 B ^b	BD +31°3767 B	M2.5 V	1260	—
GL 226 ^c	G 222-11	M2.5 V	480	—
GL 725 A ^d	HD 173739	M3 V	250	1, 2
GL 22 B	BD +66°34 B	M3 V	915	3
GL 725 B ^d	HD 173740	M3.5 V	250	1, 2
GL 873 ^e	BD +43°4305	M3.5 V	345	1, 4
GL 169.1 A ^f	Stein 2051 A	M4 V	840	4
GL 213	Ross 47	M4 V	2400	4
GL 83.1	G 3-33	M4.5 V	2010	2
GL 166 C	40 Eri C	M4.5 V	870	2

^a No mention of periodic residuals in the astrometric measurements by Heintz 1988.

^b Astrometric measurements by Mesrobian, Griese, & Titter 1972 show “no deviation from linearity within the scatter of the observations”.

^c Astrometric measurements by Heintz 1973 show “no systematic run of residuals in 12 years.”

^d Heintz 1987 shows that the astrometric data show no periodic residuals which would indicate a third member in the GL 725 A and B system.

^e The possible multiplicity of this object (EV Lac) is still a matter of debate: van de Kamp & Worth 1972 find astrometric evidence for a second body with a period of 28.9 years, and Rožman 1984 finds evidence for an eclipsing body having a period coincident with the photometric period of 4.378 days. In both cases, the derived masses of the other bodies fall between 0.01 and 0.04 M_{\odot} — if either is real, contribution to the light of the primary would be negligible. Curiously, Weis, Nations, & Upgren 1983 find no significant trends in their astrometric residuals, and Marcy & Benitz 1989 see no radial velocity variations to the $\sigma = 0.24$ km/sec level over 694 days.

^f Suspected companion disproven via higher quality data by Heintz 1990.

SPECKLE REFERENCES. — (1) Blazit, Bonneau, & 1987; (2) Henry & McCarthy 1990; (3) McCarthy et al. 1991; (4) Henry 1991.

TABLE 3.21

SPECTRA OF COMPOSITE SYSTEMS (M DWARF + LOW-MASS
SECONDARY) OBTAINED ON 1991 NOVEMBER 13

Object Name	Other Name	Spectral Type	Integ. (sec)	Duplicity of system established by...
GL 234 AB	Ross 614 AB	M4.5 V	1500	1, 2
LHS 1047 AB	GJ 1005 AB	M4 V	1380	3, 4, 5
GL 22 AC	BD +66°34 AC	M2 V	915	6, 7
GJ 1081 AB	G 96-45 AB	M3 V	720	8
G 250-29 AB	LHS 221 AB	M2.5 V	540	8, 9

DUPLICITY REFERENCES. — (1) Lippincott 1955; (2) Davey et al. 1989; (3) Ianna 1979; (4) Heintz 1987; (5) Ianna, Rohde, & McCarthy 1988; (6) Hershey 1973; (7) McCarthy et al. 1991; (8) McCarthy 1986; (9) Heintz 1986.

TABLE 3.22
MAGNITUDE DIFFERENCES FOR THE COMPONENTS OF THE
FIVE COMPOSITE SYSTEMS

Object Name	ΔV	ΔR	ΔI	ΔJ	ΔH	ΔK
GL 234 AB	2.97 ^a	2.47 ^a	1.99 ^a	1.71 ^b	1.66 ^b	1.51 ^b
LHS 1047 AB	2.83 ^a	2.35 ^a	1.90 ^a	1.58 ^a	1.56 ^a	1.50 ^c
GL 22 AC	3.75 ^a	3.11 ^a	2.51 ^a	2.10 ^a	2.11 ^d	1.94 ^d
GJ 1081 AB	1.89 ^a	1.57 ^a	1.26 ^a	1.06 ^a	1.04 ^a	1.0 ^e
G 250-29 AB	1.89 ^a	1.57 ^a	1.26 ^a	1.06 ^a	1.04 ^a	1.0 ^e

^a Estimated using the magnitude-difference relations from Probst 1981.

^b From Henry 1992.

^c From Ianna, Rohde, & McCarthy 1988.

^d From McCarthy et al. 1991.

^e From McCarthy 1992.

TABLE 3.23
COLORS OF THE COMPOSITE SYSTEMS

Object Name	$V - R$	$R - I$	$I - J$	$J - H$	$H - K$
GL 234 AB	1.31	1.71	1.68	0.60	0.29
GL 234 A	1.27	1.66	1.64	0.59	0.26
GL 234 B	1.77	2.14	1.92	0.64	0.41
LHS 1047 AB	1.21	1.58	1.42	0.57	0.29
LHS 1047 A	1.17	1.52	1.37	0.57	0.28
LHS 1047 B	1.65	1.97	1.69	0.59	0.34
GL 22 AC ^a	1.00	1.17	1.19	0.59	0.21
GL 22 A	0.97	1.13	1.15	0.59	0.19
GL 22 C	1.61	1.73	1.56	0.58	0.36
GJ 1081 AB ^b	1.15	1.47	—	—	—
GJ 1081 A	1.10	1.40	—	—	—
GJ 1081 B	1.41	1.71	—	—	—
GJ 1081 AB ^a	1.05	1.36	1.32	0.59	0.24
GJ 1081 A	1.00	1.29	1.27	0.58	0.23
GJ 1081 B	1.32	1.60	1.47	0.60	0.27
G 250-29 AB ^a	1.06	1.29	1.33	0.56	0.24
G 250-29 A	1.01	1.22	1.28	0.55	0.23
G 250-29 B	1.33	1.53	1.48	0.57	0.27

^a Values are adopted from Table 3.25. See text for discussion.

^b Values are based on Weis & Upgren 1982 photometry. See text for details.

TABLE 3.24
ABSOLUTE MAGNITUDES OF THE COMPOSITE SYSTEMS^a

Object Name	M_V	M_R	M_I	M_J	M_H	M_K
GL 234 AB	13.01	11.70	9.99	8.31	7.71	7.42
GL 234 A	13.08	11.81	10.15	8.51	7.92	7.66
GL 234 B	16.05	14.28	12.14	10.22	9.58	9.17
LHS 1047 AB	12.88	11.67	10.09	8.66	8.09	7.80
LHS 1047 A	12.96	11.79	10.26	8.89	8.32	8.04
LHS 1047 B	15.79	14.14	12.16	10.47	9.88	9.54
GJ 1081 AB ^b	11.21	10.06	8.59	—	—	—
GJ 1081 A	11.39	10.29	8.89	—	—	—
GJ 1081 B	13.28	11.86	10.15	—	—	—
G 250-29 AB ^c	10.82	9.69	8.29	—	—	—
G 250-29 A	11.00	9.92	8.59	—	—	—
G 250-29 B	12.89	11.49	9.85	—	—	—

^a GL 22 AC lacks any *VRI* photometry and is hence not listed here.

^b Values are based on Weis & Upgren 1982 photometry. See text.

^c Values are based on Dawson & Forbes 1989 photometry. See text.

TABLE 3.25

MEAN COLORS AS A FUNCTION OF SPECTRAL TYPE FOR M DWARFS

Spec.	$V - R$	$R - I$	$I - J$	$J - H$	$H - K$	Objects used in the mean
M0 V	0.87(3)	0.86(1)	1.03(3)	0.65(3)	0.15(3)	GL 270, 328, 763
M0.5 V	0.87(3)	0.91(3)	1.03(4)	0.65(4)	0.16(4)	GL 720 A, 761.2, 839, 846
M1 V	0.96(1)	1.05(1)	1.13(1)	0.63(1)	0.20(1)	GL 229
M1.5 V	0.97(1)	1.10(1)	1.14(1)	0.68(1)	0.19(1)	GL 205
M2 V	1.00(3)	1.17(3)	1.19(3)	0.59(3)	0.21(3)	GL 382, 411, 806
M2.5 V	1.06(2)	1.29(2)	1.33(2)	0.56(2)	0.24(2)	GL 226, 381
M3 V	1.05(4)	1.36(4)	1.32(4)	0.59(4)	0.24(4)	GL 251, 436, 725 A, 752 A
M3.5 V	1.15(4)	1.51(4)	1.47(4)	0.56(4)	0.24(4)	Gl 273, 643, 669 A, 725 B
M4 V	1.21(3)	1.59(3)	1.52(4)	0.54(4)	0.26(4)	GL 213, 232, 402, 699
M4.5 V	1.32(4)	1.71(4)	1.65(4)	0.57(4)	0.27(4)	GL 83.1, 166 C, 268, 669 B
M5 V	1.43(2)	1.89(2)	1.82(2)	0.59(2)	0.29(2)	GL 51; GJ 1057
M5.5 V	1.59(1)	2.01(1)	2.03(1)	0.52(1)	0.37(1)	GJ 1245 A
M6 V	1.80(3)	2.17(3)	2.25(4)	0.56(4)	0.37(4)	GL 283B, 316.1, 406; GJ 1245B
M6.5 V	2.03(2)	2.30(2)	2.31(4)	0.57(4)	0.34(4)	GJ 1111; LHS 191, 292, 523
M7 V	2.15(1)	2.41(1)	2.47(1)	0.58(1)	0.37(1)	GL 644 C
M8 V	—	—	2.95(2)	0.70(2)	0.45(2)	GL 752 B; LHS 2397a
M9 V	—	—	3.29(2)	0.71(2)	0.51(2)	LHS 2065, 2924

TABLE 3.26
MEAN ABSOLUTE MAGNITUDES AS A FUNCTION OF SPECTRAL TYPE
FOR M DWARFS

Sp. Type	M_V	M_R	M_I	M_J	M_H	M_K
M0 V	8.68(3)	7.80(3)	6.94(3)	5.92(3)	5.26(3)	5.11(3)
M0.5 V	8.89(4)	7.96(3)	7.08(4)	6.05(4)	5.40(4)	5.24(4)
M1 V	9.33(1)	8.37(1)	7.32(1)	6.19(1)	5.56(1)	5.36(1)
M1.5 V	9.14(1)	8.17(1)	7.07(1)	5.93(1)	5.25(1)	5.06(1)
M2 V	10.16(3)	9.16(3)	7.99(3)	6.80(3)	6.21(3)	6.00(3)
M2.5 V	10.45(2)	9.40(2)	8.11(2)	6.78(2)	6.23(3)	5.99(2)
M3 V	10.84(4)	9.79(4)	8.43(4)	7.11(4)	6.52(4)	6.29(4)
M3.5 V	12.05(4)	10.90(4)	9.39(4)	7.92(4)	7.36(4)	7.12(4)
M4 V	12.95(4)	11.57(3)	10.12(4)	8.60(4)	8.06(4)	7.80(4)
M4.5 V	13.04(4)	11.73(4)	10.02(4)	8.34(4)	7.80(4)	7.53(4)
M5 V	13.95(2)	12.52(2)	10.63(2)	8.82(2)	8.23(2)	7.94(2)
M5.5 V	15.10(1)	13.51(1)	11.50(1)	9.47(1)	8.95(1)	8.58(1)
M6 V	16.49(4)	14.56(3)	12.48(4)	10.22(4)	9.66(4)	9.29(4)
M6.5 V	17.14(4)	15.13(2)	12.82(4)	10.51(4)	9.94(4)	9.60(4)
M7 V	17.76(1)	15.61(1)	13.20(1)	10.73(1)	10.15(1)	9.78(1)
M8 V	18.76(2)	—	14.10(2)	11.15(2)	10.45(2)	10.01(2)
M9 V	19.29(2)	—	14.93(2)	11.65(2)	10.94(2)	10.43(2)

TABLE 3.27
RESULTS OF THE DIFFERENTIAL SPECTROSCOPY

Object Name	—Spectral Type Determined—		Adopted Sp. Type	Calculated Mass (M_{\odot})
	Spectroscopically	Photometrically		
GL 22 A	—	M2 V	M2 V	0.36 ± 0.05
G 250-29 A	—	M2 V	M2 V	unknown
GJ 1081 A	—	M2.5 V	M2.5 V	$0.27 (\pm 0.06)$
LHS 1047 A	—	M3.5 V	M3.5 V	0.17 ± 0.12
G 250-29 B	M4.5-5 V	M3.5-4.5 V	M3.5-5 V	unknown
GL 234 A	—	M4-4.5 V	M4-4.5 V	0.13 ± 0.04
GL 22 C	M4.5-5.5 V	M4-5.5	M4-5.5 V	0.12 ± 0.02
GJ 1081 B	\sim M5 V	M4.5-5 V	M4.5-5 V	0.13 ± 0.03
LHS 1047 B	M4.5-5 V	M4.5-6.5 V	M4.5-6.5 V	0.055 ± 0.032
GL 234 B	M5-6.5 V	M5.5-6 V	M5-6.5 V	0.080 ± 0.025

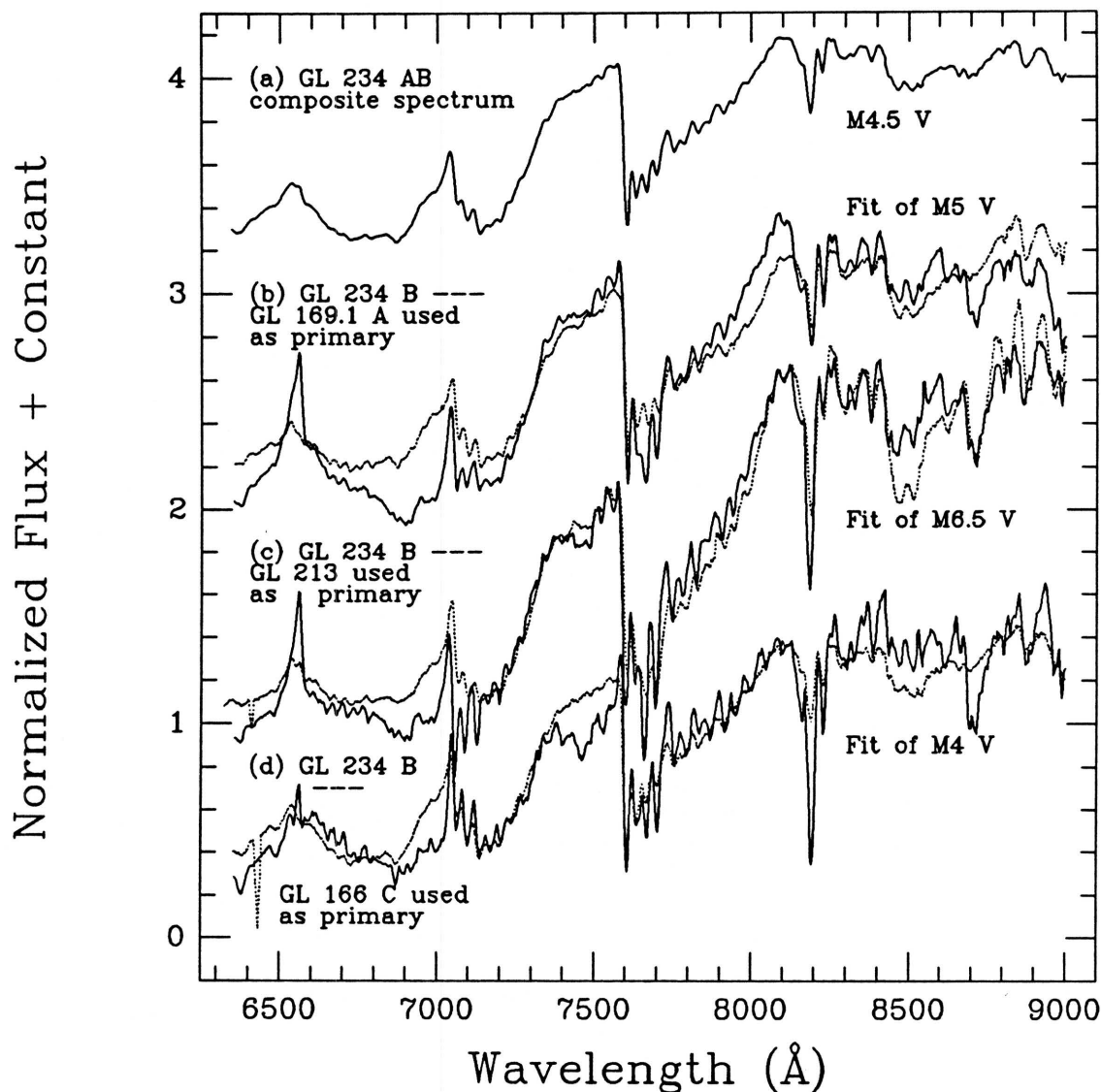


FIG. 3.21. — (a) The composite spectrum of GL 234 AB. (b) The resulting spectrum of GL 234 B, where the spectrum of GL 169.1 A has been subtracted as the spectrum of GL 234 A. The best fit, shown by the dashed line, gives a spectral type of M5 V for the secondary. (c) The resulting spectrum of GL 234 B, where the spectrum of GL 213 has been subtracted as the spectrum of GL 234 A. The best fit, which represents a very good match to this spectrum, gives a spectral type of M6.5 V. (d) The resulting spectrum of GL 234 B, where the spectrum of GL 166 C has been subtracted as the spectrum of GL 234 A. This spectrum is quite peculiar and is fit best by an M4 V — which is half a spectral subclass earlier than GL 166 C itself. See text for discussion. Integral offsets have been used in (a)-(c) to separate the spectra vertically.

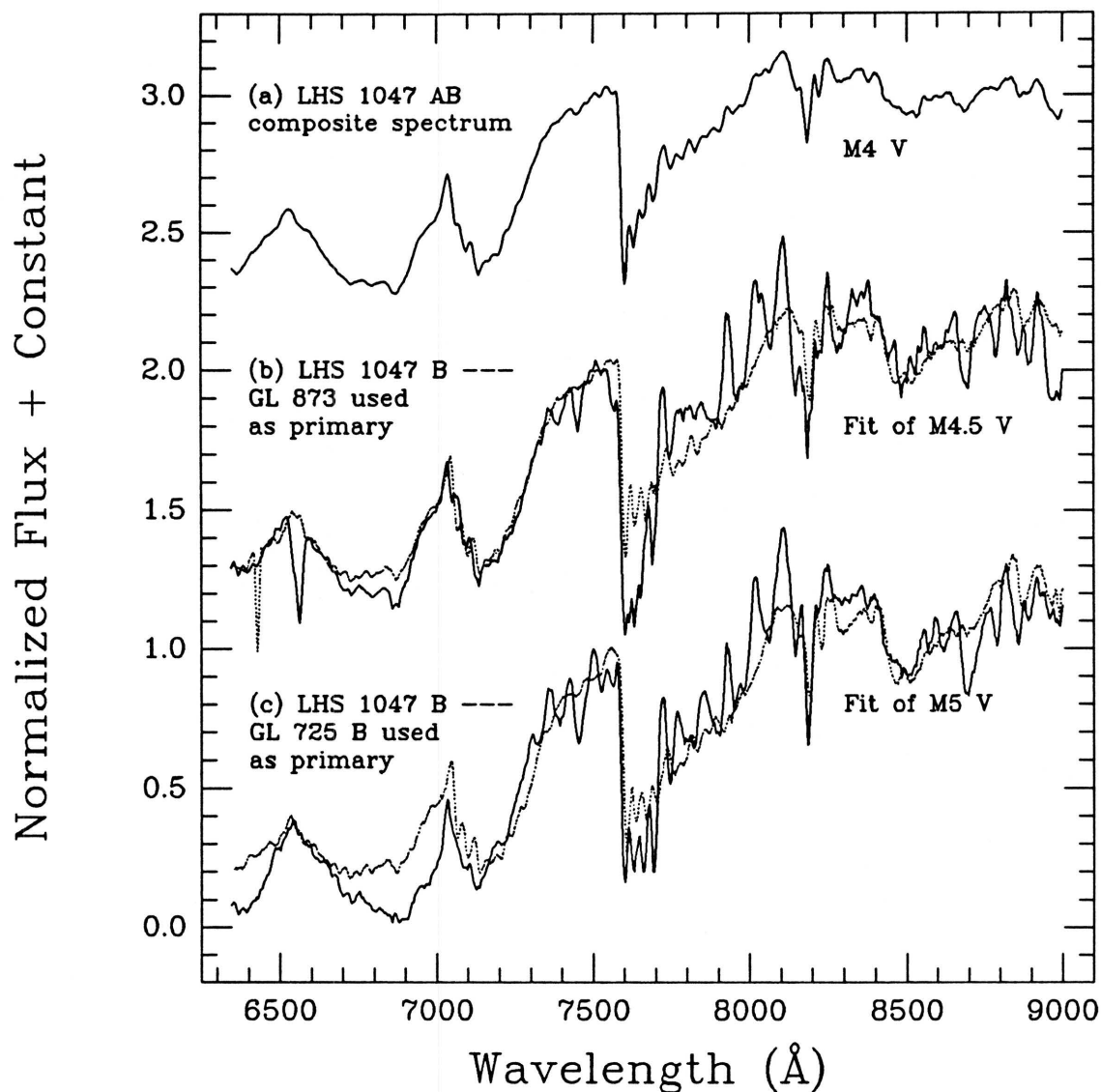


FIG. 3.22. — (a) The composite spectrum of LHS 1047 AB. (b) The resulting spectrum of LHS 1047 B, where the spectrum of GL 873 has been subtracted as the spectrum of LHS 1047 A. The best fit, shown by the dashed line, is a good general match to the spectrum and suggests a spectral type of M4.5 V. (c) The resulting spectrum of LHS 1047 B, where GL 725 B has been subtracted as the spectrum of LHS 1047 A. The best fit to this spectrum suggests a type of M5 V. Integral offsets have been used to separate the spectra vertically.

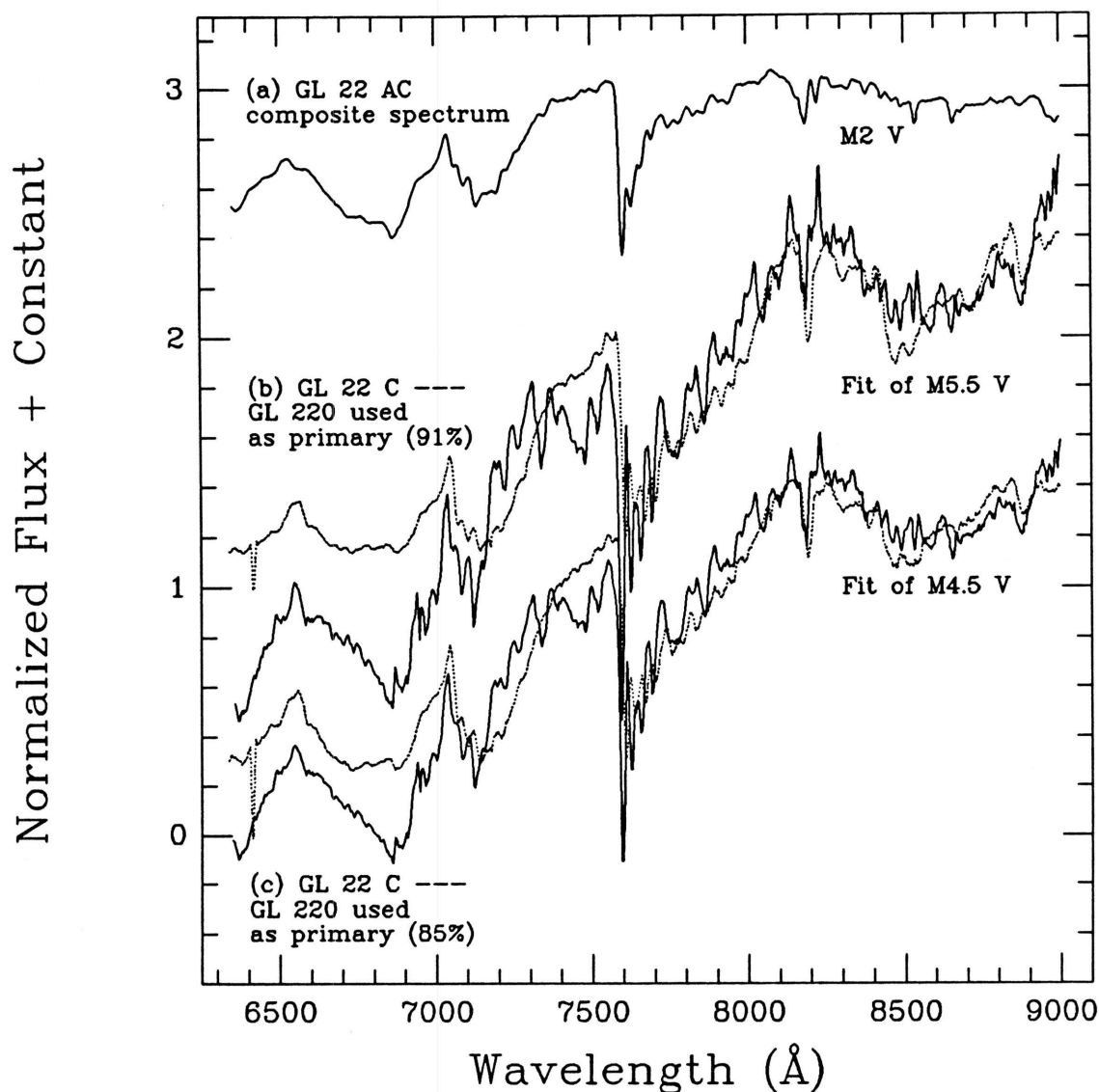


FIG. 3.23. — (a) The composite spectrum of GL 22 AC. (b) The resulting spectrum of GL 22 C, where the spectrum of GL 220 has been subtrated as that of the primary star, which is assumed to be contributing 91% of the flux in the *I* bandpass. The spectrum representing the best match (M5.5 V) does not fit the differenced spectrum below 7500 Å, largely because the flux for GL 22 C falls below zero for part of this region. (b) The resulting spectrum of GL 22 C, again using GL 220 as the primary. In this case, the primary is assumed to contribute only 85% of the total flux at *I*. The spectrum of GL 22 C now has mainly positive flux, and the best-fit spectrum (M4.5 V) provides a more convincing match. Integral offsets have again been used for clarity.

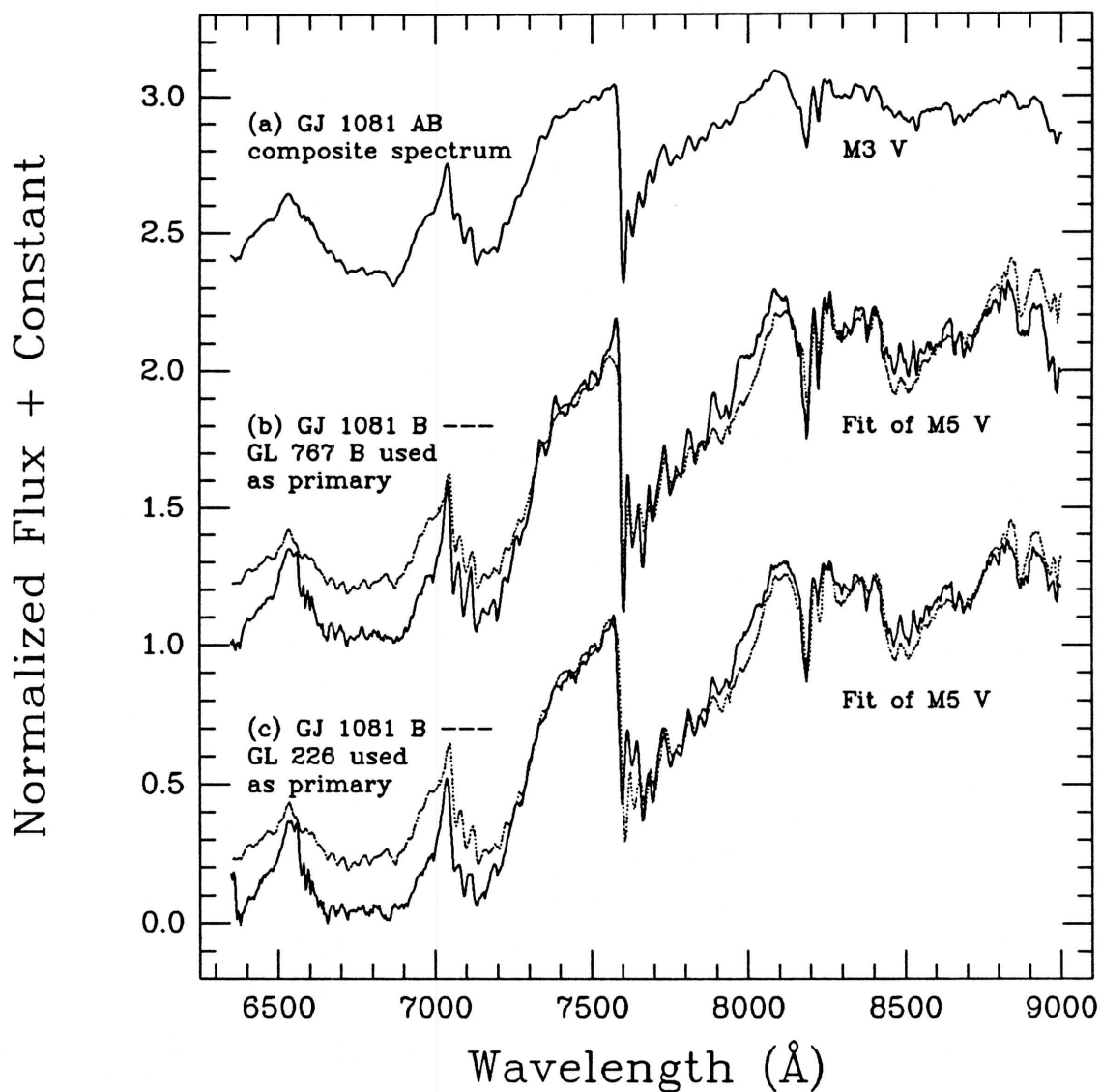


FIG. 3.24. — (a) The composite spectrum of GJ 1081 AB. (b) The resulting spectrum of GJ 1081 B, where the spectrum of GL 767 B has been subtracted as the spectrum of GJ 1081 A. The best fit (dashed line) gives a spectral type of M5 V. (c) The resulting spectrum of GJ 1081 B, where the spectrum of GL 226 has been subtracted as the spectrum of GJ 1081 A. The best fit here also gives a spectral type of M5 V. Again, integral offsets have been used for vertical separation.

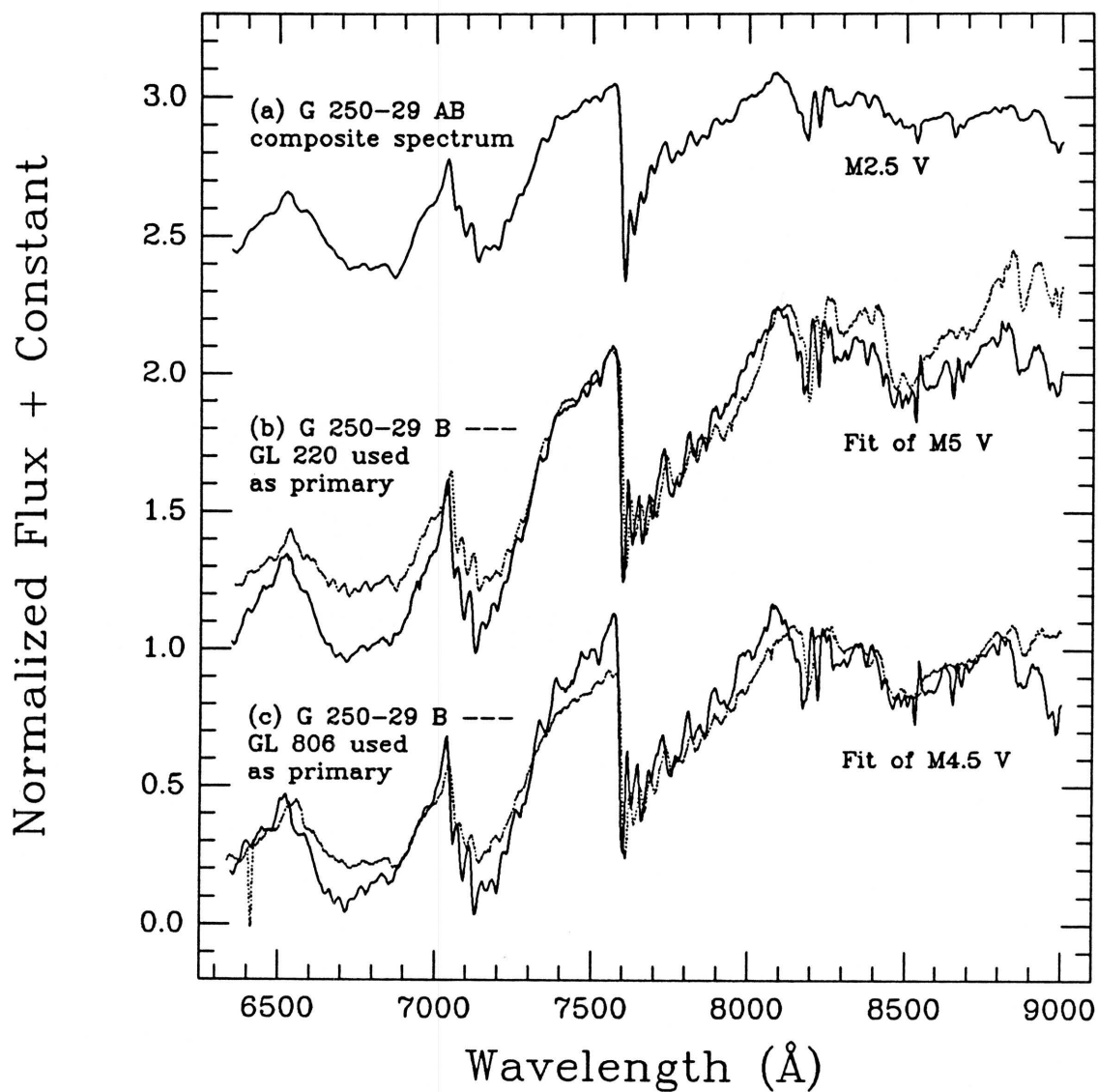


FIG. 3.25. — (a) The composite spectrum of G 250-29 AB. (b) The resulting spectrum of G 250-29 B, where the spectrum of GL 220 has been subtracted as the spectrum of G 250-29 A. The dashed line shows the best fit to the spectrum, suggesting a type of M5 V. (c) The resulting spectrum of G 250-29 B, where the spectrum of GL 806 has been subtracted as the spectrum of G 250-29 A. The best fit suggests a type of M4.5 V. Integral offsets have been added to separate the spectra vertically.

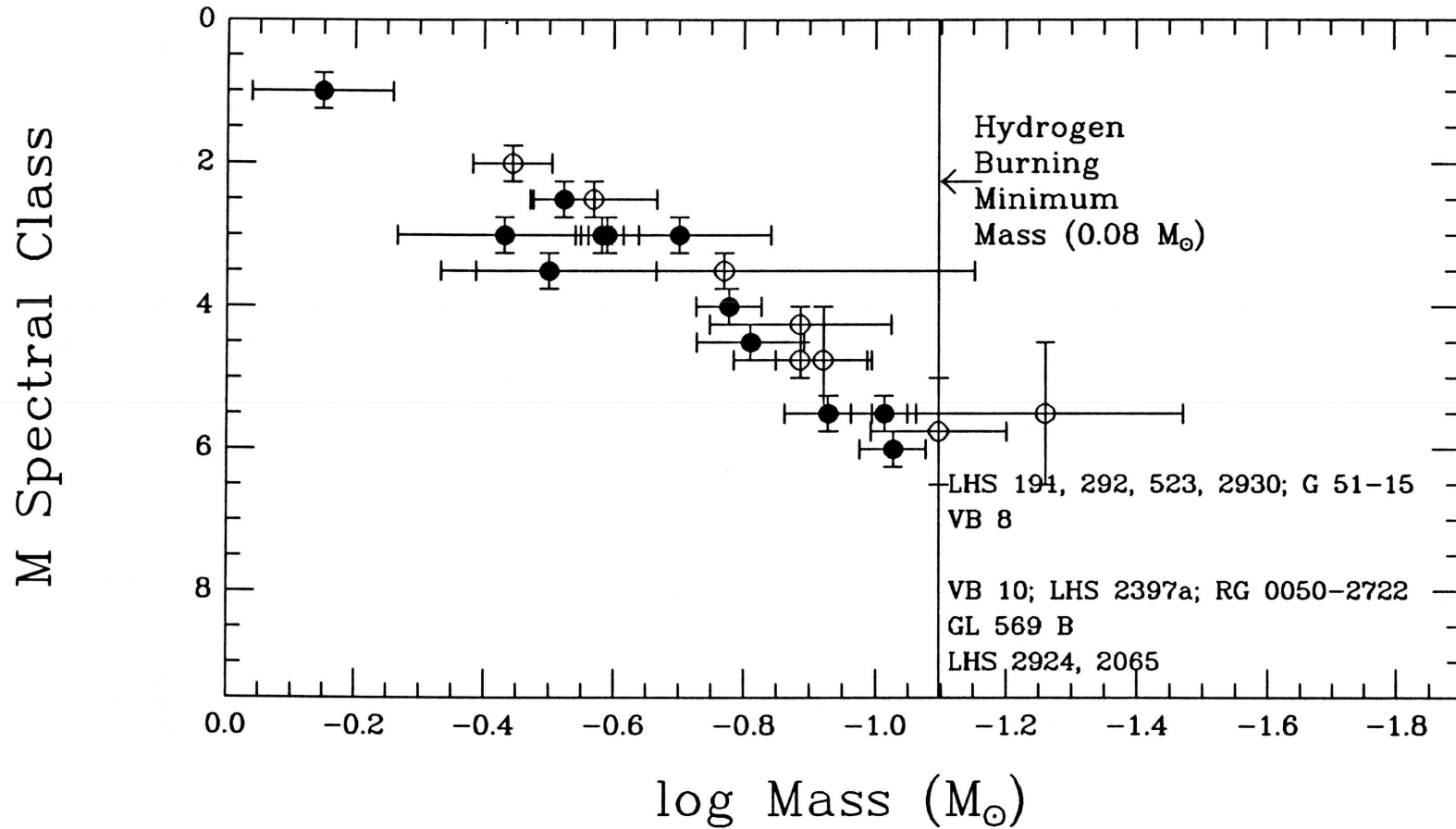


FIG. 3.26. — An adaptation of the spectral class versus mass relation for M dwarfs from Figure 3.10. The solid points are borrowed directly from Figure 3.10 except that the composite points for GL 234 AB, LHS 1047 AB, and GL 22 AC have been omitted. The open points are from Table 3.27 and represent the results of the differential spectroscopy. The aforementioned trend is confirmed based on the new data alone, and combined with the previous results suggests even more strongly that dwarfs of spectral class $\sim M7$ and later are not stars but are actually brown dwarfs.

3.5: CONCLUSIONS

The results of this chapter can be briefly summarized as follows:

- An M dwarf spectral sequence from 6300 to 9000 Å has been established, and detailed identifications have been presented for features throughout this region. Temperature-sensitive and luminosity-sensitive ratios have been used to produce quantitative classification criteria.
- The M dwarf spectral sequence has been extended into the infrared (out to 1.5 μm), and theoretical spectra have been fit to the observed 0.63-to-1.50 μm data to establish a new temperature scale for M dwarfs. The new scale agrees better with theoretical calculations of the main sequence than do previous calculations based on black-body fits.
- The 6300-to-9000 Å spectrum of GD 165 B has been obtained and compared with spectra of the other lowest luminosity objects known: LHS 2924, LHS 2065, and PC 0025+0447. Its spectrum does not resemble those of the other three objects and as such is a striking deviation from the familiar M dwarf spectral sequence. Future observations throughout the infrared are required before this object can be accurately positioned on the H-R Diagram and its true nature can be revealed.
- Differential spectroscopy has been performed on five composite systems containing a low-mass secondary. The surprising result is that these objects near the stellar/substellar break are found to have spectral types no later than M6.5, suggesting that objects of type M7 and later are bona fide brown dwarfs.

CHAPTER 4

A SEARCH FOR OTHER LOW-MASS OBJECTS

Ye little stars! Hide your diminished rays.

— Alexander Pope, Moral Essays, Epistle III, l. 282 (1731-1735)

This chapter describes the search — using photometric data provided by the CCD/Transit Instrument (CTI) — for stars of extremely low mass. The reddest objects discovered in the data bases have also been targeted spectroscopically in an attempt to assess the accuracy of the CTI photometry near the magnitude limit of the survey and to identify previously unknown, very late M dwarfs in the solar neighborhood. The selection of spectroscopic targets and the follow-up observations are discussed in §4.1.

Using this complementary spectroscopic information together with CTI photometry of all stars in the strip, a luminosity function for M dwarfs is produced. No other recent photometric determination of the faint end of the stellar luminosity function has obtained spectra to check the majority of targets found in the lowest luminosity bins as well as a sampling of stars found in the higher luminosity bins. These data can provide adequate statistics on the percentage of contamination by objects such as M giants and M subdwarfs and can also be used to verify that objects falling in the intrinsically faintest (and most crucial) bins are legitimate objects of extreme type. The derivation of the CTI luminosity

function is detailed in §4.2 along with a comparison to previously published versions of the luminosity function. Implications for the mass function are presented in §4.3. Results of this chapter are summarized in §4.4.

4.1: THE SEARCH FOR LATE-M DWARFS IN THE CTI STRIP

A thorough search of the CTI photometric data bases was begun in 1989 to identify late-K to late-M dwarfs. A subset of these objects has been observed spectroscopically with the MMT Red Channel using the setup described in the previous chapter. These spectra are used first to define a sequence of dwarf stars stretching from K5 to late-M so that a calibration of internal CTI $R - I$ and $V - I$ colors (hereafter denoted with the subscript CTI) with spectral type could be produced. (The magnitude limits and photometric calibration to a standard system are addressed in §4.3.) Once this correlation is established, an intensive search for stars later than M6 can begin.

4.1.1: Object Selection

a) Photometric Interrogations of Single-night Data

The data used for this survey rely primarily upon the R_{CTI} and I_{CTI} photometry, with V_{CTI} being utilized whenever available. During the search for spectroscopic targets, R_{CTI} and/or I_{CTI} data had not yet been entered into the data bases for $4^h30^m \leq \text{RA} \leq 6^h30^m$ and $20^h00^m \leq \text{RA} \leq 22^h30^m$, both of which are areas in and around the galactic plane. Furthermore, the region having $4^h00^m \leq \text{RA} \leq 4^h30^m$ encompasses the Taurus Molecular Cloud complex which, because of the reddening present, was excluded from the search area. Over the remaining sections of right ascension, the CTI data base known as the “pool list” (containing photometric data on all images ever identified during the

reduction process) was used to select the target objects. Objects were first selected over a range of $(R - I)_{CTI}$ color as a means of correlating $(R - I)_{CTI}$ and $(V - I)_{CTI}$ with spectral class. Later, objects with extremely red colors, typically $(R - I)_{CTI} \geq 1.50$, were the primary targets of the data base interrogations, although subsets of stars with $(R - I)_{CTI} < 1.50$ were selected as cloudy night back-up targets since brighter examples of these objects can be found throughout the strip.

After the data base interrogations, the identified red objects were visually identified on the reduced CCD images to check for merges with other objects, for photometric contamination by bright stars, or for objects lying too near the edges of the frame. If the object's image appeared to be free from these effects, a finder chart was produced. The latest object found from this data base interrogation was a dwarf of type M8.5. A color-color diagram using the $(V - I)_{CTI}$ and $(R - I)_{CTI}$ colors of the spectroscopic targets is given in Figure 4.1 to show the locus occupied by main sequence stars.

b) Photometric Interrogation of Coadded Data

Coadditions of many nights of CTI data can also be done to probe deeper than the nightly limiting magnitudes given in the "pool list." Coadditions in R_{CTI} , I_{CTI} , and sometimes V_{CTI} were performed on $\sim 2^h$ of the 24^h total in the strip. This is an extremely time-consuming process, which is why only a total of 2^h has been completed. To examine small areas having the most archived CTI data, regions spanning only $\sim 5^m$ in RA were summed at a time. In general, the coadditions at I_{CTI} included no more than 9 nights of (high-quality) data,

those at R_{CTI} had no more than 8, and those at V_{CTI} had as many as 27. It has been found that coadding 9 nights at I_{CTI} enables the survey data to probe ~ 2.2 magnitudes deeper than a single night's data, and coadding 8 nights at R_{CTI} improves the R_{CTI} limit by ~ 1.8 magnitudes. However, many of the areas have only 2 or 3 nights of I_{CTI} data and 3 or 4 of R_{CTI} , which extends the limit by only one magnitude or less.

The RA centers for each of the 5^m coadded regions are 00^h15^m , 01^h03^m , 01^h27^m , 01^h57^m , 02^h51^m , 13^h18^m , 13^h42^m , 14^h15^m , 14^h42^m , 15^h06^m , 15^h39^m , 16^h09^m , 18^h03^m , 19^h00^m , 19^h12^m , 20^h27^m , 21^h03^m , 22^h06^m , 22^h54^m and 23^h36^m . Despite the facts that some of these regions do not have both R_{CTI} and I_{CTI} photometry in the “pool list” and that the regions probe more deeply than the “pool list,” very few extremely red stars were found that had not previously been discovered during the data base interrogations. The latest of these were an M6 dwarf and an M6.5 dwarf.

c) Other Checks of the Data

Additional information can also be acquired for these objects. The finder charts can be compared to POSS prints of the same field to check visually for proper motion. This visual check is reliable only for proper motions exceeding ~ 0.2 arcsec/yr, and then only if the field has a sufficient number of stellar images to use as positional comparisons. For many of the objects observed with the Red Channel, CTI light curves have been produced to check for possible variability. However, because most of the data entered into the data bases have been V_{CTI} measurements, only light curves at V_{CTI} can currently be examined.

4.1.2: Spectra of CTI Objects

In total, 133 spectra have been obtained of CTI objects. Appendix A includes finder charts, coordinates, photometric data, spectra, and special notes on variability, proper motion, etc. for each of the spectroscopic targets. Each spectrum is typed using the least-squares minimization technique of Chapter 3, with luminosity classes being assigned through the use of color ratios. Figure 4.2 plots the values of these ratios (defined in Table 3.7) for each of the spectra having signal-to-noise ratios of ~ 7 or better. For the seventeen spectra having poorer quality data, luminosity classes are assigned by eye — but all have the appearance of dwarfs.

a) Giants and Subdwarfs

Of the 133 objects, 7 are giants. Six of these lie within $\sim 10^\circ$ of the galactic plane, and the seventh, at a galactic latitude of -31° , has $R_{CTI} \approx 11$. Light curves have been produced for six (the exception is the M4 III star CTI 192853.3+280415), and all show marked variability. These are Mira-like variables, and the brightest one, CTI 190917.7+280305, is listed in the General Catalogue of Variable Stars (Kholopov 1985) as TY Lyrae. The others have not been previously designated as variable stars.

Two of the 133 objects are found to be marginal subdwarfs — CTI 000351.3+280138 and CTI 225431.2+ 280046. No extreme, metallic hydride subdwarfs are found. All of the other 124 spectra have dwarf luminosity classifications.

b) Very Late M Dwarfs

A total of eighteen spectra have been classified as dwarfs of type M6 or later. There are twelve objects with spectral types of M6 V, four with M6.5 V, one with M7 V (CTI 115638.5+280002), and one with M8.5 V (CTI 012657.5+280202). This last object is one of the reddest dwarfs currently known; only LHS 2924, LHS 2065, PC 0025+0447, and GD 165 B are known to be of later type. Each of these should be studied more closely to see if companions are present, and if so, follow-up studies could eventually lead to all-important mass determinations for the components.

c) Objects with Large Proper Motion

The comparison of the CTI finder charts in Appendix A to the POSS E prints has revealed a number of proper motion objects with $\mu > 0.2$ arcsec/yr. Confirmation of these motions falls beyond the scope of this thesis, but it is worth noting that a few of these spectroscopic targets may have $\mu > 1.0$ arcsec/yr. As Benedict et al. (1991) have shown, a ten-night set of CTI frames taken over a 3-year baseline would be sufficient to detect stars with proper motions exceeding 0.175 arcsec/yr. Thus, CTI data alone could potentially be used to determine the motions of these high- μ suspects.

4.2: DETERMINATION OF THE LUMINOSITY FUNCTION FROM CTI DATA

The first step in determining the luminosity function is to calibrate the photometry to a standard system so that $(R - I)_{CTI}$ color and I_{CTI} magnitude can be transformed into an absolute magnitude and a distance. The completeness limit of the survey must then be judged, and the contamination of the photometric sample by non-dwarf objects must be assessed. Once these parameters are known, the data can be binned to produce a luminosity function.

4.2.1: Photometric Calibration

With the spectroscopic data completed, a subset of stars having a range of M dwarf spectral types was chosen for calibration photometry. This CCD photometry was obtained at the USNO 1.0-m reflector on UT 1992 Jun 20 by Conard C. Dahn, on 1992 Jul 1 and 2 by Hugh C. Harris, and on 1992 Jul 5 and 6 by the author in collaboration with Conard C. Dahn. The CTI objects were observed at V and I on the Kron-Cousins system (hereafter denoted by the subscript KC) and reduced according to the procedures outlined in Monet et al. (1992). A listing of the USNO photometry and the CTI photometry for each of the objects observed is given in Table 4.1. As a diagnostic check, Figure 4.3 is also presented. Here, M dwarf spectral class is plotted against $(V - I)_{KC}$ and against $(R - I)_{CTI}$. There is a trend of increasing color with later spectral type, as would be expected, on both plots, except that four points have $(R - I)_{CTI}$ colors which deviate from the trend. These same four stars have $(V - I)_{KC}$ colors which are consistent with the rest of the data. Each of these has $R_{CTI} > 19.5$,

and for three of them, the errors on $(R - I)_{CTI}$ exceed 0.5 magnitude. For subsequent analyses, these four objects have been omitted.

The remaining data can be used to determine the transformation between $(R - I)_{CTI}$ and $(V - I)_{KC}$. This is shown graphically in Figure 4.4. A weighted linear least-squares fit to the data yields the equation

$$(R - I)_{CTI} - 1.50 = a + b[(V - I)_{KC} - 3.25], \quad (4.1)$$

$$\text{where } a = -0.136 \pm 0.019$$

$$\text{and } b = 0.713 \pm 0.022.$$

This fit is shown by the solid line in Figure 4.4.

Using the CCD photometry and parallax data presented in Monet et al. (1992), a transformation from $(V - I)_{KC}$ to $M_{I_{KC}}$ can be made. These data are presented in Figure 4.5. Based on the location of objects on the color-magnitude diagram (Figure 10 of Monet et al. 1992), eighteen objects in their Table 1 have been labelled as subdwarfs and another ten as white dwarfs; these non-dwarfs are omitted from Figure 4.5. Unpublished tables of dwarf photometry covering the other data points in their Figure 10 have been kindly provided by Conrad C. Dahn and are also presented in Figure 4.5. In addition, because the CTI strip has no stars as late as M9 and because this is the point at which the $(V - I)_{KC}$ color begins to turn *bluer* with later spectral type, the two M9 V stars LHS 2924 and LHS 2065 have been omitted from Figure 4.5.

These data require a correction which depends upon the size of the errors in the trigonometric parallaxes used to calculate each $M_{I_{KC}}$. A parallax value of $\pi \pm \sigma$ is more likely to represent a star further away ($\pi - \sigma$) than a star closer ($\pi + \sigma$) because the volume of space between parallax values of π and $\pi - \sigma$ is

larger than that sampled between parallax values of π and $\pi + \sigma$. The observed values of π are thus larger than the true values, and hence the resulting absolute magnitudes will be systematically too large. Lutz & Kelker (1973) have shown that a correction can be applied which depends only upon the value of σ/π . This correction to M_{IKC} has already been applied to the individual data points in Figure 4.5. (As Lutz & Kelker (1973) have shown, trigonometric parallaxes having $\sigma/\pi > 0.175$ have indeterminate corrections, so points with large parallax errors have been omitted from Figure 4.5.) A second-order least-squares fit to these resulting points gives the relation

$$M_{IKC} - 11.50 = c + d[(V - I)_{KC} - 3.25] + e[(V - I)_{KC} - 3.25]^2, \quad (4.2)$$

$$\text{where } c = -0.816 \pm 0.037,$$

$$d = 2.334 \pm 0.053,$$

$$\text{and } e = -0.107 \pm 0.055.$$

Finally, I_{CTI} can be related to I_{KC} . A plot of ΔI vs. $(V - I)_{KC}$ (data from Table 4.1) is presented in Figure 4.6. A weighted linear least-squares fit, shown by the solid line, represents the trend well. This fit is given by

$$I_{CTI} - I_{KC} = f + g[(V - I)_{KC} - 3.25], \quad (4.3)$$

$$\text{where } f = 0.020 \pm 0.009$$

$$\text{and } g = -0.072 \pm 0.010,$$

showing that the transformation between the two systems requires a small color term. The above sequence of equations transforms the I_{CTI} and $(R - I)_{CTI}$ values for any given object into a value of M_{IKC} and a distance for that object.

A correct transformation of color into absolute magnitude is, however, of utmost importance to an accurate derivation of the luminosity function. Although obvious subdwarfs have been removed from Figure 4.5 before the determination of equation 4.2, the data used to construct this relation are based primarily upon a *kinematically* selected sample of objects (mainly objects chosen from the proper motion lists of Luyten and Giclas). On the other hand, the CTI data to which the transformation will be applied represent a *photometrically* selected sample. To address this bias, U, V, W space motions for many of the objects plotted in Figure 4.5 have been found in Gliese & Jahreiss (1991). According to Mihas & Binney (1981b), the V space motions of M dwarfs average around -15 to -19 km/sec, whereas subdwarfs have average V space motions of -150 km/sec. Figure 4.7 breaks the stars in Figure 4.5 into three different V velocity bins. Figure 4.7a shows the low-velocity sub-sample ($V > -30$ km/sec); Figure 4.7b shows the intermediate-velocity sub-sample ($-100 \text{ km/sec} < V \leq -30 \text{ km/sec}$); and Figure 4.7c shows the high-velocity sub-sample ($V < -100 \text{ km/sec}$). For each part of the figure, the second-order fit from Figure 4.5 is shown. The bright end of the low-velocity sample in Figure 4.7a falls largely *above* the previous relation, whereas the bright end of the high-velocity sample in Figure 4.7c falls largely *below*. Figure 4.8 shows the low-velocity sub-sample of Figure 4.7a and a second-order least-squares fit to the sub-sample, which is given by

$$M_{I_{KC}} - 11.50 = h + j[(V - I)_{KC} - 3.25] + k[(V - I)_{KC} - 3.25]^2, \quad (4.4)$$

$$\text{where } h = 0.003 \pm 0.014,$$

$$j = 4.254 \pm 0.044,$$

$$\text{and } k = -0.293 \pm 0.013.$$

Because of a lack of data at the faint end, this calibration should only be considered valid for $(V - I)_{KC} < 3.0$.

The calibration given by equation 4.2 is biased towards higher velocity stars; equation 4.4 is biased towards low-velocity stars. Because a photometrically selected sample will choose stars regardless of kinematics, the true calibration needed to convert the CTI colors into absolute magnitudes lies somewhere *between* the calibrations given by these two equations. Therefore, to bracket the true luminosity function, two different luminosity functions should be derived, one using equation 4.2 and the other using equation 4.4.

4.2.2: Completeness and Contamination in the Strip

a) Completeness Limit at R

In a search for red objects where the principle criterion for selection is an $R - I$ color, the limit of the survey is dictated by the magnitude limit at R . To determine the limiting R_{CTI} magnitude of the strip, objects in a very narrow range of color, $0.99 \leq (R - I)_{CTI} \leq 1.01$ (corresponding to a spectral class of $\sim M3$), have been selected from the “pool list” over the region $0^h \leq RA < 2^h$. In this region of right ascension, the galactic latitude maintains a nearly constant value of -35° . The number of objects for each 0.2-magnitude bin in R_{CTI} is shown by the solid line in Figure 4.9.

For a constant space density of stars, the ratio of star counts in a shell with thickness Δm_1 to the star counts in the next adjacent shell of thickness Δm_2 (where Δm refers to the change in apparent magnitude between the far and near

sides of the shell) is

$$\frac{V_2}{V_1} = \frac{10^{\frac{3\Delta m_2}{5}} - 1}{1 - 10^{\frac{-3\Delta m_1}{5}}}, \quad (4.5)$$

$$\text{or } \frac{V_2}{V_1} = 10^{\frac{3\Delta m}{5}} \quad \text{if } \Delta m_1 = \Delta m_2 = \Delta m. \quad (4.6)$$

For star counts out of the plane of the galaxy, however, the space density is not constant for successive shells but drops off as the perpendicular z distance from the plane increases. The density $D(z)$ of stars is well represented by the expression

$$D(z) = D_0 e^{\frac{-|z|}{\beta}} \quad (4.7)$$

where D_0 is the density of stars near the sun, z is the height of the star away from the plane, and β is the scale height. For the data examined here, this expression becomes

$$D(z) = D_0 e^{\frac{-d \sin 35^\circ}{\beta}}, \quad (4.8)$$

where d is the distance to the star from the sun. The scale height of dwarf M stars is given as 350 pc by Mihalas & Binney (1981a) and as 300 pc by Gilmore & Reid (1983). A value of $\beta = 350$ pc is adopted here, but it can be shown that a value of $\beta = 300$ pc does not change the results.

Using these two expressions, the percentage change in star counts from one bin to the next can be predicted. The dotted line in Figure 4.9 is this prediction normalized to the observed counts at $R_{CTI} = 19.1$, and the dashed line shows the prediction when normalized to the observed counts at $R_{CTI} = 18.9$. These predictions demonstrate that the CTI survey is not complete beyond $R_{CTI} = 19.5$. Based on this plot, a magnitude of $R_{CTI} = 19.0$ is chosen as a conservative estimate of the completeness limit of the CTI survey.

b) Area of Sky Covered

Based on data obtained during the interrogation for spectroscopic targets, the useable portion of the CTI strip is found (by eliminating objects falling too near the north or south edges of the CCD frames) to have an extent of $\sim 8'10''$ in declination. The northern and southern extremes of the strip are roughly $\delta_{south}(1987.5) = 27^\circ 58'25''$ and $\delta_{north}(1987.5) = 28^\circ 06'35''$. The area encompassed by the strip is given by

$$\begin{aligned} \text{Area}_{CTI} &= \frac{\text{Area}_{CTI} \text{ (steradians)}}{\text{Area}_{sky} \text{ (steradians)}} (\text{Square degrees on celestial sphere}) \\ &= \frac{\int_{\delta_{south}}^{\delta_{north}} 2\pi \cos\theta d\theta}{4\pi} (41252.96124) \text{ square degrees} \\ &= 43.3 \text{ square degrees,} \end{aligned} \tag{4.9}$$

where the value of square degrees on a sphere comes from Abell (1982).

Because of interstellar reddening near the galactic plane, the full 24^h range of right ascension will not be used. Maps of H I column densities and galaxy counts given in Burstein & Heiles (1982) give the total line-of-sight reddening as a function of galactic latitude and longitude. If the reddening material is assumed to have a scale height of ~ 100 parsecs like that of the H I, and if this material is assumed to be uniformly distributed along the line of sight, the total reddening out to a specified distance within the galaxy can be estimated. With these maps and input assumptions, plots of $E(B - V)$ as a function of right ascension along the CTI strip can be produced. These have been kindly provided by Conard C. Dahn. Assuming a distance of 100 pc, $E(B - V)$ never exceeds 0.03 magnitude for right ascensions more than 20° away from the galactic plane ($03^h 47^m \leq \text{RA} < 07^h 26^m$ and $18^h 12^m \leq \text{RA} < 21^h 51^m$), except for the region

$3^h < \text{RA} < 3^h 30^m$, where the excess reaches 0.06 magnitude. Johnson (1965) presents mean extinction data for various colors along different lines-of-sight, and his average measurement of $E(R - I)/E(B - V)$ is 0.80, if the Orion region is excluded. Therefore, only the data having $\text{RA} < 3^h 00^m$, $7^h 26^m \leq \text{RA} < 18^h 12^m$, or $\text{RA} \geq 21^h 51^m$ will be used since in these regions the data have a negligible value of $E(R - I) \leq 0.02$.

Finally, no R_{CTI} and/or I_{CTI} data exist for $21^h 51^m \leq \text{RA} < 22^h 36^m$. This, combined with the above restrictions on RA, reduces the percentage of useable area in the strip to 63.2%, or 27.4 square degrees.

c) Contamination by Non-dwarfs

Contamination of the CTI photometric data by objects which are not dwarfs has been examined in the previous section. Spectroscopy revealed 2 subdwarfs out of 133 objects. This $\sim 2\%$ contamination by subdwarfs is negligible.

A total of 7 giants was discovered among the 133 spectroscopic targets. Six fall within $\sim 10^\circ$ of the galactic plane, and the seventh is sufficiently bright that the distance derived using its $(R - I)_{CTI}$ color in the dwarf calibration equations would be conspicuously small. Thus, excluding areas near the galactic plane assures that contamination by giants is also negligible.

4.2.3: Analysis of the Photometric Data

a) Imposed Distance Limit

With the transformations to a standard system established and with completeness and contamination problems assessed, the data bases can now be interrogated. Because of the large area covered by this survey and because of the faint limiting magnitude attained, there will be a sufficient number of objects per bin in the luminosity function even if a distance limit of 100 parsecs is imposed upon the sample of stars. The reason for limiting the sample volume to this radius is twofold:

- (1) The drop in star density for areas out of the plane will be negligible at this distance. At the North Galactic Pole, the density of M dwarfs will have dropped to 72% of its value in the solar neighborhood; for areas in the strip which look more obliquely along the galactic plane, the decrease in density at 100 parsecs is even less than this. If objects much greater than 100 parsecs were to be included, the exponential factor, which for a given distance depends upon the galactic latitude and hence upon the right ascension, would have to be incorporated into the star counts to normalize the computed density to the value in the solar neighborhood. This factor depends upon the scale height, which is not accurately known and thus inserts another uncertainty into the calculations.
- (2) For distances under 100 parsecs, reddening problems will be minimized. (See discussion in §4.2.2 above.)

b) Scrutiny of the Photometrically Selected Objects via Internal Checks

For the calculation of the luminosity function, the CTI “master list” was used since this data base contains only those objects which have a high probability of being real detections (unlike the “pool list” which includes photometric information for *all* identified objects). The data were searched for all objects having $M_{I_{KC}} \geq 8.00$ and derived distances not exceeding 100 parsecs. This resulted in the discovery of 283 candidates.

The selection of candidates indicates that there are some values of right ascension which occur more frequently than would be expected from a random distribution of M dwarfs along the strip. In particular, there are twelve small regions having a preponderance of red objects, and at each of these regions a nearby, bright star was found. These stars are generally of late type themselves, and they greatly influence the photometric measurements of other objects lying near them on the sky. The identification of these affected areas resulted in the removal of 117 objects. A list of these bright stars is given in Table 4.2. CTI images show the affected region around β Geminorum (Pollux) to be $\sim 3^m 30^s$ long; a smaller area ($< 3^m$ long) around β Pegasi (Scheat) is also affected. (The other bright star mentioned in Chapter 2, β Cygni (Albireo), does not fall in the range of right ascension discussed here.) The fainter stars in Table 4.2 contaminate much smaller regions. If a total area of $\sim 7^m$ in right ascension is assumed to be unuseable because of bright stars, then the useable portion of the strip is only 27.2 square degrees, instead of 27.4. This small change in total area would increase the resulting logarithmic space densities by only 0.003, which is considered negligible.

Two additional objects were excluded because their values of R_{CTI} and $(R - I)_{CTI}$ would indicate that $V_{CTI} < 19.0$ for each, yet neither was detected at V . These two objects, CTI 002737.2+280025 and CTI 170411.6+280620 are considered spurious and are not considered further. Also, because of the large photometric uncertainties for extremely faint objects, no objects with $R_{CTI} \geq 20.0$ have been used for the determination of the luminosity function. (Although the *completeness* limit has been taken to be $R_{CTI} = 19.0$, the *limiting magnitude* is chosen to be $R_{CTI} = 20.0$.) This criterion has led to the elimination of another eight objects. Another object, CTI 103415.5+280117, has been excluded because it is merged with another object on the CCD frame.

For the remaining 155 objects, those with $M_{IKC} < 12.0$ all have I , R , and V measurements, so color criteria based on the results of Figure 4.1 can be employed to discard obviously bad data. A plot of $(V - I)_{CTI}$ vs. $(R - I)_{CTI}$ for these objects is shown in Figure 4.10. Objects lying along the locus of main sequence stars (defined by Figure 4.1) are denoted by filled circles, and those points with discrepant photometry are denoted by open circles. (Three additional points are so discrepant that they fall off the plot as shown.) Using this plot, a total of 19 objects is eliminated. To aid in further checking the validity of remaining objects, Figure 4.11 is produced. This plot shows $(B - I)_{CTI}$ vs. $(R - I)_{CTI}$ for those objects in Figure 4.10 having B_{CTI} photometry. At first glance, Figure 4.11 appears to show a second sequence of stars lying beneath the sequence defined by the majority of the objects. This second sequence, however, does not represent a sequence of giants or subdwarfs, as verified by Figure 4.12, which shows the $(B - I)_{CTI}$ vs. $(R - I)_{CTI}$ diagram for spectroscopically observed dwarfs (filled circles) and giants (open triangles). The dwarf targets are shown to have a large

scatter of $(B - I)_{CTI}$ values, and two spectroscopically identified giants having $R_{CTI} > 12.0$ do not distinguish themselves from the dwarfs on this plot. Because M giants are high amplitude variable stars and because CTI cannot acquire B and I (for example) simultaneously, it is not clear what the $(B - I)_{CTI}$ values for these objects actually represent. Over time, with the inclusion of many more nights of data into the data bases, these will reflect the mean colors of the giants over their light curves. Despite this problem with separating the luminosity classes via color-color diagrams, spectroscopy has, as noted previously, already shown that giant contamination is negligible. At a later time, light curves of all selected objects can be produced from CTI data so that any giants which may still be contaminating the counts can be removed.

Of the nine objects having $M_{IKC} \geq 12.0$, seven have been observed spectroscopically and have dwarf spectral types of M6 or later. A spectrum of CTI 022000.5+275933 has not been acquired, but because its finder chart shows it to be free from sources of photometric contamination, it is retained. A spectrum of CTI 153915.6+280445 has also not been obtained, but this object, along with CTI 174729.0+280322 (M6.5 V), falls outside of the distance limit (72 pc) of its absolute magnitude bin (see discussion below).

As a final internal check, Figure 4.13, which plots the number of remaining objects vs. right ascension, is produced. Within the (Poissonian) errors, this histogram is, as one would expect, flat. The total number of objects thus remaining is 136.

c) Scrutiny of the Photometrically Selected Objects via External Checks

As an external check of the completeness of the CTI data, the NLTT Catalogue (Luyten 1979) is used to generate a list of proper-motion selected objects lying in the CTI strip. These objects are given in Table 4.3. Column 1 gives the LP or other name of the 60 NLTT objects falling in the strip; columns 2 and 3 give the magnitudes as listed in the NLTT Catalogue; column 4 lists Luyten's color class of the object; and column 5 gives the proper motion in arcseconds per annum. Incorporating both proper motion as well as precession of the coordinates (using the precession coefficients listed in Lang 1980), the 1950 positions are updated to equinox 1987.5 coordinates (epoch 1987.5) to give a predicted CTI positional designation for each of these objects. These predicted coordinates are listed in columns 6 and 7. The CTI "master list" is then searched for objects near these locations, yielding the corresponding CTI name of the NLTT star as listed in column 8. Columns 9 and 10 list the R_{CTI} and I_{CTI} photometry of the objects.

Of the 60 objects, 58 were clearly detected by the CTI. Of the two not detected, Wolf 411 ($m_r = 11.1$) and LP 340-555 ($m_r = 11.3$) are bright enough so that saturation problems in the CCD system and subsequent CTI photometric analysis have, most likely, failed to distinguish these objects as single entities; β Gem, for example, is broken into many photometric segments by the CTI photometry routines, and the segment falling nearest the predicted position has a magnitude of only $V_{CTI} = 10.8$. There is little doubt that stars this bright could have been "missed."

Column 11 of Table 4.3 gives a note indicating if the object is used toward the construction of the CTI luminosity function (Table 4.4) and if not, why it is not used. Some fall outside of the range of RA being used for the analysis, others are too blue ($(R-I)_{CTI} < 0.60$), others are too bright ($R_{CTI} < 12.0$), and others are determined to be beyond the 100-pc cutoff (in which case the derived distance is listed). In total, there are 12 objects out of 60 which satisfy the criteria used for determination of the luminosity function. In summary, this external check shows that the CTI has detected, with 100% success, objects listed in Luyten's volumes. Therefore, the percentage of objects which should have been detected by the CTI but which were missed during photometric reductions is negligibly small. The main reason for missed objects is the incompleteness at very faint ($R_{CTI} > 19.0$) magnitudes.

4.2.4: CTI Luminosity Function and Comparison to Others

The final list of objects used in the derivation of the luminosity function is presented in Table 4.4, which is a compendium of sub-tables, one for each of the twelve half-magnitude bins between $M_{IKC} = 8.00$ to 14.00. Listed are the CTI designation for each object, the R_{CTI} magnitude and $(R-I)_{CTI}$, $(V-I)_{CTI}$, and $(B-I)_{CTI}$ colors, the derived absolute magnitudes at I_{KC} and V_{KC} , the distance and its propagated error, and the resulting value of V/V_{max} . In this last quantity, V is the volume of the sphere having a radius equal to the object's calculated distance, and V_{max} is the maximum value of V for which the object would still be included in the luminosity function — which, for all but the faintest bins, is a volume of 100-pc radius.

The first bin, centered at $M_{IKC} = 8.25$, is incomplete because non-linearity effects in the CCD make photometry for stars with $R_{CTI} < 12.0$ unreliable. The bin centered at $M_{IKC} = 12.25$ is marginally incomplete since an object having $M_{IKC} = 12.50$ and lying 100 parsecs away would have $R_{CTI} = 19.40$, fainter than the completeness limit of the strip. The three lowest luminosity bins are not complete to 100 parsecs even when the limiting magnitude of $R_{CTI} = 20.0$ is considered. These only probe to distances of 97, 72, and 53 parsecs for bin centers of $M_{IKC} = 12.75$, 13.25, and 13.75, respectively.

The average V/V_{max} values for each bin are listed in the footnotes of Table 4.4. For a randomly distributed sample of stars, the V/V_{max} average in each bin should be 0.5 since half of the objects in the bin should lie in the nearer half of the volume, and the rest should lie in the farther half. If this number is not near 0.5, then the sample is either not uniformly distributed or is incomplete. Within the errors, however, all of the bins have $V/V_{max} \sim 0.5$, with the exception of the faintest, which contains only one point. The number of objects found in each bin is summarized in Table 4.5, along with the distance probed by each (the volume is 2782 pc^3 for $d = 100 \text{ pc}$), and the logarithm of the observed luminosity function Φ_{obs} , in units of number per cubic parsec per unit M_{IKC} bin.

This “uncorrected” luminosity function is shown in Figure 4.14 (solid symbols), along with the M_{IKC} luminosity function at the South Galactic Pole (open circles) as determined by Leggett & Hawkins (1988). The error bars represent the square root of the number of stars in each bin. Note that the number of stars predicted by the two samples are virtually the same within the errors. Both luminosity functions show an upturn in the luminosity function beyond $M_{IKC} = 12.5$, though these upturns are based on usually one or two objects per

bin. The upturns are consistent with the theoretically predicted contribution by brown dwarfs to the luminosity function. The dashed line in Figure 4.14 shows the brown dwarf luminosity function calculated by Nelson, Rappaport, & Joss (1986) and normalized so that $0.08 M_{\odot} pc^{-3}$ is the total local mass density of substellar objects.

If calibration equation 4.4 (based on low-velocity parallax stars only) is used instead of equation 4.2, this changes the makeup of the first three bins of the luminosity function. The new membership of the first three bins is shown in Table 4.6. This dramatically alters the shape below $M_{IKC} = 10.0$, as shown by the open circles in Figure 4.15. The true luminosity function for $8.00 \leq M_{IKC} \leq 9.50$ falls somewhere between the solid circles and the open circles in the figure.

As presented, none of the luminosity functions in Figures 4.14 or 4.15 has been corrected for the Malmquist effect or Malmquist bias, which can be thought of as the absolute-magnitude analogue of the Lutz-Kelker. For a full description of the Malmquist corrections, see Stobie, Ishida, & Peacock (1989) and Leggett & Hawkins (1988). Once the “uncorrected” luminosity function $\Phi(M)$ has been calculated, the Malmquist correction, which depends upon the first and second derivatives of $\Phi(M)$, can be applied to the star counts in each bin. This is accomplished via the equation

$$\frac{N_{obs}}{N_{true}} = 1 + \frac{\sigma_M^2}{2} \frac{1}{\Phi(M)} \left[10^{-0.6M} (0.6 \ln 10)^2 \Phi(M) - 1.2 \ln 10 \frac{d\Phi}{dM} + \frac{d^2\Phi}{dM^2} \right], \quad (4.10)$$

where N_{obs} is the observed number of objects in the bin, N_{true} is the true number of objects, and σ_M is the typical error in absolute magnitude. Values for the quantities σ_M , N_{obs}/N_{true} , and $\log \Phi_{true}$ are also given in Table 4.5. The derivatives are computed by using the forward- and central-difference formulas

given in Conte & de Boor (1980). Figure 4.16 compares the uncorrected CTI luminosity function (solid circles and triangles) with the luminosity function once the Malmquist correction has been applied (solid squares). The absolute magnitude errors in the faintest bins are so large that accurate corrections cannot be applied.

Also shown in Figure 4.16 (open squares) is the luminosity function for objects within 5.2 parsecs of the sun and north of $\delta = -20^\circ$ (updated here but originally presented in Dahn, Liebert, & Harrington 1986). For comparison to this version of the CTI luminosity function, the 5.2-parsec sample was recomputed at I (photometry from Leggett 1992) and supplemented with the newest trigonometric parallax data from Gliese & Jahreiss (1991). The data for these objects are given in Table 4.7. All objects with $M_{I_C} \geq 7.0$, $\delta \geq -20^\circ$, and $d < 5.2$ parsecs listed in Gliese & Jahreiss (1991) are tabulated, with the exception of white dwarfs. GJ 1116 A and B and GL 412 A and B, originally included in the 5.2 parsec census, now fall outside of that volume, and GL 866 is now listed as a double star. Using Probst's equations (Chapter 3.4) together with individual infrared magnitudes determined through speckle observations, the I magnitudes for the close binaries in the list have been de-convolved into their separate components. The trigonometric parallaxes are so well known that the Lutz-Kelker correction is negligible, and the errors in the absolute magnitudes will correspondingly be small, making the Malmquist correction negligible. The largest source of error comes from the paucity of known objects — Poisson errors are indicated in Figure 4.16.

The luminosity function for nearby stars is virtually flat from $M_I = 8.5$ to 11.5 with a gradual decline to $M_I = 13.5$. This form of the luminosity function is

quite different from the CTI determination. One possible reason for this is that binaries are more easily resolved in the nearby sample, and this tends to raise the faint end of the luminosity function as lower luminosity companions are found, while lowering the brighter end as the resolved primaries shift to lower luminosity bins themselves. Henry & McCarthy (1990) argue that the difference between their luminosity function for nearby stars and luminosity functions found during more distant, magnitude-limited surveys is due solely to the inability of the more distant surveys to recognize duplicity. Reid (1991), on the other hand, models the effect of unresolved binaries and finds that this effect can not reconcile the differences between the nearby sample and the more distant ones which rely on photometric parallaxes. He suggests that the solar neighborhood has an excess of low-luminosity objects.

To address this issue, the 5.2-pc sample of Table 4.7 is re-investigated. To convert this luminosity function into a luminosity function like that derived from the CTI data, three effects must be considered. First, the photometrically derived samples are based on a volume with a much larger average distance from the sun. For the 100-pc cut-off, half-volume occurs at 79 pc. If the 5.2-pc sample were moved to this distance, many of the multiple systems would be unresolvable. Second, the 5.2-pc sample relies on accurate *trigonometric* parallaxes to compute distances, whereas *photometric* parallaxes are used in the 100-pc sample. Third, because of the cosmic scatter in the absolute magnitude vs. color relation, some of the objects in the nearby sample will have estimated distances *greater* than 5.2 pc, and some objects outside of the volume will have estimates placing them *within* 5.2 pc. As a result of these three effects, a larger volume of stars needs to be considered; those stars need to be thought of as residing at a larger distance to

determine which composite systems are no longer resolvable; and $(V - I)$ colors and I photometry for each single star or system need to be used to compute absolute magnitudes and distances.

A complete sample of M dwarfs out to 7 pc was selected from Gliese & Jahreiss (1991). (Twenty-five objects, including several binaries, between 7 and 10 pc were also selected, but for none of these did the photometrically derived distance place them within 5.2 pc.) The 7-pc sample includes 74 objects. V and I photometry was provided by Conard C. Dahn or taken from Leggett (1992) for most of these; however, photometry for GJ 1005 AB was taken from Chapter 3.4, and no I photometry was found for either G 99-49 or GL 338 AB. G 99-49 is an M4 dwarf whose trigonometric parallax places it at 5.4 pc; because of its proximity to the 5.2-pc cut-off, a distance for this object derived photometrically could place it within the 5.2-pc sample. GL 338 AB has a trigonometric parallax placing it at 6.2 pc; because this binary would have composite photometry in the more distant sample, it is likely that this object's photometrically derived distance (which would be an underestimate of the true distance) would place it within 5.2 pc. The spectral types of GL 338 A and B presented in Chapter 3.1, however, indicate that this derived absolute magnitude will likely be $M_I < 8.0$, placing it outside of the sample considered here. Regardless, these two systems would add (at most) two more points to the luminosity function described below — one at mid-M types and the other at early M. Exclusion of these does not alter the conclusions which follow.

Once the remaining entries in the 7-pc sample are considered, the resulting luminosity function contains 28 “objects” of which 15 are single stars and 13 are composites (consisting of 12 binaries and 1 triple system). This result is

compared to other luminosity functions in Figure 4.17. This photometrically derived “nearby” luminosity function differs from the true nearby luminosity function in that it now predicts a peak at $M_I \sim 9.5$ (like the CTI luminosity function) and predicts fewer objects at lower luminosities (also like the CTI luminosity function). In fact, this new result is in close agreement with the CTI luminosity function over most of the range of M_I . The major, remaining discrepancy between the two occurs at the bin centered on $M_I = 11.5$. Whereas the CTI luminosity function would predict only one object in this bin, it is found that 5 “objects” actually fall there: GL 65 AB, GL 473 AB, GJ 1245 ABC, GL 866 AB, and GL 905. Thus, 80% of the “objects” are composite — the highest frequency of binaries in the other bins is 57%. This preponderance of composite systems, together with the fact that these results involve small numbers, suggests that the overabundance at $M_I = 11.5$ is a mere statistical fluctuation. Were it not for the large number of composites, fewer objects would be found in this bin and more would fall in the adjacent bin at $M_I = 12.5$, where the CTI luminosity function predicts only a lower limit. In this case, the new luminosity function presented here would very closely mimic that from the CTI. Therefore, the true 5.2-pc luminosity function and luminosity functions like the one determined from CTI data are consistent when unresolved binarity and photometric uncertainties are considered.

Using the data presented in Table 4.4, the CTI luminosity function can also be constructed at V . This is shown in Figure 4.18 and tabulated in Table 4.8. In Figure 4.18 the CTI derivation (solid symbols) is also compared to Reid & Gilmore’s (1982) derivation (open circles) which agrees well with the CTI determination. Both show a peak in the predicted counts around $M_{V_{KC}} = 12.0$

and an increase at faint ($M_{V_{KC}} > 15.5$) luminosities.

Table 4.6 can also be used to re-derive the brighter end of the luminosity function when equation 4.4 is used instead of equation 4.2. The result (Figure 4.19) is a lowering in the predicted number of stars with $10.0 \leq M_{V_{KC}} \leq 12.5$, with a possible shift in the peak of the luminosity function toward fainter magnitudes. Again, the true function lies somewhere between the solid symbols and the open symbols on the diagram.

The Malmquist correction at V is also given in Table 4.8 and is illustrated by the solid squares in Figure 4.20. This is compared to the Wielen, Jahreiss, & Kruger (1983) luminosity function (open triangles) which is based on objects known within 20 parsecs and which is basically flat for the range $12 < M_V < 17$. The disparity between the CTI sample and a sample based on nearby stars has been discussed above.

4.3: IMPLICATIONS FOR THE MASS FUNCTION

The luminosity function can also be used to address the more fundamental question: “Does the density of M dwarfs rise for lower and lower masses and if so, does this increase predict enough mass for the faintest M dwarfs (and even brown dwarfs) to account for the local missing matter?” As basic as this question is to galactic structure, it remains very difficult to answer based on the lack of observational data — and portions of the analysis frequently revert to theory.

Most derivations of the mass function (ξ = number of stars per unit mass interval per unit volume) have relied on converting absolute magnitudes at a particular bandpass into a bolometric absolute magnitude, and then with the help of some form of the mass-luminosity relation have converted these magnitudes into masses. A slightly different approach will be attempted here — one which requires fewer steps and relies only upon empirically derived quantities.

Consider the objects listed in Table 3.10. All of these objects are within 20 parsecs and have well determined parallaxes. Several of these have I photometry listed in Leggett (1992), so absolute magnitudes at I can be computed. Several of these have composite I photometry only, but in the spirit of Table 4.7 these can be de-convolved into component magnitudes based on speckle observations. Where the components are nearly equal in magnitude and mass, the joint I magnitude has been made fainter by 0.75 mag and an average of the two masses taken. In Figure 4.21 these absolute I magnitudes are plotted as a function of mass. Regrettably, this figure has only nine points and some of those have poorly determined masses, but nonetheless, a trend of decreasing mass (M) with fainter $M_{I_{KC}}$ is evident. A weighted linear least-squares fit to these data is shown by

the solid line in the figure. Its functional form is

$$\bar{M} = 0.646 - 0.046M_I. \quad (4.11)$$

Solving this equation for the minimum hydrogen-burning mass of $\bar{M} = 0.08M_\odot$ gives $M_I = 12.3$, which is the point where the luminosity function reaches its minimum. This would give credence to the ideas that (1) the rise in the luminosity function noted beyond $M_I = 12.3$ represents the appearance of the brown dwarf component, and (2) as suggested in Chapter 3.4, objects of spectral type $\sim M7$ and later are indeed brown dwarfs.

However, this relation maps M_I linearly into mass, so the shape of the mass function (ξ) mimics that of the luminosity function (Φ). This is shown by the solid circles in Figure 4.22. The mass function rises slowly toward $\sim 0.2M_\odot$, then drops off quickly toward the end of the main sequence. A similar effect, shown by the open circles in Figure 4.22, is seen even when the mass function is derived from the nearby luminosity function of Figure 4.16. One might expect *a priori*, however, that the mass function should climb steadily for decreasing mass, meaning that lower mass objects are formed in larger numbers than high mass ones throughout the M dwarf regime.

Therefore, a second fit of the M_I vs. mass data is acquired — this time with a weighted second-order least-squares solution. This fit is shown by the dotted line in Figure 4.21 and has the form

$$\bar{M} = 1.590 - 0.231M_I + 0.009M_I^2. \quad (4.12)$$

This mapping of M_I into mass results in the mass function ξ shown by the solid circles in Figure 4.23. Here, ξ increases toward $0.17M_\odot$, drops toward the

hydrogen burning limit, then begins to increase again after $0.13M_{\odot}$. The mass function derived from the nearby luminosity function (open circles) is essentially flat (within the errors) above a mass of $0.17 M_{\odot}$ and then increases dramatically towards the hydrogen burning limit. A small change in the form of the absolute magnitude-mass relation has made a substantial difference in the shape of the mass function.

The integrated mass density is nearly identical for the two nearby mass functions presented in Figures 4.22 and 4.23 — $0.014 \pm 0.001 M_{\odot} \text{ pc}^{-3}$ for $M_I \geq 8.0$ (masses below $M \sim 0.3M_{\odot}$). Unless the upward tail seen in the CTI luminosity function is indicative of a large, previously undetected population of (substellar) objects, the missing mass in the solar neighborhood is not in the form of low-luminosity M dwarfs and brown dwarfs.

4.4: SUMMARY

The CTI data base has been used to search for previously unrecognized M dwarfs of extremely late type. In total, eighteen objects having classifications of M6 V or later were found, and the latest of these has a spectral type of M8.5, ranking it with the latest “dwarf” objects known.

The CTI data base has also been used to construct the stellar luminosity function for M dwarfs at both I and V . Both exhibit a slow rise for the early M stars, reaching a peak at $M_I \sim 9.5$ ($M_V \sim 12.0$), then declining rapidly to a minimum at $M_I \sim 12.0$ ($M_V \sim 15.5$). At fainter magnitudes there appears to be an increase in the number density which might be caused by a brown dwarf component of the luminosity function.

Comparisons of these luminosity functions to others derived by Leggett & Hawkins (1988) and Reid & Gilmore (1982) show that the same general result is found. The luminosity function for stars within 5.2 and 20 parsecs shows an essentially constant density except for the faintest bins. It has been illustrated that this effect is caused by the resolving of binaries into their individual components for the nearby surveys, whereas for the more distant surveys, these systems show up as single points in higher absolute magnitude bins.

Lastly, unless the upturn seen for the faintest magnitudes of the CTI luminosity function is suggesting a large population of still undetected objects, the missing mass, if there *is* mass missing, is *not* in the form of low-luminosity M dwarfs. Obtaining this result has, however, highlighted the current difficulty in relating the luminosity function to a mass function. Until more observational data points linking absolute magnitude with mass are measured, the difficulty

will remain. This involves the search for and follow-up investigation of more late-type objects — some of which, it is hoped, will be members of close binary systems so that dynamical masses can eventually be determined. These objects will also aid in better defining the faint end of the luminosity function. Proposed directions for this search are outlined in the next chapter.

TABLE 4.1
USNO PHOTOMETRY OF CTI M DWARFS

CTI Object No.	Spec.	I_{KC}	$(V - I)_{KC}$	I_{CTI}	$(R - I)_{CTI}$
131541.4+280227	M4	14.098±.019	2.976±.043	14.15±.01	1.21±.01
135347.7+280418	M6	15.764±.020	3.687±.054	15.75±.04	1.60±.06
141111.3+280141	M5.5	16.403±.023	3.543±.055	16.41±.06	1.43±.09
141237.7+280559	M3	14.583±.018	2.458±.042	14.66±.02	0.78±.02
141329.8+280131	M2.5	14.579±.024	2.355±.031	14.64±.01	0.73±.02
153915.6+280214 ^a	M4	18.444±.026	2.815±.058	18.62±.21	2.33±.79
153915.6+280446	M6.5	17.897±.021	4.433±.117	17.77±.11	1.92±.49
153945.1+280234	M1.5	14.044±.016	2.124±.056	14.15±.01	0.56±.01
153948.1+280322	M2	14.737±.016	2.213±.026	14.83±.01	0.65±.02
154231.3+280401	M5.5	16.705±.034	3.620±.062	16.71±.20	1.81±.28
160557.4+280437 ^a	M3	18.191±.037	2.501±.096	17.96±.20	1.55±.28
161340.2+280011	M5.5	17.306±.022	3.916±.062	17.32±.29	1.77±.41
170958.5+275905	M5.5	13.903±.024	3.674±.031	13.88±.02	1.58±.03
171818.0+280512	M5	16.830±.022	3.366±.123	16.93±.12	1.57±.18
174729.0+280322	M6.5	17.872±.022	4.271±.197	17.57±.29	2.21±.42
180120.1+280410	M2.5	14.699±.025	2.265±.028	14.79±.01	0.60±.02
180304.9+280256	M2.5	14.876±.034	2.368±.042	15.01±.01	0.76±.03
191216.8+280229 ^a	M4	17.171±.027	2.946±.057	17.40±.40	2.21±.57
202738.5+280227 ^a	M3	18.454±.107	2.527±.126	18.03±.50	2.86±.35
223752.5+275918	M1	14.763±.020	2.059±.056	14.84±.02	0.48±.03

^a Data point has been removed from subsequent analyses. See text for details.

TABLE 4.2
BRIGHT, CONTAMINATING STARS IN (OR NEAR THE EDGE OF)
THE CTI STRIP

SAO #	RA ^a	(1987.5) Dec ^a	m_V ^b	Spec ^b	Total ^c	Note
75137	02:05:11.5	+28:02:31	9.0	K7	3	BD +27°329
—	02:18:45.9	+28:00:47	11.1 ^d	M7 III ^e	5	see Appendix A
75520	02:40:49.0	+27:59:35	8.8	K7	3	BD +27°420
79434	07:29:02.1	+27:56:34	5.1	K0	18	65 Gem
79666	07:44:33.1	+28:03:25	1.2	K0	6	β Gem
80181	08:25:42.2	+27:56:07	5.8	K2	7	ϕ^1 Cnc
80511	08:54:54.8	+27:58:33	5.2	G5	2	ρ^2 Cnc
82706	13:11:17.4	+27:56:28	4.3	G0	7	β Com
85220	17:34:08.1	+27:59:50	8.8	K7	3	BD +28°2780
90732	22:42:23.5	+28:05:30	8.9	M8	39	BD Peg
90981	23:03:10.0	+28:00:53	2.6	M0	22	β Peg
91472	23:45:10.9	+28:06:29	7.9	F5	2	BD +27°4614

^a Precessed to equinox 1987.5 and updated to epoch 1987.5 using the proper motion values listed in the SAO Catalog.

^b Values taken from the SAO Catalog, unless otherwise stated.

^c Number of objects out of the 283 total whose photometry is affected by this bright star.

^d R_{CTI} magnitude.

^e From Appendix A.

TABLE 4.3

STARS FROM THE NLTT CATALOGUE WHICH SHOULD BE IN THE CTI STRIP

LP#	m _r	m _{pg}	col	μ	RA(1987.5)	Dec ^a	CTI Name	R_{CTI}^b	$(R - I)_{CTI}$	Note
294-34	16.0	17.5	m	.192	01:00:04.3	27:59:42	010005.0+275941	15.18	0.64±.13	d=176±11 pc
+27°262	7.9	8.8	G5	.534	01:38:53.2	28:02:55	013853.9+280256	(<11.1)	—	too bright
—	10.5	11.6	k	.240	01:42:56.0	27:59:38	014256.7+275937	<10.02	0.19±.01	too bright
—	11.8	12.9	k	.240	01:42:58.0	27:59:26	014257.9+275925	<10.50	0.21±.01	too bright
297-8	14.6	15.7	k	.190	02:08:59.6	28:05:06	020859.6+280504	13.57	0.82±.05	in Table 4.4
298-38	11.4	12.5	k	.284	02:49:29.0	28:03:33	024929.6+280328	<10.84	0.11±.01	too bright
298-47	10.2	11.7	m	.280	02:54:56.0	28:04:51	025456.4+280449	<10.18	0.26±.01	too blue
299-34	14.5	15.6	k	.223	03:11:49.0	28:04:45	031149.0+280442	13.77	0.06±.01	RA excluded
300-18	18.2	21.1	m	.193	03:35:32.8	28:06:10	033533.4+280608	17.25	1.02±.09	RA excluded
301-16	18.9	21.0	m	.184	03:57:50.2	28:01:10	035750.4+280105 ^c	17.47	1.41±.08	RA excluded
302-46	12.8	14.5	m	.205	04:40:41.0	27:59:26	044041.1+275919	(13.32)	—	RA excluded
R 411	11.0	12.1	k	.347	05:34:13.3	28:05:28	053413.5+280529	(<11.6)	—	RA excluded
—	14.2	15.7	m	.305	05:47:25.3	28:03:15	054725.2+280312	(14.65)	—	RA excluded
308-14	14.0	15.5	m	.197	07:02:44.2	28:02:19	070244.0+280215	13.52	0.63±.08	RA excluded
β Gem	1.1	2.2	K0	.625	07:44:34.1	28:03:28	074434.0+280331	(<10.8)	—	too bright
313-5	11.6	13.4	m	.202	09:02:10.9	28:04:37	090210.4+280434	11.40	0.72±.01	too bright
314-8	16.6	18.5	m	.227	09:28:38.2	28:06:33	092838.3+280629	16.03	0.80±.06	d=188±20 pc
+28°1779	8.9	9.8	G5	.203	09:36:06.8	28:01:46	093606.5+280149	<8.61	—	too bright
314-68	14.9	15.5	g	.238	09:48:13.5	28:03:38	094811.7+280337	14.19	-0.07±.01	too blue
315-63	17.4	20.9	m+	.193	10:17:10.5	28:02:11	101710.9+280213	16.75	1.11±.03	d=141±9 pc

TABLE 4.3 — continued

LP#	m _r	m _{pg}	col	μ	RA(1987.5)	Dec ^a	CTI Name	R_{CTI}^b	$(R - I)_{CTI}$	Note
+28°1902	6.7	7.8	K0	.186	10:34:08.7	28:01:38	103407.9+280137	(<9.3)	—	too bright
317-5	15.2	16.9	m	.390	10:45:59.2	27:58:31	104559.5+275829	14.46	0.15±.02	too blue
—	12.8	14.6	m	.210	10:53:45.7	28:02:36	105345.9+280235	<11.88	0.38±.02	too blue
317-36	17.8	19.7	m	.223	10:59:46.2	28:01:19	105945.8+280120	17.06	0.03±.06	too blue
319-8	12.8	13.1	f-g	.182	11:38:46.8	28:00:14	113846.6+280016	12.24	-0.27±.03	too blue
W 411	11.1	12.6	M1	.198	12:23:01.5	27:59:06	(not found)	—	—	too bright
321-218	17.7	19.6	m	.222	12:40:49.4	28:02:27	124049.5+280231	17.02	1.34±.04	d=102±7 pc
321-106	15.3	16.8	m	.245	12:41:54.1	28:06:18	124154.1+280620	14.69	0.05±.02	too blue
322-403	15.1	16.6	m	.185	13:01:41.9	28:03:53	130144.9+280346	13.88	0.62±.05	d=101±6 pc
322-1178	16.5	18.0	m	.228	13:15:40.2	28:02:08	131541.3+280227 ^c	15.35	1.21±.01	in Table 4.4
323-25	17.9	20.3	m	.500	13:20:15.1	28:04:06	132017.4+280347 ^d	16.76	1.20±.03	d=118±7 pc
+28°2242	10.4	11.0	G5	.220	13:35:06.2	27:59:39	133505.7+275945	(<11.5)	—	too bright
—	16.2	16.0	a	.261	13:49:10.6	27:59:03	134910.5+275904 ^e	15.64	-0.39±.06	too blue
324-30	18.3	20.3	m	.180	13:53:47.3	28:04:13	135347.7+280419 ^c	17.35	1.60±.06	in Table 4.4
325-1	18.6	20.8	m+	.186	14:11:11.1	28:01:37	141111.3+280141 ^c	17.84	1.43±.08	d=125±17 pc
325-29	18.2	20.5	m	.212	14:20:53.5	28:02:32	142053.4+280234	17.68	0.92±.08	d=315±39 pc
327-10	17.0	18.3	k-m	.196	15:04:58.1	28:01:57	150457.9+280202	16.32	1.00±.03	d=145±8 pc
—	13.3	14.8	m	.377	16:00:42.5	27:59:25	160042.7+275927	12.82	0.67±.01	in Table 4.4
331-4	17.7	19.4	m	.220	16:49:57.5	28:06:37	164956.9+280642	17.15	0.14±.10	too blue
331-23	14.2	16.0	m	.187	16:58:13.1	28:01:30	165812.6+280131	13.73	0.67±.01	in Table 4.4

TABLE 4.3 — continued

LP#	m _r	m _{pg}	col	μ	RA(1987.5) Dec ^a		CTI Name	R_{CTI}^b	$(R - I)_{CTI}$	Note
331-41	11.7	12.3	g	.278	17:04:35.7	28:03:10	170435.1+280315	<10.90	-0.27±.01	too blue
332-10	14.3	15.8	m	.287	17:14:17.6	28:06:28	171417.4+280630	13.56	0.96±.01	in Table 4.4
332-17	16.1	17.6	m	.237	17:18:34.5	28:05:47	171834.3+280550	14.85	0.86±.01	in Table 4.4
333-8	15.8	16.9	k	.244	17:41:21.1	28:01:22	174121.4+280126	15.66	-0.02±.03	too blue
333-26	14.7	16.4	m	.241	17:54:44.0	28:03:59	175443.4+280405	13.51	0.77±.01	in Table 4.4
334-3	16.1	17.6	m	.297	18:05:58.2	28:04:17	180558.5+280419	15.51	1.15±.02	in Table 4.4
334-45	17.8	19.4	m	.298	18:30:02.2	28:05:04	183002.4+280506	16.35	0.09±.11	RA excluded
—	15.3	16.4	k	.240	18:48:17.6	28:05:24	184817.9+280533	13.75	0.29±.01	RA excluded
R 712	12.6	13.2	g	.270	18:49:25.9	28:04:56	184925.5+280459	<11.70	-0.36±.01	RA excluded
340-555	11.3	12.8	m	.243	21:04:49.2	28:05:03	(not found)	—	—	RA excluded
342-7	14.6	16.3	m	.260	21:38:59.2	28:02:20	213859.6+280219	(15.14)	—	RA excluded
343-42	15.3	16.6	k-m	.183	22:17:22.0	28:04:41	221722.6+280441	14.45	—	RA excluded
344-8	11.3	11.9	g	.229	22:27:41.2	28:02:54	222741.1+280253	10.36	—	RA excluded
β Peg	2.6	4.1	M0	.237	23:03:10.0	28:00:54	230310.5+280045	<10.00	—	too bright
345-43	16.6	17.7	k	.281	23:07:06.6	28:01:35	230706.6+280135	15.78	0.60±.04	d=252±23 pc
345-49	18.1	20.2	m	.222	23:10:13.8	28:02:25	231013.8+280223	17.15	1.11±.12	d=170±31 pc
346-7	14.5	15.6	k	.198	23:20:16.2	28:06:06	232016.4+280607	13.62	0.82±.01	in Table 4.4
346-14	17.1	18.6	m	.187	23:21:33.0	28:00:40	232133.4+280040	16.35	1.08±.04	d=125±10 pc
346-43	17.5	19.4	m	.206	23:31:33.2	28:01:58	233133.1+280158	16.59	1.35±.05	in Table 4.4
346-50	14.0	15.5	m	.232	23:34:51.8	27:59:56	233452.3+275955	13.18	0.99±.01	in Table 4.4

TABLE 4.3 — continued

^a Predicted coordinates for epoch and equinox 1987.5

^b Parenthetical values refer to V_{CTI} photometry

^c In Appendix A

^d Luyten appears to have overestimated this object's proper motion. The CTI star listed in the table has been confirmed from CTI images to be the proper motion object (LP 323-25 = LHS 2723) in question.

^e In Table 2.1

TABLE 4.4
OBJECTS USED IN THE DERIVATION OF THE CTI LUMINOSITY FUNCTION
(a) $8.0 \leq M_{IKC} < 8.5$

CTI Object Name	R_{CTI}	$(R - I)_{CTI}$	$(V - I)_{CTI}$	$(B - I)_{CTI}$	M_{IKC}	M_{VKC}	dist(pc)	$\frac{V}{V_{max}}$
023847.2+280001	12.75	0.71±.01	2.18±.01	3.57±.01	8.45±.12	10.78±.13	50±3	0.13
081639.4+280502	13.88	0.69±.01	2.17±.01	3.58±.02	8.38±.12	10.68±.13	88±5	0.68
082957.2+275934	13.89	0.64±.01	2.09±.01	3.39±.01	8.20±.13	10.43±.14	98±6	0.94
094720.8+280132	13.32	0.63±.01	2.09±.01	3.49±.01	8.16±.13	10.38±.14	77±5	0.46
101140.7+275859	14.06	0.69±.01	2.16±.01	3.42±.02	8.37±.13	10.67±.13	96±6	0.88
105543.8+275850	13.49	0.65±.01	2.12±.01	3.50±.02	8.23±.13	10.47±.14	80±5	0.51
124540.8+275915	13.60	0.60±.01	2.04±.01	3.37±.03	8.06±.14	10.23±.14	93±6	0.80
154930.3+280216	13.37	0.64±.01	2.13±.01	3.74±.02	8.22±.13	10.46±.14	76±5	0.44
155023.4+280613	13.01	0.66±.01	2.15±.01	3.62±.03	8.28±.13	10.54±.13	63±4	0.25
160042.7+275927	12.82	0.67±.01	2.18±.01	3.86±.01	8.31±.13	10.58±.13	56±3	0.18
165812.6+280131	13.73	0.67±.01	2.20±.01	3.91±.02	8.30±.13	10.57±.13	86±5	0.64
224754.6+280029	13.14	0.61±.01	2.05±.01	3.38±.01	8.09±.14	10.28±.14	74±5	0.41
232230.1+280303	13.59	0.67±.01	2.17±.01	3.56±.01	8.31±.13	10.59±.13	80±5	0.51

Average $\frac{V}{V_{max}} = 0.53 \pm 0.03$.

TABLE 4.4 — continued

(b) $8.5 \leq M_{I_{KC}} < 9.0$

CTI Object Name	R_{CTI}	$(R - I)_{CTI}$	$(V - I)_{CTI}$	$(B - I)_{CTI}$	$M_{I_{KC}}$	$M_{V_{KC}}$	dist(pc)	$\frac{V}{V_{\max}}$
003238.9+280229	14.73	0.84±.01	2.36±.01	3.75±.03	8.92±.11	11.44±.11	95±5	0.86
003257.9+280102	14.39	0.75±.01	2.25±.01	3.69±.02	8.59±.12	10.97±.12	99±5	0.97
011544.7+280414	12.97	0.81±.01	2.30±.01	3.68±.07	8.82±.11	11.30±.11	45±2	0.09
011557.5+275930	14.79	0.86±.01	2.41±.01	3.80±.03	8.98±.11	11.52±.11	95±5	0.86
020859.6+280504	13.57	0.82±.01	2.32±.01	4.15±.01	8.84±.11	11.32±.11	59±3	0.21
072709.4+280352	14.71	0.83±.02	2.41±.01	3.77±.02	8.88±.11	11.38±.12	96±5	0.88
083520.9+280004	14.19	0.84±.01	2.37±.01	3.79±.03	8.92±.10	11.43±.11	74±4	0.41
093631.3+280237 ^a	14.49	0.84±.01	2.37±.01	3.87±.02	8.92±.10	11.44±.11	85±4	0.61
111007.3+275952	13.96	0.80±.01	2.30±.01	3.68±.02	8.77±.11	11.23±.11	73±4	0.39
114014.1+280624	14.81	0.85±.02	2.42±.01	3.91±.06	8.93±.11	11.45±.12	98±5	0.94
134024.0+280508	13.92	0.79±.01	2.39±.01	3.75±.02	8.72±.11	11.16±.12	73±4	0.39
135842.2+280642	14.16	0.84±.01	2.43±.01	3.82±.07	8.90±.11	11.41±.12	74±4	0.41
140051.1+280653	14.55	0.80±.01	2.36±.01	—	8.76±.12	11.22±.13	96±5	0.88
145115.0+275902	13.02	0.81±.01	2.30±.01	3.77±.01	8.81±.11	11.28±.11	46±2	0.10
154107.1+280508	13.24	0.78±.01	2.29±.01	3.78±.04	8.70±.11	11.14±.12	54±3	0.16
170759.1+280555	14.01	0.78±.01	2.33±.01	4.04±.02	8.70±.11	11.14±.12	78±5	0.47
171834.3+280550	14.85	0.86±.01	2.29±.01	3.57±.04	8.98±.11	11.52±.12	98±5	0.94
175443.4+280405	13.51	0.77±.01	2.37±.01	3.79±.02	8.67±.11	11.09±.12	63±3	0.25
225113.8+280022	14.02	0.73±.01	2.25±.01	3.71±.02	8.54±.12	10.90±.13	86±5	0.64

TABLE 4.4 — continued
(b) $8.5 \leq M_{I_{KC}} < 9.0$ (continued)

CTI Object Name	R_{CTI}	$(R - I)_{CTI}$	$(V - I)_{CTI}$	$(B - I)_{CTI}$	$M_{I_{KC}}$	$M_{V_{KC}}$	dist(pc)	$\frac{V}{V_{\max}}$
231028.2+280452	14.50	$0.84 \pm .02$	$2.38 \pm .01$	$3.78 \pm .03$	$8.90 \pm .12$	$11.41 \pm .12$	87 ± 5	0.66
232016.4+280607	13.62	$0.82 \pm .01$	$2.36 \pm .01$	$3.75 \pm .02$	$8.84 \pm .11$	$11.32 \pm .12$	60 ± 3	0.22
233843.5+280219	14.40	$0.77 \pm .01$	$2.29 \pm .01$	$3.76 \pm .02$	$8.67 \pm .12$	$11.09 \pm .12$	95 ± 5	0.86

Average $\frac{V}{V_{\max}} = 0.55 \pm 0.02$.

^a Spectrum M3 V.

TABLE 4.4 — continued

(c) $9.0 \leq M_{I_{KC}} < 9.5$

CTI Object Name	R_{CTI}	$(R - I)_{CTI}$	$(V - I)_{CTI}$	$(B - I)_{CTI}$	$M_{I_{KC}}$	$M_{V_{KC}}$	dist(pc)	$\frac{V}{V_{\max}}$
001956.9+275927	15.25	0.99±.01	2.63±.01	3.92±.04	9.43±.09	12.15±.10	90±4	0.73
002151.7+280450	14.71	1.00±.01	2.60±.01	3.92±.03	9.47±.09	12.21±.10	69±3	0.33
010332.0+280234 ^b	15.37	1.00±.01	2.56±.01	4.14±.05	9.45±.10	12.19±.10	94±4	0.83
014344.1+280344	14.72	0.87±.01	2.40±.01	3.83±.03	9.01±.10	11.56±.11	90±4	0.73
015115.8+280458 ^b	15.05	0.99±.01	2.57±.01	—	9.42±.10	12.14±.10	83±4	0.57
015723.6+275946	13.58	0.89±.01	2.43±.01	3.79±.01	9.07±.10	11.65±.10	51±2	0.13
022228.2+275853	14.85	0.96±.01	2.55±.01	3.72±.03	9.34±.10	12.03±.10	79±4	0.49
074104.7+280143	15.16	0.94±.02	2.51±.02	3.92±.05	9.25±.11	11.90±.12	96±5	0.88
075350.3+280306	14.63	0.91±.02	2.47±.01	3.97±.03	9.16±.11	11.78±.11	79±4	0.49
083524.2+280412	15.23	1.00±.01	2.60±.01	3.96±.07	9.48±.09	12.22±.10	87±4	0.66
095541.2+280148	14.71	1.00±.01	2.59±.01	4.10±.03	9.48±.09	12.23±.10	68±3	0.31
101912.3+280028	15.16	0.96±.01	2.55±.01	4.00±.04	9.33±.10	12.02±.10	91±4	0.75
103555.5+280005	15.16	0.92±.01	2.48±.01	3.88±.04	9.18±.10	11.80±.11	100±5	1.00
104642.9+280435	14.76	0.95±.01	2.55±.01	4.09±.03	9.29±.09	11.95±.10	78±3	0.47
105707.5+280223 ^c	14.17	0.88±.01	2.45±.01	3.92±.02	9.05±.10	11.62±.11	68±3	0.31
112959.7+280044	14.70	0.99±.01	2.60±.01	4.12±.03	9.43±.09	12.16±.10	70±3	0.34
115339.5+280332	15.01	0.90±.01	2.44±.01	3.90±.06	9.12±.10	11.71±.11	97±5	0.91
115350.7+280342	13.58	0.91±.01	2.47±.01	3.90±.02	9.17±.10	11.79±.10	49±2	0.12
125417.4+280002	15.05	0.95±.01	2.54±.01	3.93±.06	9.31±.10	11.98±.10	88±4	0.68
142531.5+280033	15.03	0.95±.01	2.53±.01	4.07±.03	9.28±.10	11.94±.10	89±4	0.70

TABLE 4.4 — continued
(c) $9.0 \leq M_{I_{KC}} < 9.5$ (continued)

CTI Object Name	R_{CTI}	$(R - I)_{CTI}$	$(V - I)_{CTI}$	$(B - I)_{CTI}$	$M_{I_{KC}}$	$M_{V_{KC}}$	dist(pc)	$\frac{V}{V_{\max}}$
144455.1+280618	14.82	0.88±.01	2.46±.01	3.87±.12	9.06±.10	11.64±.11	92±4	0.78
144708.9+275947	14.79	0.89±.01	2.46±.01	4.00±.03	9.09±.10	11.68±.11	88±4	0.68
151814.8+280548	14.46	0.97±.01	2.60±.01	—	9.37±.10	12.07±.11	65±3	0.27
161117.0+280426	13.74	0.96±.01	2.61±.01	4.42±.02	9.33±.09	12.02±.10	47±2	0.10
165052.8+275958	15.16	0.94±.02	2.57±.01	4.26±.06	9.26±.11	11.92±.11	95±5	0.86
171417.4+280630	13.56	0.96±.01	2.61±.01	—	9.34±.09	12.03±.10	43±2	0.08
180525.2+275914	15.17	0.97±.03	2.75±.01	4.47±.07	9.36±.13	12.06±.14	90±5	0.73
230637.3+280228	14.57	0.95±.01	2.53±.01	3.87±.03	9.30±.10	11.97±.11	71±3	0.36
233452.3+275955	13.18	0.99±.05	2.63±.04	4.03±.01	9.44±.09	12.18±.09	34±1	0.04
233855.8+280517	14.69	0.97±.02	2.58±.01	3.99±.03	9.37±.11	12.07±.12	72±4	0.37
234725.1+280306	13.15	0.87±.01	2.38±.01	3.76±.01	9.02±.10	11.58±.11	44±2	0.09

Average $\frac{V}{V_{\max}} = 0.51 \pm 0.01$.

^b Spectrum M3.5 V.

^c Spectrum M3 V.

TABLE 4.4 — continued

(d) $9.5 \leq M_{I_{KC}} < 10.0$

CTI Object Name	R_{CTI}	$(R - I)_{CTI}$	$(V - I)_{CTI}$	$(B - I)_{CTI}$	$M_{I_{KC}}$	$M_{V_{KC}}$	dist(pc)	$\frac{V}{V_{\max}}$
001251.1+280535 ^d	15.43	1.03±.02	2.67±.01	4.32±.18	9.56±.10	12.34±.11	91±4	0.75
002241.4+280145	14.86	1.07±.01	2.73±.01	4.33±.03	9.71±.09	12.55±.09	64±3	0.26
005108.5+280103	15.58	1.06±.01	2.71±.01	4.18±.05	9.66±.09	12.48±.10	92±9	0.78
021537.7+275838	15.20	1.09±.01	2.91±.01	—	9.76±.09	12.62±.10	73±3	0.39
074001.0+280406	15.11	1.10±.02	2.75±.01	4.25±.05	9.80±.10	12.68±.11	70±3	0.34
074046.2+275917	14.78	1.01±.02	2.63±.01	4.08±.03	9.51±.10	12.26±.11	69±3	0.33
080302.4+280017	15.87	1.12±.02	2.96±.01	4.54±.10	9.88±.10	12.79±.11	93±4	0.80
091237.6+280105	15.37	1.02±.01	2.64±.01	3.98±.07	9.52±.10	12.28±.10	91±4	0.75
092641.4+275836	15.24	1.03±.02	2.67±.02	3.98±.11	9.56±.11	12.33±.11	83±4	0.57
094558.7+275949	14.90	1.02±.01	2.63±.01	4.09±.04	9.53±.09	12.30±.10	72±3	0.37
095536.6+280143	14.27	1.02±.01	2.65±.01	4.12±.02	9.52±.09	12.29±.09	54±2	0.16
104631.6+280413	14.56	1.10±.01	2.77±.01	4.25±.03	9.80±.08	12.68±.09	53±2	0.15
105315.0+280523	15.30	1.04±.01	2.73±.01	4.27±.05	9.59±.09	12.39±.10	84±4	0.59
105539.5+280122	14.77	1.05±.01	2.70±.01	4.11±.03	9.64±.09	12.45±.09	64±3	0.26
120408.8+280305	15.86	1.15±.02	2.80±.01	4.98±.16	9.97±.09	12.92±.10	87±4	0.66
123808.9+280618	15.12	1.09±.02	2.76±.01	4.27±.17	9.77±.10	12.63±.10	70±3	0.34
133707.3+275935	14.73	1.02±.01	2.64±.01	4.05±.03	9.52±.09	12.28±.09	67±3	0.30
135210.6+280310	15.33	1.11±.01	2.81±.01	4.31±.08	9.84±.09	12.73±.10	74±3	0.41
135755.3+280057	15.05	1.13±.01	2.84±.01	4.31±.06	9.89±.09	12.81±.09	63±2	0.25
144733.4+280459	15.28	1.13±.01	2.86±.01	4.36±.05	9.92±.09	12.85±.10	69±3	0.33

TABLE 4.4 — continued
(d) $9.5 \leq M_{I_{KC}} < 10.0$ (continued)

CTI Object Name	R_{CTI}	$(R - I)_{CTI}$	$(V - I)_{CTI}$	$(B - I)_{CTI}$	$M_{I_{KC}}$	$M_{V_{KC}}$	dist(pc)	$\frac{V}{V_{\max}}$
154549.6+280140	15.58	1.07±.02	2.75±.01	4.16±.09	9.69±.10	12.52±.10	90±4	0.73
165228.8+275955	14.58	1.03±.01	2.73±.01	4.51±.04	9.56±.09	12.33±.10	61±3	0.23
165313.8+275950	14.62	1.06±.01	2.79±.01	4.61±.05	9.67±.09	12.49±.10	59±2	0.21
170532.0+275926	15.04	1.09±.01	2.88±.01	4.85±.07	9.78±.11	12.65±.11	67±3	0.30
172351.3+280248	15.57	1.09±.02	2.79±.01	4.54±.17	9.76±.10	12.62±.11	86±4	0.64
175221.7+280329	13.43	1.02±.01	2.77±.01	4.58±.02	9.54±.09	12.21±.09	36±1	0.05
180558.5+280419	15.51	1.15±.02	2.91±.01	4.76±.10	9.97±.10	12.92±.10	74±3	0.41
225024.0+275956 ^e	15.64	1.14±.03	2.86±.02	4.28±.06	9.94±.12	12.87±.12	80±4	0.51
235133.2+280057	15.63	1.09±.02	2.76±.01	4.10±.05	9.76±.10	12.62±.11	89±4	0.70

Average $\frac{V}{V_{\max}} = 0.43 \pm 0.01$.

^d Double star unresolved by CTI; both spectra are M3.5 V.

^e Spectrum M4 V.

TABLE 4.4 — continued

(e) $10.0 \leq M_{I_{KC}} < 10.5$

CTI Object Name	R_{CTI}	$(R - I)_{CTI}$	$(V - I)_{CTI}$	$(B - I)_{CTI}$	$M_{I_{KC}}$	$M_{V_{KC}}$	dist(pc)	$\frac{V}{V_{\max}}$
002142.1+280548 ^f	15.83	1.19±.02	2.85±.01	4.27±.11	10.10±.10	13.11±.11	80±4	0.51
003439.1+280309 ^f	15.83	1.18±.02	2.84±.01	4.24±.41	10.07±.09	13.06±.10	81±3	0.53
005100.5+280430 ^f	15.87	1.17±.02	2.86±.01	4.56±.08	10.03±.09	13.01±.10	84±4	0.59
012703.2+275835	16.00	1.19±.02	2.89±.01	4.16±.16	10.11±.10	13.12±.11	86±4	0.64
015714.5+275816	16.38	1.21±.06	2.91±.03	3.86±.10	10.17±.21	13.20±.23	98±10	0.94
021050.6+280307	16.21	1.18±.03	2.83±.02	4.47±.09	10.08±.11	13.08±.12	96±5	0.88
082852.6+280159	15.25	1.26±.01	3.00±.01	4.48±.05	10.33±.08	13.43±.09	53±2	0.15
084047.8+280234	15.64	1.17±.01	2.88±.01	4.53±.07	10.04±.09	13.02±.10	76±3	0.44
085556.5+280559	14.46	1.23±.01	3.00±.01	—	10.25±.08	13.31±.08	39±1	0.06
101111.3+275946	15.66	1.21±.01	2.90±.01	4.25±.06	10.17±.09	13.20±.09	70±3	0.34
114741.4+280311	16.63	1.27±.03	3.08±.02	4.69±.23	10.37±.11	13.49±.12	98±5	0.94
120048.6+275958	15.20	1.29±.01	3.10±.01	4.54±.08	10.43±.08	13.58±.08	49±2	0.12
131541.3+280227 ^f	15.35	1.21±.01	2.93±.01	4.64±.09	10.16±.08	13.19±.09	62±2	0.24
133723.8+280206	15.24	1.22±.01	2.94±.01	4.39±.05	10.21±.08	13.25±.09	57±2	0.19
133727.4+280628	16.37	1.20±.03	2.91±.02	4.31±.06	10.15±.13	13.17±.14	99±6	0.97
142659.1+280657	16.00	1.20±.04	2.92±.02	—	10.15±.16	13.18±.18	83±6	0.57
171253.5+280042	16.65	1.27±.04	3.12±.02	—	10.37±.16	13.48±.18	99±7	0.97
175958.0+280550	16.47	1.31±.04	3.11±.02	—	10.50±.15	13.67±.16	85±6	0.61
225852.9+280043	16.33	1.25±.04	3.25±.03	5.36±.39	10.31±.15	13.40±.17	89±6	0.70
225953.7+275905	14.57	1.18±.01	2.89±.01	4.68±.03	10.06±.09	13.05±.09	46±2	0.10

TABLE 4.4 — continued
(e) $10.0 \leq M_{I_{KC}} < 10.5$ (continued)

CTI Object Name	R_{CTI}	$(R - I)_{CTI}$	$(V - I)_{CTI}$	$(B - I)_{CTI}$	$M_{I_{KC}}$	$M_{V_{KC}}$	dist(pc)	$\frac{V}{V_{\max}}$
235317.0+280338	15.10	1.19±.01	2.88±.01	4.43±.04	10.11±.08	13.12±.09	57±2	0.19
235659.2+280243	16.15	1.29±.02	3.02±.01	4.65±.07	10.43±.11	13.58±.11	76±4	0.44

Average $\frac{V}{V_{\max}} = 0.54 \pm 0.02$.

^f Spectrum M4 V.

(f) $10.5 \leq M_{I_{KC}} < 11.0$

CTI Object Name	R_{CTI}	$(R - I)_{CTI}$	$(V - I)_{CTI}$	$(B - I)_{CTI}$	$M_{I_{KC}}$	$M_{V_{KC}}$	dist(pc)	$\frac{V}{V_{\max}}$
085445.3+280047	16.65	1.34±.06	3.07±.04	—	10.61±.20	13.83±.22	86±8	0.64
141034.2+280158 ^g	16.39	1.33±.03	3.12±.01	4.91±.21	10.58±.11	13.79±.12	78±4	0.47
223903.2+280324	16.61	1.33±.05	3.13±.04	4.57±.34	10.56±.18	13.76±.19	87±7	0.66
233133.1+280158	16.59	1.35±.05	3.39±.04	4.62±.39	10.62±.17	13.84±.19	83±7	0.57

Average $\frac{V}{V_{\max}} = 0.59 \pm 0.07$.

^g Spectrum M4.5 V.

TABLE 4.4 — continued

(g) $11.0 \leq M_{I_{KC}} < 11.5$

CTI Object Name	R_{CTI}	$(R - I)_{CTI}$	$(V - I)_{CTI}$	$(B - I)_{CTI}$	$M_{I_{KC}}$	$M_{V_{KC}}$	dist(pc)	$\frac{V}{V_{\max}}$
092248.3+280503	17.81	$1.57 \pm .18$	$3.41 \pm .03$	—	$11.34 \pm .58$	$14.87 \pm .63$	96 ± 26	0.88
124832.6+280502 ^h	16.92	$1.53 \pm .03$	$3.50 \pm .02$	$4.77 \pm .26$	$11.22 \pm .13$	$14.70 \pm .14$	68 ± 4	0.31
132116.6+280328	17.60	$1.59 \pm .05$	$3.31 \pm .03$	—	$11.40 \pm .18$	$14.96 \pm .20$	84 ± 7	0.59
135347.7+280419 ⁱ	17.35	$1.60 \pm .06$	$3.47 \pm .02$	—	$11.44 \pm .21$	$15.01 \pm .23$	73 ± 7	0.39
170958.5+275905 ^h	15.46	$1.58 \pm .03$	$3.65 \pm .01$	$5.68 \pm .13$	$11.37 \pm .12$	$14.91 \pm .13$	32 ± 2	0.03

Average $\frac{V}{V_{\max}} = 0.44 \pm 0.15$.^h Spectrum M5.5 V.ⁱ Spectrum M6 V.(h) $11.5 \leq M_{I_{KC}} < 12.0$

CTI Object Name	R_{CTI}	$(R - I)_{CTI}$	$(V - I)_{CTI}$	$(B - I)_{CTI}$	$M_{I_{KC}}$	$M_{V_{KC}}$	dist(pc)	$\frac{V}{V_{\max}}$
015625.5+280135 ^j	17.69	$1.65 \pm .07$	$3.61 \pm .04$	—	$11.60 \pm .25$	$15.25 \pm .27$	77 ± 9	0.46

Average $\frac{V}{V_{\max}} = 0.46 \pm 0.16$.^j Spectrum M6 V.

TABLE 4.4 — continued

(i) $12.0 \leq M_{I_{KC}} < 12.5$

CTI Object Name	R_{CTI}	$(R - I)_{CTI}$	$(V - I)_{CTI}$	$(B - I)_{CTI}$	$M_{I_{KC}}$	$M_{V_{KC}}$	dist(pc)	$\frac{V}{V_{\max}}$
004244.4+280140 ^k	19.30	1.94±.16	—	—	12.50±.55	16.56±.60	95±25	0.86
011826.7+280514 ^k	19.00	1.85±.21	—	—	12.23±.69	16.16±.75	98±31	0.94
015607.7+280241 ^l	18.33	1.83±.12	3.89±.08	—	12.16±.40	16.06±.43	75±14	0.42

Average $\frac{V}{V_{\max}} = 0.74 \pm 0.38$.^k Spectrum M6 V.^l Spectrum M6.5 V.(j) $12.5 \leq M_{I_{KC}} < 13.0$

CTI Object Name	R_{CTI}	$(R - I)_{CTI}$	$(V - I)_{CTI}$	$(B - I)_{CTI}$	$M_{I_{KC}}$	$M_{V_{KC}}$	dist(pc)	$\frac{V}{V_{\max}}$
000455.2+280301 ^m	18.27	1.99±.08	4.08±.06	—	12.67±.28	16.80±.31	54±7	0.17
014716.6+280142 ^m	19.12	1.95±.21	—	—	12.53±.71	16.60±.78	86±29	0.70
022000.5+275933	18.99	1.95±.19	—	—	12.53±.63	16.60±.68	81±24	0.58

Average $\frac{V}{V_{\max}} = 0.48 \pm 0.27$, based on $d_{\max} = 97$ pc.^m Spectrum M6 V.

TABLE 4.4 — continued

(k) $13.0 \leq M_{I_{KC}} < 13.5$

CTI Object Name	R_{CTI}	$(R - I)_{CTI}$	$(V - I)_{CTI}$	$(B - I)_{CTI}$	$M_{I_{KC}}$	$M_{V_{KC}}$	dist(pc)	$\frac{V}{V_{\max}}$
153915.6+280445 ⁿ	19.87	$2.14 \pm .80$	—	—	13.09 ± 2.64	17.42 ± 2.87	87 ± 106	—
174729.0+280322 ^p	19.78	$2.21 \pm .41$	—	—	13.30 ± 1.37	17.74 ± 1.49	74 ± 47	—

ⁿ No spectrum available; photometric errors are very large; object is beyond $d_{\max} = 72$ pc.^p Spectrum M6.5 V; object is just beyond $d_{\max} = 72$ pc.(l) $13.5 \leq M_{I_{KC}} < 14.0$

CTI Object Name	R_{CTI}	$(R - I)_{CTI}$	$(V - I)_{CTI}$	$(B - I)_{CTI}$	$M_{I_{KC}}$	$M_{V_{KC}}$	dist(pc)	$\frac{V}{V_{\max}}$
012657.5+280202 ^q	19.35	$2.30 \pm .24$	—	—	$13.57 \pm .80$	$18.14 \pm .87$	51 ± 19	0.89

Average $\frac{V}{V_{\max}} = 0.89 \pm 0.15$, based on $d_{\max} = 53$ pc.^q Spectrum M8.5 V.

TABLE 4.5
THE CTI LUMINOSITY FUNCTION AT I

$M_{I_{KC}}$	#	$d_{max}(\text{pc})$	$\log \Phi_{obs}$	$\overline{\sigma_M}$	$\frac{N_{obs}}{N_{true}}$	$\log \Phi_{true}$
8.25	13	100	-2.029	0.13	0.968	-2.015
8.75	22	100	-1.801	0.11	0.966	-1.786
9.25	31	100	-1.652	0.10	0.996	-1.650
9.75	29	100	-1.681	0.10	0.994	-1.678
10.25	22	100	-1.801	0.11	1.063	-1.827
10.75	4	100	-2.541	0.17	0.858	-2.475
11.25	5	100	-2.444	0.24	1.361	-2.578
11.75	1	100	-3.143	0.27	0.175	-2.386
12.25	3	100 ^a	<-2.666	0.55	—	—
12.75	3	97 ^a	<-2.626	0.54	—	—
13.25	0	72 ^a	—	0.91	—	—
13.75	1	53 ^a	<-2.316	0.80	—	—

^a Taking a limiting magnitude of $R_{CTI} = 20.0$, one magnitude fainter than the adopted completeness limit.

TABLE 4.6

REDISTRIBUTION OF OBJECTS IN THE FIRST THREE BINS OF THE CTI LUMINOSITY FUNCTION
WHEN CALIBRATION EQUATION 4.4 IS USED INSTEAD OF EQUATION 4.2 ^a

(a) $8.0 \leq M_{I_{KC}} < 8.5$

CTI Object Name	R_{CTI}	$(R - I)_{CTI}$	$(V - I)_{CTI}$	$(B - I)_{CTI}$	$M_{I_{KC}}$	$M_{V_{KC}}$	dist(pc)
011544.7+280414	12.97	0.81±.01	2.30±.01	3.68±.07	8.05±.16	10.52±.16	64±50.09
020859.6+280504	13.57	0.82±.01	2.32±.01	4.15±.01	8.08±.16	10.57±.16	83±60.21
105707.5+280223	14.17	0.88±.01	2.45±.01	3.92±.02	8.48±.15	11.05±.16	89±60.31
145115.0+275902	13.02	0.81±.01	2.30±.01	3.77±.01	8.02±.16	10.49±.17	66±50.10
232016.4+280607	13.62	0.82±.01	2.36±.01	3.75±.02	8.08±.17	10.57±.17	85±70.22
234725.1+280306	13.15	0.87±.01	2.38±.01	3.76±.01	8.42±.15	10.98±.15	57±40.09

(b) $8.5 \leq M_{I_{KC}} < 9.0$

CTI Object Name	R_{CTI}	$(R - I)_{CTI}$	$(V - I)_{CTI}$	$(B - I)_{CTI}$	$M_{I_{KC}}$	$M_{V_{KC}}$	dist(pc)
015723.6+275946	13.58	0.89±.01	2.43±.01	3.79±.01	8.52±.15	11.10±.15	66±50.13
075350.3+280306	14.63	0.91±.02	2.47±.01	3.97±.03	8.69±.17	11.30±.17	98±80.49
104642.9+280435	14.76	0.95±.01	2.55±.01	4.09±.03	8.92±.15	11.59±.15	92±60.47
115350.7+280342	13.58	0.91±.01	2.47±.01	3.90±.02	8.70±.15	11.32±.15	60±40.12
230637.3+280228	14.57	0.95±.01	2.53±.01	3.87±.03	8.95±.16	11.62±.17	84±60.36

TABLE 4.6 — continued

(c) $9.0 \leq M_{I_{KC}} < 9.5$

CTI Object Name	R_{CTI}	$(R - I)_{CTI}$	$(V - I)_{CTI}$	$(B - I)_{CTI}$	$M_{I_{KC}}$	$M_{V_{KC}}$	dist(pc)
002151.7+280450	14.71	1.00±.01	2.60±.01	3.92±.03	9.27±.14	12.01±.15	75±50.33
015115.8+280458	15.05	0.99±.01	2.57±.01	—	9.16±.16	11.88±.16	93±70.57
022228.2+275853	14.85	0.96±.01	2.55±.01	3.72±.03	9.02±.15	11.71±.16	91±60.49
083524.2+280412	15.23	1.00±.01	2.60±.01	3.96±.07	9.28±.15	12.03±.16	95±70.66
095541.2+280148	14.71	1.00±.01	2.59±.01	4.10±.03	9.28±.14	12.03±.15	75±50.31
112959.7+280044	14.70	0.99±.01	2.60±.01	4.12±.03	9.19±.14	11.92±.15	78±50.34
151814.8+280548	14.46	0.97±.01	2.60±.01	—	9.07±.16	11.77±.16	74±50.27
161117.0+280426	13.74	0.96±.01	2.61±.01	4.42±.02	9.01±.14	11.70±.14	55±40.10
171417.4+280630	13.56	0.96±.01	2.61±.01	—	9.03±.14	11.71±.15	50±30.08
233452.3+275955	13.18	0.99±.05	2.63±.04	4.03±.01	9.22±.14	11.95±.14	58±20.04
233855.8+280517	14.69	0.97±.02	2.58±.01	3.99±.03	9.07±.18	11.77±.18	82±70.37

^a These recalibrated data are re-distributed into the first three bins as follows:6 objects with $8.0 \leq M_{I_{KC}} < 8.5$, yielding $\log \Phi_{obs} = -2.365$,5 objects with $8.5 \leq M_{I_{KC}} < 9.0$, yielding $\log \Phi_{obs} = -2.444$,11 objects with $9.0 \leq M_{I_{KC}} < 9.5$, yielding $\log \Phi_{obs} = -2.102$ (or, 1 object with $10.0 \leq M_{V_{KC}} < 10.5$, yielding $\log \Phi_{obs} < -3.143$,4 objects with $10.5 \leq M_{V_{KC}} < 11.0$, yielding $\log \Phi_{obs} = -2.541$,4 objects with $11.0 \leq M_{V_{KC}} < 11.5$, yielding $\log \Phi_{obs} = -2.541$,10 objects with $11.5 \leq M_{V_{KC}} < 12.0$, yielding $\log \Phi_{obs} = -2.143$,16 objects with $12.0 \leq M_{V_{KC}} < 12.5$, yielding $\log \Phi_{obs} = -1.939$).

TABLE 4.7

LUMINOSITY FUNCTION DATA FOR OBJECTS WITH $M_I \geq 8.0$,
 $\delta > -20^\circ$, AND $d \leq 5.2$ PARSECS (WHITE DWARFS EXCLUDED)

Object	m_I	π (arcsec)	M_I
GL 699	6.77	0.5453 ± 0.0010	10.45
GL 406	9.39	0.4183 ± 0.0025	12.50
GL 411	5.32	0.3973 ± 0.0018	8.32
GL 65 A	8.31 joint	0.3807 ± 0.0043	11.81
GL 65 B	8.31 joint	0.3807 ± 0.0043	12.15
GL 905	8.84	0.3156 ± 0.0016	11.34
GL 447	8.14	0.3011 ± 0.0019	10.53
GL 866 A	8.62 joint	0.2943 ± 0.0035	11.72
GL 866 B	8.62 joint	0.2943 ± 0.0035	11.72
GL 15 A	5.94	0.2895 ± 0.0049	8.25
GL 15 B	8.25	0.2895 ± 0.0049	10.56
GL 725 A	6.44	0.2861 ± 0.0018	8.72
GL 725 B	7.13	0.2861 ± 0.0018	9.41
GJ 1111	10.53	0.2758 ± 0.0030	12.73
GL 54.1	8.90	0.2674 ± 0.0030	11.04
GL 273	7.16	0.2644 ± 0.0020	9.27
GL 860 A	6.91 joint	0.2519 ± 0.0023	9.29
GL 860 B	6.91 joint	0.2519 ± 0.0023	10.25
GL 628	7.40	0.2447 ± 0.0063	9.34
GL 234 A	8.06 joint	0.2421 ± 0.0017	10.14
GL 234 B	8.06 joint	0.2421 ± 0.0017	12.13
GL 473 A	8.92 joint	0.2322 ± 0.0043	11.45
GL 473 B	8.92 joint	0.2322 ± 0.0043	11.55
GL 83.1	9.17	0.2238 ± 0.0029	10.92
LHS 292	11.20	0.2210 ± 0.0036	12.92
GJ 1002	10.16	0.2128 ± 0.0033	11.80
GL 687	6.72	0.2127 ± 0.0020	8.36
GJ 1245 A	9.81 joint	0.2120 ± 0.0043	11.71
GJ 1245 C	9.81 joint	0.2120 ± 0.0043	13.11
GJ 1245 B	10.27	0.2120 ± 0.0043	11.90
GL 876	7.45	0.2113 ± 0.0048	9.07
GL 166 C	8.32	0.2071 ± 0.0025	9.90
GL 388	6.81	0.2039 ± 0.0028	8.36
GL 873	7.57	0.1970 ± 0.0025	9.04

TABLE 4.8
THE CTI LUMINOSITY FUNCTION AT V

$M_{V_{KC}}$	#	$d_{max}(\text{pc})$	$\log \Phi_{obs}$	$\overline{\sigma_M}$	$\frac{N_{obs}}{N_{true}}$	$\log \Phi_{true}$
10.25	>6	100	<-2.365	0.14	1.039	<-2.382
10.75	9	100	-2.189	0.13	0.896	-2.141
11.25	18	100	-1.888	0.12	1.027	-1.900
11.75	18	100	-1.888	0.11	0.931	-1.857
12.25	28	100	-1.696	0.10	1.030	-1.709
12.75	16	100	-1.939	0.10	0.963	-1.923
13.25	19	100	-1.864	0.12	1.038	-1.881
13.75	7	100	-2.298	0.15	1.182	-2.371
14.25	0	100	—	—	—	—
14.75	4	100	-2.541	0.27	1.101	-2.583
15.25	2	100	-2.842	0.25	1.595	-3.045
15.75	0	100	—	—	—	—
16.25	2	100 ^a	<-2.842	0.59	—	—
16.75	4	100 ^a	<-2.541	0.59	—	—
17.25	0	90 ^a	—	—	—	—
17.75	0	73 ^a	—	—	—	—
18.25	1	60 ^a	<-2.477	0.87	—	—

^a Taking a limiting magnitude of $R_{CTI} = 20.0$, one magnitude fainter than the adopted completeness limit.

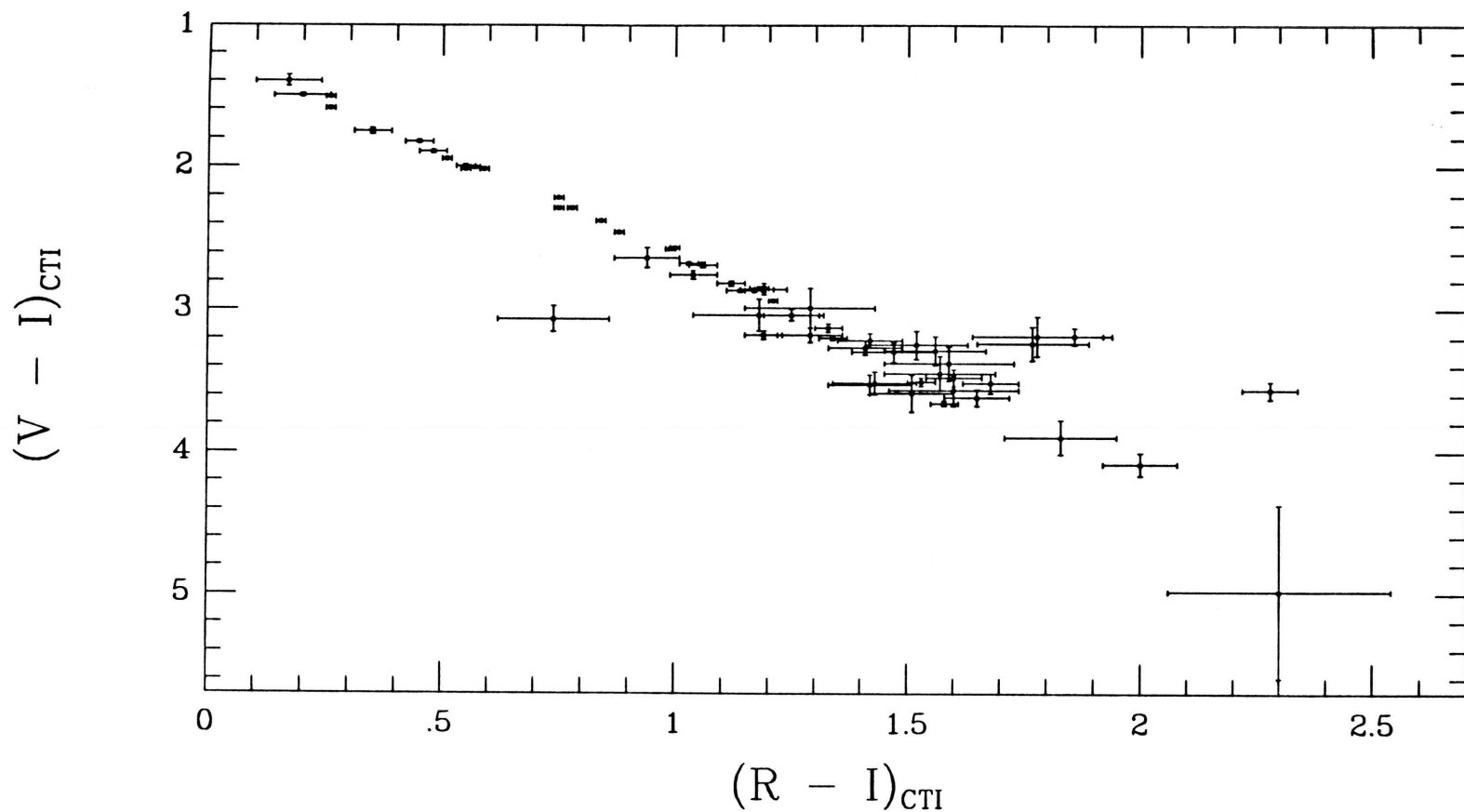


FIG. 4.1. — The $(V - I)_{CTI}$ vs. $(R - I)_{CTI}$ diagram for spectroscopic targets having $(R - I)$ errors of 0.15 magnitude or less. In this diagram, only those objects verified to be dwarfs are plotted. Also plotted at the lower right is the location of the M8.5 dwarf. Its V_{CTI} magnitude was determined through coadditions of multiple nights of CTI data.

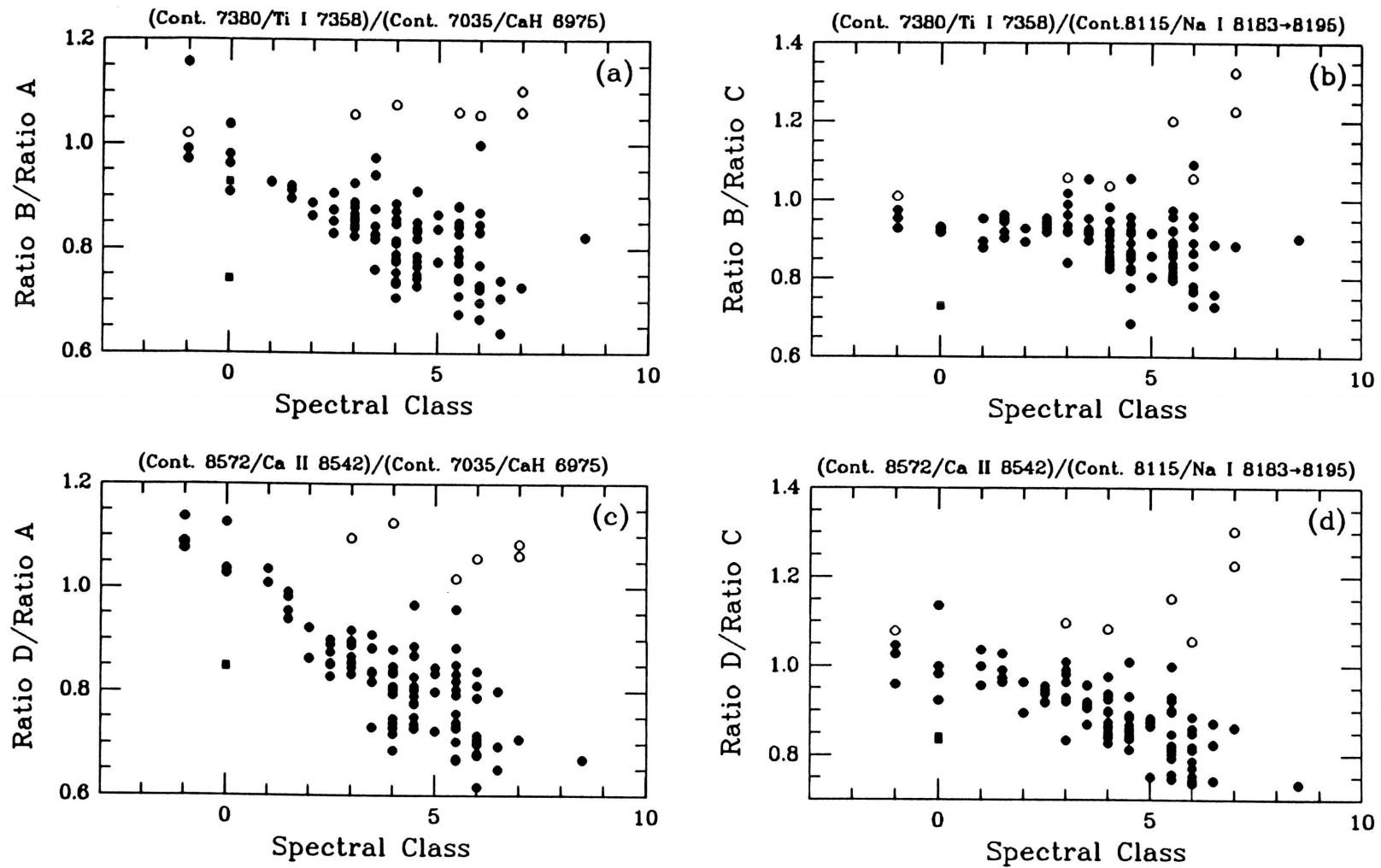


FIG. 4.2. — Color ratios determined from the spectra of the CTI targets. Dwarfs are indicated by the filled circles, giants by the open circles, and subdwarfs by the filled squares.

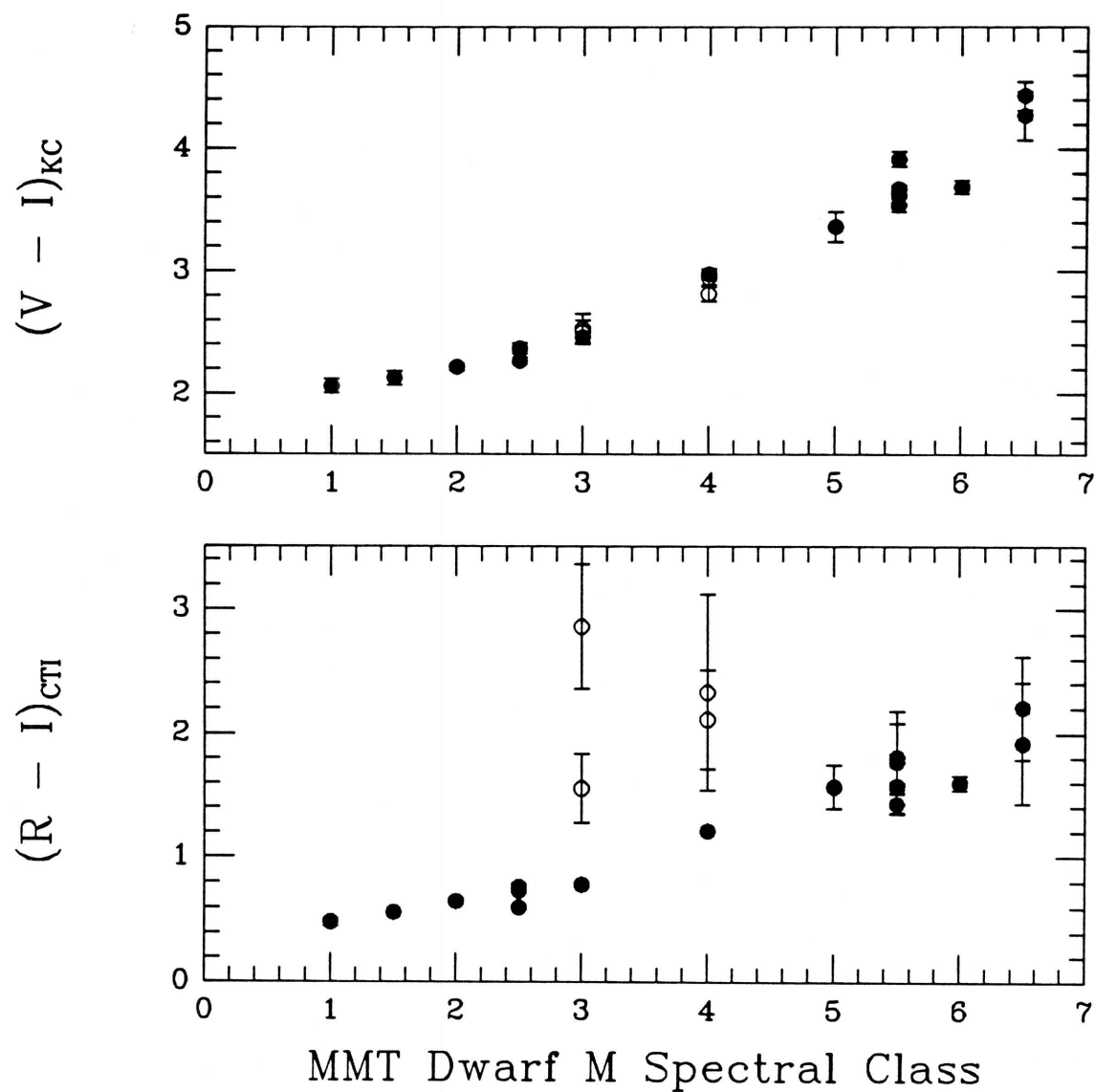


FIG. 4.3. — $(V - I)_{KC}$ and $(R - I)_{CTI}$ vs. M dwarf spectral class for those dwarfs observed photometrically at the U. S. Naval Observatory. The four discrepant points on the $(R - I)_{CTI}$ plot are labelled with open circles on both figures.

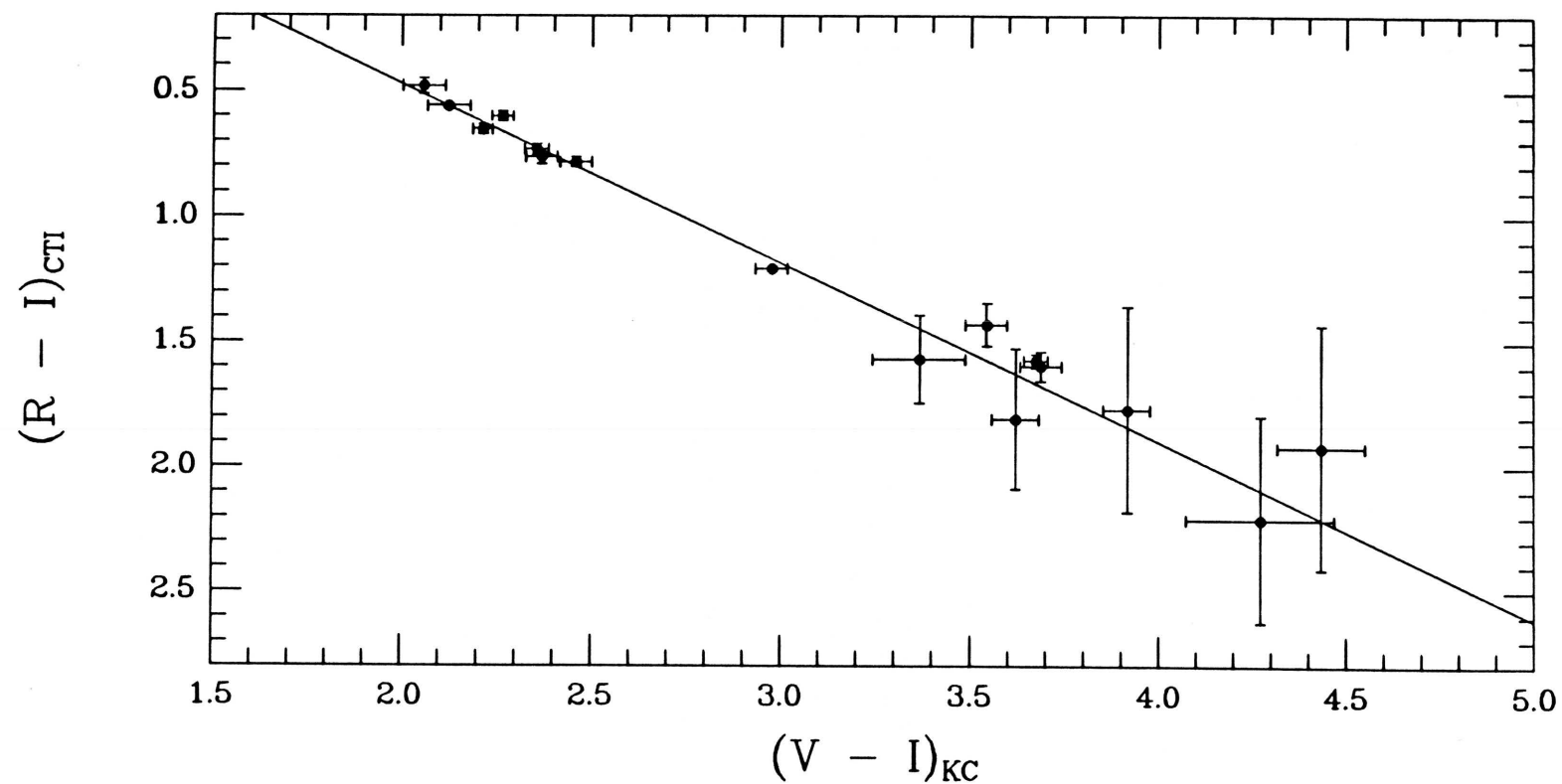


FIG. 4.4. — The $(R - I)_{CTI}$ vs. $(V - I)_{KC}$ relation as determined through photometry taken at the U. S. Naval Observatory. The solid line represents a weighted linear least-squares fit to the data.

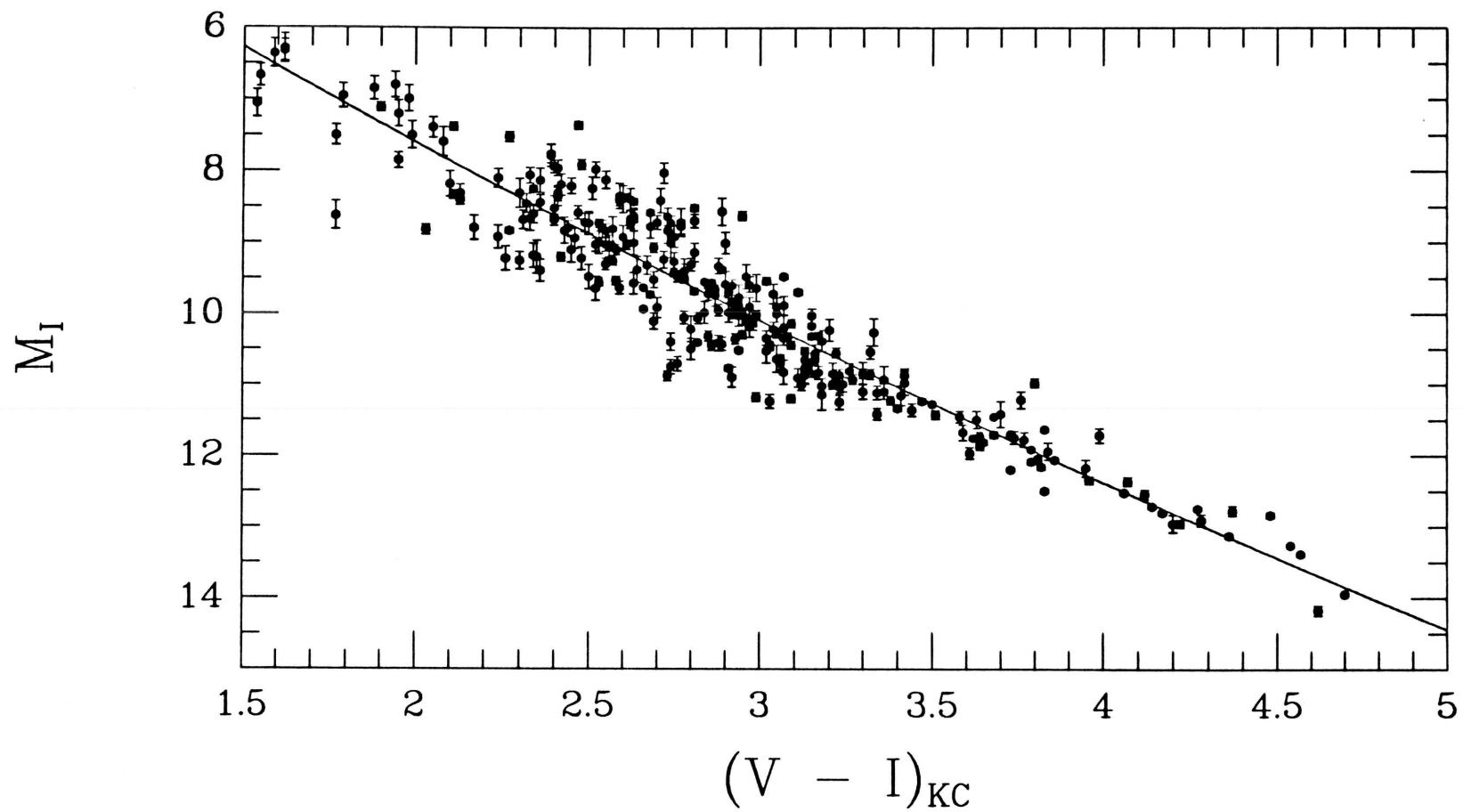


FIG. 4.5. — A plot of $M_{I_{KC}}$ vs. $(V - I)_{KC}$ for USNO parallax stars. The solid line represents a second-order least-squares fit to the data.

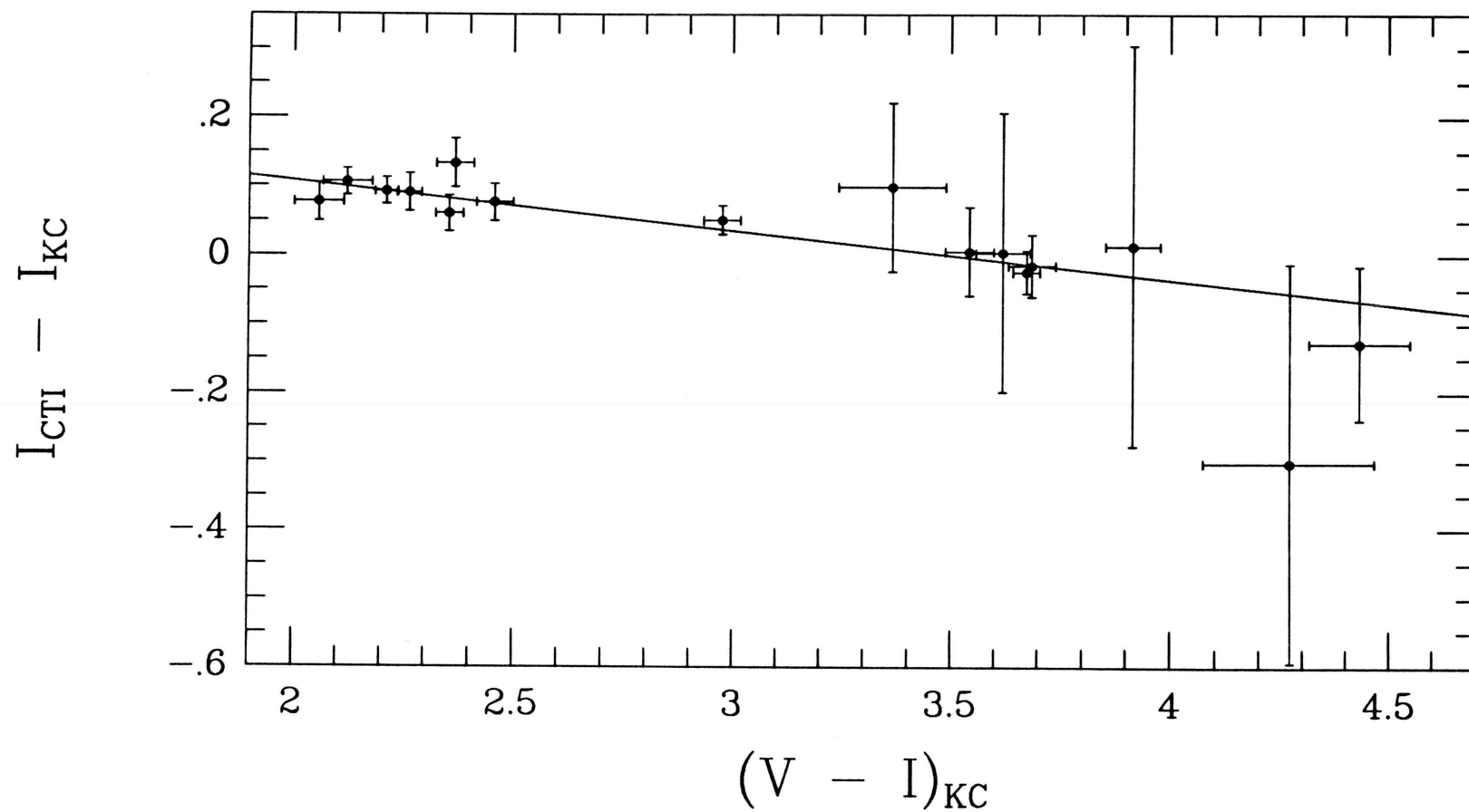


FIG. 4.6. — The ΔI vs. $(V - I)_{KC}$ diagram for CTI objects observed at the U.S. Naval Observatory. The solid line represents a weighted linear least-squares fit to the data.

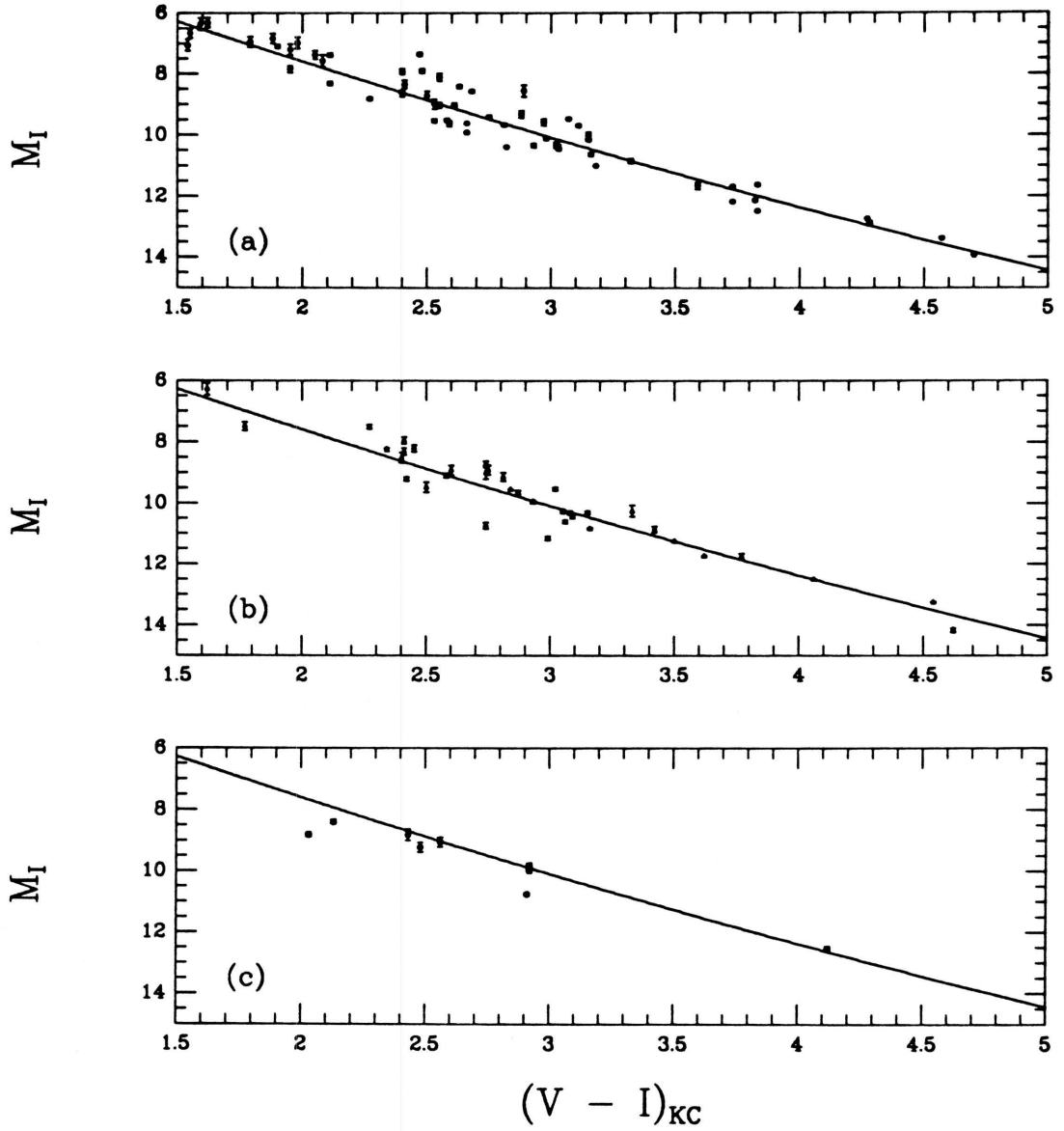


FIG. 4.7. — The fitted relation from Figure 4.5 shown for (a) low-velocity stars only, (b) intermediate-velocity stars only, and (c) high-velocity stars only. Note that the low-velocity sample tends to fall above the relation at the brighter magnitudes.

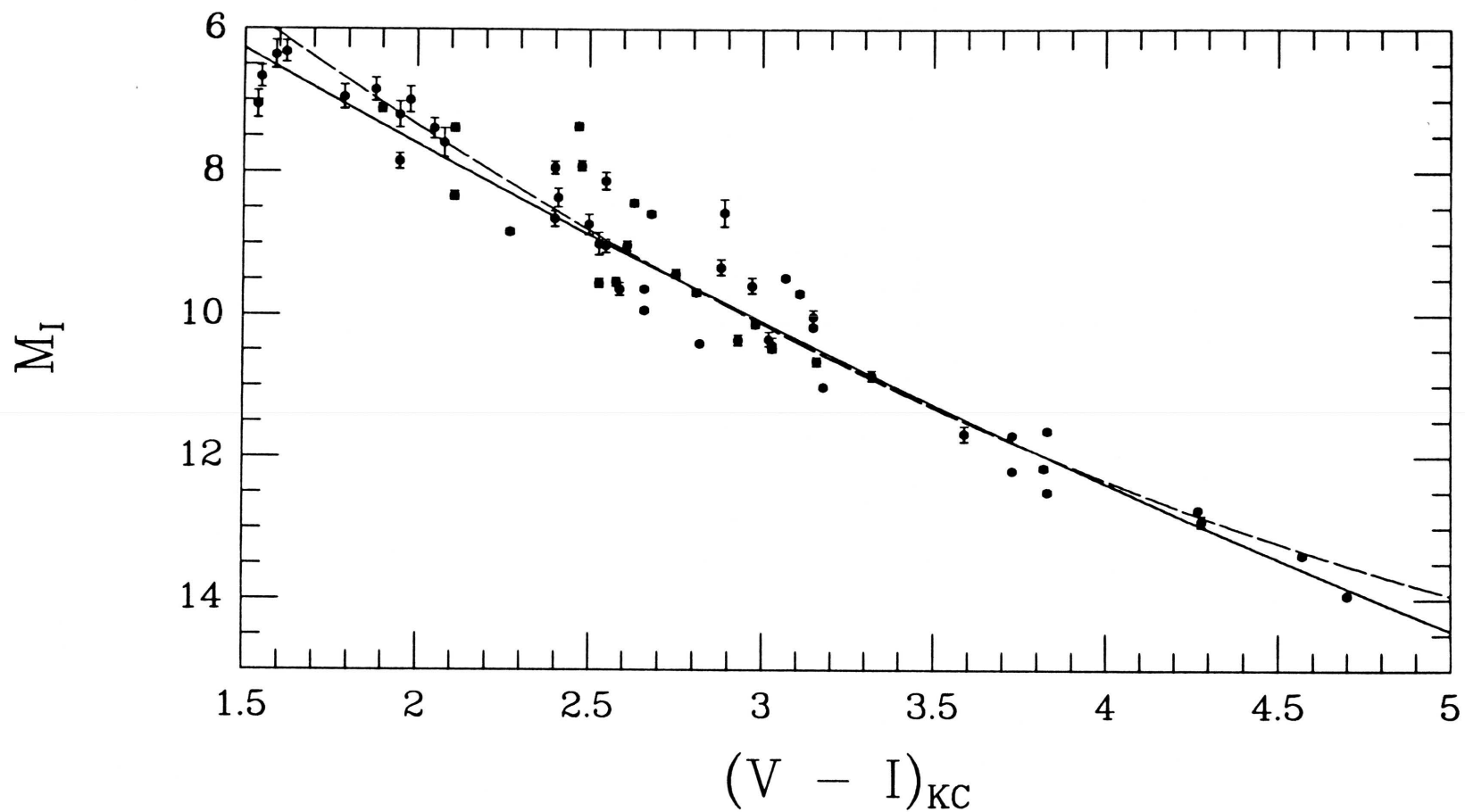


FIG. 4.8. — Figure 4.7(a) plotted with the previous relation from Figure 4.5 (solid line) and with a new second-order least-squares solution (dashed line) based on the low-velocity data only.

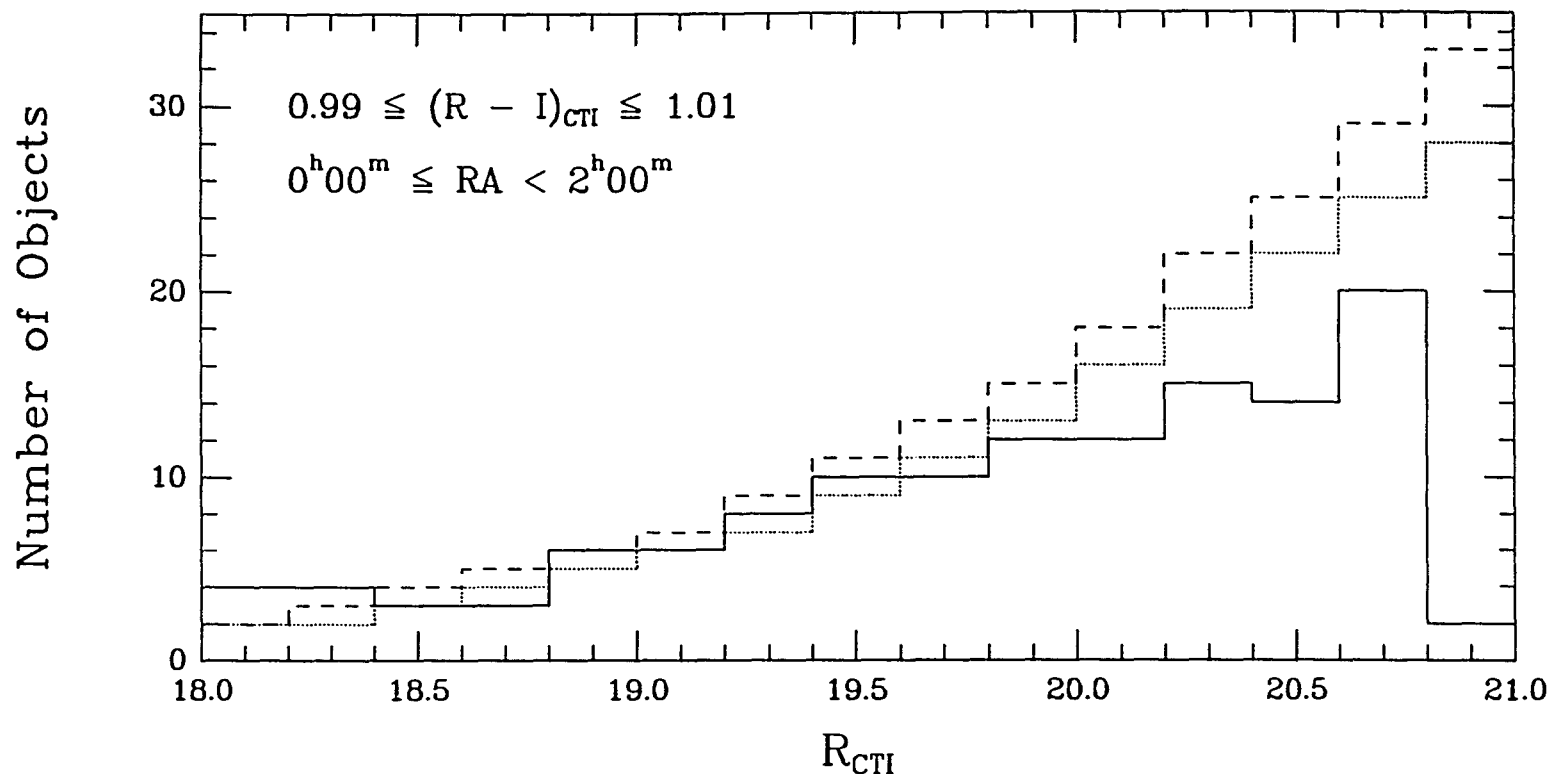


FIG. 4.9. — Observed counts of objects detected in the CTI strip with colors of $0.99 \leq (R - I)_{CTI} \leq 1.01$ and with $0^h00^m \leq RA < 2^h00^m$ (representing an almost constant galactic latitude of $b \sim 35^\circ$). Two predictions of the expected counts are shown, both of which represent the number expected per bin assuming that objects of this type have an exponential scale height of $\beta = 350$ pc: the dotted line shows the prediction normalized to the observed counts in the 19.1 magnitude bin and the dashed line shows the prediction normalized to the 18.9 magnitude bin.

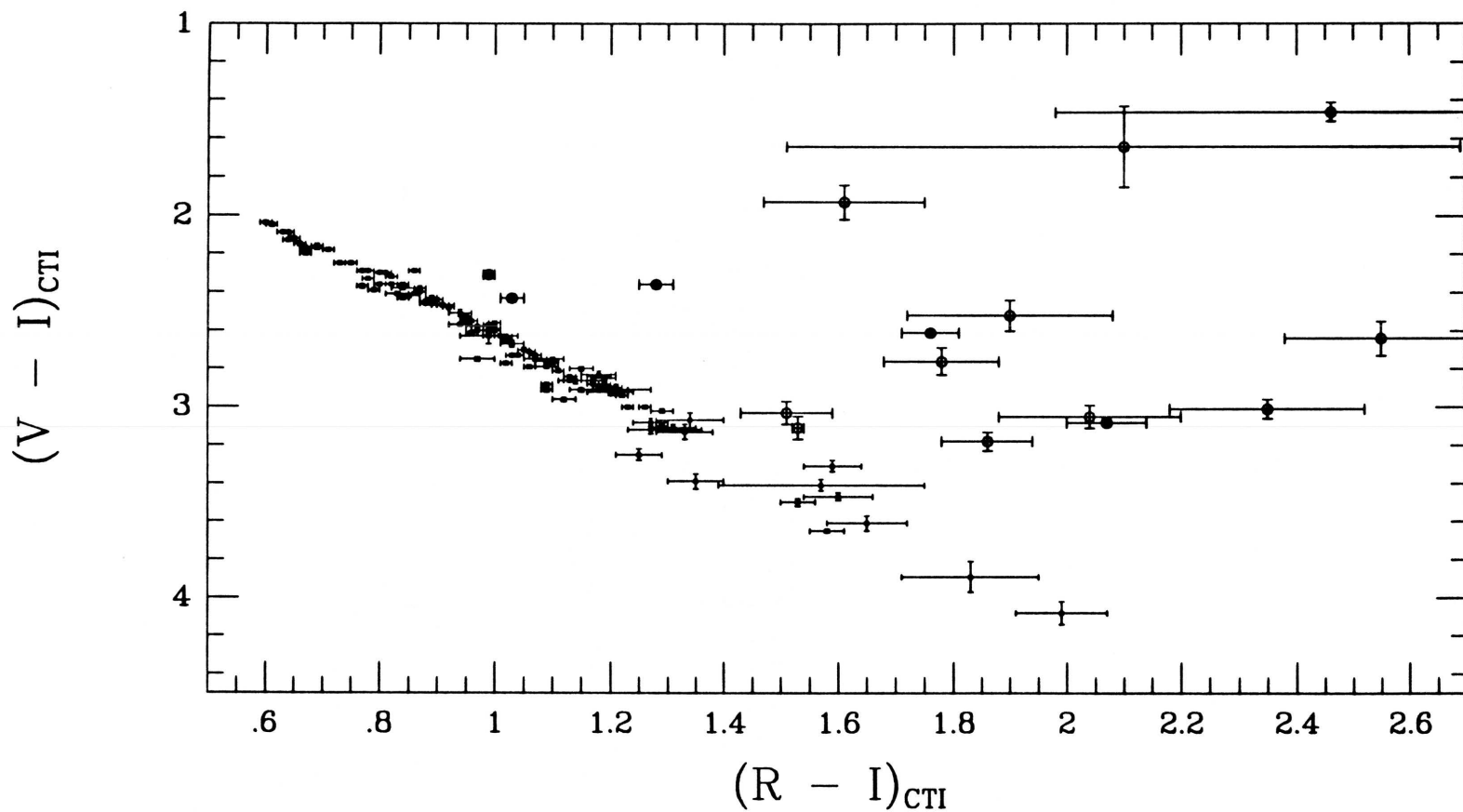


FIG. 4.10. — The $(V - I)_{CTI}$ vs. $(R - I)_{CTI}$ diagram for the final selection of objects to be used in construction of the luminosity function. The solid circles represent objects that were retained, and the open circles indicate objects that have been removed.

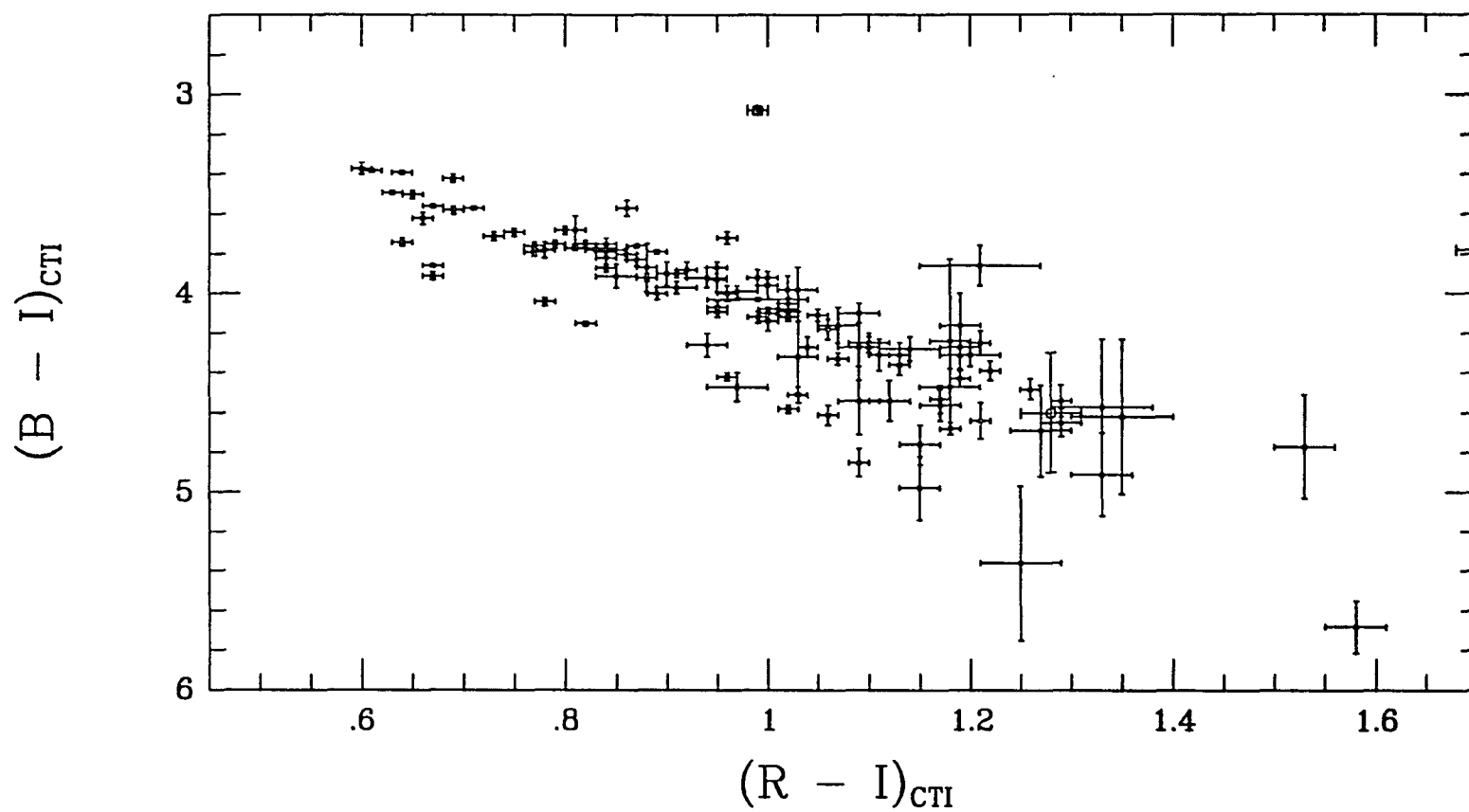


FIG. 4.11. — The $(B - I)_{CTI}$ vs. $(R - I)_{CTI}$ diagram for those objects shown in Figure 4.10.

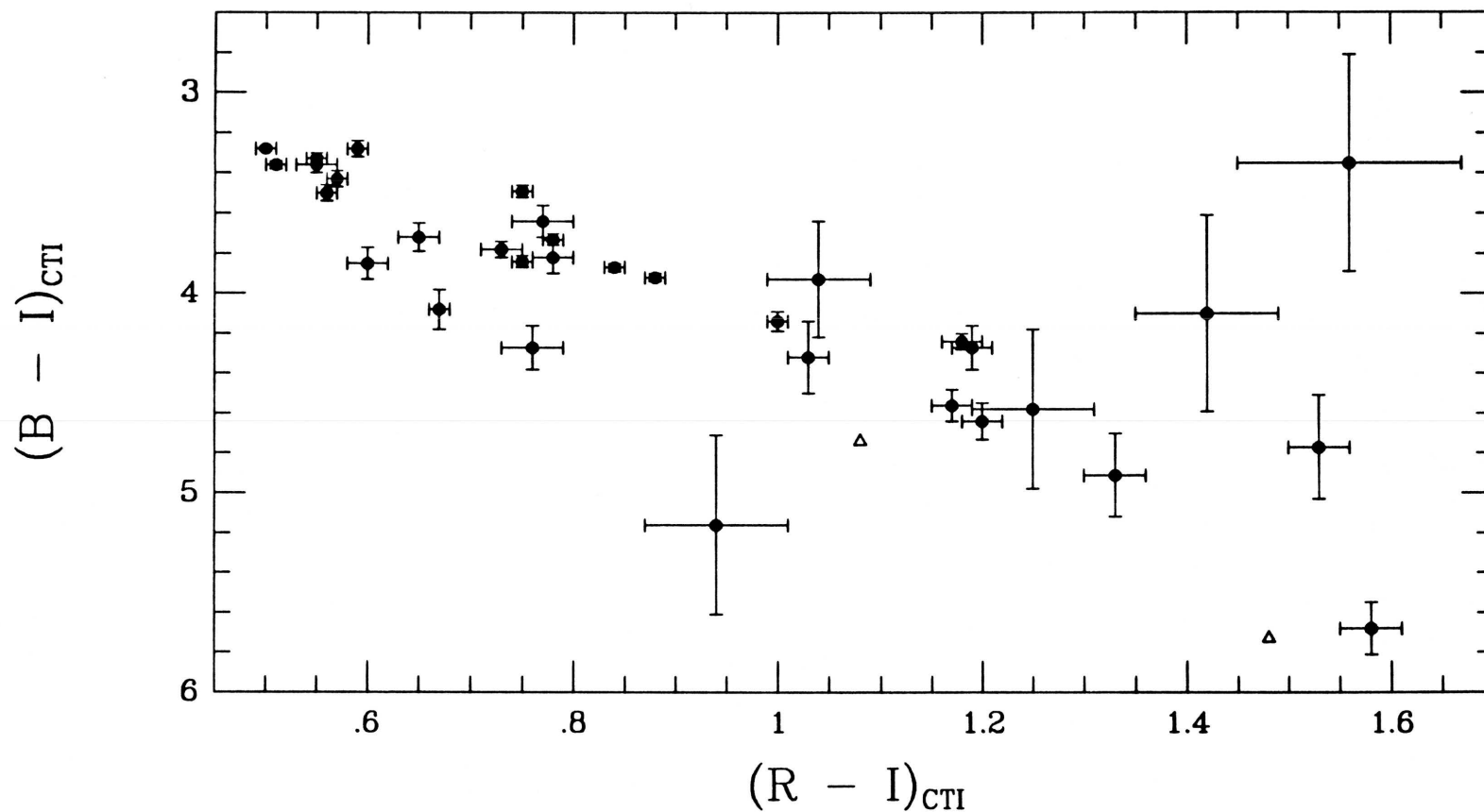


FIG. 4.12. — The $(B - I)_{CTI}$ vs. $(R - I)_{CTI}$ diagram for those spectroscopically observed objects having B_{CTI} measurements. Dwarfs are shown as filled circles, and giants are shown as open triangles. Compare this plot to Figure 4.11.

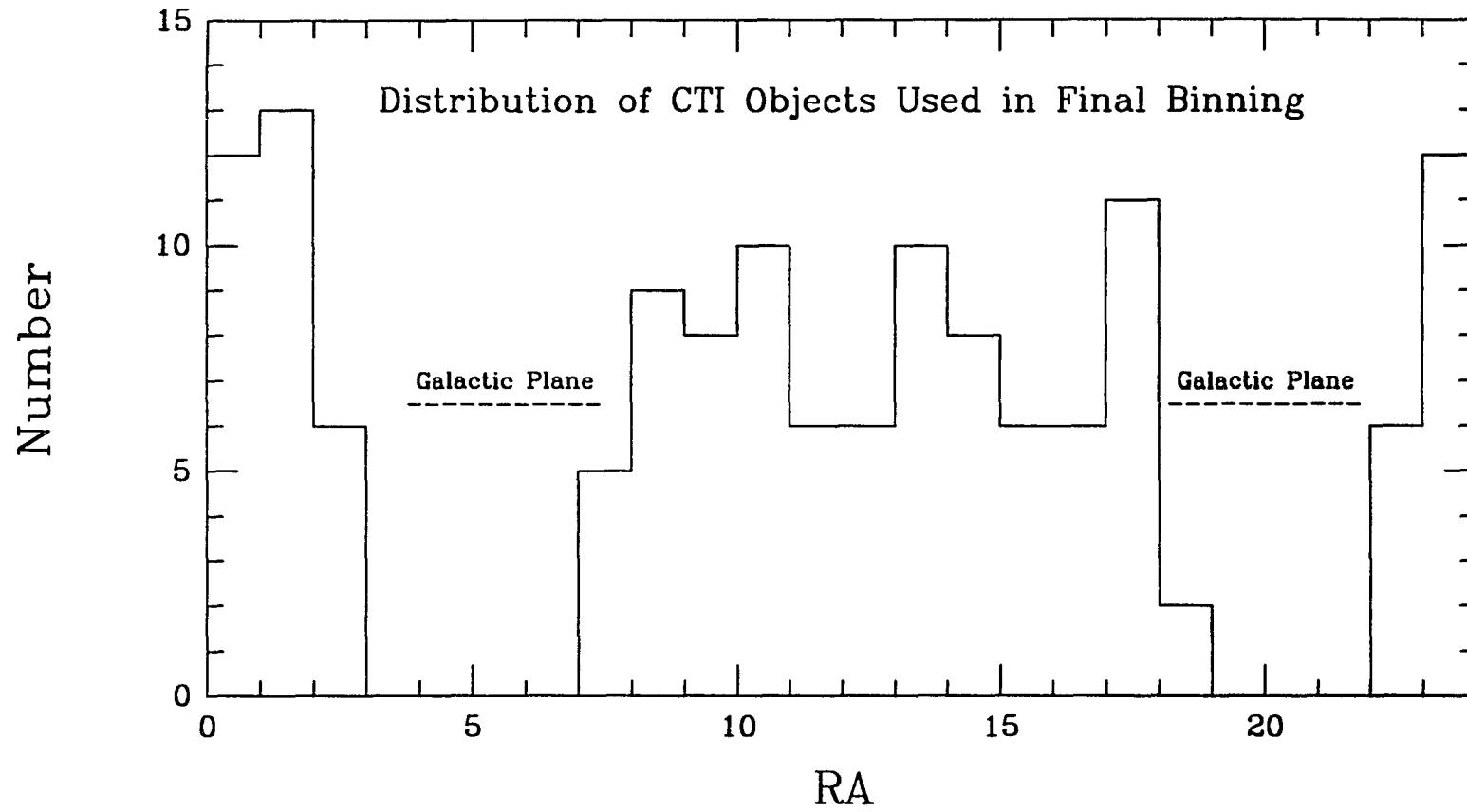


FIG. 4.13. — Histogram in right ascension of the final (136) objects to be used in construction of the luminosity function.

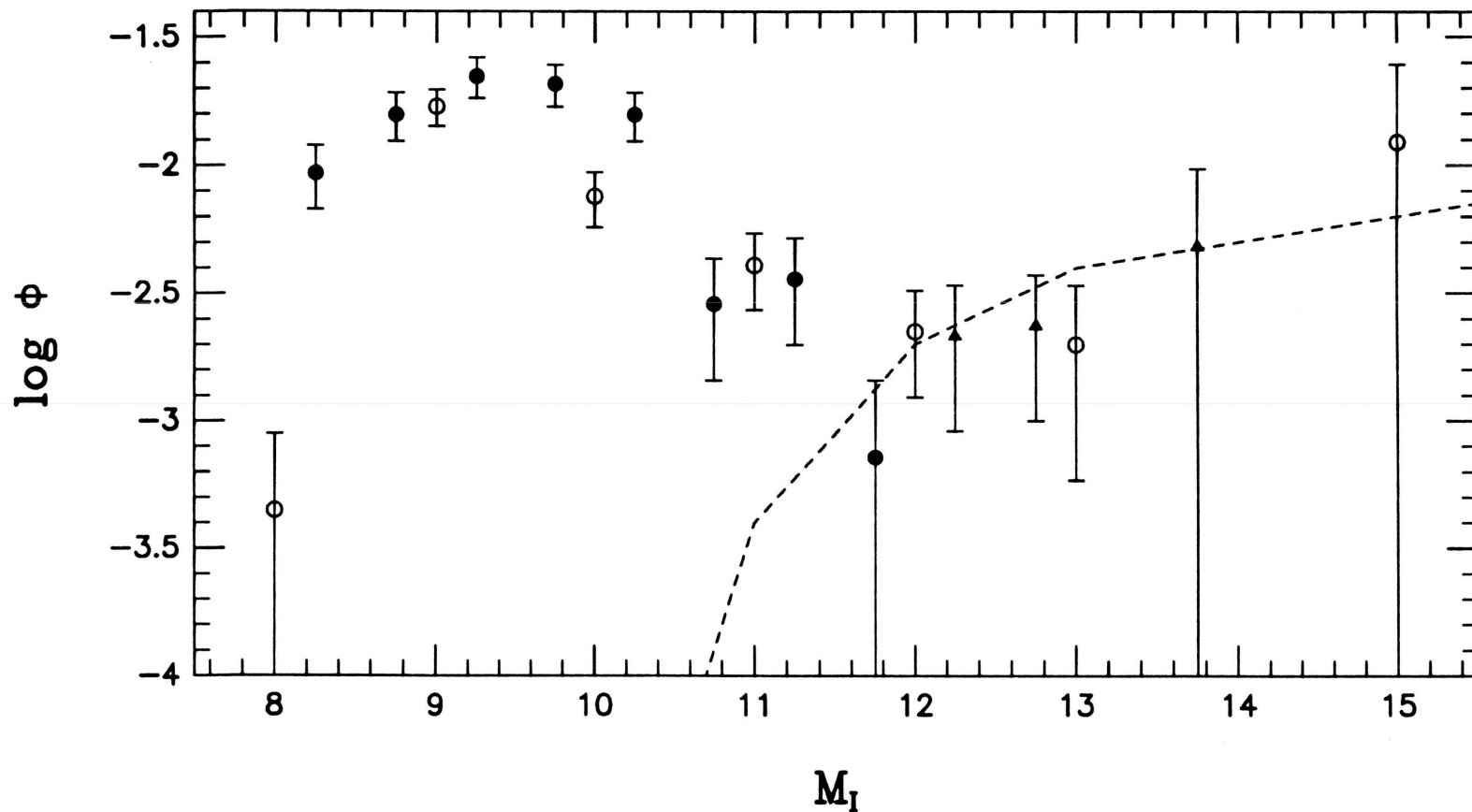


FIG. 4.14. — The (uncorrected) CTI luminosity function Φ of M dwarfs at I , given as filled circles. Filled triangles represent lower-limit points. The error bars represent the Poisson errors in each bin. The open circles show the Leggett & Hawkins (1988) luminosity function at the South Galactic Pole. Note the apparent increase in Φ at the lowest absolute magnitudes. The dashed line shows the contribution of brown dwarfs to the luminosity function as predicted by the theoretical models of Nelson, Rappaport, & Joss (1986).

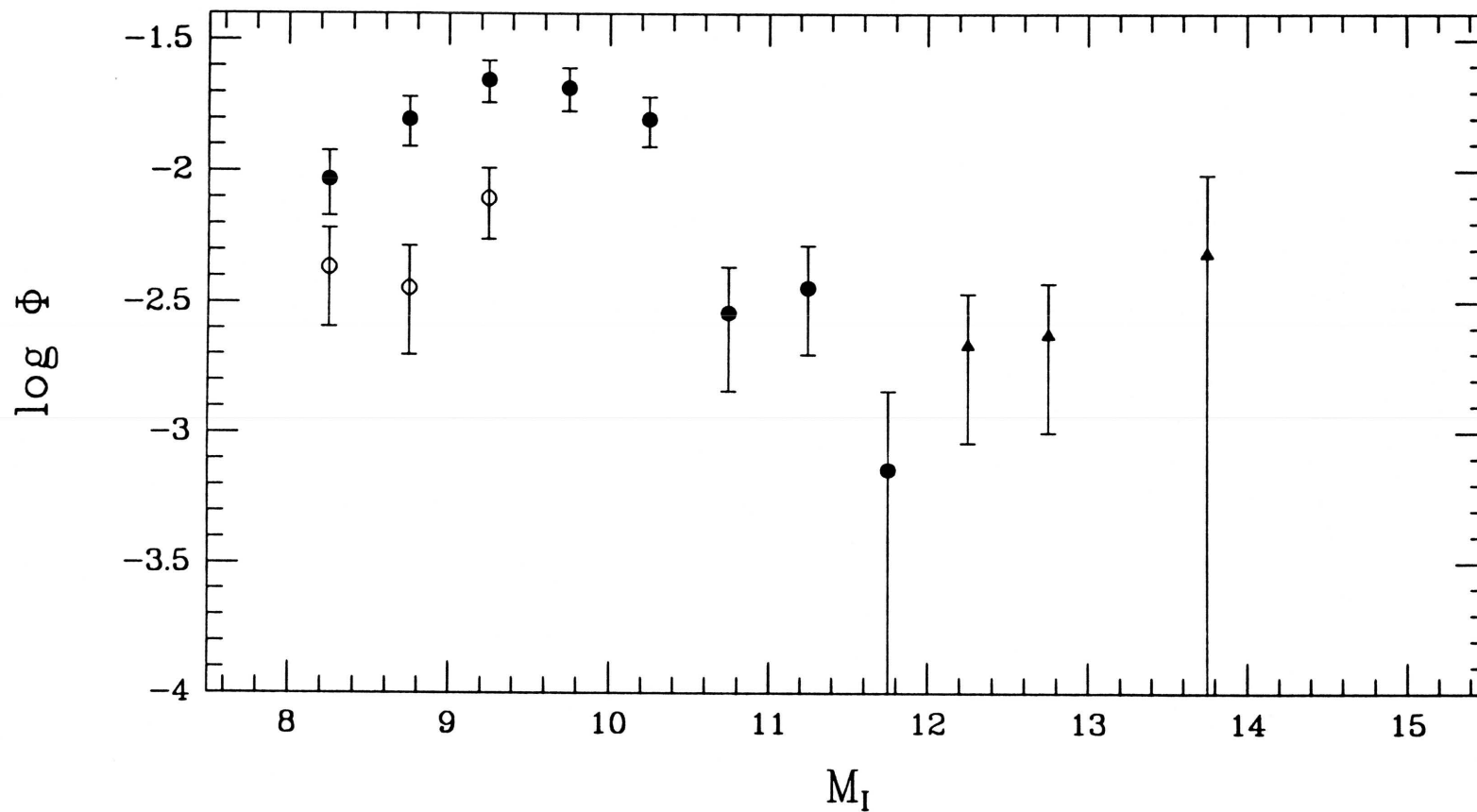


FIG. 4.15. — The CTI luminosity function from Figure 4.14. Open circles represent a recalculation of the first three luminosity bins when calibration equation 4.4 is used instead of equation 4.2. The true luminosity function for these first three bins falls somewhere *between* the open and filled circles.

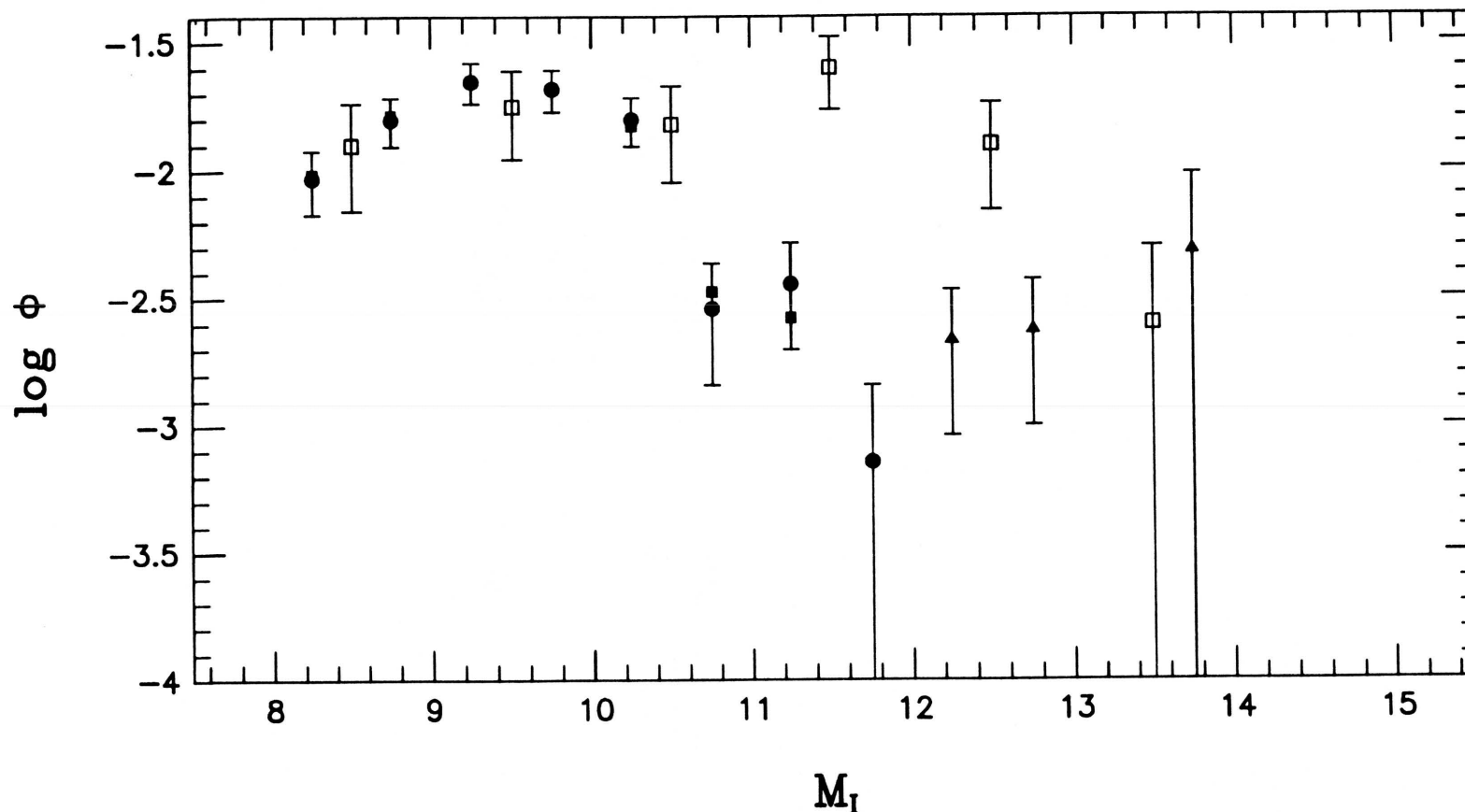


FIG. 4.16. — The CTI luminosity function at I without the Malmquist correction (filled circles and triangles) and with the correction (filled squares). For the first four points, the correction is so small that the two symbols are superposed. For the data points at $M_{I_{KC}} \geq 11.75$, large errors in the absolute magnitude give an aphysical result for the Malmquist correction, so no correction was implemented. The open squares show the luminosity function for objects within 5.2 parsecs, modified from Dahn, Liebert, and Harrington (1985) using I photometry from Leggett (1992) and updated trigonometric parallaxes from Gliese & Jahreiss (1991).

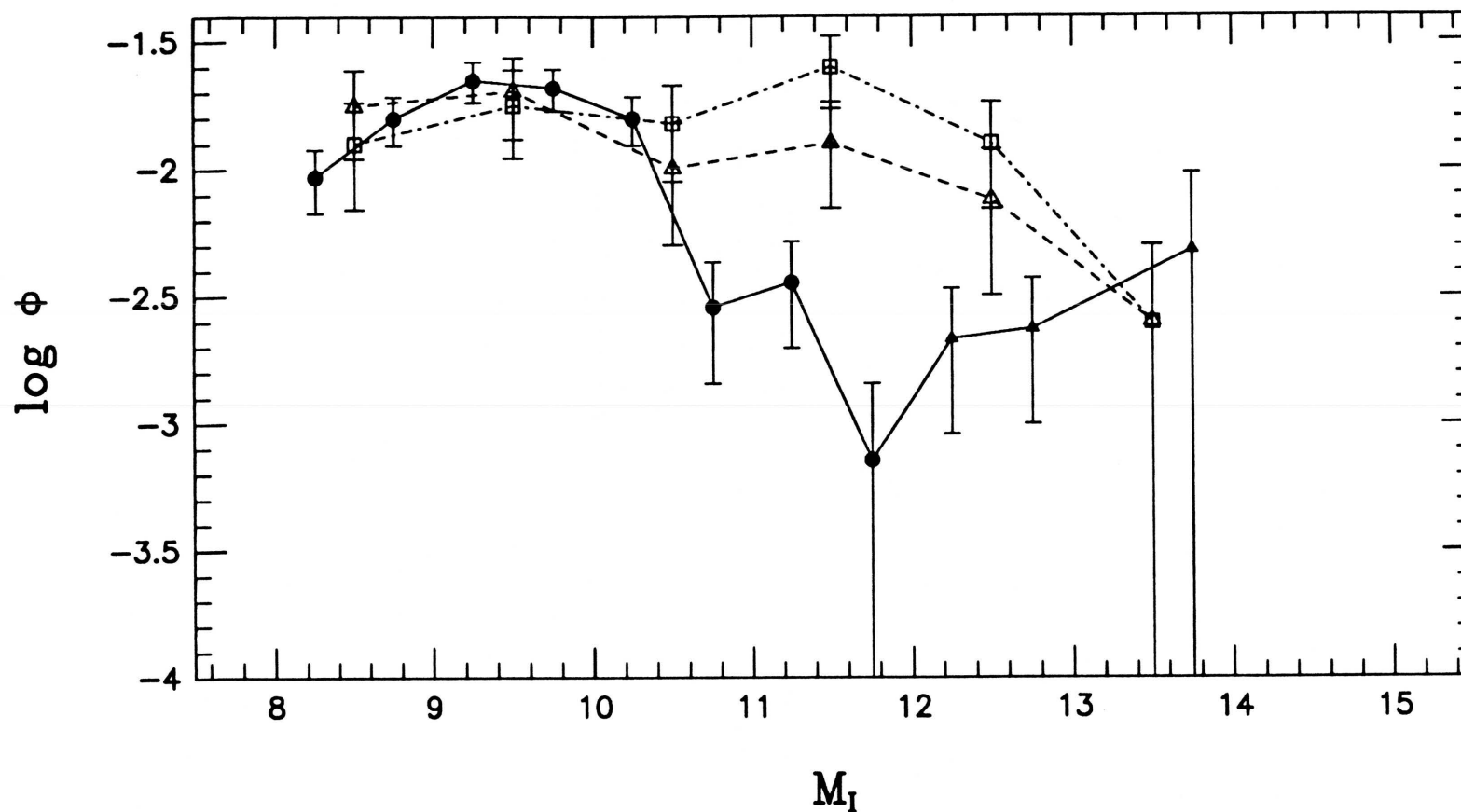


FIG. 4.17. — Comparison of the CTI luminosity function (solid symbols and solid line), the nearby luminosity function of Figure 4.16 (open squares and dot-dash line), and the nearby luminosity function when recomputed as a more distant sample derived photometrically (open triangles and dashed line). See text for discussion.

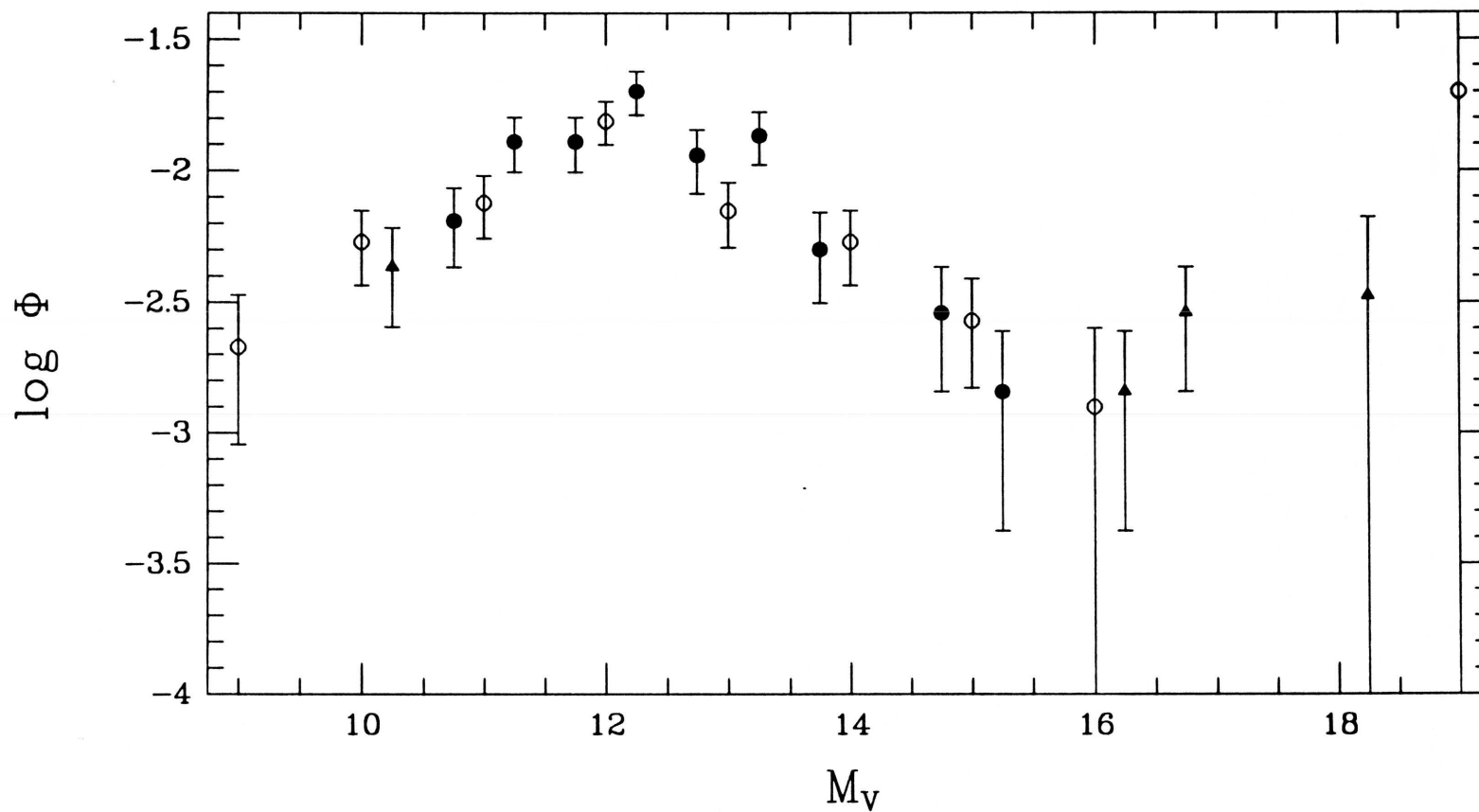


FIG. 4.18. — The (uncorrected) CTI luminosity function Φ of M dwarfs at V , given as filled circles and triangles. The open circles show the Reid & Gilmore (1982) luminosity function at the South Galactic Pole. Again, notice for both determinations the apparent increase in Φ for $M_V > 16$.

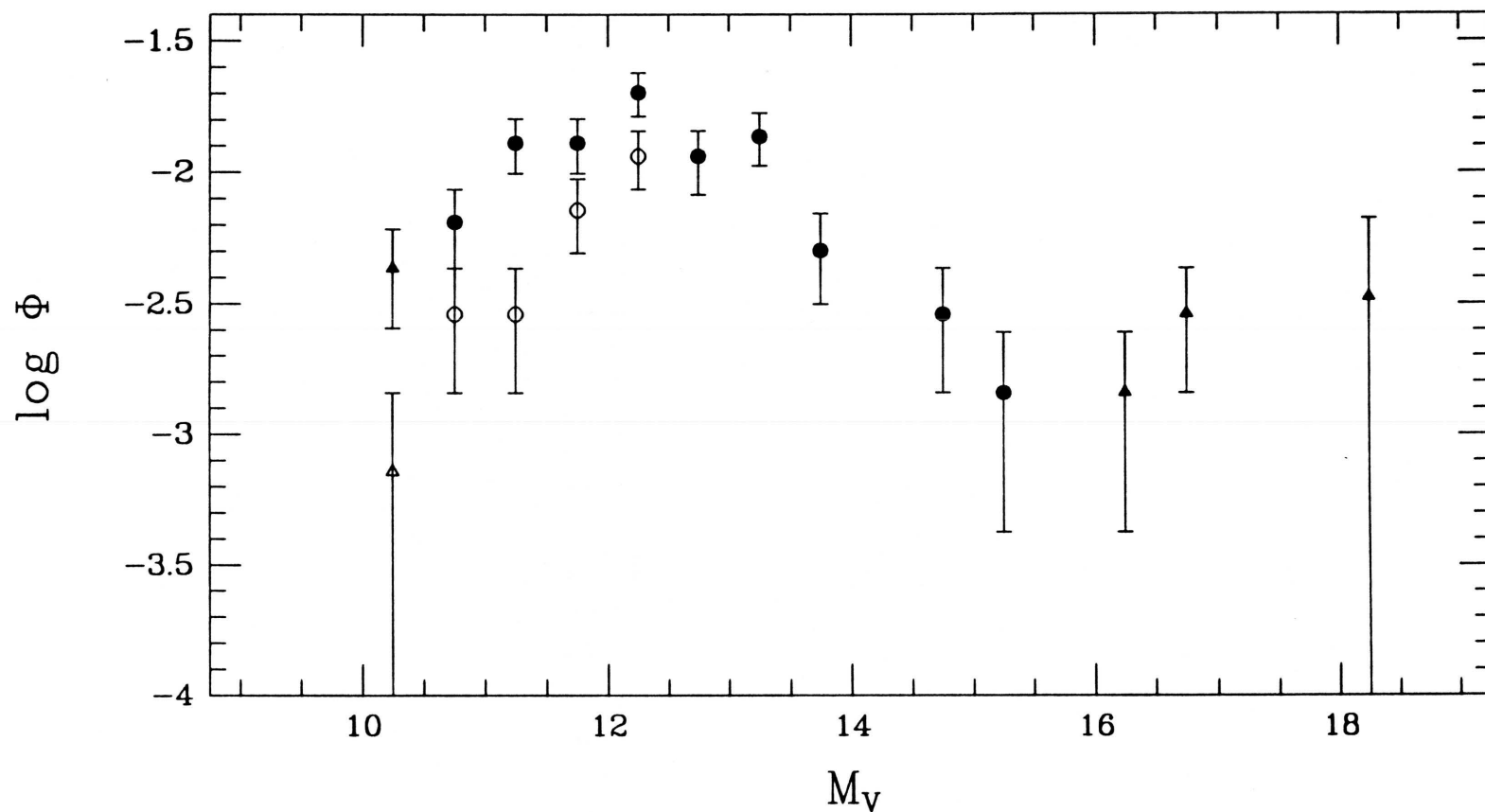


FIG. 4.19. — The CTI luminosity function from Figure 4.18 (solid circles and triangles). Open circles (and triangles for lower limits) represent a recalculation of the first five luminosity bins when calibration equation 4.4 is used instead of equation 4.2. The best estimate of the luminosity function for the first few bins falls somewhere *between* the open and solid symbols.

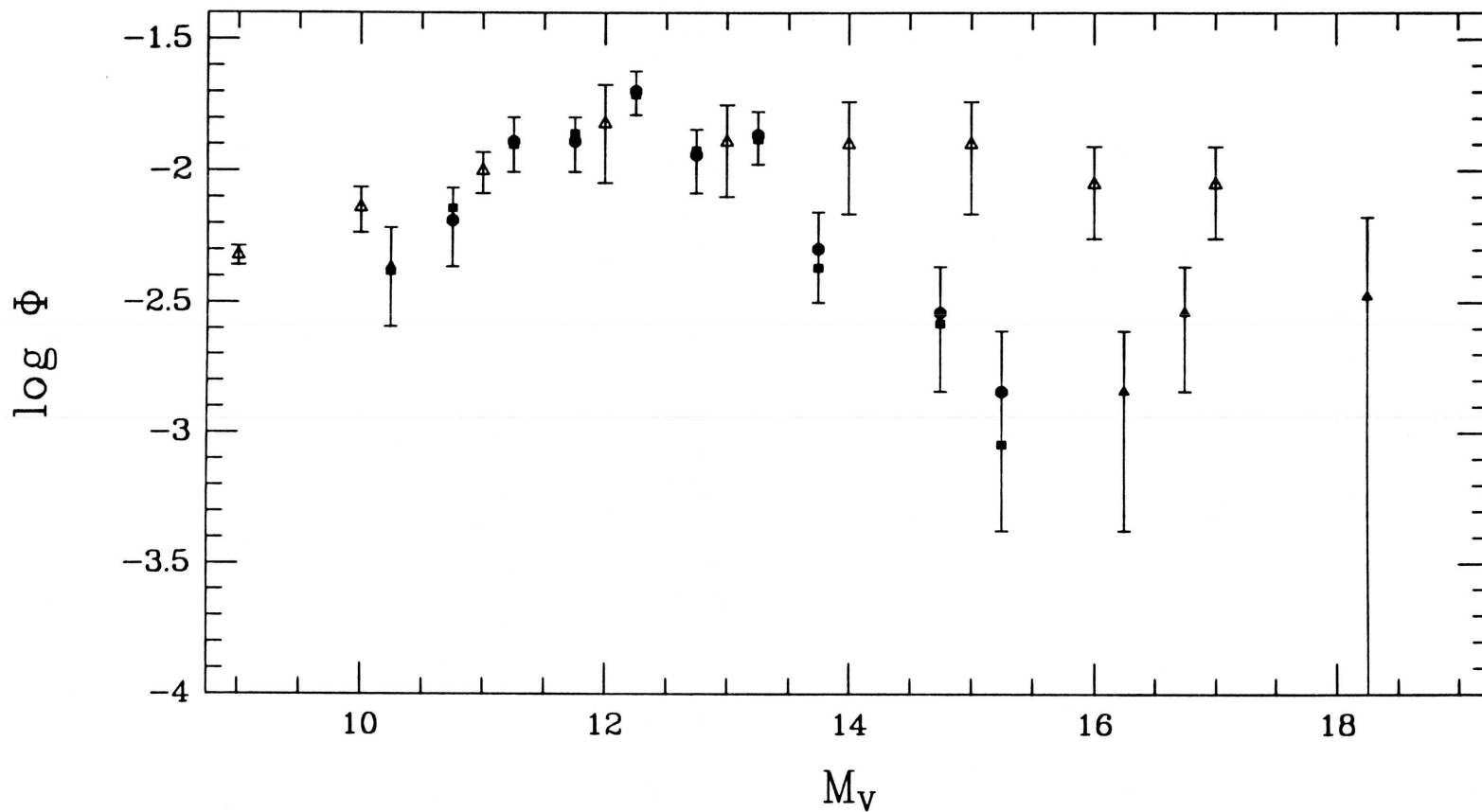


FIG. 4.20. — The CTI luminosity function shown without the Malmquist correction (solid circles and triangles) and with the correction (solid squares). For the data with $M_V \geq 16.25$, no Malmquist correction can be applied. Also shown is the Wielen, Jahreiss, & Kruger (1983) luminosity function for objects within 20 parsecs (open triangles).

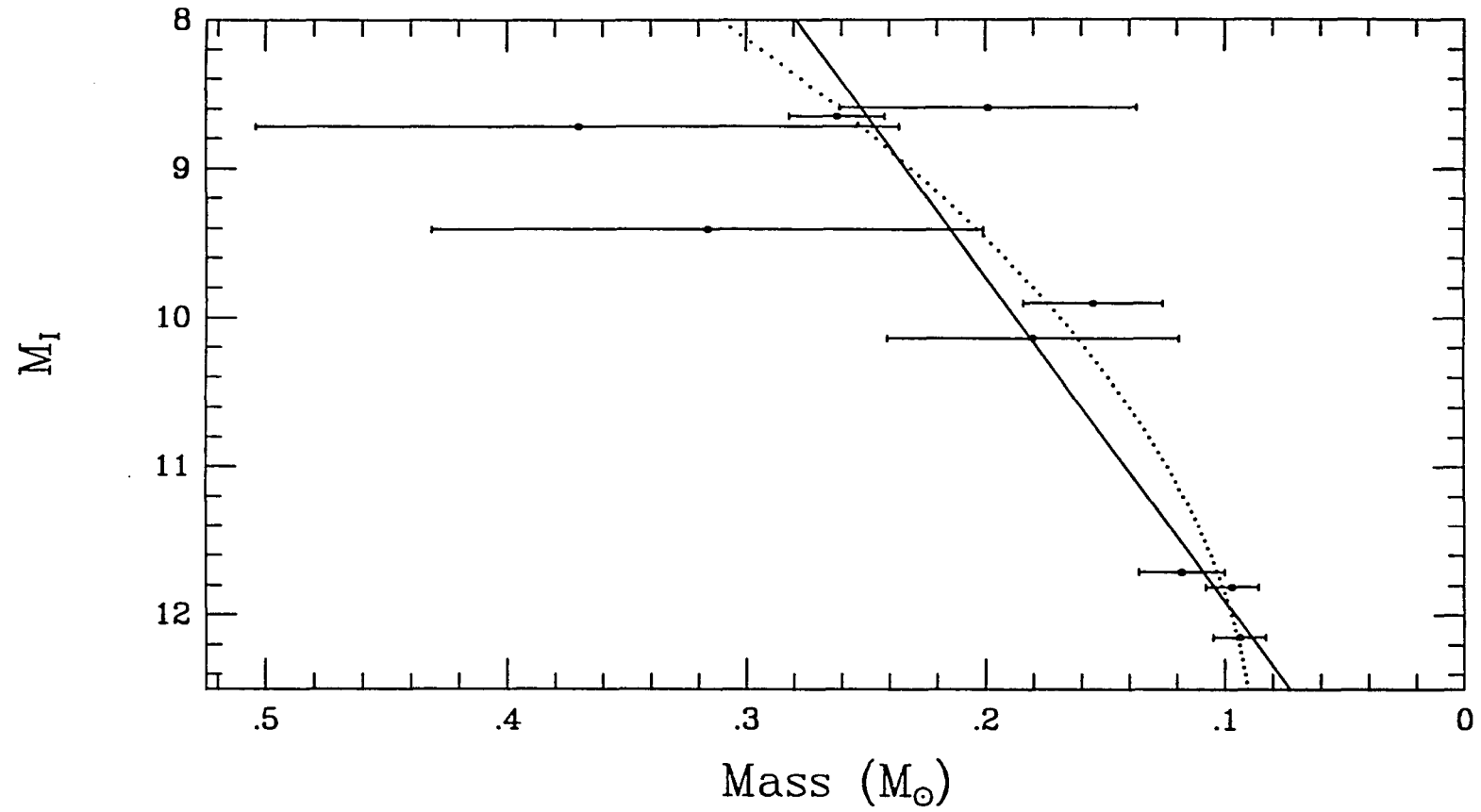


FIG. 4.21. — Plot of absolute I magnitude vs. dynamically determined mass for M dwarfs. The solid line represents a weighted linear least-squares fit to the data, and the dotted line represents a weighted second-order least-squares fit to the data.

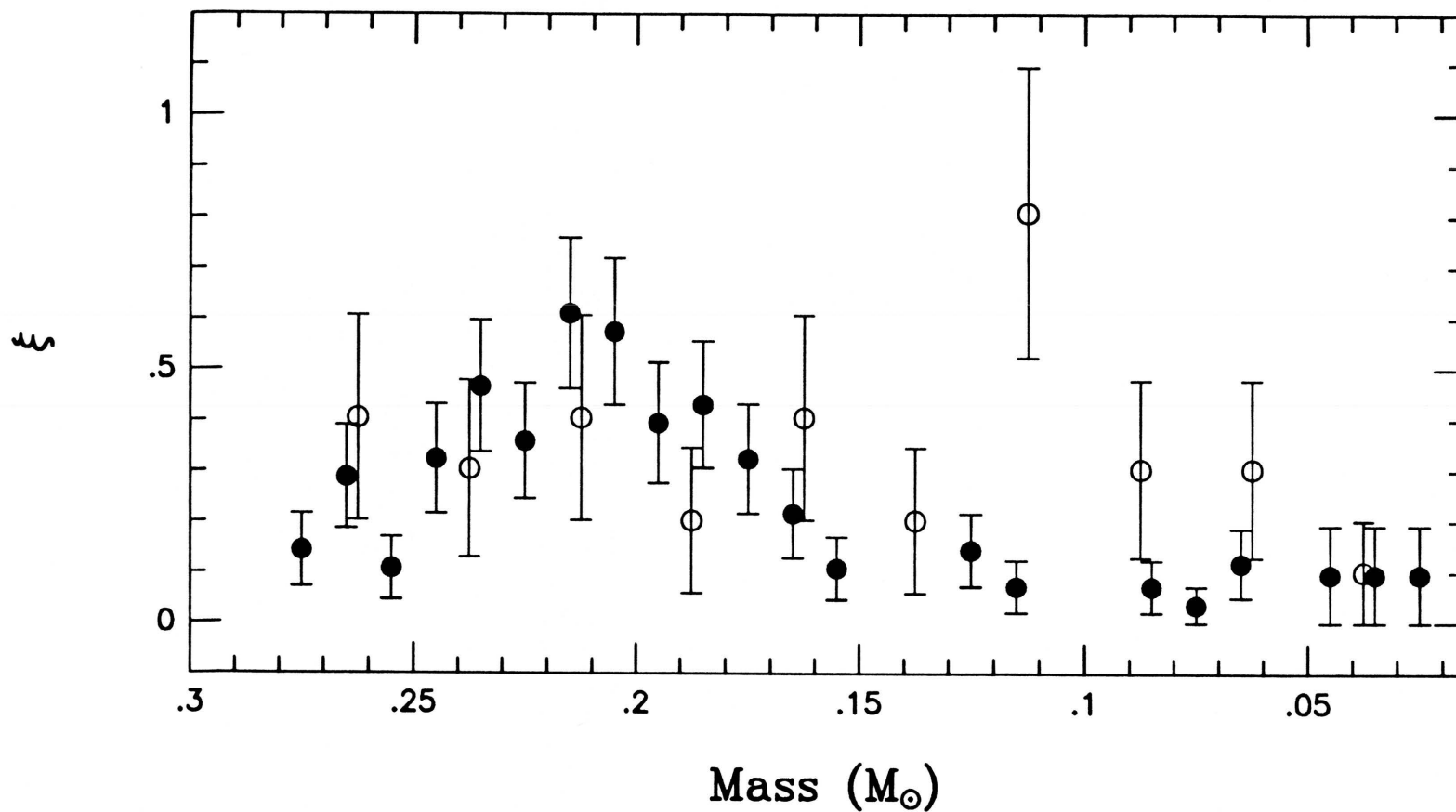


FIG. 4.22. — The derived mass function ξ (filled circles) obtained by using the CTI luminosity function of Figure 4.14 with the *linear* relation of Figure 4.21. Open circles show the mass function when the nearby luminosity function of Figure 4.16 is used. The Poisson errors in each mass bin are shown.

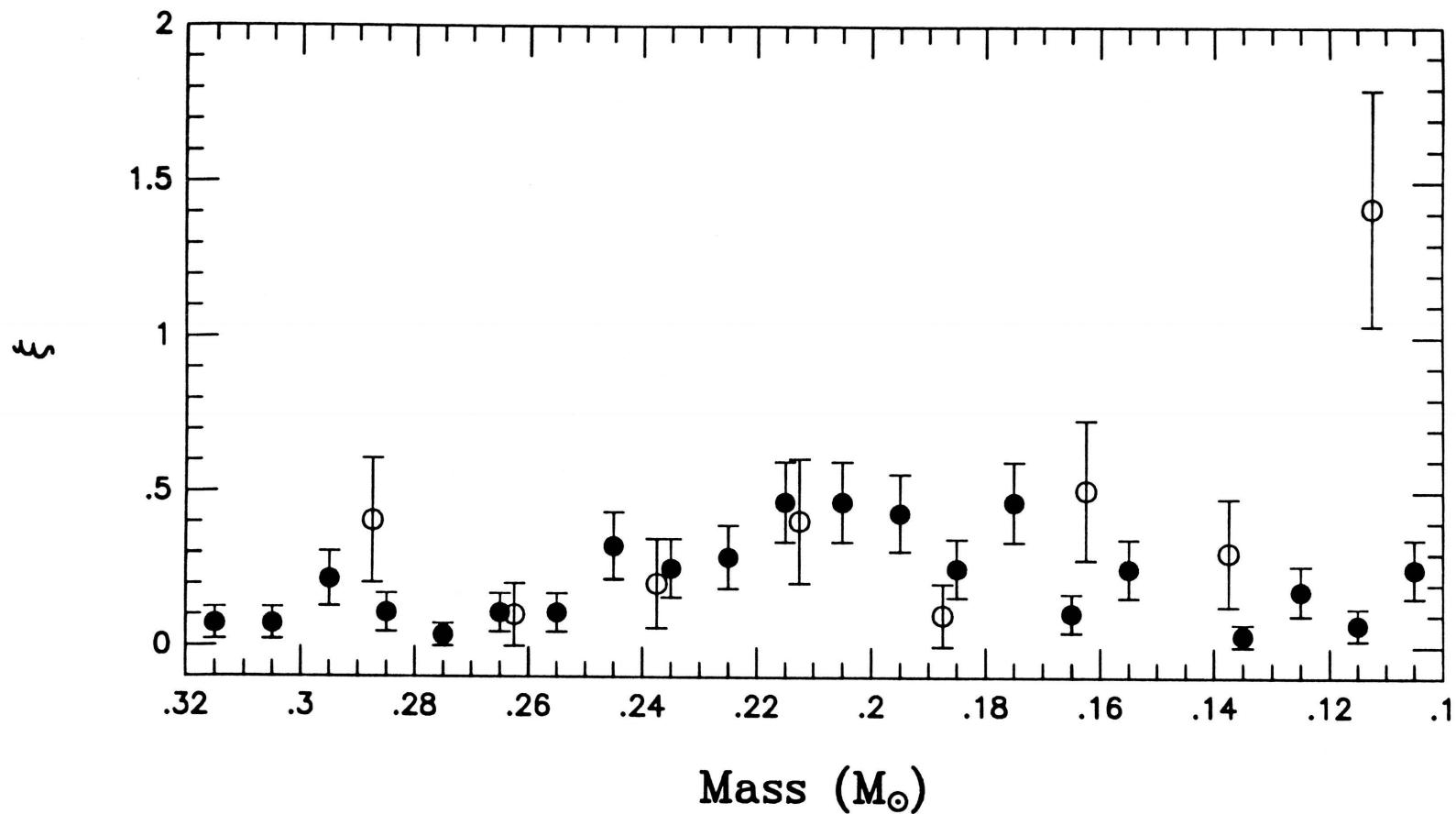


FIG. 4.23. — The derived mass function ξ (filled circles) obtained by using the CTI luminosity function of Figure 4.14 with the *second-order* relation of Figure 4.21. Open circles show the mass function resulting from this second-order relation when the nearby luminosity function of Figure 4.16 is used. The Poisson errors in each mass bin are shown.

CHAPTER 5

GOALS FOR FUTURE STUDIES

Time is the warp of the tapestry which is life... Fate...weaves the design that is never finished. A thread from here, a thread from there, another from out of the past that has waited years for the companion thread without which the picture must be incomplete. But Fate is patient. She waits a hundred or a thousand years to bring together two strands of thread whose union is essential to the fabrication of her tapestry, to the composition of the design that was without beginning and is without end.

— Edgar Rice Burroughs, Tarzan Triumphant, beginning of Chapter 1 (1932)

As the last chapter has shown, there is still much to be learned about the faint end of the stellar luminosity function. The number of extremely low luminosity objects currently known is very small, although intuition might lead one to believe that these objects are actually quite plentiful. Because of their intrinsic faintness, they can only be detected photometrically in the immediate solar vicinity. Discovering large numbers of objects like vB 8, vB 10, and LHS 2924 would require laborious, all-sky surveys. In some cases, however, the companion thread — that is, the painstaking, preliminary research — *can already be found*, and only a little effort is needed to uncover many more of these objects. This chapter thus introduces several scientific projects beneficial to the study of M dwarfs and brown dwarfs and also outlines the research interests that the author plans to pursue at the termination of this thesis.

5.1: FOLLOW-UP TO LUYTEN'S WORK

The study of the solar neighborhood is vital to our understanding of the Milky Way and of stellar systems in general. Our knowledge of the *faintest* local constituents of the Galaxy remains, however, very limited. Of all stars known within 5.2 parsecs of the sun (Batten 1992), M dwarfs comprise 68%, or 46 out of 68, of the total. This space density implies that another 281 M dwarfs should be found between 5.2 and 10 parsecs, yet only 142 are known (Gliese 1969; Gliese & Jahreiss 1979). Furthermore, this 50% incompleteness rate serves only as a lower limit because it assumes that all M dwarfs within 5.2 parsecs have been discovered — since 1986 alone, three new M dwarfs have been added to the 5.2-parsec census (Henry & McCarthy 1990). Two of these (G 208-44 B and GL 866 B) were newly identified companions to stars already known, but the other (LHS 292) was a single object whose identity as a nearby, late-M dwarf had just been recognized (Dahn, Liebert, & Harrington 1986). This shows that unresolved binarity is not the only reason that some objects have been missed.

LHS 292 is just one of more than 3500 objects listed in the LHS Catalogue (Luyten 1979), which lists all objects determined by Luyten to have proper motions exceeding 0.5 arcsecond per year. The catalog is divided into four sections:

- (1) Stars numbered LHS 1 through 73 have proper motions larger than 2 arcseconds per year and include such famous stars as Barnard's Star, 61 Cygni A and B, Arcturus, and the Alpha Centauri system. In general, these stars are relatively bright and had been studied long before 1979.
- (2) Stars numbered LHS 101 through 552 have proper motions between 1 and 2 arcseconds per year. In general, this list contains lesser-known and fainter

objects, but also includes such noteworthy stars as Sirius A and B, Procyon A and B, vB 8, and vB 10.

(3) Stars numbered LHS 1001 through 4058 have proper motions between 0.5 and 1 arcsecond per year. These stars are generally rather faint and include LHS 2924 and LHS 2065.

(4) Stars numbered LHS 5001 through 5413, which Luyten places in his Appendix I, have motions between 0.480 and 0.499 arcsecond per year. These were included because remeasurements of their proper motions might give values of $\mu \geq 0.500$ arcsecond per year, earning them true membership in the catalog.

The number of unclassified objects remaining in the catalog should be determined. Are there late-type, very nearby dwarfs which are, as had been LHS 292, lying unrecognized in this list?

To answer this question, Table 5.1 has been produced. Column 1 gives the LHS number of the object as listed in Luyten (1979). Column 2 gives the GL name (Gliese 1969, numbers from 1 to 915) or the GJ name (Gliese & Jahreiss 1979, numbers from 1001 to 2159). Column 3 gives the G number (Giclas, Burnham, & Thomas 1971; Giclas, Burnham, & Thomas 1978). (The matching of names for columns 1, 2, and 3 was accomplished by comparing the coordinates, the magnitudes, and the sizes and directions of the proper motion listed in the LHS, Gliese, and Giclas catalogs; previous cross-listings were in general not used in an attempt to avoid earlier, incorrect matches.) Column 4 gives other names; preference is given to Bayer designations, then Flamsteed designations, BD (Bonner Durchmusterung, $-22^\circ \leq \delta \leq +89^\circ$) numbers, CD (Cordoba Durchmusterung, $-89^\circ \leq \delta \leq -22^\circ$) numbers, CP (Cape Photographic, $-89^\circ \leq \delta \leq -18^\circ$) numbers,

Wolf or Ross number, other name (such as vB number), and finally variable star designation. In a few cases, this hierarchy has been ignored if a designation further down the list has become the more popular name of the object. For example, LHS 57 is listed as Barnard's Star, not as BD +4° 3561a. For coordinates and magnitudes of all LHS objects, refer to Luyten (1979); for finder charts, refer to Luyten & Albers (1979).

In the LHS Catalogue, both a photographic and a red magnitude are given, and these can be used to generate an $m_{pg} - m_R$ color. These colors are listed in column 5 of Table 5.1. In column 6 are given the spectroscopic classifications and their references, the key for which is found in the notes following the table; when found, classifications from multiple sources are given. This column of the table has relied heavily on the use of the SIMBAD data base, operated at CDS, Strasbourg, France. To aid in the compilation of column 6, a number of additional tables were produced. These complementary tables are given to facilitate cross-referencing between LHS numbers and other names when the LHS number is not known: LHS numbers are cross-listed with GL and GJ numbers in Table 5.2; with G numbers in Table 5.3; with common star names in Table 5.4; with Bayer designations in Table 5.5; with Flamsteed designations in Table 5.6; with HR numbers in Table 5.7; with BD numbers in Table 5.8; with CD numbers in Table 5.9; with CP numbers in Table 5.10; with Wolf numbers in Table 5.11; with Ross numbers in Table 5.12; with variable star designations in Table 5.13; and with other, miscellaneous names (like vB or Lalande numbers) in Table 5.14.

5.1.1: Spectroscopic Identifications of LHS Objects

For LHS 1 to 73, published spectral types were found for 97%. For two entries (LHS 17 and 40) types have not been found; two systems (LHS 8 AB and 68 AB) have composite spectra only; and two others have poor types (LHS 18 and 22). Six objects between LHS 1 and 73 have $m_{pg} - m_R \geq 2.0$, and all are classified as mid-M dwarfs. The reddest of these is LHS 2 with $m_{pg} - m_R = 2.5$ and spectral type M5-5.5 V.

For LHS 101 to 552, published spectral types were found for 79%. Twenty-seven systems have composite spectra only and another twenty have poor types. Of the 95 objects without spectroscopic identification, two (LHS 106 and 211) have $m_{pg} - m_R \geq 2.5$ and would be considered good candidates for late-type dwarfs. Figure 5.1 plots the $m_{pg} - m_R$ color against spectral type for LHS 1 through 552. There is a general trend, though the scatter is large, of increasing $m_{pg} - m_R$ color with later spectral type.

The incompleteness of the spectroscopic classifications in Table 5.1 is glaringly evident for the objects numbered LHS 1001 and higher. In this group, a total of 119 objects have $m_{pg} - m_R \geq 2.5$. These are listed in Table 5.15. To get a better census of nearby, late-type dwarfs, follow-up spectroscopy should be done on all of these which have not been classified previously. Only 46 of the objects in Table 5.15 have known spectral classifications, and 12 of these are first-time identifications by this author. Spectroscopic observations of these 12 objects were obtained with the MMT Red Channel using the previously described set-up and are summarized in Table 5.16. The spectra are presented in Figures 5.2 and 5.3.

As would be expected from a proper-motion selected sample, and as the data in Tables 5.15 and 5.16 confirm, these objects of late color class comprise two distinct groups: nearby ($d \leq 30$ pc) mid- to late-M dwarfs and more distant ($d \sim 100$ pc) subdwarfs of extreme type. The results of the observations on 1992 Feb 25 prove that objects near the end of the main sequence lie unrecognized in the LHS Catalogue — two objects comparable in type to vB 8 and one object comparable to vB 10 were identified. Furthermore, one of the subdwarfs discovered, LHS 2352, is as red as LHS 1742a (Liebert et al. 1993), the latest subdwarf known, but has even weaker bands of TiO .

Neither vB 8 ($m_{pg} - m_R = 2.2$) nor vB 10 ($m_{pg} - m_R = 1.5$), however, would have earned inclusion into Table 5.15. This indicates that other late dwarf candidates, not distinguishable by their $m_{pg} - m_R$ colors, are probably included in Table 5.1. For some of the unclassified objects, clues can be found in follow-up photometry. Specifically, additional photometry of LHS objects is presented in the following sources:

UBV: Sandage (1964); Sandage (1969); Augensen & Buscombe (1978);
 Carney (1978); Harrington & Dahn (1980); Sandage (1981); Dahn
 et al. (1982); Harrington et al. (1985); Sandage & Kowal (1986);
 Fouts & Sandage (1986); Sandage & Fouts (1987); Carney &
 Latham (1987); Dahn et al. (1988); Ryan & Norris (1991).

UBVRI: Eggen (1979); Eggen (1980); Ryan (1989).

UBVRIJHK: Carney (1983a); Carney (1983b).

BVRI: Eggen (1987).

VRI: Weis (1991).

VI: Monet et al. (1992).

Table 5.1 is, of course, also useful for uncovering objects other than M dwarfs and subdwarfs:

(1) There are 71 objects having $m_{pg} - m_R \leq 0.0$. Of the 54 with spectroscopic identifications, 52 are white dwarfs. The 17 unclassified objects are all prime white dwarf candidates.

(2) Between the extremely blue and the extremely red entries of Table 5.1 lies the majority of objects, from which will doubtless come other interesting discoveries and perhaps even new classes of stars. An example is the discovery of a rare object known as a dwarf carbon star — LHS 1555, also known as G 77-61 (Dahn et al. 1977). Within the past year, four more dwarf carbon stars have been recognized (Green, Margon, & MacConnell 1991; Green et al. 1992), and among these is LHS 1075. Spectra of LHS 1555 and LHS 1075 are shown in Figure 5.4

5.1.2: Late-type Stars in Binary and Multiple Systems

A census of nearby stars would be incomplete without an accurate knowledge of each system's multiplicity. Binary stars are necessary for mass determinations, and the recognition of low-mass companions will help to answer questions concerning the frequency and nature of late-M dwarfs, brown dwarfs, and planets. Some of the entries in Table 5.1 have been checked for binarity through astrometric, spectroscopic, photometric, imaging, and interferometric techniques. An asterisk next to the object name in column 1 of Table 5.1 indicates an object which, although listed as a single LHS entry, has been suspected or confirmed as a binary or multiple object. Each of the asterisks refers to a note given in Table 5.17, which lists, in increasing order, the LHS number (and designations

of A, B, and C given for confirmed components) with a parenthetical note giving the status of the system followed by notes and references to the suspected or confirmed multiplicity. The codes for the system status are —

Conf. = binarity or multiplicity confirmed.

As = astrometric perturbations suggest a companion.

As? = unverified astrometric perturbations suggest a companion.

As?? = dubious astrometric perturbations suggest a companion.

CPM? = nearby object may share common proper motion.

Ecl? = photometric measures suggest eclipse by unseen companion.

Flare? = possible flaring events suggest an unseen companion.

Opt = nearby companion is optical only.

Opt? = suspected companion may be optical only.

Phot? = photometry suggests excess flux due to unseen companion.

Radio? = radio emission detected from possible unseen companion.

SB = single-lined spectroscopic binary or radial velocity variable.

SB? = unverified single-lined spectroscopic binary or velocity variable.

Speck? = speckle interferometry may suggest a companion is present.

Vis? = companion was, perhaps, visually resolved but is now unseen.

As this legend suggests, the multiplicity is considered definite (Conf.) if distinct and recurrent eclipses are detected, if the object is a double-lined spectroscopic binary, or if the companion is resolved through, for example, visual, photographic, or speckle techniques and is found to be physically associated with the primary.

Among the entries in Table 5.17 are found several confirmed secondaries which lie near the stellar/substellar break: LHS 154 B (δ Tri B), LHS 417 B (GL 623 B), LHS 472 B (Wolf 1062 B), LHS 1047 B (GJ 1005 B), and LHS 3494

B (G 208-44 B). Other entries which have suspected companions in the late-M dwarf/brown dwarf/planetary regime include LHS 26 (Stein 2051 A), LHS 33 (Luyten's Star), LHS 57 (Barnard's Star), LHS 2042 (GL 319 AB), LHS 2665 (GL 494), LHS 2693 (HD 114762), LHS 3076 (G 152-31), LHS 3277 (GJ 1215), LHS 3509 (GL 777 B), LHS 3556 (GL 791.2), LHS 3853 (EV Lacertae), and LHS 5405 (G 29-38). Follow-up observations of these objects are continuing as other entries in Table 5.1 are slowly being added to these observing programs.

Newly recognized late-type stars from Table 5.16 and from subsequent observing runs can be imaged in the infrared to detect companions of even later type. With current infrared arrays, typical separations studied are on the order of 20 to 1000 AU for nearby stars. First-epoch images are taken to obtain colors of all field stars in an attempt to photometrically select red, possible low-mass secondaries. Second-epoch images are taken to check for common proper motion. Henry & Simons (Henry 1992) have begun such a systematic survey around all known, northern M dwarfs within 8 parsecs. This author plans to do a similar survey for all known, northern dwarfs of type M6.5 and later. These surveys are the infrared analogues to the photographic survey completed by van Biesbroeck (1961), who imaged fields around ~ 650 stars with proper motions of ≥ 0.75 arc-second per year. It was this survey which provided the original discoveries of vB 8 and vB 10.

5.1.3: Spectroscopic Identifications for "The Stars of Low Luminosity"

The LHS Catalogue contains only those Luyten discoveries with $\mu \geq 0.5$ arcsecond per year, though he catalogued many more objects with proper mo-

tions down to ~ 0.2 arcsecond per year. In a monograph entitled “The Stars of Low Luminosity” (Luyten 1977), all of his discoveries with large reduced proper motions ($H = m + 5 + 5 \log \mu$, which is analogous to the absolute magnitude if one believes that the size of the proper motion gives some indication of the distance) are tabulated. In total, Luyten lists 2907 objects, and the 443 having $m_{pg} - m_R \geq 3.0$ are given in Table 5.18. Amazingly, only 18 of these have been spectroscopically identified, all of which are cross-listed as LHS objects. This author plans to produce finder charts for these objects and to obtain spectra of a subset of these. The number of presently unknown, nearby M dwarfs and brown dwarf candidates contained in this list could be staggering and would have profound ramifications on our knowledge of the stellar luminosity function.

5.2: A New Proper Motion Survey

A means of discovering nearby stars is to search for objects having extremely large proper motions. Table 5.19 lists all known objects with motions exceeding ~ 3 arcseconds per year. Columns 1 and 2 give the LHS number and other names for each star, column 3 gives the proper motion, column 4 gives the V magnitude, and column 5 gives the spectral type. Note the complete absence of faint ($m_V \geq 15$) stars. When this list is compared to a similar list from a 1927 textbook by Russell, Dugan, & Stewart (see column 6 of Table 5.19), it is found that there are very few differences. Of the 35 stars listed in Table 5.19, 24 were already known in 1927. Of the 11 additions, two were discovered as companions to stars already on the list, three were discovered by Ross between 1925 and 1939, one was discovered by Luyten and Ebbighausen in 1935 (Luyten & Ebbighausen

1935), four were discovered by Luyten during the Bruce Proper Motion Survey (before 1957), and the last was discovered on Palomar plates by Luyten in 1968, before measuring machines were used (Liebert 1991). In fact, Russell, Dugan, & Stewart (1927) state emphatically that their table “is undoubtedly incomplete... there is a fair chance that photographic observations may detect some faint star with a proper motion greater than Barnard’s star, and a practical certainty that they will in future add a good many stars to the list.” Clearly, however, the intervening years have seen few additions.

The reason for this discrepancy can be understood by reviewing the two major proper motion surveys undertaken in the last 50 years — those by Giclas and co-workers at Lowell Observatory and by Luyten at the University of Minnesota. The Lowell Survey (Giclas, Burnham, & Thomas 1971; Giclas, Burnham, & Thomas 1978) covered declinations north of $\delta \sim -5^\circ$, with spotty coverage between $\delta = -5^\circ$ and -40° . The Bruce Proper Motion Survey (Luyten 1955) covered almost the entire southern hemisphere and about 30% of the northern hemisphere (Luyten 1963). Both of these surveys quote a limiting magnitude of $m_{pg} \sim 16.0$ to 16.5, though the onset of incompleteness is $m_{pg} \sim 14.5$ to 15.0 (Liebert & Probst 1987). The Luyten Palomar survey (Luyten 1963) covered declinations north of -33° (with spotty coverage for galactic latitudes $\pm 20^\circ$ from the plane) down to a limiting magnitude of $m_R \sim 20.8$; however, an algorithm for matching plates was limited to proper motions of less than 2.5 arcseconds per year (Luyten 1987; Liebert & Probst 1987). These surveys, therefore, would have completely missed the fainter, highest proper motion objects — those still unrecognized, nearby, low-luminosity, low-mass members of the solar neighborhood.

If Wolf 359 were moved out to 3.4 parsecs, its apparent magnitude would be fainter than the detection limit for the Lowell or Bruce surveys, and its proper motion of 3.25 arcseconds per year would be larger than the detection limit of the Luyten Palomar survey. Furthermore, if vB 10 and LHS 2924 were moved close enough so that their proper motions measured greater than 2.5 arcseconds per annum, they would shine dimly at $m_{pg} \sim 18.2$ and 18.7, respectively — too faint to have been detected by the Lowell or Bruce surveys — yet would lie at distances of 3.5 and 3.4 parsecs, respectively!

Table 5.20 lists objects with $\mu \geq 0.57$ arcsecond per year which are not included in the LHS Catalogue. Several of these objects are southern stars missed by the Bruce survey because of their faint apparent magnitudes. Several others were added by Luyten after fields near the galactic plane were measured. Interestingly, the first star in Table 5.20, GJ 2045, is an object which Luyten may have missed because its motion was larger than the Luyten Palomar detection limit. (However, there is a possibility that this object is actually a rediscovery of LHS 1777, whose proper motion Luyten gives as 0.971 arcsecond per year. This proper motion, together with Luyten's 1950 position of the object, coincides with the position given for GJ 2045 in Ohtani & Ichikawa (1977), where it is denoted as star #50. In this case the motion cited by Ohtani & Ichikawa must have been overestimated, which is likely since their calculation was based on comparing the object's position on a 1976 plate with the object's position on the Palomar Observatory Sky Survey *prints*.)

Ruiz, Maza, & Wischnjewsky (1988) have begun a proper motion search in the southern hemisphere by blinking ESO plates taken 3 to 7 years apart. The blinking process combined with the ESO plate limit of $m_R = 21$ means that any

faint, high- μ objects missed by Luyten can be uncovered. This new search began in 1986, and to date results on only two $5^\circ \times 5^\circ$ fields have been reported (Ruiz, Maza, & Wischnjewsky 1988; Ruiz & Maza 1990).

In the northern hemisphere, no such follow-up to Luyten's survey is underway. Evans' (1992) search for "high proper motion" stars is limited to motions of less than 0.5 arcsecond per year. The parallax survey of Perlmutter et al. (1986), whose aim is to identify a faint stellar companion (Nemesis?) to the sun, is limited to known M dwarfs listed in the Dearborn Catalogue of Faint Red Stars, which is complete to only 13th magnitude.

Again, the preliminary observations for such a project are already being taken — by, in this case, the second-generation Palomar Observatory Sky Survey (POSS II). High proper motion objects will be best detected if the time baseline between plates is relatively short. For the Luyten Palomar survey, this baseline was typically 11 to 13 years, meaning that a star at the upper detection limit of $\mu = 2.5$ arcseconds per annum would have moved $450 \mu m$ on the plate. Luyten was easily able to detect stars with $\mu \sim 0.1$ arcsecond per annum, corresponding to $18 \mu m$ on the plate. (For the APM proper motion project, Evans (1992) quotes upper and lower detection limits of 160 and $16 \mu m$, respectively.) To allow for some overlap between Luyten's candidates and newly discovered ones, the lower limit on μ for this new search should be no larger than ~ 1.5 arcseconds per annum. This would correspond to a time baseline of ≥ 1 year. Adopting Luyten's upper detection limit of $450 \mu m$ means that a star like Barnard's could be detected in ≤ 3 years.

Rejected POSS II plates, which have been discarded because of too many airplane trails or various other flaws but which are still useful for science, can

be used as epoch 1, and retakes of the same regions can be used as epoch 2. The typical amount of time between the discards and the retakes is 3 or 4 years, which satisfies the criteria stated above. Presently, there are already over 100 fields which have 2 useable, rejected plates (Reid 1991). These plates cover over 2900 square degrees to a limiting magnitude of $R = 20.8$ (Reid et al. 1991), and a subset will be used by this author for the preliminary stages of this investigation.

5.3: A New Photometric Search for Late Dwarfs

The new proper motion search mentioned above will, of course, miss those nearby objects having small tangential velocities. To discover faint, nearby M dwarfs and brown dwarf candidates with small values of μ , a photometric search is required. As Chapter 4 has shown, this search should be conducted over a large area of sky to combat the poor sampling statistics which have plagued most previous photometric surveys. Tinney and collaborators have begun such a survey by using POSS II plates covering an area of 320 square degrees. Preliminary results over 60% of this region are presented in Tinney, Mould, & Reid (1992) along with the derived luminosity and mass functions. The POSS II has an advantage over the POSS I in that for the new survey, plates are being taken in the blue (IIIa-J), the red (IIIa-F), *and* the near infrared (IVN) (Reid et al. 1991) — so a search for red stars is limited by the R magnitude of 20.8 rather than by the blue magnitude of the POSS I. An extension of the Tinney survey to even larger areas can be accomplished in tandem with the new proper motion survey outlined above. After positions and magnitudes are measured for all images on the subset of IIIa-F plates, subsequent measures can be made on the IVN plates

of the same field to generate an $R - I$ color for each matched object. The reddest of these will likewise be spectroscopically observed and then imaged in the infrared to search for companions.

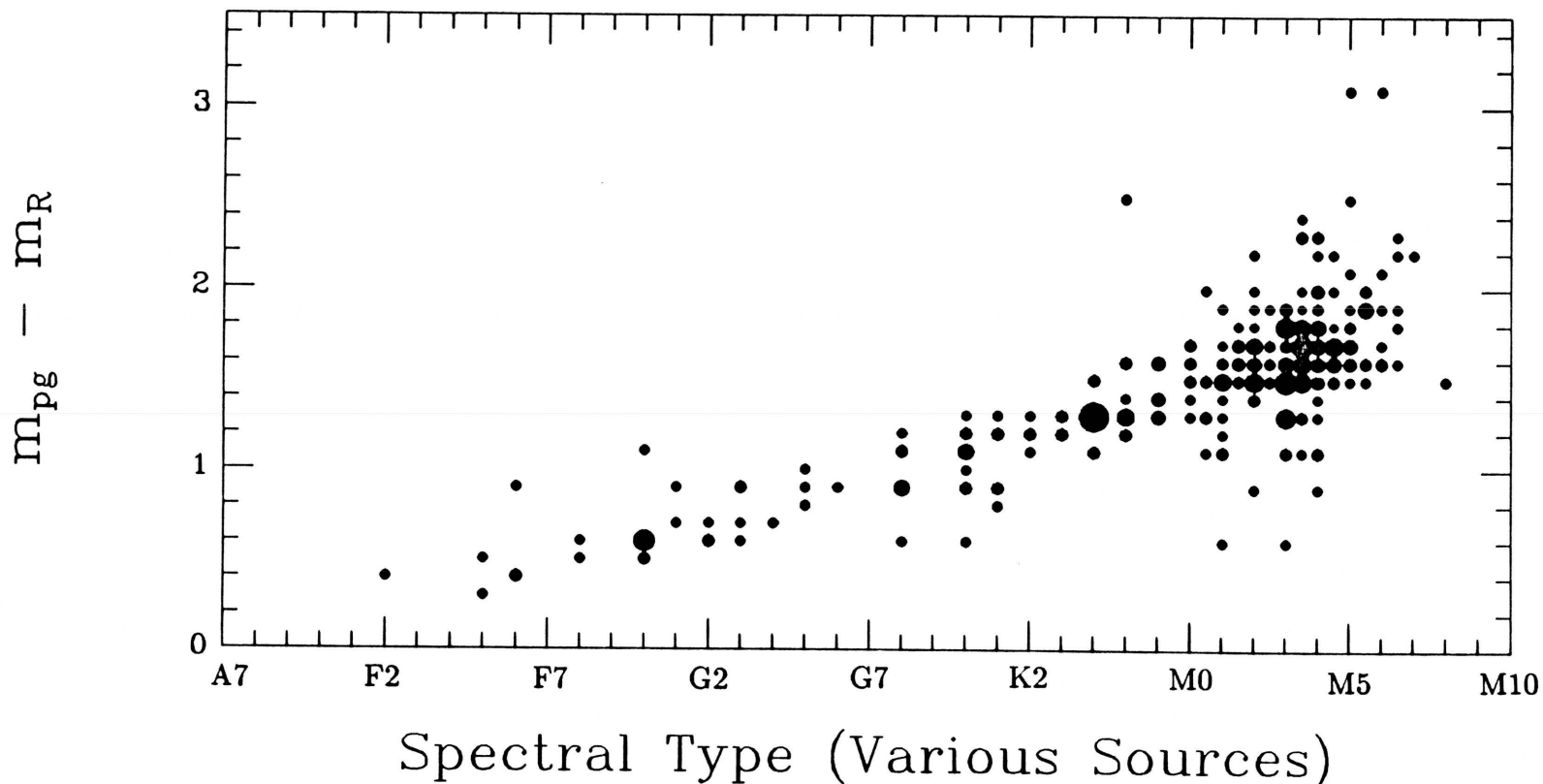


FIG. 5.1. — $m_{pg} - m_R$ color versus spectral type for those LHS stars (1 through 552) with spectral types in the literature. White dwarfs, subdwarfs, and higher luminosity stars like Arcturus are not included here. The smallest circles represent one data point each; where two data points fall together, a slightly larger circle is drawn, etc. The largest circle, at type K4, represents the superposition of eleven different points. Along the horizontal axis, tick marks are shown for every unit subclass. There are no subclasses labelled K6, K8, or K9 in accordance with Kirkpatrick, Henry, & McCarthy (1991). The scatter is large due to large color errors and to heterogeneous classifications, but nonetheless it is clear that very red candidates (later than M6) can be selected from the LHS Catalogue by using the $m_{pg} - m_R$ color as a preliminary criterion for selection.

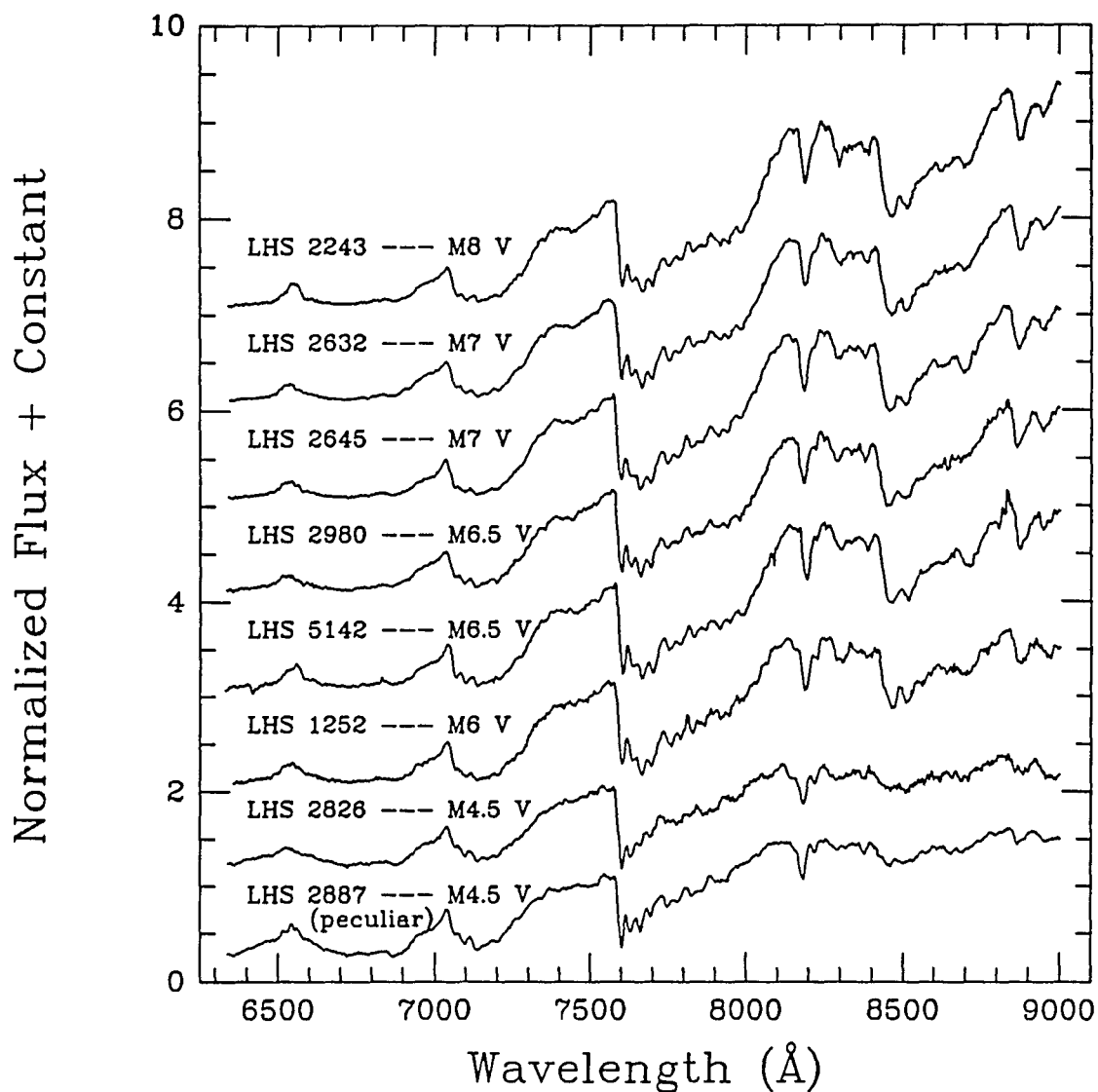


FIG. 5.2. — MMT spectra of newly identified M dwarfs from Table 5.15. Most of these have proven to be of late type, with the latest being the M8 dwarf LHS 2243. The spectrum of LHS 2887 is peculiar, relative to other M4.5 dwarfs, in that the flux between 7300 and 7600 Å is suppressed. Data for each of the spectra can be found in Table 5.16. Telluric absorption has not been removed. The flux is in units of F_{λ} , normalized to one at 7500 Å, with integral offsets added to separate the spectra along the vertical axis.

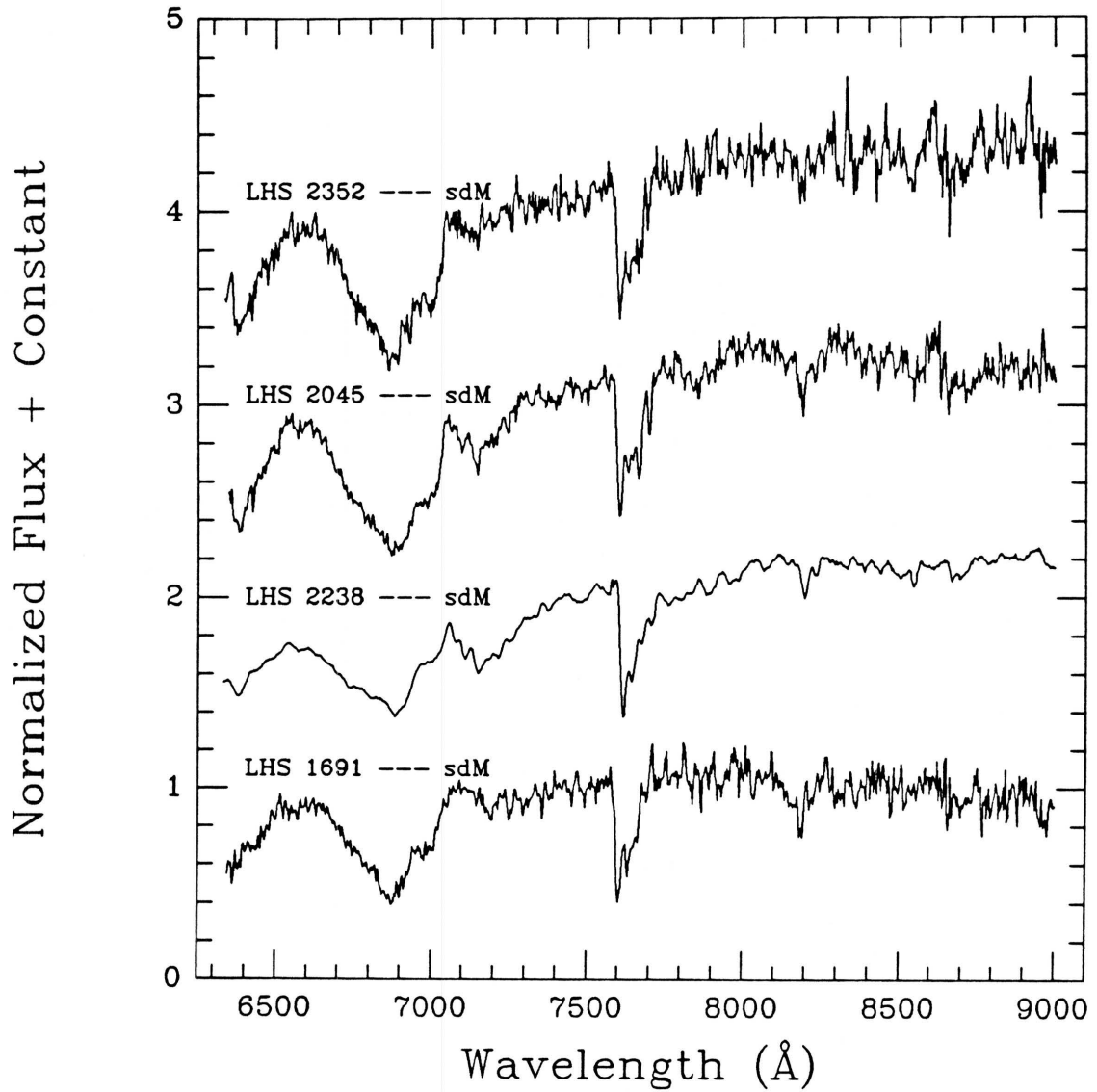


FIG. 5.3. — MMT spectra of newly identified M subdwarfs from Table 5.15. All of these are extreme metallic hydride subdwarfs, as indicated by the unmistakable *CaH* absorption between 6700 and 7000 Å. Data for each of the spectra can be found in Table 5.16. As before, telluric absorption has not been removed and the flux is in units of F_λ , normalized to one at 7500 Å, with integral offsets added to separate the spectra along the vertical axis.

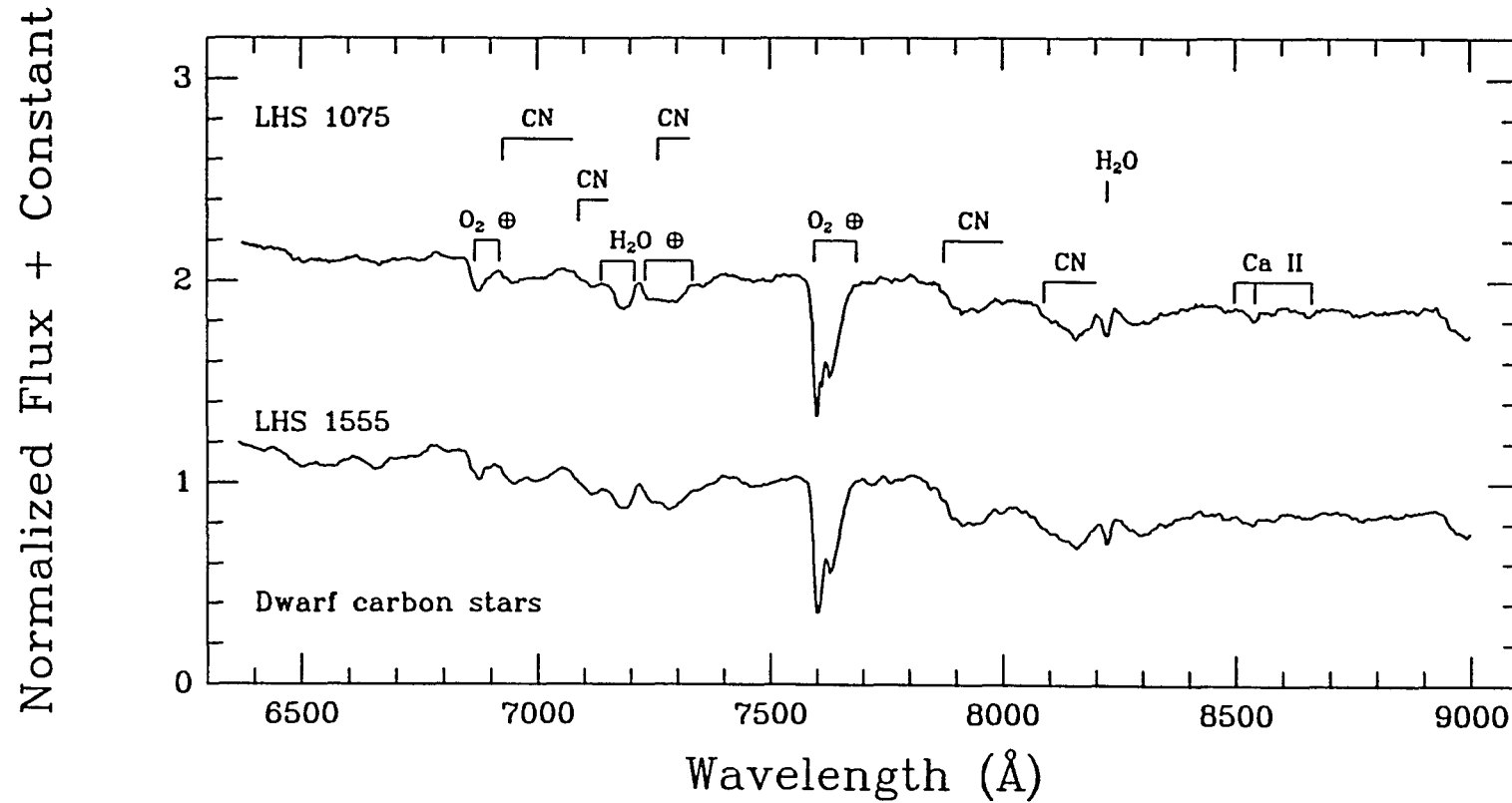


FIG. 5.4. — MMT spectra of the two LHS objects known to be dwarf carbon stars. As before, telluric lines have not been removed, but are marked in the spectra. Several stellar bands of *CN* are noticeable in this spectral region; the *CaII* triplet may even serve as a luminosity indicator to distinguish carbon dwarfs from carbon giants. Both spectra were obtained on (UT) 1991 Oct 17 with the MMT Red Channel Spectrograph. The integration time was 1200 seconds for LHS 1075 and 600 seconds for LHS 1555. The flux (F_λ) is normalized to one at 7500 Å, and an integral offset of 1 has been added to the spectrum of LHS 1075 to separate it from LHS 1555.

TABLE 5.1
THE SPECTROSCOPIC LHS CATALOG

LHS	Gliese	Giclas	Other Name	$m_{pg} - m_R$	Spectral Type and Reference
1	1	267-25	CD -37°15492	1.7	M2 V (bf), M3.5 V (bh), M3 (af), M4 V (au)
2	1002	158-27	—	2.5	M5-5.5 V (ah), M5-5.5 V (ax)
3*	15 A	171-47	BD +43°44 A	1.7	M1.5 V (ah), M2.5 V (bh), M3 V (am)
4	15 B	171-48	BD +43°44 B	2.3	M4 V (ah), M4.5 V (bh), M4 (af)
5	17	—	ζ Tuc	0.5	G0 V (bf), F9 V (be), G2 V (au)
6	19	—	β Hyi	0.7	G1 IV (bf), G2 IV (be), G2 IV (au)
7	35	1-27	van Maanen's Star	0.5	DZ8 (br), DZ7 (bn), DZ7+ (ba)
8 A*	53 A	—	μ Cas A	0.9	G5 V (be), G5 (af), sdG5 (au)
8 B*	53 B	—	μ Cas B	—	composite with LHS 8 A
9	65 A	272-61 A	—	1.9	M5.5 V (bi), M5.5 V (bh)
10	65 B	272-61 B	UV Cet	1.9	M6 V (bi), M6 V (bh)
11	83.1	3-33	TZ Ari	1.7	M4.5 V (bi), M4.5 V (ah), M5- V (ca)
12	—	3-36	Wolf 110	0.9	M4 (af), K4 (au), sdM (bm)
13	86	—	CD -51°532	0.9	K1 V (bf), K0 V (au), K1 V (be)
14	87	73-35	BD +2°348	1.7	M1.5 V (ah), M2.5 V (bh), M3 V (au)
15*	105 A	73-70	BD +6°398 A	1.2	K3 V (be), K3 (af), K5V (au)

TABLE 5.1 — continued

LHS	Gliese	Giclas	Other Name	$m_{pg} - m_R$	Spectral Type and Reference
16	105 B	73-71	BD +6°398 B	1.8	M4: V (ah), M4.5 V (bh), M4 (af), M4 (au)
17	—	—	—	1.9	—
18	1053	221-5	—	1.2	dM (bl), dM (bo), dM (ai)
19	139	—	CD -43°1028	0.9	G8 III (bf), G5 (af), G5 V (au), G8 III (be)
20	1062	160-5	Ross 578	1.4	M2 (af), sdM (bm)
21	158	—	BD +34°796	1.1	K0 (af), K1 V (bx), K1 V (au)
22	1068	—	—	1.5	“peculiar” (af)
23	166 A	—	o^2 Eri A	0.8	K1 V (be), K1 (af), K1 V (au)
24	166 B	160-60 A	o^2 Eri B	0.0	DA4 (br), DA (af)
25	166 C	160-60 B	o^2 Eri C	1.7	M4.5 V (bi), M4.5 V (ah), M5 V (bw)
26*	169.1 A	175-34 A	Stein 2051 A	1.7	M4 V (bi), M4 V (au)
27	169.1 B	175-34 B	Stein 2051 B	0.2	DC5 (br), DC5 (bn), DC (au), DQ?7 (ba)
28	184	191-19	BD +52°911	1.6	M0 V (cb), M0.5 V (bh), M1 (af)
29	191	—	Kapteyn’s Star	1.4	M1 V (ah), M0 V (bf), sd (bw), M0 (af)
30*	205	99-15	BD -3°1123	1.5	M1.5 V (bi), M1.5 V (ah), M1.5 V (ca)
31	213	102-22	Ross 47	1.7	M4 V (bi), M4+ V (ah), sdM4.5 (bh)
32	223.2	99-44	—	0.9	DZ9 (br), DZ9 (bn), DC11+(ba)
33*	273	89-19	Luyten’s Star	1.8	M3.5 V (bi), M4 V (ah), M3.5 (af)
34	293	—	—	0.6	DQ9 (br)
35	299	50-22	Ross 619	1.6	M4-4.5 V (ah), M5 V (bh), sdM5 (ab)

TABLE 5.1 — continued

LHS	Gliese	Giclas	Other Name	$m_{pg} - m_R$	Spectral Type and Reference
36	406	45-20	Wolf 359	2.1	M6 V (bi), M6 V (ah), M6 V (ca), M6 V(ax)
37*	411	119-52	BD +36°2147	1.7	M2 V (bi), M2 V (ah), M2+ V (ca)
38	412 A	176-11	BD +44°2051 A	1.6	M1 V (ah), M2 V (bh), M0.5 (af)
39	412 B	176-12	BD +44°2051 B	2.0	M5.5 V (bg), M5.5 (ai), M5 V (ad)
40	422	—	—	1.5	M (au), M3 (bp)
41	424	236-65	BD +66°717	1.5	M1 V (ah), M1.5 V (bh), M1 (af), M1 V(au)
42	—	236-80	Ross 451	1.3	sdM0 (ap), sdK (ao), sdM0.5 (bh), sdM0(au)
43	440	—	—	-0.2	DQ6 (br)
44*	451	122-51	BD +38°2285	0.9	G8 V (be), G8 (af), G8 V (au)
45	465	—	Ross 695	1.7	M3.5 V (bq), M4.5 V (bh), M3.5 (af)
46	518	62-53	Wolf 489	0.8	DZ9 (br), DZ9 (bn)
47	526	63-53	BD +15°2620	1.6	M1.5 V (ah), M3 V (bh), M3 V (am)
48	541	—	α Boo	1.1	K1 IIIb (be), K1 III (af), K2 III (au)
49	551	—	Proxima Cen	1.6	M5.5 V (ah), M6 V (bq), M5 V (au)
50	559 A	—	α Cen A	0.6	G2 V (bf), G2 V (be), G2 V (au)
51	559 B	—	α Cen B	1.3	K1 V (bf), K1 V (be), K0 V (au)
52	579.2 B	—	BD -15°4041	0.9	G8-K1 V: (bf), sdK (ao), K0 (af), sdK2 (au)
53	579.2 A	—	BD -15°4042	0.6	K0-1 V (bf), sdK (ao), K0 V (am), sdK0(au)
54	595	—	—	1.8	M4 V (bq), M5 V (cb), M3.5 (af)
55	1200	—	—	2.4	M3.5 V (al)

TABLE 5.1 — continued

LHS	Gliese	Giclas	Other Name	$m_{pg} - m_R$	Spectral Type and Reference
56	699.1	259-21	—	0.6	DA7 (br), DA7 (bn), DA (au)
57*	699	140-24	Barnard's Star	2.0	M4 V (bi), M5 V (al), sdM4.5 (bh)
58*	725 A	227-46	BD +59°1915 A	1.7	M3 V (bi), M3 V (ca), M4 V (bh), M4 V (au)
59*	725 B	227-47	BD +59°1915 B	1.8	M3.5 V (bi), M3.5 V (ca), M4.5 V (bh)
60	754	—	—	1.6	M4.5 (af), M7 (au)
61	817	—	Ross 769	1.7	M2 (af), M3 (au), sdM3 (ab)
62*	820 A	—	61 Cyg A	1.3	K5 V (bi), K5 V (ca), K5 V (be)
63*	820 B	—	61 Cyg B	1.4	K7 V (bi), K7 V (ca), K7 V (be)
64	—	231-27	Wolf 1106	1.5	sdM1.5 (bh), sdM1 (cb), sd: (bb), sdM1 (au)
65	821	—	Wolf 918	1.7	M2 V (al), M1 (af)
66	825	—	CD -39°14192	1.5	M1-2 (bf), M1 V (bh), M0 (af), M0 V (be)
67	845	—	ϵ Ind	1.3	K4-5 V (bf), K4-5 V (be), K5 V (au)
68 A*	866 A	156-31 A	EZ Aqr A	1.6	M5 V (bi), M5.5 V (ah), M5 V (bw)
68 B*	866 B	156-31 B	EZ Aqr B	—	composite with LHS 68 A
69	1276	—	—	1.8	DZ9 (br), DZ9 (bn), DZ13 (ba)
70	887	—	CD -36°15693	1.6	M2-3 V (bf), M2.5 V (bh), M0.5 (af)
71	892	—	BD +56°2966	1.3	K3 V (be), K3 (af), K3 V (am), K3 V (au)
72	—	275-90	CD -24°17814	1.5	sd (bw), K4 (af), sdM (au)
73	—	275-92	—	1.5	sd (bw), K5 (af), sdM (au)

TABLE 5.1 — continued

LHS	Gliese	Giclas	Other Name	$m_{pg} - m_R$	Spectral Type and Reference
101 A*	914 A	—	85 Peg A	0.6	G2 V (be), G5 (af), G3 V (au)
101 B*	914 B	—	85 Peg B	—	composite with LHS 101 A
102	1001	—	—	1.5	M3.5 (af)
103	1003	130-43	—	1.9	—
104	—	30-48	—	1.5	K4 (af), K4 (au)
105	—	—	—	1.6	—
106	—	—	—	> 3.1	—
107	1006 A	32-6	—	1.9	M4 (af)
108	1006 B	32-7	—	2.0	M4.5 (af)
109	—	158-53	—	1.4	sd (bw), K5 (af), sdM (au)
110	—	266-88	—	1.5	M4 (af)
111	—	266-89	—	1.5	M3.5 (af)
112	—	—	—	2.0	M5.5 V (ai), M6 V (ax)
113	1013	158-95	—	1.6	—
114 A*	22 A	243-30 A	BD +66°34 A	1.9	M2 V (bi), M2.5 V (bh), M2.5 (af)
114 B*	22 C	243-30 C	BD +66°34 C	—	composite with LHS 114 A
115	22 B	243-30 B	BD +66°34 B	1.9	M3 V (bi), M3.5 (af)
116	—	—	CD -64°12	0.9	F6 V (bf), K3 V (au)
117	1014	32-35	—	1.8	—
118 A*	25 A	—	CD -25°225 A	1.1	K1 V + G (bf), G5 (af), G8 V (be)
118 B*	25 B	—	CD -25°225 B	—	composite with LHS 118 A
119	26	69-10	Wolf 1056	1.9	M4 V (ap), M3.5 V (bh), M3 (af), M4 V (au)
120	1019	69-16	—	1.8	—

TABLE 5.1 — continued

LHS	Gliese	Giclas	Other Name	$m_{pg} - m_R$	Spectral Type and Reference
121	33	—	BD +4°123	1.1	K2 V (be), K2 (af), K2 V (am), K2 V (au)
122	34 B	—	η Cas B	1.4	K7 V (ah), M0 V (be), M0 V (bh)
123*	34 A	—	η Cas A	0.5	G0 V (be), G0 (af), G0 V (au)
124	1022	—	—	1.5	—
125	—	—	—	—	—
126	38	218-17	Wolf 33	1.6	M2 V (ap), M1 V (bh), K5 (af), M2 V (au)
127	—	268-77	—	1.4	—
128	45	—	CD -62°39	1.3	M0 V (bf), K7 V (au)
129	46	269-63	CD -28°302	1.6	M4 (af)
130	1025	70-28	—	1.3	M3.5 (af)
131	48	242-76	BD +70°68 b	1.7	M3.5 V (cb), M3.5 V (bh), M3 (af)
132	—	—	—	—	—
133	—	—	CD -46°293	1.1	sd (bw), K3 (af), sdK (au)
134	1028	268-110	—	1.7	—
135	1029	69-47	—	2.0	—
136	52	243-60	BD +63°137	1.2	M1 V (bh), K5 (af), K7 V (au)
137	52.2	132-57	Ross 322	1.7	M3 (af), M4 (ag), M4 (au)
138	54.1	268-135	YZ Cet	1.6	M5.5 V (bh), M4.5 (af), M5 V (au)
139	1034	34-15	—	1.5	—
140	1035	265-8	—	1.5	—

TABLE 5.1 — continued

LHS	Gliese	Giclas	Other Name	$m_{pg} - m_R$	Spectral Type and Reference
141	57	—	CD -42°469	1.3	M0.5 (af), M0 V (au)
142	—	272-36	CD -22°526	1.5	M1.5 (af)
144	—	—	—	1.6	sdM1-2 (ai)
145	—	—	—	0.9	—
146	71	—	τ Cet	1.1	G8 V (bf), G8 V (be), G6 (af), G8 V (au)
147	—	—	—	0.4	DC7 (br), DC7 (bn)
148	—	—	—	—	—
149	84	272-148	BD -18°359	1.6	M3 (af), M0 V (au)
150	85	—	—	1.5	—
151	1042	74-7	—	0.0	DAZ7 (br), DAZ7 (bn)
152	—	3-44	Wolf 125	1.1	dK (bo), K3 (af), dK (au)
153	91.3	134-22	—	0.0	DA9/DC (br), DC9 (bn), DA9+ (ba)
154 A*	92 A	—	δ Tri A	0.6	G0 V (be), G0 (af), G0 V (au)
154 B*	92 B	—	δ Tri B	—	composite with LHS 154 A
154a	1046	—	—	1.9	M3 (af)
155	101	174-1	Ross 21	1.6	M3.5 (af), M5 (au)
156	—	4-29	—	1.6	—
157	1050	—	—	1.5	M3 (af)
158	—	—	—	1.5	—
159	116	37-8	BD +33°529	1.4	K4 (af), sdK6 (au)
160	118	—	—	1.4	M (au)

TABLE 5.1 — continued

LHS	Gliese	Giclas	Other Name	$m_{pg} - m_R$	Spectral Type and Reference
161	—	75-47	—	1.7	—
162	—	—	—	—	—
163	120	5-7	Ross 791	1.6	M3.5 V (bh), M3.5 (af), M3 V (au)
164	—	—	—	—	—
165	—	—	—	1.1	sdK (bl)
166	124	—	ι Per	0.6	G0 V (be), G1 (af), G4 V (au)
167	130	—	CD -38°1058	1.6	M3 (af)
168	1057	77-31	—	1.9	M5 V (bi), M5 V (ah)
169	129	5-22	Wolf 134	2.0	sdM0 (bh), K3 (af), sdM0 (au)
170	—	78-26	Wolf 1324	1.4	sdK5 (ap), K4 (af), sdK5 (au)
171	136	—	ζ^1 Ret	0.6	G3-5 V (bf), G3-5 V (be), G2 V (au)
172	138	—	ζ^2 Ret	0.6	G2 (bf), G2 V (be), G1 V (au)
173	—	38-1	Ross 34	1.3	sdK5 (ap), K4 (af), sdK5 (au)
174	—	37-40	Ross 585	1.4	K5 (af)
175	—	246-38	BD +66°268	0.9	G4 (af), sdG8 (au)
176	—	—	—	1.9	M5.5 V (ai)
177	—	78-42	Wolf 194	1.7	M2 (af)
178	—	79-59	Wolf 1057	2.0	M0.5 (af)
179	151	6-30	Wolf 219	0.2	DQ8 (br), DQ8 (bn)
180	1064 A	95-57 A	BD +41°750	1.2	K1 (af), K1 V (au)

TABLE 5.1 — continued

LHS	Gliese	Giclas	Other Name	$m_{pg} - m_R$	Spectral Type and Reference
181*	1064 B	95-57 B	BD +41°750 a	1.3	K2 (af), K2 V (au)
182	1064-	95-59	—	1.7	M0: V (ah), Mp (cb), sdMp (ag)
183	1065	160-28	—	1.6	—
184	155.3	—	CD -37°1501	1.1	M3 (af)
185	157.2	7-17	—	1.3	sdM (ap), sdM (ai)
186	—	160-42	—	1.5	—
187	—	38-25	BD +32°719	1.3	K4 (af), K4 V (au)
188	163	—	—	1.5	M4.5 V (bq), M (au)
189	—	—	—	1.6	sdM4 (ai)
190	—	—	—	1.7	—
191	—	—	—	2.3	M6.5 V (bi)
192	—	—	—	1.6	sdM (bl), sd (bb), sdK7-M0 (ai)
193	—	—	—	1.5	—
194	—	—	—	0.5	DQ7 (br), DQ7 (bn)
195	—	—	CD -65°253	0.6	sdG2 (au)
196	176	8-55	BD +18°683	1.5	M2.5 V (cb), M2.5 V (bh), M3 (af)
197	—	—	—	1.8	sdM (bl), M1 V (ai)
198	1073	81-39	—	1.1	sdM1 (ai)
199	181.1	—	—	1.5	—
200*	183	—	BD -5°1123	1.1	K4 (af), K3 V (am), K3 V (au), K3 V (be)

TABLE 5.1 — continued

LHS	Gliese	Giclas	Other Name	$m_{pg} - m_R$	Spectral Type and Reference
201	***** the same object as LHS 28 *****				
202	—	—	—	1.6	—
203	190	—	—	1.8	M5 V (bq), M4 (af)
204	—	—	CD -59°1024	0.8	sd (bw), sdF6 (au)
205	1077	—	—	1.5	—
205a	—	—	—	2.9	sdM (bl), sdM (ac), sdK7-M1 (ai)
206	1080	99-10	—	1.9	M3 V (bk)
207	—	—	—	1.8	M6.5: V (ai), sdM (bl)
208	—	—	π Men	0.9	G1 V (be), G3 IV (au)
209	—	96-50	—	1.5	sdK (aq), sd (ao), K5-M0 V (ai)
210	217.2	—	CD -70°340	0.6	G8 V (bf), K0 V (au)
211	—	99-33	—	2.5	—
212	1087	99-47	V1201 Ori	0.6	DAP9 (br), DAP9 (bn), DC (au), DAP9(ba)
213	—	249-27	—	1.5	—
214	—	249-28	—	1.3	—
215	226	222-11	—	1.6	M2.5 V (bi), M2.5 (af), M3 V (au)
216	—	105-23	—	1.6	—
217	—	249-46	—	1.3	—
218	—	103-46	—	2.0	—
219 A*	244 A	—	α CMa A	-0.3	A0 V (bf), A1 V (be), A1 V (am), A1 V (au)
219 B*	244 B	—	α CMa B	—	DA2 (br), DA (au)
220	1092	87-8	vB 16	1.9	—

TABLE 5.1 — continued

LHS	Gliese	Giclas	Other Name	$m_{pg} - m_R$	Spectral Type and Reference
221 A*	—	250-29 A	—	1.5	M2.5 V (bi), M3.5 (af)
221 B*	—	250-29 B	—	—	composite with LHS 221 A
222 A*	257 A	—	CD -44°3045 A	1.8	M3.5 V (bq), M4 (au)
222 B*	257 B	—	CD -44°3045 B	—	M3 (af), M4 (au)
223	1093	109-35	—	1.8	M2 V (ai)
224	—	193-27	—	1.8	M4.5 (af)
225*	—	—	—	1.1	M3 (af)
226 A*	268 A	87-26 A	Ross 986 A	1.7	M4.5 V (bi), M4.5 V (ah), M4.5 V (ca)
226 B*	268 B	87-26 B	Ross 986 B	—	composite with LHS 226 A
227	—	—	—	1.3	< M2 (bp)
228	—	—	—	1.7	M2.5-3 V (ai)
229*	275.2 A	107-69	—	2.2	M4 V (bi), M4+: V (ai), M5 V (au)
230 A*	275.2 B	107-70 A	—	0.9	DC9 (bn), DC (br)
230 B*	275.2 C	107-70 B	—	—	DC9 (bn)
231	—	—	—	2.2	M4.5 V (ai)
232	—	112-28	—	1.1	—
233 A*	280 A	—	α CMi A	0.3	F5 IV-V (be), F4 (af), F5 IV-V (au)
233 B*	280 B	—	α CMi B	—	DA (br)
234	283 B	—	—	1.7	M6 V (bi), M6 V (ai)
235	283 A	—	—	0.1	DZQ6 (br), DZ6 (bn)
236	—	251-44	—	1.5	K4 (af)
237	288 A	—	CD -33°4113	0.6	G0 V (bf), G0 (af), G0 V (au), G0 V (be)
237a	288 B	—	vB 3	2.	—
238	289	91-11	Wolf 1421	2.2	M2 (af), M2 (au), M2 V (as)
239	1102 B	—	—	1.1	DC9 (br), DC9 (bn)
240	1102 A	—	—	0.9	DC9 (br), DC9 (bn)

TABLE 5.1 — continued

LHS	Gliese	Giclas	Other Name	$m_{pg} - m_R$	Spectral Type and Reference
241*	1104	90-25	BD +31°1684	0.7	G2 (af), G2 V (am), sdG2 (au)
242*	295	—	BD +29°1664	0.7	G4 (af), G8 V (bx), G8 V (au), G8 V (be)
243	—	—	—	2.2	M4.5 V (ai)
244	—	—	—	1.8	—
245	302	—	BD -12°2449	0.9	K0 V (bf), G7.5 V (be), G9 (af), G8 V (au)
246	—	—	—	1.5	M5.5: V (ai)
247 A*	308 A	51-13 A	—	1.6	—
247 B*	308 B	51-13 B	—	—	—
248	1111	51-15	DZ Cnc	1.6	M6.5 V (bi), M6.5 V (ah), M6.5 V (ca)
249	309	—	CD -31°6229	1.0	K0 V (bf), K0 V (be), G9 (af), K0 V (au)
250	—	234-37	—	1.3	M3 (af)
251 A*	310 A	234-38 A	BD +67°552 A	1.5	M1 V (bh), K7 (af), M1 V (au)
251 B*	310 B	234-38 B	BD +67°552 B	—	composite with LHS 251 A
252	—	234-45	—	2.2	—
253	318	—	CD -32°5613	-0.3	DA6 (br), DA (au)
254	—	—	—	1.5	M5.5 V (ai)
255	328	46-9	BD +2°2098	1.5	M0 V (bi), M0.5 V (ah), M1 V (bh), K7 (af)
256	325 A	252-24 A	BD +71°482	1.5	M1 V (bh), K7 (af), K5 V (au)
257	325 B	252-24 B	BD +71°482 a	1.5	M1 V (bh), K7 (af), M1 V (au)
258*	1118	—	—	1.3	M4: (af)
259	—	194-50	—	1.3	—
260*	338 A	195-17	BD +53°1320	1.4	M0 V (bi), M0 V (be), M0.5 V (bh)

TABLE 5.1 — continued

LHS	Gliese	Giclas	Other Name	$m_{pg} - m_R$	Spectral Type and Reference
261*	338 B	195-18	BD +53°1321	1.4	K7 V (bi), M0 V (be), M0.5 V (bh)
262	339.1	195-19	—	0.1	DXP7/DCP7 (br), DXP7 (bn), DC (au)
263	1123	—	—	1.5	—
264 A*	338.1 A	252-30 A	BD +77°361 A	1.3	K7 V (bi), K5 (af), dK (au)
264 B*	338.1 B	252-30 B	BD +77°361 B	—	composite with LHS 264A
265	—	195-22	—	1.6	—
266	—	—	—	2.9	sdM3.5: (ai)
267	—	46-34	—	1.5	—
268	345	—	CD -80°328	0.4	sd (bw), white dwarf (bv), sdG (au)
269	—	—	—	1.5	M5: V (ai)
270 A*	354 A	—	θ UMa A	0.4	F6 IV (be), F7 (af), F6 IV (au)
270 B*	354 B	—	θ UMa B	—	composite with LHS 270 A
271	1128	—	—	1.7	—
272	—	—	—	2.3	M3.5 (as), M2 (af)
273	1129	—	—	2.0	M3.5 (af)
274	369	161-80	BD -11°2741	2.0	M2 V (cb), M2 V (bh), M0.5 (af), sdM2(ab)
276	—	117-61	Wolf 335	1.8	G2 V (be), M1.5 (af)
277	377	—	CD -29°8019	1.5	M3 (af), M4 (au)
278	378	146-6	BD +48°1829	1.6	M2 (af), M2 V (au)
279	—	—	—	1.6	M4.5 V (ai)
280	380	196-9	BD +50°1725	1.3	K7 V (bi), K7 V (ah), K2 V (be), M0 V (bh)

TABLE 5.1 — continued

LHS	Gliese	Giclas	Other Name	$m_{pg} - m_R$	Spectral Type and Reference
281	1132	—	—	1.1	M4 (af)
282	—	—	—	0.5	DC9 (br), DC8 (bn)
283	—	236-34	—	1.3	—
284	—	—	—	1.3	M4.5 V (ai)
285	—	—	—	0.9	DC9 (br), DC9 (bn)
286	—	—	—	1.6	M6 V (ai)
287	1134	146-58	—	2.0	M5 V (al)
288	—	—	—	1.5	M4 (bp), sd (bg)
289	401 A	—	BD -18°3019 A	1.6	M0 V (bc), M3 V (bq), M0.5 (af), M (au)
290	401 B	—	BD -18°3019 B	0.3	DQ9 (br), DQ9 (bn), DQ9 (bc)
291	—	—	—	0.4	DQ8 (br), DQ8 (bn)
292	—	—	—	1.9	M6.5 V (bi), M6.5 V (ai), M6.5-7 V (ax)
293	1138	119-36	—	2.1	—
294*	402	44-40	Wolf 358	1.7	M4 V (bi), M4 V (ah), M4.5 V (bq)
295	403	44-42	Hubble 3	1.8	M3 (af), M4 (au)
296	—	45-27	—	1.6	—
297	—	119-57	—	1.7	M3.5 V (al), M3.5 (af)
298	415	—	BD -10°3216	1.3	K4 (af), M0 V (au)
299	—	163-59	—	1.9	—
300	—	—	—	1.1	K4 (af)

TABLE 5.1 — continued

LHS	Gliese	Giclas	Other Name	$m_{pg} - m_R$	Spectral Type and Reference
301	1146	10-17	—	1.3	—
302	—	—	—	2.2	—
303	2085	10-19	Wolf 386	1.9	M1 V (bh), M1 (af), M1 V (au)
304	427	120-45	Ross 627	0.4	DA7 (br), DA7 (bn)
305	—	10-25	Wolf 397	1.5	M0 V (bh), K5 (af), M0 V (au)
306	—	—	—	1.7	M5.5 (bq)
307	—	176-40	—	1.7	—
308	432 A	—	CD -32°8179	1.1	K0 V (bf), K0 V (be), K0 (af), K0 V (au)
309	432 B	—	vB 4	2.	—
310	436	120-68	BD +27°28217	1.8	M3 V (bi), M3 V (ah), M3.5 V (bh), M3 (af)
311	442 A	—	CD -39°7301	0.9	G3-5 V (bf), G5 V (be), G6 (af), G5 V (au)
312	—	176-53	BD +51°1696	0.6	G0 (af)
313	442 B	—	vB 5	—	—
314	443	—	—	1.6	M3.5 V (bq), M3 (af), M (au)
315	447	10-50	Ross 128	1.7	M4+ V (ah), M4.5 V (bq), M5 V (au)
316	1151	122-49	—	1.6	M5 V (al)
317	—	—	—	2.0	M4 (af)
318	—	—	—	1.3	sdM0-2 (ai)
319	453	—	CD -26°8883	1.3	K4 V (bf), K5 V (be), K4 (af), K5 V (au)
320	—	11-35	—	1.3	—

TABLE 5.1 — continued

LHS	Gliese	Giclas	Other Name	$m_{pg} - m_R$	Spectral Type and Reference
321	—	122-67	Ross 943	1.1	M0.5 (af)
322	—	—	BD -9°3468	0.5	F5 (af), F6 V (bx), F6 V (au), F5 V (be)
323	—	—	—	1.5	—
324	1156	12-30	GL Vir	2.5	dM (bt)
325	—	—	—	1.6	sd (bb), sdM0-2 (ai)
325a	—	—	—	3.1	M6 V (ad (but mis-ID'd as LHS 325))
326	—	—	—	1.6	—
327	—	—	—	1.1	K0: (af), sd (bw), sdK (au)
328	467 A	—	—	1.3	—
329	467 B	—	—	1.6	—
330	1159 B	199-17 B	—	2.5	dM (ai)
331	1159 A	199-17 A	—	1.5	dM (bl), dM (ai)
332	1158	—	—	1.3	M3 (bp)
333 A*	473 A	12-43 A	Wolf 424 A	1.7	M5.5 V (bi), M5.5 V (ah), M5.5 V (bq)
333 B*	473 B	12-43 B	Wolf 424 B	—	composite with LHS 333A
334	2093	—	—	2.8	sdM4 peculiar (ai)
335	—	—	—	1.5	sdM (bl), sdM (ai)
336	479	—	CD -51°6859	0.6	M3 V (bq), white dwarf (bv), M3 (af)
337	—	—	—	1.5	M4 (af)
338	480	60-24	Wolf 433	1.6	M4 V (bh), M3.5 (af), M4 V (au)
339	—	—	—	-0.2	DA (br)
340	480.1	—	—	1.1	M3.5 (af), M4 (au)

TABLE 5.1 — continued

LHS	Gliese	Giclas	Other Name	$m_{pg} - m_R$	Spectral Type and Reference
341	486	60-32	Wolf 437	1.6	M4 V (ah), M4.5 V (bh), M3 (af), M4 V (au)
342	—	—	—	1.5	DC9 (br), DC9 (bn)
343	—	61-21	—	1.3	sd (bb), \leq K5 V (al), K4: (af)
344	496.1	—	CD -51°7244	1.3	K5-M0 V (bf), K9 V (au)
345	—	62-15	—	1.9	—
346	—	—	—	1.5	M3.5 (af)
347	—	61-35	—	1.3	K0 (af)
348	502	—	β Com	0.6	G0 V (be), G0 (af), G0 V (au)
349	506	—	BD -17°3813	0.8	G5 V (bf), G6 V (be), G6 V (au)
350	—	149-81	Ross 1020	1.6	M3.5 (af)
351	513	63-32	—	1.7	M5 V (cb), M3.5 (af), M5 (au)
352*	514	63-34	BD +11°2576	1.1	M1 V (ah), M1 V (cb), M0.5 V (bh)
353	514.1	14-57	Ross 476	1.6	M6 V (bq), M6 V (cb), M4: (af), M6 V (au)
354	515	14-58	BD -7°3632	-0.5	DA5/DA4 (br), DA (au)
355	1171	149-94	—	1.7	—
356	—	—	—	1.5	sdM0-1 (ai)
357	1174	177-51	Ross 1026	1.1	dM (bo), M4 V (al), M3 (af), dM (au)
358	—	—	—	1.8	dM (bl), dM (ai)
359*	525	63-52	BD +18°2776	1.7	M0 (af), M1 V (au), sdK9 (ab)
360	—	—	—	1.8	sdK7-M0 (ai)

TABLE 5.1 — continued

LHS	Gliese	Giclas	Other Name	$m_{pg} - m_R$	Spectral Type and Reference
361	1179 B	—	—	1.6	DC9 (br), DC9 (bn)
362	1179 A	—	—	2.0	M4: V (bo)
363	529	—	BD -21°3781	1.3	K4-5 V (bf), M0 V (bh), K6 V (am)
364	—	165-47	—	1.6	sdM (bl)
365	—	—	—	1.2	sdM (bl), sdM (ai)
366	1182	65-39	—	2.1	—
367	—	—	—	0.6	sd (bw), sdK (au)
368	543	124-23	Wolf 534	1.8	M3 (af), M4 V (as)
369	545	124-25	Ross 848	1.8	M4 V (bh), M5 (au)
370	—	—	—	1.9	M5.5 V (ai)
371	548 A	166-27	BD +24°2733 A	1.6	M1 V (bh), M0 (af), M1 V (au)
372	548 B	166-28	BD +24°2733 B	1.6	M1.5 V (bh), M0.5 (af), M1 V (au)
373	552	135-56	BD +16°2658	1.8	M2 V (bq), M2.5 V (bh), M3 (af), M3 V (au)
374*	553	124-47	BD -7°3856	1.5	M2.5 V (bq), M1.5 V (bh), M0 (af)
375	—	—	—	2.0	—
376	—	135-67	—	1.5	M3 V (ai)
377	—	—	—	3.1	sdM5 (ai), sdM5 (ax)
378	—	—	—	0.6	DC (br), DC9 (bn)
379	563.2 B	—	CD -25°10553 B	1.3	M3 (af)
380	563.2 A	—	CD -25°10553 A	1.3	M3 (af)

TABLE 5.1 — continued

LHS	Gliese	Giclas	Other Name	$m_{pg} - m_R$	Spectral Type and Reference
381	—	—	—	1.5	—
382	—	—	—	1.3	—
383	565	—	CD -23°11940	1.3	K3 V (bf), K3 (af), K5 V (au)
384	569.1	200-62	BD +54°1716	0.9	K1 (af), K1 V (au), K1 V (am), K1 V (au)
385	—	—	—	1.5	—
386 A*	570 B	—	BD -20°4123 A	1.6	K5 V (bf), M1 V (cb), M2 V (bh), M0 V (au)
386 B*	570 C	—	BD -20°4123 B	—	composite with LHS 386 A
387	570 A	—	BD -20°4125	1.3	K4 V (bf), K4 V (be), K4 V (am), K5 V (au)
388	570.2	166-57	Ross 53	1.4	M2 V (bh), K5 (af), M2 V (au)
389	1188	15-4	Ross 1044	1.6	K7 (af)
390	—	—	—	1.2	K5 (af)
391	579	167-19	BD +25°2874	1.5	M0.5 V (bh), K7 (af), K7 V (au)
392	—	151-34	—	1.6	—
393 A*	580 A	—	BD -0°2944 A	1.1	G9 V (be), K0 (af), K0 V (am)
393 B*	580 B	—	BD -0°2944 B	—	composite with LHS 393 A
394	581	151-46	BD -7°4003	1.7	M5 V (cb), M4 V (bh), M3 (af), M5 V (au)
395	582	—	ν^2 Lup	0.7	G3-5 V (bf), G3-5 V (be), G2 V (au)
396	585	136-103	Ross 508	1.9	M5.5 V (bq), M6 V (cb), M4 V (al), M6 (au)
397	588	—	CD -40°9712	1.7	M3.5 V (bq), M3 (af), M4 (au)
398	—	—	—	1.6	sdM (bl), sdM0+: (ai)
399	589 A	137-26	Ross 513	1.9	M2.5 V (bq), M4 V (al), M4 (au)
400	589 B	137-25	—	1.7	M4.5: (af), M6 (au)

TABLE 5.1 — continued

LHS	Gliese	Giclas	Other Name	$m_{pg} - m_R$	Spectral Type and Reference
401	—	—	—	1.3	sd (bw), sdM (au)
402	1194 A	179-43 A	vB 24 a	1.6	M3 V (al), M2 V (bk)
403	1194 B	179-43 B	vB 24 b	1.5	composite with LHS 402
404	597	257-20	Ross 1057	1.8	M3 (af)
405	1195	—	BD -10°4149	0.4	F2 (af), sdF5 (bx), sdG2 (au)
406	2116	—	—	1.3	M1 (af)
407	—	—	—	2.2	sd (bb)
408	603	—	γ Ser	0.4	F6 V (be), F5 (af), F6 IV (au)
409	—	16-17	Wolf 611	1.7	sd (bw), M3.5 (af), sdM (au)
410	—	16-18	Wolf 612	2.4	sd (bw), M0: (af), sdM (au)
411	609	137-78	—	1.7	M4 V (al), M3 (af)
412	1198	153-27	Plaut 1	2.1	—
413	615	—	CD -57°6303	0.9	G8-K0 V (bf), K0 V (au)
414	—	—	—	1.7	—
415	618 A	—	CD -37°10765 A	1.6	M3 (af), M4 (au)
416	618 B	—	CD -37°10765 B	1.7	M5: (af), M7 (au)
417 A*	623 A	202-45 A	—	1.7	M2.5 V (bi), M3 V (bh), M3 (af), M3 V (au)
417 B*	623 B	202-45 B	—	—	composite with LHS 417A
418	—	138-25	—	2.5	K5 V: (al)
419*	628	153-58	BD -12°4523	2.3	M4 V (bq), M5 V (cb), M4.5 V (bh)
420	—	17-21	BD+4°3195	0.5	F8 (af), F9 V (au), F9 V (am)

TABLE 5.1 — continued

LHS	Gliese	Giclas	Other Name	$m_{pg} - m_R$	Spectral Type and Reference
421 A*	630.1 A	225-67 A	CM Dra A	1.5	M5 V (au)
421 B*	630.1 C	225-67 B	CM Dra B	—	composite with LHS 421
422	630.1 B	225-68	—	0.4	DQ8 (br), DQ8 (bn), DC (au), DQ8+ (ba)
423	—	—	—	1.3	M3: (bp), M3.5 (af)
424	—	17-28	—	1.1	—
425	—	138-59	—	1.5	M2-2.5 V (ai)
426	641	19-4	BD +0°3593	1.0	G7 V (be), G5 (af), G6 V (au), G8 V (am)
427*	643	—	BD -8°4352 C	1.7	M3.5 V (bi), M4.5 V (bq), sdM4 (cb)
428 A*	644 A	—	BD -8°4352 A	1.8	M3.5 V (bq), M4.5 V (cb), M3.5 V (bh)
428 B*	644 B	—	BD -8°4352 B	—	composite with LHS 428 A
429*	644 C	—	vB 8	2.2	M7 V (bi), M7 V (ax), M7 V (ai)
430	1209	170-12	—	1.5	M2-3: (al), M3 (af)
431	653	19-13	BD -4°4225	1.6	K5 V: (al), K5 (af), K5 V (am), K5 V (au)
432	654	19-14	BD -4°4226	1.5	M3.5 V (cb), M3.5 V: (al), M3 V (bh)
433	661 A	203-51 A	BD +45°2505 A	1.6	M3 V (bi), M3 V (cb), M4 V (bh)
434	661 B	203-51 B	BD +45°2505 B	1.6	composite with LHS 433
435	1213	203-52	BD +42°2810	1.6	K8 V (al), M1 V (bh), K5 (af), M1 V (au)
436	—	—	—	1.7	M5.5 V (ai)
437	663 A	—	CD -26°12026 A	1.2	K2: III: (bf), K0 V (be), K2 (af)
438	663 B	—	CD -26°12026 B	1.2	K2: III: (bf), K1 V (be), K1 (af)
439	664	—	CD -26°12036	1.3	K5 V (bf), K7 (af), K5 V (au), K5 V (be)
440	—	—	—	0.6	M1 (af)

TABLE 5.1 — continued

LHS	Gliese	Giclas	Other Name	$m_{pg} - m_R$	Spectral Type and Reference
441	672	—	BD +32°2896	0.6	G0 V (be), G3 (af), G1 V (am), G2 V (au)
442 A*	667 A	—	CD -34°11626 A	1.3	K4 V (bf), K3 V (be), K3 (af), K3 V (au)
442 B*	667 B	—	CD -34°11626 B	—	K5 V (be), K4 (af), K5 V (au)
443	667 C	—	CD -34°11626 C	1.6	M2 (bp), M2.5 (af), M2 V (au)
444	666 A	—	CD -46°11370 A	1.1	G8-K0 V (bf), K0 (af), G8-K0 V (be)
445	666 B	—	CD -46°11370 B	1.5	M0.5 (af), M0 V (au)
446	1216	203-63	—	1.6	—
447	673	19-24	BD +2°3312	1.3	K7 (af), K7 V (au), K7 V (am)
448	1219	139-39	—	1.6	—
449	674	—	CD -46°11540	1.8	M3 (af), M4 (au)
450*	687	240-63	BD +68°946	1.6	M3.5 V (cb), M4 V (bh), M3 (af), M4 V (au)
451	682	—	CD -44°11909	1.5	M3 (bp), M3.5 (af), M5 (au)
452*	686	170-55	BD +18°3421	1.7	M1 V (bh), M0.5 (af), M1 V (au)
453	—	—	—	2.3	sdM (aa), sdM (bl), sdM (ap), sdK5-M1 (ai)
454	693	—	—	1.5	M4.5 (bp), M (au)
455	1221	240-72	—	1.1	DXP9 (br), DXP9 (bn), DXP11 (ba)
456	—	—	—	1.5	M3: (bp)
457	1223	182-36	—	1.7	—
458*	702 A	—	70 Oph A	1.2	K0 V (be), K0 V (am), K0 V (au)
459*	702 B	—	70 Oph B	1.3	K5 (af), K4 V (am), K5 V (au)
460	1225	260-1	—	1.6	M4.5: V (ai)

TABLE 5.1 — continued

LHS	Gliese	Giclas	Other Name	$m_{pg} - m_R$	Spectral Type and Reference
461	—	204-57	—	1.5	—
462	—	204-58	—	1.5	—
463 A*	1226 A	21-10 A	—	1.3	M3.5 (af)
463 B*	1226 B	21-10 B	—	—	composite with LHS 463 A
464	712	141-4	Ross 136	1.7	M3.5 V (al), M3 (af), M4 (au)
465	1227	227-29	—	1.6	—
466	—	155-27	Wolf 1465	—	K5 (af), sdM (au)
467	—	21-23	Wolf 851	1.3	< M0 (bp), K4 (af)
468	—	22-1	—	1.1	M3: (bp), M1 (af)
469 A*	732 A	—	—	1.1	G0: (af)
469 B*	732 B	—	—	—	composite with LHS 469 A
470	740	22-10	BD +5°3993	1.5	M2 V (cb), M1 V (bh), M0 (af), M2 V (au)
471 A*	747 A	207-16 A	—	1.7	M5 V (cb), M2 V (al), M4 V (bh), M4 V (au)
471 B*	747 B	207-16 B	—	—	composite with LHS 471 A
472 A*	748 A	22-18 A	Wolf 1062 A	1.5	M3.5 V (bi), M4 V (cb), M4 V (bh)
472 B*	748 B	22-18 B	Wolf 1062 B	—	composite with LHS 472A
473	752 A	22-22 A	BD +4°4048 A	1.5	M3 V (bi), M3.5 V (al), M3 V (ah)
474*	752 B	22-22 B	vB 10	1.5	M8 V (bi), M8 V (ca), M8 V (ai)
475	—	—	—	1.5	—
476	1235	185-18	—	1.3	dM (bl), M8:: V (al)
477	764	—	σ Dra	0.9	K0 V (be), G9 (af), K0 V (au)
478 A*	766 A	185-37 A	Ross 165 A	1.7	M4.5 V (cb), M4.5 V (bh), M4 (af)
478 B*	766 B	185-37 B	Ross 165 B	—	composite with LHS 478 A
479	—	142-52	—	1.1	dK-dM (bl), dK-dM (ai)
480	769	—	—	1.8	M3 (af)

TABLE 5.1 — continued

LHS	Gliese	Giclas	Other Name	$m_{pg} - m_R$	Spectral Type and Reference
481	778	186-11	BD +22°3908	1.2	K2 (af), K1 V (au)
482*	781	230-26	Wolf 1130	1.5	M3 V (cb), M3 V (bh), K7 (af), M3 V (au)
483	—	—	—	1.3	DC9 (br), DC9 (bn), DC13 (ba)
484	776	—	CD -67°2385	0.9	G3 V (bf), G3 V (be), G2 V (au)
485	780	—	δ Pav	0.9	G6-8 V (bf), G6-8 IV (be), G5 IV (au)
486	783 A	—	CD -36°13940 A	1.2	K2 V (bf), K3 V (be), K2 (af), K3 V (au)
487	783 B	—	CD -36°13940 B	1.8	M3.5 (af)
488*	785	—	CD -27°14659	1.2	K3 V (bf), K0 V (be), K1 (af), K0 V (au)
489	—	—	—	2.0	sdM0 (ax), sdM (aa), K5-M0 V (ai)
490	—	—	BD -21°5703	0.6	F8 (af), F8 V (am), sdG0 (au)
491	—	210-19	—	1.3	dK-dM (bl), K3: V (ai)
492	1252	—	—	1.5	—
493	1251	—	—	1.5	—
494	1254	230-42	—	2.3	M3.5 V (al)
495	1256	144-25	—	2.1	M5 V: (al), M4 V (au)
496	798	—	CD -53°8617	1.2	K5 V (bf), K7 V (au)
497 A*	800 A	—	BD -19°5899 A	1.5	M2 V (bh), M1 (af), M2 V (au)
497 B*	800 B	—	BD -19°5899 B	—	composite with LHS 497 A
498	802	231-13	Wolf 1084	1.6	M5 V (bh), M5.5 (af), M5 V (ai)
499	808	—	—	1.5	M (au)
500	810 B	—	—	1.9	composite with LHS 501

TABLE 5.1 — continued

LHS	Gliese	Giclas	Other Name	$m_{pg} - m_R$	Spectral Type and Reference
501*	810 A	—	—	1.9	M3.5 (af), M5 (au)
502	811.1	—	Wolf 896	1.8	M4 V (cb), M3 V (bh), M3 (af), M4 V (au)
503	812.1	—	CD -44°14214	0.6	G0 V (bf), G0 (af), G0 V (au), G0 V (be)
504	—	—	—	1.7	—
505	—	—	—	1.3	—
506	—	—	Ross 770	1.3	K4 (af)
507	—	—	—	1.9	sdK (bl), sdM (ac), K3-5 V (ai)
508	829	126-4	Ross 775	1.8	M3.5 V (bi), M4 V (cb), M3.5 V (bh)
509	830	—	BD -13°5945	1.3	K4-5 V (bf), M0 V (cb), M0 V (bh)
510	—	—	—	1.5	M3 (af)
511 A*	831 A	26-7 A	Wolf 922 A	1.6	M4.5 V (bi), M5 V (bh), M4 (af), M4 V (au)
511 B*	831 B	26-7 B	Wolf 922 B	—	composite with LHS 511A
512	—	—	—	1.5	M2 (af)
513	836	—	—	1.7	M3.5 (af), M5 (au)
514	—	261-46	—	1.1	dM (bo)
515	—	—	—	2.5	sdM2.5 (bi), sdM0-2 (ax), sdM0-2 (ai)
516	—	—	—	1.3	—
517	849	27-16	BD -5°5715	1.6	M3.5 V (bh), M3 (af), M3 V (au)
518	—	—	—	1.3	K5: (af)
519	—	—	CD -51°13248	0.9	K0 V (au)
520*	855.1	—	ν Ind	0.6	A3 V:+F9 V (be), G0-2 V (bf), G0 V (au)

TABLE 5.1 — continued

LHS	Gliese	Giclas	Other Name	$m_{pg} - m_R$	Spectral Type and Reference
521	—	—	—	1.8	—
522*	861	18-51	Wolf 1037	1.3	K4 (af), sdK6 (au)
523	—	—	—	2.2	M6.5 V (bi), M6.5 V (ai), M6.5 V (ax)
524	1270	215-50	—	1.9	—
525 A*	863.1 A	233-17 A	BD +53°2911 A	1.6	K7 V (bi), M1 V (bh), K5 (af), M1 V (au)
525 B*	863.1 B	233-17 B	BD +53°2911 B	—	composite with LHS 525 A and C
525 C*	863.1 C	233-17 C	BD +53°2911 C	—	composite with LHS 525 A and B
526	—	—	—	1.7	M4.5 V (ai)
527	—	—	—	—	—
528	1271	67-15	—	1.7	M3 (af), M3 V (bk)
529	1275	128-7	—	0.5	DA9 (br), DA9 (bn)
530	876	156-57	BD -15°6290	—	M5 V (cb), M4.5 V (bh), M3.5 (af)
531	877	—	—	1.1	—
532	1277	—	—	1.5	—
533*	880	67-37	BD +15°4733	1.7	M1.5 V (bi), M2 V (cb), M2.5 V (bh)
534	—	241-44	—	1.5	M2 V (bk)
535	—	241-45	—	1.5	—
536	—	128-34	—	1.3	—
537	—	28-43	BD -0°4470	0.8	sdG2 (au)
538	1281	—	—	1.8	M3 (af)
539	—	—	—	—	—
540 A*	—	273-1 A	BD -14°6437 A	0.4	sdG2: (ar), F8 (af), sdF7 (am), sdG2 (au)
540 B*	—	273-1 B	BD -14°6437 B	—	composite with LHS 540 A

TABLE 5.1 — continued

LHS	Gliese	Giclas	Other Name	$m_{pg} - m_R$	Spectral Type and Reference
541	—	—	BD -14°6437 C	2.0	sdM (ac), sd (ai)
542	—	—	—	1.3	DC9 (br), DC9 (bn)
543	—	68-8	—	1.7	—
543a	—	—	—	1.7	—
544	895.4	217-11	BD +58°2605	1.2	G8 (af), K2 V (am), K0 V (au), K1 IV (be)
545	899	29-43	Wolf 1039	1.6	M2.5 (af)
546	1286	157-77	—	1.6	—
547	—	—	—	1.8	M4 (af)
548	901	29-53	Wolf 1040	1.7	M3.5: (af)
549	905	171-10	Ross 248	1.8	M5 V (ah), M5.5 V (bh), M4.5 (af)
550	908	29-68	BD +1°4774	1.6	M1.5 V (ah), M2 V (bb), M2.5 V (bh)
551	1292	129-47	—	1.3	M3 V (bk)
552	—	266-20	BD -17°6856	0.9	K2 (af), K0 V (au), K0 V (am)

TABLE 5.1 — continued

LHS	Gliese	Giclas	Other Name	$m_{pg} - m_R$	Spectral Type and Reference
1001	—	—	—	—	—
1002a	—	217-27	—	1.5	—
1003	—	267-16	—	1.7	M3.5 (af)
1004	—	130-36	Ross 679	1.3	K3 (af)
1005	915	—	—	-0.1	DAs (af)
1006	—	158-22	—	1.6	—
1007	—	—	—	1.5	—
1008	—	267-18	—	0.4	DC9 (br), DC (af)
1009	—	30-38	—	2.1	—
1010	—	—	—	1.5	—
1011	—	266-36	—	1.6	—
1012	—	267-23	—	1.6	—
1013	—	—	BD +33°4828	0.5	G2 V (be), G2 V (am), G3 (af)
1014	2	171-39	BD +44°4548	1.5	M2 V (bh), M1 (af)
1015	3	—	CD -68°2378	1.1	—
1016*	4 A	171-40 A	BD +45°4408 A	1.2	K7 (af)
1017	4 B	171-40 B	BD +45°4408 B	1.2	M0 V (ai), K7 (af), M0.5 V (bh)
1018	—	—	—	1.5	—
1019	—	—	—	1.5	—
1020	4.2 A	—	CD -49°14337 A	0.6	G1 IV (be), F7 V (bf), F8 (af)

TABLE 5.1 — continued

LHS	Gliese	Giclas	Other Name	$m_{pg} - m_R$	Spectral Type and Reference
1021	4.2 B	—	CD -49°14337 B	—	—
1022	—	30-45	—	1.7	M3.5 (af)
1023	—	158-31	—	1.6	—
1024	—	—	—	2.2	—
1025	—	266-55	—	2.1	—
1026	7	266-57	CD -27°16	1.5	M0 (af)
1027*	8	—	β Cas	0.3	F2 III-IV (be), F2 IV (am), F1 (af)
1028	—	130-49	—	-0.2	DC6 (br), DC6+ (ba)
1029	—	130-50	—	1.9	—
1030	—	—	—	—	—
1031	—	—	—	1.5	—
1032	—	—	—	2.0	—
1033	—	31-31	—	1.8	—
1034	—	—	—	1.5	—
1035	—	—	—	2.8	—
1036	—	267-45	CD -39°31	1.5	K4 (af)
1037	—	130-53	—	1.3	—
1038	1004	217-37	—	0.1	DA8 (br)
1039	—	217-38	—	1.5	—
1040 A*	11 A	241-76 A	—	1.7	M6 V (cb), M4 comp (af)
1040 B*	11 B	241-76 B	—	—	composite with LHS 1040 A

TABLE 5.1 — continued

LHS	Gliese	Giclas	Other Name	$m_{pg} - m_R$	Spectral Type and Reference
1041	—	130-56	—	1.1	—
1042	—	—	—	1.7	—
1043	—	130-57	—	2.0	—
1044	—	158-45	—	0.3	DC8 (br), DC8 (bn)
1045	—	266-72	—	1.3	—
1046	—	266-73	—	1.5	—
1047 A*	1005 A	158-50 A	—	2.2	M4 V (bi), M4 (af)
1047 B*	1005 B	158-50 B	—	—	composite with LHS 1047 A
1048	—	267-58	—	1.5	M4: (af)
1049	—	—	—	1.5	—
1050	12	30-55	—	1.7	M3.5 (af)
1051	—	—	—	1.5	—
1052	1007	31-39	—	1.9	—
1053	14	171-44	BD +40°45	1.5	M0.5 (bh), K7 (af)
1054	—	130-61	Ross 680	2.4	M2 (af), M0 (bk)
1055	—	—	—	1.5	—
1056	—	—	—	1.5	—
1057	—	266-87	—	1.3	K7 (af)
1058	—	—	—	2.2	—
1059	—	—	—	1.5	—
1060	—	—	—	2.0	—

TABLE 5.1 — continued

LHS	Gliese	Giclas	Other Name	$m_{pg} - m_R$	Spectral Type and Reference
1061	17.1	—	CD -46°76	1.6	M1 (af)
1062	—	171-51	—	1.3	—
1063	—	—	CD -53°70	1.1	K3 V (at)
1064	—	—	CD -51°89	1.5	—
1065	1010 A	242-51	—	1.3	dK (bj)
1066	1010 B	242-52	—	1.5	M4 V (ai), dK (bj)
1067	18	226-107	CD -27°108	1.1	K3 (af), K2 V (bf)
1068	—	130-68	—	1.7	—
1069	—	—	—	2.3	—
1070	2005	—	McCarthy 45	1.6	M6 V (ad), M6 V (bg)
1071	—	—	CD -51°95	0.6	G0 V (bf), G3-4 IV-V (be)
1072	—	—	—	—	—
1073	—	131-66	—	1.7	—
1074	—	—	—	2.4	—
1075	—	—	—	1.8	dwarf carbon star (ay)
1076	—	—	—	-0.2	DA5 (br)
1077	—	267-106	—	1.1	—
1078	—	167-107	CD -33°143	1.1	K3: (af)
1079	—	1-2	—	1.8	—
1080	—	—	—	1.5	—

TABLE 5.1 — continued

LHS	Gliese	Giclas	Other Name	$m_{pg} - m_R$	Spectral Type and Reference
1081	—	—	—	1.6	—
1082	—	31-52	—	1.9	K5 (af)
1083	—	—	—	1.7	—
1084	1012	31-53	—	1.7	M4 (af)
1085	—	—	—	1.6	—
1086	—	158-86	—	1.5	—
1087	—	158-87	—	1.5	—
1088	—	217-55	—	1.5	M3.5 V (ai)
1089	—	—	—	1.3	sdM (bm)
1090	—	—	—	1.5	—
1091	—	158-94	—	2.0	—
1092	—	267-121	—	1.6	—
1093	—	—	—	0.9	—
1094	—	—	CD -63°9	1.5	—
1095	—	—	—	1.5	—
1095a	—	—	—	1.6	—
1096	—	—	—	1.5	M2 (bz)
1097	—	267-128 A	CD -35°170 A	0.9	G0 (af), G3 IV (be), F8/G0 V (bf)
1098	—	267-128 B	CD -35°170 B	1.2	K1 (af)
1099	—	266-132	—	1.5	M3 (af)
1100	—	—	—	1.5	—

TABLE 5.1 — continued

LHS	Gliese	Giclas	Other Name	$m_{pg} - m_R$	Spectral Type and Reference
1101	—	242-60	—	1.3	—
1102	—	266-135	—	-0.1	DA5+ (ba)
1103	—	—	—	1.6	—
1104	—	172-11	—	1.5	—
1105	—	217-59	—	1.8	—
1106	—	158-103	BD -10°109	1.8	K7 (af)
1107	—	—	—	—	—
1108	—	267-138	—	1.6	MS (bz)
1109	—	—	—	2.5	—
1110 A*	—	267-141 A	CD -37°205 A	0.6	G5 V (be), G8 V (bf), G8 (af)
1110 B*	—	267-141 B	CD -37°205 B	—	composite with LHS 1110 A
1111	—	172-14	—	1.1	—
1112	—	270-23	BD -9°122	0.4	F5 V (bx), G0 V-VI (bu)
1113	—	270-26	—	1.3	sd? (ae)
1114	—	1-9	BD +2°84	0.6	M2.5 (af), G2 V (am)
1115	—	270-28	—	1.6	—
1116	27	—	54 Psc	1.1	K0 V (be), K1 (af), K0 V (am)
1117	—	—	—	1.6	—
1118	—	1-10	BD +9°73	1.3	K5 (af)
1119	—	267-149	—	1.5	M3 (bz)
1120	—	132-14	—	1.1	—

TABLE 5.1 — continued

LHS	Gliese	Giclas	Other Name	$m_{pg} - m_R$	Spectral Type and Reference
1121	—	—	—	—	—
1122	27.1	—	CD -44°170	1.5	M0.5 (af)
1123	29	—	CD -60°118	0.6	G1 V (be), F6/8 (bf)
1124	27.2	266-152	CD -24°263	0.9	G3-5 V (bf), G3 V (be), G6 (af)
1125	28	132-15	BD +39°154	1.2	K3 (af), K2 V (am)
1126	2012	266-157	—	0.5	DC9 (br), DX-DQ10 (ba), DC (af)
1127	—	267-157	—	1.3	K3 (af)
1128	—	270-39	—	1.1	—
1129	1017	—	—	1.5	—
1130	—	—	—	1.5	—
1131	—	—	—	1.0	DA3 (br)
1132	—	—	—	1.1	—
1133	—	1-17	—	1.5	M1 (af)
1134	—	—	—	1.6	M4 (af)
1135	—	—	—	2.5	—
1136	—	—	—	1.5	—
1137	—	1-18	—	1.6	—
1138	—	69-18	Wolf 1504	0.9	G2 (af), G5 (ag)
1139	31.5	—	CD -66°38	0.9	G3-5 V (be), G5 V (bf)
1140	—	268-38	—	1.6	—

TABLE 5.1 — continued

LHS	Gliese	Giclas	Other Name	$m_{pg} - m_R$	Spectral Type and Reference
1141	31.4	1-20	BD +1°131	1.3	K2 V (am), K2 (af)
1142	—	—	—	1.5	—
1143	—	—	—	—	—
1144	—	267-168	—	1.5	M2.5: (af)
1145	—	—	—	1.5	sdK7-M5 (ai)
1146	—	—	—	2.8	—
1147	—	—	—	1.7	—
1148	—	—	—	—	—
1149	—	—	—	1.5	M4 V (ai)
1150	—	—	—	1.9	—
1151	—	—	—	2.7	M4 V (ai)
1152	—	—	—	1.3	—
1153	—	132-32	—	1.5	—
1154	36	268-53	CD -23°315	0.9	G8/K0 V (bf), G9 (af)
1155	—	—	—	1.5	—
1156	—	69-26	—	1.1	—
1157	—	—	—	2.0	M3 V (ai)
1158	—	—	—	0.6	DC9 (br), DC9 (bc)
1159	40 A	268-60	CD - 23°332	1.2	K5 V (bf), K5 (af)
1160	40 B	—	—	1.4	—

TABLE 5.1 — continued

LHS	Gliese	Giclas	Other Name	$m_{pg} - m_R$	Spectral Type and Reference
1161	—	132-35	—	1.3	—
1162	—	132-36	—	1.3	—
1163*	42	269-49	CD -31°325	1.0	K2 V (bf), K3 (af)
1164	—	—	—	1.5	—
1165	—	268-76	—	1.5	M3 (af)
1166	—	—	—	2.9	mid-M V-VI (bm)
1167	—	242-73	BD +68°60	1.3	K3 (af)
1168	1024	32-59	—	1.7	—
1169	—	172-30	—	1.3	—
1170	—	243-48	Wolf 40	1.1	—
1171	—	269-67	—	1.5	M3.5: (af)
1172	—	69-38	—	1.7	—
1173	—	—	—	1.5	M3.5 V (ai)
1174	—	—	—	1.5	sdK7-M1 (ai)
1175	—	69-40	Wolf 1506	1.6	M3 (af)
1176	47	243-50	Wolf 44	1.7	M2.5 V (bh), M3 (af)
1177	—	—	—	1.6	—
1178	—	—	—	1.5	sd (bw)
1179*	49	243-52	BD +61°195	1.6	M1.5 V (ah), M2 V (bh), M2 V (cb), M1(af)
1180	1026 A	33-35A	—	1.5	M1.5 (af)

TABLE 5.1 — continued

LHS	Gliese	Giclas	Other Name	$m_{pg} - m_R$	Spectral Type and Reference
1181	1026 B	33-35 B	—	1.6	M3.5 (af)
1182	—	242-77	—	1.6	—
1183	51	243-55	Wolf 47	2.1	M5 V (bi), M5 V (ah), M5 V (bh), M5 (af)
1184	—	—	—	1.5	—
1185	—	132-52	—	1.9	—
1186	—	269-87	CD -35°360	0.6	G8 (af)
1187	—	—	—	1.6	M5.5 V (ai)
1188	—	—	CD -40°239	0.6	G2/3 V (bf), G2 (af)
1189	—	—	—	1.3	—
1190	—	—	—	1.5	—
1191	—	—	—	1.8	M3.5 (af)
1192	—	—	—	—	—
1193	52.1	—	CD -51°273	1.1	K2 V (bf)
1194	—	—	—	—	—
1195	—	33-39	—	1.5	—
1196	—	—	—	—	—
1197	1031	269-106	—	1.5	M3.5 (af)
1198	—	243-62	Wolf 56	1.1	K2 (af)
1199	53.2	33-40	BD +16°120	1.5	M0 V (bh), K4 (af)
1200	—	33-41	—	0.5	—

TABLE 5.1 — continued

LHS	Gliese	Giclas	Other Name	$m_{pg} - m_R$	Spectral Type and Reference
1201	—	—	—	—	—
1202	—	—	—	1.5	—
1203	—	270-154	—	1.5	M3.5 V (ai)
1204	—	33-43	—	1.6	—
1205	—	270-155	—	1.6	M4 V (ai)
1206*	—	243-63	BD +60°170	0.6	G5 (af), F9 V (am)
1207	—	269-112	—	1.3	—
1208	54	—	CD -68°47	1.1	—
1209	—	—	—	1.6	—
1210	—	—	—	1.3	—
1211	—	132-61	—	1.5	—
1212	—	2-27	—	1.7	—
1213	—	70-44	—	1.9	—
1214	—	—	—	1.6	—
1215	—	—	—	—	—
1216	—	—	—	1.5	—
1217	—	269-125	—	1.6	—
1218	—	—	—	1.8	M5 V (ai)
1219	—	—	—	0.6	DC9 (br), DC9 (bc)
1220	55	—	ν Phe	0.6	G0 V (bf), F8 V (be), G0 (af)

TABLE 5.1 — continued

LHS	Gliese	Giclas	Other Name	$m_{pg} - m_R$	Spectral Type and Reference
1221	—	34-12	—	1.3	—
1222	—	—	—	1.5	—
1223	—	—	—	1.3	—
1224	—	268-145	—	1.3	K0 (af)
1225	56	268-146	BD -16°214	1.6	K3 V (bf), K3 (af)
1226	—	2-33	—	1.5	M1 (bk)
1227	1037	33-49	Wolf 1516	0.1	DQ6/DC6 (br), DC (af), DQ5+ (ba)
1228	56.1	270-188	—	1.3	M3 (af)
1229	56.3 B	70-50	BD -1°167 B	1.1	M0 (af)
1230	56.3 B	70-51	BD -1°167 A	1.1	K2 (af), K1 V (am)
1231	—	271-34	BD -9°256	0.6	G2 (af), G2 V (am)
1232	—	269-138	—	1.7	—
1233	—	—	—	0.3	—
1234	—	219-5	Ross 9	1.5	K5 (af), K6 V (ag)
1235	—	—	—	1.5	—
1236	—	69-65 B	BD +30°206 B	1.5	M1: (af)
1237	—	69-65 A	BD +30°206 A	1.1	K1 (af)
1238	—	272-4	—	1.1	—
1239	—	—	BD +17°197	0.6	G3 V (be), G4 (af), G3 V (am)
1240	—	70-55 A	—	1.6	—

TABLE 5.1 — continued

LHS	Gliese	Giclas	Other Name	$m_{pg} - m_R$	Spectral Type and Reference
1241	—	70-55 B	—	1.5	—
1242	—	133-7	—	1.3	—
1243	—	—	—	—	—
1244	—	133-8	—	0.2	DC9 (az)
1245	—	—	CD -44°397	—	—
1246	—	33-56	BD +17°202	1.2	K2 (af)
1247	1039	269-160	—	0.2	DC7 (br)
1248	—	—	—	1.1	—
1249	—	269-161	—	1.8	M4.5 (af)
1250	—	—	—	1.5	—
1251	—	269-166	—	2.1	—
1252	—	—	—	>3.2	M6 V (bi)
1253	—	269-171	—	1.5	—
1254	—	245-25	—	1.5	—
1255	—	—	—	1.5	—
1255a	—	274-53	—	1.5	—
1256	—	271-84	—	1.1	—
1257	—	—	—	1.5	M4 V (ai)
1258	—	—	—	1.5	—
1259	—	—	—	1.5	—
1260	—	—	—	—	—

TABLE 5.1 — continued

LHS	Gliese	Giclas	Other Name	$m_{pg} - m_R$	Spectral Type and Reference
1261	—	—	—	1.5	—
1262	—	—	—	1.5	—
1263	—	—	—	—	—
1264	—	—	—	1.5	—
1265	—	—	—	3.1	—
1266	—	133-21	—	1.8	—
1267	—	—	CD -61°282	0.4	sdF8 (ak)
1268	—	—	CD -49°451	1.5	K7 (af)
1269	—	—	—	1.5	—
1270	64	271-115	—	0.1	DA7 (br), DA (af)
1271	—	272-58	—	1.1	K3 (af)
1272	—	71-24	—	1.1	—
1273	—	—	—	1.0	—
1274	—	—	—	—	—
1275	—	72-21	BD +27°262	0.8	G8 V (am)
1276	—	—	—	1.3	—
1277	—	173-14	Ross 11	1.7	K7 (af), K7 (ag)
1278	—	274-83	CD -31°682	1.1	K4: (af)
1279	—	—	CP - 68°77 B	1.5	—
1280	—	—	—	1.7	—

TABLE 5.1 — continued

LHS	Gliese	Giclas	Other Name	$m_{pg} - m_R$	Spectral Type and Reference
1281	—	—	CD -68°74	0.5	G0wF5: (bf)
1282	—	—	—	1.6	—
1283	—	244-31	BD +66°145	0.9	G5 V (am), G6 (af)
1284 A* 67 A	—	—	BD +41°328 A	0.5	G1.5 V (be), G2 V (am), G1 (af)
1284 B* 67 B	—	—	BD +41°328 B	—	composite with LHS 1284 A
1285	—	133-29	—	1.3	—
1286	—	272-81	BD -18°287	0.6	G2-3 V (bf), G1 V (am)
1287	68	—	107 Psc	0.9	K1 V (be), K1 V (am), K0 (af)
1288	—	—	CD -42°594	1.6	M0 (af)
1289	—	35-8	BD +27°273	1.1	—
1290	70	3-14	—	1.6	M2.5 V (ah), M2 V (bh)
1291	69	244-33	BD +63°229	1.5	K5 V (am), K4 (af), M0.5 V (bh)
1292	73	3-17	Wolf 1530	1.5	M3 (af)
1293	—	274-90	—	1.5	M3.5 (af)
1294	—	—	—	2.8	—
1295	—	—	—	1.6	—
1296	—	133-39	—	1.6	—
1297	75	—	BD +63°238	1.1	K0 V (be), K0 V (am), K0 (af)
1298	—	—	—	1.7	—
1299	—	—	—	3.3	—
1300	—	—	—	1.6	—

TABLE 5.1 — continued

LHS	Gliese	Giclas	Other Name	$m_{pg} - m_R$	Spectral Type and Reference
1301	—	271-163	—	1.6	—
1302	—	159-3	—	2.3	—
1303	78	271-168	Ross 555	1.7	M3.5 (af)
1304	—	—	—	2.0	—
1305	—	—	CD -42°654	1.3	G8 (af)
1306	—	—	CD -44°545 B	1.7	M0 (af)
1307	79	272-114	CD -23°693	2.1	K5-M0 V (bf), M1.5 V (bh), K7 (af)
1308	—	—	—	1.5	—
1309	—	3-27	—	1.5	—
1310	—	245-34	—	1.3	K4 (af), K5 (bk)
1311	—	—	—	1.8	—
1312	—	244-42	—	1.7	—
1313	—	244-41	—	1.7	—
1314 A*	81 A	—	χ Eri A	0.9	G8 IIIb (be), G8 IIIb (bf)
1314 B*	81 B	—	χ Eri B	—	composite with LHS 1314 A
1315	—	—	—	1.5	K3: (af)
1316	—	—	—	1.3	—
1317	—	—	—	2.9	M6.5: (ai)
1318	—	17-45	—	1.3	M4 V (ai)
1319	—	3-29	—	1.1	—
1320	—	—	—	1.1	—

TABLE 5.1 — continued

LHS	Gliese	Giclas	Other Name	$m_{pg} - m_R$	Spectral Type and Reference
1321	—	274-136	—	1.1	—
1322	—	—	—	1.1	dK-M? (bc)
1323	—	—	CD -41°556	0.6	G4 (af), G3 V (bf)
1324	—	71-47	—	1.5	—
1325	—	272-137	—	1.7	—
1326	—	—	—	1.5	—
1327	—	—	—	1.6	—
1328	—	—	—	1.5	—
1329	—	274-143	—	1.3	—
1330	—	173-34	—	1.7	—
1331	—	—	—	1.3	—
1332	—	159-34	—	2.0	—
1333	—	3-39	—	1.6	M3 (af)
1334	—	—	—	1.5	—
1335	—	35-24	BD +22°301	1.1	K2 (af)
1336	—	—	—	1.8	—
1337	84.1 A	274-145	CD -28°657 A	1.1	M0.5 (af)
1338	84.1 B	274-146	CD -28°657 B	1.2	M3.5 (af)
1339	—	274-149	CD -30°731	1.4	M3.5 (af)
1340	—	—	—	1.5	M2-3 V (ai)

TABLE 5.1 — continued

LHS	Gliese	Giclas	Other Name	$m_{pg} - m_R$	Spectral Type and Reference
1341	—	—	—	0.5	—
1342	—	—	—	—	—
1343*	84.2	134-1	—	1.3	K4 (af)
1344	—	242-81	—	1.1	K5 (af)
1345	—	—	—	1.9	—
1346	—	—	BD -17°400	1.3	K7 (af)
1347	—	—	—	2.3	M3 (af)
1348	85.1	74-4	Ross 17	1.5	M3 (af), M3 (ag)
1349	—	—	—	2.1	M5 V (ai)
1350	—	245-45	—	1.5	—
1351	—	—	—	1.5	—
1352	—	—	—	1.6	—
1353	—	—	—	1.1	—
1354	—	—	—	1.0	—
1355	—	—	—	—	—
1356	—	—	—	1.5	—
1357	88	—	—	1.7	M0 (af)
1358	—	159-46	—	1.8	—
1359	—	—	—	1.5	M4.5 V (ai)
1360	—	—	—	1.5	K2: (af)

TABLE 5.1 — continued

LHS	Gliese	Giclas	Other Name	$m_{pg} - m_R$	Spectral Type and Reference
1361	91	—	CD -32°828	1.3	M2.5 (af)
1362	—	—	—	1.5	—
1363	—	—	—	1.5	—
1364	—	—	—	1.3	—
1365	—	159-50	BD -1°306	0.6	G0 (af), G1 V (am)
1366	1045	35-35	—	1.9	—
1367	—	—	—	2.8	—
1368*	—	74-10	Ross 18	0.6	G4 (af), G2 (ag)
1369	—	73-37	Wolf 127	1.1	M1 (af)
1370	—	—	—	1.7	—
1371	90	244-56	BD +67°191	1.4	K2 V (am), K2 V (be), K2 (af)
1372	—	159-53	—	1.6	—
1373	—	—	—	1.9	M3 (af)
1374	—	—	—	1.5	—
1375	—	—	—	1.5	—
1376	—	—	—	1.7	M4 (af)
1377	—	—	CD -31°909	1.9	M4 (af)
1378	—	—	—	2.1	—
1379	93	—	CD -54°487	1.5	—
1380	—	—	—	1.3	M1: (af)

TABLE 5.1 — continued

LHS	Gliese	Giclas	Other Name	$m_{pg} - m_R$	Spectral Type and Reference
1381	—	—	—	1.8	M3 (af)
1382	—	—	BD +1°410	0.5	G0.5 IVb (be), F9 V (am)
1383	92.2	134-24	—	1.9	M4 (ag), M3 (af)
1384	—	—	—	1.5	—
1385	—	—	—	—	—
1386	—	—	—	—	—
1387	95	—	CD -26°828	0.9	G8 V (bf), G5 V (be), G6 (af)
1388	94	74-14	Ross 19	1.5	M3.5 (af)
1389	—	—	—	0.5	—
1390	—	—	—	1.6	—
1391	—	—	CD -31°943	1.1	K2-3 V (bf), K1: (af)
1392	1047 C	74-18	—	1.8	—
1393 A*	1047 A	74-19 A	—	1.8	—
1393 B*	1047 B	74-19 B	—	—	—
1394	—	—	—	1.6	—
1395	—	—	—	2.3	—
1396	—	—	—	2.5	—
1397	—	244-60	BD +70°169	1.2	K1 (af), K2 V (am)
1398	—	—	—	1.3	—
1399	—	—	—	1.5	—
1400	—	74-21	—	1.1	—

TABLE 5.1 — continued

LHS	Gliese	Giclas	Other Name	$m_{pg} - m_R$	Spectral Type and Reference
1401	—	—	—	1.7	—
1402	—	—	—	-0.8	—
1403	—	4-21	—	0.9	—
1404	—	75-9	—	1.5	M2.5: (af)
1405	—	—	—	1.1	—
1406	—	—	—	1.3	—
1407	—	—	—	1.8	M5.5 V (ai)
1408	100 C	—	—	1.3	M3 (af)
1409 A*	100 A	—	BD -20°465 A	1.2	K4 V (bf), K4 V (am), K4 (af)
1409 B*	100 B	—	BD -20°465 B	—	composite with LHS 1409 A
1410	—	36-22	—	1.1	—
1411	—	—	—	1.4	—
1412	—	—	—	1.5	—
1413	—	—	—	>2.5	—
1414	—	—	—	1.5	—
1415	—	—	—	1.4	DC/DF? (br)
1416	—	—	—	1.5	—
1417	102	36-24	—	1.9	M4+ V (ah), M4 (af), M6 V (cb)
1418	—	221-1	—	1.5	—
1419	—	73-67	BD +4°415	1.2	K4 (af)
1420	—	—	—	2.6	—

TABLE 5.1 — continued

LHS	Gliese	Giclas	Other Name	$m_{pg} - m_R$	Spectral Type and Reference
1421	—	—	—	0.9	—
1422	—	—	—	2.5	—
1423	—	—	—	1.5	—
1424	—	—	—	1.6	—
1425	—	—	—	1.3	—
1426	—	75-30	—	1.7	—
1427	—	—	—	1.6	—
1428*	—	36-28	BD +30°421	0.6	G1 V (am)
1429	—	76-20	—	0.9	—
1430	—	—	—	—	—
1431	—	—	—	1.8	—
1432	—	—	CD -30°990	0.6	F8 V (bf)
1433	—	—	—	-0.2	—
1434	—	—	—	1.8	M3.5 (af)
1435	—	75-37	—	1.6	—
1436	—	—	CD -46°790	1.1	K4 V (bf), K3 (af)
1437	—	—	—	1.5	—
1438	1051	—	Wolf 1132	1.5	M2.5 (af)
1439	109	36-31	Ross 556	1.8	M3.5 V (ah), M3.5 V (bh), M3 (af)
1440	—	—	—	1.5	—

TABLE 5.1 — continued

LHS	Gliese	Giclas	Other Name	$m_{pg} - m_R$	Spectral Type and Reference
1441	—	—	—	1.1	—
1442	1052	75-39	—	0.3	DA7 (br), DA7+ (ba)
1443	—	—	—	1.6	M5.5-6: V (ai), M5.5-6 V (ax)
1444	—	—	—	1.5	—
1445	—	—	—	2.0	—
1446	—	174-14	—	0.6	DA9/DC (br), DA11 (ba)
1447	—	—	—	-1.1	—
1448	—	—	—	1.5	—
1448a	—	74-43	—	1.8	—
1449	—	—	—	1.3	—
1450	—	—	—	2.2	—
1451	—	—	—	1.6	—
1452*	114.1	—	CD -53°570	1.1	—
1453	114	4-43	BD +15°395	1.3	K5 (af)
1454	—	—	—	1.6	—
1455	—	246-13	—	1.7	—
1456	—	246-14	—	1.6	—
1457	—	75-43	—	1.6	—
1458 A*	—	78-7 A	BD +45°669 A	0.9	G1 V (am), G5 (af)
1458 B*	—	78-7 B	BD +45°669 B	—	composite with LHS 1458 A
1459	—	—	—	1.9	M2 (af)
1460	—	75-45	—	1.5	—

TABLE 5.1 — continued

LHS	Gliese	Giclas	Other Name	$m_{pg} - m_R$	Spectral Type and Reference
1461	—	—	—	1.5	—
1462	—	—	—	2.4	M5-6: (ai)
1463	—	—	—	2.2	—
1464	—	—	—	1.5	—
1465	—	—	—	1.5	—
1466*	118.1 A	—	CD -36°1091 A	1.3	K1 V (bf), K1 (af)
1467	118.1 B	—	CD -36°1091 B	1.5	M3: (af)
1468	—	36-41	—	1.6	—
1469	—	—	—	1.8	—
1470	—	—	—	1.3	—
1471	—	—	—	1.5	—
1472	—	—	—	1.5	—
1473	—	174-18	—	1.7	—
1474	2028	—	—	-0.3	DA6 (br)
1475	119 A	174-19	Ross 364	1.6	M1 (af)
1476	119 B	174-20	Ross 365	1.7	M3 (af)
1477	—	—	—	1.9	—
1478	—	245-61	—	1.5	—
1479	—	—	—	1.1	K4 (af)
1480	—	—	—	1.9	—

TABLE 5.1 — continued

LHS	Gliese	Giclas	Other Name	$m_{pg} - m_R$	Spectral Type and Reference
1481	—	—	—	1.9	M2.5 (af)
1482	—	—	—	1.1	K4 (af)
1483	—	74-52	Ross 331	1.5	M3.5 (af)
1484	—	—	—	1.5	—
1485	—	36-48	—	1.3	—
1486	—	78-11	—	1.3	—
1487	—	75-57	BD +5°435	1.1	K2 (af), K0 V (am)
1488	—	174-27	Ross 367	1.7	M3 (af)
1489	—	—	ϵ For	0.9	G5 IV (be), G8-K0 V (bf)
1490	—	—	—	—	—
1491	—	—	—	3.3	—
1492	—	—	BD +61°513 A	0.7	G4 V (be), G4 V (am), G2 (af)
1493	—	—	—	—	—
1494	—	246-22	BD +61°513 B	—	M3 (af)
1495	—	174-31	Ross 341	1.3	M3 (af)
1496	123	76-58	BD +1°543	1.5	M1 V (bh), K5 (af)
1497	—	—	—	1.5	—
1498	—	174-33	—	1.7	—
1499	—	78-18	—	1.5	—
1500	—	—	—	—	—

TABLE 5.1 — continued

LHS	Gliese	Giclas	Other Name	$m_{pg} - m_R$	Spectral Type and Reference
1501*	—	37-26	BD +25°495	0.4	F5 (af), sdF7 (am)
1502	—	—	—	—	—
1503	—	—	—	1.0	—
1504	1055	76-62	—	1.6	—
1505	122	245-65	—	1.5	M1 V (bh)
1506	—	—	—	2.2	—
1507	125	78-19	—	1.6	M1 V(bh), M3 (af)
1508	—	5-16 B	—	1.3	—
1509	—	5-16 A	—	1.1	—
1510	—	—	—	1.5	—
1511	—	—	CD -85°33	1.5	—
1512	—	76-66	—	1.7	—
1513	—	—	—	1.6	M3.5 (af)
1514	—	—	—	1.3	—
1515 A*	127 A	—	α For A	0.5	F8 V (be), F8 V (bf), F8 (af)
1515 B*	127 B	—	α For B	—	—
1516	—	—	—	2.0	M5.5 (ai)
1517	—	—	—	1.3	—
1518	—	174-38	BD +51°697	1.3	M0 V (ag), M0 V (bh), K5 (af)
1519	—	—	—	1.5	—
1520	—	79-18	BD +8°482	1.2	K1 (af), K1 V (am)

TABLE 5.1 — continued

LHS	Gliese	Giclas	Other Name	$m_{pg} - m_R$	Spectral Type and Reference
1521	—	246-30	—	1.7	—
1522	130.1 A	174-41 A	Ross 370 A	1.5	M1.5 (af)
1523	130.1 B	174-41 B	Ross 370 B	1.7	M2 (af)
1524	—	—	—	1.7	—
1525	—	37-32	—	1.1	—
1526	—	77-41	—	1.1	—
1527	—	5-26	Ross 373	1.1	K2 (af)
1528	134	78-31	BD +37°748	1.6	M1.5 (af), M1.5 V (bh)
1529	—	—	—	1.7	—
1530	—	246-32	Ross 371	1.1	M3.5 (af)
1531	—	—	—	—	—
1532	—	77-45	—	1.1	—
1533	—	37-34	BD +33°622	1.2	K2 (af)
1534	—	—	CD -33°1180	0.8	—
1535	—	—	—	—	—
1536	—	—	—	1.5	—
1537	—	—	—	1.5	—
1538	—	79-32	—	1.3	—
1539	—	77-47	—	1.5	—
1540	1058	77-48	—	1.5	M4.5 V (ai)

TABLE 5.1 — continued

LHS	Gliese	Giclas	Other Name	$m_{pg} - m_R$	Spectral Type and Reference
1541	1059	95-30	—	1.5	—
1542	—	—	—	1.5	—
1543	—	—	—	1.6	K3 (af)
1544	—	5-34	—	2.1	—
1545	—	5-35	BD +11°468	1.4	G0 V (ag)
1546	141	77-49	BD -5°642	1.2	K5 V (am), K4 (af)
1547	—	77-50	—	0.6	DZ9/DA10 (br), DZ9 (bn), DA10+ (ba)
1548	142	—	BD -20°643	1.4	K5 V (bf), K7 V (am), K7 (af), M0.5 V (bh)
1549	1060 A	—	—	-0.6	DA5 (br), DAs (af)
1550	1060 B	—	—	1.7	M3 (af)
1551	143.2 A	—	κ Ret A	0.4	F3 IV-V (bf), F5 IV-V (be)
1552	143.2 B	—	κ Ret B	1.6	—
1553	—	221-12	—	1.6	—
1554	143.3	5-43	—	1.3	M3: V (ah), sdM3 (ag)
1555*	—	77-61	—	1.8	dwarf carbon star (an)
1556	—	—	—	1.1	—
1557*	144	—	—	ϵ Eri	1.2K2 V (be), K2 V (ca), K2 V (am)
1558	—	—	—	1.6	—
1559	—	—	—	1.1	M3: V (bs)
1560	—	—	CD -31°1454	1.0	K2: (af)

TABLE 5.1 — continued

LHS	Gliese	Giclas	Other Name	$m_{pg} - m_R$	Spectral Type and Reference
1561	—	77-64	—	1.3	—
1562	—	38-3	—	1.7	—
1563	146	—	CD -48°1011	1.2	K5-M0 V (bf), K7: (af)
1564	—	—	—	2.7	—
1565	1061	—	—	1.6	M4.5 (af)
1566	—	77-65	—	1.3	—
1567	—	—	—	1.8	M3 (af)
1568	—	6-18	—	1.3	—
1569*	147	—	10 Tau	0.6	F8 V (am), F9 V (be), G0 (af)
1570	—	—	—	1.5	—
1571	—	37-45	—	1.8	—
1572	—	—	—	1.5	—
1573	—	6-24	Wolf 204	1.5	M3.5 (af)
1574	—	6-25	Wolf 205	1.5	M3.5 (af)
1575	—	—	—	—	—
1576	—	—	—	1.5	—
1577	147.1	80-15	BD -3°592	0.5	F9 V (am), F9 V (be), F9 (af)
1578	—	—	—	1.3	—
1579	—	38-10	—	1.3	—
1580	—	—	—	1.3	—

TABLE 5.1 — continued

LHS	Gliese	Giclas	Other Name	$m_{pg} - m_R$	Spectral Type and Reference
1581	150	—	δ Eri	1.1	K0+ IV (be), K0 IV (am), G9 (af)
1582	—	160-19	—	1.9	—
1583	—	246-44	—	1.3	—
1584	—	—	CD -51°887	0.5	G1 V (be), F6 V (bf)
1585	—	38-11	—	1.3	—
1586	—	6-31	—	1.3	—
1587	—	38-12	—	1.8	—
1588	—	95-54	Ross 36	1.7	M3.5 (af)
1589	—	79-69	—	1.8	—
1590	—	160-22	—	2.0	M2.5 (af)
1591	155	—	τ^6 Eri	0.5	F3 III (be), F3-5 V (bf), F5 (af)
1592	—	—	—	1.7	—
1593	—	7-4	—	1.3	—
1594	155.1	80-22	Ross 588	1.6	M1 (af)
1595	—	—	—	1.5	—
1596	—	221-22	—	1.5	—
1597	—	175-8	Ross 566	0.6	K0 (af), K0 (bk)
1598	—	80-23	—	1.1	—
1599	—	80-24	BD +0°659	1.1	K1 (af)
1600	—	—	—	1.5	—

TABLE 5.1 — continued

LHS	Gliese	Giclas	Other Name	$m_{pg} - m_R$	Spectral Type and Reference
1602*	—	246-49	—	0.4	—
1603	—	—	CD -42°1269	1.1	K3 V (bf), K5 (af)
1604	—	—	—	3.3	—
1605	—	38-17	—	1.3	—
1606	—	—	—	0.6	K (af)
1607	—	79-75	Ross 589	1.3	K4 (af)
1608	—	80-29	—	1.8	—
1609	—	—	—	2.3	—
1610	—	6-39	Wolf 227	1.7	M4.5 (af)
1611	—	—	—	-0.2	DA9 (br), DA9 (bc)
1612	—	—	—	1.8	—
1613	155.2	246-53	BD +60°762	1.1	K0 V (am), K2 (af)
1614	—	7-12	—	0.9	—
1615	—	—	—	1.6	—
1616	157.1	6-42	Wolf 1322	1.8	M4 V (bh), M3.5 (af)
1617	—	7-16	—	0.6	DC9 (br)
1618	—	175-13	Ross 25	1.7	M3.5 (af)
1619	156.2	248-10	BD +75°154	1.2	K4 (af), K4 V (am)
1620	—	—	CD -57°806	0.5	F7 V (bf)

TABLE 5.1 — continued

LHS	Gliese	Giclas	Other Name	$m_{pg} - m_R$	Spectral Type and Reference
1621	—	175-14	—	1.3	—
1622	—	—	—	—	—
1623	—	221-26	—	1.6	—
1624	—	160-43	—	1.6	—
1625	—	—	—	>2.3	—
1625a	—	—	—	2.3	—
1626	—	—	—	1.8	—
1627	—	—	—	1.1	dM? (bc)
1628	160.2	—	BD -21°784	1.4	K5 (af)
1629	—	248-12	—	1.5	—
1630	—	—	—	2.8	—
1631	—	221-28	—	1.5	—
1632	—	—	—	2.3	sd (bb)
1633	—	—	—	1.1	—
1634	162	38-26	Ross 587	1.6	M1 (af)
1635	—	—	—	1.7	—
1636	—	—	—	0.5	DC9(br)
1637	—	247-14	—	1.3	—
1638	—	247-15	—	1.7	—
1639	—	—	—	1.5	—
1640	—	—	—	1.5	—

TABLE 5.1 — continued

LHS	Gliese	Giclas	Other Name	$m_{pg} - m_R$	Spectral Type and Reference
1641	—	—	—	1.3	—
1642*	164	175-19	Ross 28	1.8	M3.5 (af)
1643	—	222-2	—	1.5	—
1644	—	8-16	BD +21°607	0.5	F2 (af)
1645	—	82-4	—	2.0	—
1646	—	82-5	BD -6°855	0.9	—
1647	—	—	—	1.6	—
1648	—	—	—	1.9	—
1649	—	82-6	—	1.3	—
1650	167	—	CD -53°889	1.1	K5 V (bf)
1651	167.2	—	—	0.9	M0 (af)
1652	—	—	—	1.5	sdM0 (ax), K7-M0 V (ai)
1653	—	8-22	Ross 597	1.3	K3 (af)
1654	—	—	—	1.5	M4 (af)
1655	—	82-9	—	1.5	—
1656	—	—	—	1.5	—
1657	—	—	—	>2.0	—
1658	—	—	—	1.6	—
1659	—	38-30	Ross 593	1.1	M3 (af)
1660	2034	—	RR Cae	-0.2	DA8 (br)
1660a	—	—	—	>2.5	—

TABLE 5.1 — continued

LHS	Gliese	Giclas	Other Name	$m_{pg} - m_R$	Spectral Type and Reference
1661	—	82-13	—	1.1	—
1662	—	—	—	1.5	—
1663	—	248-19	—	1.7	M3 (af)
1664	—	248-18	—	1.5	—
1665	—	—	—	1.5	—
1666	—	—	—	1.6	—
1667	1070	39-9	—	1.3	—
1668	—	—	—	1.5	M3.5 (af)
1669	—	—	—	2.1	—
1670	—	—	—	-0.4	DC9 (bc), DC9 (bn), DC9 (br)
1671	—	7-39	—	1.1	—
1672	—	—	—	1.5	M2.5 (af)
1673	—	—	—	1.5	K7: (af)
1674	170	81-21	Ross 594	1.6	M4.5 (af), M7 V (cb)
1675	—	82-25	—	2.0	—
1676	—	—	—	1.5	—
1677	—	222-4	—	1.3	—
1678	—	—	—	1.5	M1.5 (af)
1679	—	247-22	—	2.0	—
1680	—	247-23	—	2.0	—

TABLE 5.1 — continued

LHS	Gliese	Giclas	Other Name	$m_{pg} - m_R$	Spectral Type and Reference
1681	—	8-41	—	1.5	—
1682	—	81-25	—	1.3	—
1683	—	175-37	Ross 31	1.2	K3 (af)
1684	171	175-39	BD +55°900	1.2	K2 V (am), K1 (af)
1685	—	—	—	1.4	—
1686	—	83-22	—	1.3	—
1687	—	—	—	1.5	M3.5 (af)
1688	172	175-42	BD +52°857	1.3	M0 V (ca), K8 V (am), M1 V (bh), K7 (af)
1689	—	82-37	Ross 398	1.1	M0 (af)
1690	—	—	—	1.8	—
1691	—	—	—	3.3	sdM (bi), sd (bb)
1692	—	8-49	—	1.5	—
1693	—	—	—	-0.7	DA8 (br)
1694	—	—	—	1.1	—
1695	—	8-50	Ross 600	1.1	K2 (af)
1696	—	81-30	BD +41°931	0.7	G2 V (am)
1697	—	175-45	—	1.7	M1 (bk)
1698	—	39-32	—	1.7	sdM1.5-2 (ai)
1699	—	—	—	1.3	—
1700	—	—	—	2.1	M0 (af)

TABLE 5.1 — continued

LHS	Gliese	Giclas	Other Name	$m_{pg} - m_R$	Spectral Type and Reference
1701	176.3	—	CD - 50°1492	0.9	K1 V (bf)
1702	—	191-11	—	1.1	sdK (bo)
1703	—	8-57	—	1.3	—
1704	—	—	—	1.1	K3: (af)
1705	—	39-37	—	1.5	—
1706	1072	85-19	—	1.8	—
1707	—	—	—	1.5	—
1708	—	81-38	BD +45°992	0.6	G1 V-VI (be), G1 V-VI (am), G2 (af)
1709	—	—	—	1.5	—
1710	—	39-40	—	0.9	M0-1 V (ai)
1711	—	—	—	1.6	—
1712	180	—	—	1.3	M3: (af)
1713	—	—	—	1.5	—
1714	—	81-42	—	1.1	K3 (af)
1715	—	39-41	—	1.7	—
1716	—	39-42	—	1.8	—
1717	—	—	—	1.1	—
1718	—	83-46	Ross 382	1.1	G8 (af), K0 (bk)
1719	—	39-43	BD +34°927	0.8	G8 V (am)
1720	—	—	—	1.5	—

TABLE 5.1 — continued

LHS	Gliese	Giclas	Other Name	$m_{pg} - m_R$	Spectral Type and Reference
1721	1074	191-15	—	1.7	M0 V (ag), M1 (af)
1722	—	39-44	—	1.3	—
1723	—	—	—	1.5	—
1724	186.1 A	—	CD -56°1071 A	0.7	G5 V (be), G0 V (bf)
1725	—	—	—	1.3	K4 (af)
1726	—	—	—	1.6	K (af)
1727	186.1 B	—	CD -56°1071 B	1.5	—
1728	—	247-45	—	1.6	—
1729	—	—	—	1.0	—
1730	—	—	—	1.8	sdM4 (ad)
1731	—	—	—	1.1	M3 (af)
1732	—	83-53	—	0.9	—
1733	—	191-21	—	1.8	—
1734	—	—	—	-0.2	DZ9?/DC9? (br)
1735	—	—	—	1.5	—
1736*	188	—	104 Tau	0.7	G4 V (be), G4 V (am), G4 (af)
1737	—	—	—	-0.8	—
1738	—	85-42	—	1.4	—
1739	—	—	—	0.2	—
1740	—	85-44	Ross 388	1.6	M3 (af)

TABLE 5.1 — continued

LHS	Gliese	Giclas	Other Name	$m_{pg} - m_R$	Spectral Type and Reference
1741	—	247-50	—	1.5	—
1742	—	86-27	—	1.9	—
1742a	—	—	—	2.9	sdM5: (ai)
1743	—	85-48	—	2.1	—
1744	—	—	BD -9°1094	1.1	K0 (af), K1 V (am)
1745	—	85-54	BD +19°869	1.3	K3 (af)
1746*	—	96-28	BD +44°1142	1.1	K3 (af), K3 (bk)
1747	—	—	—	1.5	M3: (bp)
1748	—	—	—	1.6	—
1749	—	—	—	1.5	—
1750	—	—	—	1.6	—
1751	200.1	—	—	1.1	—
1752	—	249-2	—	1.6	K4 (af)
1753	197	—	λ Aur	0.6	G2 IV-V (be), G0 V/G2 IV-V (am), G1 (af)
1754	200 A	84-45 A	BD -3°1061 A	1.3	K3 V (am), K4 (af)
1755	200 B	84-45 B	BD -3°1061 B	1.6	M2: (af)
1756	—	—	—	1.7	—
1757	—	191-29	—	1.8	—
1758	—	191-30	—	2.2	—
1759	—	86-39	Ross 65	1.1	K2 (af)
1760	—	—	—	1.6	—

TABLE 5.1 — continued

LHS	Gliese	Giclas	Other Name	$m_{pg} - m_R$	Spectral Type and Reference
1761	203	97-42	Ross 41	2.0	M4 ⁻ -4 V (ah), M3.5 (af)
1762	—	99-11	—	1.3	—
1763	204	99-12	BD -3°1110	1.2	K5 V (am), K5 (af)
1764	—	—	—	-0.2	DA (br)
1765	—	86-44	Ross 406	1.1	M3 (af)
1766	204.2	99-14	Wolf 1450	1.3	M4.5 V (bq), M4: (bp), M3.5 (af)
1767	—	—	—	1.8	—
1768	—	—	—	1.5	—
1769	207.2	—	CD - 23°2865	1.2	K3 (af), K2 V (bf)
1770	—	—	CD -46°1936 A	0.6	G6 V (bf), G8 (af)
1771	—	—	CD -46°1936 B	1.4	K3 (af)
1772	—	191-48	BD +51°1094	1.2	K2 (af)
1773	—	191-50	—	1.9	—
1774	211	—	BD +53°934	1.1	K1 V (am), K1 V (be), K1 (af)
1775	212	191-51	BD +53°935	1.5	M1 V (bh), M1 (af)
1776	—	99-24	Ross 48	1.1	K4 (af)
1777	—	—	—	1.7	M5 V (ai)
1778	—	99-27	—	1.5	—
1779	—	99-26	BD +2°1041	1.2	K3 (af), K1 V (am)
1780*	—	99-31	BD +9°946	0.6	F8f (af)

TABLE 5.1 — continued

LHS	Gliese	Giclas	Other Name	$m_{pg} - m_R$	Spectral Type and Reference
1781	—	—	vB 1	1.3	—
1782	215	249-18	BD +62°780	1.3	K5 V (ag), K7 (af)
1783	217	96-51	BD +37°1312	1.0	K0 V (am), K1 (af)
1784	—	96-52	Wolf 237	2.5	M4 (af)
1785	—	—	—	1.5	M4 V (ai)
1786	—	191-53	—	0.9	—
1787	218	—	CD -36°2458	1.5	M3.5 (bq), M3 (af)
1788	—	—	—	1.5	—
1789	—	98-25	Ross 66	1.1	M0 (af)
1790	—	102-33	—	0.6	sdG (bo), sdK: (bd)
1791	—	102-34	—	0.9	K4 (af), sdK: (bd)
1792	—	—	δ Lep	1.2	G8 III (be), G8 III-IV (bf), G8p (am)
1793	—	—	—	1.5	—
1794	220	100-44	Ross 59	1.5	M1.5 (af)
1795	—	—	—	2.2	sd (bb)
1796	224.1	—	CD -63°218	1.1	K1 III-IV (be), K1 III-IV (bf)
1797	223.3	—	CD -50°1977	1.2	K1 (af), G8 IV (be)
1798	223	99-43	BD +2°1085	1.2	K3 (af)
1799	—	192-8	—	1.3	—
1800	—	99-45	—	1.1	—

TABLE 5.1 — continued

LHS	Gliese	Giclas	Other Name	$m_{pg} - m_R$	Spectral Type and Reference
1801	—	—	—	0.3	—
1802	—	—	—	2.5	—
1803	224	—	BD +13°1036	1.8	G0 V (am), G5 IV (be), G8 (af)
1804 A*	225.2 A	—	CD -31°2902 A	1.3	K3-4 V (bf), K4p (af)
1804 B*	225.2 B	—	CD -31°2902 B	—	composite with LHS 1804 A and C
1804 C*	225.2 C	—	CD -31°2902 C	—	composite with LHS 1804 A and B
1805	—	192-13	—	1.6	—
1806	—	192-14	—	1.9	—
1807	—	—	—	2.8	—
1808	—	249-32	—	1.5	—
1809	—	192-15	—	1.6	M5 V (ai)
1810	—	—	—	1.7	—
1811	—	100-54 A	BD +19°1185 A	0.6	G1 (af), G0 V (am)
1812	—	100-54 B	BD +19°1185 B	1.2	K3 (af)
1813	—	101-16	Wolf 261	2.3	M3.5 (af)
1814	226.1	98-38	Ross 60	1.8	M3.5 (af)
1815	—	—	—	1.1	—
1816	—	—	—	2.3	—
1817	—	249-36	—	1.3	—
1818	—	—	CD -59°1224	0.8	K1 V (bf)
1819	—	106-25	Ross 413	1.3	K4 (af)
1820	—	106-26	vB 2	1.5	—

TABLE 5.1 — continued

LHS	Gliese	Giclas	Other Name	$m_{pg} - m_R$	Spectral Type and Reference
1821	—	—	—	1.3	—
1822	—	—	—	0.9	DA/DC (bo), DC9 (br)
1823	—	—	—	2.0	—
1824	—	98-46	Ross 62	1.7	M3 (af)
1825	—	—	Ross 414	1.3	M1.5 (af)
1826	—	—	—	2.6	sdM (ac)
1827	229	—	BD -21°1377	1.2	M1 V (bi), M1 V (ah), M1-2 V (bf)
1828	—	98-49	Wolf 1058	1.6	M2 (bk), M1.5 (af)
1829	—	—	—	2.5	—
1830 A*	228 A	102-53 A	BD +10°1032 A	1.7	M2.5 V (bh), M3 V (cb), M3 (af)
1830 B*	228 B	102-53 B	BD +10°1032 B	—	composite with LHS 1830 A
1831	1088	—	—	1.1	M3.5 (af)
1832	—	—	—	1.1	—
1833	—	—	—	>1.8	—
1834	—	—	—	1.5	—
1835	—	101-30	BD +47°1276	1.1	K1 (af)
1836	231.3	—	Ross 417	1.7	M4 (af), M3.5 V (bq)
1837	—	—	—	1.5	—
1838	—	105-30	—	0.3	DA9 (br)
1839	—	—	—	2.9	M4.5 V (ad)
1840	2049	—	BD -22°3005	1.3	M1.5 (af)

TABLE 5.1 — continued

LHS	Gliese	Giclas	Other Name	$m_{pg} - m_R$	Spectral Type and Reference
1841	—	—	—	1.1	sd (bw)
1842	—	—	—	1.8	—
1843	—	—	—	1.7	—
1844	—	—	—	1.5	M0.5 (af)
1845	—	—	CD -42°2503	0.8	G5 V (be), G5 V (bf)
1845a	—	—	—	2.3	—
1846	232	104-37	Ross 64	1.8	M4 V (bi), M4.5 (af), M6 V (cb)
1847	—	—	—	2.0	M2: (af)
1848	—	192-26	—	2.3	—
1849	234 A	106-49 A	Ross 614 A	1.7	M4.5 V (bi), M4.5 V (ah), M4.5 V (bh)
1850	234 B	106-49 B	Ross 614 B	—	composite with LHS 1849
1851	—	101-42	—	1.2	K4 (af)
1852	—	—	—	1.5	—
1853	—	249-51	—	1.5	—
1854	—	192-30	—	1.5	—
1855	238	—	—	1.5	M2 V (bq)
1856	—	192-32	—	1.3	—
1857	—	105-46	—	1.3	M4.5 V (ai)
1858	239	104-49	BD +17°1320	1.6	M0 V (ah), M1 V (bh), M0 (af), M1 V (cb)
1859	—	—	—	1.8	—
1860	—	104-50	—	1.8	—

TABLE 5.1 — continued

LHS	Gliese	Giclas	Other Name	$m_{pg} - m_R$	Spectral Type and Reference
1861	—	109-16	—	1.9	—
1862	—	103-51	—	1.8	—
1863	—	—	—	1.5	—
1864 A*	—	192-39 A	—	2.1	M3.5 (af)
1864 B*	—	192-39 B	—	—	composite with LHS 1864 A
1865	2050	251-16	—	1.5	K7 (af), M3.5 V (bh)
1866	—	87-3	BD +32°1398 A	1.5	K3 V (am), K2 (af)
1867	—	87-4	BD +32°1398 B	1.6	M0.5 (af)
1868*	240.1	—	BD +79°212	0.5	F8 V (be), F8 V (am)
1869	—	87-5	—	1.5	—
1870	246	87-7	—	-0.1	DA2 (br)
1871	—	110-17	—	1.7	—
1872	—	—	—	1.5	M2 (bp)
1873	—	—	—	1.1	—
1874	249	107-27	BD +47°1355	1.4	K5 (af)
1875	250 A	—	BD -5°1844 A	1.2	K4 V (be), K4 (af)
1876	250 B	—	BD -5°1844 B	1.7	M2.5 V (bi), M2.5 V (ah), M2 (af)
1877	—	—	—	1.5	—
1878	—	—	CD -28°3554	0.6	G5 IV (be), G8: (af)
1879	251	87-12	Wolf 294	1.5	M3 V (bi), M3.5 V (ah), M3.5 V (bh)
1880	—	107-34	—	1.9	—

TABLE 5.1 — continued

LHS	Gliese	Giclas	Other Name	$m_{pg} - m_R$	Spectral Type and Reference	\prec
1881	—	—	CD -56°1692	0.5	F8-G0 V (bf)	
1882	—	192-58	—	1.3	—	
1883	—	107-36	—	1.6	—	
1884	—	108-40	BD +1°1600	0.9	G8 V (am)	
1884a	—	87-15	—	1.6	—	
1885	—	250-31	—	1.5	—	
1886	—	108-43	BD -0°1520	0.6	G1 (af)	
1887	—	—	—	1.5	M2-3 (bp)	
1888	—	250-32	—	1.6	—	
1889	—	—	—	0.9	DC9 (br), DC9 (bc), DA?11 (ba)	
1890	257.1	107-42	BD +48°1469	1.3	K3 V (am), K3 (af)	
1891	—	108-48	Ross 612	0.7	G7 (af)	
1892	261	—	—	-0.2	DA8 (bn), DA (ai)	
1893	262	—	BD +29°1441	0.7	G4 V (am), G4 V (be), G1 (af)	
1894	—	—	—	1.5	K5-M0 V (ai)	
1895	263	—	Ross 54	1.7	M3.5 (af)	
1896	—	—	CD -57°1633	0.5	sd (bw)	
1897	—	250-38	—	1.5	—	
1898	—	—	—	0.6	—	
1899	—	88-9	BD +21°1528	0.9	G9 V (am), G9 V (be)	
1900	—	—	BD -14°1750	1.5	K5 (af), M0 (bp)	

TABLE 5.1 — continued

LHS	Gliese	Giclas	Other Name	$m_{pg} - m_R$	Spectral Type and Reference
1901	—	—	—	2.1	—
1902	—	—	CD -49°2676	0.8	G8 V (bf), G8 (af)
1903	—	107-55	—	1.3	—
1904	—	—	—	1.6	—
1905	—	—	—	0.9	—
1906	—	—	—	1.1	—
1906a	—	107-56	—	1.1	sdK (bd)
1907	—	193-38	—	1.3	—
1908	268.2	—	CD -63°295	1.3	—
1909	—	—	—	1.5	—
1910	—	—	BD -12°1871	0.7	G5 V (bf), G2 V (am), G3 (af)
1911 A*	269 A	—	CD -46°3046 A	1.1	K1 V (be), K3 V (bf), K2 (af)
1911 B*	269 B	—	CD -46°3046 B	—	K4 V (be)
1912	270	87-33	BD +33°1505	2.0	M0 V (bi), M0 V (ah), M0 (af), M1.5 V (bh)
1913	—	—	BD -15°1776	0.5	G6 (af)
1913a	—	107-63	—	1.1	—
1914	—	87-36	—	1.3	—
1915	—	107-67	—	1.6	sdM0-2 (ai)
1916	—	—	—	0.2	K5 (af)
1917	—	87-37	—	1.6	—
1918	—	—	—	1.3	—
1919	—	87-38	Ross 988	1.1	G5: (af)
1920	1097	112-21	—	1.3	M3 (bp)

TABLE 5.1 — continued

LHS	Gliese	Giclas	Other Name	$m_{pg} - m_R$	Spectral Type and Reference
1921	—	—	—	2.7	—
1922	—	—	CD -44°3484	1.1	K5: (af)
1923	—	—	—	1.5	M6: V (ai), M6: V (ax)
1924	—	—	—	1.1	M3 (af)
1925	—	—	—	1.5	M4.5: V (ai)
1926	—	—	vB 17	—	—
1927	2062	—	—	-0.1	DAE (br), DAe (af)
1928	1099	112-27	—	1.9	—
1929*	—	—	CD -45°3283	0.5	G0f: (af)
1930	—	—	Ross 390	0.9	G6 (af), sd (bw)
1931	—	111-18	—	1.8	—
1932	—	—	—	1.5	M3: (bp)
1933	—	88-43	Ross 394	1.7	M3 (af)
1934	—	87-48	BD +37°1748	1.1	K2 (af)
1935	—	—	—	1.9	M3 (bp)
1936	—	—	—	1.5	—
1937	—	—	—	2.8	—
1938	—	—	—	1.9	—
1939	284	—	CD -44°3675	0.9	G6 IV (bf), G6 IV (be), G8 (af)
1940	—	193-59	—	1.3	—

TABLE 5.1 — continued

LHS	Gliese	Giclas	Other Name	$m_{pg} - m_R$	Spectral Type and Reference
1941	—	193-60	—	1.3	—
1942	—	88-48	BD +18°1719	1.3	—
1943	285	50-4	Ross 882	1.1	M4.5 V (ah), M4.5 V (bq), M4 V (ax)
1944	—	—	BD +39°1998	0.5	F8 V (be), F8 V (am)
1945*	286	—	β Gem	1.1	K0 IIIb (be), K0 III (am), G8 (af)
1946	—	193-62	—	0.9	—
1947	—	193-67	—	0.9	—
1948	—	193-70	BD +54°1175	1.3	K3 (af), K4 V (am)
1949	—	50-5	—	1.8	—
1950	—	50-6	—	1.7	—
1951	1103 A	112-50	—	2.0	dM (bt)
1952	1103 B	—	—	2.0	—
1953	—	—	—	1.5	—
1954	—	193-75	—	1.1	—
1955 A*	—	—	—	1.3	M4 (af)
1955 B*	—	—	—	—	composite with LHS 1955 A
1956	1101	253-6	—	1.8	—
1957	—	—	—	1.5	M3 (af)
1958	—	111-45	—	1.2	K4 (af)
1959	294 A	—	CD -59°1773	0.8	G0 V (bf), G0 V (be)
1960 A*	294 B	—	CD -59°1774 A	1.1	—
1960 B*	294 C	—	CD -59°1774 B	—	—

TABLE 5.1 — continued

LHS	Gliese	Giclas	Other Name	$m_{pg} - m_R$	Spectral Type and Reference
1961	—	90-34	—	1.8	—
1962	—	253-2	—	1.5	—
1963	1105	111-47	—	1.1	M4 V (al)
1964	—	193-81	—	1.1	—
1965	—	—	—	1.5	—
1966	—	40-2	BD +21°1731	1.0	K0 V (am), K1 (af)
1967	—	—	—	1.1	—
1968	296	—	CD -39°3869	1.4	K[5] V (bf), K5 (af)
1969	—	—	—	1.3	—
1970	—	—	—	1.9	sdM0-2 (ai), sdM (bl), sdM (ac)
1971	—	—	—	2.3	—
1972	—	50-16	—	1.1	—
1973	—	193-83	—	1.5	—
1974	—	—	—	1.6	—
1975	—	90-39	—	1.8	sdM1.5-3 (ai)
1976	—	194-7	—	1.9	—
1977	—	40-3	—	1.8	—
1978	—	—	—	1.5	—
1979	—	—	—	1.8	—
1980	—	—	—	0.6	DC9 (br), DC9 (bc), DC9 (bn)

TABLE 5.1 — continued

LHS	Gliese	Giclas	Other Name	$m_{pg} - m_R$	Spectral Type and Reference
1981	—	—	—	1.5	—
1982	296.1	—	CD -29°5555	0.6	G4 IV-V (be), G2 V (bf)
1983	—	251-51	—	1.4	—
1984	—	251-52	BD +72°395	0.6	G2 V (am)
1985	298	—	—	1.5	—
1986	—	—	—	1.1	DC: (br)
1987	—	—	BD +32°1695	0.8	G4 V (am), G4 V (be), G4 (af)
1988	—	111-61	—	1.3	—
1989	300	—	—	1.6	M4 (af)
1990	—	—	—	1.9	—
1991 A*	301 A	—	BD -13°2439 A	1.3	K7 V comp (bi), K7 comp (af)
1991 B*	301 B	—	BD -13°2439 B	—	M0 V (bh)
1992	—	—	—	1.3	—
1993	—	251-58	—	1.7	—
1994	—	—	—	1.7	—
1995	—	—	—	1.5	—
1996	—	194-19	—	1.1	—
1997	—	—	—	1.5	K7 (af), M2 (bp)
1998	301.1	51-6	BD +31°1781	1.4	K4 V (am), K3 (af)
1999	—	—	—	1.8	—
2000	—	194-22	BD +54°1216	0.4	F4 (af), sdF6 (am)

TABLE 5.1 — continued

LHS	Gliese	Giclas	Other Name	$m_{pg} - m_R$	Spectral Type and Reference
2001	—	252-10	BD +73°407	0.9	K0 (af)
2002	—	—	—	1.5	—
2003	—	—	—	1.5	—
2004	—	—	—	1.6	—
2005	—	—	—	1.3	—
2006	—	—	—	1.6	—
2007	—	51-10	BD +33°1694	1.2	K3 (af)
2008	—	234-33	BD +66°550	1.3	K2 (af)
2009	—	—	—	1.5	—
2010	—	—	—	1.5	M3 (af), M4 (bp)
2011	1110	9-7	—	0.9	M3 V (al)
2012	—	—	—	1.6	—
2013	—	—	—	1.3	—
2014	—	115-5	—	1.1	—
2015	—	—	—	0.6	—
2016	—	115-4	BD +46°1405	1.3	K4 (af)
2017	308.2	113-40	—	1.3	K3 (af), sd (bw)
2018	308.1	234-35	—	1.5	M0 V (ag)
2019	—	52-15	—	1.3	—
2020	—	—	—	2.3	—

TABLE 5.1 — continued

LHS	Gliese	Giclas	Other Name	$m_{pg} - m_R$	Spectral Type and Reference
2021	—	—	—	1.5	—
2022	1112	51-16	—	-0.2	DA7 (br), DAs (ag)
2023	—	—	—	2.1	—
2024	—	—	—	1.5	—
2025	—	252-13	—	1.5	—
2026	—	—	—	2.7	M6 V (ad)
2027	—	9-9	—	1.5	—
2028	—	115-10	BD +42°1899	1.2	K3 (af), K2 V (am)
2029	—	9-11	—	1.1	—
2030	—	252-17	—	1.3	—
2031	—	252-19	—	1.6	—
2032	—	234-42	—	1.3	—
2033	315	9-13	BD +12°1888	1.1	K1 V (am), K1 (af)
2034	316.1	—	AZ Cnc	1.5	M6 V (bi), M6.5 V (ai), M6 V (ad)
2035	—	—	—	2.3	—
2036	—	—	BD -15°2546	0.5	F2 (af), sdF6 (am), Fw (bf)
2037	317	—	—	1.5	M3.5 (af)
2038	—	234-43	—	1.6	—
2039	—	—	—	2.9	—
2040	—	114-13	—	1.8	—

TABLE 5.1 — continued

LHS	Gliese	Giclas	Other Name	$m_{pg} - m_R$	Spectral Type and Reference
2041	—	115-18	Wolf 320	1.9	M3 (af)
2042 A*	319 A	46-1 A	BD +10°1857 A	1.4	M0 (af), M1 V (bh)
2042 B*	319 B	46-1 B	BD +10°1857 B	—	—
2043	319 C	46-2	BD +10°1857 C	1.5	M3.5 (af)
2044	—	—	—	1.5	—
2045	—	—	—	3.3	sdM (bi)
2046	—	—	—	1.8	—
2047	321	115-23	BD +42°1922	1.2	K3 V (am), K3 (af)
2048	—	47-5	—	1.7	—
2049	—	—	—	2.8	M6 V (ad)
2050	—	46-4	BD +7°2031	1.3	K4 (af), M0 V (bh)
2051	—	234-47	—	1.8	—
2052	—	—	—	2.2	—
2053	—	115-27	BD +37°1912	1.5	K5 (af), M1 V (bh)
2054	—	194-41	—	1.3	—
2055	—	114-19	BD -4°2468	1.0	G6 (af), G8 V (am)
2056	—	46-5	Ross 683	0.6	G6 (af)
2057	—	51-27	—	1.7	M3 V (ai)
2058	—	—	—	1.7	—
2059	—	9-25	—	0.9	sdK (bo)
2060	1114	9-28	Ross 622	1.6	M2 (af)

TABLE 5.1 — continued

LHS	Gliese	Giclas	Other Name	$m_{pg} - m_R$	Spectral Type and Reference
2061	—	—	—	1.5	—
2062	324 A	—	ρ^1 Cnc A	1.1	G8 V (am), G8 V (be), K0 (af)
2063	324 B	47-9	ρ^1 Cnc B	1.8	M3.5 (af), M5 V (cb)
2064	—	—	—	1.6	—
2065	—	—	—	2.9	M9 V (bi)
2066	—	234-48	—	1.1	K5: (af)
2067	—	—	—	2.7	sdM5 (bi), sdM (ac), erroneous M10 III (ad)
2068	—	—	—	0.9	<K5 V (bi)
2069	326 A	—	—	1.8	M4 V (bq), M4 (af), M3.5 V (bh)
2070	326 B	—	—	1.8	composite with LHS 2069
2071	—	—	—	1.8	—
2072	—	—	—	1.5	—
2073	—	—	—	1.5	—
2074	—	—	—	1.9	—
2075	—	—	—	1.5	dM? (bc)
2076	1116 A	9-38	EI Cnc	1.8	M5.5 V (bi), ~M5? V (al)
2077	1116 B	—	—	1.3	composite with LHS 2076
2078	330.1	9-39	BD +21°1949	1.2	K4 (af)
2079	—	—	—	2.1	—
2080	—	114-25	BD -5°2678	0.5	G0f (af)

TABLE 5.1 — continued

LHS	Gliese	Giclas	Other Name	$m_{pg} - m_R$	Spectral Type and Reference
2081	—	115-39	—	0.9	—
2082 A*	—	114-26 A	BD -3°2525	0.5	F3 (af)
2082 B*	—	114-26 B	BD -3°2525	—	composite with LHS 2082 A
2083 A*	331 B	—	ι UMa B	1.3	M1.5 (af), M1 V (bh)
2083 B*	331 C	—	ι UMa C	—	composite with LHS 2083 A
2084*	331 A	—	ι UMa A	0.3	A7 IV (be), A7 V (am), A6 (af)
2085	333	—	—	1.5	M2 V (bq), M2-3 (bp), M3 (af)
2086	—	234-51	—	-0.6	DCE? (br)
2087	—	234-52	—	1.6	DBQ (br)
2088	—	252-25	—	1.6	M4.5 V (ai)
2089	—	—	—	1.6	—
2090	—	—	—	1.9	—
2091	—	252-26	—	1.2	K3 (af)
2092	1119	115-42	—	2.2	M4 (af)
2093 A*	332 A	—	10 UMa A	0.4	F5 V (be), F5 V (am)
2093 B*	332 B	—	10 UMa B	—	G5 V (be)
2094	—	41-18	—	1.1	—
2095	—	253-18	—	1.0	K0 (af)
2096	—	—	—	2.0	—
2097	—	115-47	—	2.0	—
2098	—	—	—	2.2	—
2099	—	—	—	1.6	sdM (ac)
2100	—	—	—	2.2	sdM (ac)

TABLE 5.1 — continued

LHS	Gliese	Giclas	Other Name	$m_{pg} - m_R$	Spectral Type and Reference
2101	—	252-27	—	0.3	DC9 (br)
2102	—	234-54	—	1.3	M0-1 V (ai)
2103	—	115-50	—	1.3	—
2104	—	—	—	1.1	—
2105	—	234-55	—	1.3	M1 (af)
2106	—	—	—	1.3	—
2107	—	—	—	1.6	—
2108	—	—	BD -14°2757	0.7	G2 V (am), G3 V (bf)
2109	—	194-57	—	1.7	—
2110	—	—	—	1.5	—
2111	1121	115-57	—	1.7	—
2112	—	—	—	2.9	M4: V (ai)
2113	336	47-26	BD +33°1814	0.9	M2 V (ag)
2114 A*	337 A	—	π^1 Cnc A	0.9	G9 V (be), G9 V (am), G8 (af)
2114 B*	337 B	—	π^1 Cnc B	—	—
2115	—	—	—	1.1	—
2116	—	—	—	2.3	—
2117	—	115-63 A	—	2.1	—
2118	—	115-63 B	—	2.2	—
2119	—	46-30	—	1.3	—
2120	—	—	—	1.6	—

TABLE 5.1 — continued

LHS	Gliese	Giclas	Other Name	$m_{pg} - m_R$	Spectral Type and Reference
2121	—	47-31	—	1.1	—
2122	—	—	—	1.5	—
2123	—	253-21	—	1.6	—
2124	—	252-31	—	1.5	—
2125 A*	340 A	—	BD +29°1883 A	1.1	K3 (af), K3 V (am)
2125 B*	340 B	—	BD +29°1883 B	—	—
2126	—	252-33	—	1.6	M4.5 V (ai)
2127	—	—	—	1.5	M2: (bp)
2128	341	—	CD -51°2351	1.4	—
2129	—	46-35	—	1.5	—
2130	—	—	CD -31°7195	1.1	K2 (af), K1 V (bf)
2131	1124	116-23	BD +40°2197	1.2	K2 V (am), K3 (af)
2132	—	—	—	1.8	—
2133	—	41-35	—	1.8	—
2133a	—	—	—	1.3	—
2134	—	—	—	1.5	K5 (af)
2135	—	—	—	1.6	—
2136	—	—	—	1.6	M4: V (ai)
2137	—	161-24	BD -12°2889	1.1	K3 (af), K1-2 V (bf)
2138	—	161-25	Ross 436	1.4	K5 (af)
2139	—	—	—	1.7	—
2140	—	46-40	—	1.4	—

TABLE 5.1 — continued

LHS	Gliese	Giclas	Other Name	$m_{pg} - m_R$	Spectral Type and Reference
2141	343	41-37	Ross 83	1.7	M2 (af)
2142	—	161-30	Ross 438	1.1	K5 (af)
2143	—	—	—	2.1	—
2144	—	—	—	1.5	—
2145	347 A	161-33	Ross 439	1.6	M3.5 (af), M5 V (cb)
2146	347 B	161-34	—	1.5	—
2147	349	—	BD +6°2182	1.2	K3 V (am), K3 (af)
2148	—	—	—	1.5	—
2149	1125	48-20	—	1.3	M3.5 (af), M4 (bk)
2150	—	—	CD -46°5238	1.1	K3 (af), K2 V (bf)
2151 A*	352 A	—	Bd -12°2918 A	1.7	M3 V (bi), M3+ V (ah), M3 (af), M4 V (cb)
2152	—	—	—	1.3	—
2153	—	—	—	1.5	—
2154	351.1	41-43	Ross 84	1.1	M3 (af)
2155	353	116-36	BD +36°1970	1.6	M0.5 (af), M0.5 (af)
2156 A*	356 A	—	11 LMi A	1.1	G8 III (be), G8 IV-V (am), G8 (af)
2156 B*	356 B	—	11 LMi B	—	composite with LHS 2156 A
2157	357	—	—	2.0	M3 (af), M4 (bp)
2158	—	161-51	—	1.8	—
2159	—	161-52	—	1.1	M3.5 (af), “peculiar” (bw)
2160	—	—	—	1.8	—

TABLE 5.1 — continued

LHS	Gliese	Giclas	Other Name	$m_{pg} - m_R$	Spectral Type and Reference
2161	—	48-21	Ross 887	0.6	K4 (af), K5 (bk)
2162	—	—	—	1.3	—
2163	—	49-18	Ross 90	1.5	M0.5 (af)
2164	—	48-25	Ross 888	1.7	M0 (af), M1 (bk)
2165*	—	—	CD -38°5760	1.1	K4 (af), <M0 (bp)
2166	358	—	CD -40°5404	1.5	M3 V (bq), M3 (af), M3 (bp)
2167	—	—	—	2.1	—
2168	—	48-27	—	1.5	—
2169*	—	48-29	BD +1°2341p	0.1	A4 (af)
2170	—	48-30	—	1.5	—
2171	359	49-20	Ross 92	1.6	M4 (af)
2172	—	—	—	2.4	—
2173	361	42-17	Ross 85	1.7	M1.5 (af), M2.5 V (bh)
2174	—	—	—	1.9	—
2175	363	195-36	—	1.5	M3.5 (af)
2176	360	235-35	—	1.7	M3 (af)
2177	—	—	—	1.8	M3 (af)
2178	362	235-36	—	1.7	M3 (af)
2179	—	—	—	2.9	M5 V (ad)
2180	365	116-42	BD +43°1953	1.2	K5 V (am), <K5 V (ah), K4 (af)

TABLE 5.1 — continued

LHS	Gliese	Giclas	Other Name	$m_{pg} - m_R$	Spectral Type and Reference
2181	—	49-23	Ross 93	1.6	M4 (ag), M3 (af)
2182	367	—	CD -45°5378	1.6	M3 (af)
2183	—	116-46	—	1.5	—
2184	—	42-19	—	1.6	—
2185	—	116-48	—	1.3	—
2186	—	161-74	—	2.3	—
2187	—	—	—	1.8	—
2188*	366	252-44	Ross 434	1.6	M1.5 (af), M1.5 V (bh), M2 (au)
2189	—	—	—	1.6	—
2190	—	—	—	1.7	—
2191	—	235-40	—	2.2	—
2192	—	—	—	1.3	—
2193	—	—	—	1.1	—
2194*	—	43-3	BD +14°2151	0.4	sdF5 (am), sdF2 (ag), F0 (af)
2195	—	—	—	>1.8	—
2196	—	253-31	—	1.5	—
2197	—	235-46	—	1.7	—
2198	—	48-42	—	1.3	—
2199	—	—	—	1.6	—
2200	—	—	—	1.5	—

TABLE 5.1 — continued

LHS	Gliese	Giclas	Other Name	$m_{pg} - m_R$	Spectral Type and Reference
2201	370	—	CD -42°5678	1.4	M0 V (bf), K5 (af)
2202	—	235-48	—	1.1	—
2203	—	116-61	—	1.5	—
2204	—	—	—	1.3	—
2205	—	195-47	—	1.6	—
2206	—	42-24	—	1.8	—
2207	—	42-25	—	1.6	—
2208	—	—	CD -58°2884	1.1	K3-4 V (bf)
2209	—	—	—	1.5	—
2210	—	—	—	1.2	—
2211	373	235-49	BD +63°869	1.5	M0 (af), M1.5 V (bh)
2212	—	49-32	—	1.8	—
2213	375	—	CD -45°5627	1.8	M3.5 (af), M3.5 V (bq)
2214	—	—	—	3.0	—
2215	—	—	—	2.6	M6 V (ad)
2216	376	—	20 LMi	0.9	G2 Va (be), G8 (af), G1 V (am)
2217	—	43-24	—	1.7	—
2218	—	—	—	1.7	—
2219	—	—	—	0.5	—
2220	—	116-77	—	1.7	—

TABLE 5.1 — continued

LHS	Gliese	Giclas	Other Name	$m_{pg} - m_R$	Spectral Type and Reference
2221	—	—	CD -84°102	0.9	F8-G0 (bf)
2222	1131	235-55	—	1.5	M4 V (ai)
2223	—	—	—	1.6	—
2224	—	195-57	—	1.3	—
2225	—	146-11	—	1.3	—
2226	—	—	—	1.1	—
2227	—	—	—	1.5	—
2228	—	—	—	1.1	—
2229	—	—	—	0.9	—
2230	381	53-28	—	1.5	M2.5 V (bi), M3 V (ah), M2.5 V (bq)
2231	383	—	BD -17°3088	2.0	M1.5 V (bq), M0 (af)
2232	—	195-59	—	1.3	—
2233	—	—	—	1.5	M3.5 (af)
2234	—	43-34	BD +10°2122	1.2	K2 (af)
2235	—	43-36	—	1.6	—
2236	—	—	—	3.1	M5 V (ad)
2237	383.1	196-13	BD +53°1395	1.3	M0 V (bh), K3 (af)
2238	—	146-15	—	2.5	sdM (bi)
2239	—	235-62	—	1.5	—
2240	—	162-32	Ross 445	1.1	K3 (af)

TABLE 5.1 — continued

LHS	Gliese	Giclas	Other Name	$m_{pg} - m_R$	Spectral Type and Reference
2241	—	—	—	1.5	—
2242	—	53-38	—	-0.1	—
2243	—	—	—	3.4	M8 V (bi)
2244	386	162-38	—	1.3	M3 (af)
2245	—	118-48	—	1.3	—
2246	—	—	—	1.6	—
2247	—	—	—	1.1	—
2248	—	118-50	—	1.3	—
2249	—	146-23	—	1.5	—
2250	—	236-22	—	1.3	—
2251	—	53-40	BD -0°2326	1.1	K4 (af)
2252	—	—	—	1.8	—
2253	389 A	—	—	1.5	M3 (bp)
2254	389 B	—	—	1.5	—
2255	—	—	—	1.5	—
2256	—	—	—	1.5	—
2257	—	—	—	1.5	M4 V (ai)
2258	—	—	—	1.9	—
2259	390	162-52	BD - 9°3070	2.3	M1.5 (af), M0 V (cb)
2260	—	54-26	—	1.3	—

TABLE 5.1 — continued

LHS	Gliese	Giclas	Other Name	$m_{pg} - m_R$	Spectral Type and Reference
2261	—	—	—	1.3	—
2262	—	196-22	—	1.3	—
2263	—	196-23	—	1.5	—
2264	—	—	—	1.1	K5 (af)
2265	—	55-16	BD -5°3063	1.1	K3 (af)
2266	392 B	—	BD +49°1961 B	—	—
2267	392 B	—	BD +49°1961 B	0.5	F9 V (be), G1 V (am), G2 (af)
2268	—	146-35	—	1.8	—
2269	—	—	—	1.6	—
2270	—	118-61	—	1.6	—
2271	—	54-29	Ross 893	1.5	—
2272	393	55-24	BD +1°2447	1.7	M2 V (ah), M2 (af), M2.5 V (bh)
2273	2080	43-54	—	0.2	DC8 (br), DC (ag)
2274	—	118-66	—	1.3	—
2275	—	196-28	BD +60°1266	1.3	K4 (af)
2276	—	—	—	0.9	—
2277	—	196-29	—	1.5	—
2278	—	119-11	—	1.1	—
2279	397	146-39	BD +46°1635	1.5	K7 (af), M0.5 V (bh)
2280	—	—	—	1.6	—

TABLE 5.1 — continued

LHS	Gliese	Giclas	Other Name	$m_{pg} - m_R$	Spectral Type and Reference
2281	—	54-30	—	1.5	—
2282	—	—	—	1.7	—
2283	—	44-24	—	1.8	—
2284	—	44-25	Ross 99	0.6	K2 (af)
2285	398	44-27	RY Sex	1.8	M4 (af), M4 V (bh)
2286*	398.1	—	BD -11°2918	0.5	F7 V (be), F8 V (am), F9 (af)
2287	—	—	—	1.7	—
2288	—	—	—	2.1	—
2289	—	—	—	1.6	—
2290	—	119-22	—	1.1	—
2291	—	253-37	—	1.3	K5 (af)
2292	—	119-25	—	1.3	—
2293	—	—	—	-0.3	DQP9/DX (br)
2294	—	—	—	1.5	—
2295	399	55-35	—	2.4	M3 (af)
2296	—	—	—	1.1	M1 (af)
2297	—	—	—	1.8	M3 (af)
2298	—	55-37	—	1.5	—
2299	—	—	—	1.6	sd (bb)
2300	—	—	—	2.2	—

TABLE 5.1 — continued

LHS	Gliese	Giclas	Other Name	$m_{pg} - m_R$	Spectral Type and Reference
2301	—	—	—	1.5	—
2302	—	—	—	1.6	—
2303	—	—	—	1.6	—
2304	—	58-14	—	1.1	—
2306	—	—	—	1.5	M1 (af)
2307	—	119-29	—	2.1	M3.5 V (al)
2308	—	119-32	BD +2°2091	0.5	F8f (af)
2309	—	—	—	1.8	—
2310	—	—	—	1.5	—
2311	—	—	—	2.0	M0 (af)
2312	—	196-45	—	1.1	—
2313	—	—	—	1.6	—
2314	—	—	—	3.1	M6 V (ad)
2315	—	—	—	2.2	—
2317	—	119-37	—	1.9	—
2318	—	58-25	BD +21°2247	0.4	sdF7 (am), F8 (af)
2319	—	—	—	1.7	—
2320	—	44-43	—	1.8	—

TABLE 5.1 — continued

LHS	Gliese	Giclas	Other Name	$m_{pg} - m_R$	Spectral Type and Reference
2321	—	55-44	BD -1°2457	1.1	K4 (af), M0.5 V (bh)
2322	—	—	—	1.5	—
2323	—	—	—	1.5	—
2324	—	—	—	2.3	—
2325	—	44-46	Hubble 4	1.8	M4 (af)
2326	—	—	—	1.4	—
2327*	—	146-72	—	1.8	M2 V (al)
2328	—	163-23	—	2.1	M4 (af)
2329	—	—	—	1.5	M2: (bp)
2330	—	—	—	2.9	—
2331	405	196-51	Ross 107	1.5	M1.5 (af)
2332	—	146-75	BD +42°2163	1.2	K2 (af)
2333	1140	163-27	—	0.0	DA6 (br), DA7 (bn), DA (af)
2334	406.1	236-46	BD +70°639	1.3	M0 (af), M0.5 V (bh)
2335	—	—	—	2.8	—
2336	—	176-3	—	1.6	—
2337	—	147-11	—	1.9	—
2338	—	—	—	1.5	M3: (af)
2339	—	—	—	2.7	—
2340	—	147-13	—	1.3	—

TABLE 5.1 — continued

LHS	Gliese	Giclas	Other Name	$m_{pg} - m_R$	Spectral Type and Reference
2341	—	—	—	1.7	—
2342	—	—	—	2.4	—
2343	—	—	—	1.8	—
2344	—	58-40	—	1.3	—
2345	—	—	—	1.5	—
2346	—	—	—	1.6	—
2347	—	—	—	2.7	M5 V (ad)
2348	—	45-33	—	1.1	M3.5 (af), M2 (bk)
2349	—	196-58	Ross 108	1.3	K7 (af)
2350	—	—	—	1.9	—
2351	—	—	—	3.2	M6.5 V (ad)
2352	—	—	—	3.0	sdM (bi)
2353	—	10-2	Wolf 362	1.3	M3.5 (af)
2354	412.2	—	CD -29°8875	0.6	G1-2 V (bf), G2 V (be)
2355	—	—	—	1.7	—
2356	—	163-52	—	1.7	—
2357	—	—	—	1.1	—
2358	413.1	—	CD -23°9765	1.5	M3 (af)
2359	—	254-16	—	1.5	—
2360	—	—	—	1.5	—

TABLE 5.1 — continued

LHS	Gliese	Giclas	Other Name	$m_{pg} - m_R$	Spectral Type and Reference
2361	—	10-3	Wolf 364	1.0	K2 (af)
2362	—	—	—	1.7	—
2363	—	176-15	—	1.9	—
2364	—	—	—	0.9	DC:9 (br), DC?9 (bc), DC9: (bn)
2365	—	10-4	Wolf 365	0.6	G2f (af)
2366	414 B	119-59	BD +31°2240 B	1.8	M2 (af), M2.5 V (bh)
2367	414 A	119-60	BD +31°2240 A	1.5	K7 (af), K9 V (am), M1 V (bh)
2368	414.1 A	122-2 A	—	1.6	M3 (af), M2 V (bh)
2369	414.1 B	122-2 B	—	1.7	M3 (af), M2 V (bh)
2370	416	—	BD -14°3277	1.2	K4 V (bf), K4 (af), M0.5 V (bh)
2371	—	—	—	1.7	—
2372	—	—	—	1.6	—
2373	—	119-64	BD +36°2165	0.4	F2 (af)
2374	—	45-39	Wolf 368	1.6	M3.5 (af)
2375	—	—	—	1.6	—
2376	—	—	—	1.3	—
2377	—	—	—	2.8	—
2378	421 C	—	—	1.6	M3.5 (af), M5 V (bq)
2379	421 A	—	BD -17°3336	1.4	K7 (af), M0.5 V (bh), M1 V (bq)
2380*	421 B	—	BD -17°3337	1.4	K7 (af), M0.5 V (bh), M1 V (bq)

TABLE 5.1 — continued

LHS	Gliese	Giclas	Other Name	$m_{pg} - m_R$	Spectral Type and Reference
2381	—	10-8	—	1.9	—
2382	—	119-65	—	1.3	M0 V (al)
2383	—	10-9	Wolf 373	1.3	M3 (af)
2384	—	—	—	1.3	M2: (af)
2385	—	—	—	1.5	M4 (af)
2386	—	—	—	1.1	M3: (af)
2387	—	120-30	BD +22°2340	0.9	G5 (af)
2388	—	10-10	BD -1°2505	1.7	K5 (af)
2389	—	56-29	—	1.8	M3 (af), G5 (ag)
2390*	423 A	—	ξ UMa A	0.7	G0 V (aj), G0 V (be), G0 V (am), G0 (af)
2391*	423 B	—	ξ UMa B	0.7	G5 V (aj), G0 V (be), G0 V (am)
2392	—	10-11	—	-0.3	DC5 (br), DC? (af)
2393	423.1	163-74	BD -4°3049	0.9	G8 V (am), K0 (af)
2394	—	120-32	—	1.5	M3.5 (af)
2395	—	—	—	2.7	—
2396	—	—	—	2.2	—
2397	—	—	—	3.3	M5 V (ad)
2397a	—	—	—	2.8	M8 V (bi), M8 V (ax)
2398	—	—	—	1.5	—
2399	—	—	—	1.9	—
2400	—	—	—	1.5	—

TABLE 5.1 — continued

LHS	Gliese	Giclas	Other Name	$m_{pg} - m_R$	Spectral Type and Reference
2401	—	—	—	1.8	M3 (af)
2402 A*	428 A	—	CD -60°3532 A	1.3	K7 V (av), K5-M0 V (bf)
2402 B*	428 B	—	CD -60°3532 B	—	M0 V (aw)
2403	—	176-34	—	1.7	—
2404	—	253-49	—	1.9	M3 (af)
2405	—	253-50	—	1.8	M2.5 (af)
2406	—	10-22	Wolf 391	1.1	M2 (af)
2407	429 A	—	BD +3°2502	1.1	K0 IV (be), K) IV (am), K0 (af)
2408	429 B	10-23	BD +3°2503	1.3	K2 V (am), K3 (af)
2409	—	56-41	Wolf 395	1.3	M0 (af)
2410	—	197-14	Ross 109	1.1	K0 (af)
2411	—	120-51	—	1.3	—
2412	429.2	—	—	1.1	M2 (af)
2413	—	197-15	Ross 110 A	1.5	M3.5 (af)
2414	—	197-16	Ross 110 B	1.5	M3.5 (af)
2415	—	56-44	Wolf 398	1.1	M3 (af), M2.5 (bk)
2416	—	—	—	1.9	—
2417	429.4	—	CD -56°3980	1.1	<M0 (bp)
2418	—	120-56	—	2.2	—
2419	—	—	—	3.0	sdM4.5 (ad)
2420	—	10-29	—	1.3	—

TABLE 5.1 — continued

LHS	Gliese	Giclas	Other Name	$m_{pg} - m_R$	Spectral Type and Reference
2421	—	—	—	1.3	—
2422	430.1	120-57	BD +23°2359	1.5	M0.5 (af), M1 V (bh)
2423	431	—	—	1.5	M3.5 (af), M4.5 (bq), M3 V (bw)
2424*	—	254-24	—	0.6	G0f (af)
2425	—	—	—	1.5	M5.5 V (ad), sdM (ac)
2426	—	122-30	—	1.1	K0 (af), K0 (bk)
2427	—	—	CD -23°10062	1.8	M1 (af)
2428	—	—	—	2.4	M4 V (ai)
2429	433	—	CD -31°9113	2.5	M2.5 V (bq), M2 (af)
2430	—	122-34	—	1.8	—
2431	—	120-61	—	1.5	K7 V (al), K3: (af)
2432	—	122-36	BD +40°2442	1.3	K5 (af)
2433	—	—	CD -47°7000	1.1	K4 (af), M1 (bp)
2434	—	10-39	Ross 910	1.1	K7 (af), K7: (bk)
2435	1147	—	—	1.1	M3.5 (af)
2436*	433.2 B	—	BB +45°1947 B	1.2	K2 V (am), K3 (af)
2437*	433.2 A	—	BD +45°1947 A	0.6	G0 V (be), G0 V (am), G0 (af)
2438	—	—	—	2.0	—
2439	—	254-27	—	1.3	—
2440	—	10-42	—	0.9	—

TABLE 5.1 — continued

LHS	Gliese	Giclas	Other Name	$m_{pg} - m_R$	Spectral Type and Reference
2441	435	—	CD -43°7228	1.2	K4-5 V (bf), K4 (af)
2442	—	56-50	—	1.8	—
2443	1148	122-40	Ross 1003	1.7	M3.5 (af), M5 (ag)
2444	—	—	—	1.6	sdK5-M1 (ai)
2445	—	—	—	1.5	sdM0 (ai)
2446	—	—	—	1.5	—
2447	438	—	CD -51°5974	1.1	—
2448	—	10-45	Ross 912	1.6	M3 (af)
2449	—	122-42	—	1.1	—
2450	—	121-12	BD +26°2251	0.5	F6 (af)
2451	—	121-14	Ross 907	1.3	K5 (af), K8 V (al)
2452	—	—	—	1.5	M3.5 V (ai)
2453	—	122-45	BD +48°1964	0.6	G2 (af), G2 V (am)
2454	—	—	—	1.5	—
2455	—	11-20	—	0.3	—
2456	—	—	CD -65°1143 A	1.5	<M0 (bp)
2457	—	—	CD -65°1143 B	1.5	<M0 (bp)
2458	—	122-46	—	1.7	—
2459	445	254-29	—	1.8	M3 (af), M4 V (bh), sdM4 (cb)
2460	—	—	—	1.1	—

TABLE 5.1 — continued

LHS	Gliese	Giclas	Other Name	$m_{pg} - m_R$	Spectral Type and Reference
2461	—	197-32	—	1.3	—
2462 A*	448 A	—	β Leo A	-0.1	A3 V (be), A3 V (am), A2 (af)
2462 B*	448 B	—	β Leo B	—	composite with LHS 2462 A
2463	—	10-53	—	0.9	—
2464	—	—	—	1.5	—
2465*	449	—	β Vir	0.5	F9 V (be), F8 V (am), F8 (af)
2466	—	—	—	1.8	—
2467	—	121-27	Ross 908	0.6	G7 (af)
2468	—	—	—	1.6	—
2469	—	—	—	1.5	—
2470	452 A	—	—	1.1	M4 V (bq), M3 (af)
2470a	452 B	—	—	0.4	—
2471	—	—	—	2.4	M6 V (ai), M6: V (ax), M6.5 V (ad)
2472	452.1	12-4	Ross 119	1.6	M3.5 (af)
2473	—	—	—	1.6	M3 (af)
2474	—	—	—	1.5	K3:: (af)
2475	—	11-31	Ross 129	1.7	M1.5 (af)
2476	—	—	—	1.6	—
2477	2086	—	—	1.3	M0 (af)
2478	—	—	—	0.2	DC9 (br), DC9 (bc)
2479	—	—	—	2.9	—
2480	—	—	—	1.6	M6 V (ai)

TABLE 5.1 — continued

LHS	Gliese	Giclas	Other Name	$m_{pg} - m_R$	Spectral Type and Reference
2481	—	148-23	—	1.5	—
2482	—	12-12	Ross 122	1.6	M2.5 (af)
2483	—	—	—	2.5	—
2484	—	—	vB 6	—	—
2485	—	—	CD -41°6879	0.9	K1 V (bf), K2 (af)
2486	—	197-38	—	1.5	—
2487	—	—	—	3.5	—
2488	—	237-38	—	1.5	—
2489	—	—	—	2.2	—
2490	—	—	—	1.9	—
2491	—	122-62	—	1.5	—
2492	—	—	—	1.6	—
2493	—	—	—	1.5	—
2494	454.1	11-34	Ross 920	1.1	K4 (af)
2495	—	121-43	Wolf 1426	1.7	K7 (af)
2496	—	—	—	1.6	sd (bb)
2497	455	121-45	—	1.8	M3 (af)
2498	—	122-66	BD +43°2182	1.1	G8 V (be), G9 IV-V (am)
2499	—	—	—	1.8	—
2500	—	—	—	3.3	sdM0.5-1: (ai), sd (bb)

TABLE 5.1 — continued

LHS	Gliese	Giclas	Other Name	$m_{pg} - m_R$	Spectral Type and Reference
2501	—	122-68	—	1.1	—
2502	—	—	—	3.8	M6+ V (ad)
2503	—	198-19	—	1.6	—
2504	—	—	—	1.6	—
2505*	—	—	—	1.1	K5 (af)
2506	—	—	—	1.8	M4.5 (af)
2507	—	11-36	BD +4°2568	0.7	G4 (af), G0 V (am)
2508	—	—	—	1.6	—
2509	2090	—	—	1.1	M0 (af)
2510	—	11-37	BD -0°2532	0.9	F8 IV-V (am)
2511	—	—	—	1.1	K1: (af)
2512	—	—	—	1.7	—
2513	—	254-35	—	1.5	—
2514	—	—	—	2.2	—
2515	456	11-40	Wolf 406	1.6	M2 V (bq), M0.5 (af), M2 V (bh)
2516	—	—	—	1.7	—
2517	—	—	—	1.6	—
2518	—	11.42	Wolf 1435	1.6	M3 (af)
2519	—	—	—	1.1	—
2520	—	—	—	1.6	—

TABLE 5.1 — continued

LHS	Gliese	Giclas	Other Name	$m_{pg} - m_R$	Spectral Type and Reference
2521	—	—	—	1.5	—
2522	—	197-47	—	0.4	DA9 (br)
2523	—	—	—	1.8	—
2524*	458.1	11-45	BD -2°3481	0.9	G4 V (am)
2525	—	—	—	1.5	—
2526	—	12-24	BD +11°2439	0.9	G3 V (am)
2527	—	12-25	Wolf 1438	1.1	M1.5 (af)
2528	—	—	—	1.1	K7: (af)
2529	—	121-68	—	1.5	—
2530	—	—	—	1.3	M3 (bp)
2531*	1154	13-22	—	1.7	—
2532	—	—	—	0.4	—
2533	—	—	—	2.2	—
2534	—	—	—	-0.2	—
2535	—	—	—	1.3	—
2536	—	237-54	—	1.5	—
2537	—	12-26	—	1.8	M3: (af)
2538	—	59-9	Wolf 1439	1.3	M2.5 (af)
2539	—	—	—	1.6	—
2540	—	—	—	1.3	—

TABLE 5.1 — continued

LHS	Gliese	Giclas	Other Name	$m_{pg} - m_R$	Spectral Type and Reference
2541	1155 A	13-26 A	—	1.7	sdM3 (ag)
2542	1155 B	13-26 B	—	0.2	DAs (ag)
2543	—	—	—	1.5	—
2544	459.3	121-77	BD +29°2279	1.6	M0.5 (af), M2 V (bh)
2545	—	—	—	>2.3	M6 V (ad)
2546	—	199-7	—	2.3	—
2547	—	12-35	—	1.6	—
2548	462	123-26	BD +42°2296	1.5	K5 (af), M3 (bk), M0.5 V (bh)
2549	—	59-14	Wolf 409	1.6	M0 (bk), M0 (af)
2550	—	—	—	1.1	K3:: (af)
2551	463	237-63	Ross 690	1.7	M3 (af), M4 V (cb)
2552	1157	—	—	1.1	M3.5 : (af)
2553	—	—	CD -66°1212	1.3	G8-K0 IV (be), G8-K0 IV (bf)
2554	—	—	—	1.6	—
2555	—	—	—	1.5	K7 (af)
2555a	—	—	—	2.7	—
2556	—	123-29	BD +39°2519	0.5	G0 V (am)
2557	—	—	—	2.1	M5 V (ai)
2558	—	—	CD -48°7414	0.6	K4: (af)
2559	—	—	—	0.9	DC9 (br), DC9 (bc)
2560	—	—	CD -48°7426	0.6	G3-5 V (bf), G3-5 V (be), G6 (af)

TABLE 5.1 — continued

LHS	Gliese	Giclas	Other Name	$m_{pg} - m_R$	Spectral Type and Reference
2561	—	—	—	1.3	—
2562	—	12-37	—	1.3	—
2563	—	—	—	1.5	—
2564	—	—	BD -16°3469	0.9	K3 (af), K2 V (bf)
2565	469	12-38	Wolf 414	1.5	M3.5 (af), M4 V (bh)
2566*	469.1	13-43	BD -2°3528	0.9	G7 V (am)
2567	—	13-44 A	—	1.5	M3.5 (af)
2568	—	13-44 B	—	1.5	M3.5: (af)
2569	—	—	—	1.5	—
2570	471	12-39	BD +9°2636	1.5	K7 (af), M1 V (bh)
2571	—	198-58	—	1.8	—
2572	—	—	—	1.5	—
2573	—	—	—	2.0	—
2574	—	199-24	—	1.6	—
2575	—	12-42	Wolf 422	1.5	M2 (af)
2576	—	237-68	—	1.3	—
2577	472	—	CD -68°1095	0.9	K1 V (bf)
2578	—	—	—	1.6	—
2579	475	—	β CVn	0.6	G0 V (ca), G0 V (be), G0 V (am), G0 (af)
2580	—	—	—	1.6	—

TABLE 5.1 — continued

LHS	Gliese	Giclas	Other Name	$m_{pg} - m_R$	Spectral Type and Reference
2581	—	—	—	1.5	—
2582	476	12-44	Wolf 427	1.7	M3 (af)
2583	—	—	—	1.7	M6 V (ad)
2584	—	199-31	—	1.3	—
2585	477	—	CD -45°7872	1.6	M1 (af)
2586	—	13-47	—	1.6	M3 (af)
2587	478	—	—	1.5	M1 V (bq)
2588	—	199-33	—	1.9	—
2589	—	—	—	1.5	M5.5 V (ai), M4 V (ad)
2590	—	—	—	1.3	—
2591	—	—	—	1.5	—
2592	—	—	—	1.5	—
2593	—	60-23	—	1.3	—
2594	2095	—	—	-0.2	DA6 (br)
2595	1162	13-51	—	1.8	M3 V: (al)
2596	—	—	—	0.1	DC8 (br), sdM0: (ai), DC8 (bn)
2597	—	—	—	1.9	—
2598	—	—	—	1.9	—
2599	—	—	—	1.6	—
2600	2096	—	CD -77°568	1.3	K5 V (bf)

TABLE 5.1 — continued

LHS	Gliese	Giclas	Other Name	$m_{pg} - m_R$	Spectral Type and Reference
2601	—	—	—	0.9	—
2602	—	—	—	1.5	M5.5 V (ai)
2603	—	—	—	1.3	—
2604	482 A	—	γ Vir A	0.6	F0 V (be), F0s (af)
2605	482 B	—	γ Vir B	0.6	F0 V (be), F0s (af)
2606	—	—	—	1.5	—
2607	—	—	—	1.1	—
2608	—	—	—	1.3	—
2609	—	—	—	1.3	sdM (ac)
2610	—	255-17	—	1.7	M4.5 V (ai)
2611	—	—	—	2.0	—
2612	—	164-12	—	1.3	—
2613	—	123-55	—	1.8	—
2614	—	164-13	—	1.5	—
2615	—	—	CD -37°8082	0.8	G5 V (bf)
2616	—	60-27	—	1.8	—
2617	—	199-35	—	1.3	M2.5 V (ai)
2618	—	—	—	1.9	—
2619	—	—	—	1.6	—
2620	—	—	Ross 704	1.1	K4 (af)

TABLE 5.1 — continued

LHS	Gliese	Giclas	Other Name	$m_{pg} - m_R$	Spectral Type and Reference
2621	—	—	—	0.1	—
2622	—	—	—	1.5	—
2623	—	—	—	2.2	—
2624	—	164-17	—	1.3	—
2625	—	—	—	1.3	—
2626	—	—	—	1.3	—
2627	—	—	—	1.3	—
2628	—	—	—	1.1	—
2629	—	—	—	2.8	—
2630	—	—	—	2.0	M5 V (ai)
2631	—	—	33 Vir	1.1	K1 III-IV (be), K1 IV (am), G9 (af)
2632	—	—	—	3.1	M7 V (bi)
2633	—	123-60	Ross 991	1.3	M2.5 (af)
2634	—	14-1	—	1.6	M3 (af)
2635	—	—	—	1.5	—
2636	—	60-33	Wolf 438	1.5	M3 (af)
2637	—	123-61	—	2.2	—
2638	—	14-4	—	1.7	—
2639	—	199-41	BD +62°1257	1.3	G1 (af), G1 V (am)
2640	—	199-42	—	1.6	—

TABLE 5.1 — continued

LHS	Gliese	Giclas	Other Name	$m_{pg} - m_R$	Spectral Type and Reference
2641	—	14-5	BD +2°2585	0.9	G8 V (am)
2641a	—	—	—	1.1	—
2642	—	—	BD -16°3543	1.3	K5 (af)
2643	—	—	—	2.5	M4.5 V (ad)
2644	—	—	CD -55°4825	0.6	—
2645	—	—	—	3.2	M7 V (bi)
2646	—	199-45	—	1.5	—
2647 A*	—	—	BD -17°3723 A	0.5	K7 V (bf), sdF7 (am), F9 (af)
2647 B*	—	—	BD -17°3723 B	—	composite with LHS 2647 A
2648	—	—	—	1.5	—
2649	—	237-81	—	1.2	—
2650	—	—	—	1.6	—
2651	—	177-4	—	1.7	—
2652	—	—	—	1.3	—
2653	—	—	—	1.5	K (af)
2654	—	123-74	—	1.1	—
2655	—	—	—	1.3	—
2656 A*	491 A	—	BD -9°3595 A	1.1	K0 V (am), K0 (af)
2656 B*	491 B	—	BD -9°3595 B	—	composite with LHS 2656 A
2657	—	—	—	2.5	—
2658	—	—	—	1.8	—
2659	—	199-51	—	1.5	—
2660	—	61-26	—	1.5	—

TABLE 5.1 — continued

LHS	Gliese	Giclas	Other Name	$m_{pg} - m_R$	Spectral Type and Reference
2661	492	60-54	Wolf 457	0.5	DC9 (br), DC9 (bn), DC (af)
2662	—	—	—	1.6	—
2663	493	14-19	BD -1°2754	1.3	K8 V (am), K5 (af), M0.5 V (bh)
2664*	493.1	60-55	Wolf 461	2.2	M4.5 (af), M5 V (bh)
2665*	494	60-57	BD +13°2618	1.8	M1.5 V (ag), M1 (af), M1.5 V (bh)
2666	—	123-82	—	0.9	—
2667	—	—	—	1.9	—
2668	—	—	—	1.5	M2 (bp)
2669	—	—	CD -26°9470	0.5	G1 V (bf), F9f (af)
2670	—	177-13	—	1.3	—
2671	—	—	—	2.1	—
2672	—	123-84	—	1.3	—
2673	—	—	—	1.1	DC:/DC9 (br), DC9 (bn)
2674	—	149-33	—	1.7	—
2674a	—	—	—	1.5	—
2675	—	—	—	2.2	—
2676	—	—	—	1.8	—
2677	—	237-88	—	1.3	—
2678	—	—	CD -40°7705	0.9	K0 V (bf), G9 (af)
2679	—	149-44	—	1.3	—
2680	—	61-33	—	2.2	M3 (af), G5 (ag)

TABLE 5.1 — continued

LHS	Gliese	Giclas	Other Name	$m_{pg} - m_R$	Spectral Type and Reference
2681	—	60-67	BD +6°2697	0.9	G5 IV (be), G5 IV (am)
2682	—	14-35	—	1.3	—
2683	—	—	—	1.1	M0 (af)
2684	—	199-60	—	1.3	—
2685	—	—	—	1.5	K3: (af)
2686	—	177-25	—	1.8	—
2687	—	238-26	BD +68°714	1.1	K2 V (am), K2 (af)
2688	—	—	—	1.5	—
2689	—	63-5	BD +10°2519 A	0.6	G1 V (am), G4 (af)
2690	—	63-6	BD +10°2519 B	1.6	M0 (af)
2691	—	—	—	1.5	—
2691a	—	—	—	1.9	—
2692	—	—	—	1.1	M1 (af)
2692a	—	—	—	1.3	—
2693*	—	63-9	BD +18°2700	0.6	F9 V (am)
2694	—	—	—	1.1	—
2695	1168	61-41	—	1.8	—
2696	—	—	—	0.9	—
2697	—	—	—	1.6	—
2698	—	—	—	1.6	M3.5 (af)
2699	—	62-18	—	1.6	—
2700	—	199-64	—	1.5	—

TABLE 5.1 — continued

LHS	Gliese	Giclas	Other Name	$m_{pg} - m_R$	Spectral Type and Reference
2701	—	14-39	—	0.9	K3 (af)
2702	—	177-27	—	1.8	—
2703	—	164-53	—	1.8	—
2704	—	—	—	1.5	—
2705	—	61-44	—	1.7	—
2706	—	—	—	1.5	—
2707	—	—	—	1.5	—
2708*	—	164-55	—	0.9	K3 (bk)
2709	—	14-42	—	1.6	—
2710	—	—	—	0.6	DC9 (br), DC9 (bc)
2711	1169	149-70	—	1.5	M3.5 V (al)
2712	—	—	—	0.4	—
2713	505 A	63-18 A	BD +17°2611 A	1.2	K1 V (be), K2 V (am), K3 (af)
2714	505 B	63-18 B	BD +17°2611 B	1.5	M1 V (be), M1.5 V (bh), M0 (af)
2715	506.1	14-45	Ross 484	1.3	K3 (af), K8.5 V (bq)
2716	507 A	164-64	BD +35°2436 A	1.8	M0 (af), M1.5 V (bh)
2717	507 B	164-65	BD +35°2436 B	1.9	M3 (af), M3.5 V (bh)
2718	—	—	—	1.5	M3.5 (af)
2719	—	—	—	1.7	M6: V (ai)
2720	—	—	—	1.3	—

TABLE 5.1 — continued

LHS	Gliese	Giclas	Other Name	$m_{pg} - m_R$	Spectral Type and Reference
2721	—	—	—	1.5	—
2722	—	62-33	BD +4°2729	1.3	K2 V (am), K2 (af)
2723	—	—	—	2.4	—
2724	508.2	164-68	BD +35°2439	1.7	M1 V (ag), M1 V (bh), M2 (af)
2725	—	62-34	—	1.7	—
2726	—	—	CD -38°8457	0.4	F/Gw[A] (bf), F4 (af)
2727	—	238-35	—	1.5	—
2728 A*	509 A	164-71 A	BD +29°2405 A	1.5	K7 (af), M0 V (bh)
2728 B*	509 B	164-71 B	BD +29°2405 B	—	M0.5 V (bh)
2729	—	—	—	2.5	—
2730	—	—	—	1.5	—
2731	508.3	—	Wolf 482	1.3	K7 (af)
2732	—	—	—	2.3	—
2733	—	149-88	—	1.3	—
2734	—	—	—	1.9	—
2735	—	164-73	Ross 1011	1.1	K5 (af), K7 (bk)
2736	—	—	—	1.8	—
2737	—	—	—	-0.2	DA4 (br)
2738	—	—	—	1.6	—
2739	—	—	—	1.8	M4 (af)
2740	521.1	—	70 Vir	0.9	G2.5 Va (be), G3 (af), G5 V (am)

TABLE 5.1 — continued

LHS	Gliese	Giclas	Other Name	$m_{pg} - m_R$	Spectral Type and Reference
2741	—	14-56	—	1.9	—
2742	—	—	—	2.3	M6 V (ad)
2743	—	—	—	1.5	—
2744	—	—	—	1.3	—
2745	—	165-7	—	0.2	DZ7 (br)
2746	—	—	—	2.1	—
2747*	—	62-44	BD -1°2832	1.0	G9 V (am)
2748	—	238-39	—	1.5	—
2749	—	150-9	Ross 1020b	1.5	K3 (af)
2750	—	—	CD -42°8521	1.1	G0: (af)
2751	—	199-72	—	1.5	—
2752	—	238-42	—	1.5	—
2753	—	—	—	1.3	—
2754	2102	62-49	BD +9°2776	1.1	—
2755	—	—	—	3.0	—
2756	—	—	—	1.3	—
2757	—	—	—	1.5	M2-3 (bp)
2758	—	—	—	2.8	—
2759	—	—	CD -26°9804	1.1	K2 V (bf), K3 (af)
2760	—	—	CD -38°8635	0.6	G3 V (bf)

TABLE 5.1 — continued

LHS	Gliese	Giclas	Other Name	$m_{pg} - m_R$	Spectral Type and Reference
2761	—	150-15	—	1.3	—
2762	—	177-44	BD +47°2072	1.2	K3 (af)
2763	—	165-17	—	1.5	—
2764	—	—	—	2.3	—
2765	—	63-40	—	0.9	—
2766	518.1	62-54	BD +8°2735	0.9	M0 (ag), K4 (af)
2767	—	63-43	—	1.7	—
2768	—	—	—	1.7	—
2769	—	—	—	-0.2	DA6 (br)
2770	—	64-7	—	1.7	—
2771	—	150-25	Ross 1022	1.1	M3 (af)
2772	—	177-48	—	1.8	—
2773	521.1	62-60	BD -3°3508	1.4	K7 (af), M1 V (bh)
2774	—	63-45	—	1.8	—
2775	—	—	—	1.8	—
2776	—	—	—	2.1	M5 V (ai)
2777	—	177-52	—	1.6	—
2778	—	177-53	—	1.3	—
2779	—	—	—	1.5	—
2780	—	—	—	0.9	K0 (af)

TABLE 5.1 — continued

LHS	Gliese	Giclas	Other Name	$m_{pg} - m_R$	Spectral Type and Reference
2781	—	—	—	-0.1	—
2782	—	—	—	1.3	—
2783	—	—	—	1.7	—
2784	—	165-25	Ross 1015	1.7	M3 (af)
2785	—	177-57	—	1.3	—
2787	—	62-66	BD +5°2791	1.3	K7 (af), M2 (bk)
2788	—	223-22	—	1.5	—
2789	—	177-58	Ross 492	1.5	—
2790	—	—	—	2.2	—
2791	—	165-29	Ross 1018	1.3	—
2792	—	150-34	—	1.1	\geq M3: (al)
2793	—	—	—	1.5	sdM1: (ai)
2794	—	—	—	1.5	M3.5 (af)
2795	—	150-36	—	1.5	—
2796	—	—	—	1.7	—
2797	—	—	—	2.2	—
2798	—	—	BD +7°2690	0.6	G0-1 IV-V (be), G0 V (am), G2 (af)
2799	—	64-24	BD -5°3763	1.4	K4 (af)
2800	1178	63-54	—	0.2	DA7/DA6 (br), DA7 (bn), DA/F (ag)

TABLE 5.1 — continued

LHS	Gliese	Giclas	Other Name	$m_{pg} - m_R$	Spectral Type and Reference
2801	—	65-2	BD +7°2692	1.5	K4 (af), M0 V (bh)
2802	—	—	—	1.3	—
2803	—	—	—	1.7	M4.5: V (ai)
2804	—	64-26	—	1.6	—
2805	—	—	—	1.5	—
2806	—	—	CD -35°9019 B	1.5	K4: (af)
2807	—	—	CD -35°9019 A	0.7	G3 IV-V (be), G0 V (bf), F9 (af)
2808	—	—	—	0.5	DC9 (br), DC9 (bc)
2809	—	63-60	—	1.8	—
2810	—	—	—	2.7	—
2811	—	—	—	1.7	M3.5-4: V (ai)
2812	—	—	—	1.5	—
2813	—	—	—	1.5	—
2814	530	—	CD -23°11329	0.9	G5 V (bf), G5 V (be)
2815	—	—	CD -56°5169	0.6	G5wF8 V (bf)
2816	—	—	—	1.5	—
2817	531	—	CD -50°8092	0.9	K3 V (bf)
2818	—	—	—	1.5	—
2819	—	238-55	—	1.5	—
2820	533.1	238-54	—	1.6	M1.5 (af)

TABLE 5.1 — continued

LHS	Gliese	Giclas	Other Name	$m_{pg} - m_R$	Spectral Type and Reference
2821	533	65-12	BD +13°2721	1.5	M0 (af), M0 V (bh)
2822	—	—	—	1.8	M1 (af)
2823	—	—	—	1.5	—
2824	—	223-35	—	1.1	—
2825	—	—	—	2.6	—
2826	—	—	—	2.7	M4.5 V (bi)
2827	—	223-38	—	1.5	—
2828	—	—	—	2.3	M5.5 V (ai), M5.5 V (ax)
2829	—	—	—	1.1	—
2830	—	65-19	Ross 837	1.1	M3 (af)
2831	—	—	—	1.1	—
2832	—	64-29	—	1.3	—
2833	—	165-38	—	1.5	—
2834	534.3	—	CD -33°9467	0.9	G5 V (bf)
2835	—	64-31	—	1.3	—
2836	—	—	—	2.3	K2: (af)
2837	—	150-54	Ross 494	1.1	K5 (af)
2838	—	—	—	1.5	—
2839	—	200-14	vB 7	2.0	—
2840	—	200-15	Ross 1027	1.6	K4 (af)

TABLE 5.1 — continued

LHS	Gliese	Giclas	Other Name	$m_{pg} - m_R$	Spectral Type and Reference
2841	—	—	BD -31°10833	2.7	K7 (af)
2842	536	64-35	BD -1°2892	1.3	M1 (af)
2843	—	—	—	1.6	sdK5-M0 (ai)
2844	—	135-10	—	1.7	—
2845*	—	165-40	—	1.1	M1: (bk)
2846	—	65-22	Ross 838	0.6	G5 (af)
2847	—	—	—	2.6	M5.5: V (ai), M5 V (ad)
2848	—	—	—	1.5	M3.5 (af)
2849	537 A	200-16 A	BD +47°2112 A	1.6	M1 (af), M2 V (bh), M3 V (cb)
2850	537 B	200-16 B	BD +47°2112 B	1.6	M1 (af), M2.5 V (bh)
2851	—	—	—	0.9	—
2852	—	—	—	2.7	M0.5 (af)
2853	—	135-13	Wolf 530	1.3	M3.5 : (af)
2854	—	—	—	1.3	—
2855	—	—	—	2.6	M6 V (ad)
2856	—	—	—	0.9	DC (br)
2857	—	64-42	—	1.3	—
2858	539	—	θ Cen	1.2	K0 IIIb (bf), K0 IIIb (be), G9 III (af)
2859	—	—	—	3.1	—
2860	—	—	—	1.5	—

TABLE 5.1 — continued

LHS	Gliese	Giclas	Other Name	$m_{pg} - m_R$	Spectral Type and Reference
2861	—	165-48	—	1.3	—
2862	—	—	—	1.6	—
2863	—	64-47	—	2.4	—
2864	—	223-43	—	1.5	—
2865	540	255-51	BD +81°465	1.5	M1 (af), M0.5 V (bh)
2866	—	255-49	—	1.6	M1 (af)
2867	—	—	—	2.2	—
2868	—	255-50	—	1.5	—
2869	—	64-48	Ross 800	1.6	K5 (af), K5: (bk)
2870	539.2	—	CD -30°11195	2.1	M0 (af)
2871	—	—	CD -60°5077	0.9	G8 [V] (bf)
2872	—	—	BD -13°3834	1.6	G0: (af)
2873	—	65-33	—	1.1	—
2874	—	—	—	1.1	—
2875	—	64-52	—	1.8	M2-3: (al), M3.5 (af)
2876	—	—	—	>1.6	M6.5 V (ad)
2877	—	—	—	1.3	—
2878	—	65-35	—	1.8	—
2879	—	—	—	1.6	M3.5 (af)
2880	540.2	—	Ross 845	1.5	M4: (af), M5 V (bh)

TABLE 5.1 — continued

LHS	Gliese	Giclas	Other Name	$m_{pg} - m_R$	Spectral Type and Reference
2881	—	—	—	1.5	M1: (bp)
2882	—	200-24	—	1.8	—
2883*	—	64-60	—	1.3	K4: (af), sd (ab)
2884	—	178-10	Ross 992	1.5	M2.5 (af)
2885	—	—	—	1.6	—
2886	—	165-60	—	1.3	—
2887	—	165-61	—	2.5	M4.5 V (bi), M (by)
2888	—	135-35	—	1.3	—
2889	—	200-29	—	2.4	—
2890	—	165-62	—	1.6	—
2891 A*	542.1 A	—	CD -25°10271 A	0.5	F5 V (be), F7wF3 V (bf)
2891 B*	542.1 B	—	CD -25°10271 B	—	composite with LHS 2891 A
2892	542	—	CD -58°5564	1.1	K3 V (be), K3 V (bf)
2893	—	—	—	3.3	M1.5 (ai), sd (bb)
2894	544 A	124-24 A	BD -4°3665 A	1.1	K1 V (am), K1 (af)
2895	544 B	124-24 B	BD -4°3665 B	1.5	M4 (af), M6 V (cb)
2896	—	—	—	1.7	—
2897	—	200-31	—	1.9	—
2898	—	200-32	—	2.1	—
2899	—	124-27	—	1.9	M3 (af)
2900	545.1	—	CD -39°8857	1.1	K3-4 V (bf), K3 (af)

TABLE 5.1 — continued

LHS	Gliese	Giclas	Other Name	$m_{pg} - m_R$	Spectral Type and Reference
2901	—	178-18	—	1.2	—
2902	—	178-19	—	1.2	M1: V (ai)
2903	546	166-22	BD +30°2512	1.7	K8 V (am), K7 (af), M0.5 V (bh)
2904	—	124-29	Ross 849	1.1	K5 (af)
2905	—	135-44	—	1.3	K4 (af), K4 (ag)
2906	—	—	—	2.3	—
2907	547	65-47	BD +1°2920	0.8	G1 V (be), G1 V (am), G5 (af)
2908	—	135-47	—	1.3	M3 V (al), M1.5 (af)
2909	—	—	—	2.0	—
2910	—	—	—	1.5	—
2911	—	—	—	1.7	—
2912	—	—	—	1.6	—
2913	—	65-49	—	1.6	—
2914	549 C	200-38	Hubble 10	1.1	K1 (af)
2915	—	166-25	BD +21°2649	0.6	G0 (af), F9 V (am)
2916	—	—	—	2.1	—
2917	—	—	—	>2.0	—
2918	550.1	166-29	BD +24°2735	1.5	K4 (af), M0 V (cb), M0 V (bh)
2919	—	—	—	2.1	—
2920	—	—	—	1.5	—

TABLE 5.1 — continued

LHS	Gliese	Giclas	Other Name	$m_{pg} - m_R$	Spectral Type and Reference
2921	—	—	—	1.6	M5.5: V (ai), M5.5: V (ax)
2922	—	255-52	—	1.5	—
2923	—	—	—	1.6	—
2924	—	—	—	3.0	M9 V (bi), M9 V (ax), M9 V (ai)
2925	—	166-33	—	1.7	—
2926	—	—	CD -46°9361	1.1	K5-M0 V (bf), K5 (af), <M0 (bp)
2927	—	—	—	1.5	—
2928	—	—	—	2.1	—
2929	—	224-9	—	1.5	—
2930	—	—	—	1.7	M6.5 V (bi), M6.5 V (ai), M6.5 V (ax)
2931	554	178-31	BD +36°2500	1.1	K4 (af)
2932	553.1	—	Wolf 1478	1.7	M4 V (bq), M3 (af), M4 V (cb)
2933	—	—	CD -26°10340	0.8	G6-8 V (bf), G9 (af)
2934	—	—	—	1.6	—
2935	—	—	—	1.5	—
2936	—	200-46	—	2.2	—
2937	—	135-61	—	2.0	—
2938	—	—	CD -27°9894	0.9	K7 (af)
2939	—	—	—	2.1	—
2940	—	124-51	BD -9°3964	1.3	K4 (af)

TABLE 5.1 — continued

LHS	Gliese	Giclas	Other Name	$m_{pg} - m_R$	Spectral Type and Reference
2941	—	66-5	BD +10°2703 A	1.1	K3 (af), K2 V (am)
2942	—	66-6	BD +10°2703 B	1.5	M3: (af)
2943	—	178-37	—	1.5	—
2944	—	66-7	—	1.3	K5 (bk)
2945	555	—	BD -11°3759	2.0	M4.5 V (bq), M3 (af), M4 V (cb)
2946	—	239-21	—	1.3	—
2947	—	166-36	—	2.0	—
2948	558	166-38	BD +34°2541	1.5	K4 (af), M0.5 V (bh)
2949	—	66-10	—	1.6	—
2950	—	—	—	2.6	sd (bb)
2951	—	—	—	0.9	DC9 (br), DC9 (bc)
2952	—	223-74	—	1.5	—
2953	—	—	BD -11°3770	0.6	F5 V (be), F6 IV-V (am)
2954	—	—	—	1.3	—
2955	—	—	—	1.5	—
2956	—	66-18	Wolf 536	1.1	K3: (af)
2957	—	124-57	—	1.8	M1 (af)
2958	—	—	—	1.5	—
2959	—	201-7	—	2.1	—
2960	—	—	—	1.7	—

TABLE 5.1 — continued

LHS	Gliese	Giclas	Other Name	$m_{pg} - m_R$	Spectral Type and Reference
2961	—	—	CD -56°5542	0.9	G5-6 V (bf)
2962	—	166-40	Ross 51	1.2	K5 (af)
2963	—	178-44	Ross 993	1.2	K3 (af)
2964	—	—	—	1.5	sdM0 (ai)
2965	—	66-21	Wolf 537	1.3	M3: (af)
2966	—	—	—	0.9	—
2967	—	—	—	1.3	K5-M0 V (ai)
2968	—	66-22	BD +6°2932	0.6	G3: (af)
2969	—	—	—	0.6	G5 (af), dK (bo)
2970	—	—	CD -49°9033	1.1	K3 (af), K3 V (bf)
2971	—	—	—	1.5	—
2972	—	—	—	1.5	—
2973	—	200-58	—	1.8	—
2974	562	136-13	BD +17°2785	1.4	K7 (af), M0 V (bh)
2975	—	—	—	0.6	sdK (ab)
2976	—	239-29	—	1.5	—
2977	—	136-14	Ross 994	1.5	M0.5 (af)
2978	563	—	Ross 499	1.5	M0 (af), M2 V (bq)
2979	1185	124-72	—	1.9	M3 (af)
2980	—	—	—	3.3	M6.5 V (bi)

TABLE 5.1 — continued

LHS	Gliese	Giclas	Other Name	$m_{pg} - m_R$	Spectral Type and Reference
2981	—	—	—	2.1	—
2982	—	124-76	—	1.1	—
2983	563.3	66-31	BD +7°2850	1.3	K3 (af)
2984	—	66-32	—	-0.3	DA4 (br), DA (af)
2985	—	124-81	Wolf 553	1.9	M3.5 (af)
2986	—	—	—	1.5	—
2987	—	—	—	1.5	—
2988	—	—	—	1.1	M3 (af)
2989*	—	—	—	2.4	—
2990	—	200-59	—	1.7	—
2991	—	239-32	BD +72°659	1.3	K4 (af)
2992	—	—	—	1.5	—
2993	—	151-6	—	1.5	K2 (af)
2994	—	—	Ross 501	1.6	M0: (af)
2995	1186	136-27	—	1.5	—
2996	—	166-52	BD +23°2751	1.2	K3 (af), K3 V (am)
2997 A*	568 A	166-53 A	Ross 52 A	1.8	M3.5 (af), M5 V (cb)
2997 B*	568 B	166-53 B	Ross 52 B	—	composite with LHS 2997 A
2998	—	178-55	Ross 1041	1.6	M3.5 (af)
2999	—	66-41	Ross 1028b	1.1	M0.5 (af), M1 (bk)
3000	—	—	—	2.3	—

TABLE 5.1 — continued

LHS	Gliese	Giclas	Other Name	$m_{pg} - m_R$	Spectral Type and Reference
3001	—	—	—	1.9	M5 V (ai), M5 V (ax), M5 V (ad)
3002	—	—	—	3.5	M7 V (ai), M7: V (ax), M7 V (ad)
3003	—	—	—	3.4	M6.5 V (ad)
3004	—	—	—	1.5	—
3005	—	136-39	—	1.8	—
3006	1187	201-27	—	1.7	—
3007	—	166-58	—	-0.1	DA6 (br)
3008*	—	—	BD -21°4009	0.3	sdF7 (am), F5-6 V (bf)
3009	—	224-39	—	1.5	—
3010	—	—	—	1.8	—
3011	—	136-47	—	1.4	—
3012	—	15-1	Ross 1030a	1.3	M3.5 (af)
3013	—	—	—	1.6	—
3014	—	—	—	1.5	—
3015	—	167-12	—	1.1	—
3015a	—	151-20	—	1.8	—
3016	—	179-9	—	1.8	—
3017	—	256-20	—	1.5	—
3018	—	224-44	Ross 1051	1.5	M2 (af), M0 (bk)
3019	—	—	—	1.5	—
3020*	576	15-5	BD +16°2986	1.3	K5 (af), M0 V (bh)

TABLE 5.1 — continued

LHS	Gliese	Giclas	Other Name	$m_{pg} - m_R$	Spectral Type and Reference
3021	—	—	—	0.9	M5 V (bc)
3022	—	—	—	2.1	—
3023	—	—	—	1.3	—
3024	—	66-65	BD +9°3001	0.6	F9 V (am), F9 (af)
3025	—	—	—	1.3	—
3026	1189	167-22	BD +24°2824	1.5	—
3027	—	136-69	—	1.9	—
3028	—	—	—	1.4	—
3029	—	—	—	1.3	K5 (af)
3030	—	15-9	Ross 1047	1.7	M3 (af)
3031	—	201-37	—	1.7	—
3032	—	—	—	1.9	—
3033	—	136-76	—	2.2	>M5 V (al)
3034	2111	15-13	Ross 1038	0.6	G3 (af), G2: (ag)
3035	—	179-20	—	2.1	—
3036	—	136-77	BD +19°2939 A	0.9	G5 V (be), G5 V (am)
3037	—	136-78	BD +19°2939 B	0.9	G7 V (am)
3038	—	—	CP -21°5912	0.6	K3 (af)
3039	1190	15-15	BD -3°3746	1.5	K4 (af), M0 V (bh)
3040	—	—	—	1.5	—

TABLE 5.1 — continued

LHS	Gliese	Giclas	Other Name	$m_{pg} - m_R$	Spectral Type and Reference
3041	—	—	—	1.1	M5 V (bc)
3042	—	—	—	2.6	—
3043	—	—	—	2.0	—
3044	—	224-57	—	1.7	—
3045	—	—	—	1.4	K5 (af)
3046	—	136-85	—	1.9	—
3047	—	—	—	1.5	—
3048	—	—	—	1.3	—
3049	—	151-41	—	2.2	—
3050	—	—	—	1.5	—
3051	—	179-25	—	1.8	—
3052	—	167-32	—	1.3	—
3053	—	—	BD -18°4031	1.6	K5p (af)
3054	—	167-33 A	BD +26°2677 A	0.7	G9 (af), G8 V (am)
3055	—	167-33 B	BD +26°2677 B	—	composite with LHS 3054
3056	—	151-45	—	1.3	M3 (af)
3057	—	239-48	—	1.5	—
3058	—	167-34	—	1.6	—
3059	—	—	5 Ser A	0.5	F8 III-IV (be), F8 IV-V (am), F8 (af)
3060	—	—	5 Ser B	1.3	K4 (af), M0.5 V (bh)

TABLE 5.1 — continued

LHS	Gliese	Giclas	Other Name	$m_{pg} - m_R$	Spectral Type and Reference
3061	—	—	—	>2.2	—
3062	—	151-49	Wolf 563	1.3	K5 (af)
3063	—	—	—	1.5	—
3064*	2112	—	—	1.8	M3: (af)
3065	—	—	—	1.5	—
3066	—	—	—	1.7	—
3067	1192	15-20	BD +1°3071	1.3	K3 V (am), K3 (af)
3068	—	136-102	—	1.9	—
3069	—	201-48	—	1.3	—
3070	—	15-21	—	1.3	—
3071	—	—	CD -26°10870	1.1	K3-4 V (bf), K3 (af)
3072	—	—	—	1.5	—
3073	—	137-8	Ross 510	1.4	K5 (af)
3074	—	—	—	1.5	M2-3 (bp)
3075	—	179-33	—	1.6	—
3076*	—	152-31	—	1.8	—
3077	—	152-32	—	2.0	—
3078	—	15-25	—	1.1	—
3079	—	—	—	1.3	M3.5 (af)
3080	—	167-47	—	1.8	—

TABLE 5.1 — continued

LHS	Gliese	Giclas	Other Name	$m_{pg} - m_R$	Spectral Type and Reference
3081	—	—	—	1.3	—
3082	—	201-55	—	1.3	—
3083	1193	137-22	Ross 512	1.7	M3.5 (af)
3084	—	15-26	—	1.6	—
3085	—	—	—	1.5	—
3086	—	152-37	—	2.3	—
3087	—	—	—	1.5	M5 V (bc)
3088	—	—	—	0.9	DC?9 (br), DC?9 (bc)
3089	—	224-74	—	1.5	—
3090	—	—	—	1.5	—
3091	—	167-51	—	1.3	—
3092	590	—	—	1.1	M4 (af)
3093	592	152-40	Ross 802	1.5	M4 (af)
3094	—	—	—	1.1	—
3095	—	—	—	1.6	—
3096	—	—	—	2.3	—
3097	—	—	—	1.3	K4 (af)
3098	—	—	—	1.3	—
3099	—	—	—	2.5	sd (bb)
3100	—	—	—	1.5	—

TABLE 5.1 — continued

LHS	Gliese	Giclas	Other Name	$m_{pg} - m_R$	Spectral Type and Reference
3101	—	137-35	—	1.1	—
3102	—	—	—	1.4	—
3103	—	239-58	—	1.5	M2.5 V (ai)
3104	—	—	—	2.7	—
3105	—	224-79	—	1.5	—
3106	—	—	—	3.4	M6 V (ad)
3107	—	—	—	1.7	—
3108	—	—	—	1.5	—
3109	—	—	—	1.5	—
3110	—	152-46	Ross 804	1.1	K5 (af)
3111	—	—	—	2.9	—
3112	—	—	—	1.3	—
3113	—	—	—	1.1	—
3114	—	—	CD -46°10351	1.5	M0 (af)
3115	—	152-49	BD -13°4246	1.4	K1 (af)
3116	—	—	—	2.2	—
3117	—	152-50	—	1.3	—
3118	—	—	—	1.7	—
3119	—	—	—	1.5	M2-3 (bp)
3120	—	—	—	1.3	—

TABLE 5.1 — continued

LHS	Gliese	Giclas	Other Name	$m_{pg} - m_R$	Spectral Type and Reference
3121	—	—	—	2.8	—
3122	—	179-57	—	2.0	—
3123	—	16-11	—	1.6	—
3124	—	168-14	—	1.3	—
3125	—	—	—	1.7	—
3126	—	—	—	2.5	—
3127	602	—	χ Her	0.5	F8 V (be), F9 V (am), G0 (af)
3128	—	137-60	—	1.5	—
3129	—	180-8	Ross 806	1.5	M3 (af), M2 (bk)
3130	—	180-9	—	2.3	—
3131	—	—	39 Ser	0.6	G0 IV (be), G2 V (am)
3132	—	—	—	2.3	—
3133	—	—	—	1.6	sdM0-1 (ai), sdM (ac)
3134	—	—	—	1.7	M2-3 V (ai)
3135	—	—	—	1.5	—
3136	—	137-71	—	1.8	—
3137	—	180-17	—	1.8	—
3138	—	168-20	BD +28°2503	1.1	K0 V (am)
3139	—	225-40	—	1.5	M1.5-2 V (ai)
3140	—	—	—	1.6	—

TABLE 5.1 — continued

LHS	Gliese	Giclas	Other Name	$m_{pg} - m_R$	Spectral Type and Reference
3141	—	—	—	1.9	—
3142	—	137-74	—	1.6	—
3143	—	—	49 Lib	0.6	F7 V (bf), F8 V (be), F8 V (am)
3144	—	—	—	1.5	M3: (af)
3145	606.2	—	ρ CrB	0.6	G2 V (be), G2 V (am), G1 (af)
3146	—	180-23	Ross 808	0.1	DAV5/DA4 (br), vDA (af)
3147	—	—	—	1.5	—
3148*	609.2	—	BD +25°3020	0.8	G8 V (be), G8 V (am), G8 (af)
3149	—	—	—	1.9	M4.5: V (ai)
3150	611 B	180-27	BD +39°2947 B	2.1	—
3151	—	—	—	0.6	DC9 (br)
3152	611 A	—	BD +39°2947 A	0.9	G8 V (be), G8 V (am), K0: (af)
3153	612	180-31	BD +39°2950	1.2	K3 V (am), K3 (af)
3154	—	—	—	2.1	—
3155	612.1	180-33	BD +35°2774	1.3	K5 (af), M0 V (bh)
3156 A*	611.3 A	16-29 A	—	2.0	M3 V (ag), M3 V (bh)
3156 B*	611.3 B	16-29 B	—	—	composite with LHS 3156 A
3157	—	—	—	1.1	—
3158	1197	168-32	—	1.7	—
3159	—	—	—	1.5	—
3160	—	—	—	1.5	—

TABLE 5.1 — continued

LHS	Gliese	Giclas	Other Name	$m_{pg} - m_R$	Spectral Type and Reference
3161	—	16-32	BD +6°3169	1.1	K0 IV (be), K0 IV (am), G8 (af)
3162	—	—	—	1.5	—
3163	1199	138-8	—	-0.3	DA6 (br)
3164	—	16-34	—	1.3	K3 (af)
3165	—	—	—	—	—
3166	—	202-32	Ross 522	1.6	M0.5 (af)
3167	—	—	—	1.3	—
3168	—	—	—	2.7	—
3169	—	—	—	0.6	M3.5 (af)
3170	—	—	—	3.1	—
3171	616	—	18 Sco	0.6	G2 Va (be), G1 V (am), G3 (af)
3172 A*	—	17-8 A	BD +7°3125 A	1.4	K4 (af), K4 V (am)
3172 B*	—	17-8 B	BD +7°3125 B	—	K4 (af)
3173	—	—	—	1.8	—
3174	—	—	—	1.1	dM (ba)
3175	617 A	225-57	BD +67°935 A	1.3	M0 V (am), K7 (af), M0 V (bh)
3176	617 B	225-58	BD +67°935 B	1.6	M2.5 (af)
3177	—	—	—	1.1	—
3178	—	—	—	2.7	—
3179	—	—	—	1.8	—
3180	—	—	—	1.5	—

TABLE 5.1 — continued

LHS	Gliese	Giclas	Other Name	$m_{pg} - m_R$	Spectral Type and Reference
3181	—	—	—	2.0	—
3182	—	—	CD -47°10664	0.6	K2 V (bf), K2 (af)
3183	—	—	Ross 528	1.4	K4 (af)
3184	—	—	CD -70°1402	0.6	—
3185	618.4	—	—	1.7	M3 (af)
3186	620	—	CD -24°12677	1.6	M2 V (bq), M2 (bp), M1 (af)
3187	—	—	—	1.5	—
3188	620.2	—	—	1.5	M1-2 (bp), K5 (af)
3189	—	—	—	1.7	M5.5 V (ad)
3190	—	—	—	2.1	—
3191	622	—	BD -21°4352	1.3	M1.5 (bp), K5 (af)
3192	—	169-6	—	2.1	—
3193	—	169-7	—	1.3	—
3194	—	17-14	BD +2°3101	1.1	K2 (af)
3195	—	—	—	1.5	—
3196	—	—	—	1.9	M4.5 V (ai)
3197	—	—	—	2.6	—
3198	—	—	—	1.5	—
3199*	—	180-58	—	0.9	G5 (af)
3200	626.2	180-57	Ross 640	0.3	DZA6 (br), DF (af), DZA5+ (ba)

TABLE 5.1 — continued

LHS	Gliese	Giclas	Other Name	$m_{pg} - m_R$	Spectral Type and Reference
3201	—	180-56	—	1.3	—
3202	—	17-19	BD +3°3203	1.1	—
3203	627 A	138-34 A	BD +18°3182 A	1.2	K3 V (be), K2 V (am), K1 (af)
3204	627 B	138-34 B	BD +18°3182 B	1.2	K3 V (be)
3205	2121	153-57	—	1.1	M3 (af)
3206	—	—	—	1.3	K0:: (af)
3207	—	153-59	—	1.3	sdM1: (ai)
3208	—	226-9	—	1.3	—
3209	629	—	CD -38°11019	1.0	K0 V (bf), K1 (af)
3210	1202	138-37	—	1.3	—
3211	—	—	—	1.7	—
3212	—	225-65	—	1.5	—
3213	1203	138-39	—	1.1	—
3214	—	202-61	—	1.1	—
3215*	629.2 A	17-25	BD -3°3968 A	0.9	G5 V (am), K1 (af)
3216	—	—	—	1.5	M2 (bp)
3217	—	—	—	1.5	—
3218	—	—	—	1.7	—
3219	629.2 B	17-27	BD -3°3968 B	1.1	—
3220	—	—	—	0.9	—

TABLE 5.1 — continued

LHS	Gliese	Giclas	Other Name	$m_{pg} - m_R$	Spectral Type and Reference
3221	1204	138-43	—	1.5	—
3222	—	—	BD -14°4454	1.1	K3 (af)
3223	629.3	—	—	1.1	M1: (af), M1-2 (bp)
3224	631	—	12 Oph	1.1	K2 V (be), K2 V (am), K0 (af)
3225	—	138-44	—	1.1	—
3226	632.1	169-20	BD +31°2875	1.3	K4 (af)
3227	—	—	—	1.8	—
3228	—	—	CD -40°10550	1.1	K3 V (bf), K1 (af)
3229	—	—	—	1.9	—
3230	—	138-49	—	0.2	DA6 (br)
3231	—	—	—	-0.4	DC9 (br)
3232	—	—	—	1.5	—
3233	633	—	—	0.6	M3 (af)
3234 A*	635 A	—	ζ Her A	0.6	G0 IV (be), G0 IV (am), G0 (af)
3234 B*	635 B	—	ζ Her B	—	—
3235	634	—	CD -43°11010	1.8	M3 (af)
3236	—	138-56	—	-0.1	—
3237	—	—	—	1.6	—
3238	637.1	240-25	BD +68°883	0.9	K1 V (am), K1 (af)
3239	—	—	—	1.6	—
3240	—	138-64	—	2.3	—

TABLE 5.1 — continued

LHS	Gliese	Giclas	Other Name	$m_{pg} - m_R$	Spectral Type and Reference
3241	—	—	—	1.9	—
3242	637	—	—	1.5	—
3243	—	—	—	1.3	—
3244	639.1	—	ϵ Sco	1.1	K2.5 III (be), K2 IIIb (bf), G9 III (af)
3245	—	—	—	-0.1	—
3246	—	17-38	—	1.1	—
3247	—	—	—	1.7	—
3248	639.2	—	—	0.6	—
3249	—	—	—	2.1	—
3250	—	—	—	-0.2	DC9 (br), DC9 (bc)
3251	642	138-67	Ross 644	1.3	K7 (af), M1.5 V (bh), M1.5 V (cb)
3252	—	—	—	1.1	—
3253	—	—	vB 26	1.1	—
3254	1208	169-34	V749 Her	-0.2	DA5 (br)
3255	1207	19-7	—	1.3	M3.5 (af)
3256	—	—	—	1.5	—
3257	649	169-38	BD +25°3173	1.6	M0.5 V (bi), M0.5 (af), M2 V (bh)
3258	—	240-38	—	1.5	—
3259	—	—	—	2.3	sd (bb)
3260	651	—	BD +47°2420	1.1	G8 V (be), G8 V (am), G9 (af)

TABLE 5.1 — continued

LHS	Gliese	Giclas	Other Name	$m_{pg} - m_R$	Spectral Type and Reference
3261	—	181-24	—	1.5	—
3262	—	203-42	—	1.3	—
3263	—	—	—	1.5	—
3264	—	226-45	—	1.5	—
3265	1210	139-12	—	2.2	—
3266	—	170-19	Ross 864	1.5	K4 (af)
3267	—	181-30	Wolf 648	1.8	M3.5 (af)
3268	656	—	CD -60°6576	0.9	K2 V (bf)
3269 A*	660 A	19-15 A	—	0.9	M3.5 (af)
3269 B*	660 B	19-15 B	—	—	composite with LHS 3269 A
3270	—	—	CD -46°11288	0.9	K0 V (bf), K3 (af)
3271	660.1	19-16	—	1.1	M0 (af)
3272	1212	—	—	1.5	M3 (af)
3273	—	—	—	1.1	—
3274	—	—	—	1.5	—
3275	1214	139-21	—	2.7	—
3276	—	181-33	—	1.3	—
3277*	1215	139-29	—	1.8	—
3278	—	19-20	Wolf 672 A	-0.3	DA6 (br), DA4 (ba), DA (af)
3279	—	19-21	Wolf 672 B	2.2	M3.5 (af)
3280	—	—	—	1.5	—

TABLE 5.1 — continued

LHS	Gliese	Giclas	Other Name	$m_{pg} - m_R$	Spectral Type and Reference
3281	671	181-39	—	0.9	M1 V: (al), M3 (af)
3282	—	181-37 A	Wolf 692 A	1.6	M3 (af)
3283	—	181-37 B	Wolf 692 B	1.7	—
3284	—	—	—	1.1	M0: (af)
3285	667.1	—	CD -75°967	0.6	G2 V (be), G2 V (bf)
3286	672.1	—	—	1.5	M2 (af), M2 (bp)
3287*	675	—	BD +67°1014	1.1	K0 V (be), K0 V (am), K0 (af)
3288	—	170-37	—	1.5	—
3289	—	20-1	—	1.1	—
3290	—	—	—	0.6	M3 (af)
3291	—	—	—	1.1	M3.5 (af)
3292	1218	—	—	1.5	—
3293	—	226-62	—	1.7	—
3294	—	—	—	1.5	—
3295	—	—	—	1.5	—
3296	—	—	—	1.5	—
3297	1220	259-15	—	1.5	—
3298	—	203-71	—	2.1	—
3299	—	226-64	—	0.9	—
3300	—	—	—	1.5	—

TABLE 5.1 — continued

LHS	Gliese	Giclas	Other Name	$m_{pg} - m_R$	Spectral Type and Reference
3301	—	—	Ross 858	1.1	K4 (af), sd (bw)
3302	—	170-50	—	1.1	—
3303	—	—	—	1.5	—
3304	—	139-48	BD +6°3455	0.6	G0 V (am)
3305 A*	684 A	—	26 Dra A	0.5	G0 Ve (be), G0 V (am), G0 (af)
3305 B*	684 B	—	26 Dra B	—	—
3306	685	226-66	BD +61°1678 C	1.5	M0.5 (af), M1.5 V (bh)
3307	—	—	—	2.2	M6- V (ad)
3308	—	—	—	0.6	M4 (af)
3309	—	259-12	—	1.5	—
3310	—	—	CD -27°11772	1.1	K5 (af)
3311	—	—	—	1.3	—
3312	—	182-19	BD +37°2926	0.6	G0 V (am), G0 (af)
3313	—	204-24	—	2.0	—
3314	—	—	—	1.5	—
3315	—	20-9	Wolf 1471	1.5	M3 (af)
3316	690.1	154-8	—	1.1	M2.5 (af)
3317	—	—	—	1.1	M3 (af), M3-4 (bp)
3318	—	259-17	—	1.5	—
3319	692.1	170-61	BD +21°3198	1.1	K0 V (am)
3320	—	154-9	Ross 133	1.6	M2 (af)

TABLE 5.1 — continued

LHS	Gliese	Giclas	Other Name	$m_{pg} - m_R$	Spectral Type and Reference
3321	694	204-27	BD +43°2796	1.8	M2 (af). M3.5 V (bh)
3322	—	—	—	1.7	—
3323	—	20-12	—	1.5	—
3324	—	170-62	—	2.1	—
3325 A*	695 B	—	μ Her B	0.8	M3 (af), M3.5 V (bh), M4 V (cb)
3325 B*	695 C	—	μ Her C	—	—
3326*	695 A	—	μ Her A	0.9	G5 IV (ca), G5 IV (be), G5 IV (am)
3327	—	154-19	—	0.6	—
3328	—	240-70	—	1.5	—
3329	—	140-11	BD +4°3509	1.1	K1 (af)
3330	695.1	—	CD -33°12476	0.9	G6-8 V (bf), K0 (af)
3331	—	—	—	2.0	—
3332	—	—	—	2.3	M6.5 V (ai)
3333	—	183-5	—	2.1	M4.5-5 V (ax)
3334	—	204-32	—	1.3	M2 V (ai)
3335	2132	—	—	1.1	K4:: (af), M1-2: (bp)
3336	—	140-16	—	1.1	—
3337	—	—	CP -38°7124	0.5	G0: (af)
3338	1222	140-19	—	1.8	M3 V (al)
3339	—	—	—	1.6	M5.5 V (bi), M5.5 V (ai)
3340	—	154-34	—	0.6	G4 (af)

TABLE 5.1 — continued

LHS	Gliese	Giclas	Other Name	$m_{pg} - m_R$	Spectral Type and Reference
3341	—	228-12	—	1.1	—
3342	—	—	—	2.2	—
3343	—	204-39	—	1.7	M1 (bk)
3344	—	259-22	—	1.5	—
3345 A*	—	154-36 A	BD -13°4807 A	0.6	G3 V (bf), G2 (af)
3345 B*	—	154-36 B	BD -13°4807 B	—	—
3346	—	—	—	1.5	—
3347	—	—	CD -30°15026	0.6	G8 (af)
3348	—	—	—	1.5	—
3349	—	140-29	BD +14°3384	0.9	K0 (ag)
3350	—	182-34	—	1.3	—
3351	—	258-28	—	1.3	—
3352	—	154-41	—	1.9	—
3353	700.2	182-35	BD +26°3151	1.1	G8-K0 V (be), K0 V (am), K0 (af)
3354	—	—	—	1.6	—
3355	—	183-23	—	1.3	—
3356	701	20-22	BD -3°4233	1.4	M0.5 (af), M1.5 V (al), M2 V (bh)
3357	—	140-39	—	0.6	K2 (af)
3358	—	—	—	1.8	—
3359	1224	154-44	—	1.3	—
3360	—	—	—	1.5	—

TABLE 5.1 — continued

LHS	Gliese	Giclas	Other Name	$m_{pg} - m_R$	Spectral Type and Reference
3361	—	183-26	Wolf 816	1.1	K1 (af)
3362	—	—	—	2.0	—
3363	706	205-5	BD +38°3095	1.1	K2 V (be), K2 V (am), K2 (af)
3364	—	183-28	—	0.6	G0 (bk)
3365	—	204-48	—	1.1	K (ai)
3366	—	140-46	BD +5°3640	0.6	G8 (af), G5 (bk), sd (bw)
3367	—	—	—	1.5	—
3368	—	183-31	Wolf 830	2.0	M3.5: (af)
3369	—	140-47	—	0.6	sdK (ba)
3370	—	—	—	1.6	—
3371	—	183-32	Wolf 834	1.4	M0.5 V (al), K5 (af)
3372	—	—	—	1.5	M3.5 (af)
3373	708.2	140-49	BD +13°3578	1.3	M0 V (ag), K5 (af), M0 V (bh)
3374	708.3	21.7	—	1.8	M3: (af), M3.5 V (bh)
3375	—	140-52	—	0.6	M3 (af)
3376	—	258-33	—	1.5	—
3377	—	21-9	—	1.4	M2.5 (af)
3378	—	—	—	1.5	—
3379 A*	713 A	—	χ Dra A	0.5	F7 V (am), F8 (af)
3379 B*	713 B	—	χ Dra B	—	composite with LHS 3379 A
3380	—	227-28	—	1.3	DC:9 (br)

TABLE 5.1 — continued

LHS	Gliese	Giclas	Other Name	$m_{pg} - m_R$	Spectral Type and Reference
3381	711	—	η Ser	1.1	K2 IIIab (be), K0 III-IV (am), G8 (af)
3382	—	—	—	1.7	sdM (aa), sdM (bm), sdM (ap)
3383	—	—	—	1.1	M3: (af)
3384	2135	155-15	—	0.2	DA7 (br)
3385	—	205-20	—	1.7	M1 (bk)
3386	—	227-30	—	1.6	—
3387	—	141-8	BD +8°3689	0.9	G7 V (am), G6 (af)
3388	—	141-9	BD +8°3692	0.9	G9 V (am), K0 (af)
3389	—	—	—	1.6	—
3390	—	—	—	2.1	sdM (bm)
3391	—	259-31	—	1.5	—
3392	718	183-44	BD +22°3406	1.3	K4 V (am), K5 (af)
3393	—	21-28	Wolf 1463	1.3	K7 (af)
3394	720 A	205-30	BD +45°2743	1.3	M0.5 V (bi), M0 (af), M2 V (bh)
3395	720 B	205-32	vB 9	1.6	—
3396	—	155-26	—	1.3	—
3397	—	—	—	0.6	K3 (af)
3398	2138	155-29	—	1.5	—
3399	—	141-24	—	0.6	sdM (ba)
3400	723	155-30	Wolf 1466	1.5	M0.5 (af)

TABLE 5.1 — continued

LHS	Gliese	Giclas	Other Name	$m_{pg} - m_R$	Spectral Type and Reference
3401	—	206-38 A	BD +31°3330 A	1.2	K0 (af)
3402	—	206-38 B	BD +31°3330 B	1.6	M0 (af)
3403	724	155-33	BD -13°5069	1.5	M0 (af), M2 (bp)
3404	1230 B	—	—	1.5	—
3405	1230 A	184-19	—	1.3	—
3406	—	—	—	2.2	—
3407	—	—	CD -40°12743	1.3	K4 (af)
3408	—	—	—	0.6	G9 (af)
3409	—	—	—	2.0	sdM4 (ai)
3410	—	229-16	—	1.1	—
3411	—	—	—	1.5	—
3412	728	184-29	BD +17°3729	1.6	K7 (af), M1.5 V (bh)
3413	—	—	—	1.5	—
3414	729	—	Ross 154	1.7	M4 (af), M4.5 V (bh), M4.5 V (cb)
3415	—	141-41	—	1.1	—
3416	—	141-42	—	1.1	M4 V (ai)
3417	731	184-35	Ross 160	1.5	M0 (af), M1.5 V (bh)
3418	—	—	—	1.5	—
3419	—	22.5	—	0.6	—
3420	—	205-40	—	1.7	—

TABLE 5.1 — continued

LHS	Gliese	Giclas	Other Name	$m_{pg} - m_R$	Spectral Type and Reference
3421	—	—	—	1.3	—
3422	—	—	—	1.3	—
3423	739	—	CD -48°12818	1.7	M3 (af)
3424	742	260-15	—	-0.1	DXP5 (br), DAP4+ (ba)
3425	—	184-42	BD +18°3911	0.6	G8 (af)
3426	—	22-12	BD +5°4011	0.9	K3 (bk)
3427	—	—	BD -20°5385	0.7	G6 V (bf)
3428	741	—	—	1.7	M4: (af)
3429	—	205-55	—	1.7	—
3430	—	22-14	—	0.9	—
3431	—	22-15	BD +7°3967	1.3	K5 (af)
3432	745 A	184-48	Ross 730	1.6	M1 (af), M2 V (bh), sdM2 (cb)
3433	745 B	184-49	Ross 731	1.6	M1.5 (af), M2 V (bh), sdM2 (cb)
3434	1231	207-18	—	1.8	—
3435	—	185-8	—	1.5	—
3436	—	261-1	—	1.5	—
3437	747.1	—	Ross 727	1.3	M3 (af)
3438	1232	142-11	—	1.3	M4 V: (al)
3439	747.3	—	CD -47°12773	1.3	K5-M0 V (bf), K7 (af)
3440	—	—	BD +49°2959 a	0.9	G4 V (be), G4 V (am), G4 (af)

TABLE 5.1 — continued

LHS	Gliese	Giclas	Other Name	$m_{pg} - m_R$	Spectral Type and Reference
3441	—	—	BD +49°2959	0.7	G4 V (be), G4 V (am), G2 (af)
3442	—	142-12	—	1.3	—
3443	—	—	—	1.5	M3 (af), M3 (bp)
3444	—	22-20	BD -0°3676	0.4	sdF7 (am)
3445	—	185-12	Ross 733	1.5	M3 (af)
3446	—	185-13	Ross 734	1.5	M3.5 (af)
3447	748.2 A	22-21 A	BD +1°3942 A	1.1	K7 V (bi), K4 (af), K7 (bk)
3448	748.2 B	22-21 B	Bd +1°3942 B	1.3	M0 V (bi)
3449	—	—	—	1.1	M2: (af)
3450	—	125-4	BD +41°3306	1.2	K1 (af), K0 V (am)
3451	—	—	—	1.8	—
3452	—	—	—	1.7	—
3453	—	—	—	0.6	M3 (af)
3454	—	—	—	1.5	—
3455	—	—	—	1.7	—
3456	756	185-19	Ross 163	1.6	M1 (af)
3457	1236	22-26	—	1.6	M4 V (al), M2-3 (bp)
3458	—	125-6	BD +33°3433	1.4	K5 (af)
3459	—	207-30	—	1.6	—
3460	—	—	CD -45°13178	0.5	F3-5w (bf), sd (bw)

TABLE 5.1 — continued

LHS	Gliese	Giclas	Other Name	$m_{pg} - m_R$	Spectral Type and Reference
3461	1238	261-6	—	1.7	—
3462	—	—	—	1.9	—
3463*	759	—	31 Aql	0.9	G8 IV (be), G8 IV (am), G6 (af)
3464	—	—	BD +24°3737	0.6	F7 V (be), F6 V (am), F8 (af)
3465	1237	208-22	BD +49°3009	1.1	K3 (af)
3466	762.1	229-33	BD +58°1929	1.2	K1 V (be), K1 V (am), K2 (af)
3467	—	125-13	BD +35°3659 sf	0.4	F6 (af)
3468	—	—	CD -28°15936	0.6	K0+F/G (bf)
3469	—	—	BD +32°3474	0.6	G0 V (be), G0 V (am)
3470	763	23-5	BD +4°4157	1.3	M0 V (bi), K7 (af), M0.5 V (bh)
3471	762	—	—	1.7	—
3472	—	229-35	Wolf 1108	1.8	M3 (af)
3473	—	125-24 A	—	1.5	—
3474	—	125-24 B	—	1.5	—
3475	—	—	—	1.5	—
3476	—	—	—	1.6	M2.5: (af)
3477	—	—	—	2.0	—
3478	—	125-27	—	1.3	—
3479	1242	23-8	—	1.6	—
3480	—	—	—	2.8	—

TABLE 5.1 — continued

LHS	Gliese	Giclas	Other Name	$m_{pg} - m_R$	Spectral Type and Reference
3481	—	—	—	2.5	—
3482	767 A	125-31 A	BD +31°3767 A	1.6	M0.5 V (bi), M0.5 (af), K5 V (al)
3483	767 B	125-31 B	BD +31°3767 B	1.7	M2.5 V (bi), M1 V (al), M2:: (af)
3484	—	—	—	1.5	<M0 (bp)
3485	—	208-39	—	1.5	—
3486	—	—	—	1.7	M0 (af)
3487	—	—	—	1.6	—
3488	—	—	—	1.9	—
3489	—	125-35	—	1.5	M3 (af)
3490	768	—	α Aql	0.1	A7 V (be), A7 IV-V (am), A5 (af)
3491	—	—	CD -59°7305	0.6	G8 V (bf)
3492	—	—	—	1.6	—
3493	—	92-34	—	1.3	—
3494 A*	1245 A	208-44 A	V1581 Cyg A	1.5	M5.5 V (bi), M5+ V (ah)
3494 B*	1245 C	208-44 B	V1581 Cyg B	—	composite with LHS 3494 A
3495	1245 B	208-45	—	1.6	M6 V (bi)
3496	—	—	—	1.5	—
3497	—	125-45	—	1.3	—
3498	—	—	—	1.6	—
3499	—	230-18	Wolf 1122	1.6	M2 (af)
3500	—	—	—	1.9	—

TABLE 5.1 — continued

LHS	Gliese	Giclas	Other Name	$m_{pg} - m_R$	Spectral Type and Reference
3501	772	92-40	—	-0.1	DA6 (br), DAs (af)
3502	773 A	—	BD -12°5594 A	1.8	K4 V (bf), K7 (af), M1.5 V (bh)
3503	773 B	—	BD -12°5594 B	1.5	—
3504	—	—	—	1.6	M3: (af)
3505	—	23-19	—	1.1	—
3506	—	186-7	—	1.3	—
3507	775.1	—	BD +15°4026	0.9	G7 V (am), G8 (af)
3508	773.6	—	CD -50°12780	1.2	K4 V (bf)
3509*	777 B	125-55	BD +29°3872 B	1.8	M4 V (ai), M4: (af), M6 V (be)
3510	777 A	—	BD +29°3872 A	1.1	G8 IV-V (am), G6 IV (be), G8 (af)
3511	1248	23-24	—	1.3	—
3512	774 B	—	—	1.5	—
3513	774 A	—	—	1.5	—
3514	—	—	—	1.3	—
3515	779	—	15 Sge	0.6	G1 V (be), G1 V (am), F9 (af)
3516	—	—	—	1.8	—
3517	776.1	—	—	1.5	K4: (af)
3518	—	230-25	Wolf 1129	1.8	M3.5 (af)
3519	—	143-26	—	1.1	—
3520	—	—	—	1.9	—

TABLE 5.1 — continued

LHS	Gliese	Giclas	Other Name	$m_{pg} - m_R$	Spectral Type and Reference
3521	—	—	—	1.6	K3 (af)
3522	—	—	—	1.5	—
3523	781.1 B	—	—	1.6	M3.5 (af)
3524	781.1 A	—	—	2.0	M3 (af)
3525	—	—	—	1.5	—
3526	782	—	BD -20°5833	1.5	K4 Vp (bf), K5 (af), M0 V (bh)
3527	786	261-19	BD +76°785	1.3	K7 V (bi), K7 (af), M0.5 V (bh)
3528	—	—	—	2.0	—
3529	783.2 A	143-34	BD +15°4074 A	1.1	K1 V (am), K1 (af)
3530	783.2 B	143-35	BD +15°4074 B	1.5	—
3531	784	—	CD -45°13677	1.3	M1-2 V (bf), M0 (af)
3532	784.2 B	24-9	V1412 Aql	0.2	DQ7 (br), DC? (ag), DQ7+ (ba)
3533	784.2 A	24-10	—	1.6	M5 V (ag)
3534	—	—	—	1.5	—
3535	—	—	—	1.6	—
3536	—	143-41	—	1.3	K2 (bk)
3537	788	—	BD +66°1281	0.6	G3 V (be), G3 V (am), G1 (af)
3538	—	—	—	1.5	—
3539	—	—	—	2.3	—
3540	788.2	—	—	1.3	K4 (af)

TABLE 5.1 — continued

LHS	Gliese	Giclas	Other Name	$m_{pg} - m_R$	Spectral Type and Reference
3541	—	—	—	0.1	—
3542	788.1	—	CD -58°7734	1.5	—
3543	—	230-37	—	1.1	—
3544	—	143-48	—	1.3	—
3545	—	261-22	—	1.6	—
3546	—	—	—	1.5	—
3547	—	261-23	—	1.5	—
3548	—	—	—	1.7	sdM0 (ai), sd (bb)
3549	1253	230-40	Wolf 1069	1.6	M5 (af)
3550	—	24-15	BD +9°4529	0.6	sdF7 (am), F8 (af)
3551	—	—	—	1.1	—
3552	—	—	—	1.5	—
3553	791	—	CD -28°16676	1.9	M3 (af)
3554	790	—	CD -31°17597	0.9	G5-8 V (be), G6-8 V (bf), G8 (af)
3555	—	—	—	2.2	—
3556*	791.2	24-16	HU Del	2.2	M4.5 V (bi), M4 V (ag), M6 V (cb)
3557*	—	24-17	—	0.9	K2 (bk)
3558*	793	262-15	—	1.6	M3 (af), M3 V (bh)
3559	792	209-33	Ross 188	1.8	M4 (af)
3560	—	—	—	1.5	—

TABLE 5.1 — continued

LHS	Gliese	Giclas	Other Name	$m_{pg} - m_R$	Spectral Type and Reference
3561	—	24-19	—	1.1	M1 (bk)
3562	794	186-31	Wolf 1346	-0.2	DA3 (br)
3563	—	—	—	1.1	—
3564	—	24-20	—	1.8	—
3565 A*	1255 A	261-28 A	BD +75°752 A	0.9	K0-1 V + G5-6 (be), K0 V (am), K0 V (ag)
3565 B*	1255 B	261-28 B	BD +75°752 B	—	composite with LHS 3565 A and C
3565 C*	1255 C	261-28 C	BD +75°752 C	—	composite with LHS 3565 A and B
3566	—	—	—	2.3	M6 V (ad)
3567	—	186-35	—	1.5	—
3568 A*	795 A	24-23 A	BD +4°4510 A	1.2	K5 V (am), K5 V (al), K4 (af)
3568 B*	795 B	24-23 B	BD +4°4510 B	—	—
3569	794.2	—	ϕ^2 Pav	0.4	F8 V (be)
3570	796	—	CD -24°16193	0.9	G8-K0 V (bf), G8 V (be), G8 (af)
3571	—	—	—	1.5	—
3572	1257	—	BD -22°5504	1.1	K5 V (bf), K5 (af)
3573	—	144-29	—	1.3	—
3574	1258	210-31	Ross 766	1.2	K7 (af), M3 V (bh)
3575	—	—	—	2.1	—
3576	804	144-34	BD +19°4499	1.3	K7 (af), M1.5 V (bh)
3577*	806	209-41	—	1.5	M2 V (bi), M3 V (bh), M3 V (cb)
3578	807	—	η Cep	1.0	K0 IV (be), K0 IV (am), G8 (af)
3579	2150	25-1	—	1.1	—
3580	—	—	—	1.5	—

TABLE 5.1 — continued

LHS	Gliese	Giclas	Other Name	$m_{pg} - m_R$	Spectral Type and Reference
3581	—	—	—	1.5	—
3582	—	—	CD -47°13548	1.3	M0.5 (af)
3583	—	—	—	1.5	—
3584	—	25-3	BD +10°4379	1.3	K2 (ag)
3585	—	—	—	1.5	—
3586	—	262-27	—	0.9	K7 (af)
3587	—	144-40	Ross 258	1.6	M3 (af)
3588	—	—	—	1.1	—
3589	—	187-8	—	1.1	DC9 (br)
3590	—	231-17	BD +52°2815	1.3	K5 (af)
3591	—	210-38	—	1.7	—
3592	1255-	261-29	BD +74°889	0.8	G8 V (am), G8 (af)
3593	—	25-8	—	2.2	—
3594	—	—	—	1.8	—
3595*	809	231-19	BD +61°2068	1.6	M0 V (bi), M1 (af), M2 V (bh)
3596	—	—	BD -3°5059	1.2	K5 (af), sd (bw)
3597	—	—	—	1.5	—
3598	1259	144-44	BD +12°4499	1.3	K5 (af), K5 V (ag)
3599	—	25-9	—	0.9	M3 V (ai)
3600	—	—	—	1.5	—

TABLE 5.1 — continued

LHS	Gliese	Giclas	Other Name	$m_{pg} - m_R$	Spectral Type and Reference
3601	812 B	—	vB 11	1.1	DC9 (br), DC9 (bn), DC13 (ba)
3602	812 A	—	Ross 193	1.7	M3 (af)
3603	—	—	—	1.3	—
3604	—	25-10	—	0.9	—
3605	813	187-9	Wolf 1373	1.6	M3 (af)
3606	—	—	—	1.8	sdK5-M0 (ai)
3607	—	25-11	Wolf 901	1.2	K5 (af)
3608	—	—	CD -70°1800	0.9	G1 IV-V (bf), G1 IV-V (be)
3609 A*	815 A	210-48 A	—	1.5	M2 (af), M3 V (bh), M3 V (cb)
3609 B*	815 B	210-48 B	—	—	composite with LHS 3609 A and C
3609 C*	815 C	210-48 C	—	—	composite with LHS 3609 A and B
3610	—	144-50	—	1.9	—
3611	—	—	—	1.5	—
3612	816	—	Wolf 906	1.5	M2.5 (af)
3613	—	—	CD -47°13670	1.4	—
3614	—	—	—	1.5	M3: (af)
3615	—	—	—	1.5	—
3616	—	—	—	1.7	—
3617	—	—	—	1.8	—
3619	—	144-58	—	1.5	—
3620	—	—	—	1.3	sdM (ac)

TABLE 5.1 — continued

LHS	Gliese	Giclas	Other Name	$m_{pg} - m_R$	Spectral Type and Reference
3621	—	144-60	—	1.3	—
3622	—	144-61	—	1.3	—
3623	—	—	—	1.3	M1.5 (af)
3624	818	25-16	BD +6°4741	1.2	K4 (af)
3625	—	144-62	BD +1°4614	1.1	K5 (af), K5 (bk)
3626	—	—	—	1.5	—
3627	—	—	—	1.5	—
3628	—	—	—	1.8	sdM (bm)
3629	—	—	CD -47°13695	0.9	G8 (bf), K1 (af)
3630	—	—	—	1.7	—
3631	—	261-38	BD +73°925	1.2	K1 V (am), K2 (af)
3632	—	—	—	1.5	—
3633	—	—	—	1.7	—
3634	—	—	—	1.6	—
3635*	818.1	—	CD -73°1547	1.3	F8-G0 V (be), F8-G0 V (bf)
3636	—	—	—	-0.3	DA9 (br), DA9 (ba)
3637 A*	—	187-30 A	Ross 825 A	1.3	K3 (af), K3+ (ag)
3637 B*	—	187-30 B	Ross 825 B	—	composite with LHS 3637 A
3638	—	212-29	—	1.1	—
3639	—	—	CD -44°14334	1.6	M1 (af)
3640	—	—	BD +17°4519	1.4	sdF8 (am), F9 (af)

TABLE 5.1 — continued

LHS	Gliese	Giclas	Other Name	$m_{pg} - m_R$	Spectral Type and Reference
3641	—	145-23	vMa 72	1.6	M3.5 (af)
3642	—	261-39	—	1.5	—
3643	—	—	—	1.5	—
3644	—	—	—	1.5	—
3645	—	—	—	1.7	—
3646	—	211-15	—	1.1	—
3647	—	—	—	1.5	—
3648	—	—	—	2.0	—
3649	—	231-39	Ross 197	0.9	K3 (af)
3650	—	—	—	1.3	K3 (af)
3651	—	145-35	—	1.1	—
3652	825.1	—	CD -61°6571	-0.6	G5 V (be)
3653	—	187-39	—	1.8	—
3654	—	—	—	1.6	G5 (af)
3655*	825.4 A	—	CD -26°15541 A	0.9	G5 V (bf), G5 V (be), K5 (af)
3656	825.4 B	—	CD -26°15541 B	1.2	—
3657	826.1	—	BD -20°6185	1.2	K5 V (bf), K7 (af), M0 V (bh)
3658	—	—	—	1.5	—
3659	—	—	—	1.5	—
3660	—	—	—	1.5	—

TABLE 5.1 — continued

LHS	Gliese	Giclas	Other Name	$m_{pg} - m_R$	Spectral Type and Reference
3661	—	—	—	1.9	—
3662	—	—	—	1.7	—
3663	—	—	—	1.5	—
3664	—	—	—	1.5	—
3665	—	—	—	1.8	—
3666	826.2	—	—	1.5	M2 (af)
3667	—	145-37	—	1.3	K7 (af)
3668	—	—	—	1.5	—
3669	—	—	—	1.3	—
3670	—	231-42	—	1.3	—
3671	—	—	—	1.5	—
3672	—	—	—	1.3	—
3673	—	187-43	—	2.1	—
3674	827	—	γ Pav	0.4	F7 V (bf), F6 V (be)
3675	827.1	—	CD -56°8316	0.9	K3 V (bf)
3676	—	231-44	vB 29	1.6	—
3677	—	25-32	Ross 778	1.8	M0.5 (af), M2 (bk)
3678	—	212-39	BD +45°3561	0.9	G8 V (am)
3679	—	—	—	1.6	M1.5: (af)
3680	—	126-5	—	1.8	—

TABLE 5.1 — continued

LHS	Gliese	Giclas	Other Name	$m_{pg} - m_R$	Spectral Type and Reference
3681	—	—	—	3.1	—
3682 A*	—	26-5 A	Wolf 921 A	1.5	K4: (af)
3682 B*	—	26-5 B	Wolf 921 B	—	composite with LHS 3682 A
3683	—	—	—	2.3	—
3684	—	—	—	1.7	M3: V (ai)
3685	832	—	CD -49°13515	1.5	M2-3 V (bf), M3 (af)
3686	—	26-14 A	—	1.5	—
3687	836.2	261-45	—	0.0	—
3688	—	26-14 B	—	1.5	—
3689	—	26-13	Wolf 923	1.3	M3.5 (af)
3690	—	—	—	1.5	M4.5 V (ai)
3691	—	—	—	1.5	—
3692	—	—	CD -50°13411	0.9	G3 V (bf)
3693	—	215-2	Wolf 926	1.8	M3.5 (af)
3694	—	—	—	1.1	—
3695	—	93-25	—	2.2	—
3696	—	26-21	BD -2°5588	1.1	K0 (af)
3697	—	—	—	1.7	—
3698	—	188-15	—	1.5	—
3699 A*	—	231-53 A	Ross 200 A	1.7	M3 (af)
3699 B*	—	231-53 B	Ross 200 B	—	composite with LHS 3699 A
3700	—	213-9	—	1.6	M3 (bk)

TABLE 5.1 — continued

LHS	Gliese	Giclas	Other Name	$m_{pg} - m_R$	Spectral Type and Reference
3701	—	—	—	1.5	—
3702	836.4	—	Ross 206	1.7	M1.5: (af)
3703	836.5	126-27	—	-0.2	DQ6 (br), DQ6 (ba)
3704	—	188-24	BD +24°4460	1.1	—
3705	—	212-56	BD +43°4035	1.1	M1.5 (af), M2 (bk)
3706	—	26-29	—	1.3	K3 (af)
3707 A*	836.9 A	—	CD -58°8156 A	1.5	—
3707 B*	836.9 B	—	CD -58°8156 B	—	—
3708	1263	26-30	Wolf 940	2.1	M3.5 (af)
3709	—	—	—	1.3	—
3710	—	—	—	1.5	—
3711	—	212-59	Wolf 945	1.5	M4 (af)
3712	—	—	—	1.9	—
3713	—	188-26	—	1.6	—
3714	—	—	—	—	—
3715	—	—	—	1.5	M3.5 (af)
3716	—	—	—	—	composite with LHS 3715
3717	838.1 A	93-40	BD +5°4874	1.2	K3 V (am), K3 (af)
3718	—	—	—	1.5	—
3719	—	—	—	1.6	—
3720	838.1 B	93-41	—	2.0	—

TABLE 5.1 — continued

LHS	Gliese	Giclas	Other Name	$m_{pg} - m_R$	Spectral Type and Reference
3721	—	—	—	1.5	—
3722	—	18-1	—	1.7	—
3723	—	—	—	1.3	M4.5 V (ai)
3724	—	—	—	2.1	—
3725	—	188-28	—	1.6	—
3726	—	—	—	—	—
3727	839	215-20	—	1.3	M0.5 V (bi), M1 V (bh), K7 (af)
3728	—	—	—	—	—
3729	—	215-21	—	1.5	—
3730	—	215-22	Wolf 1567	1.3	K5 (af)
3731*	—	188-30	Wolf 1143	0.6	G2 (af)
3732	—	—	—	1.5	K3:: (af), sd (bw)
3733	—	—	—	1.1	—
3734	—	—	—	1.1	sdM (ba)
3735	—	—	—	1.5	—
3736	—	—	—	1.5	—
3737	—	—	BD +29°4550	0.4	F8 V-VI (be), sdF8 (am)
3738	—	—	—	1.7	—
3739	—	—	—	1.8	—
3740	—	—	—	1.5	—

TABLE 5.1 — continued

LHS	Gliese	Giclas	Other Name	$m_{pg} - m_R$	Spectral Type and Reference
3741	842	—	CD -60°7821	1.1	—
3742	—	18-14	BD +9°4955	1.1	K4 (af)
3743	—	188-37	—	1.5	—
3744	843	—	—	1.6	M3 (af)
3745	846	18-16	BD +0°4810	1.3	M0.5 V (bi), M0.5 V (ah), M0.5 V (al)
3746	—	—	—	1.5	M3.5 (af)
3747	—	—	—	1.5	—
3748	—	—	—	1.5	—
3749	—	264-17	—	1.5	—
3750	847 A	—	—	1.5	—
3751	847 B	—	—	1.5	—
3752	—	—	—	-0.1	DA5 (br)
3753	—	—	—	0.6	—
3754	—	—	—	1.5	—
3755	—	—	—	1.5	—
3756	—	—	—	2.1	M3.5 (af)
3757	—	—	—	1.5	—
3758	—	232-54	BD +52°3112	1.1	G8 V (am)
3759	—	—	—	1.8	—
3760	—	18-31	Wolf 990	1.6	M4 (af)

TABLE 5.1 — continued

LHS	Gliese	Giclas	Other Name	$m_{pg} - m_R$	Spectral Type and Reference
3761	—	—	—	—	—
3762	—	—	—	2.8	—
3763	—	—	—	1.1	—
3764	848.3 A	27-14 A	Wolf 1328 A	1.5	M0 (af)
3765	848.3 B	27-14 B	Wolf 1328 B	1.6	—
3766	—	—	CD -79°878	1.5	—
3767	—	126-60	BD +22°4567	1.3	K3 (af)
3768	—	—	—	3.6	sd (bb)
3769	—	—	—	—	—
3770 A*	—	126-62 A	BD +17°4708 A	0.6	sdF8 (am), F2 (af)
3770 B*	—	126-62 B	BD +17°4708 B	—	composite with LHS 3770 A
3771	851.1	188-46	BD +30°4633	1.3	K4 (af), M0 V (ag), M0 V (bh)
3772	—	—	—	1.7	—
3773	—	18-36	Wolf 1014	1.6	M3 (af)
3774	—	—	—	1.3	—
3775	—	—	—	1.5	—
3776	1265	—	—	1.8	M4 (af)
3777	—	—	—	1.1	—
3778	—	—	—	1.0	—
3779	—	—	—	-0.2	DC?8 (br), DC?8+ (ba)
3780	—	—	Wolf 1332	0.9	K2 (af)

TABLE 5.1 — continued

LHS	Gliese	Giclas	Other Name	$m_{pg} - m_R$	Spectral Type and Reference
3781	851.1	127-11	—	1.5	M0.5 V (ag), M0.5 V (bh)
3782	851.2	—	CD -41°14804	0.6	G5 V (bf), G5 V (be)
3783	1266	241-1	—	1.1	dK (bo)
3784	—	188-51	—	2.1	—
3785	—	—	—	2.5	—
3786	—	—	BD +12°4797	0.6	G2 V (be), G2 V (am), G2 (af)
3787	852 A	—	Wolf 1561	1.7	M4: (af), M4.5 V (bh)
3788	852 B	—	—	1.6	M5 (af), M5 V (bh)
3789	—	—	—	—	—
3790 A*	853 A	—	CD -54°9222 A	0.6	G3 V (bf), G3 V (be)
3790 B*	853 B	—	CD -54°9222 B	—	composite with LHS 3790 A
3791	—	—	—	1.3	K2: (af)
3792	—	—	CD -42°15867	1.5	K3 (af)
3793	—	—	—	1.6	—
3794	—	—	—	-0.1	DZ5 (br)
3795	—	18-42	—	1.3	—
3796	—	189-11	—	2.3	—
3797	—	189-12	Wolf 1216	2.2	K3 (af)
3798	—	—	—	1.5	K4 (af)
3799	—	—	—	1.7	M4 (af)
3800	—	—	—	—	—

TABLE 5.1 — continued

LHS	Gliese	Giclas	Other Name	$m_{pg} - m_R$	Spectral Type and Reference
3801	—	18-45	—	1.1	—
3802	855	—	CD -57°8454	1.5	—
3803	—	—	—	1.5	—
3804	—	—	—	1.5	M3.5 (af)
3805	—	—	—	—	—
3806	—	—	—	1.5	—
3807	858	—	—	1.3	K1 (af)
3808	—	18-48 A	Wolf 1201 A	1.8	—
3809	—	18-48 B	Wolf 1201 B	1.9	—
3810	—	215-46	—	1.3	—
3811	—	—	—	1.3	—
3812	—	232-71	Ross 666	1.1	A2 (ag)
3813	—	—	—	1.5	K3: (af)
3814*	860 A	232-75 A	BD +56°2783 A	1.7	M3 V (bi), M3.5 V (ah), M3 (af)
3815	860 B	232-75 B	BD +56°2783 B	1.8	M4 V (bi), M4: (af), M4.5 V (bh)
3816	—	—	—	2.2	—
3817	862	—	CD -30°19175	1.2	K4 (af)
3818	—	215-49	—	1.5	—
3819	—	—	—	1.6	—
3820	—	—	—	1.7	—

TABLE 5.1 — continued

LHS	Gliese	Giclas	Other Name	$m_{pg} - m_R$	Spectral Type and Reference
3821	—	—	—	-0.1	—
3822	—	263-21	—	1.3	—
3823	—	189-23	—	1.7	—
3824	—	—	—	1.1	—
3825	—	27-32	—	1.3	—
3826	—	—	—	1.5	—
3827	—	—	—	1.5	—
3828	863	18-56	BD +8°4887	1.6	M2 V (bh)
3829	—	241-12	—	1.3	—
3830	—	241-13	—	1.3	—
3831	—	—	—	1.5	—
3832	—	—	—	—	—
3833*	864	27-36	BD -1°4323	1.6	M0 (af), M1.5 V (bh)
3834	—	—	—	2.1	—
3835	—	189-28	—	1.6	—
3836	—	—	—	1.6	—
3837	—	—	—	>3.1	—
3838	—	67-8	BD +9°5076	1.1	K2 (af), K0 V (ag)
3839*	865	—	—	1.3	M3 V (bw)
3840	—	27-38	—	1.6	—

TABLE 5.1 — continued

LHS	Gliese	Giclas	Other Name	$m_{pg} - m_R$	Spectral Type and Reference
3841	—	—	—	—	—
3842	—	—	—	1.5	—
3843	—	—	—	1.8	—
3844	—	—	—	1.6	—
3845	—	—	—	1.1	M5: V (bc)
3846	—	156-43	—	1.9	—
3847	—	27-45	Ross 288	0.9	K0 (af)
3848	—	—	—	1.5	—
3849	—	—	—	1.5	—
3850	—	—	—	1.6	M5 V (ai)
3851	872 A	—	ξ Peg A	0.5	F6 III-IV (be), F7 V (am), F8 (af)
3852	872 B	—	ξ Peg B	1.5	M1 (af)
3853*	873	216-16	BD +43°4305	1.8	M3.5 V (bi), M4- V (ah), M3.5 (af)
3854	—	128-3	—	1.7	—
3855	874	—	—	1.5	M3 (af)
3856	—	—	—	1.6	—
3857	1273	67-23	—	0.1	DA5 (br), DA (ag)
3858	—	241-24	—	1.5	—
3859	1274	189-38	—	1.8	—
3860	—	28-20	—	1.7	—

TABLE 5.1 — continued

LHS	Gliese	Giclas	Other Name	$m_{pg} - m_R$	Spectral Type and Reference
3861	875.1	128-8	—	1.7	M3.5 V (bh)
3862	—	128-10	BD +30°4824	1.5	K5 (af)
3863	—	—	—	1.8	M4.5 V (ai)
3864	—	—	σ Peg A	0.5	F7 IV (be), F6 V or F7 IV (am), F7 (af)
3865	—	28-21	σ Peg B	1.7	M3: (af)
3866	—	—	—	2.8	—
3867	—	67-30	—	0.9	—
3868	—	—	—	1.3	sdM (bm)
3869*	—	128-11	Ross 237	1.1	G8 (af)
3870	—	—	—	-0.2	—
3871	878	233-31	Ross 226	1.9	M3 (af)
3872	—	156-63	—	2.1	—
3873	—	—	—	2.6	—
3874	878.1 A	156-65	BD -8°5980 A	0.9	G6 (af), G6 V (am)
3875	878.1 B	156-64	BD -8°5980 B	0.1	—
3876	—	—	—	1.5	—
3877	—	241-31	—	1.7	—
3878	—	—	—	1.5	—
3879	—	189-53	—	1.3	—
3880	—	—	—	1.1	—

TABLE 5.1 — continued

LHS	Gliese	Giclas	Other Name	$m_{pg} - m_R$	Spectral Type and Reference
3881	—	241-32	BD +68°1345 B	1.5	—
3882	—	241-33	BD +68°1345 A	1.1	K0 V (am), K0 (af)
3883	—	—	—	2.1	—
3884	—	—	—	1.5	—
3885	884	—	CD -23°17699	1.5	K5-M0 V (bf), K7 (af) M0.5 V (bh)
3886	—	—	—	1.8	—
3887	—	—	—	1.5	—
3888	—	—	Ross 781	1.3	K3 (af)
3889	—	—	CD -55°9220	1.5	sd (bw)
3890	—	—	—	—	—
3891	—	—	—	—	—
3892	—	67-42	—	2.0	K7 (af), K7 (bk)
3893	—	—	—	1.7	—
3894	—	241-42	BD +67°1498	0.7	G6 V (am), G8 (af)
3895	—	—	—	1.5	—
3896	—	—	—	1.5	—
3897	—	28-34	—	1.1	K3 (af)
3898	—	275-6	—	2.1	M1 (af)
3899	889.1	28-39	—	1.1	M0 V (al), M0 V (ag)
3900	—	28-41	BD -3°5577	1.3	K3 V (am), K3 (af)

TABLE 5.1 — continued

LHS	Gliese	Giclas	Other Name	$m_{pg} - m_R$	Spectral Type and Reference
3901	—	—	—	—	—
3902	—	—	—	1.5	M5 V (ai)
3903	—	190-13	—	1.3	—
3904	891	275-13	CD -26°16501	1.3	M2.5 (af)
3905	—	275-14	—	1.7	—
3906	—	—	—	1.5	—
3907	—	—	—	1.1	—
3908	—	—	—	—	—
3909	—	—	—	1.5	—
3910	—	—	—	1.6	—
3911	—	—	—	1.1	M4.5 V (ai)
3912	—	—	CD -63°1596	0.6	G8 V (be), G8 V (bf)
3913	—	157-32	BD -9°6149	0.5	F9 V (am), F9 V (be)
3914	—	157-33	BD -9°6150	0.9	G3 V (am), G3 V (be)
3915	—	—	—	1.5	—
3916	—	—	—	1.3	—
3917	—	157-35	—	0.1	DZ8 (br), DZ7+ (ba)
3918	—	—	—	1.8	M1 (af)
3919	—	—	—	1.4	—
3920	—	—	γ Psc	1.0	G8 III (am), K0 III: (be), G8 (af)

TABLE 5.1 — continued

LHS	Gliese	Giclas	Other Name	$m_{pg} - m_R$	Spectral Type and Reference
3921	—	—	CD -67°2593	1.1	K2-4 (bf)
3922	—	—	CD -67°2594	1.1	K2-3 [V] (bf)
3923	—	190-17	—	2.0	—
3924	—	—	—	1.5	—
3925	—	—	—	1.5	—
3926	—	—	—	2.7	—
3927	—	275-29	—	1.8	K4: (af)
3928	—	—	—	—	—
3929	—	157-44	—	1.8	K5 (af)
3930	—	217-1	—	1.7	—
3931	—	128-48	BD +28°4562	1.2	K1 V (am), K2 (af)
3932	—	273-15	—	1.8	K4 (af)
3933	—	—	—	3.0	—
3934	—	—	—	1.3	—
3935	—	—	—	1.9	—
3936	894.4	190-20	BD +43°4445	0.8	K1 V (am), G9 (af)
3937	—	—	—	1.6	sdM1-3 (ai)
3938	—	242-32	—	1.5	—
3939	894.5	157-54	BD -11°6064	1.1	K2 V (am), K2 (af)
3940	—	—	—	1.6	—

TABLE 5.1 — continued

LHS	Gliese	Giclas	Other Name	$m_{pg} - m_R$	Spectral Type and Reference
3941	—	157-59	—	1.9	—
3942	—	190-22	BD +33°4707	1.1	—
3943	—	29-30	Wolf 1038	1.1	M0 (af)
3944	—	—	—	1.5	sdM0 (ai)
3945	—	68-16	Ross 291	1.3	K5: (af)
3946	—	128-61	—	1.3	K3 (af)
3947	2155	29-33	—	1.1	M0.5 V (bi), sdM (ag), sdM (bt)
3948	—	29-35	—	1.8	—
3948a	—	275-46	—	1.5	—
3949	—	—	—	1.5	—
3950	—	—	—	0.9	M5: V (bc)
3951	—	190-24	—	1.3	—
3952	—	29-36	—	1.3	—
3953	—	157-64	—	1.5	—
3954	—	—	—	2.8	—
3955	—	—	—	1.5	—
3956	—	—	—	1.5	—
3957	—	190-26	—	1.6	—
3958	—	—	—	2.7	—
3959	—	—	—	1.5	M3: (af)
3960	—	68-22	Ross 674	1.1	K4 (af)

TABLE 5.1 — continued

LHS	Gliese	Giclas	Other Name	$m_{pg} - m_R$	Spectral Type and Reference
3961	—	—	—	1.3	M5: V (bc)
3962	—	—	—	0.9	—
3963	—	—	—	1.7	—
3964	—	—	—	—	—
3965	896 A	68-24 A	BD +19°5116 A	1.8	M4- V (ah), M3 (af), M4 V (bh)
3966	896 B	68-24 B	BD +19°5116 B	1.9	M4+ V (ah), M4.5 (af), M5 V (bh)
3967	—	241-57	—	1.1	—
3967a	—	157-69	—	1.3	—
3968	—	128-73	—	1.3	—
3969	—	—	—	1.6	—
3970	—	—	—	2.0	—
3971	—	—	—	—	—
3972	—	—	—	1.5	—
3973	—	—	—	2.2	—
3974	—	—	—	1.9	—
3975	—	—	—	1.5	K0 (af)
3976	—	—	BD +30°4982 A	0.6	F9 V (be), G2 V (am)
3977	—	—	BD +30°4982 B	1.7	M3: (af)
3978	—	—	—	1.8	—
3979	—	29-49	Wolf 1533	1.5	M2 (af)
3980	—	171-5	—	1.5	M0 (af)

TABLE 5.1 — continued

LHS	Gliese	Giclas	Other Name	$m_{pg} - m_R$	Spectral Type and Reference
3981	—	29-51	—	1.3	—
3982*	—	68-31	BD +17°4946	0.9	G6 (af), G5 V (am)
3983	—	—	—	—	—
3984	—	—	—	—	—
3985	—	—	—	1.6	—
3986	—	29-55	—	1.1	K3 (bk)
3987	—	—	—	2.5	mid-M (ai)
3988	1287	—	—	1.5	—
3989	—	—	—	0.6	—
3990	—	273-95	—	1.7	—
3991	—	171-8	—	1.7	—
3992	—	—	—	1.5	—
3993	—	157-90	—	1.3	—
3994	902	—	CD -73°1672	1.1	K3 V (be), K4 V (bf)
3995*	904	—	ι Psc	0.4	F8 (af), F7 V (be), F7-8 V (am)
3996	—	—	—	—	—
3997	—	—	—	1.9	—
3998	—	—	—	1.5	—
3999	—	—	—	1.5	M2 (af)
4000	—	275-83	—	1.5	—

TABLE 5.1 — continued

LHS	Gliese	Giclas	Other Name	$m_{pg} - m_R$	Spectral Type and Reference
4001	—	—	—	1.5	—
4002	—	171-11	—	1.5	M3 V (ai)
4003	1289	130-4	—	1.1	M5 V (al)
4004	—	241-66	BD +57°2787	0.6	G2 V (am), G2 V (be)
4005	—	157-93	BD -8°6177	0.6	—
4005a	—	217-18	—	1.1	—
4006	—	241-68	Ross 676	1.1	M1.5 (af), M1 (bk)
4007	—	68-38	—	1.7	—
4008	—	130-8	BD +28°4634	1.2	K0 (af), K2 V (am)
4009	—	273-130	—	2.1	—
4010	—	—	—	1.6	sdM0 (ai), sd (bb)
4011	—	273-134	—	1.9	—
4012	—	—	—	1.5	—
4013	—	—	CD -42°16457	0.2	A3 V (bf), A2 V (be), A3 (af)
4014	—	273-137	—	1.7	K3: (af)
4015	907	171-19	Ross 249	1.7	M2 V (al), M1.5 (af)
4016	—	275-106	—	1.3	M3.5: (af)
4017	—	29-66	—	1.1	—
4018	—	130-11	—	1.3	—
4019	—	130-15	—	0.6	DA9 (br), DA8+ (ba)
4020	—	29-72	BD +2°4723	0.8	G7 V (am)

TABLE 5.1 — continued

LHS	Gliese	Giclas	Other Name	$m_{pg} - m_R$	Spectral Type and Reference
4021	—	273-147	—	1.7	—
4022	—	29-73	—	1.3	M1 (bk)
4023	—	—	—	1.5	—
4024	—	—	—	2.0	—
4025	—	—	—	—	—
4026	—	—	—	1.3	—
4027	908.2	—	—	1.9	M3.5 (af), M4 V (ai)
4028	—	—	—	1.5	—
4029	—	—	—	1.5	—
4030	—	31-11	Wolf 1046	1.3	K4: (af)
4031	—	—	CD -62°1464	1.1	K3 V[w] (bf)
4032	—	273-151	—	1.8	—
4033	—	—	—	-1.0	—
4034	—	—	—	1.8	—
4035	—	—	—	2.0	—
4036	—	158-2	—	1.5	M3:: (af)
4037	—	266-1	—	0.9	K3: (af)
4038	—	—	—	1.5	M4 (af)
4039	—	275-121 B	—	1.8	M3.5 (af)
4040	—	275-121 A	—	0.0	DA (br), DAs (af)

TABLE 5.1 — continued

LHS	Gliese	Giclas	Other Name	$m_{pg} - m_R$	Spectral Type and Reference
4041	—	—	—	-0.1	DA (br), DA (af)
4042	—	—	—	-0.2	—
4043	—	171-27	—	0.0	DQ6 (br), DQ6+ (ba)
4044	—	130-24	BD +27°4642	0.9	K1 (af), K1 V (am)
4045	—	130-25	—	1.8	—
4046	—	31-15	—	1.5	—
4047	912	31-17	BD -6°6318	2.1	M2 (af)
4048	—	266-8	CD -27°16491	1.1	—
4049	—	31-18	—	1.8	—
4050	—	273-183	—	1.3	—
4051	—	158-15	—	1.6	—
4052	—	242-44	—	1.5	—
4053	—	242-45	—	1.5	—
4054	913	171-29	BD +45°4378	1.6	M0.5 V (bh), K7 (af)
4055	—	266-21	BD -20°6684	0.8	G8 V (bf), G7 V (am), G8 (af)
4056	—	171-33	—	1.5	—
4057	—	—	—	1.9	M5 V (ai)
4058	—	267-11	—	1.6	M4 (af)

TABLE 5.1 — continued

LHS	Gliese	Giclas	Other Name	$m_{pg} - m_R$	Spectral Type and Reference
5001	—	266-42	BD -21°6537	1.5	G2-3 V (bf), G0 (af)
5001a	—	32-9	BD +18°24	1.1	K5 (bk)
5002	—	—	—	-0.3	—
5003	—	—	—	0.6	—
5004	—	31-43	—	1.1	—
5004a	—	—	—	1.6	M3: (af)
5005	—	—	—	1.6	—
5006	—	242-55	—	1.3	—
5007	—	242-56	—	1.1	K5 (af), K5 (bk)
5008	—	—	—	1.5	—
5009	—	217-56	—	1.3	—
5010	—	32-30	—	1.1	—
5011	—	32-31	—	2.1	—
5012	—	32-36	—	0.9	K7: (bk)
5013	—	242-64	—	1.3	—
5014	—	—	—	1.5	—
5015	—	—	—	1.1	—
5016	—	69-31	—	-0.2	DA5 (br), DA (ag), DA5+ (ba)
5017	—	132-40	—	1.1	—
5018	—	—	—	0.3	—
5019	50	270-118	BD -10°216	1.1	K7 (af)
5020	—	—	—	1.5	—

TABLE 5.1 — continued

LHS	Gliese	Giclas	Other Name	$m_{pg} - m_R$	Spectral Type and Reference
5021	—	—	—	1.7	—
5022	—	—	—	1.5	—
5023	—	—	—	0.6	DC9/DC?9 (br), DC10 (ba)
5024	—	—	—	0.6	DC9 (br), DC12 (ba)
5025	—	—	—	0.8	—
5026	—	243-59	Wolf 53	1.5	M3.5 (af)
5027	53.1 A	34-2 A	BD +22°176 A	1.3	K4 V (am), K4 (af)
5028	53.1 B	34-2 B	BD +22°176 B	—	M3 (af)
5029	—	—	—	1.3	—
5030	—	243-67	—	1.3	—
5031	—	269-140	—	1.6	—
5032	—	—	—	1.9	—
5033	—	272-15	—	1.1	—
5033a	—	—	—	1.6	—
5034	—	—	—	1.5	—
5035	58.2	34-32	BD +20°226	1.1	K2 V (am), K3 (af)
5036	—	—	CD -52°305	1.1	—
5037	—	271-102	—	1.1	—
5037a	—	72-23	—	1.7	—
5038	—	271-130	—	1.3	K4: (af)
5039	—	3-13	Wolf 1065	1.1	K3 (af), K3 (bk)
5040	—	—	—	0.1	—

TABLE 5.1 — continued

LHS	Gliese	Giclas	Other Name	$m_{pg} - m_R$	Spectral Type and Reference
5041	—	—	—	1.5	—
5042	—	—	—	3.2	—
5043	—	274-106	—	2.0	—
5044	—	133-47	—	1.3	—
5045	—	—	—	1.5	—
5046	—	—	—	>2.1	—
5047	—	—	—	2.7	—
5048	—	71-51	BD +3°275 B	1.9	M1.5 (af)
5049	—	71-50	BD +3°275 A	1.3	K4 (af)
5050	—	173-37	—	1.2	—
5051	—	35-30	—	1.3	—
5051a	—	—	BD +23°303	0.9	G8 IV (be)
5051b	—	244-59	BD +64°312	0.9	G8 (af)
5052	—	—	—	2.9	—
5053	—	—	—	1.1	—
5054	—	—	—	1.8	—
5055	—	—	—	1.5	—
5056	—	—	—	1.1	—
5057	—	—	—	1.6	—
5058	—	—	—	1.7	—
5059	—	—	—	1.3	—
5060	—	—	—	1.5	—

TABLE 5.1 — continued

LHS	Gliese	Giclas	Other Name	$m_{pg} - m_R$	Spectral Type and Reference
5061	—	75-44	—	1.1	—
5062	—	—	—	2.4	—
5063	—	—	BD -11°569	0.9	—
5064	—	76-48	—	-0.2	DA8 (br), DAwk (ag)
5065	—	—	—	1.3	—
5066	—	—	—	1.3	—
5067	—	—	—	1.5	—
5068	—	—	—	1.3	—
5069	—	—	—	1.7	—
5070	—	—	—	0.1	—
5071	—	—	—	1.8	—
5072	—	—	—	1.6	M2 (af)
5073	—	78-35	—	1.5	—
5074	—	77-66	—	1.7	—
5075	—	79-54	—	1.1	—
5076	—	—	—	1.7	—
5077	—	—	—	1.5	—
5078	—	—	—	1.5	—
5079	—	160-17	—	1.3	—
5080	—	221-20	—	1.5	—

TABLE 5.1 — continued

LHS	Gliese	Giclas	Other Name	$m_{pg} - m_R$	Spectral Type and Reference
5081	—	221-21	—	1.5	M0 (af)
5082	—	—	—	>1.9	—
5083	—	—	—	1.5	—
5084	—	—	—	0.6	—
5085	—	175-7	—	0.9	—
5087	156	160-35	BD -7°699	1.5	M0.5 V (bq), K7 (af)
5088	—	80-38	—	1.3	—
5089	—	—	—	1.6	—
5090	—	—	—	1.6	—
5091	—	175-17	Ross 27	1.9	M3.5 (af)
5092	—	160-53	—	1.3	—
5093	—	247-20	—	1.8	—
5094	—	—	—	1.5	—
5095	—	8-35	—	1.1	—
5096	—	39-14	—	0.9	—
5097	—	—	—	2.3	—
5098	—	—	—	1.3	M1 (af)
5098a*	—	—	CD -38°1631	1.3	G5: (af)
5099	—	—	—	1.3	—
5100	—	8-54	—	1.7	—

TABLE 5.1 — continued

LHS	Gliese	Giclas	Other Name	$m_{pg} - m_R$	Spectral Type and Reference
5101	—	84-42	BD +0°989	1.7	M0 (ag), M0 (bp)
5102	—	—	—	1.1	—
5103	—	—	—	1.3	—
5104	—	—	—	1.1	—
5105	—	—	—	1.5	—
5106	—	—	—	1.5	—
5107	—	99-16	BD -0°981	1.1	G5 V (am)
5108	—	86-45	—	1.3	—
5109	—	—	Wolf 1457	1.6	M4 (af)
5110	—	97-55	—	1.5	—
5112	—	—	CD -46°2096	1.5	M0 (af)
5113	—	106-35	—	1.7	—
5115	—	—	—	1.5	—
5116	—	103-34	BD +27°1124	1.1	K1 (af), K2 V (am)
5117	—	105-41	—	1.3	—
5118	—	—	—	2.0	—
5119	—	250-19	—	1.1	K0 (af)
5120	—	108-37	—	2.2	—

TABLE 5.1 — continued

LHS	Gliese	Giclas	Other Name	$m_{pg} - m_R$	Spectral Type and Reference
5121	—	107-32	—	1.8	—
5122	—	—	—	1.7	—
5122a	—	107-58	—	1.1	—
5123	—	89-7	—	1.8	—
5124	—	—	BD -12°1914	1.2	K3 (af), K3 V (bf)
5125	—	—	—	1.3	—
5126	—	—	—	2.2	—
5126a	—	251-43	—	1.5	—
5127	1100	—	Ross 391	1.5	M0.5 (af)
5128	—	50-8	—	1.4	—
5129	—	—	—	2.3	—
5130	290	—	BD +80°238	0.9	G8 V (be), G9 (af)
5131	—	90-36	Wolf 1059	0.6	—
5132	—	—	—	1.5	—
5133	—	40-7 A	BD +21°1764 A	1.1	—
5134	—	40-7 B	BD +21°1764 B	1.5	—
5135	—	—	—	1.3	—
5136	—	113-24	BD -3°2288	0.6	G4 (af)
5137	—	—	—	1.7	—
5138	—	—	—	-0.1	—
5139	—	115-11	—	1.6	—
5139aA*	314 A	—	BD -22°2345 A	0.8	G3-5 V (bf), G6 IV (be), G6 (af)
5139aB*	314 B	—	BD -22°2345 B	—	—
5140	—	9-19	—	0.9	—

TABLE 5.1 — continued

LHS	Gliese	Giclas	Other Name	$m_{pg} - m_R$	Spectral Type and Reference
5141	—	—	—	1.5	—
5142	—	—	—	3.8	M6 V (bi)
5143	—	—	—	2.1	—
5144	—	41-26	—	1.5	—
5145	—	—	—	1.8	—
5146	—	—	—	2.4	—
5146a	—	—	—	1.5	—
5146b	—	47-28	—	2.7	—
5147	—	—	—	1.1	—
5148	—	—	—	1.5	—
5149	—	—	CD -57°2585	1.1	K/M V (bf)
5150	—	253-23	—	1.5	—
5151	—	—	—	1.1	—
5152	—	48-15	—	1.6	—
5153	—	161-38	BD -4°2639	1.9	—
5154	—	—	—	1.3	—
5155	—	—	—	1.7	—
5156	—	—	—	1.5	—
5157	—	195-46	—	1.7	—
5158	—	49-27	Ross 96	1.2	K3 (af)
5159	—	48-52	—	1.8	—
5160	—	—	—	1.9	—

TABLE 5.1 — continued

LHS	Gliese	Giclas	Other Name	$m_{pg} - m_R$	Spectral Type and Reference
5161	—	116-70	—	1.8	—
5162	—	116-71	—	1.7	M0 V (al)
5163 A	—	195-52 A	BD +56°1421 A	1.0	G8 IV-V (am)
5163 B	—	195-52 B	BD +56°1421 B	—	—
5164	—	43-22	—	1.5	—
5165	—	—	—	3.2	—
5166	—	—	—	2.1	—
5166a	379.2	—	CD -36°6180	0.6	G3 V (bf), G1 (af)
5166b	—	—	—	1.6	—
5167*	388	54-23	BD +20°2465	1.6	M3.5 V (ah), M3.5 (af), M3.5 V (bh)
5168	—	118-51	—	1.1	—
5168a	—	—	BD -16°3030	0.9	G8 V (bf), K0 (af)
5169	—	—	—	2.1	—
5170	—	196-24	—	1.5	—
5171	—	44-19	—	1.1	—
5171a	—	196-31	—	1.3	—
5172	—	—	—	—	—
5173	—	—	—	1.8	—
5174	—	—	—	2.1	—
5175	—	—	—	1.3	—
5176	—	—	—	1.5	M3-4 (bp)
5177	—	58-22	—	1.3	—
5178	—	—	—	1.7	—
5179	—	—	—	2.4	—
5180	—	—	BD -13°3242	1.5	K3 V (bf)
5180a	1139	253-40	BD +76°404	1.3	K4 (af)

TABLE 5.1 — continued

LHS	Gliese	Giclas	Other Name	$m_{pg} - m_R$	Spectral Type and Reference
5181	—	119-42	BD +28°1952	1.1	—
5182	—	—	—	1.5	—
5183	—	—	—	1.3	—
5184	—	—	—	1.6	—
5185	—	176-4	—	1.1	—
5186	—	—	—	1.7	—
5187	—	—	—	1.3	—
5188	—	—	CD -30°8970	1.3	K5 (af)
5189	—	—	—	1.5	—
5190	—	—	—	2.4	—
5191	—	56-34	BD +15°2325	1.1	K2 (af)
5192	—	120-49	—	1.6	—
5193	—	—	—	1.8	—
5194	—	—	—	0.1	—
5195	—	120-67	Ross 904	1.1	K1 (af), G8± (ag)
5196	—	—	—	1.9	—
5197	—	—	—	1.4	—
5198	—	57-21	—	1.5	—
5199	—	—	—	1.4	—
5200	—	57-24	—	1.7	—

TABLE 5.1 — continued

LHS	Gliese	Giclas	Other Name	$m_{pg} - m_R$	Spectral Type and Reference
5201	—	—	—	1.5	—
5202	—	—	—	0.4	—
5203	—	237-37	Ross 452	0.9	G4 (af)
5204	—	—	—	1.7	—
5205	—	—	—	1.5	M3 (af)
5206	454	—	BD -9°3413	0.9	G8-M0 IV (be), K0 IV (am), G8 (af)
5207	—	122-64	—	1.3	—
5208	—	—	—	1.5	—
5209	—	—	—	1.6	—
5210	—	—	—	1.7	—
5211	—	59-3	—	1.5	—
5212	—	237-56	—	0.0	DC8 (br)
5213	—	12-29	—	1.4	—
5214	—	—	—	1.5	—
5215 A*	—	237-62 A	BD +74°493 A	1.1	G5 (af)
5215 B*	—	237-62 B	BD +74°493 B	—	composite with LHS 5215 A
5215a	—	253-59	—	1.5	—
5216	—	123-33	—	0.9	M1 (bk)
5217	—	—	—	1.5	—
5217a	—	148-66	—	1.5	—
5218	—	—	BD -13°3557	1.2	K3-4 V (bf), K5 (af)
5219	—	12-45	Wolf 429	1.5	M3.5: (af)
5220	—	—	—	1.3	—

TABLE 5.1 — continued

LHS	Gliese	Giclas	Other Name	$m_{pg} - m_R$	Spectral Type and Reference
5221	—	—	—	1.5	—
5222	—	—	—	-0.3	—
5223	—	—	—	1.1	—
5224	—	—	—	1.3	M1-2 (bp)
5225	—	13-52	—	1.3	—
5226	—	—	—	1.5	—
5227	—	—	—	1.8	—
5228	—	14-2	—	1.6	M1 (af)
5229	—	14-3	—	1.1	—
5230	—	123-63	—	1.8	—
5230a	—	—	—	1.5	—
5231	—	14-17	—	1.5	—
5232	—	—	—	1.8	—
5233	—	—	—	2.0	—
5234	—	238-21	—	1.5	—
5235	—	—	—	2.1	—
5236	—	—	—	1.7	—
5237	—	—	—	1.7	—
5238	—	149-40	—	1.6	M3 (af)
5239	—	—	—	2.3	—
5240	—	—	—	1.5	—

TABLE 5.1 — continued

LHS	Gliese	Giclas	Other Name	$m_{pg} - m_R$	Spectral Type and Reference
5241	—	—	—	1.6	—
5242	—	—	—	1.3	—
5243	—	62-27	—	0.9	—
5244	—	—	—	1.5	—
5245	—	164-72	—	1.1	—
5246	—	—	—	2.1	—
5247	—	—	CD -27°9236	1.4	K7 (af)
5248	—	—	—	1.5	—
5249	512 A	14-55 A	Ross 486 A	1.6	M3.5 (af), M4 V (bh)
5250	512 B	14-55 B	ROss 486 B	1.7	M4 (af)
5251	—	63-31	—	1.7	—
5252	—	—	—	1.7	—
5253	—	62-56	—	1.8	M3 (af)
5254	—	63-48	Wolf 491	0.9	M0 (af)
5255	—	—	CD -57°5188	1.1	M0 (bp)
5256	—	177-61	—	1.3	—
5257	—	223-27	—	1.3	—
5258	—	—	—	1.5	—
5259	—	—	—	2.0	—
5260	—	—	—	1.7	—

TABLE 5.1 — continued

LHS	Gliese	Giclas	Other Name	$m_{pg} - m_R$	Spectral Type and Reference
5261	—	—	CD -45°8786	0.6	G0: (af), G2 V (bf)
5262	—	—	—	1.5	—
5263	—	—	—	1.1	—
5264	—	—	—	—	—
5265	—	—	—	1.5	—
5266	—	165-51	BD +30°2490	1.2	K7 (af)
5267	—	165-53	—	1.9	—
5268	—	150-74	—	1.7	—
5269	—	—	—	1.7	—
5270	—	124-26	—	0.1	—
5271	—	178-21	—	1.6	—
5272	—	—	—	1.1	—
5273	—	—	—	2.5	—
5274	—	—	—	1.5	—
5275	—	—	—	1.1	M1.5 (bp)
5276	—	—	—	1.6	—
5277	—	—	—	1.5	—
5278	—	166-44	—	2.1	—
5279*	567	—	BD +19°2881	1.1	K2 V (be), K2 V (am), G8 (af)
5280	—	—	—	1.5	—

TABLE 5.1 — continued

LHS	Gliese	Giclas	Other Name	$m_{pg} - m_R$	Spectral Type and Reference
5281	—	—	—	1.3	—
5282	—	—	—	1.3	—
5283	—	151-13	—	0.9	—
5284	—	—	—	1.1	—
5285	—	66-55	Ross 1030b	1.1	K0 (af)
5286	—	—	—	1.3	—
5287	—	201-33	—	1.5	—
5288	—	—	—	1.7	—
5289	—	256-19	—	1.5	—
5289a	—	151-28	BD -7°3963	0.5	—
5290	—	136-74	Ross 996	1.6	M2 (af)
5291	—	—	—	2.0	—
5292	—	179-24	—	1.7	—
5293	—	—	—	1.3	—
5294	—	136-93	BD +15°2847	1.1	K2 (ag)
5295	—	—	—	1.1	K5 (af)
5296	—	—	—	2.4	—
5296a	—	—	—	0.9	—
5297	—	—	—	1.1	—
5298	—	—	—	1.1	—
5299	—	—	—	1.3	—
5299a	599 A	—	CD -37°10500 A	0.6	G6 V (be), G6 IV (bf), G9 (af)
5299b	599 B	—	CD -37°10500 B	-0.1	DA (af)
5300	—	—	—	1.5	—

TABLE 5.1 — continued

LHS	Gliese	Giclas	Other Name	$m_{pg} - m_R$	Spectral Type and Reference
5301	—	16-10	—	1.3	—
5302	—	—	—	1.5	—
5303	—	—	—	2.2	—
5304	—	137-66	—	1.1	—
5305	—	225-42	—	1.5	—
5306	—	152-69	—	1.3	—
5307	608	225-43	BD +62°1446	1.5	M0 V (ag)
5308	—	—	—	2.2	—
5309	—	16-26	—	1.3	—
5310	—	—	—	-0.4	—
5311	—	137-81	BD +11°2910 B	1.6	—
5312	610	—	BD -20°4399	1.1	K3-4 V (bf), K3 (af)
5313	—	137-82	BD +11°2910 A	0.9	—
5314	—	168-33	—	1.6	—
5315	616.2	202-36	BD +55°1823	1.5	M1.5 (af), M1.5 V (bh), M1 V (cb)
5316	—	—	—	1.3	—
5317	—	169-15	—	2.0	M1 (bk)
5318	—	180-61	—	1.3	—
5318a	—	169-18	BD +31°2873	0.5	—
5319	—	202-68	—	1.1	M2.5 (bk)
5320	—	—	—	1.3	M1-2 (bp)

TABLE 5.1 — continued

LHS	Gliese	Giclas	Other Name	$m_{pg} - m_R$	Spectral Type and Reference
5321	—	—	—	1.9	—
5322	—	—	—	1.5	—
5323	—	181-16	—	1.6	—
5324	655	170-17	Ross 863	1.5	M3 V (al), M3 (af)
5325	—	—	—	1.8	—
5326	—	265-34	—	1.8	—
5327	—	181-42 A	—	1.8	—
5328	—	181-42 B	—	2.2	—
5329	—	—	—	1.8	—
5330	—	240-64 A	—	1.3	—
5331	—	240-64 B	—	1.3	—
5332	—	140-37	—	1.8	—
5333	—	—	BD -22°4585	1.1	K1 V (bf)
5334	—	154-51	—	0.9	K4 (af)
5335	—	205-18	—	1.6	—
5336	—	—	—	2.0	—
5337	—	21-12	—	0.9	M0 (af)
5337a	2137	—	CD -28°14630	1.3	K[2] V (bf)
5338	—	—	—	1.3	—
5339	—	21-22	—	0.6	—
5340	—	141-25	Ross 138	1.1	K5: (af)

TABLE 5.1 — continued

LHS	Gliese	Giclas	Other Name	$m_{pg} - m_R$	Spectral Type and Reference
5341	—	—	—	1.5	—
5342	—	155-40	—	1.1	—
5343	—	141-48	—	0.8	—
5344	—	—	—	1.5	—
5345	—	259-39	—	1.3	—
5346	—	—	CD -63°1418	1.1	—
5347	757	—	CD -22°13916	1.3	K4 (af), M1 (bp)
5348	—	—	—	2.7	—
5349	—	—	—	1.7	—
5350	—	—	—	1.3	—
5350aA*	771 A	—	β Aql A	1.1	G8 IV (be), G7 (af)
5350aB*	771 B	—	β Aql B	—	M3 (af)
5351	—	—	—	1.3	—
5351aA*	773.3 A	—	BD -10°5238 A	0.5	F8 V (be)
5351aB*	773.3 B	—	BD -10°5283 B	—	composite with LHS 5351aA
5352	—	143-20	Wolf 863	1.5	K7 (af)
5353	—	—	27 Cyg	0.9	K0 IV (be), K0 IV (am)
5354	1250	125-62	—	1.9	—
5355	—	—	—	1.5	—
5356	—	—	—	2.2	—
5357	—	210-29	—	1.1	—
5358	—	—	—	1.7	—
5358a	806.1 B	—	ϵ Cyg B	1.6	M3 (af)
5358b*	806.1 A	—	ϵ Cyg A	1.1	K0 III (be), G8 (af)
5359	—	—	—	1.3	—
5360	—	—	—	3.0	—

TABLE 5.1 — continued

LHS	Gliese	Giclas	Other Name	$m_{pg} - m_R$	Spectral Type and Reference
5361	—	261-35	—	1.3	—
5362	—	212-12	—	1.3	—
5363	2151	—	—	0.6	—
5364	—	212-21	—	1.1	—
5365	—	212-24	—	1.2	K3 (af)
5366	—	—	—	1.5	—
5367	—	187-28	—	1.7	—
5368	825.3	25-25	BD -0°4195	1.3	K3 (af)
5369	—	—	—	1.5	—
5370	—	212-37	—	1.3	—
5371	—	—	—	1.5	—
5372	—	—	—	1.8	—
5373	—	—	—	1.6	—
5374	838.6	—	—	1.5	M1 (af)
5375	—	188-32	Wolf 1147	1.6	M3 (af)
5376	—	188-33	—	1.5	—
5377	—	—	CD -53°9029	0.4	G0 V (be), G0 V (bf)
5378	—	18-23	—	1.6	—
5379	—	18-25	Wolf 983	1.6	M3 (af)
5380	—	—	—	2.1	—

TABLE 5.1 — continued

LHS	Gliese	Giclas	Other Name	$m_{pg} - m_R$	Spectral Type and Reference
5381	—	—	—	1.5	—
5382	—	—	—	1.5	—
5383	—	—	—	1.5	—
5383a	—	215-44	—	1.1	—
5384	—	—	—	—	—
5385	—	18-46	—	1.2	—
5386	1268	232-69	—	1.8	—
5387	—	—	—	1.5	—
5388	—	215-48	—	1.5	—
5389	—	—	—	1.3	—
5390	—	—	—	1.5	—
5391	—	128-2	Ross 236	1.1	G8 (af), G8 (bk)
5392	—	—	—	—	—
5393	—	—	—	1.2	—
5394	—	—	—	1.8	—
5395	—	241-36	—	1.5	—
5396	—	—	—	1.6	—
5397	—	—	—	1.5	—
5398	—	233-47	—	1.1	K7 (bk)
5399 A*	—	—	CD -45°14980 A	1.3	K3 V (bf), K3 (af)
5399 B*	—	—	CD -45°14980 B	—	composite with LHS 5399 A
5400	—	242-30	—	1.5	—
5400aA*	—	29-21 A	BD +4°4994 A	1.1	K1 (af)
5400aB*	—	29-21 B	BD +4°4994 B	—	composite with LHS 5400aA

TABLE 5.1 — continued

LHS	Gliese	Giclas	Other Name	$m_{pg} - m_R$	Spectral Type and Reference
5401	—	157-50	—	1.1	—
5402	—	157-58	—	0.9	—
5403	—	—	—	1.3	—
5404	895.1	—	CD -46°14649	1.5	M0 (af)
5405*	895.2	29-38	—	0.0	DA (ag)
5406	—	171-1	Ross 247	1.5	M3 (af)
5407	—	—	—	1.5	—
5408	—	273-83	—	1.3	—
5409	—	30-22	—	1.3	—
5410	—	158-14	BD -10°6206	0.6	G4 (af)
5411	—	129-48	—	2.0	—
5412	—	30-31	Wolf 1050	1.1	K3: (af)
5413	—	—	—	2.3	—

TABLE 5.1 — continued

Legend for the spectral-type references:

aa = Ake & Greenstein 1980
 ab = Bartkevičius 1984
 ac = Bessell 1982
 ad = Bessell 1991
 ae = Bessell & Wickramasinghe 1979
 af = Bidelman 1985
 ag = Bidelman & Lee 1975
 ah = Boeshaar 1976
 ai = Boeshaar 1992
 aj = Bopp 1987
 ak = Carney 1979
 al = Cowley & Hartwick 1982
 am = Cowley, Hiltner, & Witt 1967
 an = Dahn, Liebert, Kron, Spinrad, & Hintzen 1977
 ao = Dawson & de Robertis 1988
 ap = Dawson & de Robertis 1988a
 aq = Dawson & de Robertis 1988b
 ar = Dawson & de Robertis 1989
 as = Doyle & Butler 1990
 at = Eggen 1971

TABLE 5.1 — continued

au	=	Eggen 1979
av	=	Evans, Menzies, & Stoy 1957
aw	=	Evans, Menzies, & Stoy 1959
ax	=	Giampapa & Liebert 1986
ay	=	Green, Margon, & MacConnell 1991
az	=	Greenstein 1984
ba	=	Greenstein 1986
bb	=	Hartwick, Cowley, & Mould 1984
bc	=	Hintzen 1986
bd	=	Hintzen & Jensen 1979
be	=	Hoffleit & Jaschek 1982; Hoffleit, Saladyga, & Wlasuk 1983
bf	=	Houk 1978; Houk 1988; Houk & Cowley 1975; Houk & Smith-Moore 1988
bg	=	Ianna & Bessell 1986
bh	=	Joy & Abt 1974
bi	=	this thesis.
bj	=	Klemola, Harlan, & Wirtanen 1981
bk	=	Lee 1984
bl	=	Liebert, Dahn, Gresham, & Strittmatter 1979
bm	=	Liebert, Dahn, Harris, Allard, & Kirkpatrick 1993
bn	=	Liebert, Dahn, & Monet 1988
bo	=	Liebert & Strittmatter 1977
bp	=	MacConnell 1983

TABLE 5.1 — continued

bq	= Mathioudakis & Doyle 1991
br	= McCook & Sion 1987
bs	= Oswalt, Hintzen, & Luyten 1988
bt	= Petit 1979
bu	= Przybylski & Kennedy 1965
bv	= Reid 1982
bw	= Rodgers & Eggen 1974
bx	= Roman 1955
by	= Sanduleak & Pesch 1988
bz	= Thé & Staller 1974
ca	= Turnshek, Turnshek, Craine, & Boeshaar 1985
cb	= Veeder 1974

TABLE 5.2
CROSS-LIST: GLIESE (GL/GJ) — LHS

GL #	LHS #	GL #	LHS #	GL #	LHS #
1	1	34 B	122	67 A	1284 A
2	1014	35	7	67 B	1284 B
3	1015	36	1154	68	1287
4 A	1016	38	126	69	1291
4 B	1017	40 A	1159	70	1290
4.2 A	1020	40 B	1160	71	146
4.2 B	1021	42	1163	73	1292
7	1026	45	128	75	1297
8	1027	46	129	78	1303
11 A	1040 A	47	1176	79	1307
11 B	1040 B	48	131	81 A	1314 A
12	1050	49	1179	81 B	1314 B
14	1053	50	5019	83.1	11
15 A	3	51	1183	84	149
15 B	4	52	136	84.1 A	1337
17	5	52.1	1193	84.1 B	1338
17.1	1061	52.2	137	84.2	1343
18	1067	53 A	8 A	85	150
19	6	53 B	8 B	85.1	1348
22 A	114 A	53.1 A	5027	86	13
22 B	115	53.1 B	5028	87	14
22 C	114 B	53.2	1199	88	1357
25 A	118 A	54	1208	90	1371
25 B	118 B	54.1	138	91	1361
26	119	55	1220	91.3	153
27	1116	56	1225	92 A	154 A
27.1	1122	56.1	1228	92 B	154 B
27.2	1124	56.3 A	1230	92.2	1383
28	1125	56.3 B	1229	93	1379
29	1123	57	141	94	1388
31.4	1141	58.2	5035	95	1387
31.5	1139	64	1270	100 A	1409 A
33	121	65 A	9	100 B	1409 B
34 A	123	65 B	10	100 C	1408

TABLE 5.2 — continued
CROSS-LIST: GLIESE (GL/GJ) — LHS

GL #	LHS #	GL #	LHS #	GL #	LHS #
101	155	144	1557	184	28
102	1417	146	1563	186.1 A	1724
105 A	15	147	1569	186.1 B	1727
105 B	16	147.1	1577	188	1736
109	1439	150	1581	190	203
114	1453	151	179	191	29
114.1	1452	154	5087	197	1753
116	159	155	1591	200 A	1754
118	160	155.1	1594	200 B	1755
118.1 A	1466	155.2	1613	200.1	1751
118.1 B	1467	155.3	184	203	1761
119 A	1475	156.2	1619	204	1763
119 B	1476	157.1	1616	204.2	1766
120	163	157.2	185	205	30
122	1505	158	21	207.2	1769
123	1496	160.2	1628	211	1774
124	166	162	1634	212	1775
125	1507	163	188	213	31
127 A	1515 A	164	1642	215	1782
127 B	1515 B	166 A	23	217	1783
129	169	166 B	24	217.2	210
130	167	166 C	25	218	1787
130.1 A	1522	167	1650	220	1794
130.1 B	1523	167.2	1651	223	1798
133	5072	169.1 A	26	223.2	32
134	1528	169.1 B	27	223.3	1797
136	171	170	1674	224	1803
138	172	171	1684	224.1	1796
139	19	172	1688	225.2 A	1804 A
141	1546	176	196	225.2 B	1804 B
142	1548	176.3	1701	226	215
143.2 A	1551	180	1712	226.1	1814
143.2 B	1552	181.1	199	228 A	1830 A
143.3	1554	183	200	228 B	1830 B

TABLE 5.2 — continued
CROSS-LIST: GLIESE (GL/GJ) — LHS

GL #	LHS #	GL #	LHS #	GL #	LHS #
229	1827	283 B	234	319 B	2042 B
231.3	1836	284	1939	319 C	2043
232	1846	285	1943	321	2047
234 A	1849	286	1945	324 A	2062
234 B	1850	288 A	237	324 B	2063
238	1855	288 B	237a	325 A	256
239	1858	289	239	325 B	257
240.1	1868	290	5130	326 A	2069
244 A	219 A	294 A	1959	326 B	2070
244 B	219 B	294 B	1960 A	328	255
246	1870	294 C	1960 B	330.1	2078
249	1874	295	242	331 A	2084
250 A	1875	296	1968	331 B	2083 A
250 B	1876	296.1	1982	331 C	2083 B
251	1879	298	1985	332 A	2093 A
257 A	222 A	300	1989	332 B	2093 B
257 B	222 B	301 A	1991 A	333	2085
257.1	1890	301 B	1991 B	336	2113
261	1892	301.1	1998	337 A	2114 A
262	1893	302	245	337 B	2114 B
263	1895	308 A	247 A	338 A	260
268 A	226 A	308 B	247 B	338 B	261
268 B	226 B	308.1	2018	338.1 A	264 A
268.2	1908	308.2	2017	338.1 B	264 B
269 A	1911 A	309	249	339.1	262
269 B	1911 B	310 A	251 A	340 A	2125 A
270	1912	310 B	251 B	340 B	2125 B
273	33	314 A	5139aA	341	2128
275.2 A	229	314 B	5139aB	343	2141
275.2 B	230 A	315	2033	345	268
275.2 C	230 B	316.1	2034	347 A	2145
280 A	233 A	317	2037	347 B	2146
280 B	233 B	318	253	349	2147
283 A	235	319 A	2042 A	351.1	2154

TABLE 5.2 — continued
CROSS-LIST: GLIESE (GL/GJ) — LHS

GL #	LHS #	GL #	LHS #	GL #	LHS #
352 A	2151 A	392 A	2267	428 A	2402 A
352 B	2151 B	392 B	2266	428 B	2402 B
353	2155	393	2272	429 A	2407
354 A	270 A	397	2279	429 B	2408
354 B	270 B	398	2285	429.2	2412
356 A	2156 A	398.1	2286	429.4	2417
356 B	2156 B	399	2295	430.1	2422
357	2157	401 A	289	431	2423
358	2166	401 B	290	432 A	308
359	2171	402	294	432 B	309
360	2176	403	295	433	2429
361	2173	405	2331	433.2 A	2437
362	2178	406	36	433.2 B	2436
363	2175	406.1	2334	435	2441
365	2180	411	37	436	310
366	2188	412 A	38	438	2447
367	2182	412 B	39	440	43
369	274	412.2	2354	442 A	311
370	2201	413.1	2358	442 B	313
373	2211	414 A	2367	443	314
375	2213	414 B	2366	445	2459
376	2216	414.1 A	2368	447	315
377	277	414.1 B	2369	448 A	2462 A
378	278	415	298	448 B	2462 B
379.2	5166a	416	2370	449	2465
380	280	421 A	2379	451	44
381	2230	421 B	2380	452 A	2470
383	2231	421 C	2378	452 B	2470a
383.1	2237	422	40	452.1	2472
386	2244	423 A	2390	453	319
388	5167	423 B	2391	454	5206
389 A	2253	423.1	2393	454.1	2494
389 B	2254	424	41	455	2497
390	2259	427	304	456	2515

TABLE 5.2 — continued
CROSS-LIST: GLIESE (GL/GJ) — LHS

GL #	LHS #	GL #	LHS #	GL #	LHS #
458.1 A	2524 A	506	349	542	2892
458.1 B	2524 B	506.1	2715	542.1 A	2891 A
459.3	2544	507 A	2716	542.1 B	2891 B
462	2548	507 B	2717	543	368
463	2551	508.2	2724	544 A	2894
465	45	508.3	2731	544 B	2895
467 A	328	509 A	2728 A	545	369
467 B	329	509 B	2728 B	545.1	2900
469	2565	512 A	5249	546	2903
469.1	2566	512 B	5250	547	2907
471	2570	512.1	2740	548 A	371
472	2577	513	351	548 B	372
473 A	333 A	514	352	549 C	2914
473 B	333 B	514.1	353	550.1	2918
475	2579	515	354	551	49
476	2582	518	46	552	373
477	2585	518.1	2766	553	374
478	2587	521.1	2773	553.1	2932
479	336	525	359	554	2931
480	338	526	47	555	2945
480.1	340	529	363	558	2948
482 A	2604	530	2814	559 A	50
482 B	2605	531	2817	559 B	51
486	341	533	2821	562	2974
491 A	2656 A	533.1	2820	563	2978
491 B	2656 B	534.3	2834	563.2 A	380
492	2661	536	2842	563.2 B	379
492	2663	537 A	2849	563.3	2983
493.1	2664	537 B	2850	565	383
494	2665	539	2859	567	5279
496.1	344	539.2	2870	568 A	2997 A
502	348	540	2865	568 B	2997 B
505 A	2713	540.2	2880	569.1	384
505 B	2714	541	48	570 A	387

TABLE 5.2 — continued
CROSS-LIST: GLIESE (GL/GJ) — LHS

GL #	LHS #	GL #	LHS #	GL #	LHS #
570 B	386 A	615	413	641	426
570 C	386 B	616	3171	642	3251
570.2	388	616.2	5315	643	427
576	3020	617 A	3175	644 A	428 A
579	391	617 B	3176	644 B	428 B
579.2 A	53	618 A	415	644 C	429
579.2 B	52	618 B	416	649	3257
580 A	393 A	618.4	3185	651	3260
580 B	393 B	620	3186	653	431
581	394	620.2	3188	654	432
582	395	622	3191	655	5324
585	396	623 A	417 A	656	3268
588	397	623 B	417 B	660 A	3269 A
589 A	399	626.2	3200	660 B	3269 B
589 B	400	627 A	3203	660.1	3271
590	3092	627 B	3204	661 A	433
592	3093	628	419	661 B	434
595	54	629	3209	663 A	437
597	404	629.2 A	3215	663 B	438
599 A	5299a	629.2 B	3219	664	439
599 B	5299b	629.3	3223	666 A	444
602	3127	630.1 A	421 A	666 B	445
603	408	630.1 B	422	667 A	442 A
606.2	3145	630.1 C	421 B	667 B	442 B
608	5307	631	3224	667 C	443
609	411	632.1	3226	667.1	3285
609.2	3148	633	3233	671	3281
610	5312	634	3235	672	441
611 A	3152	635 A	3234 A	672.1	3286
611 B	3150	635 B	3234 B	673	447
611.3 A	3156 A	637	3242	674	449
611.3 B	3156 B	637.1	3238	675	3287
612	3153	639.1	3244	682	451
612.1	3155	639.2	3248	684 A	3305 A

TABLE 5.2 — continued
CROSS-LIST: GLIESE (GL/GJ) — LHS

GL #	LHS #	GL #	LHS #	GL #	LHS #
684 B	3305 B	731	3417	771 B	5350aB
685	3306	732 A	469 A	772	3501
686	452	732 B	469 B	773 A	3502
687	450	739	3423	773 B	3503
690.1	3316	740	470	773.3 A	5351aA
692.1	3319	741	3428	773.3 B	5351aB
693	454	742	3424	773.6	3508
694	3321	745 A	3432	774 A	3513
695 A	3326	745 B	3433	774 B	3512
695 B	3325 A	747 A	471 A	775.1	3507
695 C	3325 B	747 B	471 B	776	484
695.1	3330	747.1	3437	776.1	3517
699	57	747.3	3439	777 A	3510
699.1	56	748 A	472 A	777 B	3509
700.2	3353	748 B	472 B	778	481
701	3356	748.2 A	3447	779	3515
702 A	458	748.2 B	3448	780	485
702 B	459	752 A	473	781	482
706	3363	752 B	474	781.1 A	3524
708.2	3373	754	60	781.1 B	3523
708.3	3374	756	3456	782	3526
711	3381	757	5347	783 A	486
712	464	759	3463	783 B	487
713 A	3379 A	762	3471	783.2 A	3529
713 B	3379 B	762.1	3466	783.2 B	3530
718	3392	763	3470	784	3531
720 A	3394	764	477	784.2 A	3533
720 B	3395	766 A	478 A	784.2 B	3532
723	3400	766 B	478 B	785	488
724	3403	767 A	3482	786	3527
725 A	58	767 B	3483	788	3537
725 B	59	768	3490	788.1	3542
728	3412	769	480	788.2	3540
729	3414	771 A	5350aA	790	3554

TABLE 5.2 — continued
CROSS-LIST: GLIESE (GL/GJ) — LHS

GL #	LHS #	GL #	LHS #	GL #	LHS #
791	3553	820 A	62	848.3 B	3765
791.2	3556	820 B	63	849	517
792	3559	821	65	851.1	3771
793	3558	825	66	851.2	3782
794	3562	825.1	3652	851.5	3781
794.2	3569	825.3	5368	852 A	3787
795 A	3568 A	825.4 A	3655	852 B	3788
795 B	3568 B	825.4 B	3656	853 A	3790 A
796	3570	826.1	3657	853 B	3790 B
798	496	826.2	3666	855	3802
800 A	497 A	827	3674	855.1	520
800 B	497 B	827.1	3675	858	3807
802	498	829	508	860 A	3814
804	3576	830	509	860 B	3815
806	3577	831 A	511 A	861	522
806.1 A	5358b	831 B	511 B	862	3817
806.1 B	5358a	832	3685	863	3828
807	3578	836	513	863.1 A	525 A
808	499	836.2	3687	863.1 B	525 B
809	3595	836.4	3702	863.1 C	525 C
810 A	501	836.5	3703	864	3833
810 B	500	836.9 A	3707 A	865	3839
811.1	502	836.9 B	3707 B	866 A	68 A
812 A	3602	838.1 A	3717	866 B	68 B
812 B	3601	838.1 B	3720	872 A	3851
812.1	503	838.6	5374	872 B	3852
813	3605	839	3727	873	3853
815 A	3609 A	842	3741	874	3855
815 B	3609 B	843	3744	875.1	3861
815 C	3609 C	845	67	876	530
816	3612	846	3745	877	531
817	61	847 A	3750	878	3871
818	3624	847 B	3751	878.1 A	3874
818.1	3635	848.3 A	3764	878.1 B	3875

TABLE 5.2 — continued
CROSS-LIST: GLIESE (GL/GJ) — LHS

GL #	LHS #	GJ #	LHS #	GJ #	LHS #
880	533	1001	102	1050	157
884	3885	1002	2	1051	1438
887	70	1003	103	1052	1442
889.1	3899	1004	1038	1053	18
891	3904	1005 A	1047 A	1055	1504
892	71	1005 B	1047 B	1057	168
894.4	3936	1006 A	107	1058	1540
894.5	3939	1006 B	108	1059	1541
895.1	5404	1007	1052	1060 A	1549
895.2	5405	1010 A	1065	1060 B	1550
895.4	544	1010 B	1066	1061	1565
896 A	3965	1012	1084	1062	20
896 B	3966	1013	113	1064 A	180
899	545	1014	117	1064 B	181
901	548	1017	1129	1064-	182
902	3994	1019	120	1065	183
904	3995	1022	124	1068	22
905	549	1024	1168	1070	1667
907	4015	1025	130	1072	1706
908	550	1026 A	1180	1073	198
908.2	4027	1026 B	1181	1074	1721
912	4047	1028	134	1077	205
913	4054	1029	135	1080	206
914 A	101 A	1031	1197	1087	212
914 B	101 B	1034	139	1088	1831
915	1005	1035	140	1092	220
		1037	1227	1093	223
		1039	1247	1097	1920
		1042	151	1099	1928
		1045	1366	1100	5127
		1046	154a	1101	1956
		1047 A	1393 A	1102 A	240
		1047 B	1393 B	1102 B	239
		1047 C	1392	1103 A	1951

TABLE 5.2 — continued
CROSS-LIST: GLIESE (GL/GJ) — LHS

GJ #	LHS #	GJ #	LHS #	GJ #	LHS #
1103 B	1952	1159 B	330	1214	3275
1104	241	1162	2595	1215	3277
1105	1963	1168	2695	1216	446
1110	2011	1169	2711	1218	3292
1111	248	1171	355	1219	448
1112	2022	1174	357	1220	3297
1114	2060	1178	2800	1221	455
1116 A	2076	1179 A	362	1222	3338
1116 B	2077	1179 B	361	1223	457
1118	258	1182	366	1224	3359
1119	2092	1185	2979	1225	460
1121	2111	1186	2995	1226 A	463 A
1123	263	1187	3006	1226 B	463 B
1124	2131	1188	389	1227	465
1125	2149	1189	3026	1230 A	3405
1128	271	1190	3039	1230 B	3404
1129	273	1192	3067	1231	3434
1131	2222	1193	3083	1232	3438
1132	281	1194 A	402	1235	476
1134	287	1194 B	403	1236	3457
1138	293	1195	405	1237	3465
1139	5180a	1197	3158	1238	3461
1140	2333	1198	412	1242	3479
1146	301	1199	3163	1245 A	3494 A
1147	2435	1200	55	1245 B	3495
1148	2443	1202	3210	1245 C	3494 B
1151	316	1203	3213	1248	3511
1154	2531	1204	3221	1250	5354
1155 A	2541	1207	3255	1251	493
1155 B	2542	1208	3254	1252	492
1156	324	1209	430	1253	3549
1157	2552	1210	3265	1254	494
1158	332	1212	3272	1255 A	3565 A
1159 A	331	1213	435	1255 B	3565 B

TABLE 5.2 — continued
CROSS-LIST: GLIESE (GL/GJ) — LHS

GJ #	LHS #	GJ #	LHS #	GJ #	LHS #
1255 C	3565 C	2005	1070	2138	3398
1255-	3592	2012	1126	2150	3579
1256	495	2028	1474	2151	5363
1257	3572	2034	1660	2155	3947
1258	3574	2049	1840		
1259	3598	2050	1865		
1263	3708	2062	1927		
1265	3776	2080	2273		
1266	3783	2085	303		
1268	5386	2086	2477		
1270	524	2090	2509		
1271	528	2093	334		
1273	3857	2095	2594		
1274	3859	2096	2600		
1275	529	2102	2754		
1276	69	2111	3034		
1277	532	2112	3064		
1281	538	2116	406		
1286	546	2121	3205		
1287	3988	2132	3335		
1289	4003	2135	3384		
1292	551	2137	5337a		

TABLE 5.3
CROSS-LIST: GICLAS (G) — LHS

G #	LHS #	G #	LHS #	G #	LHS #
1-2	1079	6-42	1616	10-25	305
1-9	1114	7-4	1593	10-29	2420
1-10	1118	7-12	1614	10-39	2434
1-17	1133	7-16	1617	10-42	2440
1-18	1137	7-17	185	10-45	2448
1-20	1141	7-39	1671	10-50	315
1-27	7	8-16	1644	10-53	2463
2-27	1212	8-22	1653	11-20	2455
2-33	1226	8-35	5095	11-31	2475
3-13	5039	8-41	1681	11-34	2494
3-14	1290	8-49	1692	11-35	320
3-17	1292	8-50	1695	11-36	2507
3-27	1309	8-54	5100	11-37	2510
3-29	1319	8-55	196	11-40	2515
3-33	11	8-57	1703	11-42	2518
3-36	12	9-7	2011	11-45 A	2524 A
3-39	1333	9-9	2027	11-45 B	2524 B
3-44	152	9-11	2029	12-4	1472
4-21	1403	9-13	2033	12-12	2482
4-29	156	9-19	5140	12-24	2526
4-43	1453	9-25	2059	12-25	2527
5-7	163	9-28	2060	12-26	2537
5-16	1509	9-38	2076	12-29	5213
5-22	169	9-39	2078	12-30	324
5-26	1527	10-2	2353	12-35	2547
5-34	1544	10-4	2365	12-37	2562
5-35	1545	10-8	2381	12-38	2565
5-43	1554	10-9	2383	12-39	2570
6-18	1568	10-10	2388	12-42	2575
6-24	1573	10-11	2392	12-43 A	333 A
6-25	1574	10-17	301	12-43 B	333 B
6-30	179	10-19	303	12-44	2582
6-31	1586	10-22	2406	12-45	5219
6-39	1610	10-23	2408	13-22 A	2531 A

TABLE 5.3 — continued
CROSS-LIST: GICLAS (G) — LHS

G #	LHS #	G #	LHS #	G #	LHS #
13-22 B	2531 B	15-26	3084	19-7	3255
13-26 A	2541	16-10	5301	19-13	431
13-26 B	2542	16-11	3123	19-14	432
13-43	2566	16-17	409	19-15 A	3269 A
13-44 A	2567	16-18	410	19-15 B	3269 B
13-44 B	2568	16-26	5309	19-16	3271
13-47	2586	16-29 A	3156 A	19-20	3278
13-51	2595	16-29 B	3156 B	19-21	3279
13-52	5225	16-32	3161	19-24	447
14-1	2634	16-34	3164	20-1	3289
14-2	5228	17-8 A	3172 A	20-9	3315
14-3	5229	17-8 B	3172 B	20-12	3323
14-4	2638	17-14	3194	20-22	3356
14-5	2641	17-19	3202	21-7	3374
14-17	5231	17-21	420	21-9	3377
14-19	2663	17-25	3215	21-10 A	463 A
14-35	2682	17-27	3219	21-10 B	463 B
14-39	2701	17-28	424	21-12	5337
14-42	2709	17-38	3246	21-18	3393
14-45	2715	18-1	3722	21-22	5339
14-55 A	5249	18-14	3742	21-23	467
14-55 B	5250	18-16	3745	22-1	468
14-56	2741	18-23	5378	22-5	3419
14-57	353	18-25	5379	22-10	470
14-58	354	18-31	3760	22-12	3426
15-1	3012	18-36	3773	22-14	3430
15-4	389	18-42	3795	22-15	3431
15-5	3020	18-45	3801	22-18 A	472 A
15-9	3030	18-46	5385	22-18 B	472 B
15-13	3034	18-48 A	3808	22-20	3444
15-15	3039	18-48 B	3809	22-21 A	3447
15-20	3067	18-51	522	22-21 B	3448
15-21	3070	18-56	3828	22-22 A	473
15-25	3078	19-4	426	22-22 B	474

TABLE 5.3 — continued
CROSS-LIST: GICLAS (G) — LHS

G #	LHS #	G #	LHS #	G #	LHS #
22-26	3457	27-14 B	3765	31-11	4030
23-5	3470	27-16	517	31-15	4046
23-8	3479	27-32	3825	31-17	4047
23-19	3505	27-36	3833	31-18	4049
23-24	3511	27-38	3840	31-31	1033
24-9	3532	27-45	3847	31-39	1052
24-10	3533	28-20	3860	31-43	5004
24-15	3550	28-21	3865	31-52	1082
24-16	3556	28-34	3897	31-53	1084
24-17	3557	28-39	3899	32-6	107
24-19	3561	28-41	3900	32-7	108
24-20	3564	28-43	537	32-9	5001a
24-23 A	3568 A	29-21 A	5400aA	32-30	5010
24-23 B	3568 B	29-21 B	5400aB	32-31	5011
25-1	3579	29-30	3943	32-35	117
25-3	3584	29-33	3947	32-36	5012
25-8	3593	29-35	3948	32-59	1168
25-9	3599	29-36	3952	33-35 A	1180
25-10	3604	29-38	5405	33-35 B	1181
25-11	3607	29-43	545	33-39	1195
25-16	3624	29-49	3979	33-40	1199
25-25	5368	29-51	3981	33-41	1200
25-32	3677	29-53	548	33-43	1204
26-5 A	3682 A	29-55	3986	33-49	1227
26-5 B	3682 B	29-66	4017	33-56	1246
26-7 A	511 A	29-68	550	34-2 A	5027
26-7 B	511 B	29-72	4020	34-2 B	5028
26-13	3689	29-73	4022	34-12	1221
26-14 A	3686	30-22	5409	34-15	139
26-14 B	3688	30-31	5412	34-32	5035
26-21	3696	30-38	1009	35-8	1289
26-29	3706	30-45	1022	35-24	1335
26-30	3708	30-48	104	35-30	5051
27-14 A	3764	30-55	1050	35-35	1366

TABLE 5.3 — continued
CROSS-LIST: GICLAS (G) — LHS

G #	LHS #	G #	LHS #	G #	LHS #
36-22	1410	41-18	2094	46-34	267
36-24	1417	41-26	5144	46-35	2129
36-28	1428	41-35	2133	46-40	2140
36-31	1439	41-37	2141	47-5	2048
36-41	1468	41-43	2154	47-9	2063
36-48	1485	42-17	2173	47-26	2113
37-8	159	42-19	2184	47-28	5146b
37-26	1501	42-24	2206	47-31	2121
37-32	1525	42-25	2207	48-15	5152
37-34	1533	43-3	2194	48-20	2149
37-40	174	43-22	5164	48-21	2161
37-45	1571	43-24	2217	48-25	2164
38-1	173	43-34	2234	48-27	2168
38-3	1562	43-36	2235	48-29	2169
38-10	1579	43-54	2273	48-30	2170
38-11	1585	44-19	5171	48-42	2198
38-12	1587	44-24	2283	48-52	5159
38-17	1605	44-25	2284	49-18	2163
38-25	187	44-27	2285	49-20	2171
38-26	1634	44-40	294	49-23	2181
38-30	1659	44-42	295	49-27	5158
39-9	1667	44-43	2320	49-32	2212
39-14	5096	44-46	2325	50-4	1943
39-32	1698	45-20	36	50-5	1949
39-37	1705	45-27	296	50-6	1950
39-40	1710	45-33	2348	50-8	5128
39-41	1715	45-39	2374	50-16	1972
39-42	1716	46-1 A	2042 A	50-22	35
39-43	1719	46-1 B	2042 B	51-6	1998
39-44	1722	46-2	2043	51-10	2007
40-2	1966	46-4	2050	51-13 A	247 A
40-3	1977	46-5	2056	51-13 B	247 B
40-7 A	5133	46-9	255	51-15	248
40-7 B	5134	46-30	2119	51-16	2022

TABLE 5.3 — continued
CROSS-LIST: GICLAS (G) — LHS

G #	LHS #	G #	LHS #	G #	LHS #
51-27	2057	60-55	2664	63-53	47
52-15	2019	60-57	2665	63-54	2800
53-28	2230	60-67	2681	63-60	2809
53-38	2242	61-21	343	64-7	2770
53-40	2251	61-26	2660	64-24	2799
54-23	5167	61-33	2680	64-26	2804
54-26	2260	61-35	347	64-29	2832
54-29	2271	61-41	2695	64-31	2835
54-30	2281	61-44	2705	64-35	2842
55-16	2265	62-15	345	64-42	2857
55-24	2272	62-18	2699	64-47	2863
55-35	2295	62-27	5243	64-48	2869
55-37	2298	62-33	2722	64-52	2875
55-44	2321	62-34	2725	64-60	2883
56-29	2389	62-44	2747	65-2	2801
56-34	5191	62-49	2754	65-12	2821
56-41	2409	62-53	46	65-19	2830
56-44	2415	62-54	2766	65-22	2846
56-50	2442	62-56	5253	65-33	2873
57-21	5198	62-60	2773	65-35	2878
57-24	5200	62-66	2787	65-39	366
58-14	2304	63-5	2689	65-47	2907
58-22	5177	63-6	2690	65-49	2913
58-25	2318	63-9	2693	66-5	2941
58-40	2344	63-18 A	2713	66-6	2942
59-3	5211	63-18 B	2714	66-7	2944
59-9	2538	63-31	5251	66-10	2949
59-14	2549	63-32	351	66-18	2956
60-23	2593	63-34	352	66-21	2965
60-24	338	63-40	2765	66-22	2968
60-27	2616	63-43	2767	66-31	2983
60-32	341	63-45	2774	66-32	2984
60-33	2636	63-48	5254	66-41	2999
60-54	2661	63-52	359	66-55	5285

TABLE 5.3 — continued
CROSS-LIST: GICLAS (G) — LHS

G #	LHS #	G #	LHS #	G #	LHS #
66-65	3024	71-51	5048	77-45	1532
67-8	3838	72-21	1275	77-47	1539
67-15	528	72-23	5037 _a	77-48	1540
67-23	3857	73-35	14	77-49	1546
67-30	3867	73-37	1369	77-50	1547
67-37	533	73-67	1419	77-61	1555
67-42	3892	73-70	15	77-64	1561
68-8	543	73-71	16	77-65	1566
68-16	3945	74-4	1348	77-66	5074
68-22	3960	74-7	151	78-7 A	1458 A
68-24 A	3965	74-10	1368	78-7 B	1458 B
68-24 B	3966	74-14	1388	78-11	1486
68-31	3982	74-18	1392	78-18	1499
68-38	4007	74-19 A	1393 A	78-19	1507
69-10	119	74-19 B	1393 B	78-26	170
69-16	120	74-21	1400	78-31	1528
69-18	1138	74-43	1448 _a	78-35	5073
69-26	1156	74-52	1483	78-42	177
69-31	5016	75-9	1404	79-18	1520
69-38	1172	75-30	1426	79-32	1538
69-40	1175	75-37	1435	79-54	5075
69-47	135	75-39	1442	79-59	178
69-65 A	1237	75-43	1457	79-69	1589
69-65 B	1236	75-44	5061	79-75	1607
70-28	130	75-45	1460	80-15	1577
70-44	1213	75-47	161	80-22	1594
70-50	1229	75-57	1487	80-23	1598
70-51	1230	76-20	1429	80-24	1599
70-55 A	1240	76-48	5064	80-29	1608
70-55 B	1241	76-58	1496	80-38	5088
71-24	1272	76-62	1504	81-21	1674
71-45	1318	76-66	1512	81-25	1675
71-47	1324	77-31	168	81-30	1696
71-50	5049	77-41	1526	81-38	1708

TABLE 5.3 — continued
CROSS-LIST: GICLAS (G) — LHS

G #	LHS #	G #	LHS #	G #	LHS #
81-39	198	87-36	1914	99-10	206
81-42	1714	87-37	1917	99-11	1762
82-4	1645	87-38	1919	99-12	1763
82-5	1646	87-48	1934	99-14	1766
82-6	1649	88-9	1899	99-15	30
82-9	1655	88-43	1933	99-16	5107
82-13	1661	88-48	1942	99-24	1776
82-25	1675	89-7	5123	99-26	1779
82-37	1689	89-19	33	99-27	1778
83-22	1686	90-25	241	99-31	1780
83-46	1718	90-34	1961	99-33	211
83-53	1732	90-36	5131	99-43	1798
84-42	5101	90-39	1975	99-44	32
84-45 A	1754	91-11	238	99-45	1800
84-45 B	1755	92-34	3493	99-47	212
85-19	1706	92-40	3501	100-44	1794
85-42	1738	93-25	3695	100-54 A	1811
85-44	1740	93-40	3717	100-54 B	1812
85-48	1743	93-41	3720	101-16	1813
85-54	1745	95-30	1541	101-30	1835
86-27	1742	95-54	1588	101-42	1851
86-39	1759	95-57 A	180	102-22	31
86-44	1765	95-57 B	181	102-33	1790
86-45	5108	95-59	182	102-34	1791
87-3	1866	96-28	1746	102-53 A	1830 A
87-4	1867	96-50	209	102-53 B	1830 B
87-5	1869	96-51	1783	103-34	5116
87-7	1870	96-52	1784	103-46	218
87-8	220	97-42	1761	103-51	1862
87-12	1879	97-55	5110	104-37	1846
87-15	1884a	98-25	1789	104-49	1858
87-26 A	226 A	98-38	1814	104-50	1860
87-26 B	226 B	98-46	1824	105-23	216
87-33	1912	98-49	1828	105-30	1838

TABLE 5.3 — continued
CROSS-LIST: GICLAS (G) — LHS

G #	LHS #	G #	LHS #	G #	LHS #
105-41	5117	112-50	1951	118-51	5168
105-46	1857	113-24	5136	118-61	2270
106-25	1819	113-40	2017	118-66	2274
106-26	1820	114-13	2040	119-11	2278
106-35	5113	114-19	2055	119-22	2290
106-49 A	1849	114-25	2080	119-25	2292
106-49 B	1850	114-26 A	2082 A	119-29	2307
107-27	1874	114-26 B	2082 B	119-32	2308
107-32	5121	115-4	2016	119-36	293
107-34	1880	115-5	2014	119-37	2317
107-36	1883	115-10	2028	119-42	5181
107-42	1890	115-11	5139	119-52	37
107-55	1903	115-18	2041	119-57	297
107-56	1906a	115-23	2047	119-59	2366
107-58	5122a	115-27	2053	119-60	2367
107-63	1913a	115-39	2081	119-64	2373
107-67	1915	115-42	2092	119-65	2382
107-69	229	115-47	2097	120-30	2387
107-70 A	230 A	115-50	2103	120-32	2394
107-70 B	230 B	115-57	2111	120-45	304
108-37	5120	115-63 A	2117	120-49	5192
108-40	1884	115-63 B	2118	120-51	2411
108-43	1886	116-23	2131	120-56	2418
108-48	1891	116-36	2155	120-57	2422
109-16	1861	116-42	2180	120-61	2431
109-35	223	116-46	2183	120-67	5195
110-17	1871	116-48	2185	120-68	310
111-18	1931	116-61	2203	121-12	2450
111-45	1958	116-70	5161	121-14	2451
111-47	1963	116-71	5162	121-27	2467
111-61	1988	116-77	2220	121-43	2495
112-21	1920	117-61	276	121-45	2497
112-27	1928	118-48	2245	121-68	2529
112-28	232	118-50	2248	121-77	2544

TABLE 5.3 — continued
CROSS-LIST: GICLAS (G) — LHS

G #	LHS #	G #	LHS #	G #	LHS #
122-2 A	2368	124-51	2940	129-48	5411
122-2 B	2369	124-57	2957	130-4	4003
122-30	2426	124-72	2979	130-8	4008
122-34	2430	124-76	2982	130-11	4018
122-36	2432	124-81	2985	130-15	4019
122-40	2443	125-4	3450	130-24	4044
122-42	2449	125-6	3458	130-25	4045
122-45	2453	125-13	3467	130-36	1004
122-46	2458	125-24	3473	130-43	103
122-49	316	125-27	3478	130-49	1028
122-51	44	125-31 A	3482	130-50	1029
122-62	2491	125-31 B	3483	130-53	1037
122-64	5207	125-35	3489	130-56	1041
122-66	2498	125-45	3497	130-57	1043
122-67	321	125-55	3509	130-61	1054
122-68	2501	125-62	5354	130-68	1068
123-26	2548	126-4	508	131-66	1073
123-29	2556	126-5	3680	132-14	1120
123-33	5216	126-27	3703	132-15	1125
123-55	2613	126-60	3767	132-32	1153
123-60	2633	126-62 A	3770 A	132-35	1161
123-61	2637	126-62 B	3770 B	132-36	1162
123-63	5230	127-11	3781	132-40	5017
123-74	2654	128-2	5391	132-52	1185
123-82	2666	128-3	3854	132-57	137
123-84	2672	128-7	528	132-61	1211
124-23	368	128-8	3861	133-7	1242
124-25	369	128-10	3862	133-8	1244
124-24 A	2894	128-11	3869	133-21	1266
124-24 B	2895	128-34	536	133-29	1285
124-26	5270	128-48	3931	133-39	1296
124-27	2899	128-61	3946	133-47	5044
124-29	2904	128-73	3968	134-1	1343
124-47	374	129-47	551	134-22	153

TABLE 5.3 — continued
CROSS-LIST: GICLAS (G) — LHS

G #	LHS #	G #	LHS #	G #	LHS #
134-24	1383	137-82	5313	141-25	5340
135-10	2844	138-8	3163	141-41	3415
135-13	2853	138-25	418	141-42	3416
135-35	2888	138-34 A	3203	141-48	5343
135-44	2905	138-34 B	3204	142-11	3488
135-47	2908	138-37	3210	142-12	3442
135-56	373	138-39	3213	142-52	479
135-61	2937	138-43	3221	143-20	5352
135-67	376	138-44	3225	143-26	3519
136-13	2974	138-49	3230	143-34	3529
136-14	2977	138-56	3236	143-35	3530
136-27	2995	138-59	425	143-41	3536
136-39	3005	138-64	3240	143-48	3544
136-47	3011	138-67	3251	144-25	495
136-69	3027	139-12	3265	144-29	3573
136-74	5290	139-21	3275	144-34	3576
136-76	3033	139-29	3277	144-40	3587
136-77	3036	139-39	448	144-44	3598
136-78	3037	139-48	3304	144-50	3610
136-85	3046	140-11	3329	144-58	3619
136-93	5294	140-16	3336	144-60	3621
136-102	3068	140-19	3338	144-61	3622
136-103	396	140-24	57	144-62	3625
137-8	3073	140-29	3349	145-23	3641
137-22	3083	140-37	5332	145-35	3651
137-25	400	140-39	3357	145-37	3667
137-26	399	140-46	3366	146-6	278
137-35	3101	140-47	3369	146-11	2225
137-60	3128	140-49	3373	146-15	2238
137-66	5304	140-52	3375	146-23	2249
137-71	3136	141-4	464	146-35	2268
137-74	3142	141-8	3387	146-39	2279
137-78	411	141-9	3388	146-58	287
137-81	5311	141-24	3399	146-72	2327

TABLE 5.3 — continued
CROSS-LIST: GICLAS (G) — LHS

G #	LHS #	G #	LHS #	G #	LHS #
146-75	2332	152-49	3115	157-50	5401
147-11	2337	152-50	3117	157-54	3939
147-13	2340	152-69	5306	157-58	5402
148-23	2481	153-27	412	157-59	3941
148-66	5217a	153-57	3205	157-64	3953
149-33 A	2674 A	153-58	419	157-69	3967a
149-33 B	2674 B	153-59	3207	157-77	546
149-40	5238	154-8	3316	157-90	3993
149-44	2679	154-9	3320	157-93	4005
149-70	2711	154-19	3327	158-2	4036
149-81	350	154-34	3340	158-14	5410
149-88	2733	154-36 A	3345 A	158-15	4051
149-94	355	154-36 B	3345 B	158-22	1006
150-9	2749	154-41	3352	158-27	2
150-15	2761	154-44	3359	158-31	1023
150-25	2771	154-51	5334	158-45	1044
150-34	2792	155-15	3384	158-50 A	1047 A
150-36	2795	155-26	3396	158-50 B	1047 B
150-54	2837	155-27	466	158-53	109
150-74	5268	155-29	3398	158-86	1086
151-6	2993	155-30	3400	158-87	1087
151-13	5283	155-33	3403	158-94	1091
151-20	3015a	155-40	5342	158-95	113
151-28	5289a	156-31 A	68 A	158-103	1106
151-34	392	156-31 B	68 B	159-3	1302
151-41	3049	156-43	3846	159-34	1332
151-45	3056	156-57	530	159-46	1358
151-46	394	156-63	3872	159-50	1365
151-49	3062	156-64	3875	159-53	1372
152-31	3076	156-65	3874	160-5	20
152-32	3077	157-32	3913	160-17	5079
152-37	3086	157-33	3914	160-19	1582
152-40	3093	157-35	3917	160-22	1590
152-46	3110	157-44	3929	160-28	183

TABLE 5.3 — continued
CROSS-LIST: GICLAS (G) — LHS

G #	LHS #	G #	LHS #	G #	LHS #
160-35	5087	164-72	5245	167-33	3054
160-42	186	164-73	2735	167-34	3058
160-43	1624	165-7	1745	167-47	3080
160-53	5092	165-17	2763	167-51	3091
160-60 A	24	165-25	2784	168-14	3124
160-60 B	25	165-29	2791	168-20	3138
161-24	2137	165-38	2833	168-32	3158
161-25	2138	165-40	2845	168-33	5314
161-30	2142	165-47	364	169-6	3192
161-33	2145	165-48	2861	169-7	3193
161-34	2146	165-51	5266	169-15	5317
161-38	5153	165-53	5267	169-18	5318a
161-51	2158	165-60	2886	169-20	3226
161-52	2159	165-61	2887	169-34	3254
161-74	2186	165-62	2890	169-38	3257
161-80	274	166-22	2903	170-12	430
162-32	2240	166-25	2915	170-17	5324
162-38	2244	166-27	371	170-19	3266
162-52	2259	166-28	372	170-37	3288
163-23	2328	166-29	2918	170-50	3302
163-27	2333	166-33	2925	170-55	452
163-52	2356	166-36	2947	170-61	3319
163-59	299	166-38	2948	170-62	3324
163-74	2393	166-40	2962	171-1	5406
164-12	2612	166-44	5278	171-5	3980
164-13	2614	166-52	2996	171-8	3991
164-17	2624	166-53 A	2997 A	171-10	549
164-53	2703	166-53 B	2997 B	171-11	4002
164-55	2708	166-57	388	171-19	4015
164-64	2716	166-58	3007	171-27	4043
164-65	2717	167-12	3015	171-29	4054
164-68	2724	167-19	391	171-33	4056
164-71 A	2728 A	167-22	3026	171-39	1014
164-71 B	2728 B	167-32	3052	171-40 A	1016

TABLE 5.3 — continued
CROSS-LIST: GICLAS (G) — LHS

G #	LHS #	G #	LHS #	G #	LHS #
171-40 B	1017	176-3	2336	179-57	3122
171-44	1053	176-4	5185	180-8	3129
171-47	3	176-11	38	180-9	3130
171-48	4	176-12	39	180-17	3137
171-51	1062	176-34	2403	180-23	3146
172-11	1104	176-40	307	180-27	3150
172-14	1111	176-53	312	180-31	3153
172-30	1169	177-4	2651	180-33	3155
173-14	1277	177-13	2670	180-56	3201
173-34	1330	177-25	2686	180-57	3200
173-37	5050	177-27	2702	180-58	3199
174-1	155	177-44	2762	180-61	5318
174-14	1446	177-48	2772	181-16	5323
174-18	1473	177-51	357	181-24	3261
174-19	1475	177-52	2777	181-30	3267
174-20	1476	177-53	2778	181-33	3276
174-27	1488	177-57	2785	181-37	3282
174-31	1495	177-58	2789	181-39	3281
174-33	1498	177-61	5256	181-42 A	5327
174-38	1518	178-10	2884	181-42 B	5328
174-41 A	1522	178-18	2901	182-19	3312
174-41 B	1523	178-19	2902	182-34	3350
175-7	5085	178-21	5271	182-35	3353
175-8	1597	178-31	2931	182-36	457
175-13	1618	178-37	2943	183-5	3333
175-14	1621	178-44	2963	183-23	3355
175-17	5091	178-55	2998	183-26	3361
175-19	1642	179-9	3016	183-28	3364
175-34 A	26	179-20	3035	183-31	3368
175-34 B	27	179-24	5292	183-32	3371
175-37	1683	179-25	3051	183-44	3392
175-39	1684	179-33	3075	184-19	3405
175-42	1688	179-43 A	402	184-29	3412
175-45	1697	179-43 B	403	184-35	3417

TABLE 5.3 — continued
CROSS-LIST: GICLAS (G) — LHS

G #	LHS #	G #	LHS #	G #	LHS #
184-42	3425	189-28	3835	193-67	1947
184-48	3432	189-38	3859	193-70	1948
184-49	3433	189-53	3879	193-75	1954
185-8	3435	190-13	3903	193-81	1964
185-12	3445	190-17	3923	193-83	1973
185-13	3446	190-20	3936	194-7	1976
185-18	476	190-22	3942	194-19	1996
185-19	3456	190-24	3951	194-22	2000
185-37 A	478 A	190-26	3957	194-41	2054
185-37 B	478 B	191-11	1702	194-50	259
186-7	3506	191-15	1721	194-57	2109
186-11	481	191-19	28	195-17	260
186-31	3562	191-21	1733	195-18	261
186-35	3567	191-29	1757	195-19	262
187-8	3589	191-30	1758	195-22	265
187-9	3605	191-48	1772	195-36	2175
187-28	5367	191-50	1773	195-46	5157
187-30 A	3637 A	191-51	1775	195-47	2205
187-30 B	3637 B	191-53	1786	195-52 A	5163 A
187-39	3653	192-8	1799	195-52 B	5163 B
187-43	3673	192-13	1805	195-57	2224
188-15	3698	192-14	1806	195-59	2232
188-24	3704	192-15	1809	196-9	280
188-26	3713	192-26	1848	196-13	2237
188-28	3725	192-30	1854	196-22	2262
188-30	3731	192-32	1856	196-23	2263
188-32	5375	192-39 A	1864 A	196-24	5170
188-33	5376	192-39 B	1864 B	196-28	2275
188-37	3743	192-58	1882	196-29	2277
188-46	3771	193-27	224	196-31	5171a
188-51	3784	193-38	1907	196-45	2312
189-11	3796	193-59	1940	196-51	2331
189-12	3797	193-60	1941	196-58	2349
189-23	3823	193-62	1946	197-14	2410

TABLE 5.3 — continued
CROSS-LIST: GICLAS (G) — LHS

G #	LHS #	G #	LHS #	G #	LHS #
197-15	2413	201-7	2957	207-16 A	471 A
197-16	2414	201-27	3006	207-16 B	471 B
197-32	2461	201-33	5287	207-18	3434
197-38	2486	201-37	3031	207-30	3459
197-47	2522	201-48	3069	208-22	3465
198-19	2503	201-55	3082	208-39	3485
198-58	2571	202-32	3166	208-44 A	3494 A
199-7	2546	202-36	5315	208-44 B	3494 B
199-17 A	331	202-45 A	417 A	208-45	3495
199-17 B	330	202-45 B	417 B	209-33	3559
199-24	2574	202-61	3214	209-41	3577
199-31	2584	202-68	5319	210-19	491
199-33	2588	203-42	3262	210-29	5357
199-35	2617	203-51 A	433	210-31	3574
199-41	2639	203-51 B	434	210-38	3591
199-42	2640	203-52	435	210-48 A	3609 A
199-45	2646	203-63	446	210-48 B	3609 B
199-51	2659	203-71	3298	211-15	3646
199-60	2684	204-24	3313	212-12	5362
199-64	2700	204-27	3321	212-21	5364
199-72	2751	204-32	3334	212-24	5365
200-14	2839	204-39	3343	212-29	3638
200-15	2840	204-48	3365	212-37	5370
200-16 A	2849	204-57	461	212-39	3678
200-16 B	2850	204-58	462	212-56	3705
200-24	2882	205-5	3363	212-59	3711
200-29	2889	205-18	5335	213-9	3700
200-31	2897	205-20	3385	215-2	3693
200-32	2898	205-30	3394	215-20	3727
200-38	2914	205-32	3395	215-21	3729
200-46	2936	205-40	3420	215-22	3730
200-58	2973	205-55	3429	215-44	5383a
200-59	2990	206-38 A	3401	215-46	3810
200-62	384	206-38 B	3402	215-48	5388

TABLE 5.3 — continued
CROSS-LIST: GICLAS (G) — LHS

G #	LHS #	G #	LHS #	G #	LHS #
215-49	3818	224-57	3044	231-17	3590
215-50	524	224-74	3089	231-19	3595
216-16	3853	224-79	3105	231-27	64
217-1	3930	225-40	3139	231-39	3649
217-11	544	225-42	5305	231-42	3670
217-18	4005a	225-43	5307	231-44	3676
217-27	1002a	225-57	3175	231-53 A	3699 A
217-37	1038	225-58	3176	231-53 B	3699 B
217-38	1039	225-65	3212	232-54	3758
217-55	1088	225-67 A	421 A	232-69	5386
217-56	5009	225-67 B	421 B	232-71	3812
217-59	1105	225-68	422	232-75 A	3814
218-17	126	226-9	3208	232-75 B	3815
219-5	1234	226-45	3264	233-17 A	525 A
221-1	1418	226-62	3293	233-17 B	525 B
221-5	18	226-64	3299	233-17 C	525 C
221-12	1553	226-66	3306	233-31	3871
221-20	5080	226-107	1067	233-47	5398
221-21	5081	227-28	3380	234-33	2008
221-22	1596	227-29	465	234-35	2018
221-26	1623	227-30	3386	234-37	250
221-28	1631	227-46	58	234-38 A	251 A
222-2	1643	227-47	59	234-38 B	251 B
222-4	1677	228-12	3341	234-42	2032
222-11	215	229-16	3410	234-43	2038
223-22	2788	229-33	3466	234-45	252
223-27	5257	229-35	3472	234-47	2051
223-35	2824	230-18	3499	234-48	2066
223-38	2827	230-25	3518	234-51	2086
223-43	2864	230-26	482	234-52	2087
223-74	2952	230-37	3543	234-54	2102
224-9	2929	230-40	3549	234-55	2105
224-39	3009	230-42	494	235-35	2176
224-44	3018	231-13	498	235-36	2178

TABLE 5.3 — continued
CROSS-LIST: GICLAS (G) — LHS

G #	LHS #	G #	LHS #	G #	LHS #
235-40	2191	240-38	3258	242-81	1344
235-46	2197	240-63	450	243-30 A	114 A
235-48	2202	240-64 A	5330	243-30 B	115
235-49	2211	240-64 B	5331	243-30 C	114 B
235-55	2222	240-72	455	243-48	1170
235-62	2239	241-1	3783	243-50	1176
236-22	2250	241-12	3829	243-52	1179
236-34	283	241-13	3830	243-55	1183
236-46	2334	241-24	3858	243-59	5026
236-65	41	241-31	3877	243-60	136
236-80	42	241-32	3881	243-62	1198
237-37	5203	241-33	3882	243-63	1206
237-38	2488	241-36	5395	243-67	5030
237-54	2536	241-42	3894	244-31	1283
237-56	5212	241-44	534	244-33	1291
237-62 A	5215 A	241-45	535	244-41	1313
237-62 B	5215 B	241-57	3967	244-42	1312
237-63	2551	241-66	4004	244-56	1371
237-68	2576	241-68	4006	244-59	5051b
237-81	2649	241-76 A	1040 A	244-60	1397
237-88	2677	241-76 B	1040 B	245-25	1254
238-21	5234	242-30	5400	245-34	1310
238-26	2687	242-32	3938	245-45	1350
238-35	2727	242-44	4052	245-61	1478
238-39	2748	242-45	4053	245-65	1505
238-42	2752	242-51	1065	245-71	5072
238-54	2820	242-52	1066	246-13	1455
238-55	2819	242-55	5006	246-14	1456
239-21	2946	242-56	5007	246-22	1494
239-29	2976	242-60	1101	246-30	1521
239-32	2991	242-64	5013	246-32	1530
239-48	3057	242-73	1167	246-38	175
239-58	3103	242-76	131	246-44	1583
240-25	3238	242-77	1182	246-49	1602

TABLE 5.3 — continued
CROSS-LIST: GICLAS (G) — LHS

G #	LHS #	G #	LHS #	G #	LHS #
246-53	1613	252-17	2030	256-20	3017
247-14	1637	252-19	2031	257-20	404
247-15	1638	252-24 A	256	258-28	3351
247-20	5093	252-24 B	257	258-33	3376
247-22	1679	252-25	2088	259-12	3309
247-23	1680	252-26	2091	259-15	3297
247-45	1728	252-27	2101	259-17	3318
247-50	1741	252-30 A	264 A	259-21	56
248-10	1619	252-30 B	264 B	259-22	3344
248-12	1629	252-31	2124	259-31	3391
248-18	1664	252-33	2126	259-39	5345
248-19	1663	252-44	2188	260-1	460
249-2	1752	253-2	1962	260-15	3424
249-18	1782	253-6	1956	261-1	3436
249-27	213	253-18	2095	261-6	3461
249-28	214	253-21	2123	261-19	3527
249-32	1808	253-23	5150	261-22	3545
249-36	1817	253-31	2196	261-23	3547
249-46	217	253-37	2291	261-28 A	3565 A
249-51	1853	253-40	5180a	261-28 B	3565 B
250-19	5119	253-49	2404	261-28 C	3565 C
250-29 A	221 A	253-50	2405	261-29	3592
250-29 B	221 B	253-59	5215a	261-35	5361
250-31	1885	254-16	2359	261-38	3631
250-32	1888	254-24	2424	261-39	3642
250-38	1897	254-27	2439	261-45	3687
251-16	1865	254-29	2459	261-46	514
251-43	5126a	254-35	2513	262-15	3558
251-44	236	255-17	2610	262-27	3586
251-51	1983	255-49	2866	263-21	3822
251-52	1984	255-50	2868	264-17	3749
251-58	1993	255-51	2865	265-8	140
252-10	2001	255-52	2922	265-34	5326
252-13	2025	256-19	5289	266-1	4037

TABLE 5.3 — continued
CROSS-LIST: GICLAS (G) — LHS

G #	LHS #	G #	LHS #	G #	LHS #
266-8	4048	268-38	1140	271-163	1301
266-20	552	268-53	1154	271-168	1303
266-21	4055	268-60	1159	272-4	1238
266-36	1011	268-76	1165	272-15	5033
266-42	5001	268-77	127	272-58	1271
266-55	1025	268-110	134	272-61 A	9
266-57	1026	268-135	138	272-61 B	10
266-72	1045	268-145	1224	272-36	142
266-73	1046	268-146	1225	272-81	1286
266-87	1057	269-49	1163	272-102	5037
266-88	110	269-63	129	272-114	1307
266-89	111	269-67	1171	272-137	1325
266-132	1099	269-87	1186	272-148	149
266-135	1102	269-106	1197	273-1 A	540 A
266-152	1124	269-112	1207	273-1 B	540 B
266-157	1126	269-125	1217	273-15	3932
267-11	4058	269-138	1232	273-83	5408
267-16	1003	269-140	5031	273-95	3990
267-18	1008	269-160	1247	273-130	4009
267-23	1012	269-161	1249	273-134	4011
267-25	1	269-166	1251	273-137	4014
267-45	1036	269-171	1253	273-147	4021
267-58	1048	270-23	1112	273-151	4032
267-106	1077	270-26	1113	273-183	4050
267-107	1078	270-28	1115	274-53	1255a
267-121	1092	270-39	1128	274-83	1278
267-128 A	1097	270-118	5019	274-90	1293
267-128 B	1098	270-154	1203	274-106	5043
267-138	1108	270-155	1205	274-136	1321
267-141 A	1110 A	270-188	1228	274-143	1329
267-141 B	1110 B	271-34	1231	274-145	1337
267-149	1119	271-84	1256	274-146	1338
267-157	1127	271-115	1270	274-149	1339
267-168	1144	271-130	5038	275-6	3898

TABLE 5.3 — continued
CROSS-LIST: GICLAS (G) — LHS

G #	LHS #
275-13	3904
275-14	3905
275-29	3927
275-46	3948a
275-83	4000
275-90	72
275-92	73
275-106	4016
275-121 B	4039
275-121 A	4040

TABLE 5.4
CROSS-LIST: COMMON NAME — LHS

Common Name	LHS #
Achird	122/123
Als[c]hai[r]n	5350aAB
Altair	3490
A[l]thafi	477
Alula Australis/El Acola	2390/2391
Arcturus	48
Caph	1027
Chara	2579
Chort	2858
Denebola	2462 AB
Fornacis	1515 AB
Gienah Cygni	5358b
Keid/Kied	23/24/25
Marfak ^a	8 AB
Pollux	1945
Porrina	2604/2605
Procyon	233 AB
Proxima Centauri	49
Rana	1557
Rigel Kentaurus	50/51
Sirius	219 AB
Talit[h]a	2083 AB/2084
Zavijava	2465

^a This name is not unique to LHS 8 AB.

TABLE 5.5
CROSS-LIST: BAYER DESIGNATION — LHS

Bayer	LHS #	Bayer	LHS #	Bayer	LHS #
α Aql	3490	σ^2 Eri B	24	ζ^1 Ret	171
β Aql A	5350aA	σ^2 Eri C	25	ζ^2 Ret	172
β Aql B	5350aB	τ^6 Eri	1591	κ Ret A	1551
λ Aur	1753	χ Eri A	1314 A	κ Ret B	1552
α Boo	48	χ Eri B	1314 B	ϵ Sco	3244
β Cas	1027	α For A	1515 A	γ Ser	408
η Cas A	123	α For B	1515 B	η Ser	3381
η Cas B	122	ϵ For	1489	δ Tri A	154 A
μ Cas A	8 A	β Gem	1945	δ Tri B	154 B
μ Cas B	8 B	ζ Her A	3234 A	ζ Tuc	5
α Cen A	50	ζ Her B	3234 B	θ UMa A	270 A
α Cen B	51	μ Her A	3326	θ UMa B	270 B
θ Cen	2858	μ Her B	3325 A	ι UMa A	2084
η Cep	3578	μ Her C	3325 B	ι UMa B	2083 A
τ Cet	146	χ Her	3127	ι UMa C	2083 B
α CMa A	219 A	β Hyi	6	ξ UMa A	2390
α CMa B	219 B	ϵ Ind	67	ξ UMa B	2391
α CMi A	233 A	ν Ind	520	β Vir	2465
α CMi B	233 B	β Leo A	2462 A	γ Vir A	2604
π^1 Cnc A	2114 A	β Leo B	2462 B	γ Vir B	2605
π^1 Cnc B	2114 B	δ Lep	1792		
ρ^1 Cnc A	2062	ν^2 Lup	395		
ρ^1 Cnc B	2063	π Men	208		
β Com	348	γ Pav	3674		
ρ CrB	3145	δ Pav	485		
β CVn	2579	ϕ^2 Pav	3569		
ϵ Cyg A	5358b	ξ Peg A	3851		
ϵ Cyg B	5358a	ξ Peg B	3852		
σ Dra	477	σ Peg A	3864		
χ Dra A	3379 A	σ Peg B	3865		
χ Dra B	3379 B	ι Per	166		
δ Eri	1581	ν Phe	1220		
ϵ Eri	1557	γ Psc	3920		
σ^2 Eri A	23	ι Psc	3995		

TABLE 5.6
CROSS-LIST: FLAMSTEED DESIGNATION — LHS

Flamst.	LHS #	Flamst.	LHS #	Flamst.	LHS #
31 Aql	3463	61 Dra	477	49 Peg B	3865
53 Aql	3490	12 Eri A	1515 A	85 Peg A	101 A
60 Aql A	5350aA	12 Eri B	1515 B	85 Peg B	101 B
60 Aql B	5350aB	18 Eri	1557	6 Psc	3920
15 Aur	1753	23 Eri	1581	17 Psc	3995
16 Boo	48	27 Eri	1591	54 Psc	1116
11 Cas	1027	40 Eri A	23	107 Psc	1287
24 Cas A	123	40 Eri B	24	171 Pup	237
24 Cas B	122	40 Eri C	25	18 Sco	3171
30 Cas A	8 A	78 Gem	1945	26 Sco	3244
30 Cas B	8 B	1 Her	3127	5 Ser A	3059
5 Cen	2858	40 Her A	3234 A	5 Ser B	3060
3 Cep	3578	40 Her B	3234 B	39 Ser	3131
52 Cet	146	72 Her	441	41 Ser	408
9 CMa A	219 A	86 Her A	3326	58 Ser	3381
9 CMa B	219 B	86 Her B	3325 A	15 Sge	3515
10 CMi A	233 A	86 Her C	3325 B	10 Tau	1569
10 CMi B	223 B	83 Leo A	2407	104 Tau	1736
55 Cnc A	2062	83 Leo B	2408	8 Tri A	154 A
55 Cnc B	2063	94 Leo A	2462 A	8 Tri B	154 B
81 Cnc A	2114 A	94 Leo B	2462 B	9 UMa A	2084
81 Cnc B	2114 B	15 Lep	1792	9 UMa B	2083 A
43 Com	348	49 Lib	3143	9 UMa C	2083 B
15 CrB	3145	11 LMi A	2156 A	10 UMa A	2093 A
8 CVn	2579	11 LMi B	2156 B	10 UMa B	2093 B
27 Cyg	5353	20 LMi	2216	25 UMa A	270 A
53 Cyg A	5358b	12 Oph	3224	25 UMa B	270 B
53 Cyg B	5358a	36 Oph A	437	53 UMa A	2390
61 Cyg A	62	36 Oph B	438	53 UMa B	2391
61 Cyg B	63	70 Oph A	458	5 Vir	2465
26 Dra A	3305 A	70 Oph B	459	29 Vir A	2604
26 Dra B	3305 B	46 Peg A	3851	29 Vir B	2605
44 Dra A	3379 A	46 Peg B	3852	33 Vir	2631
44 Dra B	3379 B	49 Peg A	3864	61 Vir	349
				70 Vir	2740

TABLE 5.7
CROSS-LIST: HR — LHS

HR #	LHS #	HR #	LHS #	HR #	LHS #
6	1020	1083 A	1551	3522 B	2063
21	1027	1083 B	1552	3569	2084
77	5	1084	1557	3579 A	2093 A
98	6	1101	1569	3579 B	2093 B
159 A	118 A	1136	1581	3650 A	2114 A
159 B	118 B	1173	1591	3650 B	2114 B
166	1116	1325	23	3775 A	270 A
173	1124	1614	200	3775 B	270 B
176	1123	1656	173	3815 A	2156 A
219	123	1729	1753	3815 B	2156 B
222	121	1925	1774	3951	2216
321 A	8 A	2022	208	4098	2267
321 B	8 B	2035	1792	4158	2286
370	1220	2067	1803	4328	2354
483 A	1284 A	2083	1797	4374	2391
483 B	1284 B	2102	1796	4375	2390
493	1287	2401	1868	4414 A	2407
509	146	2491 A	219 A	4414 B	2408
511	1297	2491 B	219 B	4458	308
566 A	1314 A	2576	1878	4486 A	2437
566 B	1314 B	2643	1893	4486 B	2436
637	13	2692	1899	4523	311
660 A	154 A	2943 A	233 A	4534 A	2462 A
660 B	154 B	2943 B	233 B	4534 B	2462 B
672	1382	2990	1945	4540	2465
683	1387	2997	5130	4550	44
753	15	2998	1939	4587	5206
914	1489	3018	237	4657	322
937	166	3138	1959	4710	2553
963 A	1515 A	3259	245	4734	2560
963 B	1515 B	3384	249	4785	2579
1006	171	3430 A	5139aA	4825	2604
1008	19	3430 B	5139aB	4826	2605
1010	172	3522 A	2062	4849	2631

TABLE 5.7 — continued
CROSS-LIST: HR — LHS

HR #	LHS #	HR #	LHS #	HR #	LHS #
4983	348	6401	438	7875	3569
5019	349	6402	437	7898	3570
5072	2740	6416	444	7949 A	5358b
5183	2798	6426 A	442 A	7949 B	5358a
5189	2807	6426 B	442 B	7957	3578
5209	2814	6458	441	8061	3635
5288	2858	6518	3287	8085	62
5340	48	6573 A	3305 A	8086	63
5356 A	2891 A	6573 B	3305 B	8148 A	3655
5356 B	2891 B	6623	3326	8148 B	3656
5384	2907	6752	458	8181	3674
5455	2953	6806	3363	8387	67
5459	50	6869	3381	8477	3782
5460	51	6927 A	3379 A	8501 A	3790 A
5553	5279	6927 B	3379 B	8501 B	3790 B
5568	387	7293	3440	8515	520
5659 A	3036	7294	3441	8665 A	3851
5659 B	3037	7373	3463	8665 B	3852
5694 A	3059	7386	3464	8697 A	3864
5694 B	3060	7462	477	8697 B	3865
5699	395	7557	3490	8829	3912
5864 A	5299a	7602 A	5350aA	8832	71
5864 B	5299b	7602 B	5350aB	8852	3920
5911	3131	7637 A	5351aA	8969	3995
5914	3127	7637 B	5351aB	9088 A	101 A
5933	408	7644	484	9088 B	101 B
5954	3143	7665	485	9107	1013
5968	3145	7670 A	3510		
6014	3161	7670 B	3509		
6060	3171	7672	3515		
6171	3224	7689	5353		
6212 A	3234 A	7703	486		
6212 B	3234 B	7722	488		
6241	3244	7783	3537		

TABLE 5.8
CROSS-LIST: BD — LHS

BD #	LHS #	BD #	LHS #
-22°2345 A	5139aA	-17°3336	2379
-22°2345 B	5139aB	-17°3337	2380
-22°3005	1840	-17°3723 A	2647 A
-22°4585	5333	-17°3723 B	2647 B
-22°5504	3572	-17°3813	349
-22°13916	5347	-17°6856	552
-21°784	1628	-16°214	1225
-21°1377	1827	-16°295	146
-21°3781	363	-16°1591 A	219 A
-21°4009	3008	-16°1591 B	219 B
-21°4352	3191	-16°3030	5168a
-21°5703	490	-16°3469	2564
-21°6537	5001	-16°3543	2642
-20°465 A	1409 A	-16°4196	3143
-20°465 B	1409 B	-15°1776	1913
-20°643	1548	-15°2546	2036
-20°1211	1792	-15°4041	52
-20°4123 A	386 A	-15°4042	53
-20°4123 B	386 B	-15°6290	530
-20°4125	387	-14°1750	1900
-20°4399	5312	-14°2757	2108
-20°5385	3427	-14°3277	2370
-20°5833	3526	-14°4454	3222
-20°6185	3657	-14°6437 A	540 A
-20°6684	4055	-14°6437 B	540 B
-19°5899 A	497 A	-14°6437 C	541
-19°5899 B	497 B	-13°2439 A	1991 A
-18°287	1286	-13°2439 B	1991 B
-18°359	149	-13°3242	5180
-18°3019 A	289	-13°3557	5218
-18°3019 B	290	-13°3834	2872
-18°4031	3053	-13°4246	3115
-17°400	1346	-13°4807 A	3345 A
-17°3088	2231	-13°4807 B	3345 B

TABLE 5.8 — continued
CROSS-LIST: BD — LHS

BD #	LHS #	BD #	LHS #
-13°5069	3403	-9°3964	2940
-13°5945	509	-9°6149	3913
-12°1871	1910	-9°6150	3914
-12°1914	5124	-8°4352 A	428 A
-12°2449	245	-8°4352 B	428 B
-12°2889	2137	-8°4352 C	427
-12°2918 A	2151 A	-8°5980 A	3874
-12°2918 B	2151 B	-8°5980 B	3875
-12°4523	419	-8°6177	4005
-12°5594 A	3502	-7°699	5087
-12°5594 B	3503	-7°780	23
-11°569	5063	-7°781 A	24
-11°2741	274	-7°781 B	25
-11°2918	2286	-7°3632	354
-11°3759	2945	-7°3856	374
-11°3770	2953	-7°3963	5289a
-11°6064	3939	-7°4003	394
-10°109	1106	-7°4242	3171
-10°216	5019	-6°855	1646
-10°728	1581	-6°6318	4047
-10°3216	298	-5°642	1546
-10°4149	405	-5°1123	200
-10°5238 A	5351aA	-5°1844 A	1875
-10°5238 B	5351aB	-5°1844 B	1876
-10°6206	5410	-5°2678	2080
-9°122	1112	-5°3063	2265
-9°256	1231	-5°3763	2799
-9°697	1557	-5°5715	517
-9°1094	1799	-4°2468	2055
-9°3070	2259	-4°2639	5153
-9°3413	5206	-4°3049	2393
-9°3468	322	-4°3665 A	2894
-9°3595 A	2656 A	-4°3665 B	2895
-9°3595 B	2656 B	-4°4225	431

TABLE 5.8 — continued
CROSS-LIST: BD — LHS

BD #	LHS #	BD #	LHS #
-4°4226	432	-0°2532	2510
-3°592	1577	-0°2601 A	2604
-3°1061 A	1754	-0°2601 B	2605
-3°1061 B	1755	-0°2944 A	393 A
-3°1110	1763	-0°2944 B	393 B
-3°1123	30	-0°3676	3444
-3°2288	5136	-0°4195	5368
-3°2525 A	2082 A	-0°4470	537
-3°2525 B	2082 B	+0°659	1599
-3°3508	2773	+0°989	5101
-3°3746	3039	+0°3593	426
-3°3968 A	3215	+0°4810	3745
-3°3968 B	3219	+1°131	1141
-3°4233	3356	+1°410	1382
-3°5059	3596	+1°543	1496
-3°5577	3900	+1°1600	1884
-2°3481	2524	+1°2341p	2169
-2°3528	2566	+1°2447	2272
-2°4211	3224	+1°2920	2907
-2°4599	3381	+1°3071	3067
-2°5588	3696	+1°3942 A	3447
-1°167 A	1230	+1°3942 B	3448
-1°167 B	1229	+1°4774	550
-1°306	1365	+2°84	1114
-1°2457	2321	+2°348	14
-1°2505	2388	+2°1041	1779
-1°2754	2663	+2°1085	1798
-1°2832	2747	+2°2098	255
-1°2892	2842	+2°2489	2465
-1°4323	3833	+2°2585	2641
-0°572	1569	+2°2944 A	3059
-0°981	5107	+2°2944 B	3060
-0°1520	1886	+2°3101	3194
-0°2326	2251	+2°3312	447

TABLE 5.8 — continued

CROSS-LIST: BD — LHS

BD #	LHS #	BD #	LHS #
+2°3482 A	458	+6°398 B	16
+2°3482 B	459	+6°2182	2147
+2°4648	3920	+6°2697	2681
+2°4723	4020	+6°2932	2968
+3°275 A	5049	+6°2986	3020
+3°275 B	5048	+6°3169	3161
+3°2502	2407	+6°3455	3304
+3°2503	2408	+6°4357 A	5350aA
+3°3203	3202	+6°4357 B	5350aB
+4°123	121	+6°4741	3624
+4°415	1419	+7°2031	2050
+4°2568	2507	+7°2690	2798
+4°2729	2722	+7°2692	2801
+4°3195	420	+7°2850	2983
+4°3509	3329	+7°3125 A	3172 A
+4°3561a	57	+7°3125 B	3172 B
+4°4048 A	473	+7°3967	3431
+4°4048 B	474	+8°482	1520
+4°4157	3470	+8°2735	2766
+4°4510 A	3568 A	+8°3689	3387
+4°4510 B	3568 B	+8°3692	3388
+4°4994 A	5400aA	+8°4236	3490
+4°4994 B	5450aB	+8°4887	3828
+4°5035	3995	+9°73	1118
+4°435	1487	+9°946	1780
+5°1668	33	+9°2636	2570
+5°1739 A	233 A	+9°2776	2754
+5°1739 B	233 B	+9°3001	3024
+5°2791	2787	+9°4529	3550
+5°3640	3366	+9°4955	3742
+5°3993	470	+9°5076	3838
+5°4011	3426	+9°5122 A	3864
+5°4874	3717	+9°5122 B	3865
+6°398 A	15	+10°1032 A	1830 A

TABLE 5.8 — continued
CROSS-LIST: BD — LHS

BD #	LHS #	BD #	LHS #
+10°1032 B	1830 B	+15°2325	5191
+10°1857 A	2042 A	+15°2383 A	2462 A
+10°1857 B	2042 B	+15°2383 B	2462 B
+10°1857 C	2043	+15°2620	47
+10°2122	2234	+15°2847	5294
+10°2468	2631	+15°4026	3507
+10°2519 A	2689	+15°4074 A	3529
+10°2519 B	2690	+15°4074 B	3530
+10°2703 A	2941	+15°4733	533
+10°2703 B	2942	+16°120	1199
+10°4379	3584	+16°2658	373
+11°468	1545	+16°2849	408
+11°2439	2526	+16°4121	3515
+11°2576	352	+17°197	1239
+11°2910 A	5313	+17°202	1246
+11°2910 B	5311	+17°1320	1858
+11°3833	3463	+17°2611 A	2713
+11°4875 A	3851	+17°2611 B	2714
+11°4875 B	3852	+17°2785	2974
+12°1888	2033	+17°3729	3412
+12°4499	3598	+17°4519	3640
+12°4797	3786	+17°4708 A	3770 A
+13°1036	1803	+17°4708 B	3770 B
+13°2618	2665	+17°4946	3982
+13°2721	2821	+18°24	5001a
+13°3024	3131	+18°683	196
+13°3578	3373	+18°779	1736
+13°4614	3625	+18°1719	1942
+14°2151	2194	+18°2700	2693
+14°2621	2740	+18°2776	359
+14°3384	3349	+18°3182 A	3203
+15°395	1453	+18°3182 B	3204
+15°2003 A	2114 A	+18°3421	452
+15°2003 B	2114 B	+18°3911	3425

TABLE 5.8 — continued
CROSS-LIST: BD — LHS

BD #	LHS #	BD #	LHS #
+19°279	287	+24°2733 B	372
+19°869	1745	+24°2735	2918
+19°1185 A	1811	+24°2824	3026
+19°1185 B	1812	+24°3737	3464
+19°2777	48	+24°4460	3704
+19°2881	5279	+25°495	1501
+19°2939 A	3036	+25°2874	391
+19°2939 B	3037	+25°3020	3148
+19°4499	3576	+25°3173	3257
+19°5116 A	3965	+26°2251	2450
+19°5116 B	3966	+26°2677 A	3054
+20°85	1116	+26°2677 B	3055
+20°226	5035	+26°3151	3353
+20°2465	5167	+26°4734 A	101 A
+21°607	1644	+26°4734 B	101 B
+21°1528	1899	+27°262	1275
+21°1731	1966	+27°273	1289
+21°1764 A	5133	+27°1124	5116
+21°1764 B	5134	+27°2888 A	3326
+21°1949	2078	+27°2888 B	3325 A
+21°2247	2318	+27°2888 C	3325 B
+21°2649	2915	+27°4642	4044
+21°3198	3319	+27°28217	310
+22°176 A	5027	+28°1463	1945
+22°176 B	5028	+28°1660 A	2062
+22°301	1335	+28°1660 B	2063
+22°2340	2387	+28°1952	5181
+22°3406	3392	+28°2193	348
+22°3908	481	+28°2503	3138
+22°4567	3767	+28°4562	3931
+23°303	5051a	+28°4634	4008
+23°2359	2422	+29°1441	1893
+23°2751	2996	+29°1664	242
+24°2733 A	371	+29°1883 A	2125 A

TABLE 5.8 — continued
CROSS-LIST: BD — LHS

BD #	LHS #	BD #	LHS #
+29°1883 B	2125 B	+32°1964	2216
+29°2091	2308	+32°2132 A	2390
+29°2279	2544	+32°2132 B	2391
+29°2405 A	2728 A	+32°2896	441
+29°2405 B	2728 B	+32°3474	3469
+29°3872 A	3510	+33°529	159
+29°3872 B	3509	+33°622	1533
+29°4550	3737	+33°1505	1912
+30°206 A	1237	+33°1694	2007
+30°206 B	1236	+33°1814	2113
+30°421	1428	+33°2663	3145
+30°2490	5266	+33°3433	3458
+30°2512	2903	+33°4018 A	5358b
+30°4633	3771	+33°4018 B	5358a
+30°4824	3862	+33°4707	3942
+30°4982 A	3976	+33°4828	1013
+30°4982 B	3977	+34°796	21
+31°1684	241	+34°927	1719
+31°1781	1998	+34°2541	2948
+31°2238a	2366	+35°2436 A	2716
+31°2240 A	2367	+35°2436 B	2717
+31°2240 B	2366	+35°2439	2724
+31°2873	5318a	+35°2774	3155
+31°2875	3226	+35°3659sf	3467
+31°2884 A	3234 A	+35°3959	5353
+31°2884 B	3234 B	+36°1970	2155
+31°3330 A	3401	+36°1979 A	2156 A
+31°3330 B	3402	+36°1979 B	2156 B
+31°3767 A	3482	+36°2147	37
+31°3767 B	3483	+36°2165	2373
+32°719	187	+36°2500	2931
+32°1398 A	1866	+37°748	1528
+32°1398 B	1867	+37°1312	1783
+32°1695	1987	+37°1748	1934

TABLE 5.8 — continued
CROSS-LIST: BD — LHS

BD #	LHS #	BD #	LHS #
+37°1912	2053	+43°2182	2498
+37°2926	3312	+43°2796	3321
+38°2285	44	+43°4035	3705
+38°3095	3363	+43°4305	3853
+38°4343	62	+43°4445	3936
+38°4344	63	+44°1142	1746
+39°154	1125	+44°2051 A	38
+39°1248	1753	+44°2051 B	39
+39°1998	1944	+44°4548	1014
+39°2519	2556	+45°669 A	1458 A
+39°2947 A	3152	+45°669 B	1458 B
+39°2947 B	3150	+45°992	1708
+39°2950	3153	+45°1947 A	2437
+40°45	1053	+45°1947 B	2436
+40°2197	2131	+45°2505 A	433
+40°2442	2432	+45°2505 B	434
+41°328 A	1284 A	+45°2743	3394
+41°328 B	1284 B	+45°3561	3678
+41°750	180	+45°4378	4054
+41°750a	181	+45°4408 A	1016
+41°931	1696	+45°4408 B	1017
+41°3306	3450	+46°1405	2016
+42°1899	2028	+46°1635	2279
+42°1922	2047	+47°1276	1835
+42°1956 A	2093 A	+47°1355	1874
+42°1956 B	2093 B	+47°2072	2762
+42°2163	2332	+47°2112 A	2849
+42°2296	2548	+47°2112 B	2850
+42°2321	2579	+47°2420	3260
+42°2648	3127	+48°1469	1890
+42°2810	435	+48°1707 A	2084
+43°44 A	3	+48°1707 B	2083 A
+43°44 B	4	+48°1707 C	2083 B
+43°1953	2180	+48°1829	278

TABLE 5.8 — continued

CROSS-LIST: BD — LHS

BD #	LHS #	BD #	LHS #
+48°1964	2453	+56°2783 A	3814
+49°857	166	+56°2783 B	3815
+49°1961 A	2267	+56°2966	71
+49°1961 B	2266	+57°150 A	123
+49°2959	3441	+57°150 B	122
+49°2959a	3440	+57°2787	4004
+49°3009	3465	+58°3	1027
+50°1725	280	+58°1929	3466
+51°697	1518	+58°2605	544
+51°1094	1772	+59°1915 A	58
+51°1696	312	+59°1915 B	59
+52°857	1688	+60°170	1206
+52°911	28	+60°762	1613
+52°1401 A	270 A	+60°1266	2275
+52°1401 B	270 B	+61°195	1179
+52°2815	3590	+61°513 A	1492
+52°3112	3758	+61°513 B	1494
+53°934	1774	+61°1678 A	3305 A
+53°935	1775	+61°1678 B	3305 B
+53°1320	260	+61°2050	3578
+53°1321	261	+61°2068	3595
+53°1395	2237	+62°780	1782
+53°2911 A	525 A	+62°1257	2639
+53°2911 B	525 B	+62°1446	5307
+53°2911 C	525 C	+63°229	1291
+54°223 A	8 A	+63°238	1297
+54°223 B	8 B	+63°869	2211
+54°1175	1948	+64°312	5051b
+54°1216	2000	+66°34 A	114 A
+54°1716	384	+66°34 B	115
+55°900	1684	+66°34 C	114 B
+55°1823	5315	+66°137	136
+56°1421 A	5163 A	+66°145	1283
+56°1421 B	5163 B	+66°268	175

TABLE 5.8 — continued
CROSS-LIST: BD — LHS

BD #	LHS #	BD #	LHS #
+66°550	2008	+75°752 C	3565 C
+66°717	41	+76°404	5180a
+66°1281	3537	+76°785	3527
+67°191	1371	+77°361 A	264 A
+67°552 A	251 A	+77°361 B	264 B
+67°552 B	251 B	+79°212	1868
+67°935 A	3175	+80°238	5130
+67°935 B	3176	+81°465	2865
+67°1014	3287		
+67°1498	3894		
+68°60	1167		
+68°714	2687		
+68°883	3238		
+68°946	450		
+68°1345 A	3882		
+68°1345 B	3881		
+69°1053	477		
+70°68b	131		
+70°169	1397		
+70°639	2334		
+71°482	256		
+71°482a	257		
+72°395	1984		
+72°659	2991		
+72°839 A	3379 A		
+72°839 B	3379 B		
+73°407	2001		
+73°925	3631		
+74°493 A	5215 A		
+74°493 B	5215 B		
+74°889	3592		
+75°154	1619		
+75°752 A	3565 A		
+75°752 B	3565 B		

TABLE 5.9
CROSS-LIST: CD — LHS

CD #	LHS #	CD #	LHS #
-85°33	1511	-63°1596	3912
-84°102	2221	-62°39	128
-80°195	208	-62°1464	4031
-80°328	268	-61°282	1267
-79°878	3766	-61°6571	3652
-77°15	6	-60°118	1123
-77°568	2600	-60°3532 A	2402 A
-75°967	3285	-60°3532 B	2402 B
-73°1547	3635	-60°5077	2871
-73°1672	3994	-60°6576	3268
-70°340	210	-60°7508	3569
-70°1402	3184	-60°7821	3741
-70°1800	3608	-59°1024	204
-68°47	1208	-59°1224	1818
-68°74	1281	-59°1773	1959
-68°1095	2577	-59°1774 A	1960 A
-68°2378	1015	-59°1774 B	1960 B
-67°2385	484	-59°2351	2128
-67°2593	3921	-59°7305	3491
-67°2594	3922	-58°2884	2208
-66°38	1139	-58°5564	2892
-66°1212	1553	-58°7734	3542
-66°2367	485	-58°8156 A	3707 A
-65°253	195	-58°8156 B	3707 B
-65°1143 A	2456	-57°806	1620
-65°1143 B	2457	-57°1633	1896
-65°3918	3674	-57°2585	5149
-64°12	116	-57°5188	5255
-63°9	1094	-57°6303	413
-63°112 A	1551	-57°8454	3802
-63°112 B	1552	-56°1071 A	1724
-63°218	1796	-56°1071 B	1727
-63°295	1908	-56°1692	1881
-63°1418	5346	-56°3980	2417

TABLE 5.9 — continued
CROSS-LIST: CD — LHS

CD #	LHS #	CD #	LHS #
-56°5169	2815	-49°14337 A	1020
-56°5542	2961	-49°14337 B	1021
-56°8316	3675	-48°1011	1563
-55°4825	2644	-48°7414	2558
-55°9220	3889	-48°7426	2560
-54°487	1379	-48°12818	3423
-54°9222 A	3790 A	-47°7000	2433
-54°9222 B	3790 B	-47°9919	395
-53°70	1063	-47°10664	3182
-53°570	1452	-47°12773	3439
-53°889	1650	-47°13548	3582
-53°8617	496	-47°13670	3613
-53°9029	5377	-47°13695	3629
-52°305	5036	-46°76	1061
-52°394 A	1314 A	-46°293	133
-52°394 B	1314 B	-46°346	1220
-51°89	1064	-46°790	1436
-51°95	1091	-46°1936 A	1770
-51°273	1193	-46°1936 B	1771
-51°532	13	-46°2096	5112
-51°887	1584	-46°3046 A	1911 A
-51°5974	2447	-46°3046 B	1911 B
-51°6859	336	-46°5238	2150
-51°7244	344	-46°9361	2926
-51°13248	519	-46°10351	3114
-50°1492	1701	-46°11288	3270
-50°1977	1797	-46°11370 A	444
-50°8092	2817	-46°11370 B	445
-50°12780	3508	-46°11540	449
-50°13411	3692	-46°14649	5404
-49°451	1268	-45°1841	29
-49°2676	1902	-45°3283	1929
-49°9033	2970	-45°5378	2182
-49°13515	3685	-45°5627	2213

TABLE 5.9 — continued
CROSS-LIST: CD — LHS

CD #	LHS #	CD #	LHS #
-45°7872	2585	-40°9712	397
-45°8786	5261	-40°10550	3228
-45°13178	3460	-40°12743	3407
-45°13677	3531	-39°31	1036
-45°14980 A	5399 A	-39°3869	1968
-45°14980 B	5399 B	-39°7301	311
-44°170	1122	-39°8857	2900
-44°397	1245	-39°14192	66
-44°545 B	1306	-38°1058	167
-44°3045 A	222 A	-38°1631	5098a
-44°3045 B	222 B	-38°5760	2165
-44°3484	1922	-38°8457	2726
-44°3675	1939	-38°8635	2760
-44°11909	451	-38°11019	3209
-44°14214	503	-37°205 A	1110 A
-44°14334	3639	-37°205 B	1110 B
-43°1028	19	-37°1501	184
-43°7228	2441	-37°8082	2615
-43°11010	3235	-37°10500 A	5299a
-42°469	141	-37°10500 B	5299b
-42°594	1288	-37°10765 A	415
-42°654	1305	-37°10765 B	416
-42°1269	1603	-37°15492	1
-42°2503	1845	-36°1091 A	1466
-42°5678	2201	-36°1091 B	1467
-42°8521	2750	-36°2458	1787
-42°15867	3792	-36°6180	5166a
-42°16457	4013	-36°13940 A	486
-41°556	1323	-36°13940 B	487
-41°6879	2485	-36°15693	70
-41°14804	3782	-35°170 A	1097
-40°239	1188	-35°170 B	1098
-40°5404	2166	-35°360	1186
-40°7705	2678	-35°9019 A	2807

TABLE 5.9 — continued
CROSS-LIST: CD — LHS

CD #	LHS #	CD #	LHS #
-35°9019 B	2806	-29°1177 B	1515 B
-35°9260	2858	-29°5555	1982
-34°11285	3244	-29°8019	277
-34°11626 A	442 A	-29°8875	2354
-34°11626 B	442 B	-28°302	129
-34°11626 C	443	-28°657 A	1337
-33°143	1078	-28°657 B	1338
-33°1180	1534	-28°987	1489
-33°4113	237	-28°3554	1878
-33°9467	2834	-28°14630	5337a
-33°12476	3330	-28°15936	3468
-32°828	1361	-28°16676	3553
-32°5613	253	-27°16	1026
-32°8179	308	-27°108	1067
-31°325	1163	-27°9236	5247
-31°682	1278	-27°9894	2938
-31°909	1377	-27°11772	3310
-31°943	1391	-27°14659	488
-31°1454	1560	-27°16491	4048
-31°2902 A	1804 A	-26°828	1387
-31°2902 B	1804 B	-26°8883	319
-31°2902 C	1804 C	-26°9470	2669
-31°6229	249	-26°9804	2759
-31°7195	2130	-26°10340	2933
-31°9113	2429	-26°10870	3071
-31°10833	2841	-26°12026 A	437
-31°17597	3554	-26°12026 B	438
-30°731	1339	-26°12036	439
-30°990	1432	-26°15541 A	3655
-30°8970	5188	-26°15541 B	3656
-30°11195	2870	-26°16501	3904
-30°15026	3347	-25°225 A	118 A
-30°19175	3817	-25°225 B	118 B
-29°1177 A	1515 A	-25°10271 A	2891 A

TABLE 5.9 — continued
CROSS-LIST: CD — LHS

CD #	LHS #
-25°10271 B	2891 B
-25°10553 A	380
-25°10553 B	379
-24°263	1124
-24°12677	3186
-24°16193	3570
-24°17814	72
-23°315	1154
-23°325	1159
-23°693	1307
-23°1565	1591
-23°2865	1769
-23°9765	2358
-23°10062	2427
-23°11329	2814
-23°11940	383
-23°17699	3885
-22°526	142
-22°3005	1840
-22°6442 A	5139aA
-22°6442 B	5139aB
-22°12618	5333
-22°13916	5347
-22°14919	3572

TABLE 5.10
CROSS-LIST: CP — LHS

CP #	LHS #	CP #	LHS #
-85°38	1511	-63°234 B	1552
-84°263	2221	-63°498	1796
-80°161	208	-63°703	1908
-80°349	268	-63°4514	5346
-70°1190	3766	-63°4862	3912
-77°16	6	-62°75	128
-77°859	2600	-62°265	172
-75°1368	3285	-62°6446	4031
-73°2192	3635	-61°122	1267
-73°2299	3994	-61°6537	3652
-72°2690	520	-60°46	1123
-70°447	210	-60°2911 A	2402 A
-70°2196	3184	-60°2911 B	2402 B
-70°2814	3608	-60°5215	2871
-68°41	1208	-60°5483 A	50
-68°77 A	1281	-60°5483 B	51
-68°77 B	1279	-60°6718	3268
-68°1684	2577	-60°7419	3569
-68°3597	1015	-60°7528	3741
-67°3703	484	-59°444	204
-67°3959	3921	-59°584	1818
-67°3960	3922	-59°944	1959
-66°53	1139	-59°1362	2128
-66°1752	2553	-59°7535	3491
-66°3474	485	-58°1695	2208
-65°13	5	-58°5131	5255
-65°361	195	-58°5467	2892
-65°1714 A	2456	-58°7893 A	3707 A
-65°1714 B	2457	-58°7893 B	3707 B
-65°2751	3674	-57°612	1620
-64°51	116	-57°1139	1896
-63°51	1094	-57°1976	5149
-63°217	171	-57°7690	413
-63°234 A	1551	-57°10015	67

TABLE 5.10 — continued
CROSS-LIST: CP — LHS

CP #	LHS #	CP #	LHS #
-56°767	1724	-49°11858 A	1020
-56°768	1727	-49°11858 B	1021
-56°1199	1881	-48°376	1563
-56°4554	2417	-48°4791	2558
-56°5970	2815	-48°4799	2560
-56°6368	2961	-47°7075	395
-56°9645	3675	-47°7610	3182
-55°5262	2644	-47°9196	3439
-54°10055 A	3790 A	-47°9633	3629
-54°10055 B	3790 B	-46°29	1061
-53°77	1063	-46°127	1220
-53°672	1650	-46°254	1436
-53°9928	496	-46°609 A	1770
-53°10224	5377	-46°609 B	1771
-52°187	5036	-46°1360 A	1911 A
-52°241 A	1314 A	-46°1360 B	1911 B
-52°241 B	1314 B	-46°3701	2150
-51°48	1071	-46°6822	2926
-51°162	1193	-46°7681	3114
-51°282	13	-46°8446	3270
-51°443	1584	-46°8513 A	444
-51°4413	2447	-46°8513 B	445
-51°5356	336	-46°8664	449
-51°5750	344	-45°1588	1929
-51°11806	519	-45°3978	2182
-50°637	1701	-45°6592	5261
-50°869	1797	-45°9704	3460
-50°6387	2817	-45°9899	3531
-50°11256	3508	-45°10407 A	5399 A
-50°11576	3692	-45°10407 B	5399 B
-49°211	1268	-44°228 B	1306
-49°1163	1902	-44°612	29
-49°7339	2970	-44°1190 A	222 A
-49°11439	3685	-44°1190 B	222 B

TABLE 5.10 — continued
CROSS-LIST: CP — LHS

CP #	LHS #	CP #	LHS #
-44°1617	1922	-36°296 A	1466
-44°1829	1939	-36°296 B	1467
-44°9918	503	-36°4124	5166a
-43°354	19	-36°9037 A	486
-43°5524	2441	-36°9037 B	487
-42°366	1603	-36°9694	70
-42°915	1845	-35°60	1097
-42°4101	2201	-35°108	1186
-42°9607	4013	-35°3546	2834
-41°183	1323	-35°5974	2807
-41°5653	2485	-35°6109	2858
-41°9759	3782	-34°6635	3244
-40°98	1188	-34°6803 A	442 A
-40°3789	2166	-34°6803 B	442 B
-40°7021	397	-33°1748	237
-40°7392	3228	-33°4608	3330
-40°8627	3407	-32°3122	308
-39°6	1036	-31°92	1163
-39°1929	1968	-31°273	1391
-39°5265	311	-31°976 A	1804 A
-39°6278	2900	-31°976 B	1804 B
-39°8920	66	-31°976 C	1804 C
-38°463	5098a	-31°2448	249
-38°5760	2165	-31°2717	2130
-38°5484	2726	-31°6268	3554
-38°5542	2760	-30°324	1432
-38°6422	3209	-30°5103	3347
-38°7124	3337	-30°6641	3817
-37°57 A	1110 A	-29°362 A	1515 A
-37°57 B	1110 B	-29°362 B	1515 B
-37°3945	1	-29°2316	1982
-37°5339	2615	-29°3437	2354
-37°6571 A	5299a	-28°302	1489
-37°6571 B	5299b	-28°1525	1878

TABLE 5.10 — continued

CROSS-LIST: CP — LHS

CP #	LHS #	CP #	LHS #
-28°6572	5337a	-22°7859	3572
-28°6957	3468	-21°5830	3008
-27°25	1067	-21°5912	3038
-27°4721	5247	-21°6162	3191
-27°5682	3310		
-27°6972	488		
-26°214	1387		
-26°4626	319		
-26°4871	2669		
-26°5012	2759		
-26°5300	2933		
-26°5457	3071		
-26°5858 A	437		
-26°5858 B	438		
-26°5863	439		
-26°7193 A	3655		
-26°7193 B	3656		
-25°64 A	118 A		
-25°64 B	118 B		
-25°5397 A	2891 A		
-25°5397 B	2891 B		
-24°60	1124		
-24°7050	3570		
-23°95	1154		
-23°101	1159		
-23°215	1307		
-23°414	1591		
-23°829	1769		
-23°5802	2814		
-23°5999	383		
-23°8259	3885		
-22°3752 A	5139aA		
-22°3752 B	5139aB		
-22°6738	5333		

TABLE 5.11
CROSS-LIST: WOLF — LHS

Wolf	LHS #	Wolf	LHS #	Wolf	LHS #
12	1125	279	1835	433	338
24 A	123	287	1858	437	341
24 B	122	294	1879	438	2636
25	121	308	2016	440	2641
28	7	315	2028	457	2661
33	126	320	2041	461	2664
40	1170	324	2078	462	2665
44	1176	335	276	477	2689
46	1179	358	294	478	2690
47	1183	359	36	482	2731
53	5026	362	2353	485a	354
54	136	364	2361	487	2747
56	1198	365	2365	489	46
57	1206	368	2374	491	5254
109 A	5049	373	2383	496	2787
109 B	5048	376	2388	497	359
110	12	385	5191	498	47
113	1335	386	303	503	2799
124	14	391	2406	504	2801
125	152	393	2407	530	2853
127	1369	394	2408	534	368
134	169	395	2409	536	2956
194	177	397	305	537	2965
204	1573	398	2415	540	2968
205	1574	406	2515	553	2985
219	179	408	2544	561	3039
225 A	180	409	2549	562	394
225 B	181	414	2565	563	3062
227	1610	417	2570	620	3138
232	1745	422	2575	623	255
237	1784	424 A	333 A	629	427
261	1813	424 B	333 B	630 A	428 A
262 A	1811	427	2582	630 B	428 B
262 B	1812	429	5219	635	431

TABLE 5.11 — continued
CROSS-LIST: WOLF — LHS

Wolf	LHS #	Wolf	LHS #	Wolf	LHS #
636	432	1037	522	1325	1528
648	3267	1038	3943	1328 A	3764
672 A	3278	1039	545	1328 B	3765
672 B	3279	1040	548	1329	517
692 A	3282	1041	4005	1332	3780
692 B	3283	1046	4030	1340	3745
718	447	1050	473	1346	3562
760	3304	1055	473	1373	3605
816	3361	1056	119	1421	238
830	3368	1057	178	1426	2495
834	3371	1058	1828	1435	2518
851	467	1059	3549	1437	2526
863	5352	1061	419	1438	2527
865	3507	1062 A	472 A	1429	2538
866	3515	1062 B	472 B	1448	2872
867	481	1065	5039	1449	1763
873	3529	1069	3549	1450	1766
891	3596	1084	498	1453	30
896	502	1106	64	1457	5109
901	3607	1108	3472	1463	3393
906	3612	1122	3499	1465	466
918	65	1129	3518	1466	3400
921 A	3682 A	1130	482	1471	3315
921 B	3682 B	1132	1438	1478	2932
922 A	511 A	1143	3731	1481	2945
922 B	511 B	1147	5375	1504	1138
923	3689	1148	3737	1506	1175
926	3693	1184	3771	1515	1199
940	3708	1201 A	3808	1516	1227
945	3711	1201 B	3809	1530	1292
962	3742	1216	3797	1533	3979
983	5379	1322	1616	1561	3787
990	3760	1323	159	1567	3730
1014	3773	1324	170		

TABLE 5.12
CROSS-LIST: ROSS — LHS

Ross	LHS #	Ross	LHS #	Ross	LHS #
5	1053	84	2154	200 B	3699 B
9	1234	85	2173	206	3702
11	1277	86 A	3345 A	226	3871
17	1348	86 B	3345 B	236	5391
18	1368	90	2163	237	3869
19	1388	92	2171	247	5406
21	155	93	2181	248	549
25	1618	96	5158	249	4015
27	5091	99	2284	257	3576
28	1642	107	2331	258	3587
31	1683	108	2349	270 A	3770 A
33	196	109	2410	270 B	3770 B
34	173	110 A	2413	279	3833
36	1588	110 B	2414	288	3847
41	1761	119	2472	291	3945
47	31	122	2482	311	1118
48	1776	127	2527	318	131
49	1780	128	315	319	1175
51	2962	129	2475	322	137
52 A	2997 A	130	373	331	1483
52 B	2997 B	131	3310	335	1533
53	388	133	3320	341	1495
54	1895	136	464	345	1518
55	1900	138	5340	364	1475
58	5124	154	3414	365	1476
59	1794	160	3417	367	1488
60	1814	162	5347	370 A	1522
62	1824	163	3456	370 B	1523
64	1846	165 A	478 A	371	1530
65	1759	165 B	478 B	373	1527
66	1789	188	3559	382	1718
79 A	1830 A	193	3602	388	1740
79 B	1830 B	197	3649	390	1930
83	2141	200 A	3699 A	391	5127

TABLE 5.12 — continued
CROSS-LIST: ROSS — LHS

Ross	LHS #	Ross	LHS #	Ross	LHS #
394	1933	512	3083	651 A	3447
398	1689	513	399	651 B	3448
406	1765	522	3166	652	473
413	1819	528	3183	666	3812
414	1825	529	3191	668 A	525 A
417	1836	555	1303	668 B	525 B
419	1867	556	1439	668 C	525 C
422	1886	566	1597	671	533
434	2188	578	20	674	3960
436	2138	584	5087	676	4006
437	2137	585	174	679	1004
438	2142	587	1634	680	1054
439	2145	588	1594	682	2050
440 A	2151 A	589	1607	683	2056
440 B	2151 B	591	187	690	2551
445	2240	593	1659	695	45
446	2272	594	1674	697	2564
447	2334	597	1653	704	2620
451	42	600	1695	705	2642
452	5203	612	1891	713	3393
458	2665	614 A	1849	719	3400
476	353	614 B	1850	720	3403
484	2715	619	35	727	3437
486 A	5249	622	2060	730	3432
486 B	5250	623	255	731	3433
490	352	624 A	2082 A	733	3445
491	2766	624 B	2082 B	734	3446
492	2789	626	2308	747	3458
494	2837	627	304	751 A	497 A
495	5266	637	2518	751 B	497 B
499	2978	640	3200	765	3590
501	2994	641	3215	766	3574
508	396	644	3251	769	61
510	3073	650	3444	770	506

TABLE 5.12 — continued
CROSS-LIST: ROSS — LHS

Ross	LHS #	Ross	LHS #	Ross	LHS #
775	508	903	2422	1030b	5285
778	3677	904	5195	1038	3034
780	530	905	310	1041	2998
781	3888	906	2430	1044	389
786	537	907	2451	1047	3030
791	163	908	2467	1051	3018
800	2869	910	2434	1057	404
802	3093	912	2448	1069a	3499
804	3110	920	2494	1069b	482
806	3129	943	321		
808	3146	985	2731		
819	3315	986 A	226 A		
825 A	3637 A	986 B	226 B		
825 B	3637 B	988	1919		
828	3590	990	1934		
835	2821	991	2633		
837	2830	992	2884		
838	2846	993	2963		
844	2872	994	2977		
845	2880	996	5290		
848	369	999	3194		
849	2904	1001	3366		
854	3186	1003	2443		
858	3301	1008	2724		
860	3257	1011	2735		
863	5324	1015	2784		
864	3266	1018	2791		
873	1616	1020	350		
882	1943	1020b	2749		
887	2161	1022	2771		
888	2164	1026	357		
889	2169	1027	2840		
893	2271	1028b	2999		
899	2373	1030a	3012		

TABLE 5.13
CROSS-LIST: VARIABLE STAR DESIGNATION — LHS

Variable	LHS #	Variable	LHS #	Variable	LHS #
GQ And	4	YZ CMi	1943	V577 Mon A	1849
GX And	3	AZ Cnc	2034	V577 Mon B	1850
HH And	549	DX Cnc	248	V1054 Oph A	428 A
V1298 Aql	474	EI Cnc	2076	V1054 Oph B	428 B
V1412 Aql	3532	TY CrB	3146	V2133 Oph	3224
EZ Aqr A	68 A	V1513 Cyg	482	V2215 Oph	439
EZ Aqr B	68 B	V1581 A	3494 A	V1201 Ori	212
FG Aqr	3787	V1581 B	3494 B	EQ Peg	3965
FR Aqr	3602	HU Del	3556	GT Peg	3861
TZ Ari	11	AS Dra A	5215 A	II Peg	4044
VX Ari	1439	AS Dra B	5215 B	SX Phe	4013
QY Aur A	226 A	CM Dra A	421 A	ZZ Psc	5405
QY Aur B	226 B	CM Dra B	421 B	MQ Ser	3059
RR Cae	1660	CR Dra	5315	RY Sex	2285
V388 Cas	1183	DY Eri	23	V1216 Sgr	3414
V547 Cas A	114 A	V749 Her	3254	CF UMa ^a	44 B ^a
V547 Cas B	114 B	V774 Her	3392	SZ UMa	41
V645 Cen	49	EV Lac	3853	WX UMa	39
DO Cep	3815	AD Leo	5167	FI Vir	315
VW Cep A	3565 A	CN Leo	36	FL Vir A	333 A
VW Cep B	3565 B	SV LMi A	2156 A	FL Vir B	333 B
VW Cep C	3565 C	SV LMi B	2156 B	FN Vir	2664
UV Cet	10	BF Lyn	2131	GL Vir	324
YZ Cet	138	AX Mic	66	GQ Vir	2880

^a This object may not be real. See entry for LHS 44 in Table 5.17.

TABLE 5.14
CROSS-LIST: MISCELLANEOUS NAME — LHS

vB #	LHS #	Name	LHS #
1	1781	Barnard's Star	57
2	1820	Hubble 1	126
3	237a	Hubble 3	295
4	309	Hubble 4	2325
5	313	Hubble 10	2914
6	2484	Kapteyn's Star	29
7	2839	Kruger 60 A	3814
8	429	Kruger 60 B	3815
9	3395	Lacaille 9352	70
10	474	Lalande 21185	37
11	3601	Lalande 27137	5279
12	541	Lalande 39866 A	3568 A
16	220	Lalande 39866 B	3568 B
17	1926	Luyten's Star	33
24a	402	McCarthy 45	1070
24b	403	Plaut 1	412
26	3253	Stein 2051 A	26
29	3676	Stein 2051 B	27
		van Maanen's Star	7

TABLE 5.15

LHS OBJECTS BETWEEN 1001 AND 5413 WITH $m_{pg} - m_R \geq 2.5$

LHS #	Spec.	Dist.(pc)	LHS #	Spec.	Dist.(pc)
1035	—	—	2049	M6 V	—
1109	—	—	2065	M9 V	8.5 ± 0.1^a
1135	—	—	2067	sdM5	—
1146	—	—	2112	M4: V	—
1151	M4 V	—	2179	M5 V	—
1166	sdM	80.0 ± 7.8^a	2214	—	—
1252	M6 V	—	2215	M6 V	—
1265	—	—	2236	M5 V	—
1294	—	—	2238	sdM	—
1299	—	—	2243	M8 V	—
1317	M6.5: V	—	2314	M6 V	24.3 ± 1.4^a
1367	—	—	2330	—	—
1396	—	—	2335	—	—
1413	—	—	2339	—	—
1420	—	40.2 ± 1.8^a	2347	M5 V	—
1422	—	—	2351	M6.5 V	—
1491	—	—	2352	sdM	—
1564	—	—	2377	—	—
1604	—	14.7 ± 0.4^a	2397	M5 V	—
1630	—	—	2397a	M8 V	14.3 ± 0.4^a
1660a	—	—	2419	sdM4.5	—
1691	sdM	—	2429	M2 V	11.8 ± 1.1^c
1742a	sdM5:	74.6 ± 5.6^a	2479	—	—
1784	M4	31.3 ± 13.6^b	2487	—	—
1802	—	26.9 ± 0.8^a	2500	sdM0.5-1:	—
1807	—	—	2502	M6+ V	—
1826	sdM	—	2555a	—	—
1829	—	—	2629	—	—
1839	M4.5 V	—	2632	M7 V	—
1921	—	36.2 ± 1.3^a	2643	M4.5 V	—
1937	—	—	2645	M7 V	—
2026	M6 V	19.6 ± 0.2^a	2657	—	—
2039	—	—	2729	—	—
2045	sdM	90.1 ± 7.4	2755	—	—

TABLE 5.15 — continued

LHS #	Spec.	Dist.(pc)	LHS #	Spec.	Dist.(pc)
2758	—	—	3197	—	—
2810	—	—	3275	—	13.1 ± 0.9^d
2825	—	—	3478	—	33.2 ± 4.1^d
2826	M4.5 V	—	3481	—	149 ± 16^a
2841	K7	50.0 ± 19.9^b	3681	—	—
2847	M5.5: V	—	3762	—	—
2852	M0.5	30.3 ± 12.7^b	3768	—	—
2855	M6 V	—	3785	—	43.5 ± 1.7^a
2859	—	—	3837	—	—
2887	M4.5 V	—	3866	—	—
2893	M1.5	—	3873	—	—
2924	M9 V	11.0 ± 0.2^a	3926	—	—
2950	—	—	3933	—	—
2980	M7 V	—	3954	—	—
3002	M7 V	—	3958	—	—
3003	M6.5 V	—	3987	—	—
3042	—	—	5042	—	—
3099	—	—	5047	—	—
3104	—	—	5057	—	—
3106	M6 V	—	5142	M6 V	—
3111	—	—	5146b	—	—
3121	—	—	5165	—	—
3126	—	—	5273	—	—
3168	—	172 ± 21^a	5348	—	—
3170	—	—	5360	—	110 ± 36^a
3178	—	141 ± 20^a			

^a Trigonometric parallax from Monet et al. 1992.

^b Trigonometric parallax from Jenkins 1963.

^c Trigonometric parallax from Jenkins 1952.

^d Trigonometric parallax from Harrington & Dahn 1980.

TABLE 5.16
SPECTROSCOPIC OBSERVATIONS OF OBJECTS LISTED IN TABLE 5.15

LHS Number	Other Name	Adopted Sp.Type	Date Obs.(UT)	Integ. (sec)
2243	LP 315-53	M8 V	1992 Feb 25	2386
2632	LP 321-222	M7 V	1992 Feb 25	2390
2645	LP 218-8	M7 V	1992 Feb 25	2385
2980	LP 441-17	M6.5 V	1992 Feb 25	2388
5142	LP 606-35	M6.5 V	1990 Jan 21	900
1252	LP 587-65	M6 V	1991 Nov 13	2400
2826	LP 912-32	M4.5 V	1992 Feb 15	888
2887	G 165-61	M4.5 V	1992 Feb 25	354
2352	LP 263-78	sdM	1992 Feb 25	2387
2045	LP 545-45	sdM	1990 Nov 23	1200
2238	G 146-15	sdM	1992 Feb 25	300
1691	LP 415-315	sdM	1991 Nov 13	1200

TABLE 5.17
LIST OF CONFIRMED OR SUSPECTED MULTIPLE SYSTEMS
GIVEN AS SINGLE LHS ENTRIES

LHS 3 (SB?) — Spectroscopic binary with range of 30 km/s (Joy 1047). No radial velocity variations detected at the $\sigma = 1.3$ km/s level over 4 years by Pettersen & Griffin (1980) or at the $\sigma = 0.22$ km/s level over 1000 days by Marcy & Benitz (1989). No evidence of a companion via infrared speckle imaging down to a limiting magnitude of $M_K = 11.1$ at a separation of 0.6 arcsecond (Henry & McCarthy 1990).

LHS 8 AB (Conf.) — Astrometric binary (Wagman 1961) of period 18.5 years (Lippincott & Wyckoff 1964). Companion detected at 0.98 arcsecond separation by McCarthy (1983); the mass is $0.15 M_\odot$.

LHS 15 (As) — Astrometric binary of period 50 years (Lippincott 1973). Martin & Ianna (1975) find a 60-year period and a companion mass of $0.12 M_\odot$. Companion not detected by photographic speckle interferometry (Hartkopf & McAlister 1984) or by infrared speckle techniques down to $K = 7.8$ (McCarthy 1986).

LHS 26 (As) — Astrometric binary of period 23 years; secondary is probably substellar (Strand 1977). Companion not detected by infrared speckle imaging (McCarthy 1986; Henry 1991), but would be fainter than the detection limits.

LHS 30 (Speck?) — Star may be resolved at a position angle of 25° and $\Delta m_K = 5.2$ (Henry 1991). No astrometric perturbations suspected (Lippincott 1974; Breakiron, Upgren, & Weis 1982). Young, Sadjadi, & Harlan (1987) find radial velocities to be constant to the $\sigma = 4.4$ km/s level over 43 days; Marcy & Benitz (1989) find it to be constant to the $\sigma = 0.23$ km/s level over 553 days.

LHS 33 (As) — Astrometric binary with possible 2-year period; companion could be planetary (Hershey & Lippincott 1982). No radial velocity variations detected to the $\sigma = 0.32$ km/s level over 1197 days (Marcy & Benitz 1989). Possible detection of companion via infrared speckle imaging at 1.6 microns, with separation changing from 0.49 to 0.34 arcsecond over 8 months, by Henry & McCarthy (1990). Later speckle studies find no companion at a level 5.3 magnitudes fainter at K than the primary for separations between 1 and 10 AU (Henry 1991).

TABLE 5.17 — continued

LHS 37 (As?) — Previous astrometric perturbations suggested a planetary companion with period of 22 years (Hershey & Lippincott 1984), but re-analysis of former data augmented by new astrometric results shows essentially flat residuals with no clear periodicity (Heintz 1991). Marcy & Benitz (1989) report no radial velocity variations to a level of $\sigma = 0.19$ km/s over 1196 days. No evidence of a companion via infrared speckle imaging down to a limiting magnitude of $M_K = 10.9$ at a separation of 0.8 arcsecond (Henry & McCarthy 1990).

LHS 44 (Flare?) — The otherwise unseen companion, designated as CF UMa, has only been detected during what are reported to be flaring events, though Heintz (1984) is skeptical that the flares are real. Schaefer (1989) suggests that the flares are rare flashes of the G star itself. Griffin (1984) notes no radial velocity variations to a level of $\sigma = 0.15$ km/s over 10 years. Duquennoy & Mayor (1991) see no velocity variations to a level of $\sigma = 0.33$ km/s over 4646 days.

LHS 57 (As) — Astrometric perturbations suggest either one planet-sized body in a highly elliptical orbit (van de Kamp 1969a), two such bodies in circular orbits (van de Kamp 1969b), or a solar system having from three to five planets (Jensen & Ulrych 1973). No evidence via infrared speckle imaging of companions down to $M_K = 11.7$ (Henry & McCarthy 1990). Marcy & Benitz (1989) noted no radial velocity variations to a level of $\sigma = 0.23$ km/s over 1383 days.

LHS 58/59 (As?) — Only slight evidence for astrometric perturbations (Eichhorn & Alden 1960; Kamper 1966; van de Kamp, Gökkaya, & Heintz 1968). Henry (1991) notes no companions down to $M_K = 10.7$ at separations of 1 to 10 AU.

LHS 62/63 (As?) — Astrometric perturbations with a period of 4.8 years discussed by Strand (1957). Astrometric perturbation of 6 years found by Deich (1978) and Deich & Orlova (1977), with additional perturbations of 7 and 12 years suggested. See additional discussion of perturbations by Josties (1981). Heintz (1988) sees no periodic astrometric perturbations in either component over 75 years. No detections via speckle interferometry (McAlister et al. 1987). Campbell, Walker, & Yang (1988) find no radial velocity variations to the $\sigma = 10.2$ m/s level around LHS 62. Marcy & Benitz (1989) find no radial velocity variations to the $\sigma = 0.21$ km/s level in either LHS 62 or 63.

TABLE 5.17 — continued

LHS 68 AB (Conf.) — Duplicity independently discovered through infrared speckle interferometry by Leinert, Jahreiss, & Haas (1986) and McCarthy (1986). Binariness not suspected through astrometry (Ianna 1979).

LHS 101 AB (Conf.) — Visual binary with 26.27-year period and semi-major axis of 0.83 arcsecond (Hall 1949). Verified through infrared speckle interferometry by McCarthy (1983).

LHS 114 AB (Conf.) — Astrometric perturbation first discussed by Alden (1947); period of 16 years determined by Hershey (1973). Partially resolved photographically by McNamara (1984) and confirmed through infrared speckle imaging by McCarthy et al. (1991).

LHS 118 AB (Conf.) — Visual double star of period 25 years (Eggen 1956a).

LHS 123 (As??) — Periodic astrometric perturbations noted but considered inconclusive (van de Kamp & Flather 1955). No perturbation seen by Strand (1969). Spectroscopic orbit with 9.2-day period determined by Abt & Levy (1976) but refuted by Morbey & Griffin (1987). Radial velocity not seen to vary to the $\sigma = 13.7$ m/s level by McMillan & Smith (1987).

LHS 154 AB (Conf.) — Spectroscopic binary of period 9.9 days (Pierce 1924). Astrometric perturbations noted by Binnendijk (1950). Gómez & Abt (1982) unable to see spectral lines from the secondary, concluding that it was at least a late M star. Detected as a double-lines spectroscopic binary by Duquennoy & Mayor (1991).

LHS 181 (SB) — Carney & Latham (1987) report this companion to LHS 180 is itself a spectroscopic binary with a range of 19.83 km/s.

LHS 200 (SB?) — Reported by Gliese (1969) as a spectroscopic binary. No evidence of variable radial velocity (Kamper 1985). No evidence for astrometric perturbations over 23 years (Heintz 1987).

LHS 219 AB (Conf.) — Astrometric perturbation announced in 1844 by Friedrich Bessel. The companion, Sirius B, was first sighted visually by Alvan Clark in 1862.

LHS 221 AB (Conf.) — Companion first suggested by Borgman (see Heintz 1986) and resolved by infrared speckle interferometry (McCarthy 1986).

TABLE 5.17 — continued

LHS 222 AB (Conf.)	— Visual binary noted by Luyten (1941).
LHS 225 (Opt?)	— Kuiper (Bidelman 1985) gives two spectral types. “Secondary” is probably the companion 3 arcseconds distant listed in Luyten (1955).
LHS 226 AB (Conf.)	— Given as a spectroscopic binary in Joy (9147). Astrometric perturbations show evidence for an 18-year period (Appelbaum 1992). Perturbations not seen by Lippincott & Worth (1976). Seen as a double-lined spectroscopic binary by Tomkin & Pettersen (1986); period of 10.4 days. Double M dwarf.
LHS 229 (As)	— Astrometric binary with period of 0.94 year (Harrington, Christy, & Strand 1981). No companion found down to $M_K = 12.0$ via infrared speckle interferometry (McCarthy 1986).
LHS 230 AB (Conf.)	— Partially resolved white dwarf pair of period 20.5 years (Harrington, Christy, & Strand 1981).
LHS 233 AB (Conf.)	— Astrometric perturbations noted by Auwers in 1861. The companion, Procyon B, was first sighted visually in 1896 by Schaeberle.
LHS 241 (SB?)	— Listed as a possible radial velocity variable in Carney & Latham (1987) and Stryker et al. (1985), the object shows no systematic trends in its astrometric residuals (Heintz 1973), and Lu et al. (1987) find no evidence for binarity via speckle interferometry.
LHS 242 (As)	— Small, periodic perturbation noted in the astrometric residuals (Hershey 1980).
LHS 247 AB (Conf.)	— Equal magnitude binary with 0.6-arcsecond separation (Eggen 1979).
LHS 251 AB (Conf.)	— Astrometric perturbations suggest an unseen companion with period of 23 years (Lippincott 1973). Companion resolved at $M_K = 5.8$ by infrared speckle interferometry by McCarthy (1986).
LHS 258 (Opt?)	— Given as a possible double in Gliese & Jahreiss (1979). “Secondary” is probably the companion 6 arcseconds distant listed in Luyten (1955).

TABLE 5.17 — continued

LHS 260/261 (Speck?) — Morbey & Griffin (1987) refute earlier findings by Abt & Levy (1976) that both stars are spectroscopic binaries. However, Chang (1972) finds LHS 261 to be overmassive; Kirkpatrick, Henry, & McCarthy (1991) find LHS 261 to have an earlier (bluer) spectral type than its primary, LHS 260; and Henry (1991) suspects that one or both of these stars is resolved via infrared speckle imaging.

LHS 264 AB (Conf.) — Visual binary seen by Worley (1962a) and Heintz (1974). Orbital period is given as 50 years by Baize (1964).

LHS 270 AB (Conf.) — Visual binary with 5-arcsecond separation.

LHS 294 (As??) — Earlier reports of astrometric perturbations not verified by Alden (1951) or Lippincott (1974). Infrared speckle techniques find no companion at K down to 4 magnitudes fainter than the primary at a separation of 1 AU (Henry 1991).

LHS 333 AB (Conf.) — Visual binary (see Reuyl 1941). Confirmation via infrared speckle imaging by Henry et al. (1992).

LHS 352 (As?) — Astrometric perturbation with 15- to 20-year period suggested (Bieger 1964). No perturbation seen in follow-up work (Lippincott & Borgman 1979). Infrared speckle imaging finds no companion at K down to 4.7 magnitudes fainter than the primary (Henry 1991).

LHS 359 (As/Opt) — Astrometric perturbation with 1000-day period noted by Osvalds (1957). Optical companion (Burt & Weis 1976), 1 magnitude fainter than the primary, seen at a separation of 20 arcseconds by Worley (1962b).

LHS 374 (Opt) — Optical companion (Burt & Weis 1976), 3 magnitudes fainter than the primary, noted by Worley (1962b).

LHS 386 AB (Conf.) — Possible double lines seen in spectra, and radial velocity variations noted (Marcy, Lindsay, & Wilson 1987). Period of 308 days found (Duquennoy & Mayor 1988; Marcy & Benitz 1989). Companion resolved by infrared speckle interferometry by Mariotti et al. (1990).

LHS 393 AB (Conf.) — Visual binary with rapid motion (Eggen 1956b).

TABLE 5.17 — continued

LHS 417 AB (Conf.) — Astrometric binary of period 3.72 years (Lippincott & Borgman 1978). Companion detected through infrared speckle interferometry (McCarthy 1983; McCarthy & Henry 1987). Derived mass indicates an object near the stellar/substellar break (Marcy & Moore 1989).

LHS 419 (SB?) — Listed as a spectroscopic binary in Joy (1947). No convincing astrometric perturbations reported (Heintz 1988). No evidence for a companion seen to $M_K = 11.6$ at a separation of 0.5 arcsecond by Henry & McCarthy (1990).

LHS 421 AB (Conf.) — Found to be an eclipsing binary (Eggen & Sandage 1967) of period 1.6 days (Lacy 1977). A binary M dwarf system.

LHS 427 (SB) — Noted as a spectroscopic binary by Joy (1947). Unresolved via speckle interferometric methods at 7000 and 8000 Å by Blazit, Bonneau, & Foy (1987).

LHS 428 AB (Conf.) — Discovered as a visual binary by Kuiper (1934). Period of 1.715 years determined by Voûte (1946). Resolved with a separation of 0.2 arcsecond at 7000 and 8000 Å via speckle interferometry (Blazit, Bonneau, & Foy 1987). Astrometric measurements indicate the fainter component to be ~ 2 to 3 times more massive than the primary! (Fleischer 1957; Weis 1982).

LHS 429 (As) — Astrometric perturbation seen by Harrington, Kallarakal, & Dahn (183). Companion 1 arcsecond away and 3 magnitudes fainter than the primary at 2.2 microns reported by McCarthy, Probst, & Low (1985) via infrared speckle interferometry. Non-confirmation of the object at 2.2 microns by Perrier & Mariotti (1987) suggests that the earlier “detection” was due to an “airmass-induced differential seeing effect.” Companion also not found via direct imaging at K and L' (Skrutskie, Forrest, & Shure 1987).

LHS 442 AB (Conf.) — Visual double (see Hirst 1950).

LHS 450 (As/SB) — Astrometric evidence for a companion by van de Kamp & Lippincott (1949). Period of 26.37 years determined by Lippincott (1977). Companion not detected at 7000 Å between separations of 0.05 to 1 arcsecond and $\Delta m < 3$ (Blazit, Bonneau, & Foy 1987). Companion also not detected via infrared speckle imaging down to $\Delta m = 3.5$ at H and K (Henry & McCarthy 1990). Apparently unrelated to the astrometric binary (Lippincott 1978), this star is also listed as a probable spectroscopic binary by Wilson (1967).

TABLE 5.17 — continued

LHS 452 (As?) — Astrometric perturbation reported by Bieger (1964) but questioned by Heintz (1976).

LHS 458/459 (As) — Astrometric perturbation suggests a third component with period of 17 years (Reuyl & Holmberg 1943). Very slight evidence for an astrometric companion with 13-year period (Wagman 1951)

LHS 463 AB (Conf.) — Visual double with confirmed common proper motion (Vilkki 1984).

LHS 469 AB (Conf.) — Double star with 12-arcsecond separation (Gliese 1969; Luyten 1979).

LHS 471 AB (Conf.) — Double star resolved at a separation of 0.148 arcsecond by Blazit, Bonneau, & Foy (1987).

LHS 472 AB (Conf.) — Astrometric perturbation with period of 2.3 years discovered by Harrington (1977). Companion detected at 2.2 microns and 0.17 arcsecond separation by McCarthy (1983). Duquennoy & Mayor (1991) give a period of 878 days and a secondary mass of $0.09 M_{\odot}$.

LHS 474 (As?) — Astrometric perturbation with 4.9-year period suggested by Harrington, Kallarakal, & Dahn (1983). Perturbation not confirmed by Monet et al. (1992). No companion found to $M_K = 12.2$ from 5 to 10 AU via infrared speckle imaging (Henry 1991).

LHS 478 AB (Conf.) — Visual binary (Kuiper 1936).

LHS 482 (SB) — Noted as a spectroscopic binary by Joy (1947).

LHS 488 (SB?) — Given as “probably SB” in Gliese (1969).

LHS 497 AB (Conf.) — Visual binary with optical companions (Eggen 1956b; Gliese 1969).

LHS 501 (Opt?) — “May have a 16-mag. companion, 2 arcseconds distant” (Luyten 1979).

TABLE 5.17 — continued

LHS 511 AB (Conf.) — Astrometric perturbation with 1.9-year period reported by Lippincott (1979) and confirmed by McNamara, Ianna, & Fredrick (1987). Companion has a mass of $0.12 M_{\odot}$. Resolved at 2.2 microns by McCarthy (1983) and at 7000 \AA and a separation of 0.2 arcsecond by Blazit, Bonneau, & Foy (1987).

LHS 520 (Vis?) — Suggested to be a binary with almost equal components separated by 0.1 arcsecond (Finsen 1941). Gliese (1969), who assigns the binary a designation of GL 855.1 AB, remarks that the separation was 0.1 arcsecond in 1928, but that the companion “not seen since 1933.” Duplicity questioned by Evans, Menzies, & Stoy (1957) and Przybylski (1962). Also listed as a double star in The Bright Star Catalogue (Hoffleit & Jaschek 1982). Other data suggest that the star is actually single (Lambert & McWilliam 1986). A prime target for speckle interferometric measurements.

LHS 522 (SB) — Listed as a spectroscopic binary in Joy (1947).

LHS 525 ABC (Conf.) — Close binary measured at 0.47-arcsecond separation by McAlister et al. (1989). A proper motion companion 10 arcseconds distant was first noted by Kuiper, and it and the close double were listed as separate entries in the LFT Catalogue (LFT 1724/1725 — Luyten 1955) and in the LTT Catalogue (LTT 16615/16616 — Luyten 1961). Inexplicably, the distant companion was dropped in the compilation of the LHS Catalogue (Luyten 1979). For completeness, LHS 525 is listed here as a triple.

LHS 533 (SB?) — Listed as a spectroscopic binary in Joy (1947) and Wilson (1967). No periodic astrometric perturbations seen by Binnendijk (1950) or Alden (1957), though Lippincott & Hershey (1983) mention weak evidence for a ~ 5 -year period. Blazit, Bonneau, & Foy (1987) see no companion at 7700 \AA via speckle interferometry, and Marcy & Benitz (1989) see no velocity variations down to a level of $\sigma = 0.21 \text{ km/s}$ over 1112 days.

LHS 540 AB (Conf.) — Visual binary measured at separations of 0.72 arcsecond by Worley (1957) and 0.21 arcsecond by Kuiper (1961).

LHS 1016 (SB) — Listed as a spectroscopic binary in Joy (1947).

TABLE 5.17 — continued

LHS 1027 (Opt?/SB?) — A companion, ADS 107 B, with $\Delta m = 11.3$ and separation of 31.3 arcseconds noted in The Bright Star Catalogue (Hoffleit & Jaschek 1982). This companion is given as optical only in the LFT and LTT Catalogues (Luyten 1955; 1961), although Proust, Ochsenbein, & Pettersen (1981) indicate that there is “slow orbital motion.” LHS 1027 is also listed as a spectroscopic binary with 27-day period (Mellor 1927), although Abt (1965) found the radial velocity to be constant to a level of $\sigma = 2.5$ km/s.

LHS 1040 AB (Conf.) — Visual double, but the only two recorded observations are from 1935 and 1954 (see Lippincott 1983). Because Δm is small, no astrometric perturbations expected, and none found over 50 years (Heintz 1990).

LHS 1047 AB (Conf.) — Astrometric perturbation first noted by Ianna (1979). Companion subsequently confirmed visually (Heintz 1987) and by infrared speckle interferometry by Ianna, Rohde, & McCarthy (1988). The companion has a period of 4.63 years and a mass of $0.055 \pm 0.032 M_{\odot}$, indicating that it is possibly substellar.

LHS 1110 AB (Conf.) — Nearly equal-magnitude binary with 0.2 arcsecond separation (Lutyn 1979; Eggen 1987).

LHS 1163 (SB?) — Originally reported as a spectroscopic binary (Joy 1947), but not supported by Evans, Menzies, & Stoy (1957).

LHS 1179 (SB?) — Reported as “probably a spectroscopic binary” by Joy & Mitchell (1948). Neither Uppgren et al. (1985) nor Heintz (1986) mention astrometric perturbations. This star has common proper motion with LHS 1183.

LHS 1206 (SB) — A spectroscopic binary with a velocity range of 17.3 km/s (Carney & Latham 1987) and a period near 1600 days (Jasniewicz & Mayor 1988). Lu et al. (1987) find no evidence for a companion via speckle interferometry.

LHS 1284 AB (Conf.) — Astrometric perturbation with 18.5-year period noted by Lippincott & Lanning (1976). Companion resolved via infrared speckle interferometry; period revised to 19.5 years (Lippincott, Braun, & McCarthy 1983).

TABLE 5.17 — continued

LHS 1314 AB (Conf.) — Visual binary with a large visual magnitude difference of ~ 7.0 (Eggen 1956b).

LHS 1343 (As?) — Astrometry shows “systematic but so far not periodic residuals” (Heintz 1987).

LHS 1368 (SB?) — Listed as a possible radial velocity variable, with an observed range of 2.5 km/s, in Carney & Latham (1987).

LHS 1393 AB (Conf.) — Listed as a double of 1 arcsecond separation in Gliese & Jahreiss (1979).

LHS 1409 AB (Conf.) — Visual double of separation 0.6 arcsecond (Jeffers, van den Bos, & Greeby 1963).

LHS 1428 (SB?) — Listed as a possible radial velocity variable in Carney & Latham (1987). See also individual velocity measurements in Abt & Levy (1969).

LHS 1452 (Opt) — Listed as part of a common proper motion pair in Gliese (1969), although no companion is listed in Luyten (1979). The Preliminary Version of the Third Catalogue of Nearby Stars (Gliese & Jahreiss 1991) confirms that the companion is not physically related to LHS 1452.

LHS 1458 AB (Conf.) — Visual binary (see Heintz & Borgman 1984) with a 171.5-year period (Heintz 1984).

LHS 1466 (SB?) — Listed as a spectroscopic binary in Gliese (1969).

LHS 1501 (SB?) — Listed in Carney & Latham (1987) as a possible radial velocity variable with an observed range of 5.7 km/s. Lu et al. (1987) find no evidence for a companion via speckle interferometry.

LHS 1515 AB (Conf.) — Visual binary (see Eggen 1956b); separation was 2.4 arcseconds in 1975 (Holden 1975).

LHS 1555 (SB) — Variable radial velocity, with an amplitude of at least 30 km/s noted by Dearborn et al. (1986); the period is 245.5 days.

TABLE 5.17 — continued

LHS 1557 (As?/Speck?) — Astrometric perturbation with a 25-year period found (van de Kamp 1974), though disputed by Heintz (1978). Resolved via speckle interferometry by Blazit et al. (1977) at 7000 Å but unconfirmed by Hartkopf & McAlister (1984).

LHS 1569 (SB?) — Listed as a possible spectroscopic binary in Duquennoy & Mayor (1991).

LHS 1602 (SB?) — Listed in Carney & Latham (1987) as a possible radial velocity variable with an observed velocity range of 5.1 km/s.

LHS 1642 (As?) — Some evidence of a short-period astrometric perturbation (Hershey 1980); unresolved by infrared speckle imaging (Henry 1991).

LHS 1736 (Vis?/Speck?) — Although given the double star designation ADS 3701 and frequently referred to as a visual binary (e.g., Flather 1957), Hartkopf & McAlister (1984) note that the pair has never been split by speckle interferometric methods despite the fact that various orbits predict the companion to be easily observable. Heintz & Borgman (1984) note that twenty measurements of the position angle are so scattered that no orbit represents them well; they conclude that the companion is spurious. However, Tokovinin (1985) reports splitting the pair at a separation of 0.04 arcsecond as measured by a photographic phase-grating interferometer. Further studies are warranted.

LHS 1746 (Opt?) — Luyten (1979) notes a possibly optical companion 2 arcseconds away.

LHS 1780 (SB?) — Listed as a possible radial velocity variable, with an observed range of 5.1 km/s, in Carney & Latham (1987).

LHS 1804 ABC (Conf.) — Visual triple with separations of 2.42 arcseconds for AC and 0.82 arcsecond for AB (Wilson 1982).

LHS 1830 AB (Conf.) — Visual binary with 1-arcsecond separation (van de Kamp 1950).

LHS 1864 AB (Conf.) — Visual double. The common proper motion companion, $\Delta m_V = 2.5$, lies 1.8 arcseconds away and is seen on some of the USNO parallax plates (Dahn et al. 1988).

TABLE 5.17 — continued

LHS 1868 (SB??) — Listed as a single-lined spectroscopic binary with a 60-day period in Abt & Levy (1976). Morbey & Griffin (1987) show that a re-analysis of the same data supports no claim for real velocity variations. McAlister (1978) finds no evidence for a companion via speckle interferometry.

LHS 1911 AB (Conf.) — Visual binary which Eggen (1965) describes as “a puzzling pair” whose orbit determination gives a total mass of $0.05 M_{\odot}$!

LHS 1929 (Opt?) — Possibly optical companion noted by Kuiper (Bidelman 1985) at a separation of 7 arcseconds; spectral type of companion given as “K?”.

LHS 1945 (Opt) — Although listed as ADS 6335, all companions are optical (Hoffleit & Jaschek 1982; Luyten 1979). No companions found via infrared speckle imaging (Henry 1991).

LHS 1955 AB (Conf.) — Noted as a double star with 0.8-arcsecond separation (Luyten 1979; Eggen 1987).

LHS 1960 AB (Conf.) — Noted as a double with 2-arcsecond separation (Gliese 1969; Luyten 1979).

LHS 1991 AB (Conf./SB?) — Visual binary with 64.65-year period (Heintz 1974). There is a possibility of a third component since the pair is listed as a spectroscopic binary by Duquennoy & Mayor (1991), who give the period as 195 days and the mass of the tertiary as $0.10 M_{\odot}$.

LHS 2042 AB (Conf./SB) — A close visual double with separation of 2 arcseconds (Worley 1962b). A third common proper motion component, LHS 2043, may not be bound to LHS 2042 AB (van de Kamp & Burton 1962). Wilson (1967) notes that LHS 2042 is a possible spectroscopic binary, suggesting a fourth member of the system. The velocity variations are confirmed by Duquennoy & Mayor (1988), who find a period of 21 days and suggest that the unseen companion would most likely have a spectral type around M7.

LHS 2082 AB (Conf.) — A double-lined spectroscopic binary whose orbital parameters are presented in Latham et al. (1988). See also Greenstein & Saha (1986).

LHS 2083 AB (Conf.) — Visual double with a separation of ~ 0.2 arcsecond in 1970 (van Beisbroeck 1974). The period is 39 years (Eggen 1956b).

TABLE 5.17 — continued

LHS 2084 (SB) — Given as a spectroscopic binary (Abt 1965) with semi-amplitude of 6.0 km/s and period of 11 years. Another component, apparently unrelated to the spectroscopic binary, is suggested at a separation of 1 arcsecond by speckle interferometry at 5000 Å (Morgan, Beckman, & Scaddan 1980).

LHS 2093 AB (Conf.) — Visual binary discovered by Kuiper (see van de Kamp 1947); period is 22.2 years (Underhill 1963).

LHS 2114 AB (Conf.) — A double-lined spectroscopic binary whose duplicity was first reported visually by Finsen (1959). See Griffin (1982) for a concise review of this pair. The period is 986.5 days (Heintz 1984).

LHS 2125 AB (Conf.) — Visual binary with 34.2-year period (Lippincott 1958).

LHS 2151 AB (Conf.) — Visual binary observed by Kuiper (1943); astrometric perturbation also noted by Tifft (1955).

LHS 2156 AB (Conf.) — Visual binary with $\Delta m \sim 8.5$ (Eggen 1956b). Period of 201.0 years (Duquennoy & Mayor 1991).

LHS 2165 (Vis?) — Kuiper's observation of this star has the note "close binary?" (Bidelman 1985).

LHS 2169 (SB) — Listed as a spectroscopic binary, with an observed velocity range of 6.9 km/s, in Carney & Latham (1987).

LHS 2188 (As?) — Astrometric perturbation with period of 460 days suggested by Alden (1951) but not confirmed by later measurements (Alden et al. 1957; Titter, Mesrobian, & Upgren 1972).

LHS 2194 (SB) — Listed as a probable spectroscopic binary of period ~ 7600 days by Abt & Levy (1969). Stryker et al. (1985) list it as a certain binary. Carney & Latham (1987) refer to it as a possible radial velocity variable with an observed range of 4.7 km/s.

TABLE 5.17 — continued

LHS 2286 (Opt) — Duquennoy & Mayor (1991) list this as GL 398.1 A and B and denote it as a common proper motion pair (although, see their “Note added in proof”). Luyten (1979), however, lists the 10.5-magnitude component as an optical companion only. Gliese (1969) gives the 1958 separation of the faint star from the bright star as 14.4 arcseconds at a position angle of 75° . Assuming no proper motion for the faint component and taking the proper motion per annum of 0.722 arcsecond at $\theta = 159.5^\circ$ for LHS 2286 (Luyten 1979), the separation of the companion is predicted to be 24.2 arcseconds at $\theta = 15.8^\circ$ during 1987. This is in very close agreement with Sinachopoulos’ (1988) measurement of $\rho = 23.95$ arcseconds and $\theta = 12.02^\circ$ during 1987. Thus, the two stars are physically unrelated. (Curiously, Duquennoy & Mayor (1991) find that this unrelated star is a spectroscopic binary with a velocity range of 20 km/s.)

LHS 2327 (As) — Astrometric perturbation with 6.7-year period noted by Behall & Harrington (1976). Mass of the unseen secondary would be around $0.16 M_\odot$. The binary has not been resolved via infrared speckle imaging (Henry 1991).

LHS 2380 (SB) — Listed as a spectroscopic binary, range 40 km/s, by Joy (1947).

LHS 2390 (SB) — A spectroscopic binary of period 669.2 days with velocity range of ~ 16 km/s (Berman 1931). Derived mass of the secondary is $0.31 M_\odot$ (Heintz 1967). Faint component not seen via speckle interferometry (Hartkopf & McAlister 1984; Henry 1991). This star is also a companion to LHS 2391.

LHS 2391 (SB) — A spectroscopic binary of period 3.98 days with a velocity range of ~ 10 km/s (Berman 1931).

LHS 2402 AB (Conf.) — Visual binary (Evans, Menzies, & Stoy 1957; Evans, Menzies, & Stoy 1959) with 4-arcsecond separation and 300-year period (Luyten 1979).

LHS 2424 (SB?) — Listed as a possible radial velocity variable, with an observed range of 2.8 km/s, in Carney & Latham (1987).

LHS 2436 (SB) — Listed as a spectroscopic binary of period 23.5 days (see Gliese 1969; Bakos 1974). Radial velocity curve presented in Duquennoy & Mayor (1991). Unresolved at 7000 \AA via speckle interferometry by Blazit, Bonneau, & Foy (1987).

TABLE 5.17 — continued

LHS 2437 (SB) — Listed as a spectroscopic binary of period 3.4 days by Bakos (1974).

LHS 2462 AB (Conf.) — Luyten (1979) notes that the 15.5-magnitude neighbor listed in Aitken (1932) is a physical companion.

LHS 2465 (SB?) — Campbell, Walker, & Yang (1988) list this as a possible, small-amplitude velocity variable, as do Duquennoy & Mayor (1991), though Heintz (1991) makes no mention of astrometric perturbations. Hartkopf & McAlister (1984) find no evidence for a companion via speckle interferometry.

LHS 2505 AB (Conf.) — Visual binary with $\Delta m = 2$ and separation of 0.8 arcsecond (see Eggen 1987).

LHS 2524 (Opt?) — Luyten (1979) notes a faint companion 2 arcseconds distant at $\theta = 5^\circ$. Duquennoy & Mayor (1991) find constant radial velocity, to the 0.42-km/s level, over 2362 days.

LHS 2531 (Opt) — Optical companion 5 arcseconds east of LHS 2531 according to Weis & Uppgren (1982).

LHS 2566 (SB) — A spectroscopic binary with a well determined orbit and a period of 25.9 days (Latham et al. 1988). This is confirmed by Jasiewicz & Mayor (1988) who find that there is a 90% chance that the secondary has a mass between 0.10 and 0.25 M_\odot .

LHS 2647 AB (Conf./SB) — Component B is 1.9 arcseconds distant, with $\Delta m = 4.5$; the A component itself is a spectroscopic binary with a well determined period of 12.4 days. The mass of this unconfirmed C component is between 0.14 and 0.60 M_\odot (Mayor & Turon 1982).

LHS 2656 AB (Conf.) — Visual pair separated by 1.5 arcseconds (Eggen 1956b).

LHS 2664 (SB) — No astrometric perturbations now suspected (Heintz & Borgman 1984). Listed as a possible spectroscopic binary in Gliese (1969) and Pettersen (1991). Joy (1947) gives it as a spectroscopic binary with a range of 54 km/s.

LHS 2665 (SB) — Given as a spectroscopic binary with a period of 1348 days in Duquennoy & Mayor (1991). The secondary, with a computed mass of 0.04 M_\odot , is an excellent brown dwarf candidate.

TABLE 5.17 — continued

LHS 2693 (SB) — Variations in the radial velocity noted by Latham et al. (1989), who find a period of 84 days and a companion mass given by $M \sin i = 0.011 \pm 0.001 M_{\odot}$. This mass falls in the regime of brown dwarfs for inclinations greater than 8° , and investigations have been launched in an effort to put constraints upon the possible values of $\sin i$. Robinson et al. (1990) find no evidence for eclipses in the system, meaning that the orbital inclination is less than 89° . From high-precision radial velocity measures, Cochran, Hatzes, & Hancock (1991) derived rotational and macroturbulent velocities consistent with $\sin i_{\text{rot}} \leq 0.14$. If the orbital and rotational axes are nearly aligned, this suggests a companion mass in the stellar regime. Lack of periodic photometric variations also support the pole-on orientation. However, other interpretations of the data are also possible. This system clearly deserves further study.

LHS 2708 (SB?) — Listed in Carney & Latham (1987) as a possible radial velocity variable with an observed range of 2.9 km/s.

LHS 2728 AB (Conf.) — A double with a period of 229.0 years (Amburster 1978). Binarity confirmed via speckle observations by McAlister et al. (1989) — separation 1.3 arcseconds.

LHS 2747 (SB?) — Listed in Carney & Latham (1987) as a possible radial velocity variable with an observed range of 2.5 km/s.

LHS 2845 (Vis?) — Luyten (1979) notes that this “could be a close double.”

LHS 2883 (Opt?) — Rodgers & Eggen (1974) note a faint, probably optical companion 1 arcsecond away.

LHS 2891 AB (Conf.) — Visual binary with a separation of 3 arcseconds (Eggen 1987; Luyten 1979; Gliese 1969).

LHS 2989 (Vis?) — Luyten (1979) lists this as a companion to LHS 2990 and adds that LHS 2989 “may itself be double again.”

LHS 2997 AB (Conf.) — Binary of 0.6-arcsecond separation as confirmed through speckle observations (McCarthy 1986; McAlister et al. 1989). Period is 34.1 years (Heintz 1990).

LHS 3008 (As) — Luyten (1979) notes, without reference, that this star has an invisible companion with a period of ~ 1300 days.

TABLE 5.17 — continued

LHS 3020 (SB?/As) — Noted as a possible spectroscopic binary by Dyer (1954). Astrometric perturbations noted by Alden et al. (1957), who suggest a 700-day period. No companion seen at 7500 Å via speckle interferometry by Bonneau et al. (1986).

LHS 3064 (Vis?) — Eggen (1980) notes that “in good seeing, this appears as a possible double of equal components.”

LHS 3076 (As) — Astrometric perturbations of period 5.96 years noted by Harrington & Dahn (1988); mass of the secondary is around $0.1 M_{\odot}$. Companion not seen via infrared speckle imaging (Henry 1991).

LHS 3148 (SB) — A spectroscopic binary of period 4451 days (Duquennoy & Mayor 1991). Unresolved at 6000 and 7500 Å via speckle interferometry by Bonneau et al. (1986).

LHS 3156 AB (Conf./SB) — There is a 14th-magnitude common proper motion companion 2 arcseconds away which is not noted by Luyten (1979) presumably because it is variable — it is frequently invisible on the Sproul plate series (Lippincott 1983). A third component could be present since the primary is a noted spectroscopic binary with range 36 km/s (Joy 1947).

LHS 3172 AB (Conf.) — Visual binary with 2-arcsecond (and increasing) separation (see Heintz & Borgman 1984; Heintz 1975; Heintz 1956; Worley 1956).

LHS 3199 (SB?) — Listed in Carney & Latham (1987) as a possible radial velocity variable with an observed range of 3.5 km/s.

LHS 3215 (SB) — A spectroscopic binary (whose effects are unrelated to its companion, LHS 3219, 19.5 arcminutes away). The close companion has a period of 133.3 days (Mayor & Turon 1982).

LHS 3234 AB (Conf./As?) — A visual binary first detected by William Herschel. The magnitude difference of the pair is 2.6, the period is 34.33 years, and the mass of the secondary is $0.78 M_{\odot}$ (Lippincott 1981). Though Baize (1967) finds evidence for a third component, of mass $\sim 0.19 M_{\odot}$ and spectral type around M4 or M5, Lippincott (1981) sees no astrometric perturbations which would indicate more than two stars in the system. Radial velocity data by Scarfe et al. (1983) rule out the companion proposed by Baize, but have difficulty ruling out a third body all together.

TABLE 5.17 — continued

LHS 3269 AB (Conf.) — Visual binary of 0.6-arcsecond separation. Because the masses are assumed to be equal, Lippincott (1983) sees no astrometric indication of the orbital motion. The period is 33.5 years (Heintz 1991).

LHS 3277 (As) — Astrometric perturbation with a period of 10 years noted by Christy (1978). Two alternative solutions for the masses of the components are given in Dahn et al. (1988): the first solution yields masses of 0.13 and 0.09 M_{\odot} for the components, and the second yields masses of 0.14 and 0.04 M_{\odot} . In either case, the secondary, which has not been imaged via infrared speckle techniques (Henry 1991), would be an excellent brown dwarf candidate.

LHS 3287 (SB?) — Noted as a spectroscopic binary with range of 28 km/s in Gliese (1969). Nineteen measurements of the radial velocity over 860 days show no evidence for variations to the $\sigma = 2.6$ km/s level (Beavers & Eitter 1986).

LHS 3305 AB (Conf.) — A visual binary of period 74 years and 1.5-arcsecond separation (Hall 1948).

LHS 3325 AB (Conf.) — Visual binary of period 43.2 years (Heintz 1987).

LHS 3326 (As) — Heintz (1987) finds this to be a “new unresolved binary of large amplitude” with a period of 63 years and $a = 0.248$ arcsecond.

LHS 3345 AB (Conf.) — Visual binary of 0.43-arcsecond separation (see Carney & Latham 1987).

LHS 3379 AB (Conf.) — A spectroscopic binary of period 280 days; companion confirmed via speckle interferometry. See Tomkin et al. (1987) for a review of this system.

LHS 3463 (Vis?/SB?) — Although a companion with $\Delta m = 3.5$ and a separation of 105.6 arcseconds is listed by Hoffleit & Jaschek (1982), Luyten (1979) makes no mention of a second object. LHS 3463 is also listed as a probable velocity variable in Evans, Menzies, & Stoy (1957) and as a possible spectroscopic binary in Duquenois & Mayor (1991). No companion has been found via speckle interferometry by either Bonneau et al. (1980) or Lu et al. (1987).

LHS 3494 AB (Conf.) — Astrometric perturbations first noted by Harrington & Kallarakal (1982). Companion, whose mass is near the stellar/substellar break, confirmed by McCarthy et al. (1988).

TABLE 5.17 — continued

LHS 3509 (Vis?) — Heintz (1988) notes that a plate taken on 1971.42 shows a faint companion of magnitude ~ 15.5 with a separation of 4.4 arcseconds and position angle of 114° . A deep-field exposure by Harrington in 1973 shows no object, whether it be a fixed background star or a common proper motion companion. Heintz's conclusion is that the object is variable and possibly a flaring, third member of the LHS 3509/3510 system. McAlister et al. (1987) find no tertiary component via speckle interferometry.

LHS 3556 (As) — Astrometric perturbation first noted by Harrington (1971). The companion has a period of 1.49 years and a mass in the range 0.06 to $0.11 M_\odot$.

LHS 3557 (SB?) — Listed in Carney & Latham (1987) as a possible radial velocity variable with an observed range of 3.2 km/s.

LHS 3558 (Opt?/As?) — Worley (1962b) notes a possibly optical companion at 35 arcseconds with $\Delta m = 2$. Also, a very uncertain astrometric perturbation is noted by van de Kamp & Lippincott (1949).

LHS 3565 ABC (Conf.) — A W Ursae Majoris-type eclipsing variable with a period of 0.278 days. The two components have masses of 0.9 and $0.25 M_\odot$ (Hill 1989). Astrometric orbital motion with a period of 30.45 years was investigated by Hershey (1975); this third component with $\Delta m = 2.9$ and mass of $0.58 M_\odot$, was confirmed visually by Heintz (see Hershey 1975) at a separation of 0.6 arcsecond from the eclipsing pair. LHS 3592 is listed by Heintz (1978) as a very distant, common proper motion, fourth component of this system.

LHS 3568 AB (Conf./SB) — A visual binary of period 37.0 years (Morel 1969). The A component of the system has been shown to be a spectroscopic binary with a period of 2.5 years by Duquennoy (1987), who claims to have detected lines from the tertiary in the spectrum of A at periastron. Duquennoy's estimate of the tertiary's mass ($0.28 M_\odot$) is disputed by Heintz (1989), who supports a mass less than $0.2 M_\odot$.

LHS 3577 (As?) — Lippincott (1979) notes an astrometric perturbation with a period of 6.3 years. Marcy & Benitz (1989) find no statistically significant velocity variations, and McCarthy (1986) finds no evidence for a companion at 2.2 microns.

TABLE 5.17 — continued

LHS 3595 (SB?/As?) — Listed by Wilson (1967) as a probable spectroscopic binary with range of 11.0 km/s. Heintz (1981) also finds a variation with a range of 15 km/s. Variable proper motion, with a period of 17 years, suspected by Lippincott & Worth (1976), but not confirmed by Heintz (1991). Five radial velocity measurements over an eight-day period by Young, Sadjadi, & Harlan (1987) show no evidence of variation. Henry (1991) sees no companion down to $M_K = 11.0$.

LHS 3609 ABC (Conf.) — Known as a visual binary (see Lippincott 1975), the primary star was also found to be a 3.2756-day double-lined spectroscopic binary by Fekel, Bopp, & Lacy (1978). The masses of this triple system are 0.9, 0.6, and 0.5 M_\odot as determined by Russell & Gatewood (1980) and 0.4, 0.3, and 0.3 M_\odot as determined by Duquennoy & Mayor (1988).

LHS 3635 (Vis?/CPM?) — Although listed in Gliese (1969) as a close double star, both Hoffleit & Jaschek (1982) and Eggen (1987) call it an unconfirmed binary. Gliese (1969) also lists a common proper motion, third component at a separation of ~ 8 arcseconds; no such object is noted in the Bruce Proper Motion Survey (Luyten 1963).

LHS 3637 AB (Conf.) — Shown to be a visual double with common proper motion by Vilkki (1984).

LHS 3655 (SB?) — Listed as a spectroscopic binary in Gliese (1969) and Augensen & Buscombe (1978). The object is unresolved at 7000 Å via speckle interferometry by Blazit, Bonneau, & Foy (1987).

LHS 3682 AB (Conf.) — Both Kuiper (Bidelman 1985) and Luyten (1979) list this as a close visual double.

LHS 3699 AB (Conf.) — Luyten (1979) notes this as a visual binary of 2-arcsecond separation and $\Delta m = 3$.

LHS 3707 AB (Conf.) — A double star whose orbit is somewhat uncertain — periods range from 6.32 to 12.65 years (Finsen & Worley 1970). The longer period makes for better agreement between the trigonometric, dynamical, and photometric parallaxes.

LHS 3731 (SB?) — Listed in Carney & Latham (1987) as a possible radial velocity variable with an observed range of 3.9 km/s.

TABLE 5.17 — continued

LHS 3770 AB (Conf./SB) — Lu et al. (1987) discovered via speckle interferometry a companion at a separation of 0.205 arcsecond and position angle of 126.7° . The primary is also listed as a spectroscopic binary with an observed range of 11.9 km/s in Carney & Latham (1987). The period of this suspected tertiary around LHS 3770 A is 219.38 days (Latham et al. 1988).

LHS 3790 AB (Conf.) — Visual double star (Eggen 1956b).

LHS 3814 (As??) — Systematic runs in the residuals of the orbital and mass-ratio solutions of Krüger 60 AB led Lippincott (1953) to propose, “with great caution,” a companion to A having a period of 16 years and mass between 0.009 and $0.025 M_\odot$. Heintz (1986) does not find a continuation of these trends in later data.

LHS 3833 (Opt?) — Worley (1962b) lists a possible companion 15 arcseconds distant with $\Delta m = 4$. This companion is too faint to be measured on plates taken by Upgren & Kuzma (1983).

LHS 3839 (Opt?) — Luyten (1979) notes that this star might have a common proper motion companion 13 arcseconds distant.

LHS 3853 (As?/Ecl?/Speck?) — van de Kamp & Worth (1972) find astrometric evidence for a second body with a period of 28.9 years and mass between 0.01 and $0.03 M_\odot$. Rožman (1984) finds evidence for an eclipsing body (mass $\leq 0.04 M_\odot$) having a period coincident with EV Lacertae’s photometric period of 4.378 days. However, Weis, Nations, & Upgren (1983) find no significant trends in their astrometric residuals; Marcy & Benitz (1989) see no radial velocity variations to the $\sigma = 0.24$ km/s level over 694 days; Blazit, Bonneau, & Foy (1987) are unable to resolve a companion at 7700 \AA via speckle interferometry; and Henry (1991) sees no companion to $M_K \sim 10.8$ via infrared speckle imaging, though earlier results (Henry & McCarthy 1990) suggest a possible companion with $\Delta m \sim 4$ at a separation of 0.4 arcsecond. Young, Sadjadi, & Harlan (1987) also list it as a possible, low-amplitude spectroscopic binary.

LHS 3869 (SB?) — Listed in Carney & Latham (1987) as a possible radial velocity variable with an observed range of 3.0 km/s.

TABLE 5.17 — continued

LHS 3982 (As/SB) — An astrometric perturbation with a period of ~ 12 years noted by Russell & Gatewood (1975). LHS 3982 is also listed as a spectroscopic binary with an observed range of 8.75 km/s by Carney & Latham (1987). Observations by Hartkopf & McAlister (1984) have not revealed either companion via speckle interferometry.

LHS 3995 (SB?) — Listed as a possible spectroscopic binary in Duquennoy & Mayor (1991).

LHS 5098a (Opt?) — Kuiper (Bidelman 1985) notes close companions to this star; they are probably optical only.

LHS 5139a AB (Conf./As/SB) — A visual double star of separation 1.9 arcseconds; the period has had estimates of 214 years (see Eggen 1956b), 140-145 years (Abt, Sanwal, & Levy 1980), and 123 years (Heintz 1990). There is also an astrometric perturbation with a period of ~ 35 years (Eggen 1956b), and Abt, Sanwal, & Levy (1980) note small-amplitude velocity variations with a period of ~ 500 days.

LHS 5163 AB (Conf.) — Lutyen (1979) notes a 14.5-magnitude companion at a separation of 1.5 arcseconds. Kuiper (Bidelman 1985) also noted that this was a close double.

LHS 5167 (As?/Speck?/Radio?) — Variable proper motion first noted by Reuyl (1943) and verified with subsequent data by Lippincott (1969). The companion, at 0.08-arcsecond separation, was resolved at 7800 Å via speckle interferometry by Balega, Bonneau, & Foy (1984). However, the companion was not found to a limit of $M_K = 11.0$ via infrared speckle imaging (Henry 1991). Likewise, Marcy & Benitz (1989) find no radial velocity variations to the $\sigma = 0.20$ km/s level over 1224 days. Heintz (1990) discounts all previously reported astrometric perturbations and notes that the alleged interferometric confirmation must be spurious. Curiously, Robinson, Slee, & Little (1976) report a weak radio emission source 1.85 arcminutes southeast of AD Leonis which they interpret as a companion object with a linear separation of ~ 550 AU.

LHS 5215 AB (Conf.) — A double-lined spectroscopic binary apparently containing two G-type stars with a period of 5.41 days (Greenstein, Hack, & Struve 1957). See also recent observations by Mayor & Mazeh (1987).

TABLE 5.17 — continued

LHS 5279 (SB) — A single-lined spectroscopic binary with a well determined orbit of period 125.37 days (Kamper & Lyons 1981; Beavers & Salzer 1983). The companion has not been verified through speckle interferometry by either Hartkopf & McAlister (1984) or Blazit, Bonneau, & Foy (1987) at 7000 and 7500 Å.

LHS 5350a AB (Conf./SB?) — A visual binary with a separation of 12 arcseconds (Eggen 1956b). Campbell, Walker, & Yang (1988) see possible radial velocity variations in component A, but state that the observed acceleration could be caused by B alone. Duquennoy & Mayor (1991) find the velocity to be constant over 3927 days.

LHS 5351a AB (Conf.) — A visual double (see van den Bos 1963) with a period of 9.70 years, $\Delta m = 0.5$, and total mass of $2.1 M_{\odot}$ (Baize 1992). The visual orbit presented in Duquennoy & Mayor (1991) has a period of 1790 days — half as long as that computed by Baize.

LHS 5358b (SB) — Listing this object as a spectroscopic binary, Hartkopf & McAlister (1984) find no companion via speckle interferometry.

LHS 5399 AB (Conf./As?) — A visual double star with a separation of 1.3 arcseconds and $\Delta m = 2.0$ (Holden 1978). An astrometric perturbation with period of 1170 days also suspected (van Altena & Sawada 1983).

LHS 5400a AB (Conf.) — A visual double star with $\Delta m = 0.9$ (e.g., see Worley 1957 and van den Bos 1958).

LHS 5405 (Phot?) — Excess infrared radiation between 2 and 5 microns detected for this white dwarf by Zuckerman & Becklin (1987) who attribute it to a possible 1200 K brown dwarf companion. Infrared imaging by Tokunaga et al. (1988) does not resolve the companion, implying that the separation from the primary is < 5.6 AU or that the excess is caused by dust. Slit scans by Haas & Leinert (1990) show an “extension” of G 29-38 which suggests a companion at 0.23-arcsecond (3.2-AU) separation. Photometry of G 29-38 at 10 microns by Graham et al. (1990) shows a flux level which is three times larger than predicted by the suspected brown dwarf — thus favoring a model based on dust. Infrared broad- and narrow-band data by Tokunaga, Becklin, & Zuckerman (1990) confirm the strong emission at 10 microns and further suggest that the excess radiation comes from orbiting particulate matter.

TABLE 5.18

POSSIBLE VERY LATE TYPE STARS, BROWN DWARF CANDIDATES,
AND EXTREME SUBDWARFS FROM *THE STARS OF LOW*
LUMINOSITY (LUYTEN 1977)

LP #	RA (1950)	Dec	$m_{pg} - m_R$	Note
704-43	0:02	-11	3.7	
704-45	0:03	-10	3.3	
704-58	0:04	-9	3.0	
524-78	0:07	+8	3.3	
704-59	0:09	-10	3.3	
824-434	0:11	-20	> 3.1	LHS 106; real?
824-385	0:11	-25	3.1	
192-47	0:12	+40	3.1	
404-64	0:13	+20	3.2	
348-50	0:14	+26	3.1	
824-442	0:17	-22	3.0	
585-22	0:22	-2	3.0	
349-21	0:24	+23	3.2	
465-27	0:27	+10	3.4	
465-38	0:29	+9	3.2	
765-71	0:30	-18	3.0	
645-52	0:33	-3	3.4	
405-39	0:35	+16	3.6	
150-33	0:36	+49	3.2	
465-63	0:37	+11	3.0	
350-6	0:45	+22	3.3	
406-45	0:55	+18	3.0	
766-89	0:58	-19	3.5	
938-71	1:00	-37	> 2.9	LHS 132
526-62	1:03	+4	3.1	
647-13	1:07	-3	3.1	
407-20	1:10	+19	3.1	
467-31	1:13	+13	3.7	
407-27	1:14	+19	3.3	
587-65	1:25	+1	> 3.2	LHS 1252, M6 (this thesis)
708-98	1:31	-11	3.7	
708-117	1:32	-9	3.1	LHS 1265
648-86	1:42	-7	3.1	

TABLE 5.18 — continued

LP #	RA (1950)	Dec	$m_{pg} - m_R$	Note
828-71	1:43	-23	3.0	
828-72	1:44	-23	3.0	
352-43	1:46	+26	3.3	LHS 1299
529-6	1:55	+6	3.1	
589-14	1:58	+2	3.1	
651-63	2:01	-2	3.1	
353-21	2:11	+26	3.3	
829-42	2:14	-22	3.0	
52-51	2:15	+66	3.0	
885-45	2:16	-27	3.4	
353-59	2:22	+23	3.5	
353-61	2:23	+23	3.2	
245-42	2:25	+34	3.0	
410-39	2:28	+20	3.7	
245-57	2:34	+36	3.1	
245-62	2:35	+36	3.2	
710-82	2:41	-14	3.1	
651-13	2:45	-8	3.0	
471-17	2:47	+11	3.2	
830-59	2:51	-23	3.2	
471-43	3:01	+12	3.2	
53-48	3:13	+67	3.1	
54-4	3:14	+63	3.1	
412-31	3:18	+18	3.4	
532-71	3:19	+3	3.2	
832-9	3:21	-25	3.2	
54-20	3:32	+66	3.2	
533-23	3:33	+5	3.2	
832-29	3:33	-22	3.3	
888-37	3:34	-30	3.2	
300-23	3:35	+32	3.3	
713-22	3:38	-9	3.1	
54-23	3:38	+64	3.8	
533-49	3:40	+6	3.0	
248-18	3:44	+35	3.0	

TABLE 5.18 — continued

LP #	RA (1950)	Dec	$m_{pg} - m_R$	Note
889-3	3:47	-32	3.1	LHS 1604
593-68	3:48	-1	3.3	
889-13	3:53	-27	3.0	
833-38	4:03	-21	3.0	
54-45	4:09	+69	3.7	
302-9	4:17	+32	3.0	
302-27	4:25	+31	3.0	
302-34	4:31	+30	3.0	
84-37	4:35	+60	3.3	
157-34	4:47	+45	3.1	
776-26	4:50	-19	3.1	Comp. to LP 119-41, 5'' away
536-23	4:54	+3	3.7	
84-55	4:55	+61	3.0	
536-25	4:56	+5	3.7	
776-44	5:00	-20	3.3	
892-18	5:10	-27	3.2	
892-27	5:13	-28	3.1	
85-28	5:22	+62	3.0	
119-42	5:23	+55	3.0	
477-33	5:28	+9	3.1	
538-3	5:30	+4	3.5	
837-11	5:34	-25	3.2	
538-7	5:35	+6	3.2	
159-8	5:35	+49	3.1	
893-16	5:43	-32	3.2	
538-21	5:43	+4	3.0	
538-22	5:44	+5	3.0	
538-24	5:44	+3	3.3	
894-4	5:56	-31	> 3.2	
719-7	5:58	-10	3.0	
159-41	5:59	+46	3.3	
779-8	5:59	-17	> 3.0	
159-47	6:01	+47	3.5	
779-28	6:08	-17	3.1	
121-4	6:10	+52	> 3.6	
121-11	6:18	+50	3.3	

TABLE 5.18 — continued

LP #	RA (1950)	Dec	$m_{pg} - m_R$	Note
121-16	6:21	+51	3.4	
121-21	6:22	+52	3.1	
160-38	6:30	+50	3.8	
720-30	6:36	-12	3.4	
895-31	6:42	-31	3.6	
205-32	6:46	+41	3.3	
308-23	7:03	+28	3.2	
308-27	7:06	+31	3.3	
161-260	7:09	+47	3.0	
482-18	7:16	+13	3.0	
123-9	7:27	+54	3.1	
256-25	7:28	+37	3.3	
365-19	7:29	+26	3.7	
123-46	7:46	+54	3.0	
366-23	7:53	+21	3.0	
366-28	7:54	+23	3.2	
545-37	8:36	+2	3.0	
545-45	8:41	+6	3.3	LHS 2045, sdM (this thesis)
606-35	8:49	+0	3.8	LHS 5142, M6.5 (this thesis)
165-5	8:56	+46	3.4	
901-4	8:56	-31	3.5	
165-28	9:05	+48	3.3	
903-32	9:07	-33	3.3	
547-10	9:11	+7	3.1	
369-27	9:16	+22	3.1	
727-47	9:17	-14	3.1	
427-31	9:18	+15	3.4	
125-69	9:19	+54	3.1	
427-38	9:22	+17	3.8	
547-46	9:23	+3	3.2	
667-26	9:25	-7	3.0	
314-28	9:34	+27	3.0	
548-15	9:35	+5	3.1	
314-44	9:36	+29	3.0	
488-15	9:36	+12	3.2	
846-23	9:38	-26	3.5	

TABLE 5.18 — continued

LP #	RA (1950)	Dec	$m_{pg} - m_R$	Note
548-29	9:43	+4	3.2	
370-59	9:45	+21	3.1	
314-69	9:46	+31	3.1	
370-69	9:48	+25	3.1	
166-28	9:48	+44	> 2.9	Real? Not in LHS Catalogue
608-54	9:52	-0	3.5	
609-1	9:53	+1	3.5	
315-11	9:54	+26	3.7	
315-13	9:55	+30	3.4	
315-15	9:55	+29	3.5	
609-19	9:58	+1	3.3	
166-56	9:58	+45	3.8	
609-24	10:00	-0	3.2	LHS 5165
609-25	10:00	+0	3.0	
903-27	10:04	-28	3.2	
609-34	10:05	+0	3.0	
789-28	10:05	-19	3.0	
167-7	10:05	+48	3.3	
903-34	10:07	-29	3.1	
212-34	10:07	+40	3.4	
315-40	10:08	+27	3.0	Comp. to LP 315-39, 14'' away
789-44	10:11	-15	3.2	
315-49	10:12	+27	3.3	
212-40	10:12	+40	3.1	
315-53	10:13	+28	3.4	LHS 2243, M8 (this thesis)
489-65	10:16	+9	3.1	
790-24	10:24	-18	3.2	
904-21	10:25	-29	3.5	
490-28	10:26	+12	3.0	
551-3	10:41	+5	3.4	
611-5	10:42	+1	3.3	
551-13	10:46	+5	3.1	LHS 2314, M6 (Bessell 1991)
551-18	10:48	+7	3.5	
551-30	10:53	+6	3.2	
731-72	10:53	-12	3.0	
905-32	10:54	-28	3.1	

TABLE 5.18 — continued

LP #	RA (1950)	Dec	$m_{pg} - m_R$	Note
731-78	10:56	-14	3.5	
263-62	10:59	+35	3.3	
551-63	11:03	+4	3.2	LHS 2351, M6.5 (Bessell 1991)
263-78	11:04	+33	3.0	LHS 2352, sdM (this thesis)
168-70	11:07	+46	3.1	
672-19	11:14	-9	3.6	
672-65	11:16	-3	> 2.9	
732-20	11:17	-14	3.3	LHS 2397, M5 (Bessell 1991)
672-70	11:19	-4	3.3	
732-23	11:20	-12	3.1	
215-4	11:20	+42	3.0	
672-73	11:20	-4	3.4	
264-47	11:20	+34	3.2	
374-43	11:22	+24	3.1	
672-35	11:22	-6	3.2	
672-37	11:24	-6	3.0	
612-55	11:25	-0	3.2	
793-2	11:29	-19	3.8	
673-10	11:31	-5	3.0	
169-59	11:32	+47	3.5	
433-20	11:33	+19	3.1	
907-10	11:36	-28	> 3.4	
793-56	11:40	-19	3.1	
533-34	11:41	+4	3.1	
907-20	11:42	-30	3.6	
433-60	11:46	+16	3.0	
907-301	11:52	-31	> 3.0	
434-13	11:56	+16	3.0	
907-48	11:56	-27	3.5	LHS 2487
794-8	11:58	-19	3.0	
434-29	12:00	+17	3.3	LHS 2500, sdM0.5-1: (Boes. '92)
907-63	12:00	-33	3.2	
434-33	12:00	+17	3.8	LHS 2502, M6+ (Bessell 1991)
434-36	12:01	+15	3.7	
376-6	12:01	+22	3.2	
266-10	12:02	+36	3.1	

TABLE 5.18 — continued

LP #	RA (1950)	Dec	$m_{pg} - m_R$	Note
734-22	12:03	-11	3.1	
434-46	12:04	+16	3.1	
494-38	12:04	+13	3.2	Comp. BD + 13°2493, 66'' away
376-19	12:05	+20	3.0	
734-77	12:06	-10	3.4	
908-27	12:08	-30	3.0	
908-33	12:11	-27	3.1	
266-28	12:13	+32	3.1	
434-75	12:13	+16	3.1	
170-90	12:17	+46	3.2	
908-47	12:17	-31	> 3.0	
555-15	12:21	+5	3.2	
496-1	12:41	+9	3.1	
853-33	12:43	-23	3.0	
321-222	12:44	+32	3.1	LHS 2632, M7 (this thesis)
853-43	12:46	-27	3.0	
496-23	12:47	+13	3.2	
217-82	12:48	+40	3.1	Comp. 102'' away
171-70	12:48	+48	3.1	
218-8	12:50	+40	3.2	LHS 2645, M7 (this thesis)
616-45	12:55	-3	3.2	
796-36	13:01	-21	3.5	
616-75	13:03	-1	3.2	
797-5	13:06	-16	3.2	
497-35	13:12	+9	3.2	
854-46	13:15	-22	3.3	
677-20	13:16	-4	3.3	
497-58	13:16	+13	3.0	
677-65	13:17	-9	3.2	
218-81	13:18	+42	> 3.1	
737-25	13:20	-9	3.3	
737-26	13:21	-11	3.2	
677-41	13:25	-4	3.1	Comp. to LP 677-40, 8'' away
497-97	13:26	+9	3.8	Comp. BD + 10°2550, 79'' away
497-105	13:28	+10	3.4	

TABLE 5.18 — continued

LP #	RA (1950)	Dec	$m_{pg} - m_R$	Note
855-33	13:31	-24	3.0	LHS 2755
855-39	13:34	-24	3.0	
855-41	13:34	-22	3.8	
911-38	13:36	-28	> 2.9	
855-49	13:36	-25	3.0	
438-46	13:41	+20	3.0	
911-56	13:43	-31	3.1	
558-46	13:45	+5	3.1	
381-4	13:45	+26	3.1	
912-12	13:46	-31	3.4	
498-70	13:47	+9	3.1	
738-16	13:48	-12	3.0	
558-51	13:48	+3	3.2	
558-52	13:49	+7	3.2	
912-24	13:49	-29	3.0	
220-13	13:54	+43	3.2	
912-47	14:02	-33	3.4	
912-49	14:03	-30	3.2	LHS 2859
499-39	14:06	+12	3.0	
912-63	14:09	-31	4.0	Largest $m_{pg} - m_R$ in the list
913-5	14:09	-28	3.1	
499-47	14:09	+10	3.2	
799-31	14:10	-21	3.1	
559-57	14:10	+7	3.2	
799-33	14:12	-21	3.1	
220-71	14:15	+44	3.1	
499-62	14:15	+13	3.4	Comp. to LP 499-63, 20'' away
440-7	14:16	+20	3.3	LHS 2893, M1.5 (Boeshaar '92)
913-10	14:17	-30	3.3	
134-7	14:21	+51	3.5	
620-17	14:25	-1	3.1	
620-19	14:26	+1	3.3	
271-25	14:26	+33	3.0	LHS 2924, M9 (this thesis)
325-56	14:31	+29	3.0	
440-52	14:36	+18	3.1	LHS 377, sdM5 (Giampapa & Liebert 1986)

TABLE 5.18 — continued

LP #	RA (1950)	Dec	$m_{pg} - m_R$	Note
560-62	14:37	+3	3.0	
271-50	14:38	+37	3.2	
271-53	14:39	+33	3.0	
858-19	14:41	-26	3.0	Comp. to LP 858-18, 12'' away
914-14	14:41	-32	3.4	
914-16	14:42	-29	3.3	
271-61	14:45	+36	3.0	
326-27	14:45	+26	3.1	
441-17	14:45	+16	3.3	LHS 2980, M6.5 (this thesis)
175-31	14:46	+49	3.1	
272-5	14:48	+35	3.0	
175-36	14:48	+50	3.2	
382-40	14:54	+23	3.4	
441-34	14:54	+18	3.5	LHS 3002, M7 (Boeshaar 1992)
801-38	14:56	-17	> 3.0	
801-39	14:56	-18	3.5	
222-23	14:56	+41	3.2	
326-61	14:57	+31	3.0	
621-62	15:01	+0	3.4	
681-56	15:02	-3	3.1	
176-12	15:11	+48	3.2	
742-41	15:16	-14	3.1	
562-29	15:16	+5	3.0	
327-309	15:16	+28	3.0	
742-18	15:23	-10	3.5	
273-25	15:25	+37	3.3	
176-46	15:26	+46	3.0	
273-32	15:28	+33	3.0	
623-7	15:32	-0	3.2	
803-9	15:33	-19	3.1	
273-46	15:35	+35	3.0	Comp. to LP 273-45, 13.5'' away
683-26	15:39	-3	3.6	
916-19	15:39	-33	3.4	LHS 3106, M6 (Bessell 1991)
223-47	15:42	+44	3.2	
684-37	15:45	-3	3.4	

TABLE 5.18 — continued

LP #	RA (1950)	Dec	$m_{pg} - m_R$	Note
803-33	15:45	-19	4.0	Largest $m_{pg} - m_R$ in the list
803-34	15:45	-15	3.2	
860-36	15:47	-23	3.0	
328-55	15:50	+27	3.4	
743-49	15:50	-13	3.0	
860-47	15:51	-24	3.0	
860-49	15:53	-22	3.0	
274-27	15:53	+36	3.0	
178-1	16:12	+48	3.2	
275-10	16:13	+37	3.1	
861-50	16:15	-26	3.5	LHS 3170
505-3	16:17	+12	3.6	
565-3	16:17	+5	3.2	
745-4	16:19	-11	3.1	
225-14	16:21	+39	3.0	
178-15	16:21	+49	> 3.0	
178-18	16:23	+45	3.2	
625-14	16:24	-2	3.0	
745-9	16:24	-12	3.2	
445-45	16:37	+17	3.1	
626-13	16:50	+0	3.3	
746-30	16:53	-14	3.4	
746-32	16:54	-13	3.4	
566-29	17:01	+3	3.0	
566-33	17:01	+3	3.0	
179-42	17:15	+45	3.2	
508-2	17:28	+12	3.2	
688-2	17:30	-7	> 2.9	
688-11	17:37	-6	3.0	
508-20	17:39	+9	3.1	
508-41	17:50	+11	3.2	
688-32	17:51	-7	3.3	
508-45	17:51	+9	3.3	
508-46	17:52	+12	3.1	
181-17	18:02	+46	3.7	

TABLE 5.18 — continued

LP #	RA (1950)	Dec	$m_{pg} - m_R$	Note
228-23	18:04	+44	3.1	
140-34	18:36	+55	3.0	
813-4	19:34	-18	3.1	
925-33	19:39	-32	3.1	
869-29	19:42	-24	3.0	
925-44	19:45	-32	3.2	
870-14	19:51	-21	3.1	
926-41	20:08	-29	3.0	
754-37	20:13	-11	3.2	
754-41	20:14	-10	3.3	
575-18	20:27	+6	3.4	Comp. to LP 575-17, 77'' away
815-50	20:39	-20	3.1	
515-42	20:40	+13	3.1	
756-10	20:48	-12	3.1	
636-23	20:51	+1	3.0	LHS 5360; Comp. 2.5'' away
928-32	20:52	-28	3.0	
696-17	20:53	-6	3.0	
756-22	20:53	-12	3.1	
696-20	20:54	-5	3.1	
756-34	21:00	-11	3.2	
756-46	21:05	-10	3.0	
517-21	21:14	+14	3.1	
697-19	21:14	-5	> 3.2	
397-13	21:15	+25	3.0	
697-24	21:17	-3	3.0	
873-36	21:20	-25	3.3	
697-32	21:21	-7	3.6	
697-33	21:22	-4	> 3.0	
929-54	21:27	-31	3.1	LHS 3681
929-63	21:31	-31	3.3	
458-7	21:31	+19	3.2	
398-24	21:39	+25	3.1	
930-29	21:40	-32	3.2	
818-27	21:41	-18	3.2	
578-40	21:47	+9	3.4	
458-51	21:49	+20	3.3	

TABLE 5.18 — continued

LP #	RA (1950)	Dec	$m_{pg} - m_R$	Note
759-1	21:53	-11	3.0	
819-18	21:59	-14	3.3	
759-17	21:59	-11	> 3.2	
519-21	22:01	+14	3.0	
759-25	22:02	-11	3.7	
699-33	22:03	-4	3.1	
699-36	22:04	-4	3.5	
639-30	22:06	-2	3.4	
287-32	22:08	+33	3.1	
819-42	22:08	-19	3.6	LHS 3768
76-8	22:11	+68	3.2	
519-45	22:12	+12	3.0	
819-60	22:13	-20	3.1	
819-61	22:13	-18	3.0	
819-68	22:17	-17	3.3	
700-5	22:19	-2	3.0	
700-56	22:35	-5	> 3.1	LHS 3837
934-57	22:37	-31	3.1	
876-53	22:40	-21	3.2	
761-44	22:43	-13	3.4	
821-15	22:43	-15	3.2	
761-46	22:43	-13	3.1	
289-4	22:44	+38	3.2	
400-63	22:47	+25	3.4	
761-61	22:49	-9	3.6	
877-4	22:51	-23	3.1	
521-43	22:52	+14	3.2	
521-44	22:52	+10	3.0	
345-18	22:53	+28	3.4	
521-56	22:56	+11	3.3	
289-34	22:57	+37	3.0	
581-47	22:57	+8	3.2	
401-41	23:01	+27	3.1	
877-10	23:01	-25	3.4	
238-39	23:14	+39	3.2	
702-59	23:14	-4	3.2	

TABLE 5.18 — continued

LP #	RA (1950)	Dec	$m_{pg} - m_R$	Note
522-33	23:17	+11	3.0	LHS 3933
762-9	23:19	-9	3.3	
702-87	23:22	-4	3.1	
702-91	23:23	-5	3.0	
290-32	23:24	+36	3.0	
878-47	23:28	-26	3.0	
402-58	23:34	+21	> 2.9	
763-39	23:35	-10	3.1	
763-41	23:35	-12	3.3	
763-51	23:39	-8	3.2	
763-67	23:45	-8	3.3	
403-11	23:46	+27	3.0	
879-22	23:47	-26	3.4	
583-58	23:48	+7	3.2	
823-59	23:49	-15	3.2	
763-15	23:50	-8	3.2	
192-8	23:53	+41	3.1	
824-420	23:56	-26	3.1	
824-75	23:59	-22	3.1	

TABLE 5.19
OBJECTS WITH THE HIGHEST PROPER MOTIONS (AS OF 1992)

LHS #	Other Name	$\mu("yr^{-1})$	m_V^a	Spec.	In 1927 list? ^b
57	Barnard's Star	10.27	9.5	M4	✓
29	Kapteyn's Star	8.73	8.8	M1	✓
44	BD +38°2285	7.04	6.5	G5	✓
70	CD -36°15693	6.90	7.4	M2	✓
1	CD -37°15492	6.08	8.6	M3	✓
35	Ross 619	5.40	12.8	M4.5	
62	61 Cyg A	5.20	5.2	K5	✓
63	61 Cyg B	5.20	6.0	K7	✓
37	BD +36°2147	4.78	7.5	M2	✓
36	Wolf 359	4.71	13.5	M6	✓
67	ϵ Ind	4.69	4.7	K5	✓
38	BD +44°2051 A	4.53	8.8	M1	✓
39	BD +44°2051 B	4.53	14.5	M5	
23	σ^2 Eri A	4.08	4.4	K0	✓
24	σ^2 Eri B	4.08	9.5	DA	✓
25	σ^2 Eri C	4.08	11.2	M4.5	✓
46	Wolf 489	3.87	14.7	DZ	✓
49	α Cen C	3.85	11.1	M5.5	✓
33	Luyten's Star	3.76	9.8	M3.5	
8 A	μ Cas A	3.75	5.2	G5	✓
8 B	μ Cas B	3.75	>8.2	?	
50	α Cen A	3.69	0.0	G2	✓
51	α Cen B	3.69	1.3	K0	✓
53	BD -15°4042	3.68	9.0	G6	✓
52	BD -15°4041	3.68	9.4	K0	✓

TABLE 5.19 — continued

LHS #	Other Name	$\mu("yr^{-1})$	m_V^a	Spec.	In 1927 list? ^b
56	GL 699.1	3.62	14.3	DA	
66	CD $-39^{\circ}14192$	3.46	6.7	M0	✓
9	GL 65 A	3.36	12.5	M5.5	
10	GL 65 B	3.36	13.0	M6	
68 A	GL 866 A	3.25	12	M5	
68 B	GL 866 B	3.25	12	M5	
42	Ross 451	3.20	11	K4	
19	CD $-43^{\circ}1028$	3.14	4.3	G7	✓
20	Ross 578	3.06	13.0	M2	
7	van Maanen's Star	2.98	12.4	DZ	✓

^a Magnitudes are from Gliese 1969.

^b Refers to Table XV in Russell, Dugan, & Stewart 1927.

TABLE 5.20
 OBJECTS WITH PROPER MOTIONS EXCEEDING $0.57''\text{yr}^{-1}$
 WHICH ARE NOT INCLUDED IN THE LHS CATALOGUE

Name	RA (1950)	Dec	Spec.	m_V	$\mu(''\text{yr}^{-1})$	Ref.
GJ 2045	05:39:45.5	-05:29:42	?	~ 14.9	~ 3	1 (star 50)
ER 8	13:10:03.6	-47:12:13	wd	~ 17.2	2.128	2
LP 251-35	05:18:38	+38:12:24	sdM	~ 18.0	1.725	3,4
unnamed	$\sim 11:30$	~ -30	?	—	~ 1.1	5
ER 2	?	?	dM	~ 12.7	1.04	6
ESO 320-24	?	?	K6	~ 15	0.969	7
CD $-32^\circ 828$	02:11:40	-32:16:00	M?	~ 10.2	0.942	8 (GL 91)
unnamed	$\sim 11:30$	~ -30	?	—	~ 0.80	5
ER 6	?	?	dM	~ 16.3	0.78	6
unnamed	$\sim 11:30$	~ -30	?	—	~ 0.65	5
LP 114-28	01:54:19	+52:53:48	?	~ 17.3	0.708	3
LP 304-36	05:07:08	+27:09:18	?	~ 18.0	0.675	3
LP 868-34	19:03:47	-24:19:06	?	~ 17.8	0.654	3
LP 111-19	23:53:55	+52:54:18	?	~ 16.6	0.597	3
CD $-27^\circ 101$	00:19:52	-27:18:18	K3	8.3	0.591	8 (GL 17.2)
LP 662-7	07:14:47	-04:55:18	?	15.6	0.590	3
Ross 29 A	04:09:27	+50:24:12	M5:	~ 15	0.572	8 (GL 165
Ross 29 B	04:09:27	+50:24:12	?	?	0.572	8 A & B)

REFERENCES. — (1) Ohtani & Ichikawa 1977; (2) Ruiz, Maza, Wischnjewsky, & González 1986; (3) Luyten & Hughes 1982; (4) Liebert et al. 1993; (5) Ruiz, Maza, Mendez, & Wischnjewsky 1988; (6) Ruiz & Maza 1987; (7) Ruiz, Maza, Wischnjewsky, & González 1988; (8) Gliese 1969.

CHAPTER 6

SUMMARY

Nature is wont to hide herself.

— Heraclitus, On the Universe, fragment 10 (c. 540 - c. 480 B.C.)

...And thus does the lowest luminosity stellar component of our galaxy remain largely hidden, but this thesis has attempted to lay some of the ground-work upon which a more complete understanding of these objects can be based. Briefly:

- A spectroscopic sequence obtained at wavelengths between 6000 and 9000 Å has been established for dwarfs of type K5 to M9. In total, 125 spectra comprise this set of standards, among which a few representative subdwarf and giant spectra are given for comparison. Atomic and molecular features usable as criteria for spectral and luminosity classification are tabulated.
- To supplement this spectral sequence, a few of the objects were also observed in the near infrared. The resulting 0.6-to-1.5 micron sequence of dwarf stars shows many temperature-sensitive features which can be used for spectral classification. This wavelength region is a logical choice for studies of M dwarfs since these objects emit their peak fluxes there.
- Recently, model atmospheres for M dwarfs have been produced which more closely duplicate observed spectroscopic properties. The modelled spectra have

been fit against the observed sequence in the red and near-infrared to produce a new temperature scale for main sequence M stars — previous temperature determinations relied almost exclusively on fitting a blackbody to observed spectra or spectrophotometry. The new determination, however, brings the temperature scale into much better agreement with theoretical models of the main sequence and assigns the later dwarfs hotter temperatures that had previously been estimated.

- One spectrum was uncovered which can not be predicted by current atmospheric theory. This peculiar object, GD 165 B, though now in a class by itself, may represent the first clear example of a numerous population of brown dwarfs. Its spectrum is compared to those of late M dwarfs and of planets in an attempt to link the two sets of objects. This object should also be spectroscopically studied in the near infrared.
- A search for low-mass stars and brown dwarf candidates was conducted using the data bases provided by the CTI. This search uncovered many late M dwarfs but only two objects of type M7 or later, demonstrating the difficulty which exists in trying to find objects of faint absolute magnitude.
- Luminosity functions have been produced at I and at V which are in excellent agreement with previous determinations using photometric surveys of the field. There is a striking difference, however, between these luminosity functions and the luminosity function calculated for nearby stars. It has been shown that this difference is largely based on the fact that binaries are much more easily resolved in the nearby sample. The resulting mass function is difficult to estimate due to the lack of observational data on the M_I vs. Mass plane, but unless the upward tail seen in the CTI luminosity function is indicative of a still undetected, large

population of objects, M dwarfs and brown dwarfs do not comprise the local missing mass.

Somewhat unexpectedly, this thesis has also uncovered several lines of evidence which point to the conclusion that some of the objects currently referred to as “M dwarfs” may actually be the brown dwarfs researchers have fought so hard to find. It has been shown that:

- If the trend of decreasing mass with later spectral type is extrapolated linearly to the hydrogen-burning limit, it suggest that objects typed as $\sim M7$ and later are brown dwarfs.
- Differential spectroscopy on composite systems with low-mass secondaries indicates that two prime brown dwarf candidates, LHS 1047 B and Ross 614 B, have spectral types no later than $\sim M6.5$.
- The minimum in the CTI luminosity function occurs at $M_I \sim 12.5$, with the number density of objects rising for fainter magnitudes. Other studies have suggested that this is the contribution from substellar objects. The CTI objects comprising this upward tail in the luminosity function all have spectral types of M6 or later.
- When the trend of M_I with mass is linearly extrapolated to the stellar cutoff of $0.08M_{\odot}$, the resulting magnitude is found to be $M_I = 12.3$, corresponding to the minimum in the luminosity function and giving credence to the idea that the subsequent rise is caused by a population of brown dwarfs. Again, these CTI objects having $12.5 < M_I < 13.5$ have been classified as late M dwarfs.

This upward tail in the luminosity function can be verified only if the census of nearby objects is more accurately known at lower luminosities. Luyten’s extensive lists of proper motion objects should be studied in a systematic way

to uncover possibly nearby objects. Such a systematic search is currently under-way to obtain spectroscopic identifications of objects which Luyten found to be extremely red.

These proper motion surveys have not been, however, sensitive to those objects having extremely large motions. As a result, faint objects having very high values of μ will have escaped detection, and such objects are likely to be members of the immediate solar vicinity. A project to search for these candidates will commence in the near future.

Nearby objects do not necessarily have to exhibit large proper motions, so even these surveys will miss some of the sun's neighbors. An all-sky photometric survey, preferably in the infrared and to very faint magnitudes, is perhaps marginally feasible, with the most complete search — an all-sky parallax survey to faint magnitudes — being unthinkable.

For the present at least, Nature keeps herself hidden. Faint, previously unrecognized M dwarfs continue to be discovered in the solar neighborhood, and the possibility still exists that the Sun could have a brown dwarf companion which has so far gone undetected. Slowly, more is being learned about the physics of and the interconnections between the lowest mass stars, brown dwarfs, and planets. The years ahead promise to provide many new insights into the composition of our own galactic environs... and of our Universe in general.

APPENDIX A

FINDER CHARTS FOR CTI SPECTROSCOPIC TARGETS

Each of the following pages is divided into three sections: a finder chart for every CTI target which was spectroscopically observed at the Multiple Mirror Telescope (MMT) during the course of the thesis, the spectrum of the object, and a section of notes relating to that object. These targets are listed in order of increasing right ascension, beginning with 0^h .

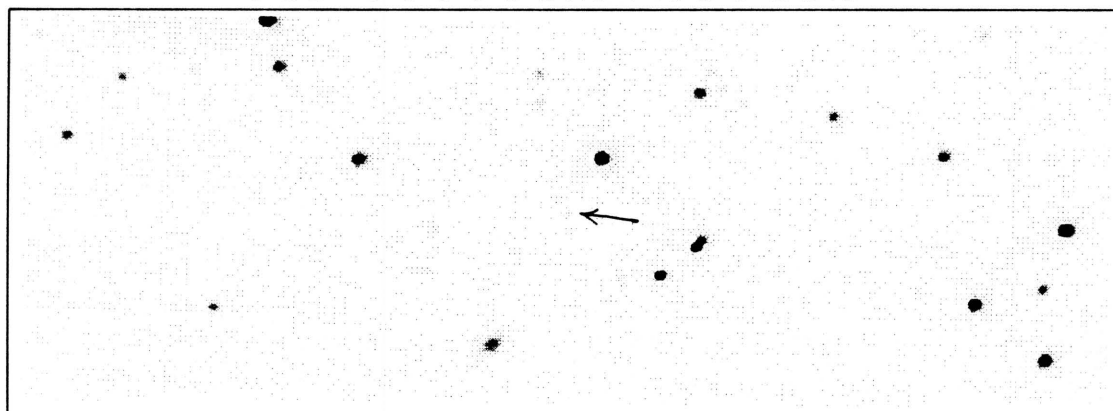
Above each finder chart is printed the CTI designation — a code, denoted by hhmmss.s+ddmmss, giving the coordinates (in equinox 1987.5) of each object. The box enclosing each finder chart is 8 arcminutes long and 3 arcminutes wide. North is at the top and east is to the left. The finders are made from reduced CTI frames taken at the filter position and on the date listed below the chart. Finders made from coadded frames do not have a specific date listed and in general are slightly more magnified than finders made from a single night's data.

All of the spectra were obtained at the MMT using the setup described in Chapter 3. The vertical scale is in units of F_λ normalized to one at 7500 \AA . The exposure time and date of observation are given above each spectrum. Spectra taken on or before 1990 May 23 have a dead column at wavelength $\sim 6410 \text{ \AA}$ and a partially dead column at $\sim 8075 \text{ \AA}$. Features useful as temperature and luminosity indicators in this spectral region are discussed in Chapter 3.

Below each spectrum is listed the object's 1950 coordinates, the spectral type

as determined via the least-squares minimization technique, and the photometry. The R_{CTI} , $(R - I)_{CTI}$, and $(V - I)_{CTI}$ values were taken directly from the CTI data base; the I_{KC} and $(V - I)_{KC}$ values are estimates based on the values of the CTI photometry together with the photometric calibrations presented in Chapter 4. In some cases, this Kron-Cousins photometry was actually measured at the U.S. Naval Observatory in Flagstaff, Arizona, in which case a note is added saying, "Actual USNO VI photometry." The notes also contain information regarding variability for the giants as well as proper motions for those objects which appear to have moved (as measured by eye) since the original Palomar Sky Survey.

CTI 000055.2+280432



CTI FINDER CHART

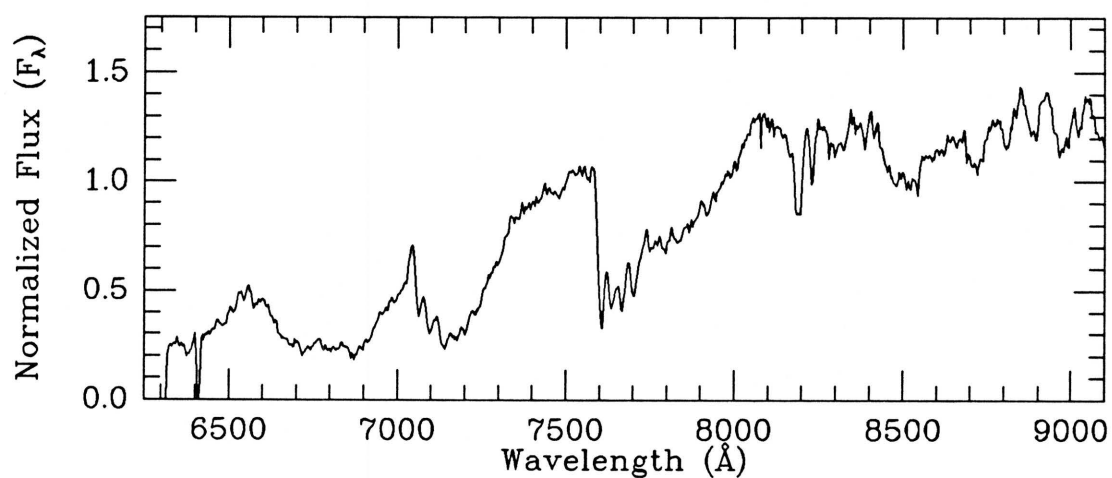
V filter

Obs. (UT) 1987 Oct 20

MMT SPECTRUM

Exposure: 2100 sec

Obs. (UT) 1989 Jul 14

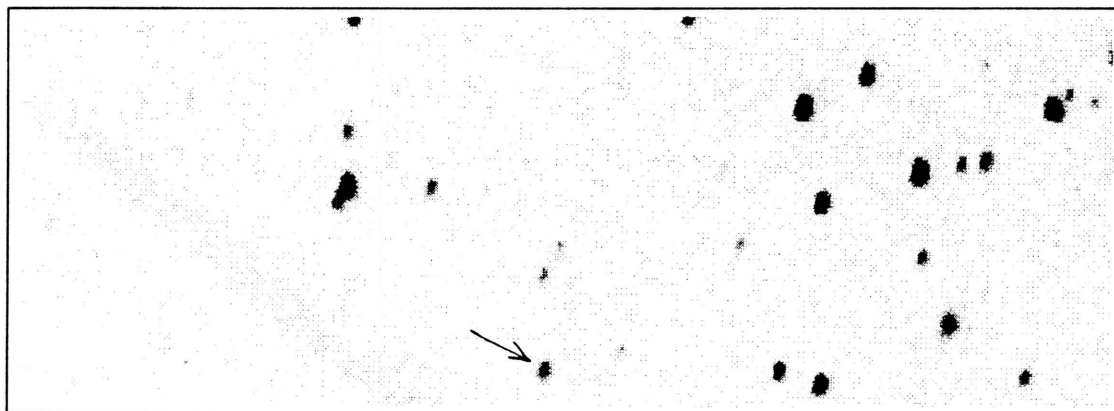
Coordinates: α (1950) = 23:59:00.0 δ (1950) = +27:52:00

Spectral Type: M4.5 V

Photometry: $I_{\text{KC}} = 16.29$ $R_{\text{CTI}} = 17.57$ $(V-I)_{\text{KC}} = 3.17 \pm 0.16$ $(R-I)_{\text{CTI}} = 1.29 \pm 0.07$ $(V-I)_{\text{CTI}} = 3.17 \pm 0.05$

Notes:

CTI 000139.9+275821



CTI FINDER CHART

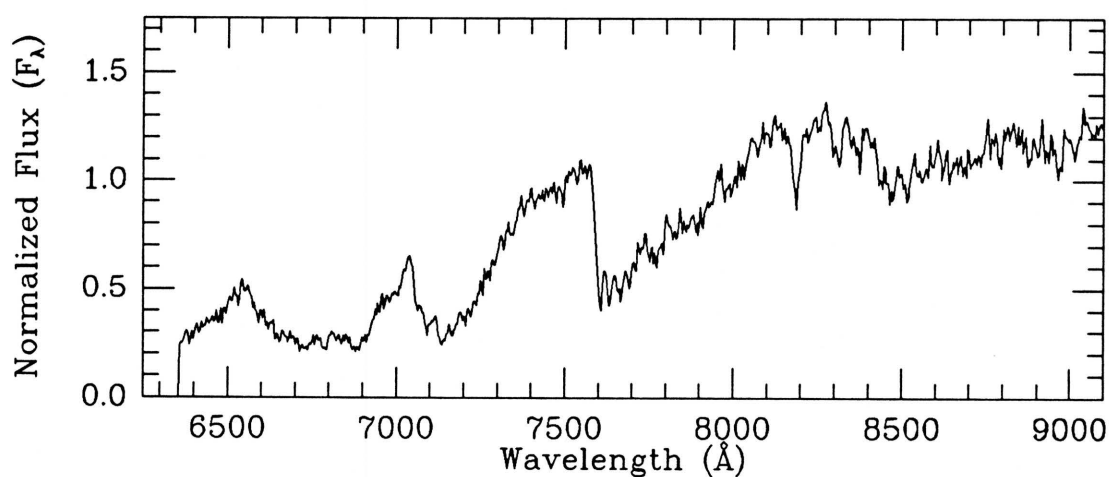
I filter

Obs. (UT) 1988 Nov 01

MMT SPECTRUM

Exposure: 1800 sec

Obs. (UT) 1991 Jun 24

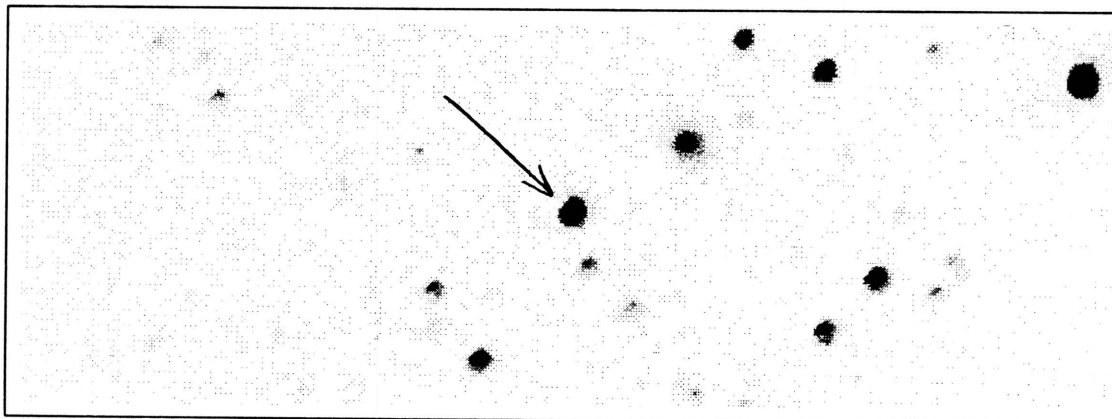
Coordinates: α (1950) = 23:59:44.5 δ (1950) = +27:45:49

Spectral Type: M4.5 V

Photometry: $I_{KC} = 16.56$ $R_{CTI} = 18.39$ $(V-I)_{KC} = 3.98 \pm 0.18$ $(R-I)_{CTI} = 1.86 \pm 0.08$ $(V-I)_{CTI} = 3.18 \pm 0.06$

Notes:

CTI 000351.3+280138



CTI FINDER CHART

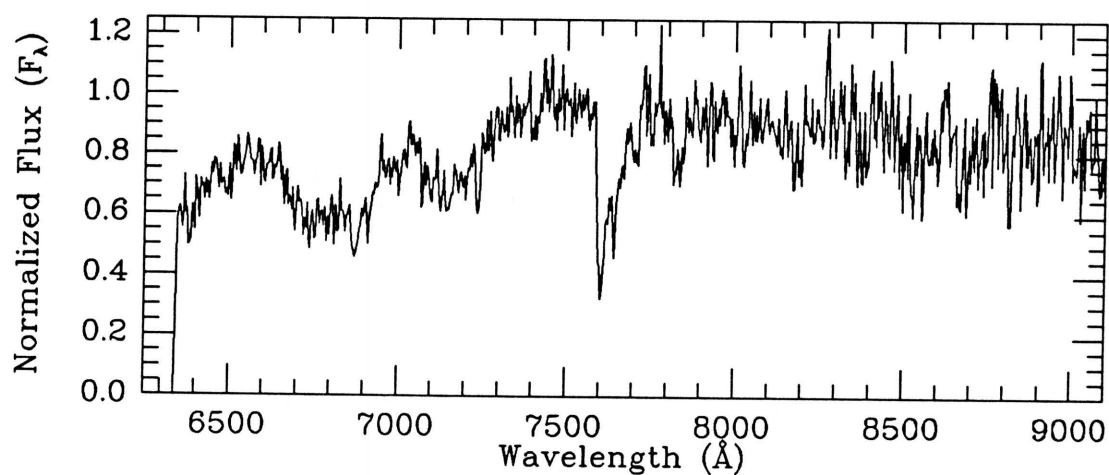
I filter

Obs. (UT) 1989 Nov 03

MMT SPECTRUM

Exposure: 360 sec

Obs. (UT) 1990 Nov 22

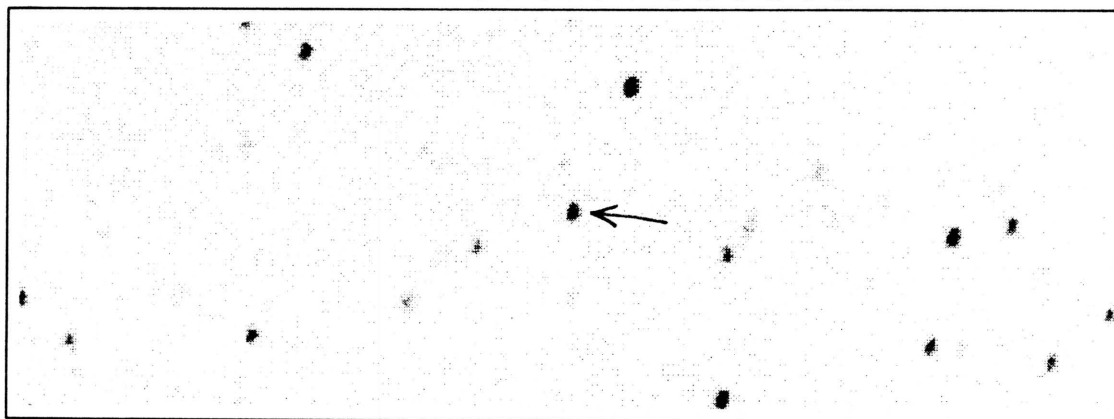
Coordinates: α (1950) = 00:01:55.7 δ (1950) = +27:49:06

Spectral Type: sdM0

Photometry: I_{KC} = unknown R_{CTI} = 14.05 $(V-I)_{KC}$ =unknown $(R-I)_{CTI}$ =0.50 \pm 0.01 $(V-I)_{CTI}$ =1.91 \pm 0.01

Notes:

CTI 000455.2+280301



CTI FINDER CHART

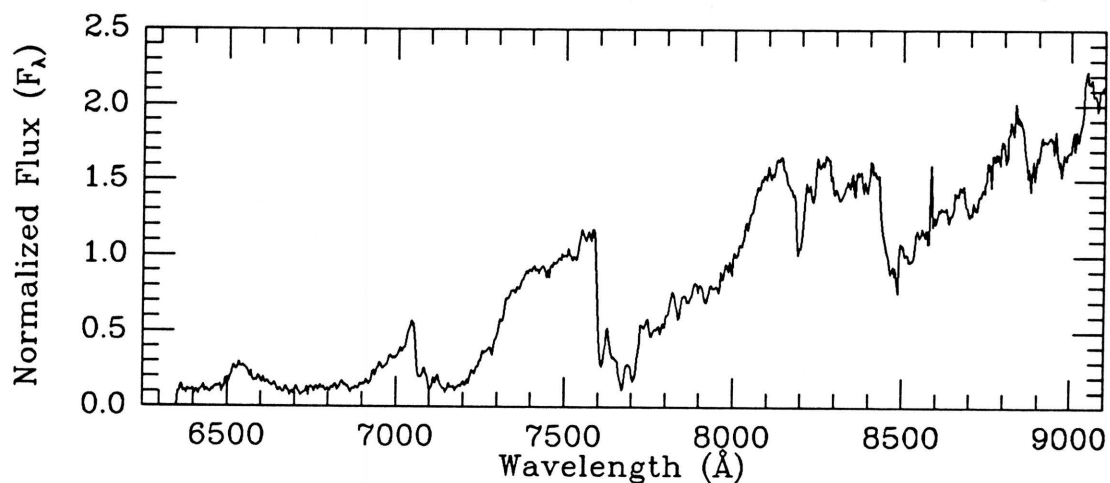
I filter

Obs. (UT) 1988 Nov 01

MMT SPECTRUM

Exposure: 2700 sec

Obs. (UT) 1990 Sep 13

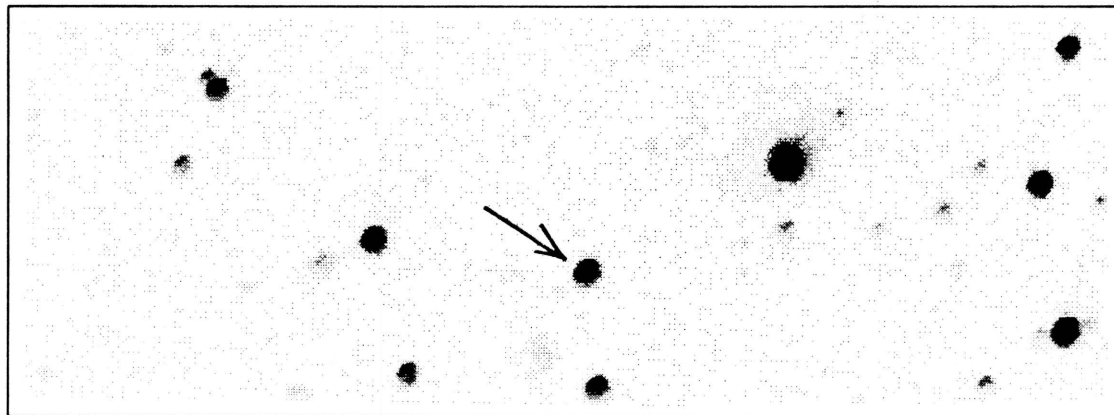
Coordinates: α (1950) = 00:02:59.5 δ (1950) = +27:50:29

Spectral Type: M6 V

Photometry: $I_{KC} = 16.28$ $R_{CTI} = 18.27$ $(V-I)_{KC} = 4.18 \pm 0.19$ $(R-I)_{CTI} = 2.00 \pm 0.08$ $(V-I)_{CTI} = 4.08 \pm 0.08$

Notes: Large proper motion? Object not found on POSS E print.

CTI 000537.5+275850



CTI FINDER CHART

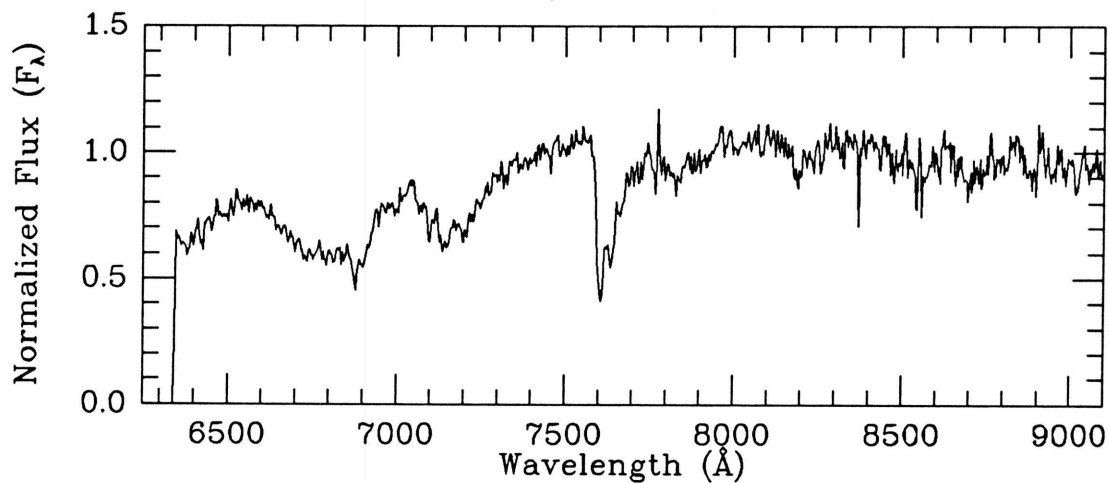
I filter

Obs. (UT) 1989 Nov 03

MMT SPECTRUM

Exposure: 900 sec

Obs. (UT) 1990 Nov 22

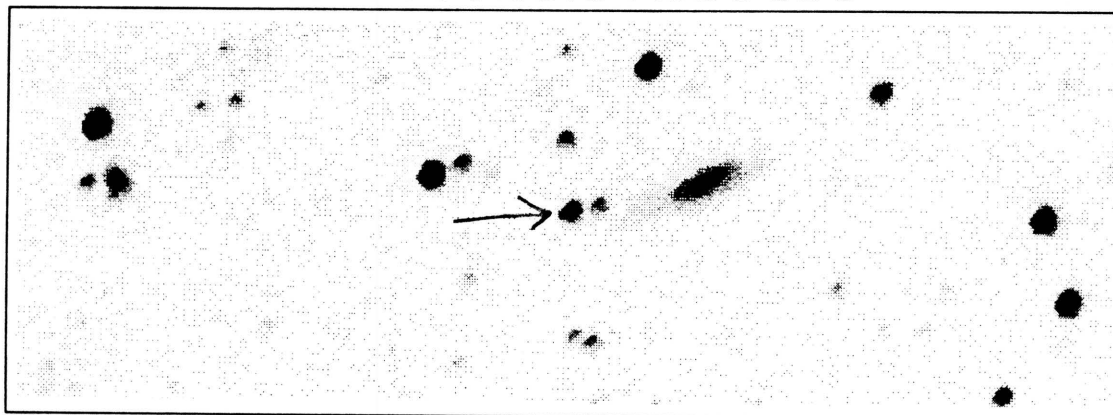
Coordinates: α (1950) = 00:03:41.2 δ (1950) = +27:46:18

Spectral Type: M1 V

Photometry: $I_{KC} = 14.28$ $R_{CTI} = 14.91$ $(V-I)_{KC} = 2.11 \pm .10$ $(R-I)_{CTI} = 0.55 \pm .01$ $(V-I)_{CTI} = 2.01 \pm .01$

Notes:

CTI 000928.8+280436



CTI FINDER CHART

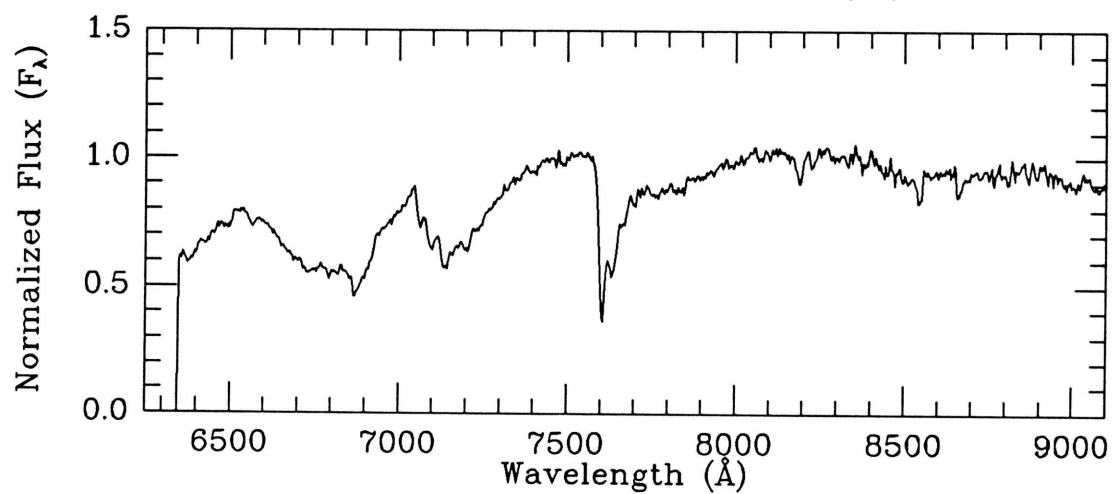
I filter

Obs. (UT) 1989 Nov 03

MMT SPECTRUM

Exposure: 1500 sec

Obs. (UT) 1990 Nov 23

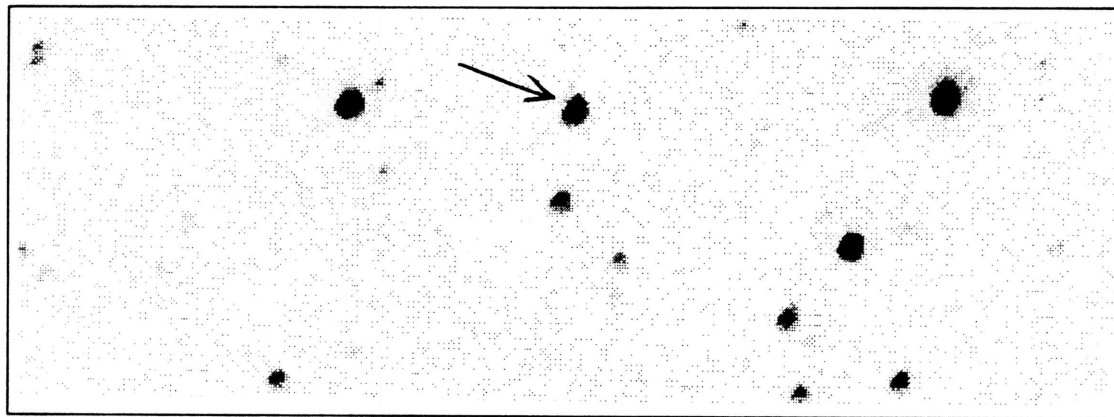
Coordinates: α (1950) = 00:07:32.5 δ (1950) = +27:52:05

Spectral Type: M1.5 V

Photometry: $I_{KC} = 14.72$ $R_{CTI} = 15.37$ $(V-I)_{KC} = 2.17 \pm 0.10$ $(R-I)_{CTI} = 0.59 \pm 0.01$ $(V-I)_{CTI} = 2.01 \pm 0.01$

Notes:

CTI 001251.1+280535 A



CTI FINDER CHART

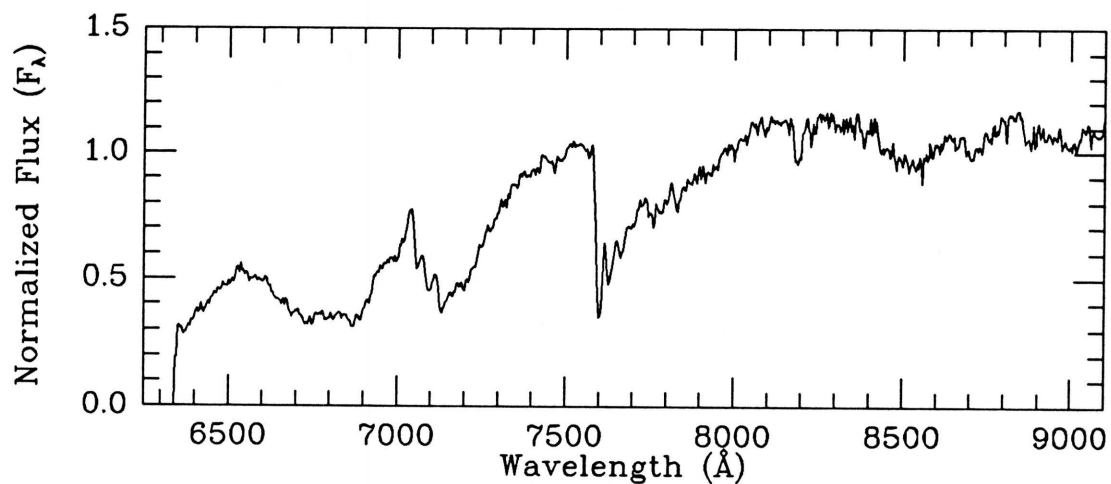
I filter

Obs. (UT) 1989 Nov 03

MMT SPECTRUM

Exposure: 1170 sec

Obs. (UT) 1990 Nov 22

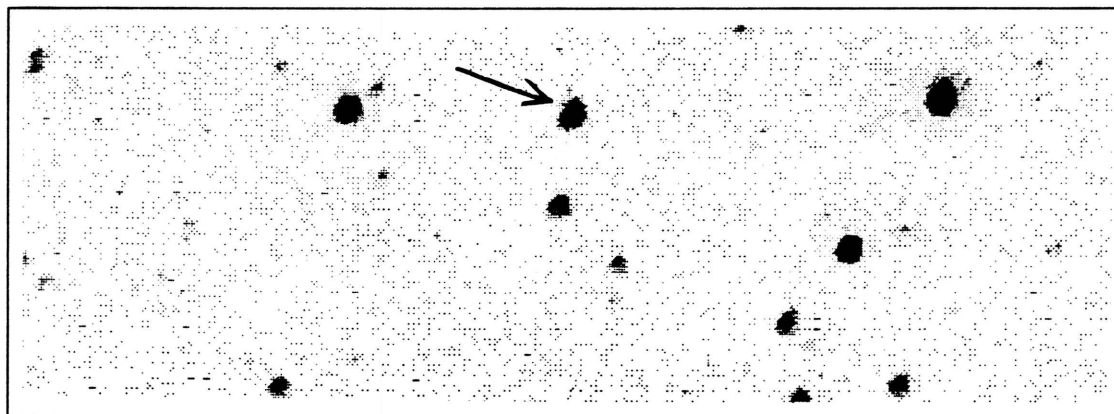
Coordinates: α (1950) = 00:10:54.4 δ (1950) = +27:53:04

Spectral Type: M3.5 V

Photometry: $I_{KC} = 14.33$ $R_{CTI} = 15.44$ $(V-I)_{KC} = 2.80 \pm 0.12$ $(R-I)_{CTI} = 1.03 \pm 0.02$ $(V-I)_{CTI} = 2.67 \pm 0.01$

Notes: Close double star (see next page). Photometry is a composite of both stars.

CTI 001251.1+280535 B



CTI FINDER CHART

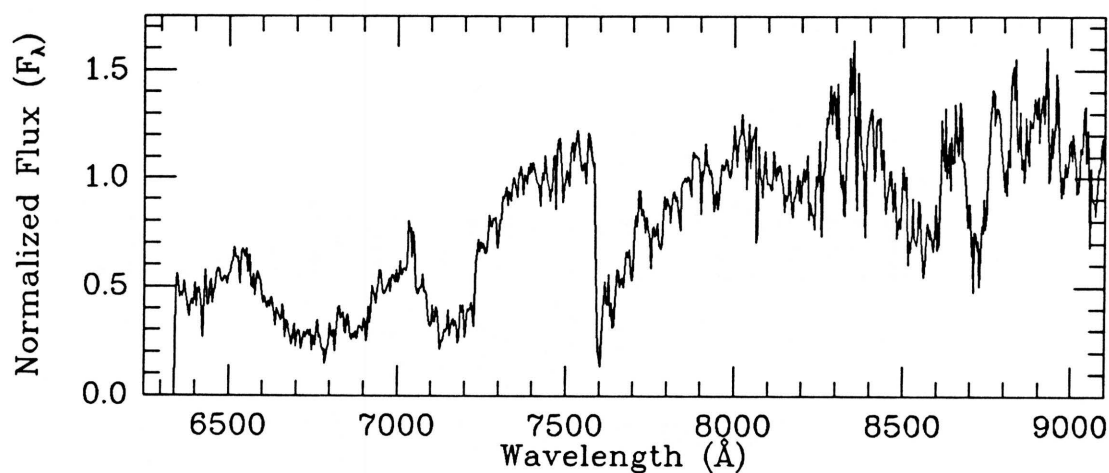
I filter

Obs. (UT) 1989 Nov 03

MMT SPECTRUM

Exposure: 1170 sec

Obs. (UT) 1990 Nov 22

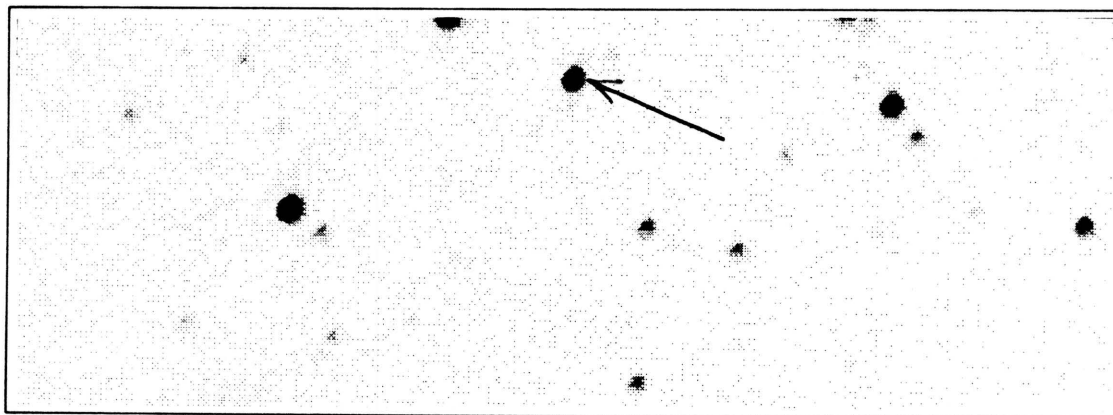
Coordinates: α (1950) = 00:10:54.4 δ (1950) = +27:53:04

Spectral Type: M3.5: V

Photometry: $I_{KC} = 14.33$ $R_{CTI} = 15.44$ $(V-I)_{KC} = 2.80 \pm 0.12$ $(R-I)_{CTI} = 1.03 \pm 0.02$ $(V-I)_{CTI} = 2.67 \pm 0.01$

Notes: Close double star (see previous page). Photometry is a composite of both stars.

CTI 002142.1+280548



CTI FINDER CHART

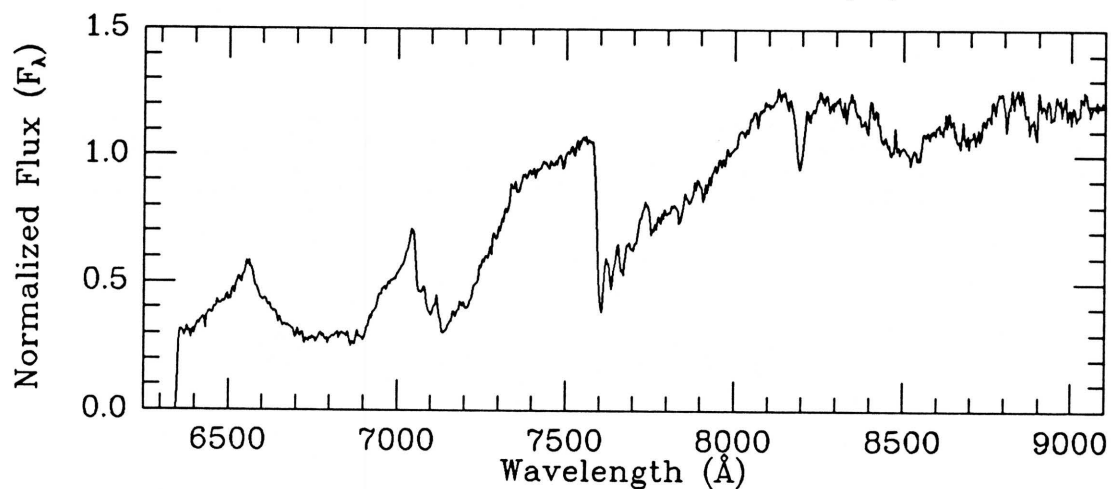
I filter

Obs. (UT) 1989 Nov 03

MMT SPECTRUM

Exposure: 1500 sec

Obs. (UT) 1990 Nov 23

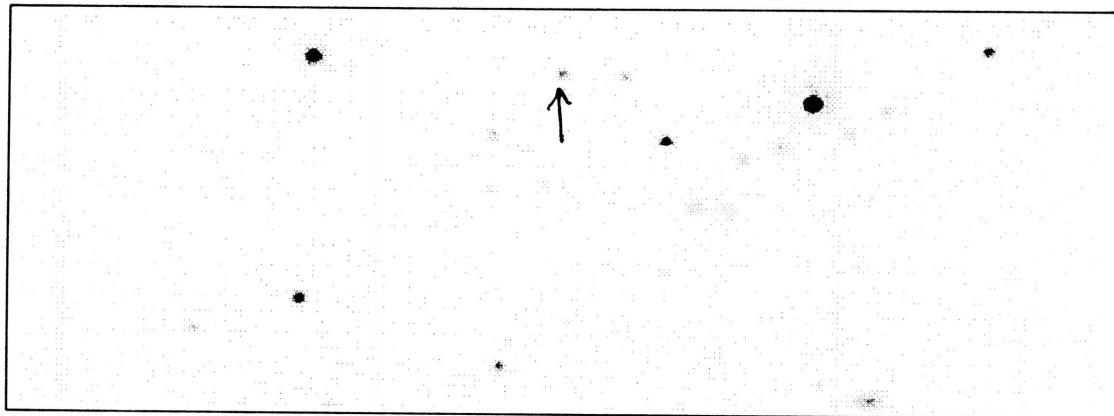
Coordinates: α (1950) = 00:19:44.4 δ (1950) = +27:53:19

Spectral Type: M4 V

Photometry: $I_{\text{KC}} = 14.57$ $R_{\text{CTI}} = 15.83$ $(V-I)_{\text{KC}} = 3.03 \pm 0.12$ $(R-I)_{\text{CTI}} = 1.19 \pm 0.02$ $(V-I)_{\text{CTI}} = 2.85 \pm 0.02$

Notes:

CTI 002352.0+280605



CTI FINDER CHART

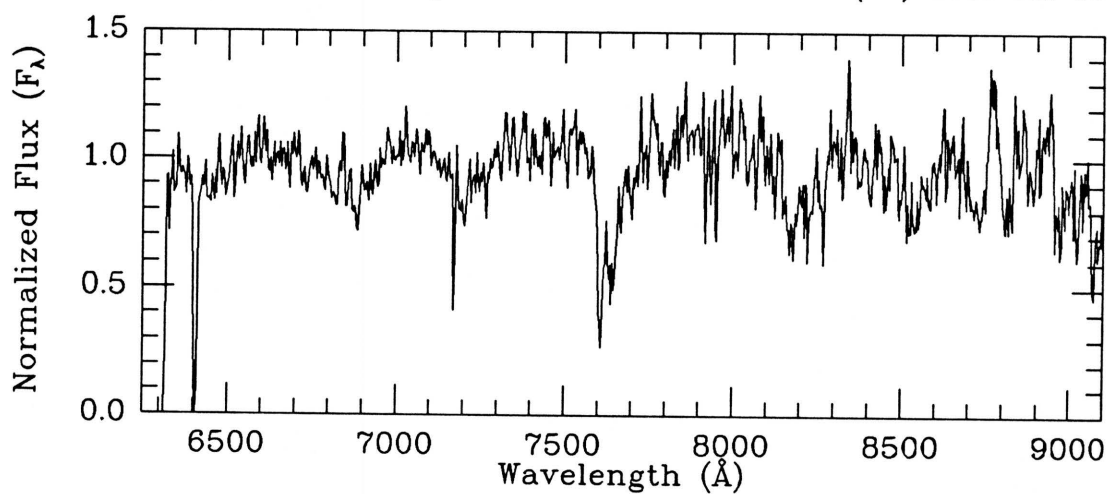
V filter

Obs. (UT) 1987 Oct 20

MMT SPECTRUM

Exposure: 300 sec

Obs. (UT) 1989 Jul 13

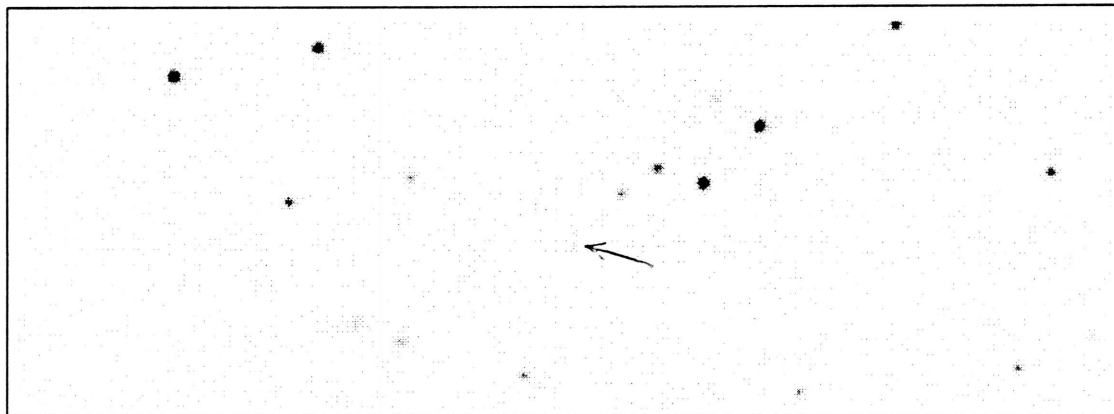
Coordinates: α (1950) = 00:21:54.1 δ (1950) = +27:53:37

Spectral Type: K7 V

Photometry: $I_{\text{KC}} = 16.85$ $R_{\text{CTI}} = 16.98$ $(V-I)_{\text{KC}} = 1.57 \pm 0.14$ $(R-I)_{\text{CTI}} = 0.17 \pm 0.07$ $(V-I)_{\text{CTI}} = 1.40 \pm 0.04$

Notes:

CTI 002603.4+275922



CTI FINDER CHART

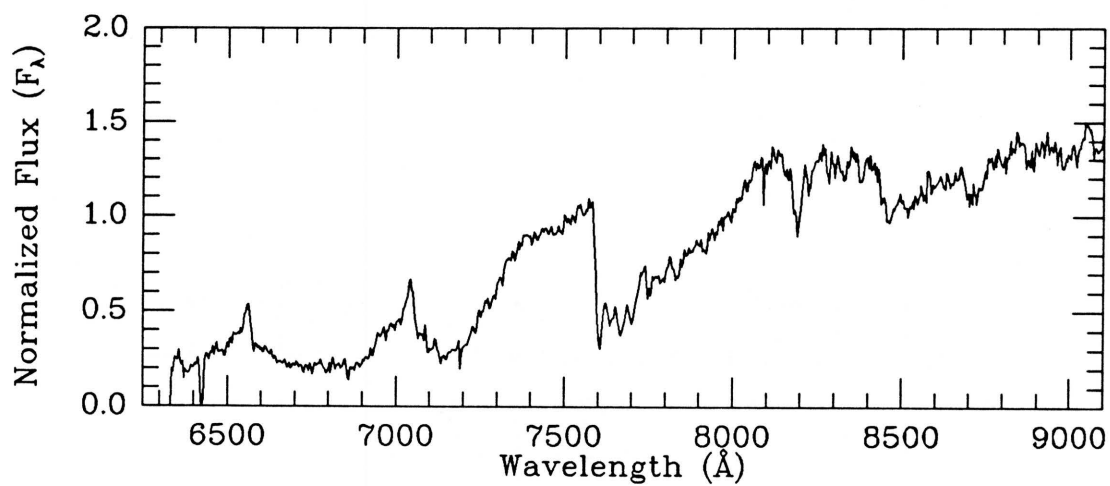
V filter

Obs. (UT) 1987 Oct 20

MMT SPECTRUM

Exposure: 2100 sec

Obs. (UT) 1990 Jan 22

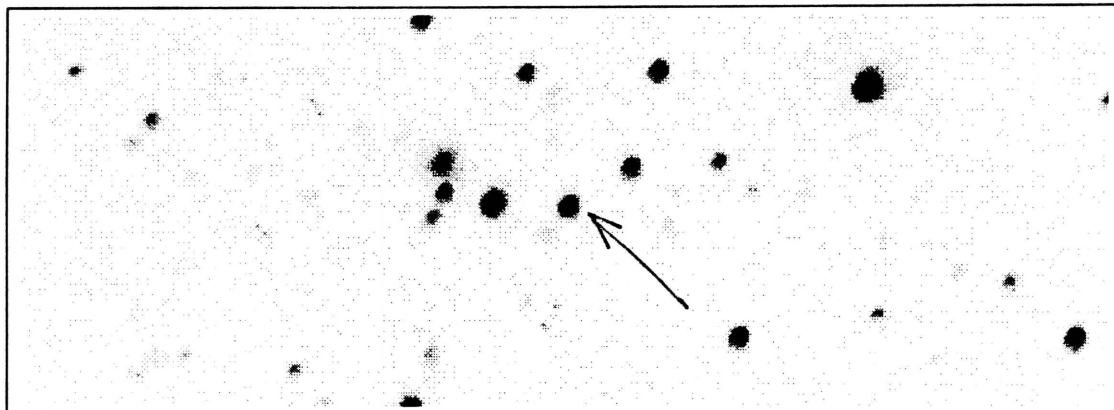
Coordinates: α (1950) = 00:24:05.2 δ (1950) = +27:46:55

Spectral Type: M5.5 V

Photometry: $I_{\text{KC}} = 16.50$ $R_{\text{CTI}} = 17.90$ $(V-I)_{\text{KC}} = 3.35 \pm 0.16$ $(R-I)_{\text{CTI}} = 1.42 \pm 0.07$ $(V-I)_{\text{CTI}} = 3.21 \pm 0.05$

Notes:

CTI 003439.1+280309



CTI FINDER CHART

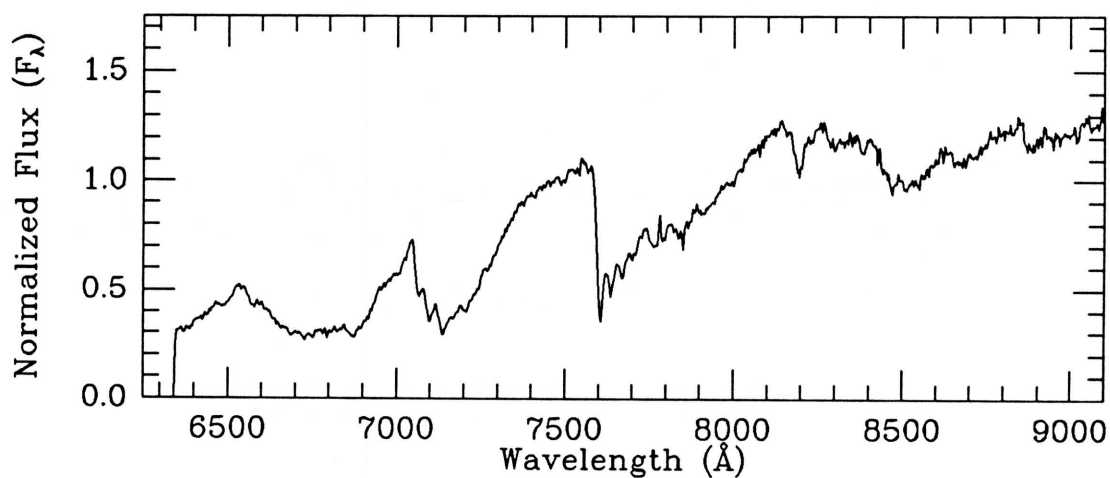
I filter

Obs. (UT) 1989 Nov 03

MMT SPECTRUM

Exposure: 1200 sec

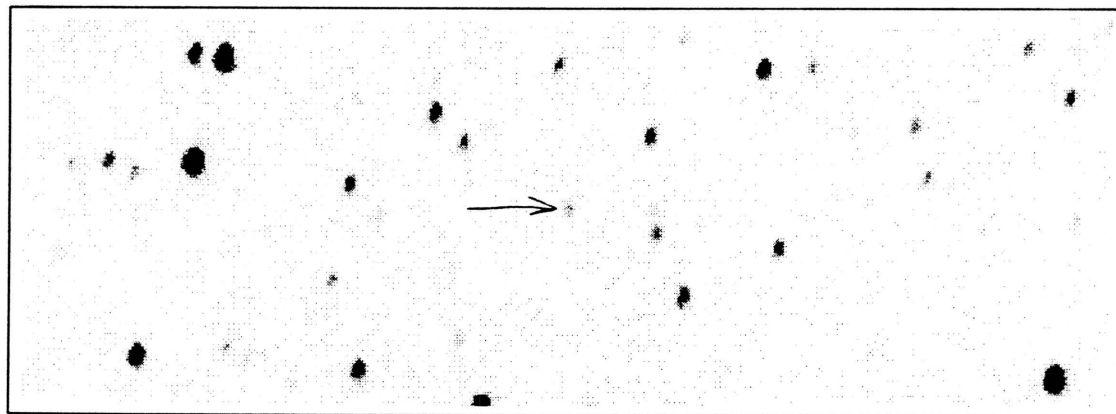
Obs. (UT) 1990 Nov 23

Coordinates: α (1950) = 00:32:39.9 δ (1950) = +27:50:45

Spectral Type: M4 V

Photometry: $I_{KC} = 14.58$ $R_{CTI} = 15.83$ $(V-I)_{KC} = 3.01 \pm 1.12$ $(R-I)_{CTI} = 1.18 \pm 0.02$ $(V-I)_{CTI} = 2.84 \pm 0.01$ Notes: Small proper motion (~ 0.2 arcsec/yr) to the SE
evident when chart is compared to POSS E print.

CTI 004244.4+280140



CTI FINDER CHART

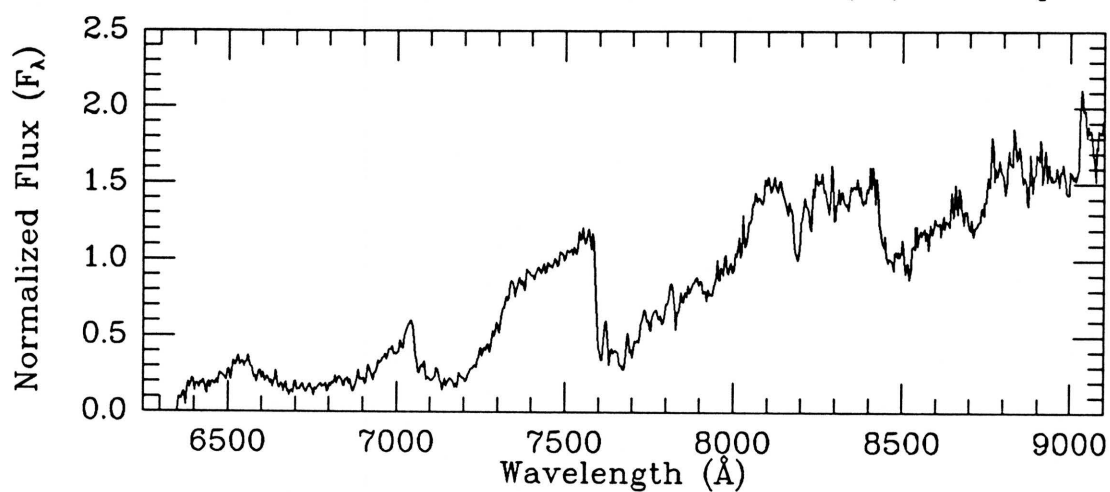
I filter

Obs. (UT) 1988 Nov 01

MMT SPECTRUM

Exposure: 2700 sec

Obs. (UT) 1990 Sep 13

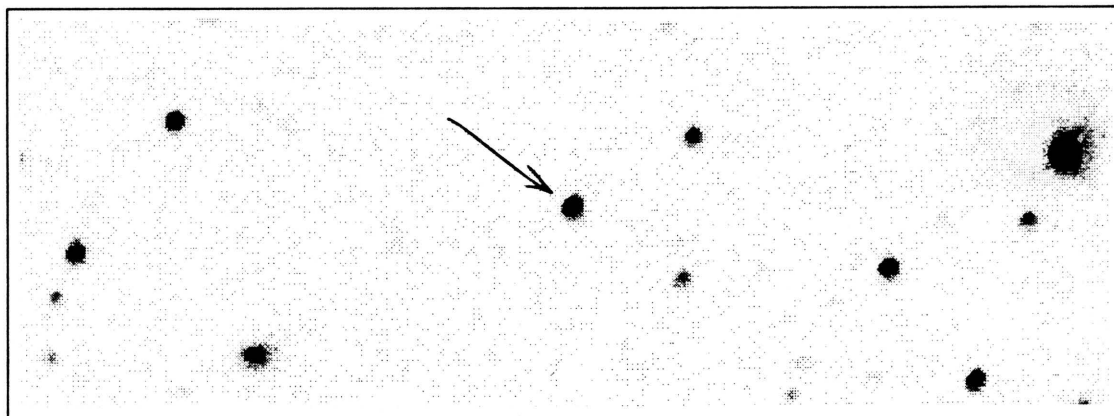
Coordinates: α (1950) = 00:40:44.3 δ (1950) = +27:49:21

Spectral Type: M6 V

Photometry: $I_{KC} = 17.43$ $R_{CTI} = 19.30$ $(V-I)_{KC} = 4.10 \pm 0.27$ $(R-I)_{CTI} = 1.94 \pm 0.16$ $(V-I)_{CTI} = \text{unknown}$

Notes: Object not found on the POSS E print; large proper motion?

CTI 004406.7+280336



CTI FINDER CHART

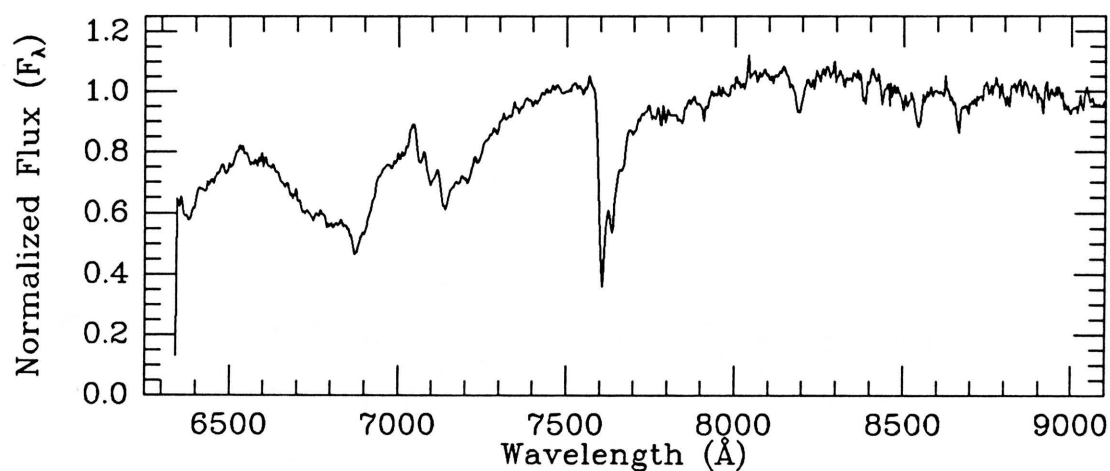
I filter

Obs. (UT) 1989 Nov 03

MMT SPECTRUM

Exposure: 1200 sec

Obs. (UT) 1990 Nov 23

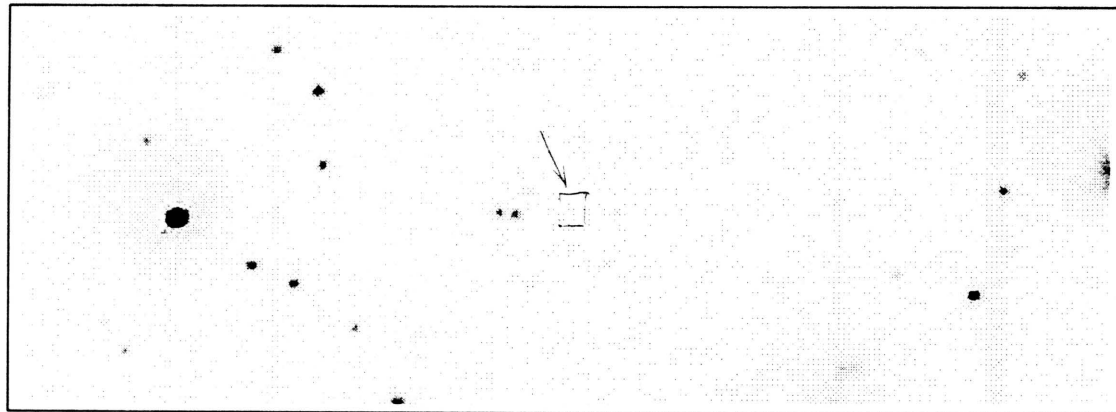
Coordinates: α (1950) = 00:42:06.4 δ (1950) = +27:51:18

Spectral Type: M1.5 V

Photometry: $I_{KC} = 14.69$ $R_{CTI} = 15.32$ $(V-I)_{KC} = 2.14 \pm 0.10$ $(R-I)_{CTI} = 0.57 \pm 0.01$ $(V-I)_{CTI} = 2.00 \pm 0.01$

Notes:

CTI 004525.7+280437



CTI FINDER CHART

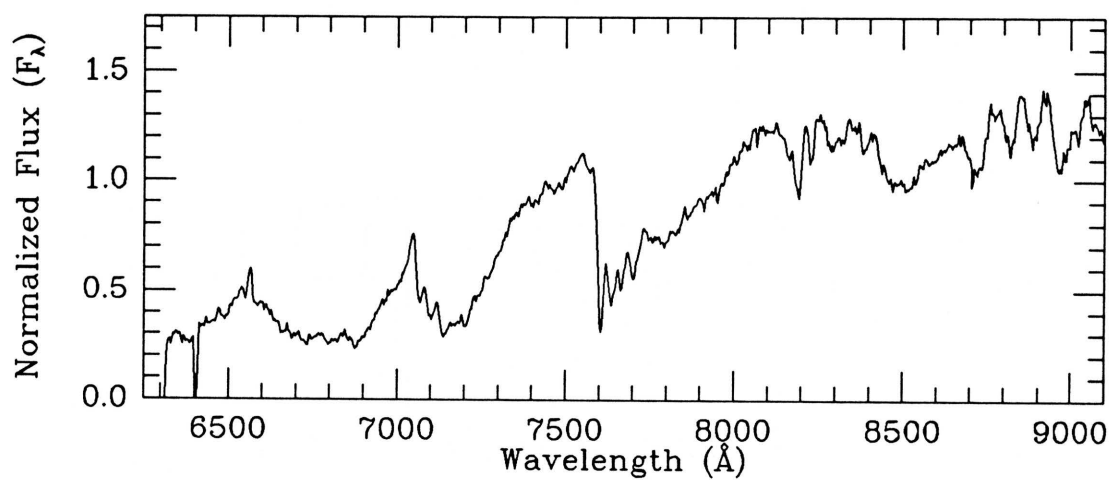
V filter

Obs. (UT) 1987 Oct 20

MMT SPECTRUM

Exposure: 2100 sec

Obs. (UT) 1989 Jul 13

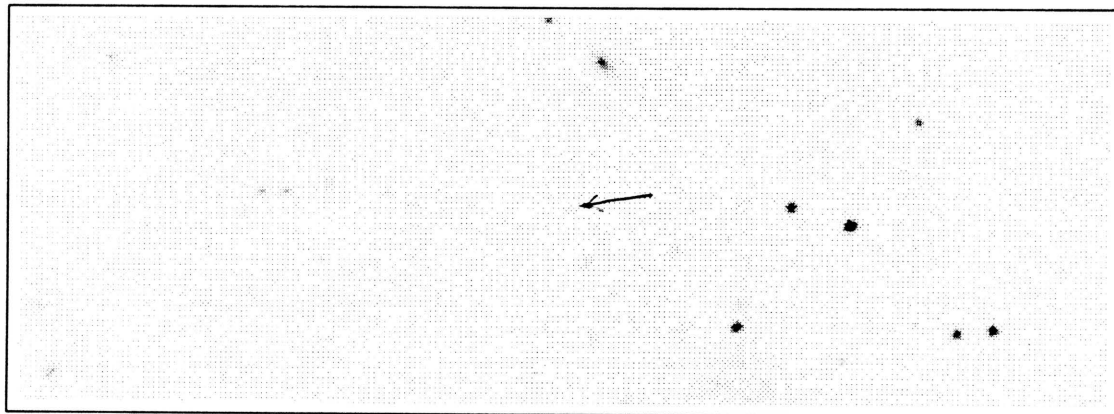
Coordinates: α (1950) = 00:43:25.3 δ (1950) = +27:52:19

Spectral Type: M4.5 V

Photometry: $I_{KC} = 16.12$ $R_{CTI} = 17.30$ $(V-I)_{KC} = 3.03 \pm 0.13$ $(R-I)_{CTI} = 1.19 \pm 0.04$ $(V-I)_{CTI} = 3.17 \pm 0.03$

Notes:

CTI 004911.4+275952



CTI FINDER CHART

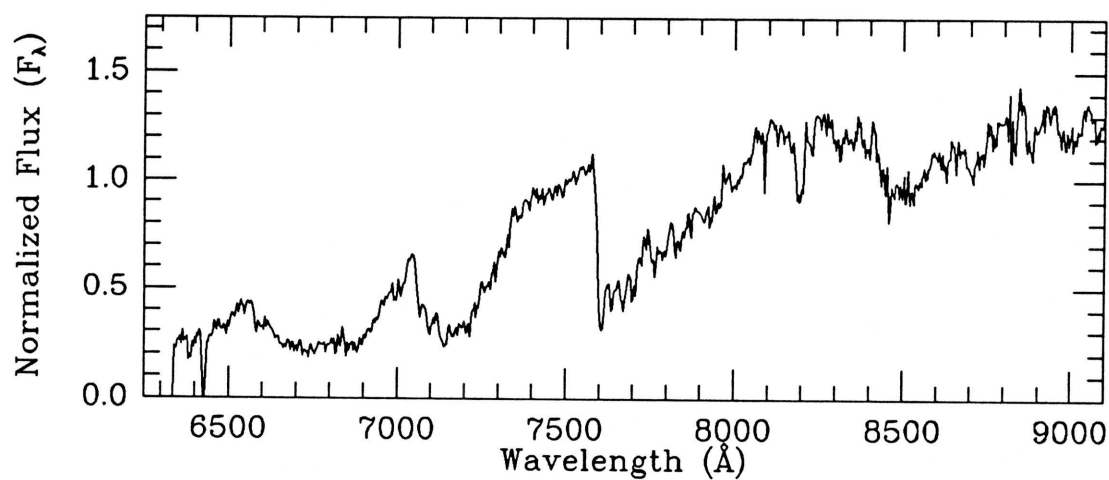
V filter

Obs. (UT) 1987 Oct 20

MMT SPECTRUM

Exposure: 2700 sec

Obs. (UT) 1990 Jan 22

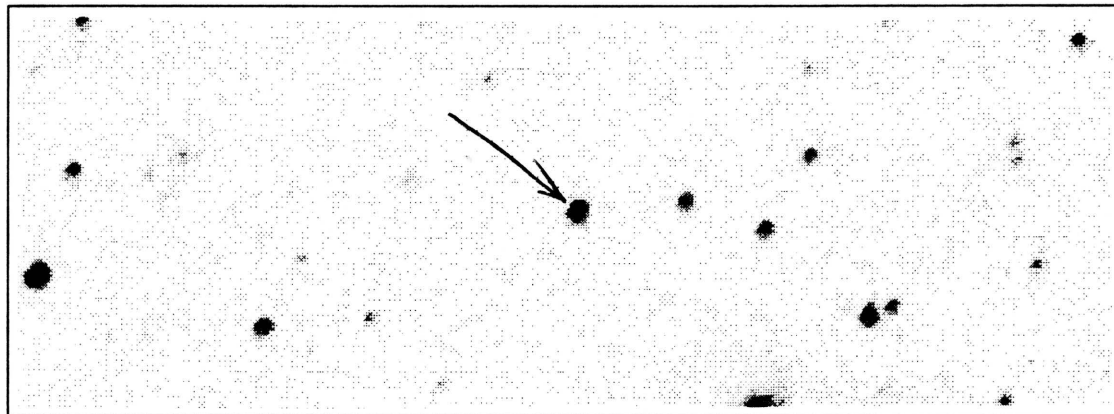
Coordinates: α (1950) = 00:47:10.6 δ (1950) = +27:47:37

Spectral Type: M4.5 V

Photometry: $I_{KC} = 16.90$ $R_{CTI} = 18.33$ $(V-I)_{KC} = 3.43 \pm 0.18$ $(R-I)_{CTI} = 1.47 \pm 0.09$ $(V-I)_{CTI} = 3.29 \pm 0.07$

Notes:

CTI 005100.5+280430



CTI FINDER CHART

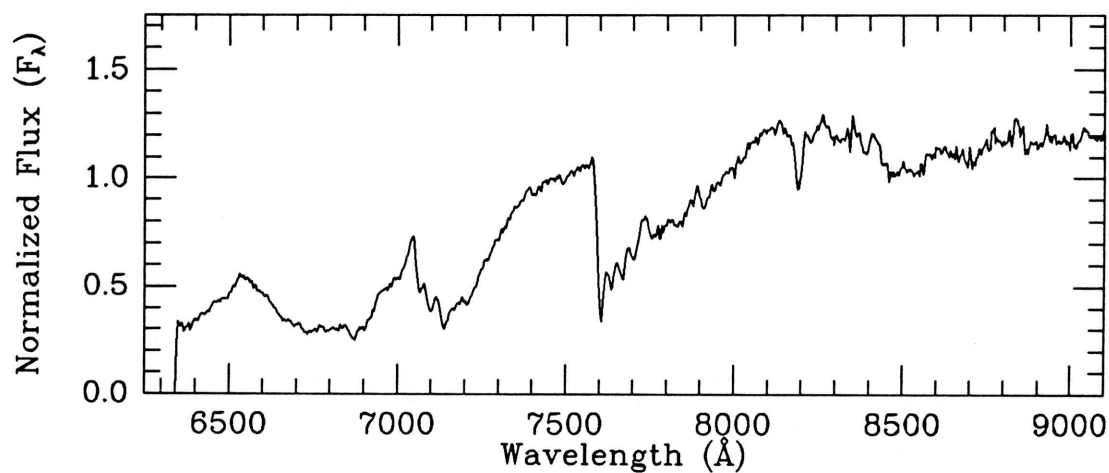
I filter

Obs. (UT) 1989 Nov 03

MMT SPECTRUM

Exposure: 1200 sec

Obs. (UT) 1990 Nov 23

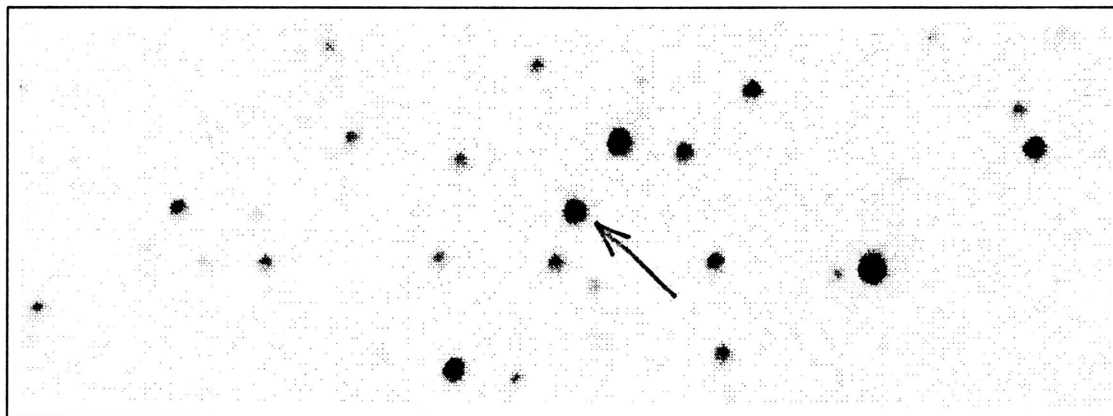
Coordinates: α (1950) = 00:48:59.5 δ (1950) = +27:52:16

Spectral Type: M4 V

Photometry: $I_{\text{KC}} = 14.64$ $R_{\text{CTI}} = 15.87$ $(V-I)_{\text{KC}} = 3.00 \pm 0.12$ $(R-I)_{\text{CTI}} = 1.17 \pm 0.02$ $(V-I)_{\text{CTI}} = 2.86 \pm 0.01$

Notes:

CTI 010332.0+280234



CTI FINDER CHART

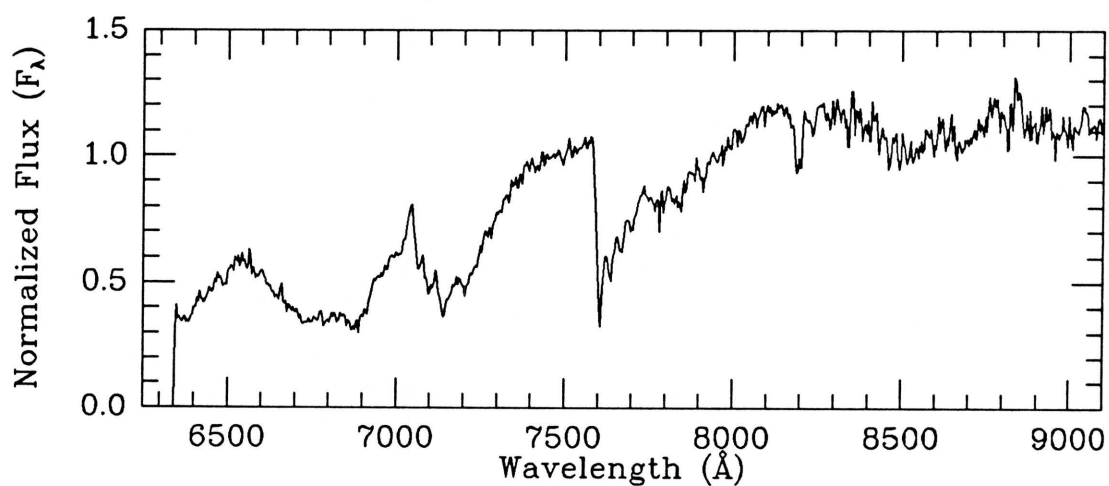
I filter

Obs. (UT) 1989 Nov 03

MMT SPECTRUM

Exposure: 1200 sec

Obs. (UT) 1990 Nov 23

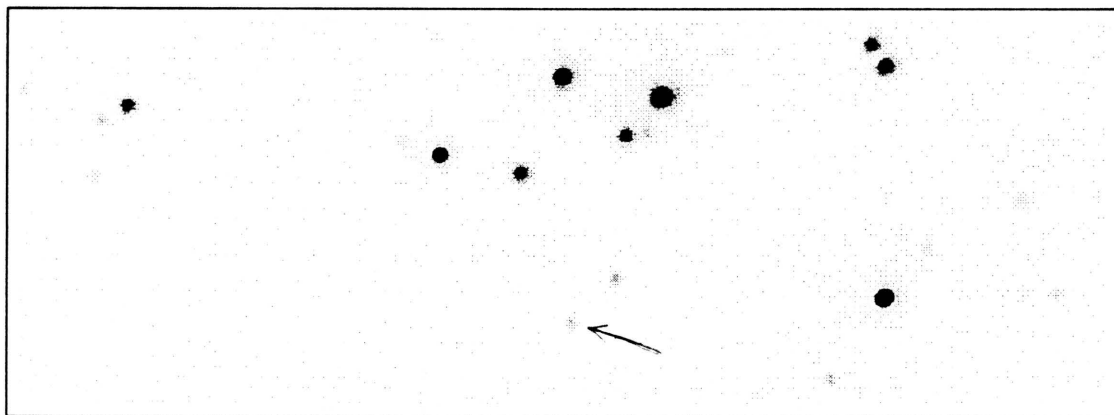
Coordinates: α (1950) = 01:01:29.6 δ (1950) = +27:50:30

Spectral Type: M3.5 V

Photometry: $I_{KC} = 14.29$ $R_{CTI} = 15.37$ $(V-I)_{KC} = 2.75 \pm 0.12$ $(R-I)_{CTI} = 1.00 \pm 0.01$ $(V-I)_{CTI} = 2.56 \pm 0.01$

Notes:

CTI 011708.6+275850



CTI FINDER CHART

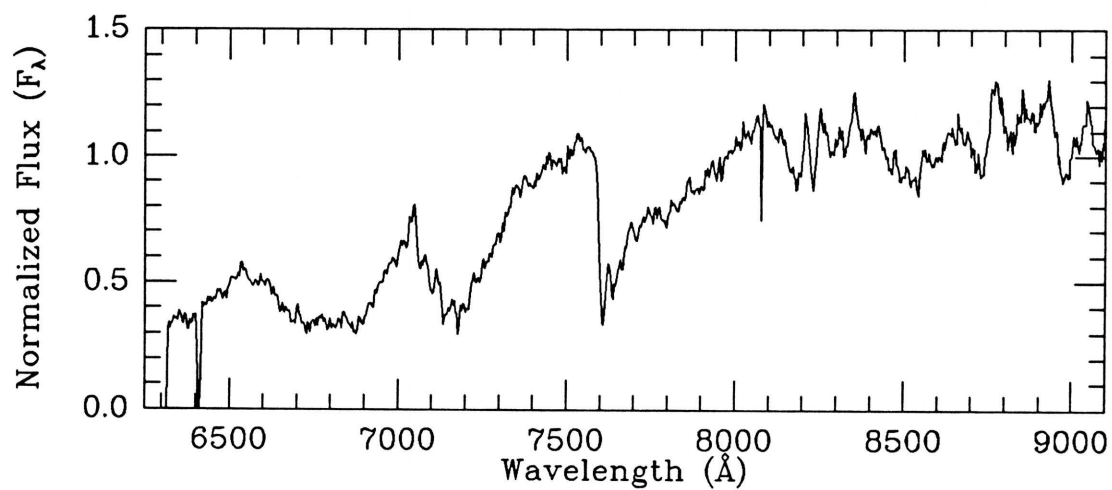
V filter

Obs. (UT) 1987 Oct 20

MMT SPECTRUM

Exposure: 1200 sec

Obs. (UT) 1989 Jul 14

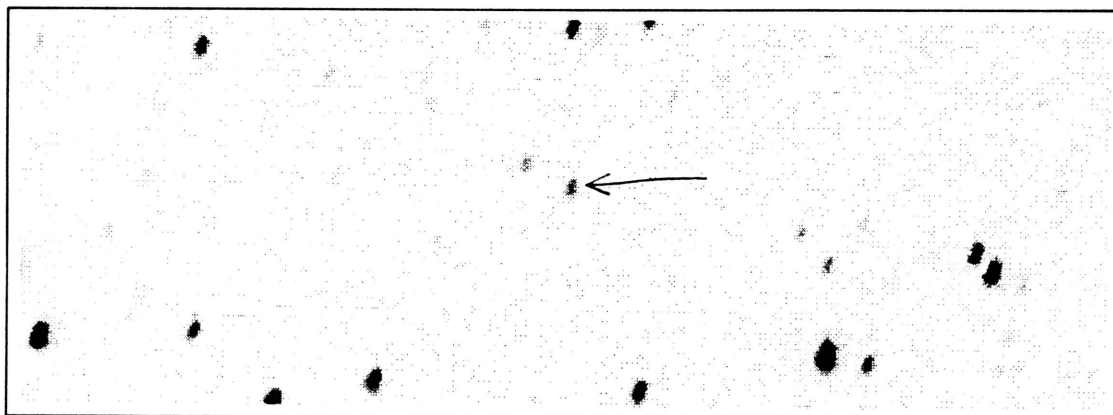
Coordinates: α (1950) = 01:15:04.7 δ (1950) = +27:46:59

Spectral Type: M3.5 V

Photometry: $I_{KC} = 15.96$ $R_{CTI} = 17.00$ $(V-I)_{KC} = 2.81 \pm 0.14$ $(R-I)_{CTI} = 1.04 \pm 0.05$ $(V-I)_{CTI} = 2.75 \pm 0.03$

Notes:

CTI 011826.7+280514



CTI FINDER CHART

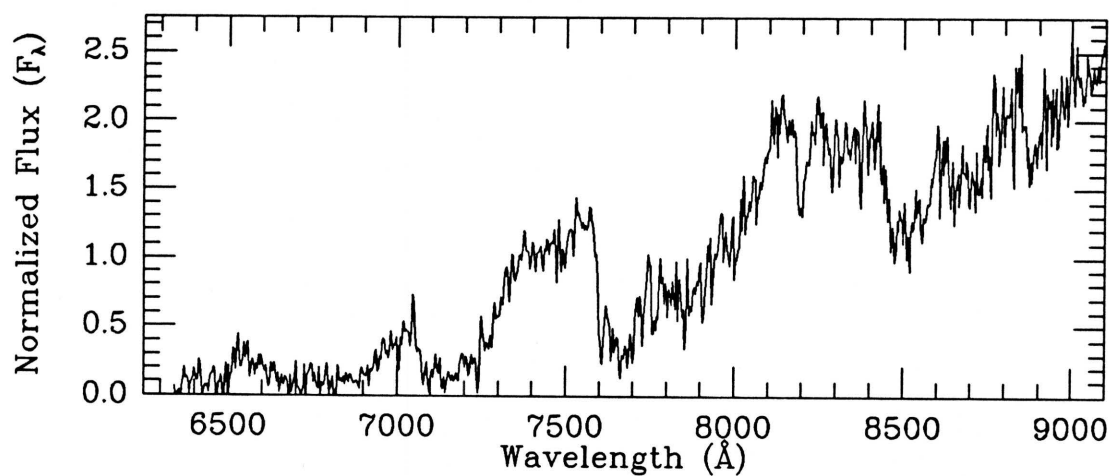
I filter

Obs. (UT) 1988 Nov 01

MMT SPECTRUM

Exposure: 4200 sec

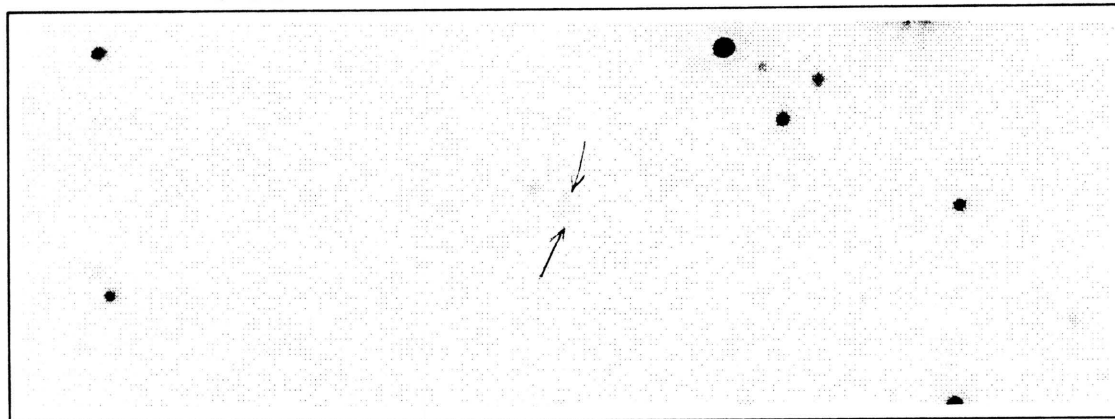
Obs. (UT) 1990 Nov 23

Coordinates: α (1950) = 01:16:22.6 δ (1950) = +27:53:25

Spectral Type: M6 V

Photometry: $I_{KC} = 17.22$ $R_{CTI} = 19.01$ $(V-I)_{KC} = 3.97 \pm 0.33$ $(R-I)_{CTI} = 1.85 \pm 0.21$ $(V-I)_{CTI} = \text{unknown}$ Notes: Proper motion of ~ 1 arcsec/yr to the WSW suspected from comparison to POSS E print.

CTI 012023.2+280320 A



CTI FINDER CHART

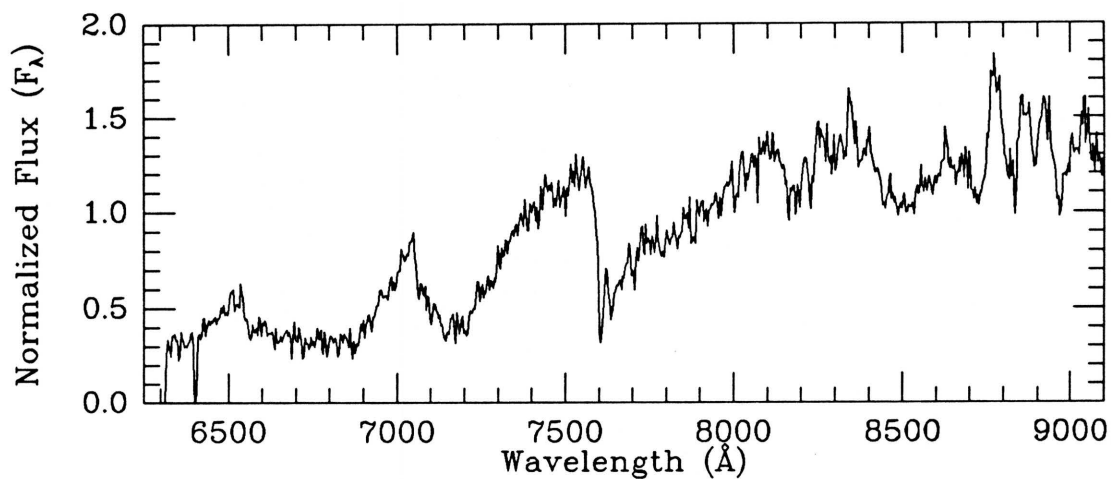
V filter

Obs. (UT) 1987 Oct 20

MMT SPECTRUM

Exposure: 1500 sec

Obs. (UT) 1989 Jul 13

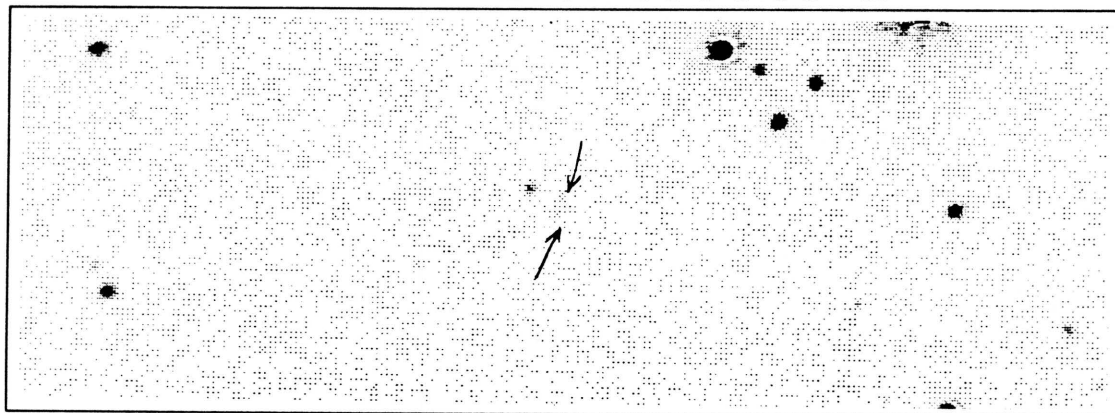
Coordinates: α (1950) = 01:18:18.9 δ (1950) = +27:51:33

Spectral Type: M4 V

Photometry: $I_{KC} = 17.25$ $R_{CTI} = 17.93$ $(V-I)_{KC} = 2.38 \pm 0.20$ $(R-I)_{CTI} = 0.74 \pm 0.12$ $(V-I)_{CTI} = 3.06 \pm 0.09$

Notes: Close double star (see next page). Photometry is a composite of both stars.

CTI 012023.2+280320 B



CTI FINDER CHART

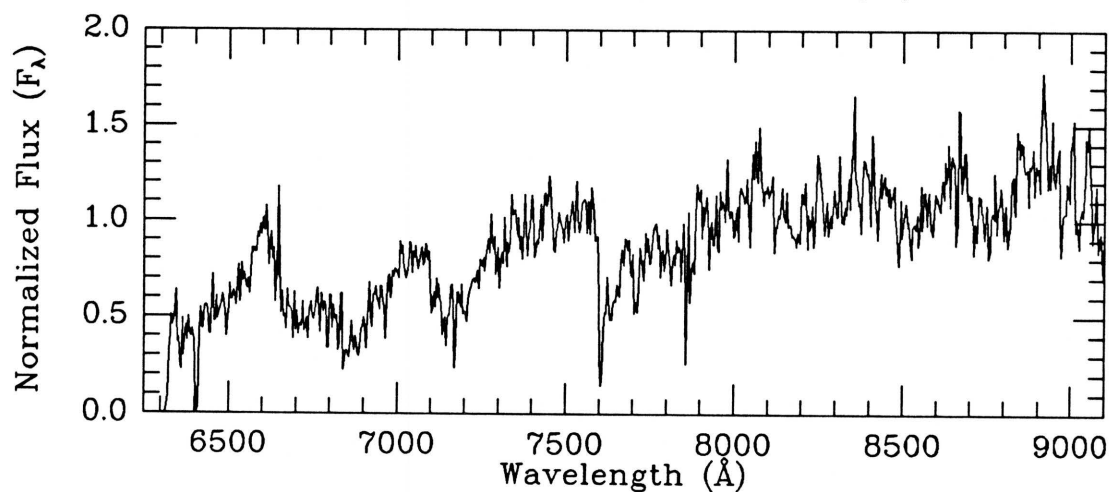
V filter

Obs. (UT) 1987 Oct 20

MMT SPECTRUM

Exposure: 1500 sec

Obs. (UT) 1989 Jul 13

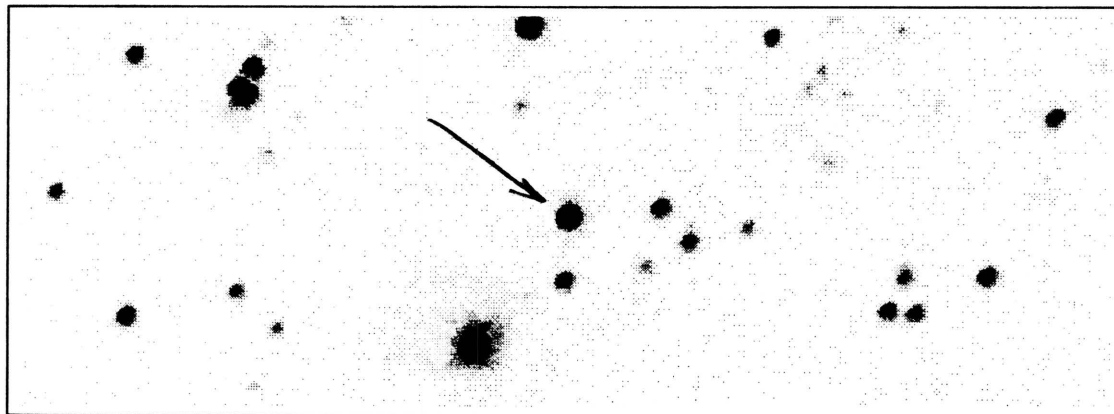
Coordinates: α (1950) = 01:18:18.9 δ (1950) = +27:51:33

Spectral Type: M3:V

Photometry: $I_{KC} = 17.25$ $R_{CTI} = 17.93$ $(V-I)_{KC} = 2.38 \pm 0.20$ $(R-I)_{CTI} = 0.74 \pm 0.12$ $(V-I)_{CTI} = 3.06 \pm 0.09$

Notes: Close double star (see previous page). Photometry is a composite of both stars.

CTI 012303.4+280449



CTI FINDER CHART

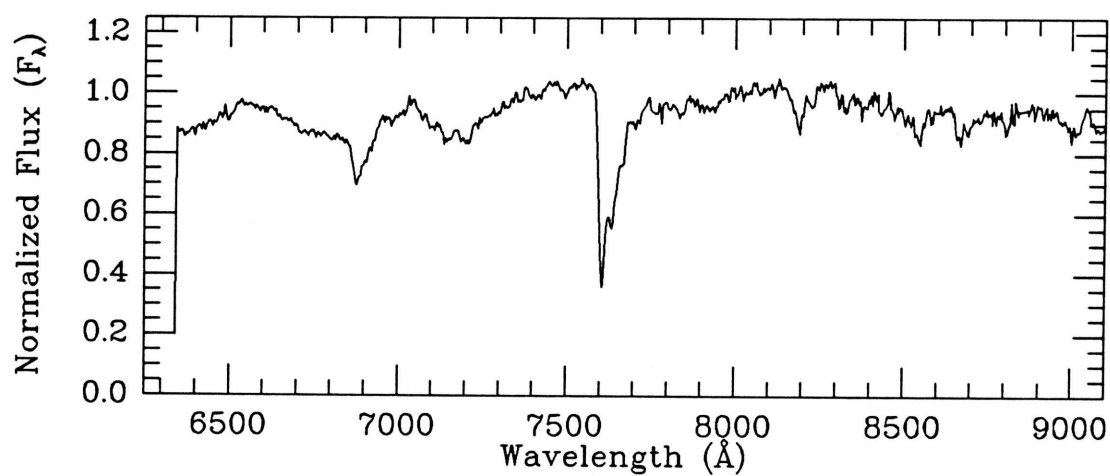
I filter

Obs. (UT) 1989 Nov 03

MMT SPECTRUM

Exposure: 600 sec

Obs. (UT) 1990 Nov 23

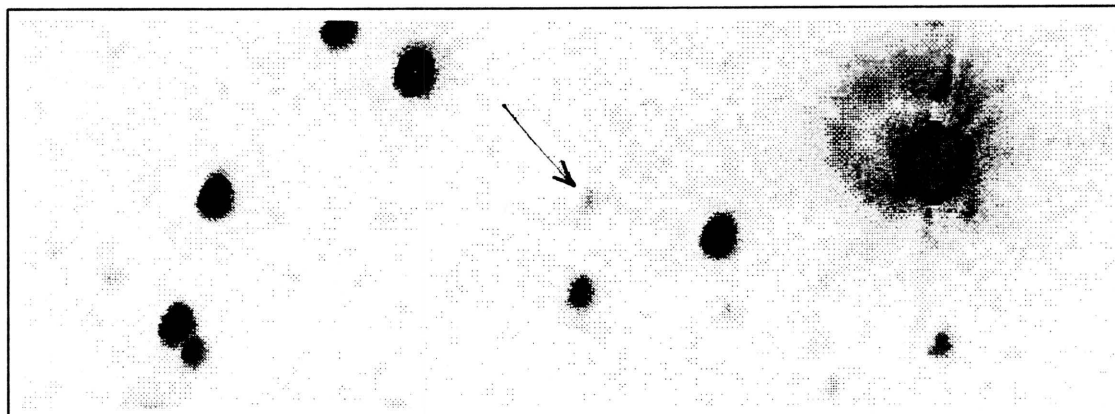
Coordinates: α (1950) = 01:20:58.8 δ (1950) = +27:53:05

Spectral Type: M0 V

Photometry: $I_{\text{KC}} = 12.87$ $R_{\text{CTI}} = 13.28$ $(V-I)_{\text{KC}} = 1.70 \pm 0.09$ $(R-I)_{\text{CTI}} = 0.26 \pm 0.01$ $(V-I)_{\text{CTI}} = 1.51 \pm 0.01$

Notes:

CTI 012517.7+280101



CTI FINDER CHART

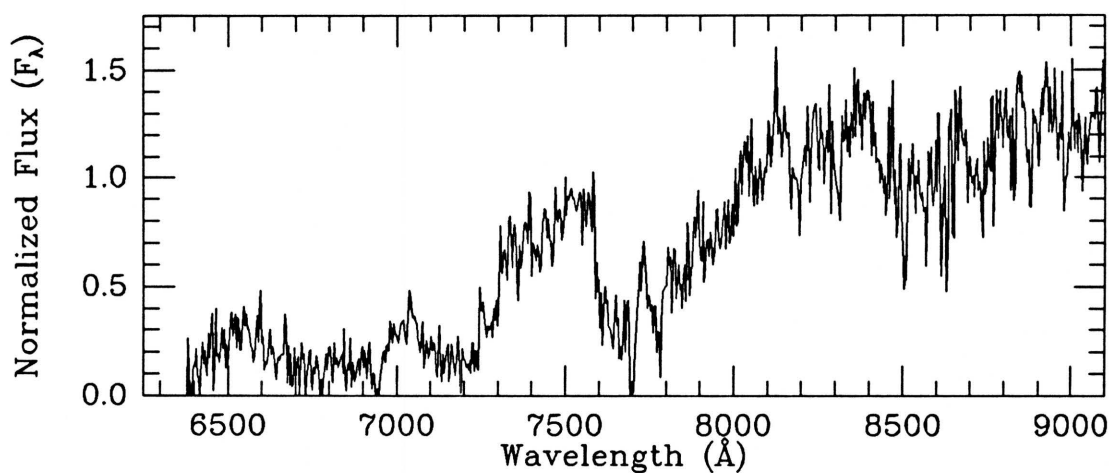
I filter

Coadded frame

MMT SPECTRUM

Exposure: 3000 sec

Obs. (UT) 1991 Oct 17

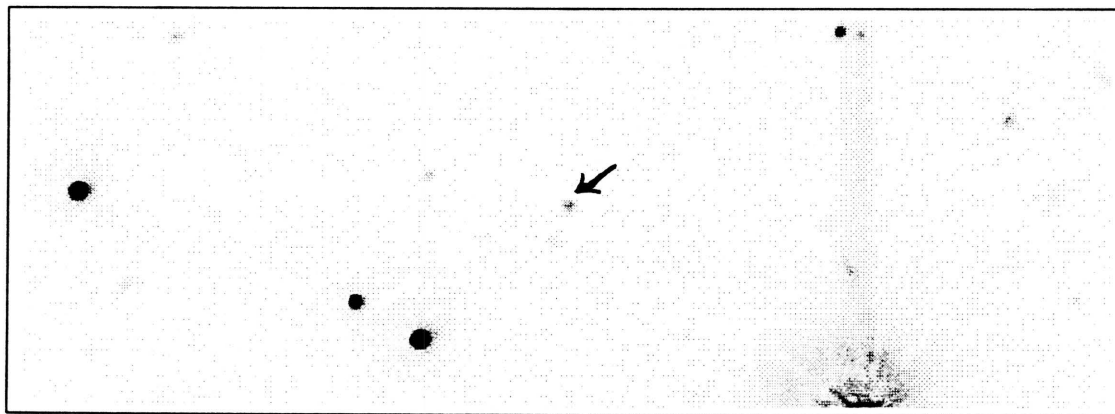
Coordinates: α (1950) = 01:23:12.9 δ (1950) = +27:49:20

Spectral Type: M6 V

Photometry: I_{KC} = unknown R_{CTI} = unknown $(V-I)_{KC}$ =unknown $(R-I)_{CTI}$ =unknown $(V-I)_{CTI}$ =3.88:

Notes:

CTI 012517.7+280245



CTI FINDER CHART

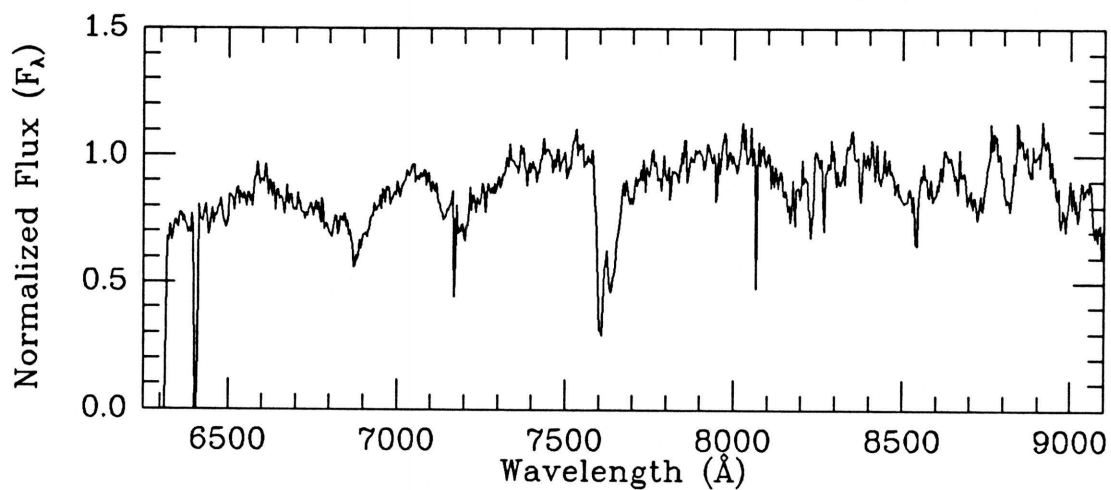
V filter

Coadded frame

MMT SPECTRUM

Exposure: 300 sec

Obs. (UT) 1989 Jul 13

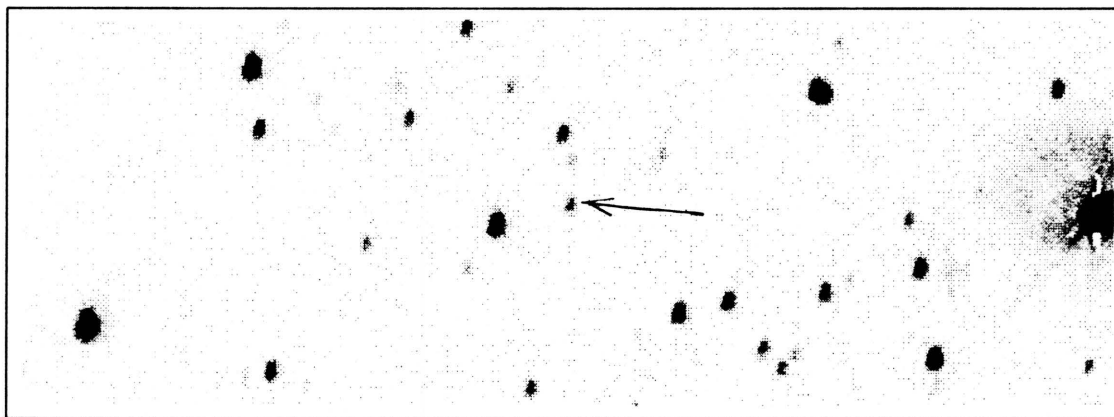
Coordinates: α (1950) = 01:23:12.9 δ (1950) = +27:51:04

Spectral Type: M0 V

Photometry: $I_{KC} = 17.50$ $R_{CTI} = 17.78$ $(V-I)_{KC} = 1.82 \pm 0.11$ $(R-I)_{CTI} = 0.35 \pm 0.04$ $(V-I)_{CTI} = 1.75 \pm 0.02$

Notes:

CTI 012657.5+280202



CTI FINDER CHART

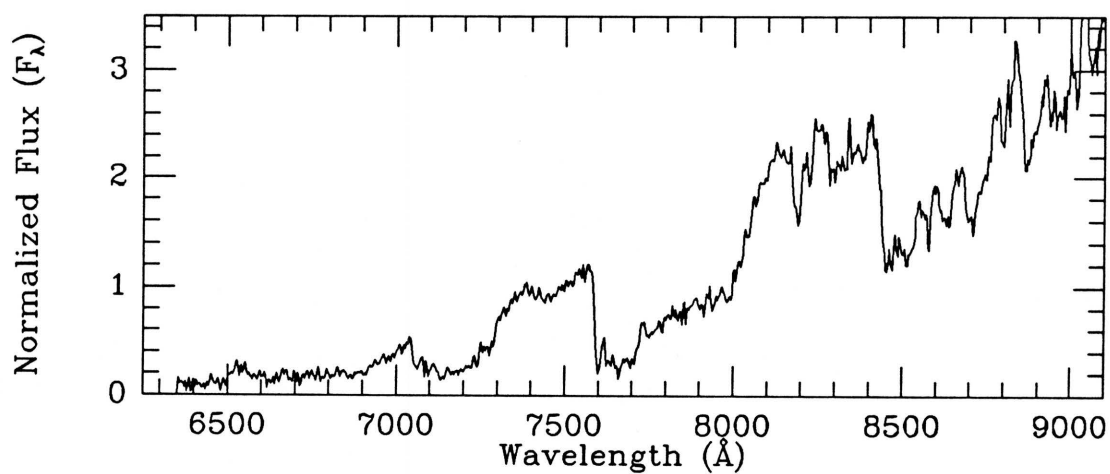
I filter

Obs. (UT) 1988 Nov 01

MMT SPECTRUM

Exposure: 3900 sec

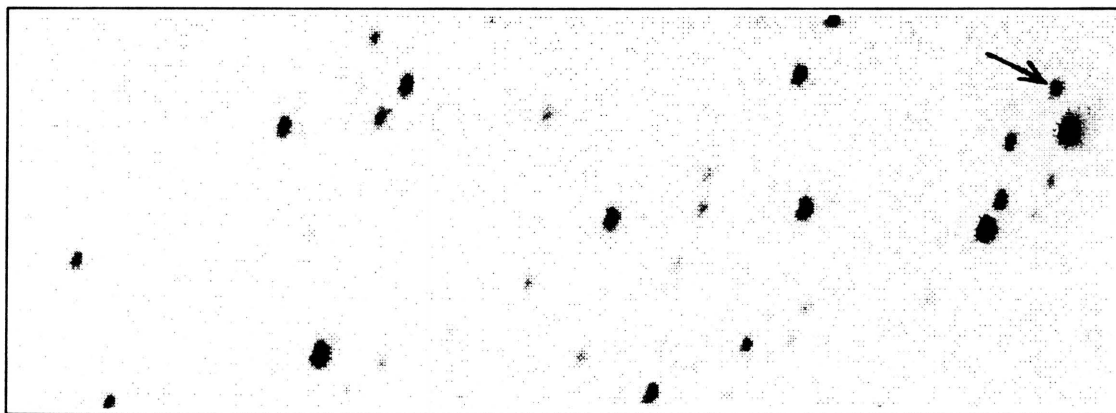
Obs. (UT) 1990 Sep 13

Coordinates: α (1950) = 01:24:52.5 δ (1950) = +27:50:23

Spectral Type: M8.5 V

Photometry: $I_{\text{KC}} = 17.10$ $R_{\text{CTI}} = 19.35$ $(V-I)_{\text{KC}} = 4.61 \pm 0.38$ $(R-I)_{\text{CTI}} = 2.30 \pm 0.24$ $(V-I)_{\text{CTI}} = \text{unknown}$ Notes: Not seen on POSS E, either because of large motion
or because of faintness. Latest dwarf found in CTI strip.

CTI 013743.0+280553:



CTI FINDER CHART

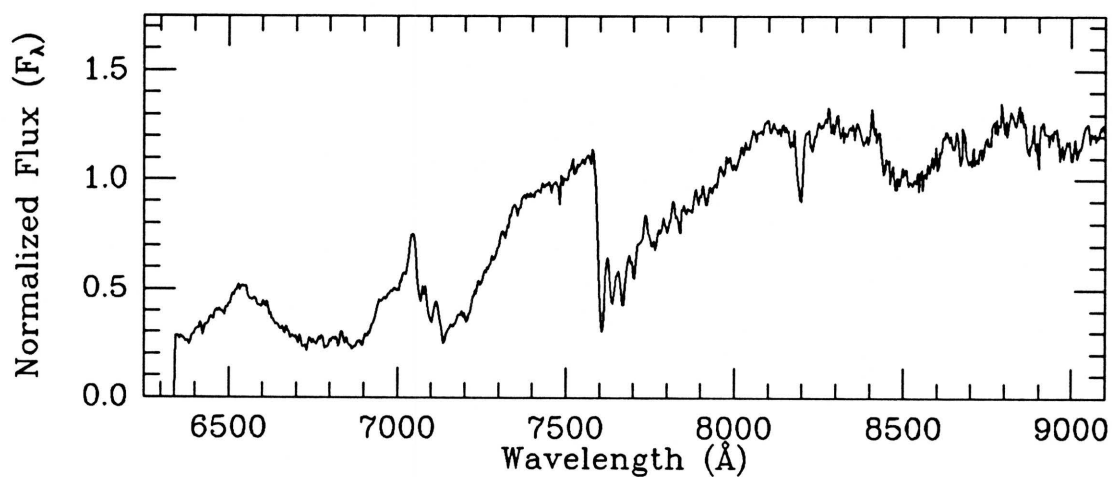
I filter

Obs. (UT) 1988 Nov 01

MMT SPECTRUM

Exposure: 1500 sec

Obs. (UT) 1990 Nov 22

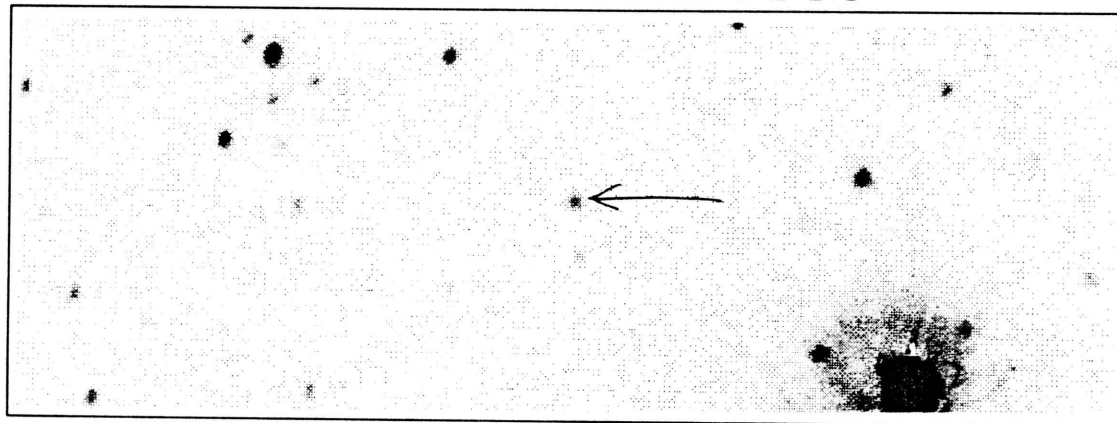
Coordinates: α (1950) = 01:37:37: δ (1950) = +27:54:28:

Spectral Type: M4.5 V

Photometry: I_{KC} = unknown R_{CTI} = unknown $(V-I)_{KC}$ =unknown $(R-I)_{CTI}$ =unknown $(V-I)_{CTI}$ =unknown

Notes: Proper motion of ~ 0.4 arcsec/yr E evident when chart compared to POSS E. Not a color-selected object. Position measured from nearby reference star and is thus uncertain.

CTI 014716.6+280142



CTI FINDER CHART

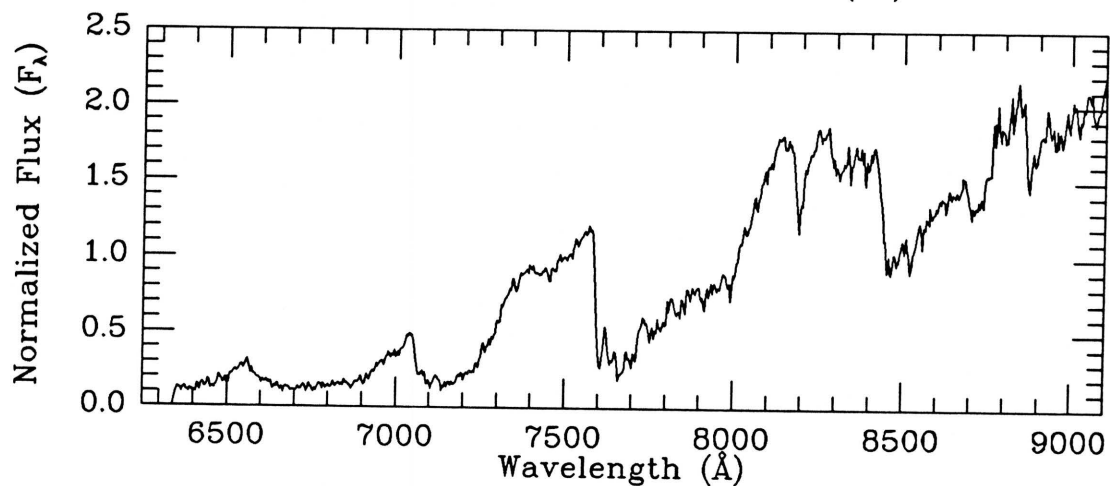
I filter

Obs. (UT) 1988 Nov 01

MMT SPECTRUM

Exposure: 3900 sec

Obs. (UT) 1990 Nov 22

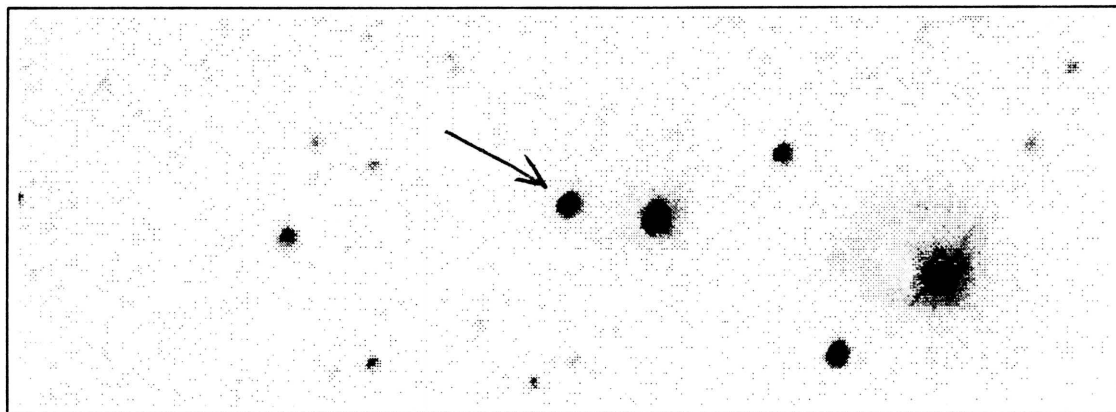
Coordinates: α (1950) = 01:45.09.4 δ (1950) = +27:50:30

Spectral Type: M6 V

Photometry: $I_{KC} = 17.23$ $R_{CTI} = 19.12$ $(V-I)_{KC} = 4.11 \pm 0.35$ $(R-I)_{CTI} = 1.95 \pm 0.22$ $(V-I)_{CTI} = \text{unknown}$

Notes: POSS E shows star ~ 1 arcmin ESE of arrowed position, but no object corresponding to CTI star. If this is the same star at different epochs, proper motion is ~ 2 arcsec/yr.

CTI 015115.8+280458



CTI FINDER CHART

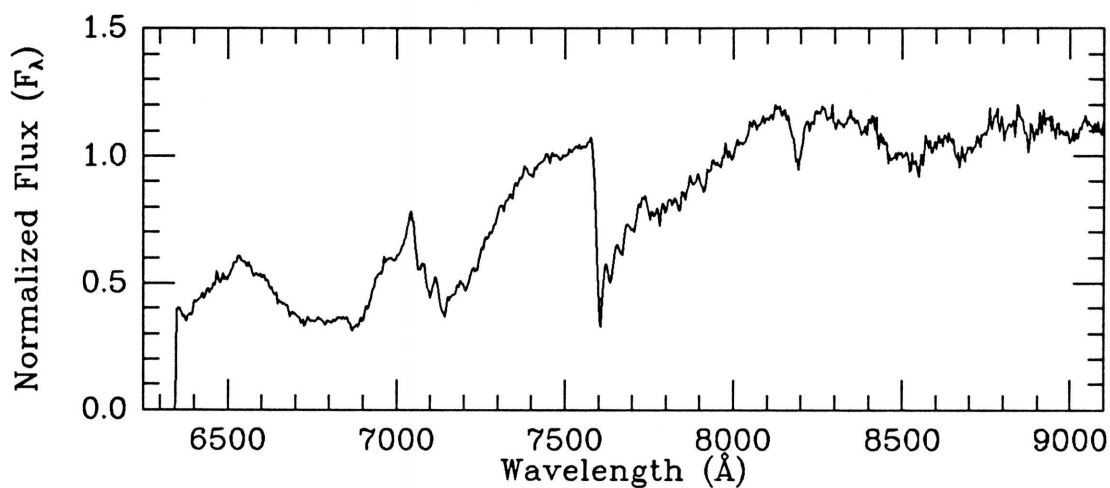
I filter

Obs. (UT) 1989 Nov 03

MMT SPECTRUM

Exposure: 1200 sec

Obs. (UT) 1990 Nov 23

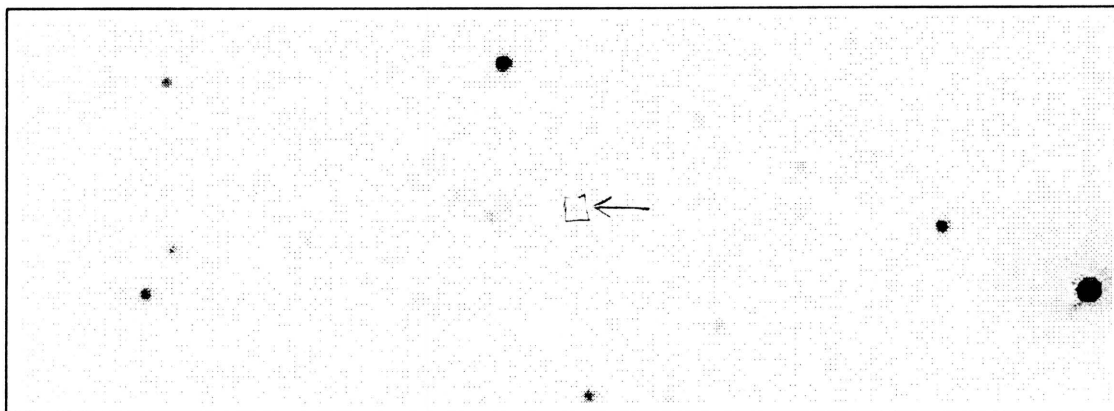
Coordinates: α (1950) = 01:49:08.2 δ (1950) = +27:53:52

Spectral Type: M3.5 V

Photometry: $I_{KC} = 13.97$ $R_{CTI} = 15.05$ $(V-I)_{KC} = 2.74 \pm 1.1$ $(R-I)_{CTI} = 0.99 \pm 0.1$ $(V-I)_{CTI} = 2.57 \pm 0.1$

Notes:

CTI 015338.5+280036



CTI FINDER CHART

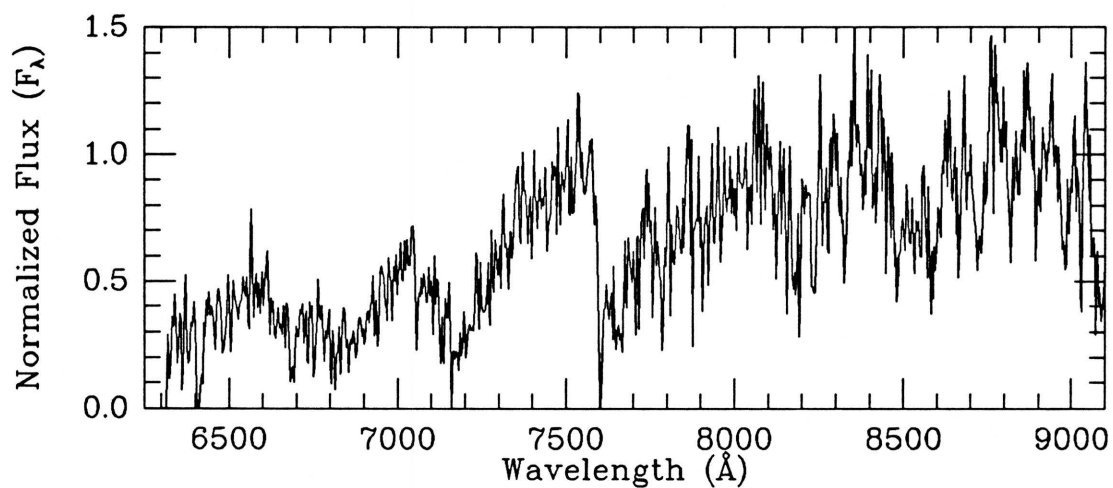
V filter

Obs. (UT) 1987 Oct 20

MMT SPECTRUM

Exposure: 300 sec

Obs. (UT) 1989 Jul 14

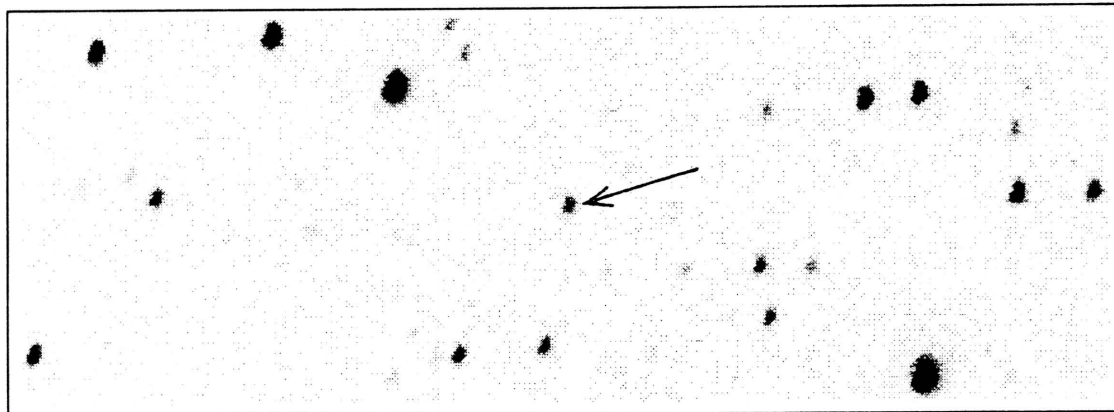
Coordinates: α (1950) = 01:51:30.7 δ (1950) = +27:49:33

Spectral Type: M3.5 V

Photometry: $I_{KC} = 17.20$ $R_{CTI} = 18.32$ $(V-I)_{KC} = 3.01 \pm .23$ $(R-I)_{CTI} = 1.18 \pm .14$ $(V-I)_{CTI} = 3.03 \pm .11$

Notes:

CTI 015607.7+280241



CTI FINDER CHART

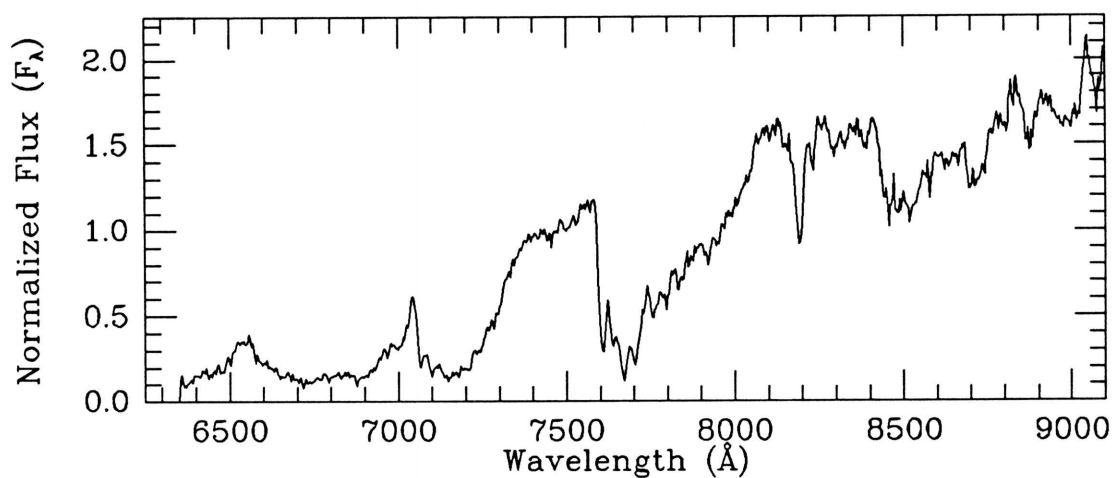
I filter

Obs. (UT) 1988 Nov 01

MMT SPECTRUM

Exposure: 1500 sec

Obs. (UT) 1990 Sep 13

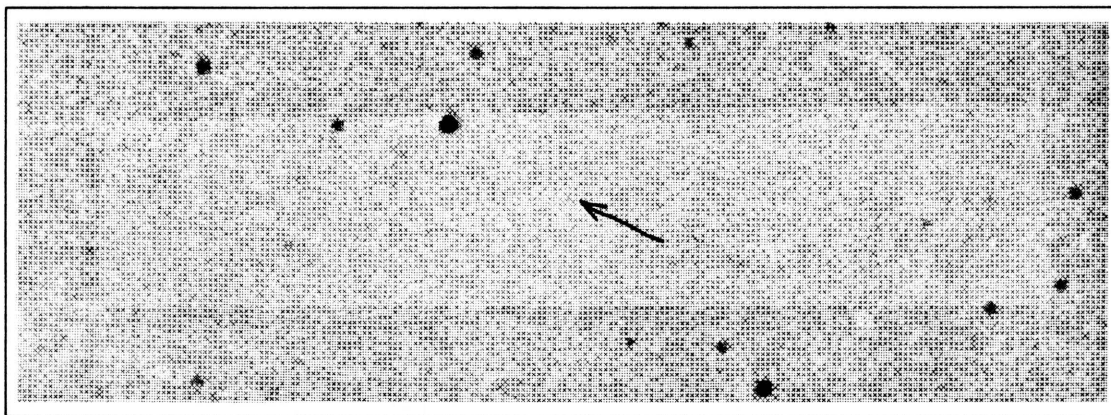
Coordinates: α (1950) = 01:53:59.6 δ (1950) = +27:51:42

Spectral Type: M6.5 V

Photometry: $I_{KC} = 16.53$ $R_{CTI} = 18.33$ $(V-I)_{KC} = 3.94 \pm .22$ $(R-I)_{CTI} = 1.83 \pm .12$ $(V-I)_{CTI} = 3.89 \pm .12$

Notes:

CTI 015625.5+280135



CTI FINDER CHART

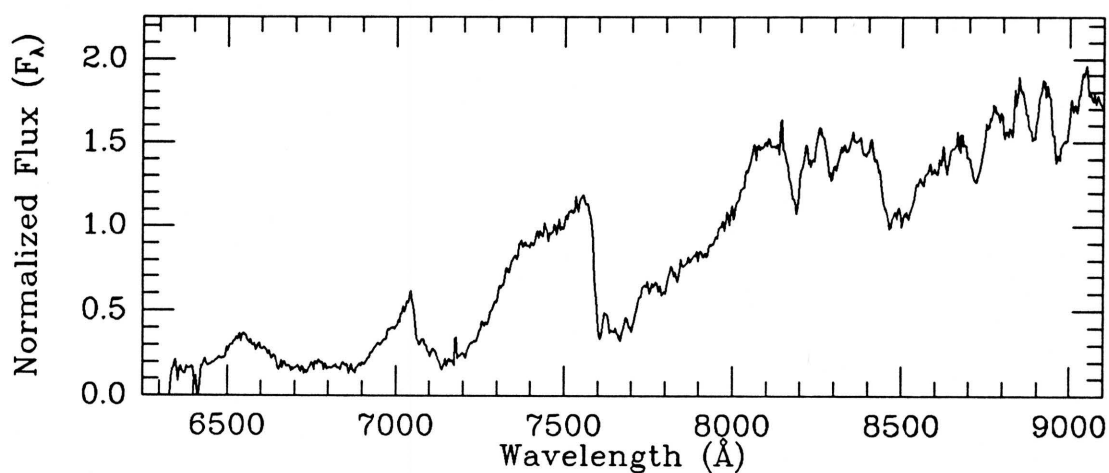
V filter

Obs. (UT) 1987 Oct 20

MMT SPECTRUM

Exposure: 1800 sec

Obs. (UT) 1989 Jul 10

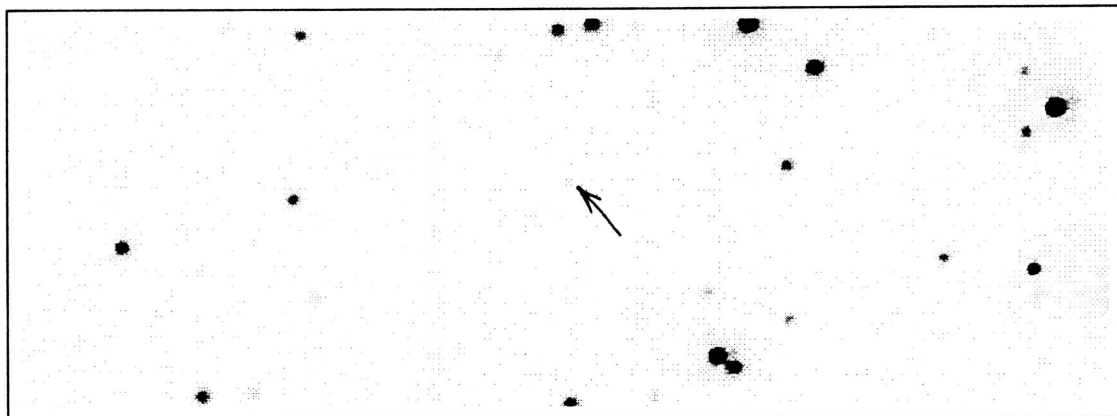
Coordinates: α (1950) = 01:54:17.4 δ (1950) = +27:50:37

Spectral Type: M6 V

Photometry: $I_{KC} = 16.04$ $R_{CTI} = 17.69$ $(V-I)_{KC} = 3.68 \pm 0.17$ $(R-I)_{CTI} = 1.65 \pm 0.07$ $(V-I)_{CTI} = 3.61 \pm 0.06$

Notes:

CTI 015706.0+280519



CTI FINDER CHART

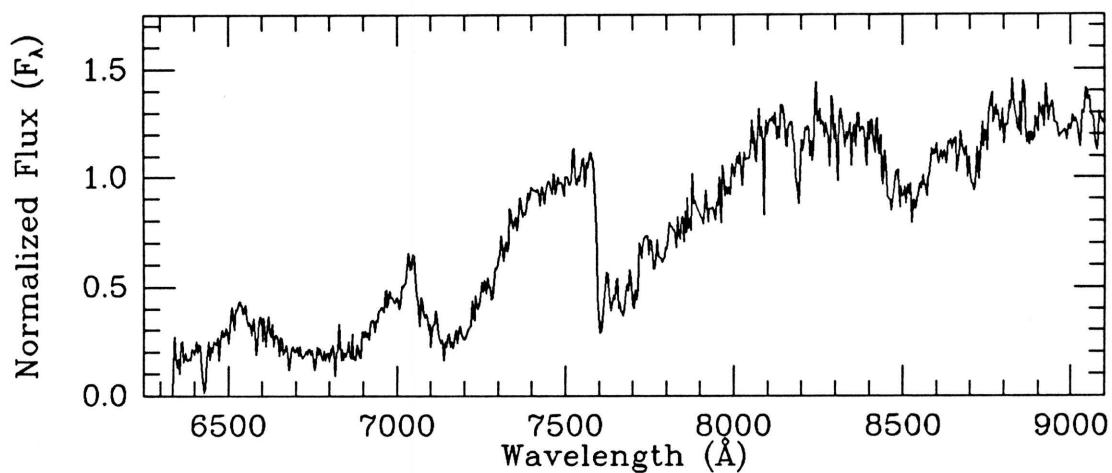
V filter

Obs. (UT) 1987 Oct 20

MMT SPECTRUM

Exposure: 2361 sec

Obs. (UT) 1990 Jan 22

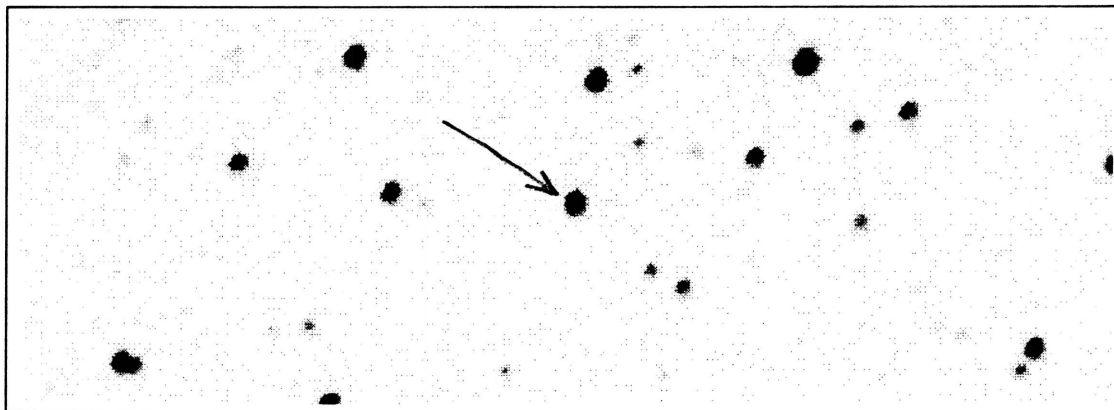
Coordinates: α (1950) = 01:54:57.8 δ (1950) = +27:54:22

Spectral Type: M4.5 V

Photometry: $I_{KC} = 17.01$ $R_{CTI} = 18.55$ $(V-I)_{KC} = 3.60 \pm .24$ $(R-I)_{CTI} = 1.59 \pm .14$ $(V-I)_{CTI} = 3.37 \pm .12$

Notes:

CTI 015812.8+280439



CTI FINDER CHART

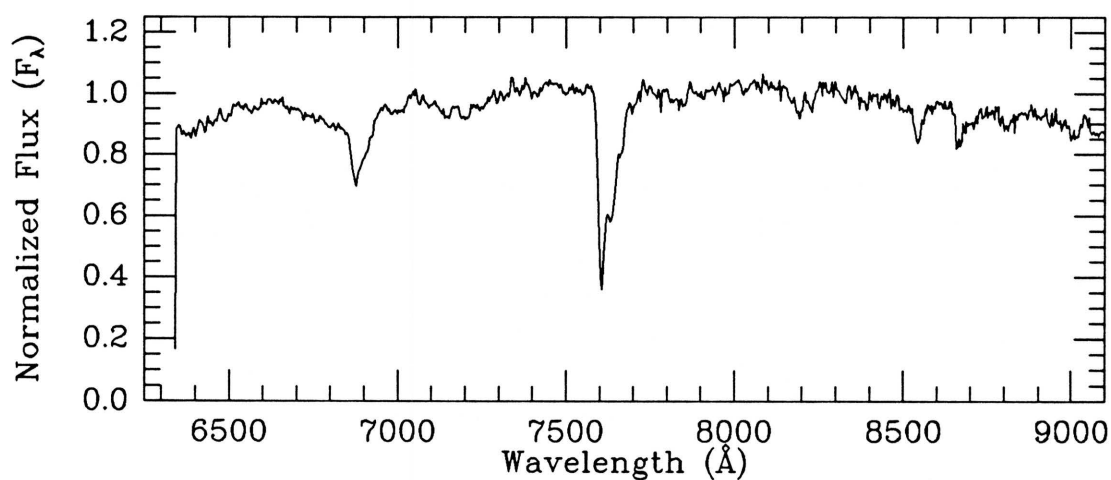
I filter

Obs. (UT) 1989 Nov 03

MMT SPECTRUM

Exposure: 900 sec

Obs. (UT) 1990 Nov 23

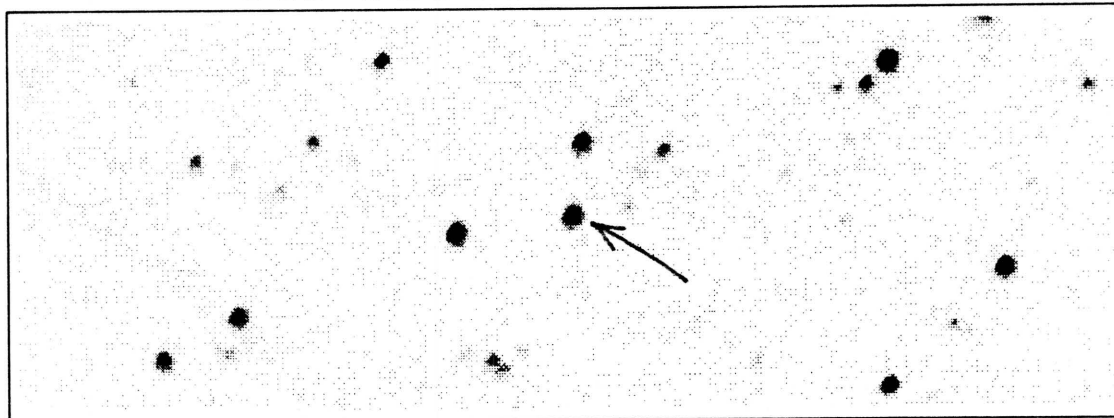
Coordinates: α (1950) = 01:56:04.5 δ (1950) = +27:53:43

Spectral Type: K7 V

Photometry: $I_{KC} = 14.18$ $R_{CTI} = 14.46$ $(V-I)_{KC} = 1.61 \pm 0.13$ $(R-I)_{CTI} = 0.20 \pm 0.06$ $(V-I)_{CTI} = 1.50 \pm 0.01$

Notes:

CTI 015825.4+280120



CTI FINDER CHART

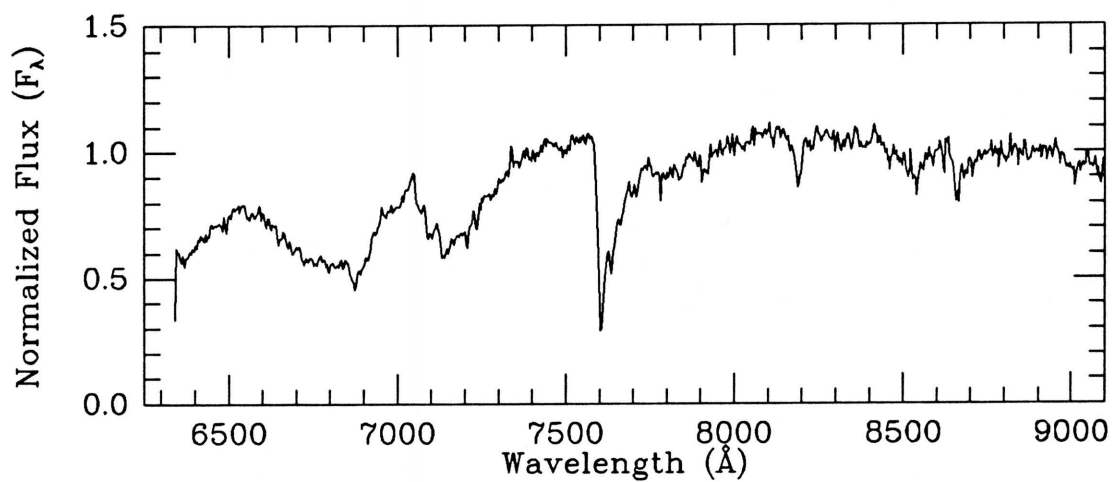
I filter

Obs. (UT) 1989 Nov 03

MMT SPECTRUM

Exposure: 1200 sec

Obs. (UT) 1990 Nov 23

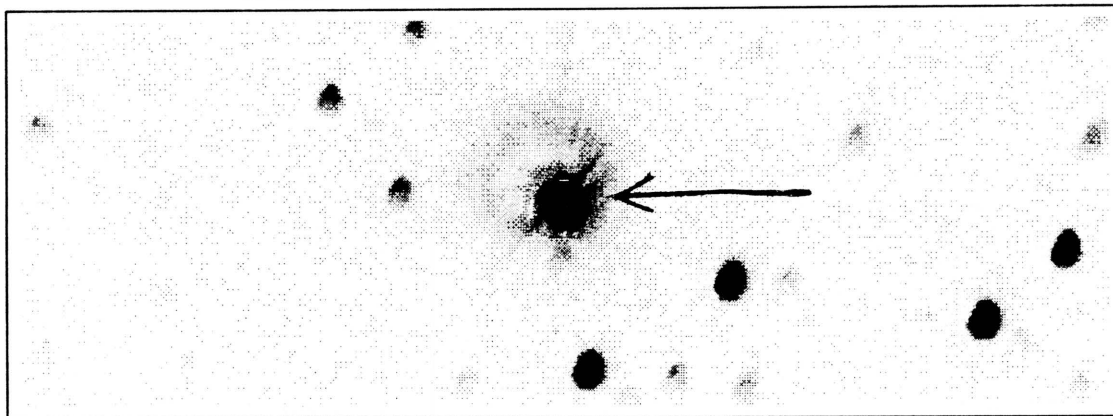
Coordinates: α (1950) = 01:56:17.1 δ (1950) = +27:50:25

Spectral Type: M1.5 V

Photometry: $I_{\text{KC}} = 14.85$ $R_{\text{CTI}} = 15.45$ $(V-I)_{\text{KC}} = 2.11 \pm 0.11$ $(R-I)_{\text{CTI}} = 0.55 \pm 0.02$ $(V-I)_{\text{CTI}} = 1.99 \pm 0.01$

Notes:

CTI 021845.9+280047



CTI FINDER CHART

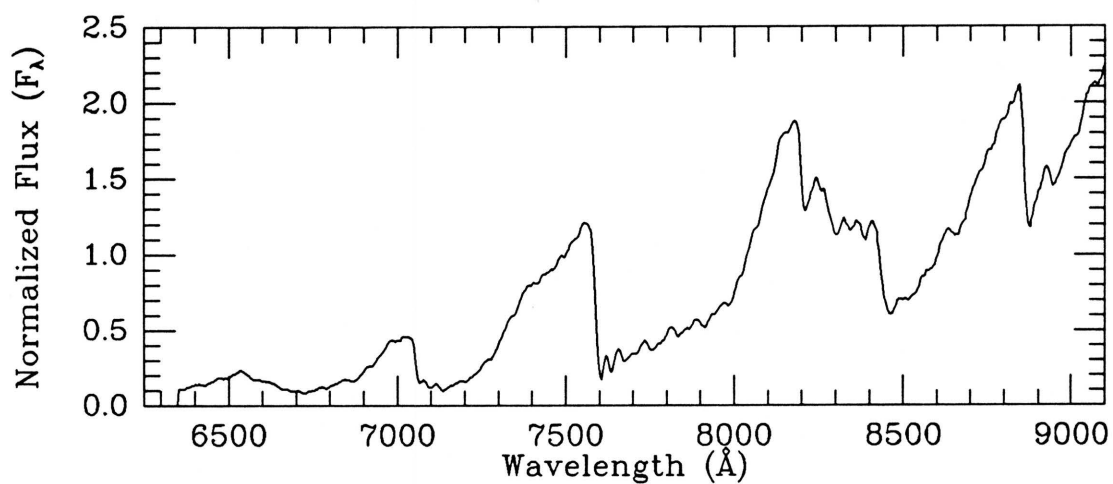
I filter

Obs. (UT) 1988 Sep 13

MMT SPECTRUM

Exposure: 390 sec

Obs. (UT) 1990 Nov 23

Coordinates: α (1950) = 02:16:35.6 δ (1950) = +27:50:27

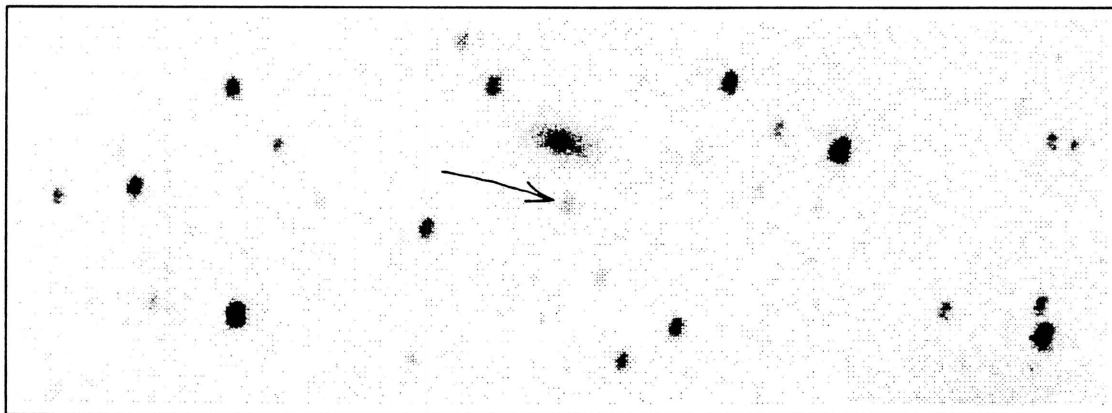
Spectral Type: M7 III

Photometry: I_{KC} = unknown R_{CTI} = 11.12 $(V-I)_{KC}$ =unknown $(R-I)_{CTI}=1.75\pm.01$ $(V-I)_{CTI}=4.08\pm.01$

Notes: CTI measurement of I, and possibly R, saturated. A Mira variable whose 19 CTI V measures range from 12.8 to 13.9.

Not listed in General Cat. of Variable Stars (Kholopov 1985).

CTI 023210.0+280313



CTI FINDER CHART

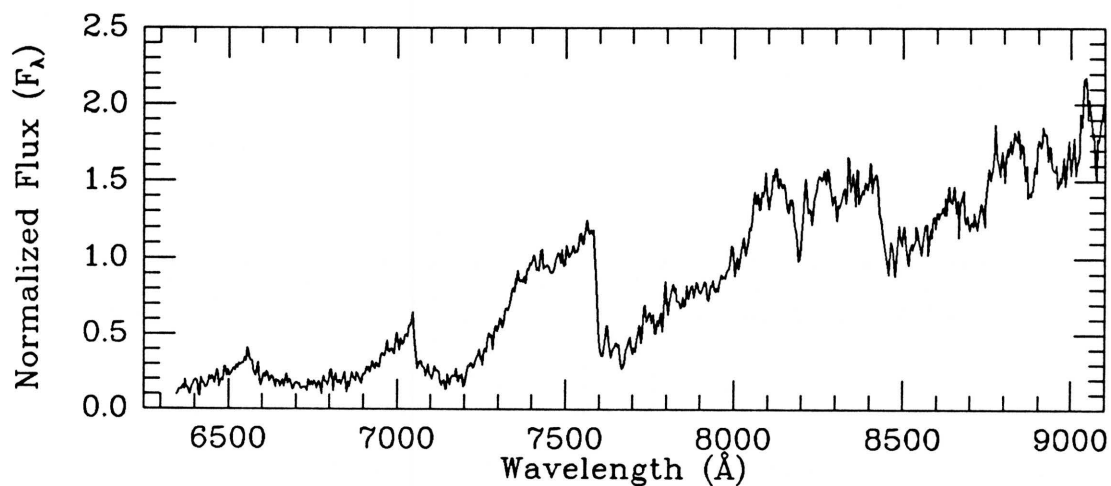
I filter

Obs. (UT) 1988 Nov 01

MMT SPECTRUM

Exposure: 2100 sec

Obs. (UT) 1990 Sep 13

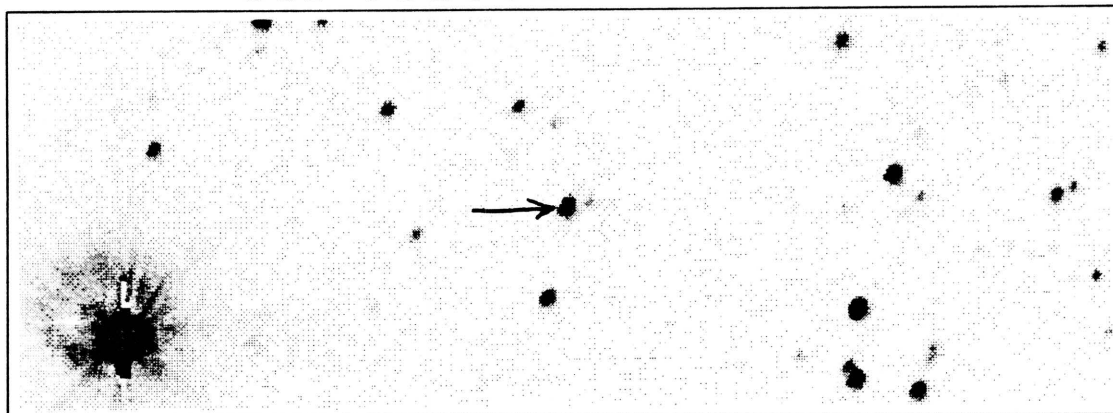
Coordinates: α (1950) = 02:29:58.4 δ (1950) = +27:53:19

Spectral Type: M6 V

Photometry: $I_{\text{KC}} = 17.58$ $R_{\text{CTI}} = 19.30$ $(V-I)_{\text{KC}} = 3.90 \pm 0.37$ $(R-I)_{\text{CTI}} = 1.80 \pm 0.24$ $(V-I)_{\text{CTI}} = 2.89 \pm 0.86$

Notes: Comparison to the POSS E print suggests that this object may have a proper motion of ~ 1.5 arcsec/yr to the north.

CTI 031502.6+280315



CTI FINDER CHART

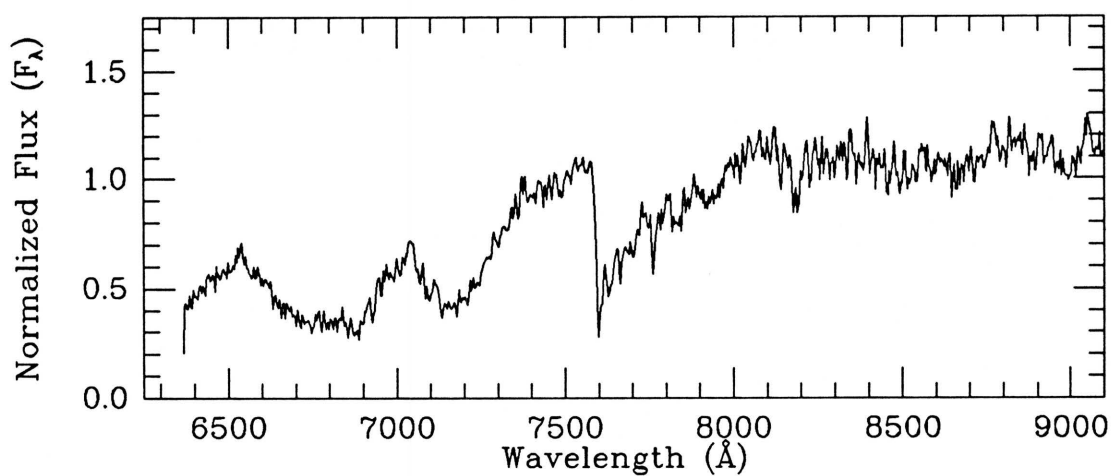
I filter

Obs. (UT) 1989 Nov 03

MMT SPECTRUM

Exposure: 300 sec

Obs. (UT) 1991 Oct 17

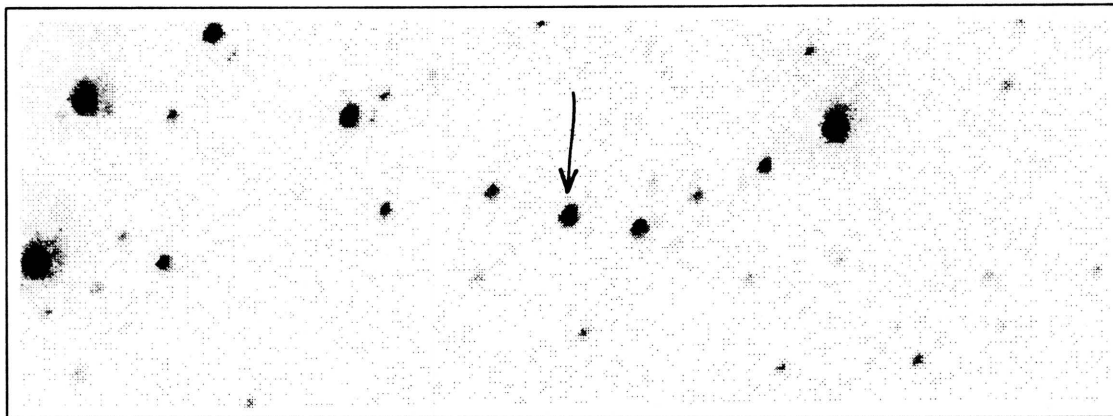
Coordinates: α (1950) = 03:12:47.4 δ (1950) = +27:54:57

Spectral Type: M3.5 V

Photometry: $I_{KC} = 14.84$ $R_{CTI} = 15.95$ $(V-I)_{KC} = 2.84 \pm 0.12$ $(R-I)_{CTI} = 1.06 \pm 0.03$ $(V-I)_{CTI} = 2.68 \pm 0.02$

Notes:

CTI 032442.5+280400



CTI FINDER CHART

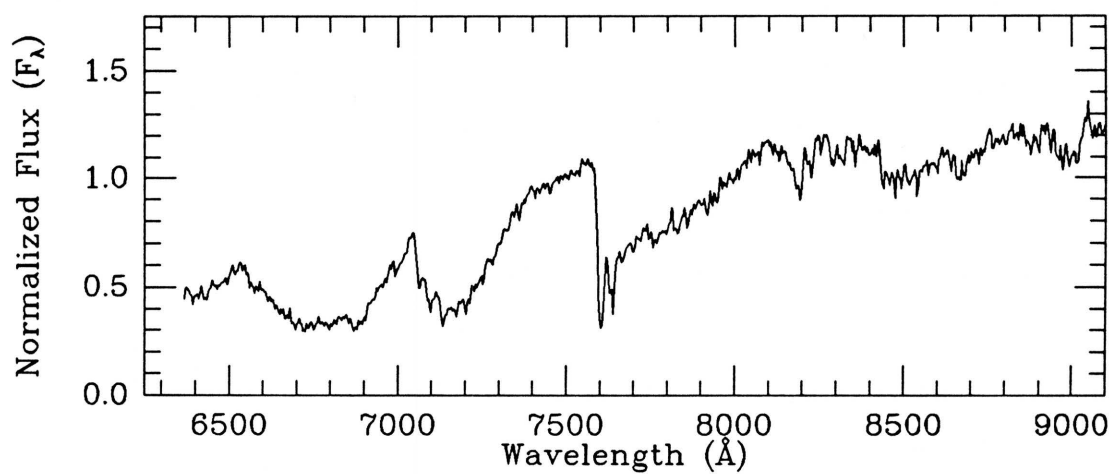
I filter

Obs. (UT) 1989 Nov 03

MMT SPECTRUM

Exposure: 300 sec

Obs. (UT) 1991 Oct 17

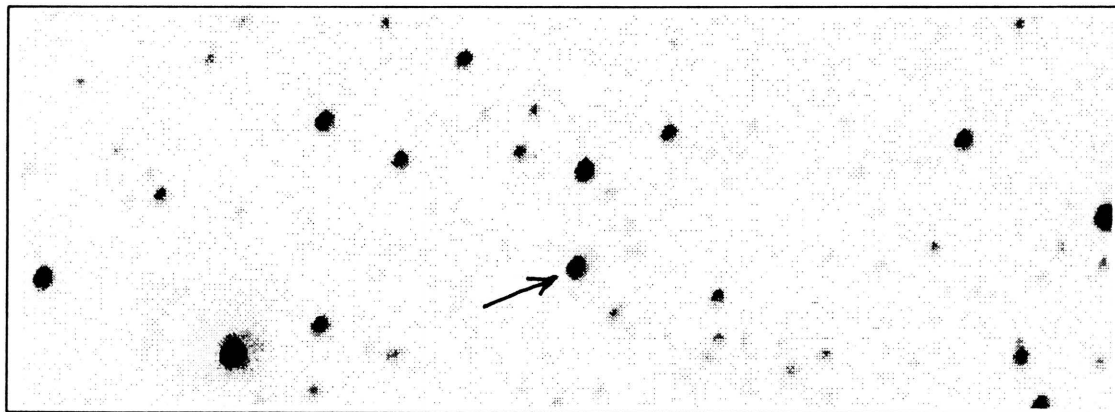
Coordinates: α (1950) = 03:22:26.5 δ (1950) = +27:56:06

Spectral Type: M4 V

Photometry: $I_{KC} = 14.77$ $R_{CTI} = 15.95$ $(V-I)_{KC} = 2.92 \pm 0.13$ $(R-I)_{CTI} = 1.12 \pm 0.03$ $(V-I)_{CTI} = 2.81 \pm 0.02$

Notes:

CTI 032659.6+275912



CTI FINDER CHART

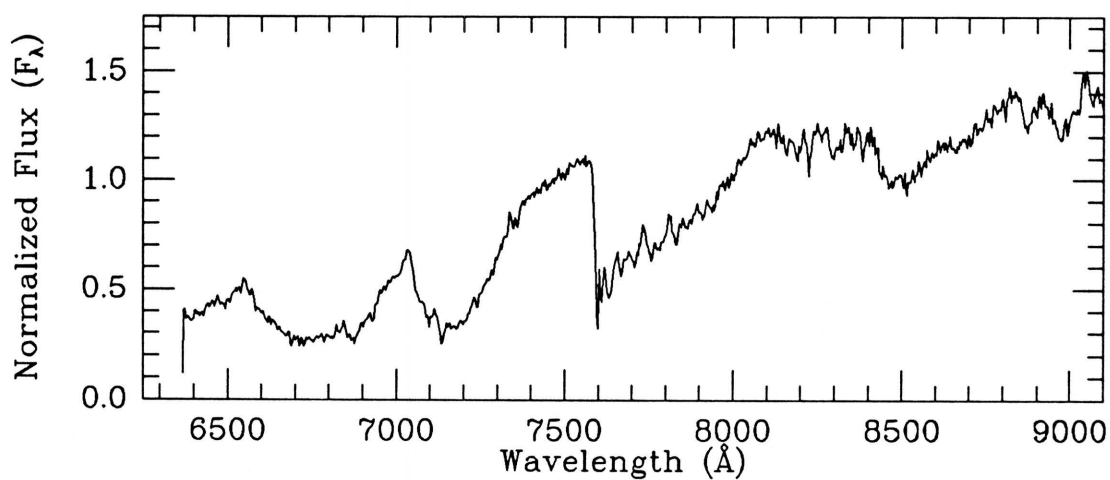
I filter

Obs. (UT) 1989 Nov 03

MMT SPECTRUM

Exposure: 300 sec

Obs. (UT) 1991 Oct 17

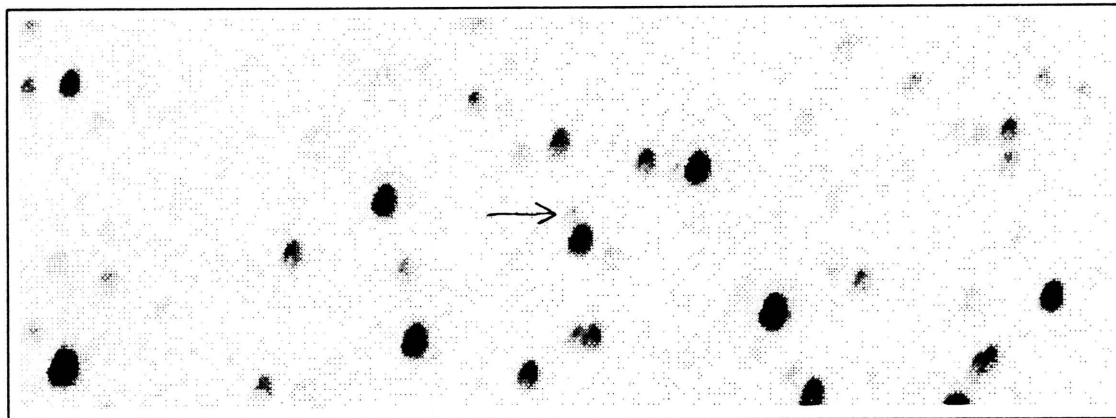
Coordinates: α (1950) = 03:24:43.5 δ (1950) = +27:51:24

Spectral Type: M4.5 V

Photometry: $I_{KC} = 14.25$ $R_{CTI} = 15.67$ $(V-I)_{KC} = 3.24 \pm 0.13$ $(R-I)_{CTI} = 1.34 \pm 0.03$ $(V-I)_{CTI} = 3.19 \pm 0.02$

Notes:

CTI 034036.8+280248



CTI FINDER CHART

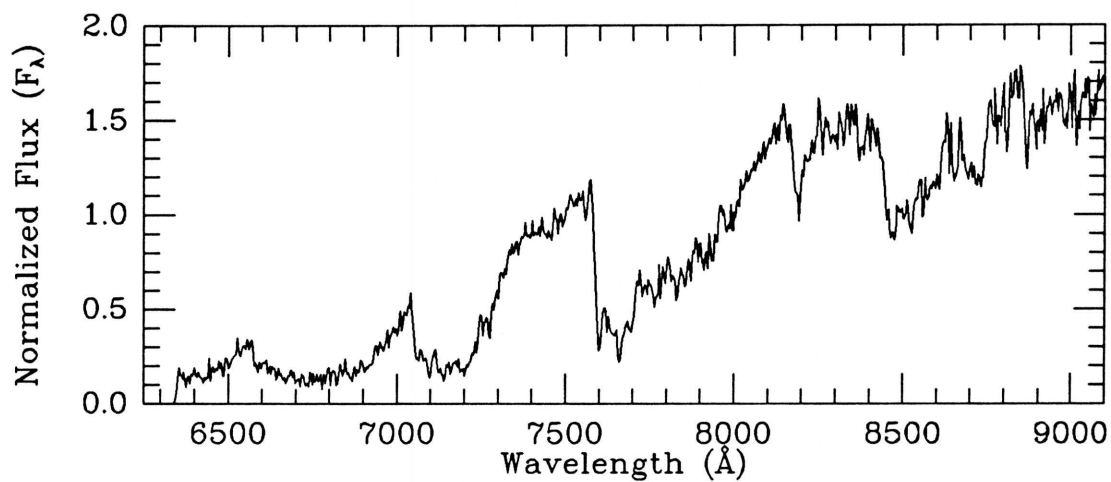
I filter

Obs. (UT) 1988 Sep 13

MMT SPECTRUM

Exposure: 2700 sec

Obs. (UT) 1990 Nov 22

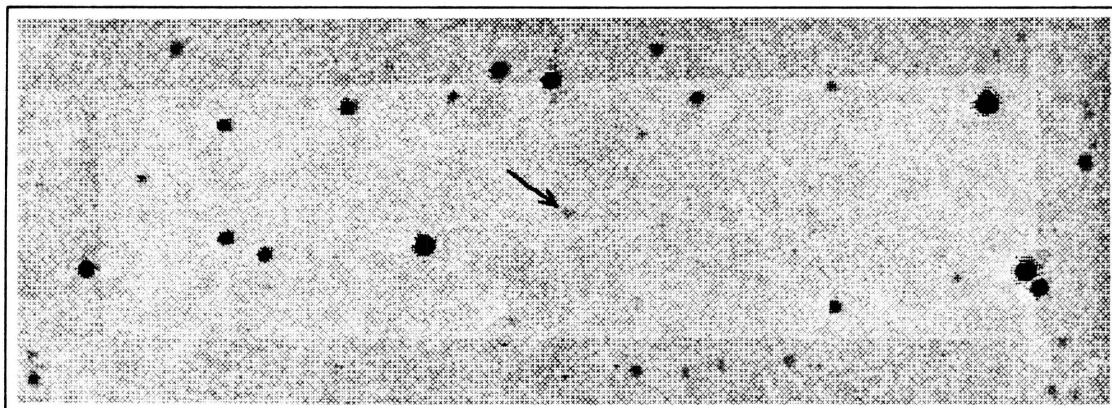
Coordinates: α (1950) = 03:38:19.7 δ (1950) = +27:55:35

Spectral Type: M6 V

Photometry: $I_{\text{KC}} = 17.88$ $R_{\text{CTI}} = 19.96$ $(V-I)_{\text{KC}} = 4.43 \pm 0.61$ $(R-I)_{\text{CTI}} = 2.17 \pm 0.41$ $(V-I)_{\text{CTI}} = \text{unknown}$

Notes:

CTI 034607.4+280109



CTI FINDER CHART

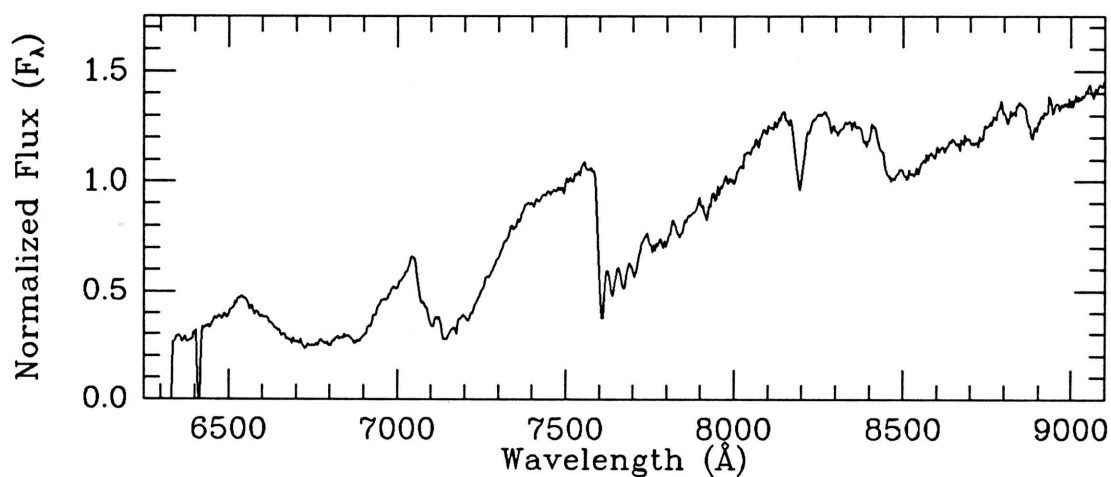
V filter

Obs. (UT) 1987 Oct 20

MMT SPECTRUM

Exposure: 2400 sec

Obs. (UT) 1990 Jan 20

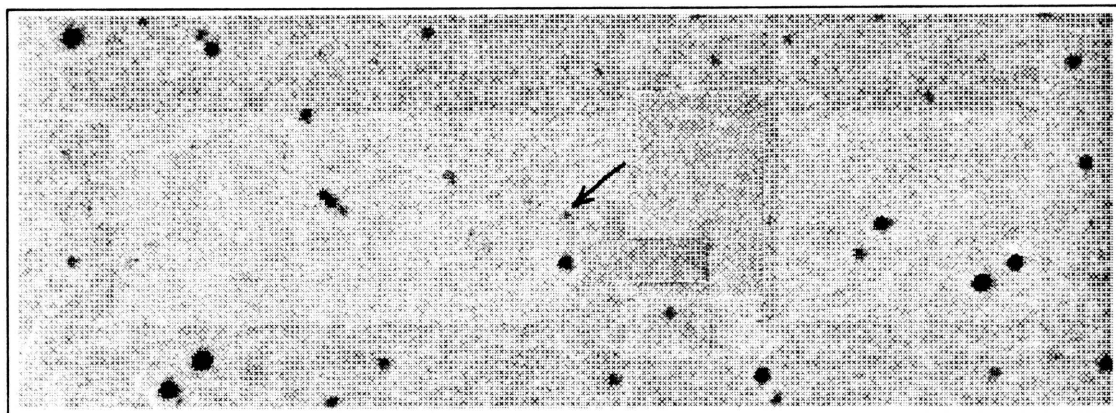
Coordinates: α (1950) = 03:43:50.0 δ (1950) = +27:54:11

Spectral Type: M4.5 V

Photometry: $I_{KC} = 15.71$ $R_{CTI} = 16.97$ $(V-I)_{KC} = 3.11 \pm 0.15$ $(R-I)_{CTI} = 1.25 \pm 0.06$ $(V-I)_{CTI} = 3.03 \pm 0.04$

Notes:

CTI 035750.4+280105



CTI FINDER CHART

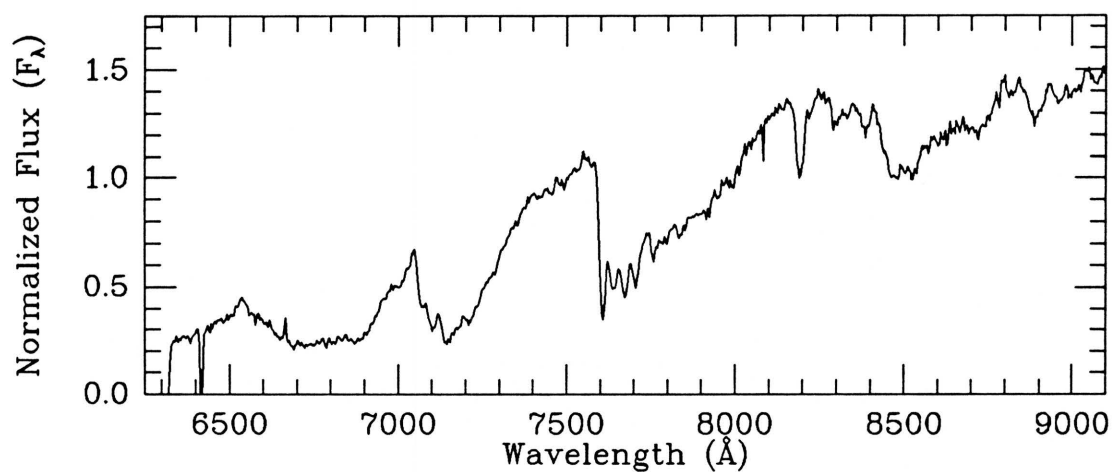
V filter

Obs. (UT) 1987 Oct 20

MMT SPECTRUM

Exposure: 2700 sec

Obs. (UT) 1990 Jan 21

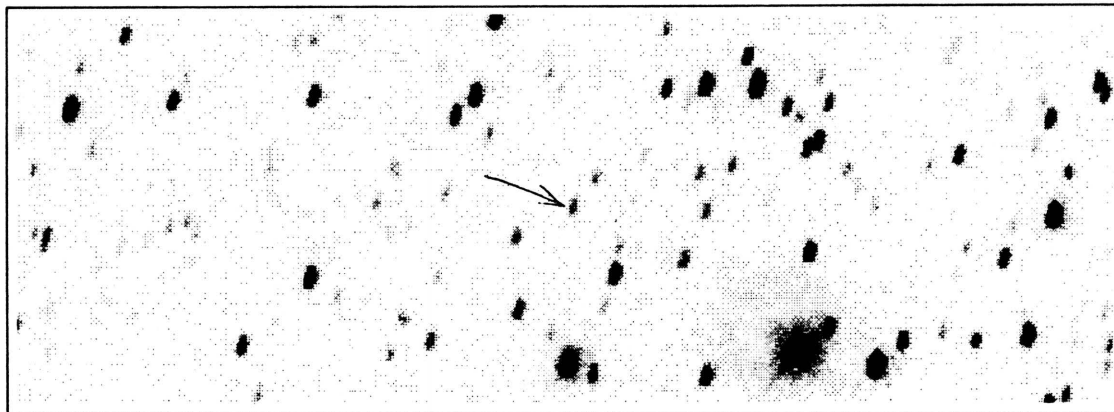
Coordinates: α (1950) = 03:55:32.3 δ (1950) = +27:54:40

Spectral Type: M5 V

Photometry: $I_{KC} = 16.06$ $R_{CTI} = 17.47$ $(V-I)_{KC} = 3.34 \pm 0.17$ $(R-I)_{CTI} = 1.41 \pm 0.08$ $(V-I)_{CTI} = 3.26 \pm 0.05$

Notes:

CTI 064951.4+280442



CTI FINDER CHART

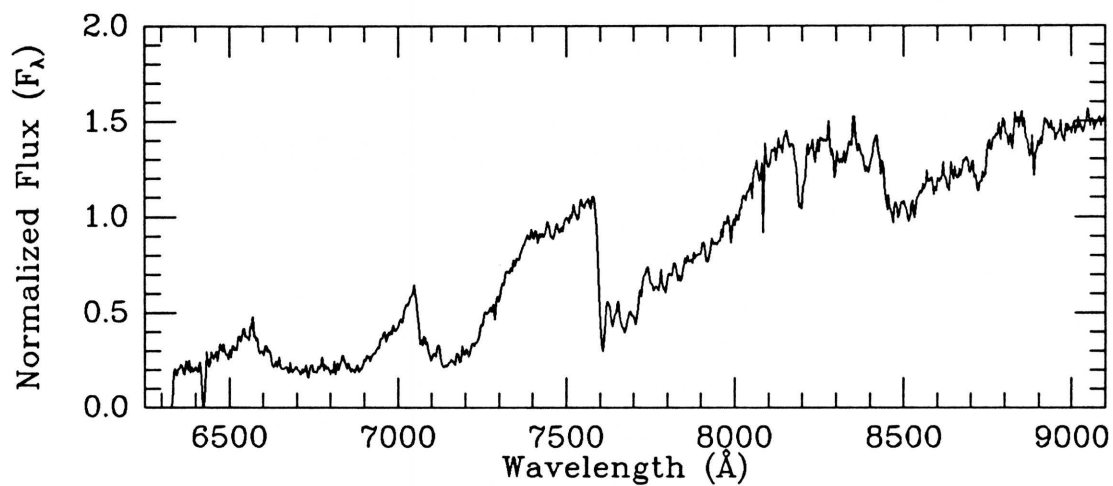
I filter

Obs. (UT) 1989 Mar 07

MMT SPECTRUM

Exposure: 2700 sec

Obs. (UT) 1990 Jan 21

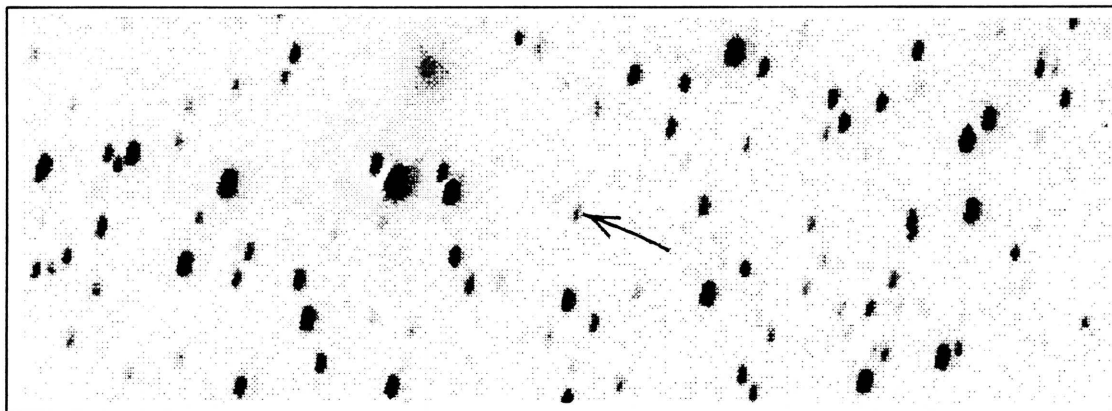
Coordinates: α (1950) = 06:47:29.9 δ (1950) = +28:07:21

Spectral Type: M5.5 V

Photometry: $I_{KC} = 17.22$ $R_{CTI} = 18.99$ $(V-I)_{KC} = 3.94 \pm 0.59$ $(R-I)_{CTI} = 1.83 \pm 0.40$ $(V-I)_{CTI} = 3.29 \pm 0.40$

Notes:

CTI 065150.8+280311



CTI FINDER CHART

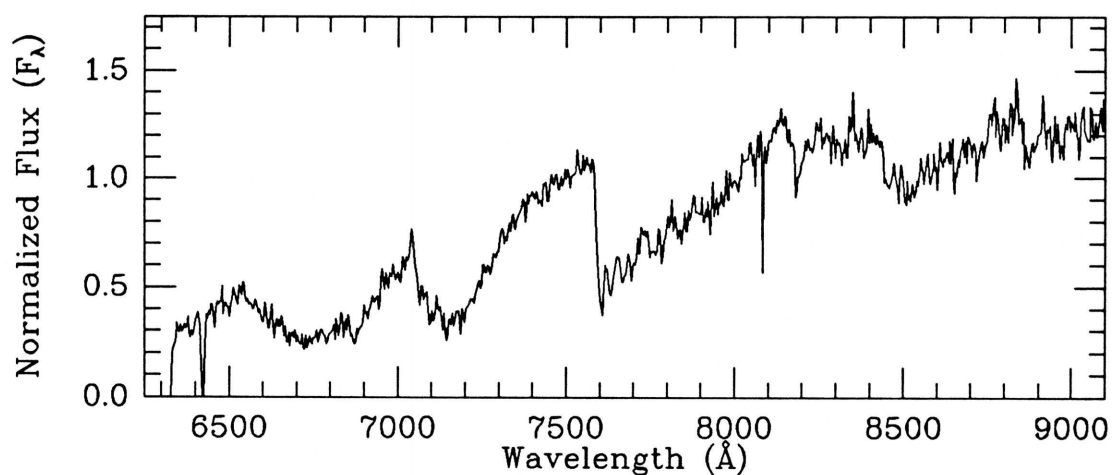
I filter

Obs. (UT) 1989 Mar 07

MMT SPECTRUM

Exposure: 2700 sec

Obs. (UT) 1990 Jan 21

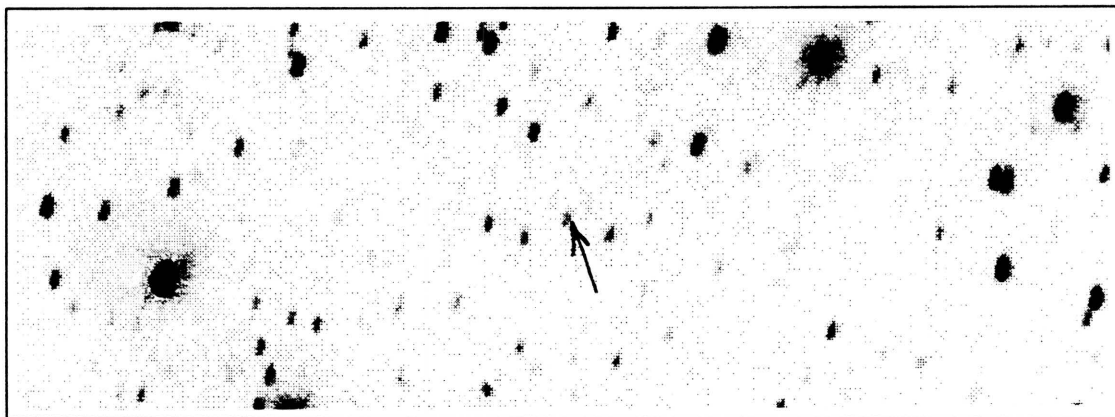
Coordinates: α (1950) = 06:49:29.4 δ (1950) = +28:05:56

Spectral Type: M5.5 V

Photometry: I_{KC} = unknown R_{CTI} = unknown $(V-I)_{KC}$ = unknown $(R-I)_{CTI} > 1.93$: $(V-I)_{CTI} = 3.04 \pm .07$

Notes:

CTI 065950.5+280228



CTI FINDER CHART

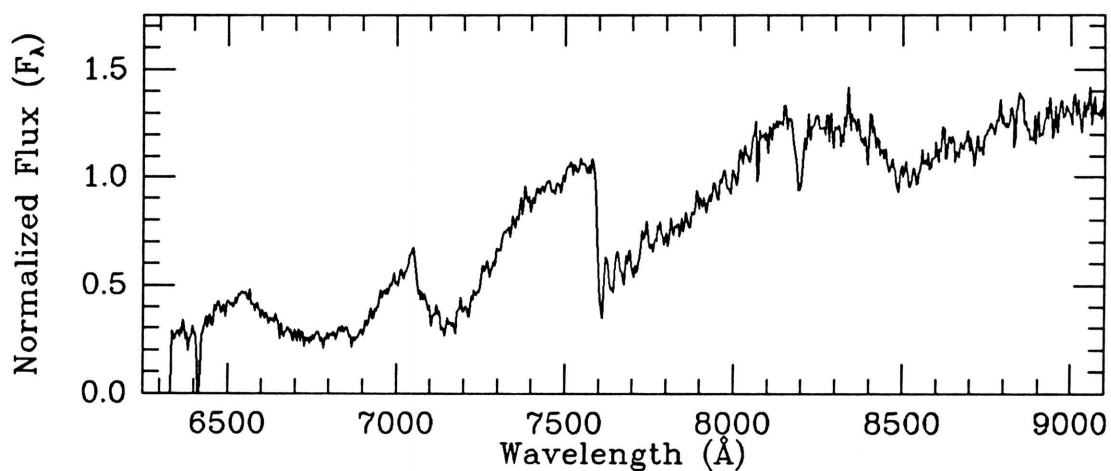
I filter

Obs. (UT) 1989 Mar 07

MMT SPECTRUM

Exposure: 2700 sec

Obs. (UT) 1990 Jan 20

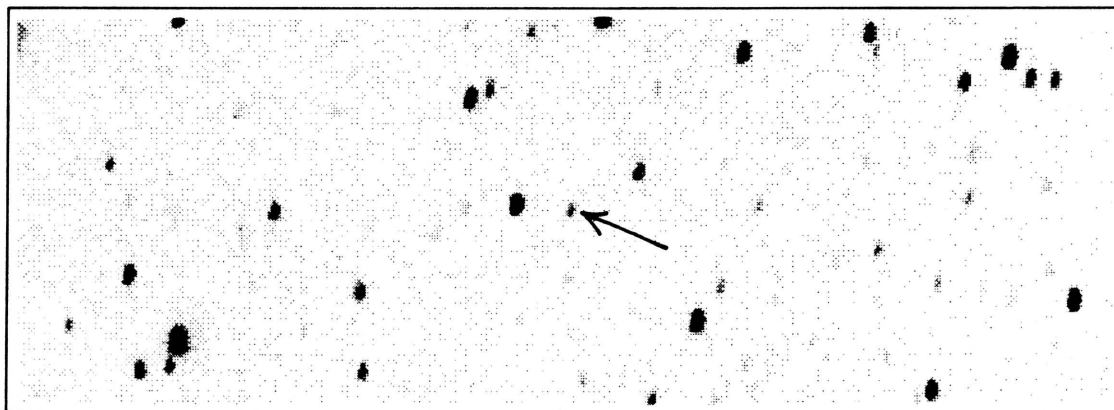
Coordinates: α (1950) = 06:57:29.4 δ (1950) = +28:05:38

Spectral Type: M4.5 V

Photometry: $I_{KC} = 17.47$ $R_{CTI} = \text{unknown}$ $(V-I)_{KC} = \text{unknown}$ $(R-I)_{CTI} = \text{unknown}$ $(V-I)_{CTI} = 2.98 \pm 0.07$

Notes:

CTI 072401.3+280238



CTI FINDER CHART

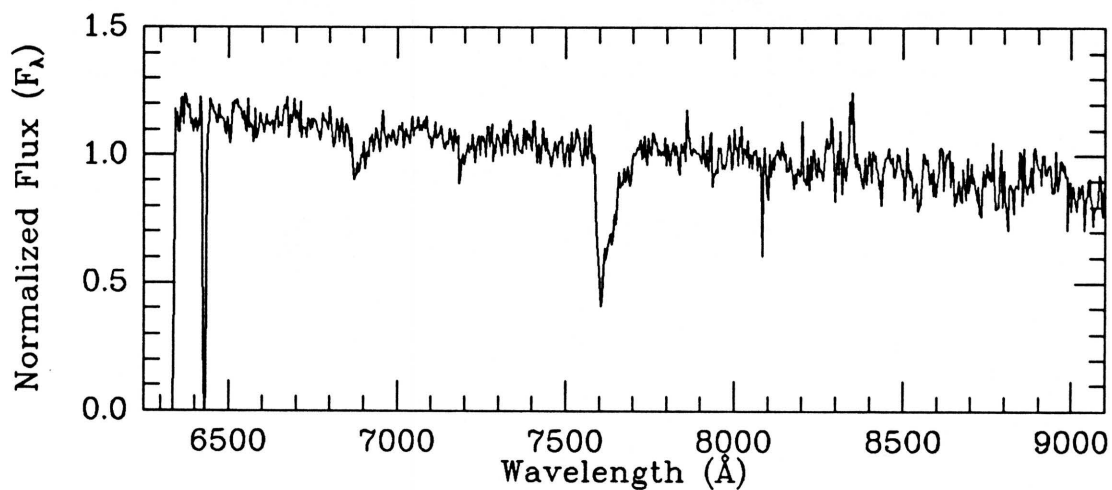
I filter

Obs. (UT) 1989 Mar 07

MMT SPECTRUM

Exposure: 1500 sec

Obs. (UT) 1990 Jan 21

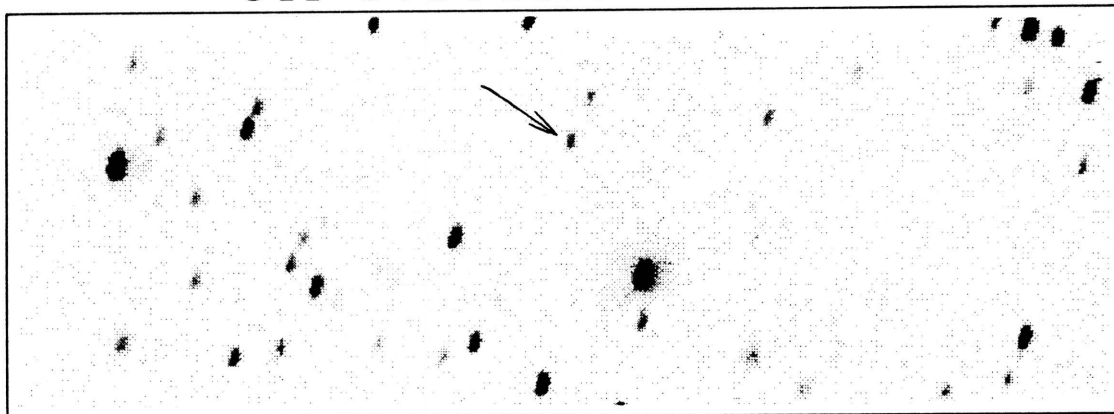
Coordinates: α (1950) = 07:21:41.0 δ (1950) = +28:07:04

Spectral Type: <K5 V

Photometry: I_{KC} = unknown R_{CTI} = unknown $(V-I)_{KC}$ =unknown $(R-I)_{CTI}$ >2.12: $(V-I)_{CTI}$ =0.82±.02

Notes:

CTI 075013.2+280613



CTI FINDER CHART

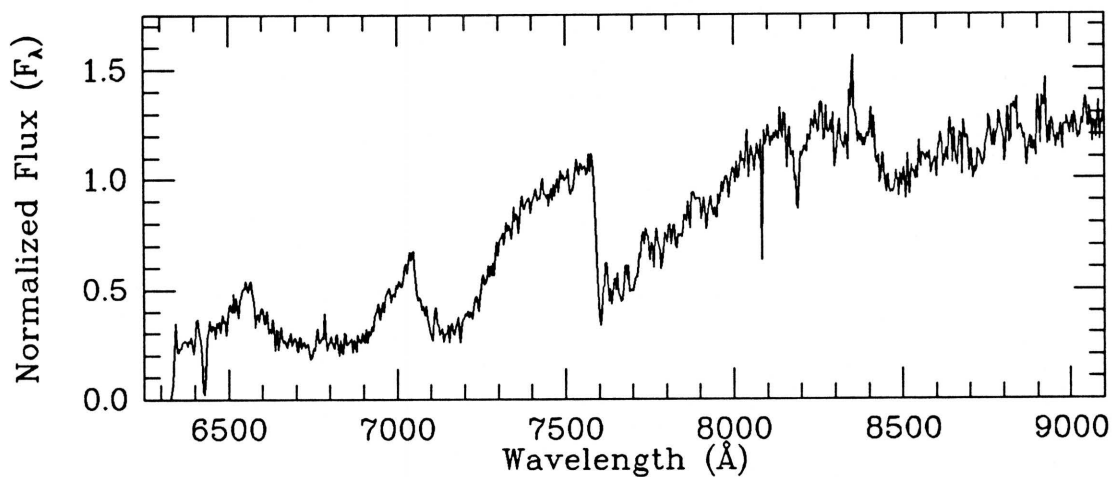
I filter

Obs. (UT) 1989 Mar 07

MMT SPECTRUM

Exposure: 2700 sec

Obs. (UT) 1990 Jan 21

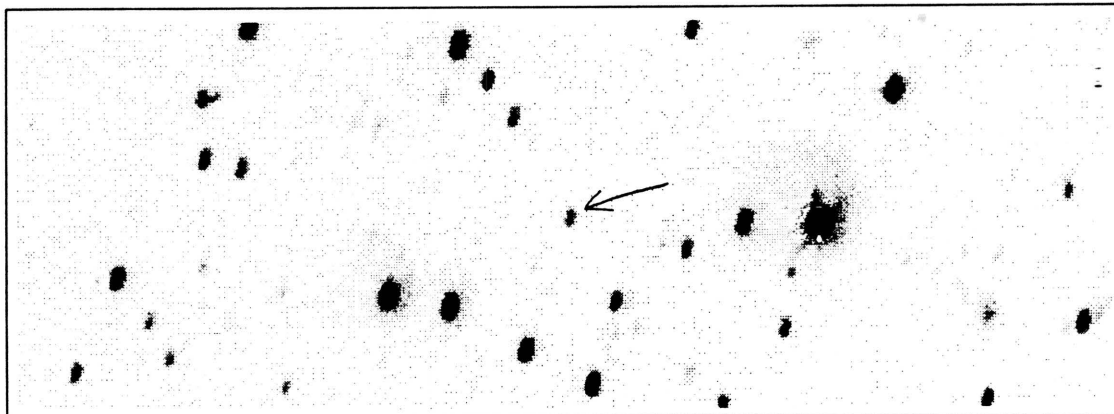
Coordinates: α (1950) = 07:47:54.1 δ (1950) = +28:11:57

Spectral Type: M4.5 V

Photometry: $I_{KC} = 17.32$ $R_{CTI} = 19.00$ $(V-I)_{KC} = 3.81 \pm .40$ $(R-I)_{CTI} = 1.74 \pm .26$ $(V-I)_{CTI} = 2.96 \pm .20$

Notes:

CTI 075723.2+280533



CTI FINDER CHART

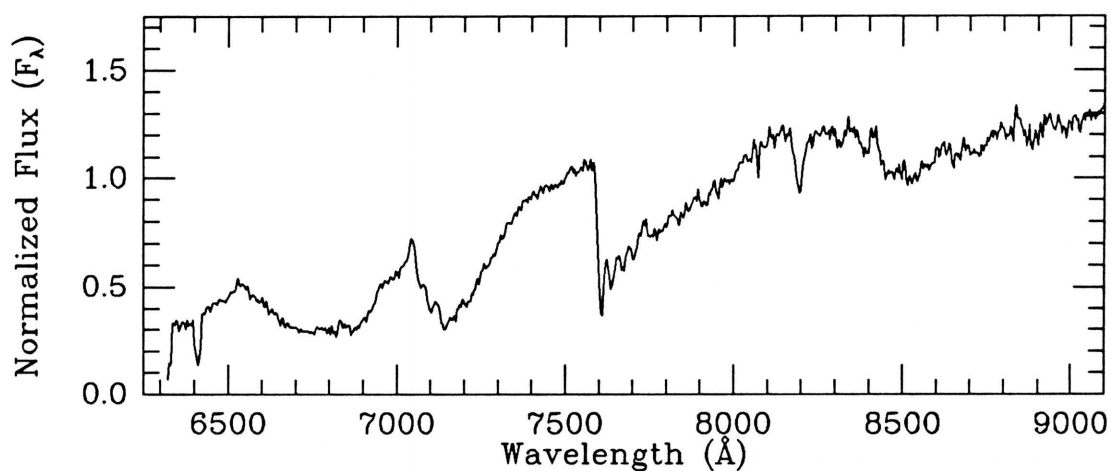
I filter

Obs. (UT) 1989 Mar 07

MMT SPECTRUM

Exposure: 2700 sec

Obs. (UT) 1990 Jan 20

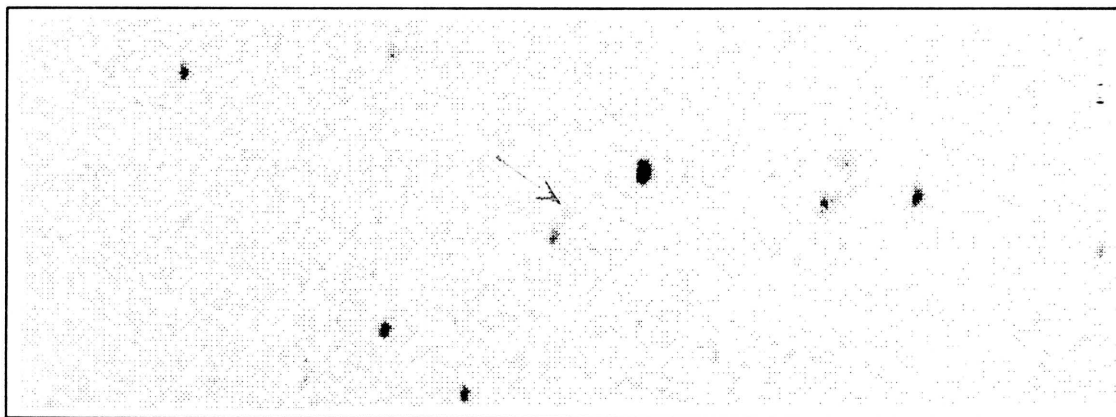
Coordinates: α (1950) = 07:55:04.5 δ (1950) = +28:11:38

Spectral Type: M4 V

Photometry: $I_{KC} = 16.66$ $R_{CTI} = 18.98$ $(V-I)_{KC} = 4.68 \pm 0.28$ $(R-I)_{CTI} = 2.35 \pm 0.16$ $(V-I)_{CTI} = 3.01 \pm 0.16$

Notes:

CTI 081722.3+280138



CTI FINDER CHART

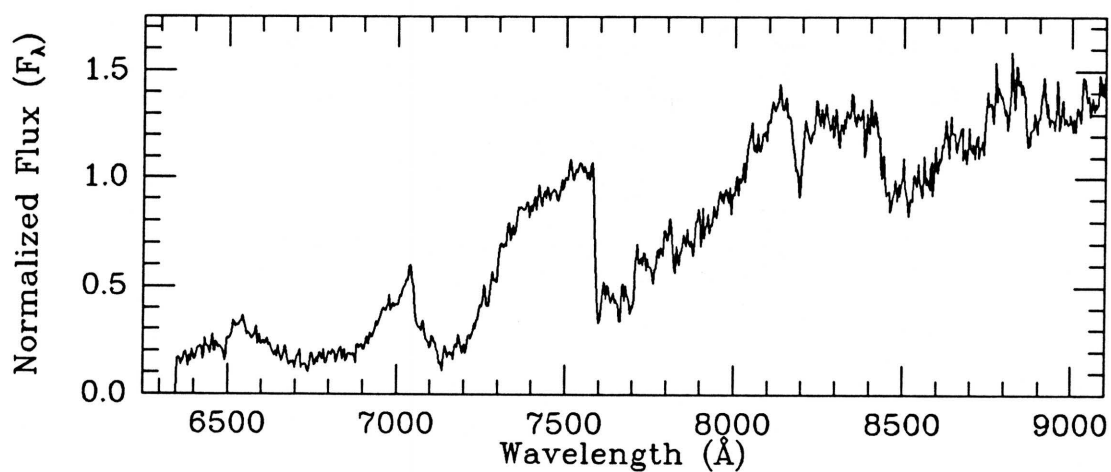
I filter

Obs. (UT) 1989 Jan 31

MMT SPECTRUM

Exposure: 3900 sec

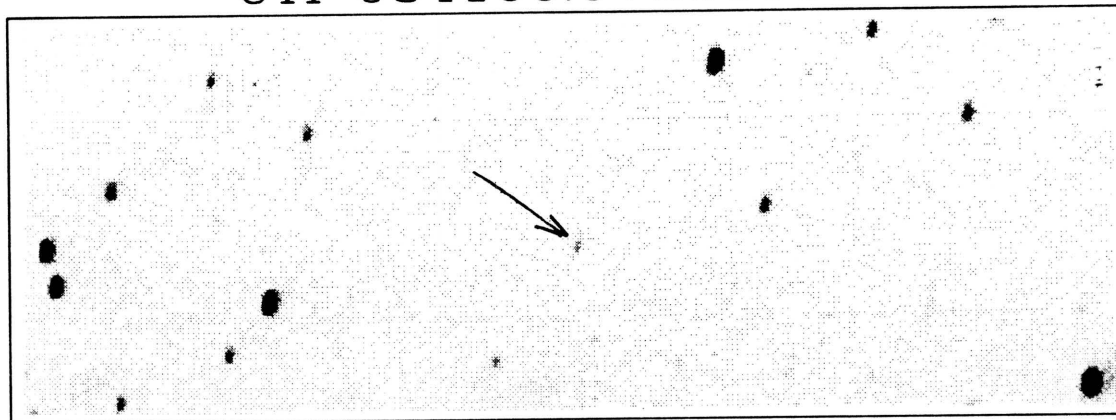
Obs. (UT) 1990 Nov 22

Coordinates: α (1950) = 08:15:04.9 δ (1950) = +28:08:39

Spectral Type: M5.5 V

Photometry: $I_{KC} = 17.25$ $R_{CTI} = 18.97$ $(V-I)_{KC} = 3.87 \pm 0.24$ $(R-I)_{CTI} = 1.78 \pm 0.14$ $(V-I)_{CTI} = 3.18 \pm 0.14$ Notes: Comparison to POSS E print suggests small (~ 0.2 arcsec/yr) proper motion to the SE.

CTI 084106.0+280016



CTI FINDER CHART

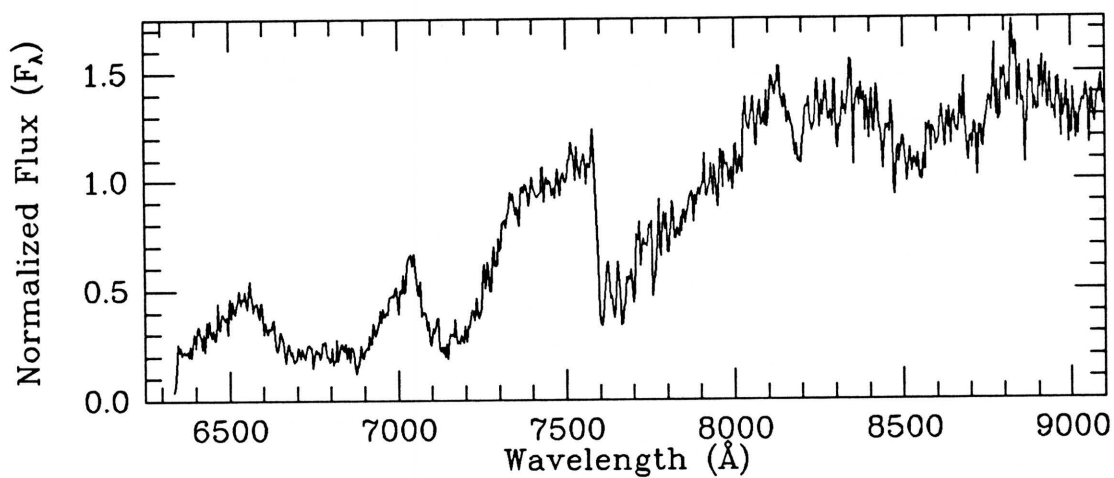
I filter

Obs. (UT) 1989 Jan 31

MMT SPECTRUM

Exposure: 3900 sec

Obs. (UT) 1990 Nov 22

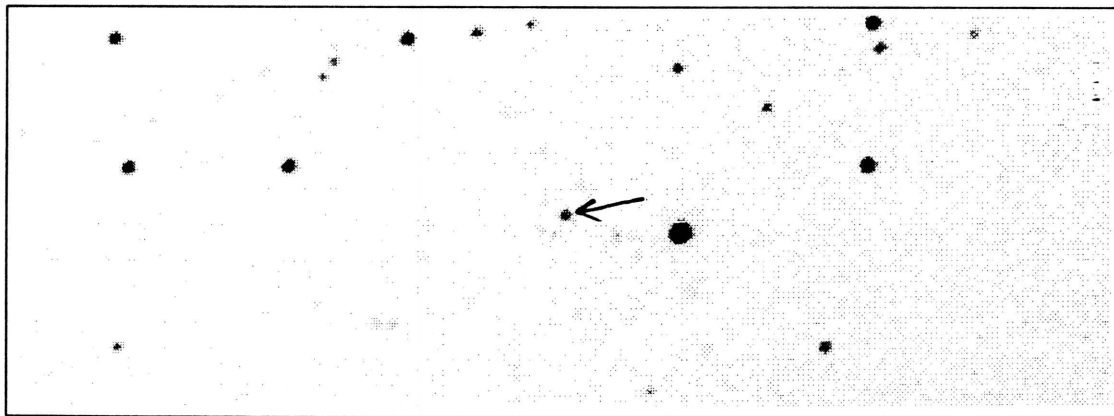
Coordinates: α (1950) = 08:38:50.2 δ (1950) = +28:08:19

Spectral Type: M5.5 V

Photometry: $I_{KC} = 17.88$ $R_{CTI} = 19.61$ $(V-I)_{KC} = 3.93 \pm .41$ $(R-I)_{CTI} = 1.82 \pm .27$ $(V-I)_{CTI} = 2.79 \pm .29$

Notes:

CTI 090120.6+280439



CTI FINDER CHART

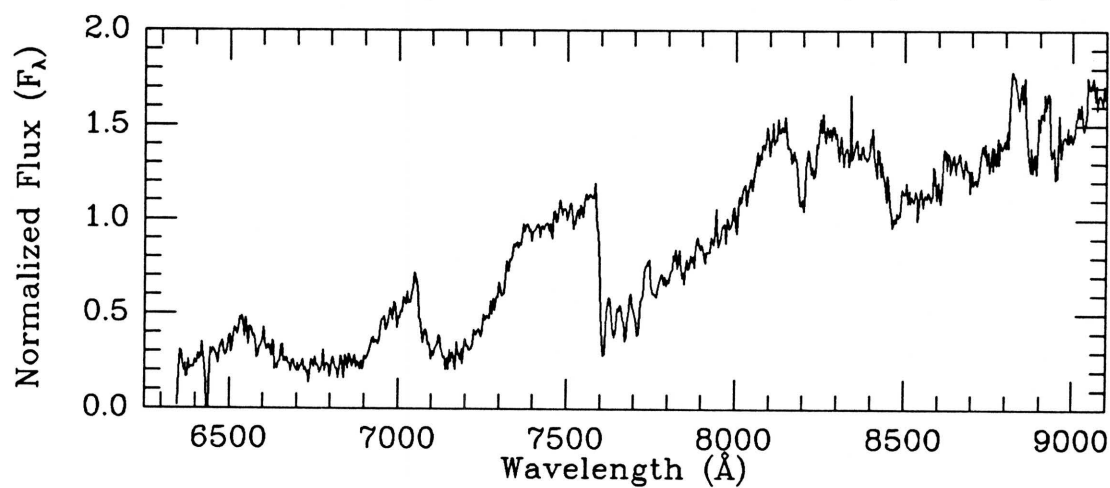
Clear filter

Obs. (UT) 1989 Apr 07

MMT SPECTRUM

Exposure: 3900 sec

Obs. (UT) 1990 May 04

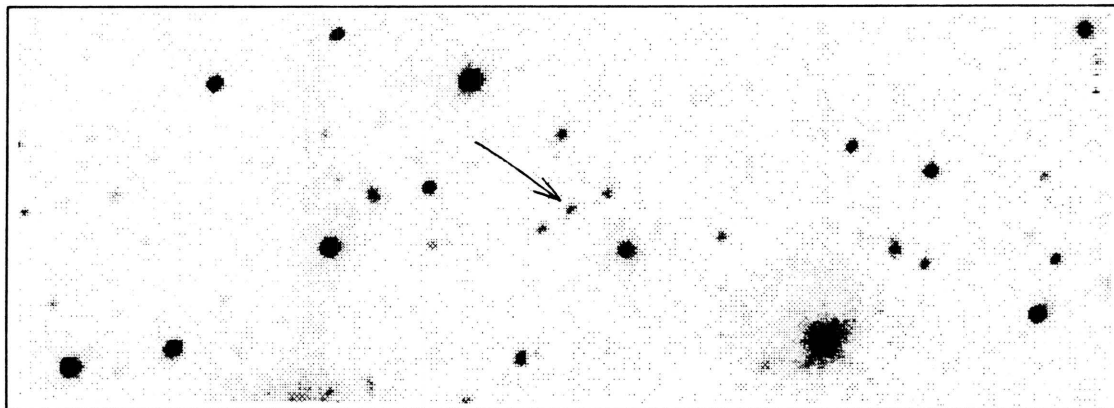
Coordinates: α (1950) = 08:59:06.4 δ (1950) = +28:13:31

Spectral Type: M5.5 V

Photometry: $I_{KC} = 16.86$ $R_{CTI} = 18.50$ $(V-I)_{KC} = 3.73 \pm 0.16$ $(R-I)_{CTI} = 1.68 \pm 0.06$ $(V-I)_{CTI} = 3.51 \pm 0.07$

Notes:

CTI 090928.9+280323



CTI FINDER CHART

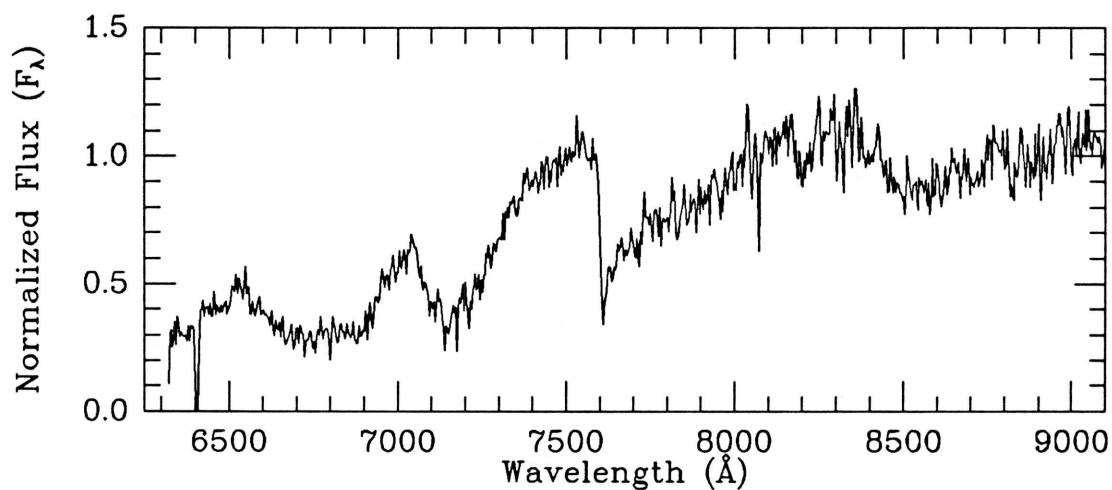
Clear filter

Obs. (UT) 1989 Apr 07

MMT SPECTRUM

Exposure: 2700 sec

Obs. (UT) 1990 Jan 20

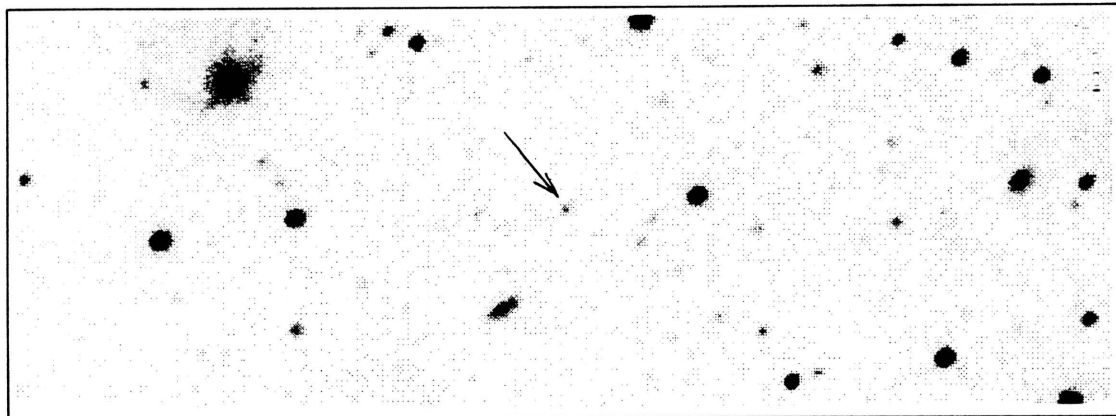
Coordinates: α (1950) = 09:07:15.4 δ (1950) = +28:12:34

Spectral Type: M3.5 V

Photometry: $I_{KC} = 18.20$ $R_{CTI} = 19.74$ $(V-I)_{KC} = 3.67 \pm 0.84$ $(R-I)_{CTI} = 1.64 \pm 0.58$ $(V-I)_{CTI} = 2.39 \pm 0.09$

Notes:

CTI 091716.8+280532



CTI FINDER CHART

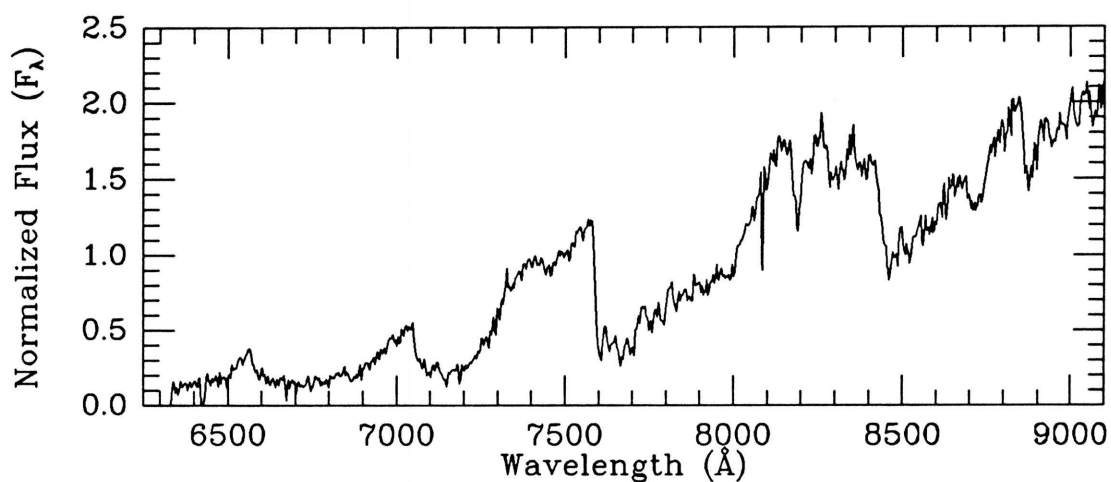
Clear filter

Obs. (UT) 1989 Apr 07

MMT SPECTRUM

Exposure: 3900 sec

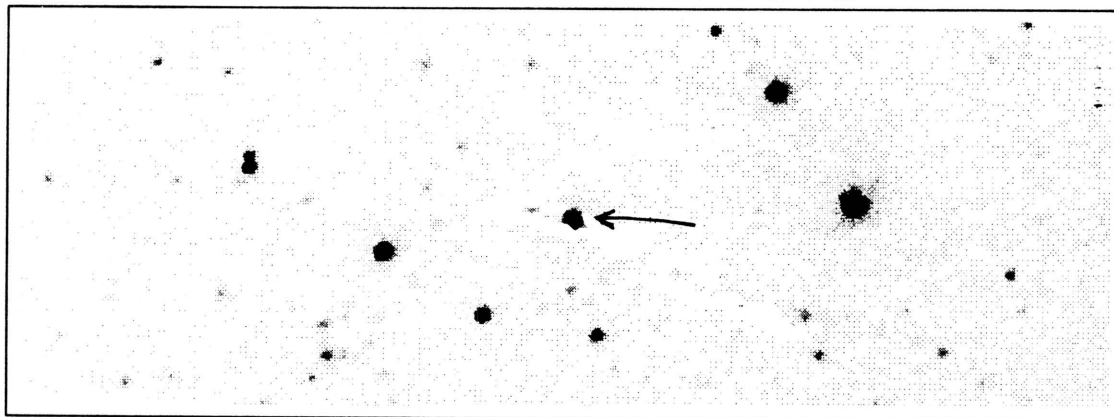
Obs. (UT) 1990 Jan 21

Coordinates: α (1950) = 09:15:03.9 δ (1950) = +28:15:00

Spectral Type: M6 V

Photometry: $I_{\text{KC}} = 17.79$ $R_{\text{CTI}} = 19.37$ $(V-I)_{\text{KC}} = 3.71 \pm 1.04$ $(R-I)_{\text{CTI}} = 1.67 \pm 0.72$ $(V-I)_{\text{CTI}} = 2.58 \pm 1.01$ Notes: Comparison to POSS E prints suggests small (~ 0.2 arcsec/yr) proper motion to the north.

CTI 092053.7+280101



CTI FINDER CHART

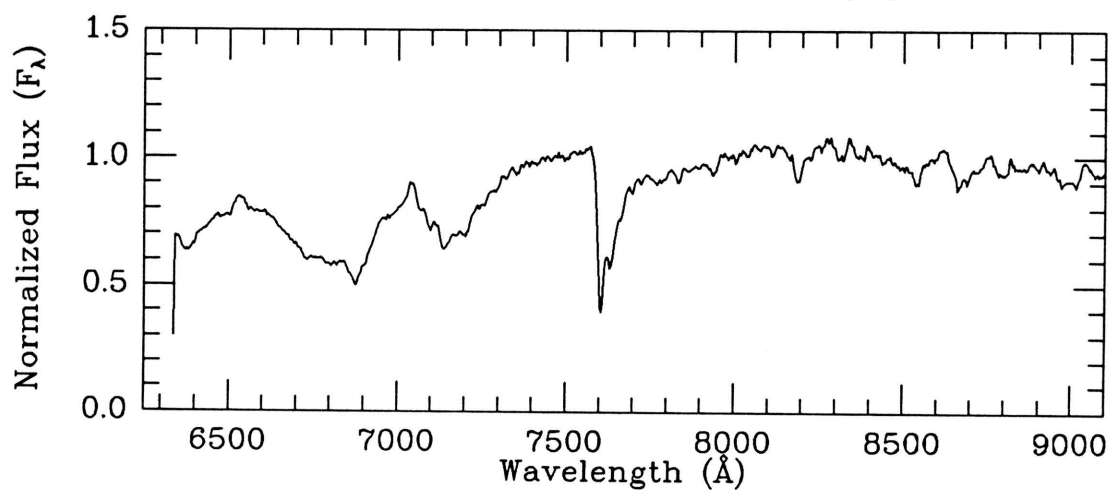
Clear filter

Obs. (UT) 1989 Apr 07

MMT SPECTRUM

Exposure: 600 sec

Obs. (UT) 1991 Mar 14

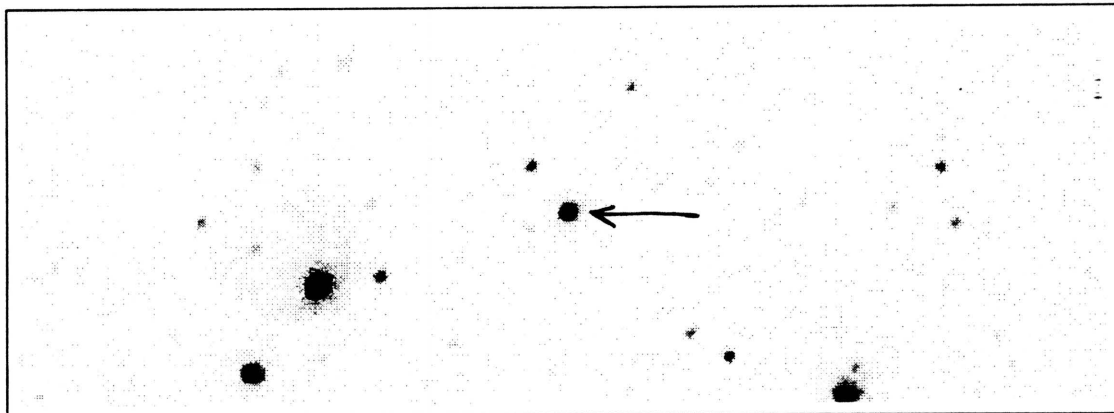
Coordinates: α (1950) = 09:18:41.2 δ (1950) = +28:10:36

Spectral Type: M1.5 V

Photometry: $I_{KC} = 13.60$ $R_{CTI} = 14.22$ $(V-I)_{KC} = 2.05 \pm 0.10$ $(R-I)_{CTI} = 0.51 \pm 0.01$ $(V-I)_{CTI} = 1.94 \pm 0.01$

Notes:

CTI 092423.0+280044



CTI FINDER CHART

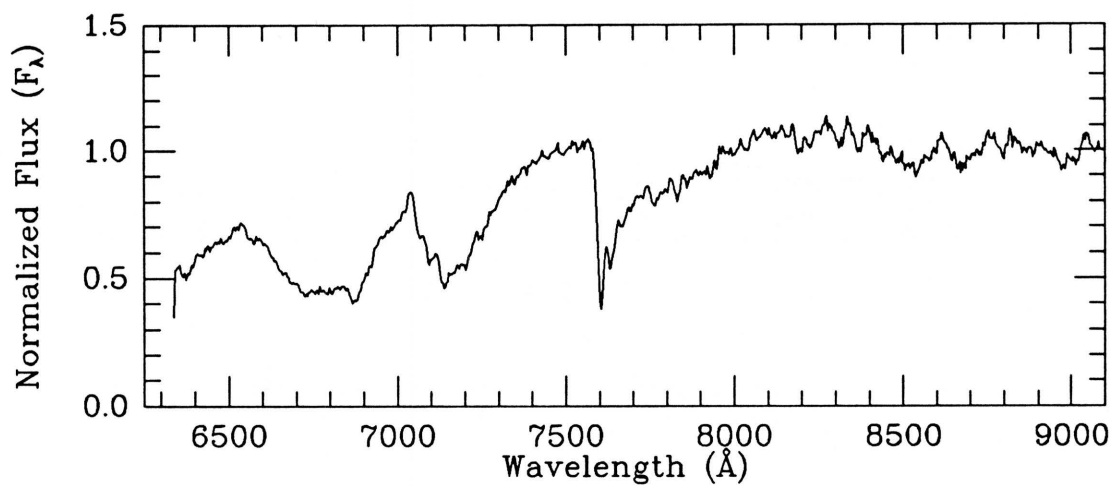
Clear filter

Obs. (UT) 1989 Apr 07

MMT SPECTRUM

Exposure: 1500 sec

Obs. (UT) 1991 Mar 14

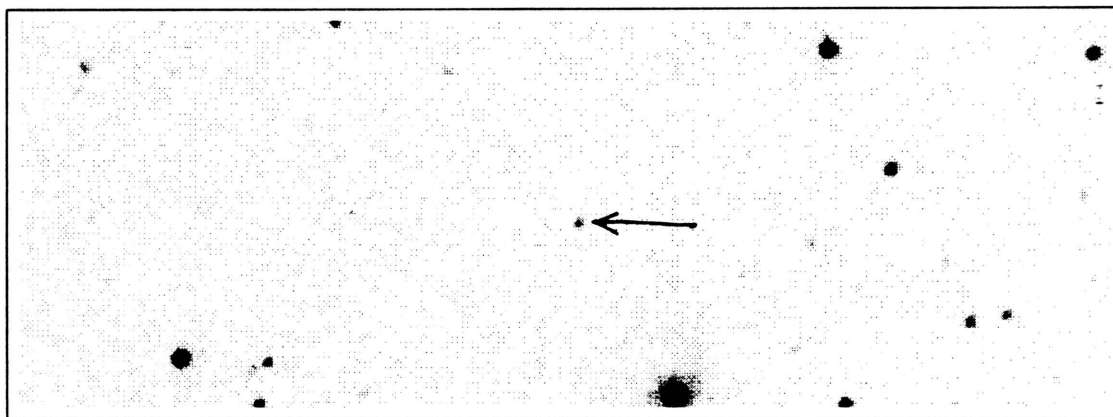
Coordinates: α (1950) = 09:22:10.8 δ (1950) = +28:10:27

Spectral Type: M3 V

Photometry: $I_{KC} = 13.93$ $R_{CTI} = 14.78$ $(V-I)_{KC} = 2.40 \pm 1.1$ $(R-I)_{CTI} = 0.75 \pm 0.1$ $(V-I)_{CTI} = 2.21 \pm 0.1$

Notes:

CTI 092539.9+280018



CTI FINDER CHART

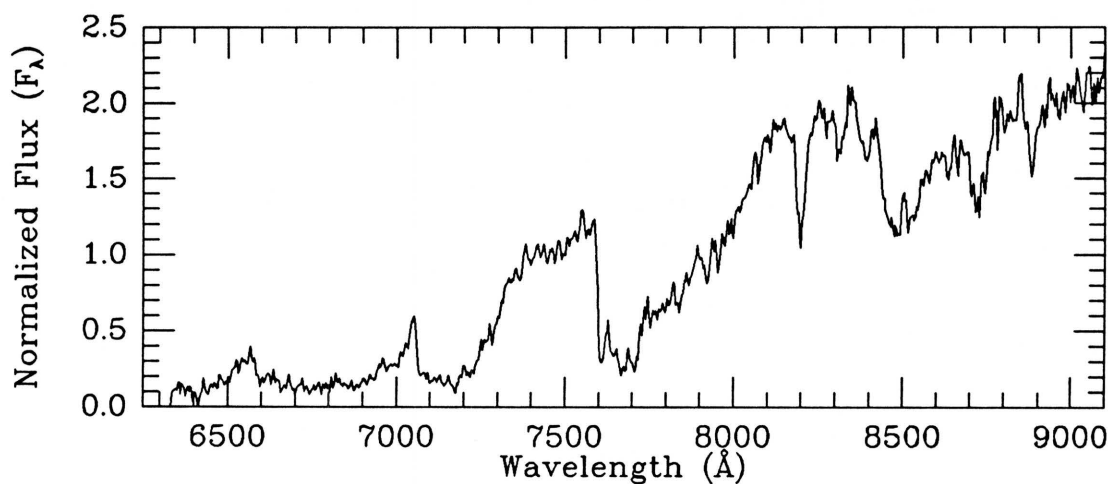
Clear filter

Obs. (UT) 1989 Apr 07

MMT SPECTRUM

Exposure: 2700 sec

Obs. (UT) 1990 Jan 20

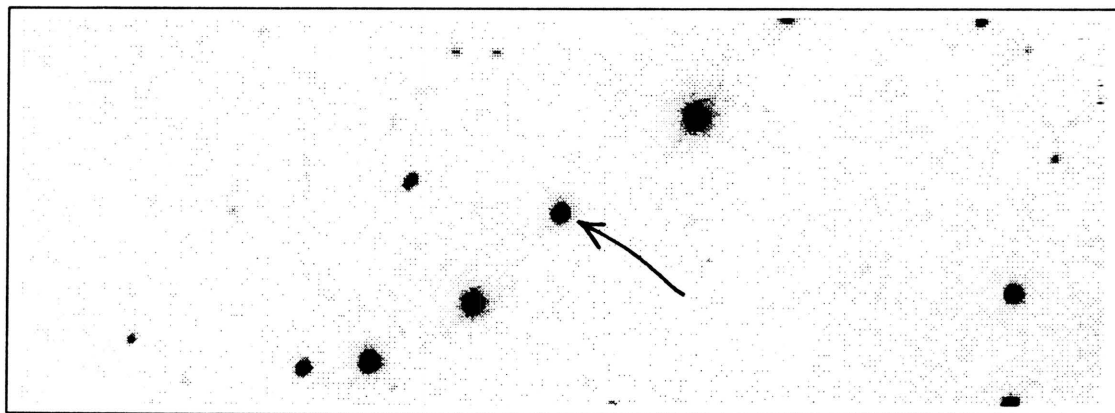
Coordinates: α (1950) = 09:23:27.8 δ (1950) = +28:10:03

Spectral Type: M6.5 V

Photometry: $I_{KC} = 17.47$ $R_{CTI} = 19.45$ $(V-I)_{KC} = 4.25 \pm .79$ $(R-I)_{CTI} = 2.05 \pm .54$ $(V-I)_{CTI} = \text{unknown}$

Notes: Object not found on POSS E plate, either because of large proper motion or because of faintness.

CTI 093631.3+280237



CTI FINDER CHART

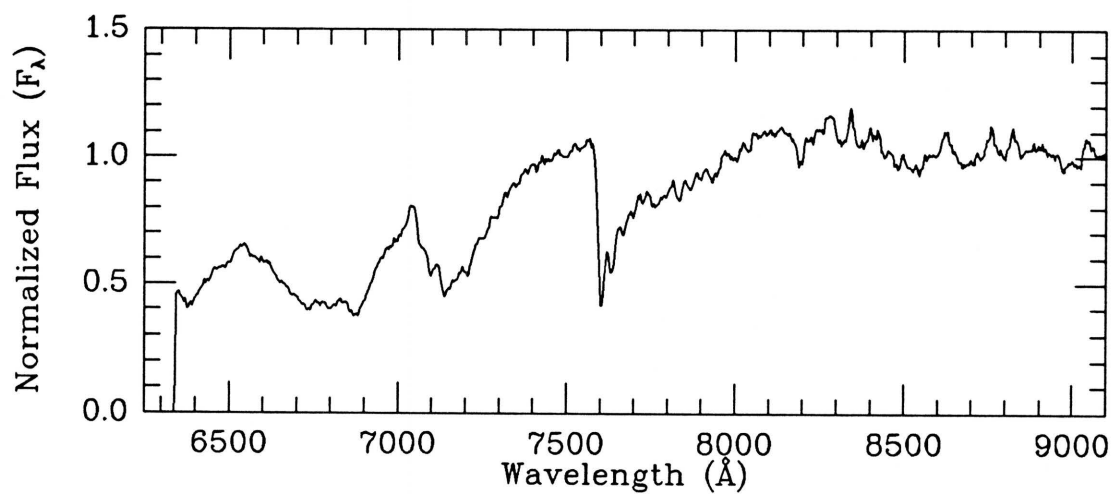
Clear filter

Obs. (UT) 1989 Apr 07

MMT SPECTRUM

Exposure: 600 sec

Obs. (UT) 1991 Mar 14

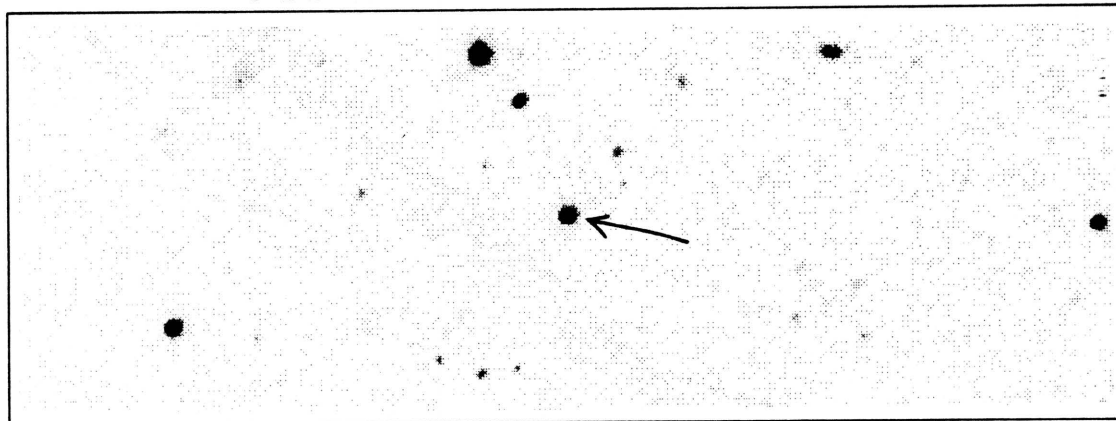
Coordinates: α (1950) = 09:34:20.2 δ (1950) = +28:12:44

Spectral Type: M3 V

Photometry: $I_{KC} = 13.53$ $R_{CTI} = 14.49$ $(V-I)_{KC} = 2.52 \pm 0.11$ $(R-I)_{CTI} = 0.84 \pm 0.01$ $(V-I)_{CTI} = 2.37 \pm 0.01$

Notes:

CTI 100219.5+280036



CTI FINDER CHART

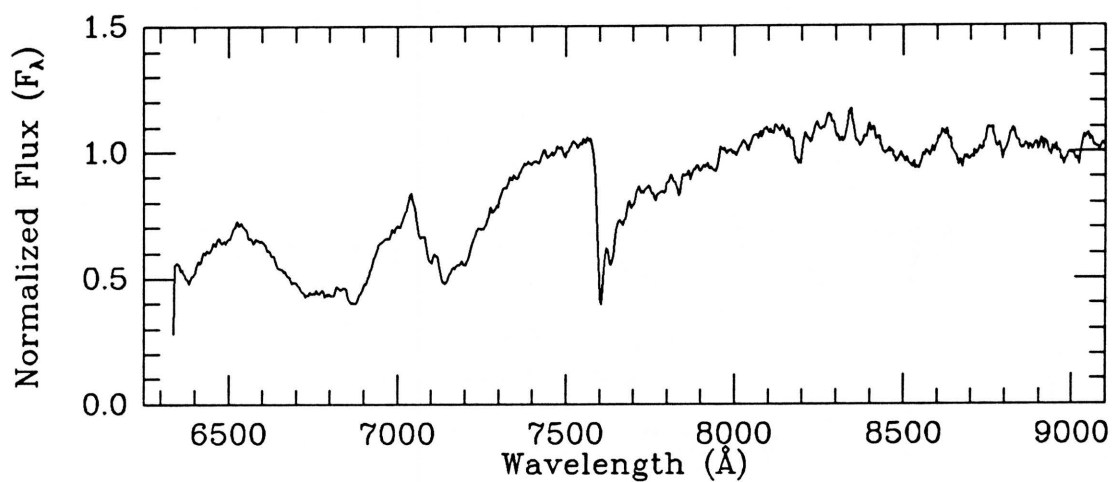
Clear filter

Obs. (UT) 1989 Apr 07

MMT SPECTRUM

Exposure: 600 sec

Obs. (UT) 1991 Mar 14

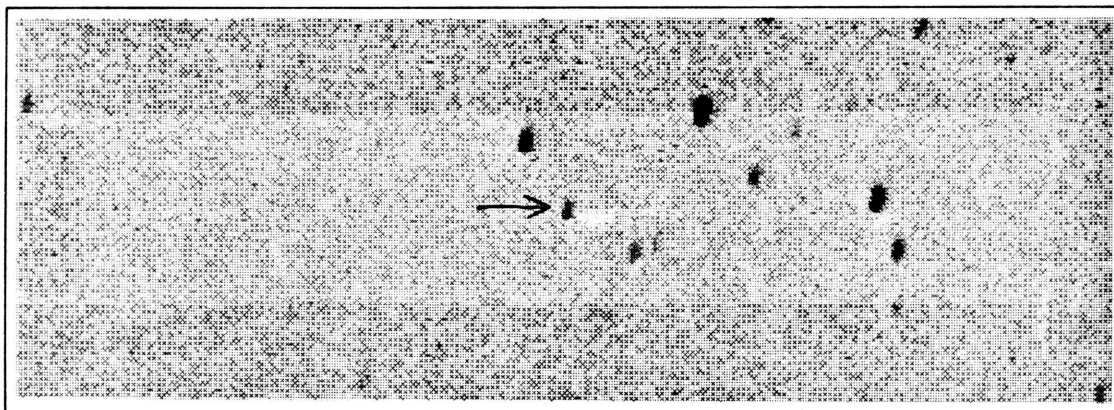
Coordinates: α (1950) = 10:00:11.0 δ (1950) = +28:11:29

Spectral Type: M3 V

Photometry: $I_{KC} = 14.04$ $R_{CTI} = 14.91$ $(V-I)_{KC} = 2.44 \pm 1.1$ $(R-I)_{CTI} = 0.78 \pm 0.01$ $(V-I)_{CTI} = 2.28 \pm 0.01$

Notes:

CTI 102840.0+280331



CTI FINDER CHART

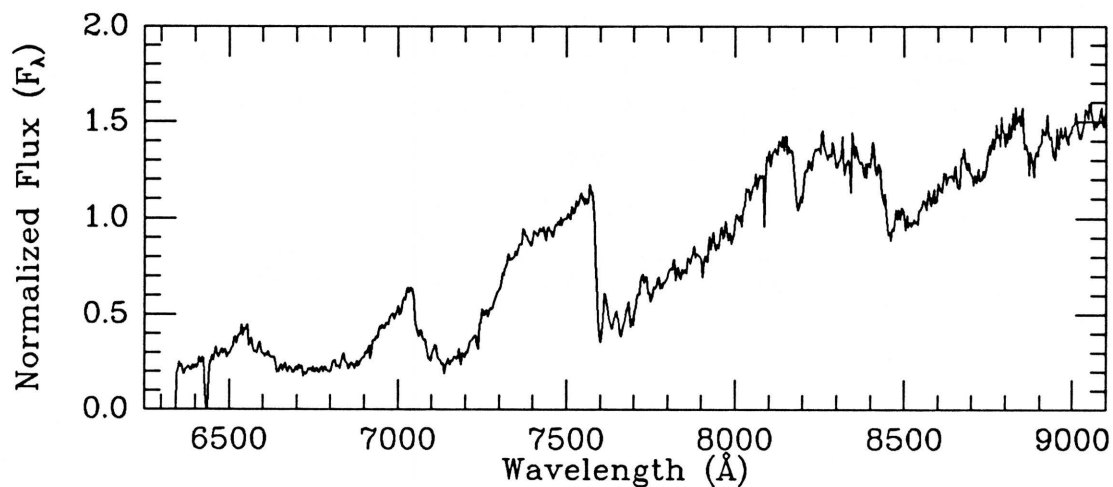
I filter

Obs. (UT) 1988 Mar 18

MMT SPECTRUM

Exposure: 2700 sec

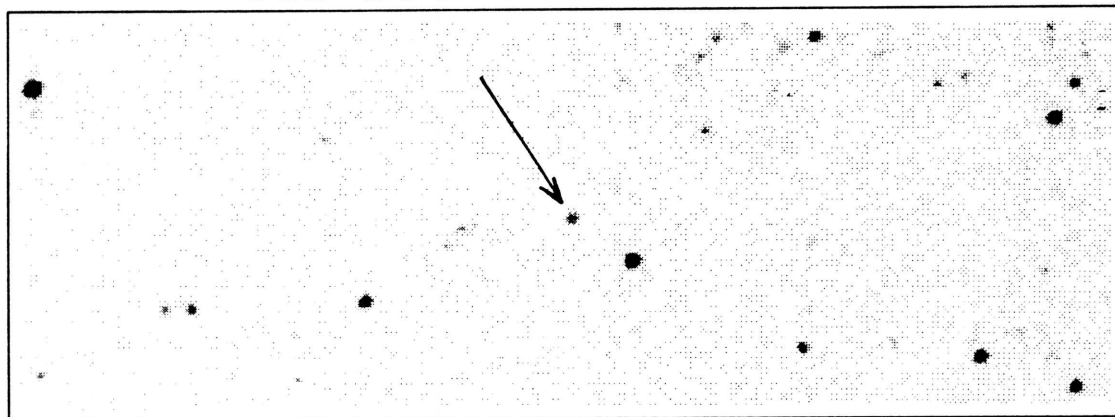
Obs. (UT) 1990 Jan 21

Coordinates: α (1950) = 10:26:34.2 δ (1950) = +28:15:03

Spectral Type: M5.5 V

Photometry: $I_{KC} = 17.03$ $R_{CTI} = 18.50$ $(V-I)_{KC} = 3.50 \pm 0.20$ $(R-I)_{CTI} = 1.52 \pm 0.11$ $(V-I)_{CTI} = 3.24 \pm 0.10$ Notes: Comparison to POSS E print suggests a proper motion of ~ 0.2 arcsec/yr to the west.

CTI 103000.3+280432



CTI FINDER CHART

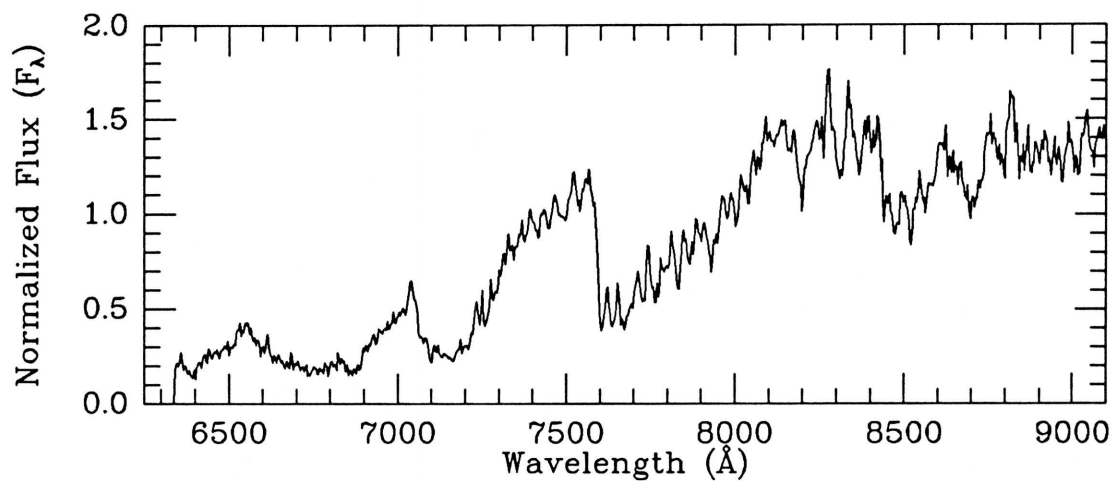
Clear filter

Obs. (UT) 1989 Apr 07

MMT SPECTRUM

Exposure: 3900 sec

Obs. (UT) 1991 Mar 14

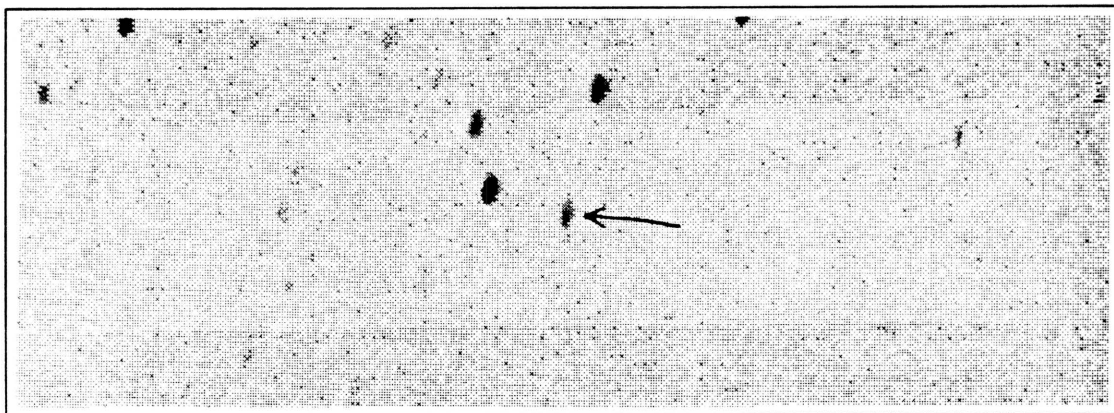
Coordinates: α (1950) = 10:27:54.6 δ (1950) = +28:16:05

Spectral Type: M5.5 V

Photometry: $I_{KC} = 17.14$ $R_{CTI} = 18.51$ $(V-I)_{KC} = 3.35 \pm 0.18$ $(R-I)_{CTI} = 1.42 \pm 0.09$ $(V-I)_{CTI} = 3.52 \pm 0.07$

Notes:

CTI 105201.6+280448



CTI FINDER CHART

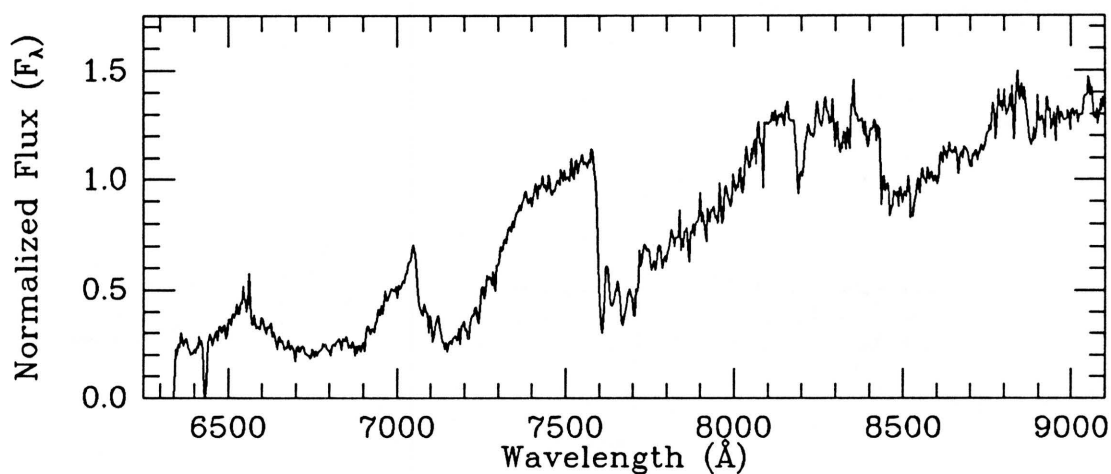
I filter

Obs. (UT) 1988 Mar 18

MMT SPECTRUM

Exposure: 3900 sec

Obs. (UT) 1990 Jan 21

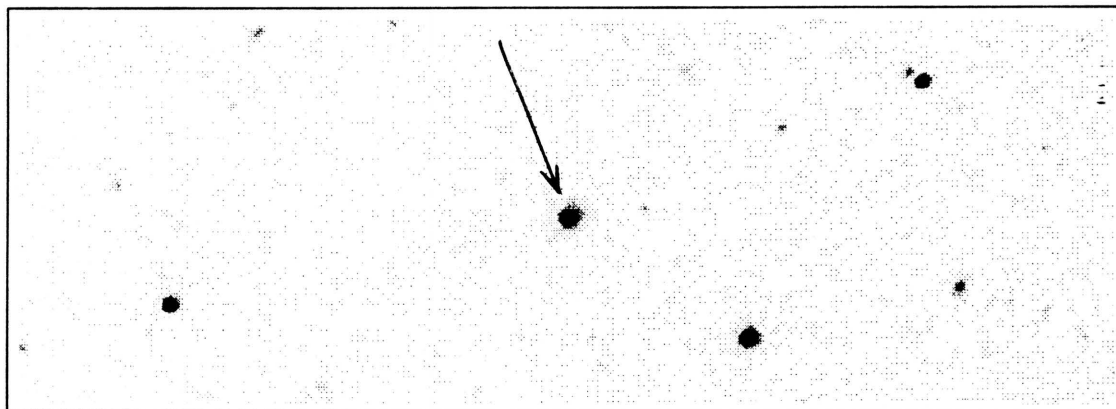
Coordinates: α (1950) = 10:49:58.4 δ (1950) = +28:16:46

Spectral Type: M5 V

Photometry: $I_{KC} = 16.96$ $R_{CTI} = 18.47$ $(V-I)_{KC} = 3.55 \pm .21$ $(R-I)_{CTI} = 1.56 \pm .11$ $(V-I)_{CTI} = 3.28 \pm .10$

Notes: On the POSS E print there are two objects near the position of the CTI star, neither of which appears on the POSS O print. A third epoch image is needed for μ determination.

CTI 105707.5+280223



CTI FINDER CHART

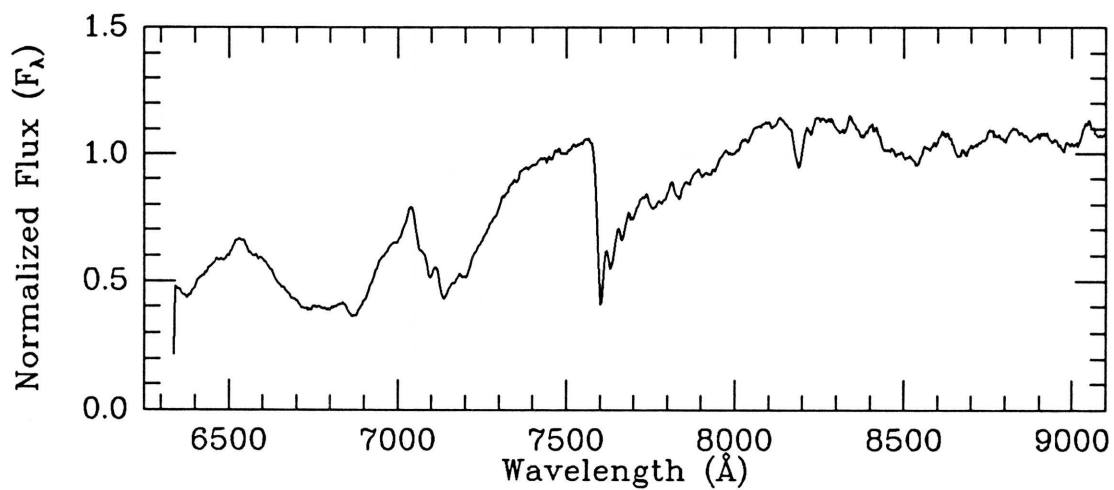
Clear filter

Obs. (UT) 1989 Apr 07

MMT SPECTRUM

Exposure: 600 sec

Obs. (UT) 1991 Mar 14

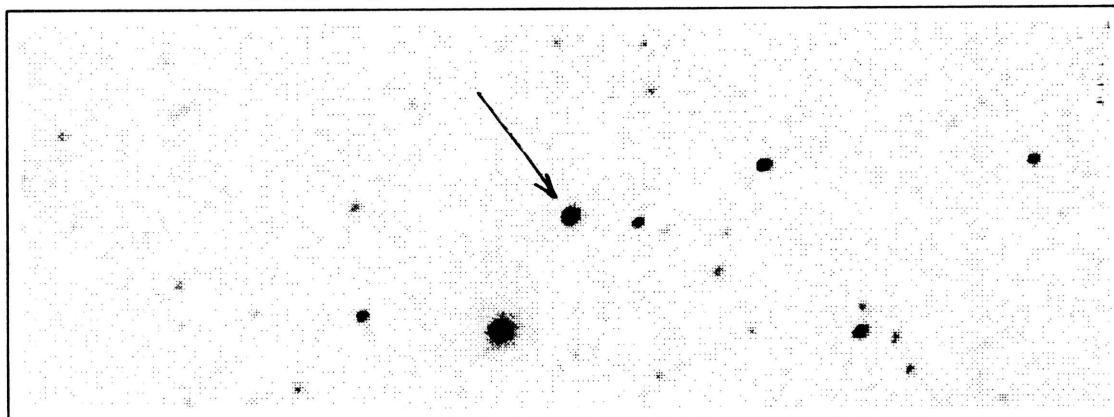
Coordinates: α (1950) = 10:55:04.8 δ (1950) = +28:14:26

Spectral Type: M3 V

Photometry: $I_{KC} = 13.16$ $R_{CTI} = 14.17$ $(V-I)_{KC} = 2.58 \pm 0.11$ $(R-I)_{CTI} = 0.88 \pm 0.01$ $(V-I)_{CTI} = 2.45 \pm 0.01$

Notes:

CTI 105802.4+280251



CTI FINDER CHART

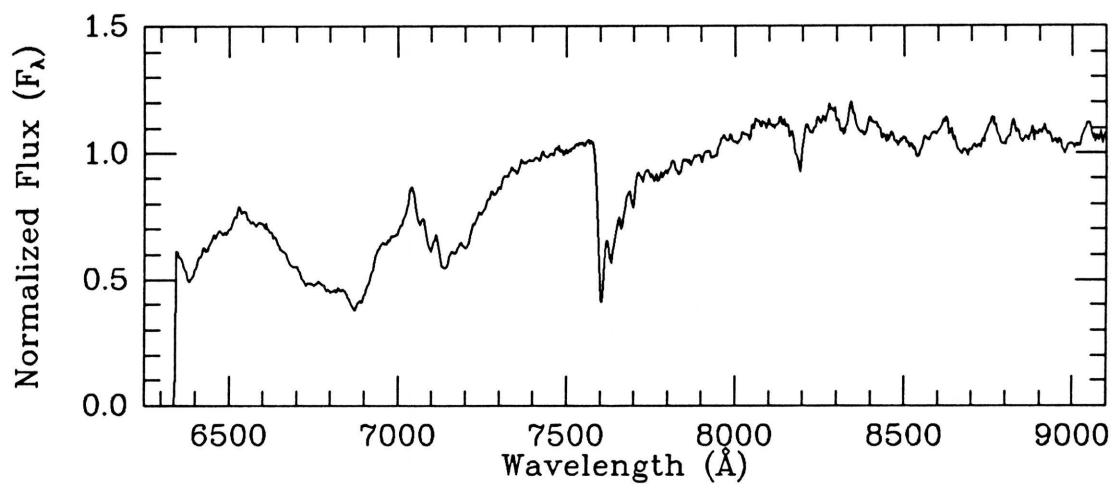
Clear filter

Obs. (UT) 1989 Apr 07

MMT SPECTRUM

Exposure: 600 sec

Obs. (UT) 1991 Mar 14

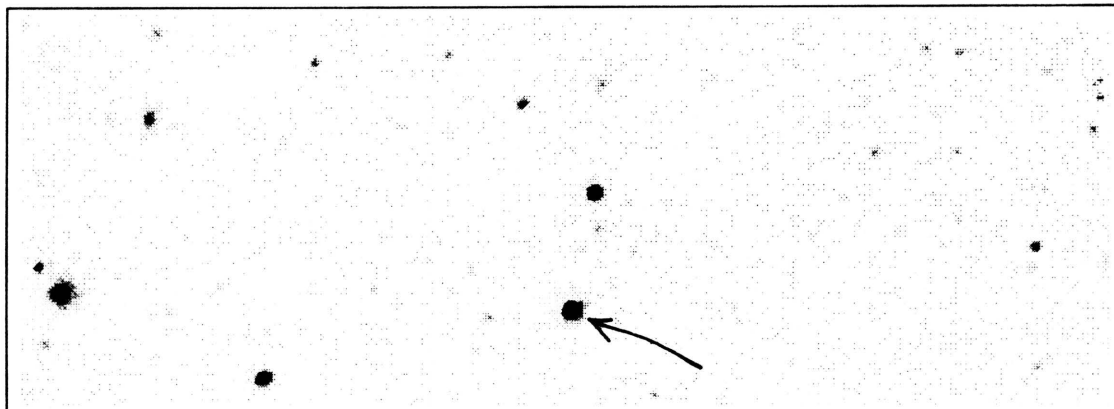
Coordinates: α (1950) = 10:55:59.8 δ (1950) = +28:14:54

Spectral Type: M2.5 V

Photometry: $I_{KC} = 13.84$ $R_{CTI} = 14.69$ $(V-I)_{KC} = 2.40 \pm .11$ $(R-I)_{CTI} = 0.75 \pm .01$ $(V-I)_{CTI} = 2.28 \pm .01$

Notes:

CTI 111035.6+275951



CTI FINDER CHART

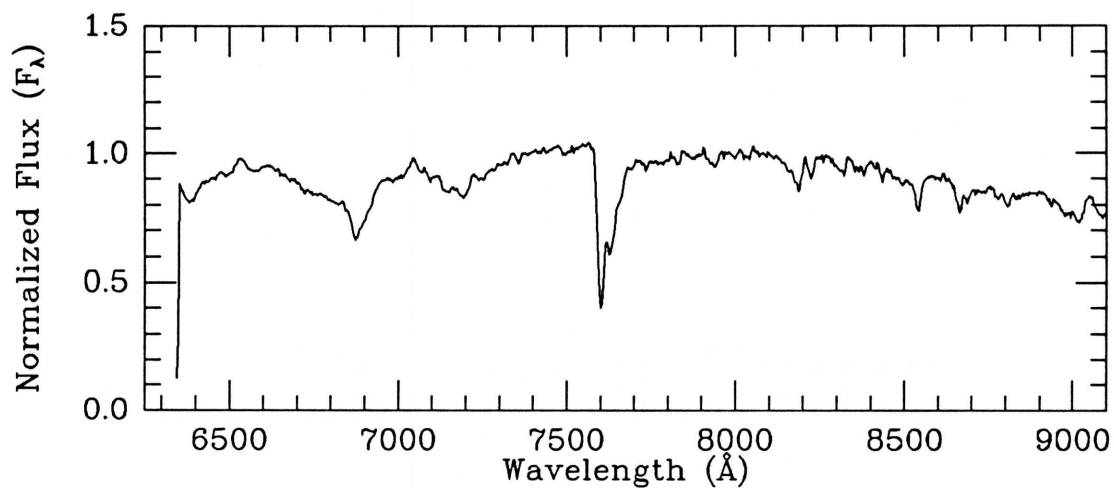
Clear filter

Obs. (UT) 1989 Apr 07

MMT SPECTRUM

Exposure: 900 sec

Obs. (UT) 1991 May 07

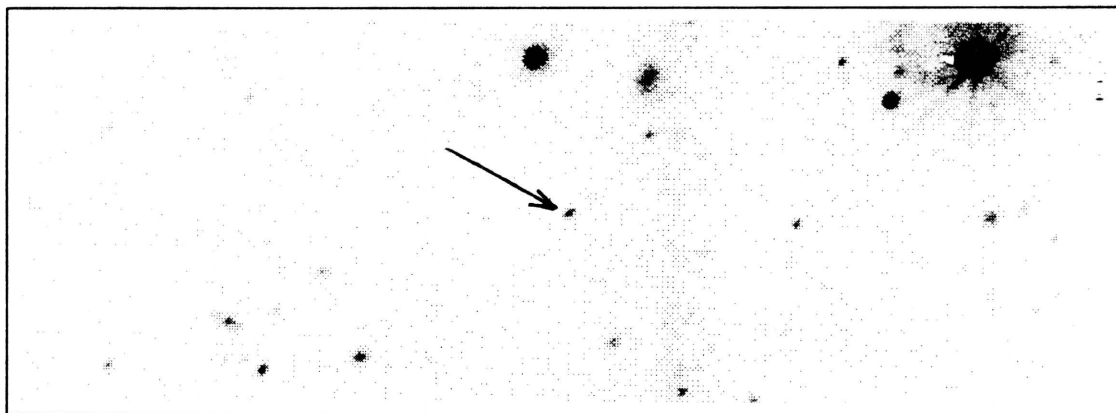
Coordinates: α (1950) = 11:08:34.5 δ (1950) = +28:12:05

Spectral Type: K7 V

Photometry: $I_{KC} = 13.93$ $R_{CTI} = 14.29$ $(V-I)_{KC} = 1.70 \pm 0.09$ $(R-I)_{CTI} = 0.26 \pm 0.01$ $(V-I)_{CTI} = 1.59 \pm 0.01$

Notes:

CTI 112443.6+280426



CTI FINDER CHART

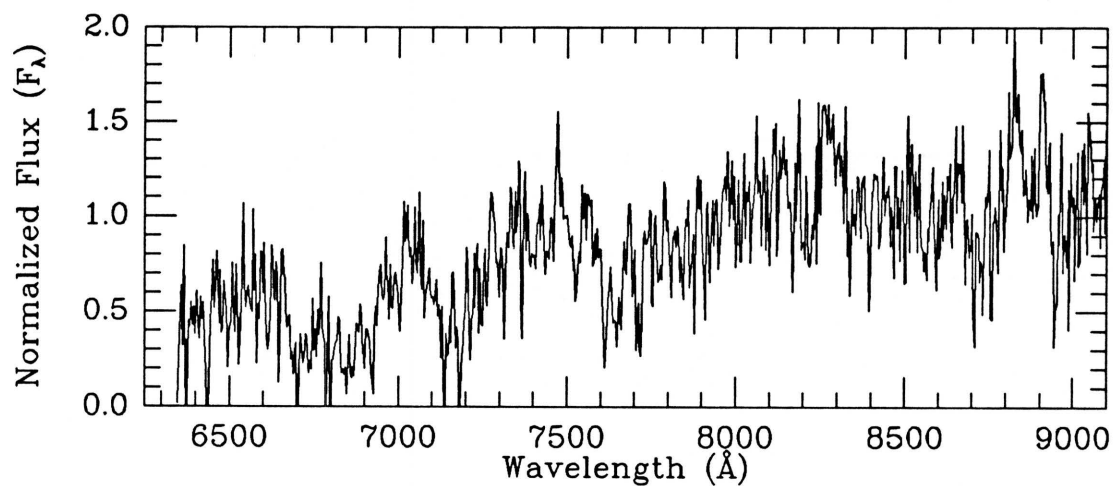
Clear filter

Obs. (UT) 1989 Apr 07

MMT SPECTRUM

Exposure: 1500 sec

Obs. (UT) 1990 May 04

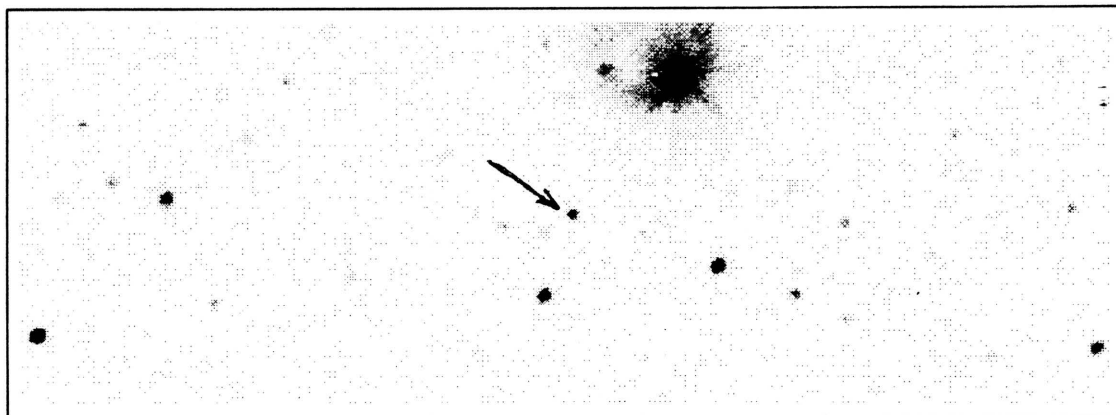
Coordinates: α (1950) = 11:22:44.1 δ (1950) = +28:16:48

Spectral Type: M3: V

Photometry: $I_{KC} = 17.24$ $R_{CTI} = 18.95$ $(V-I)_{KC} = 3.85 \pm 0.22$ $(R-I)_{CTI} = 1.77 \pm 0.12$ $(V-I)_{CTI} = 3.23 \pm 0.12$

Notes:

CTI 112750.0+280406



CTI FINDER CHART

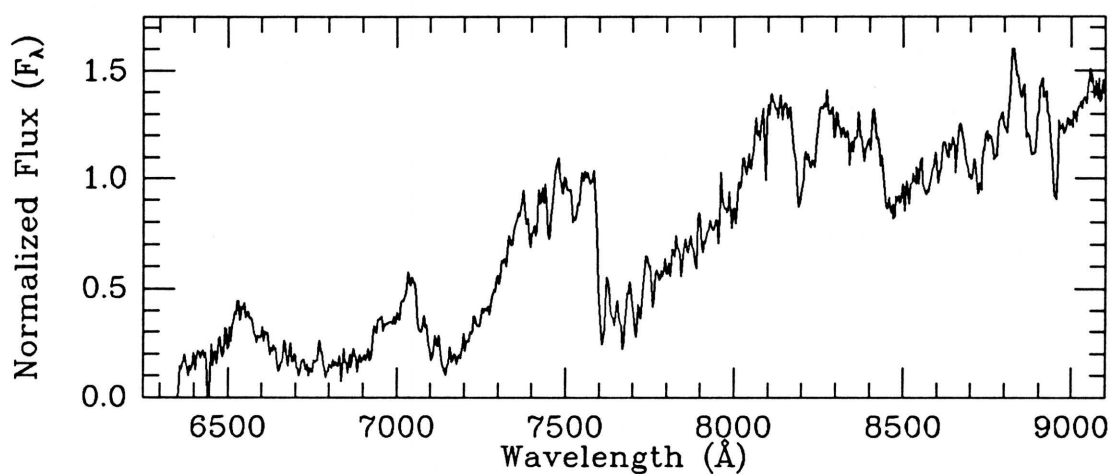
Clear filter

Obs. (UT) 1989 Apr 07

MMT SPECTRUM

Exposure: 3900 sec

Obs. (UT) 1990 May 04

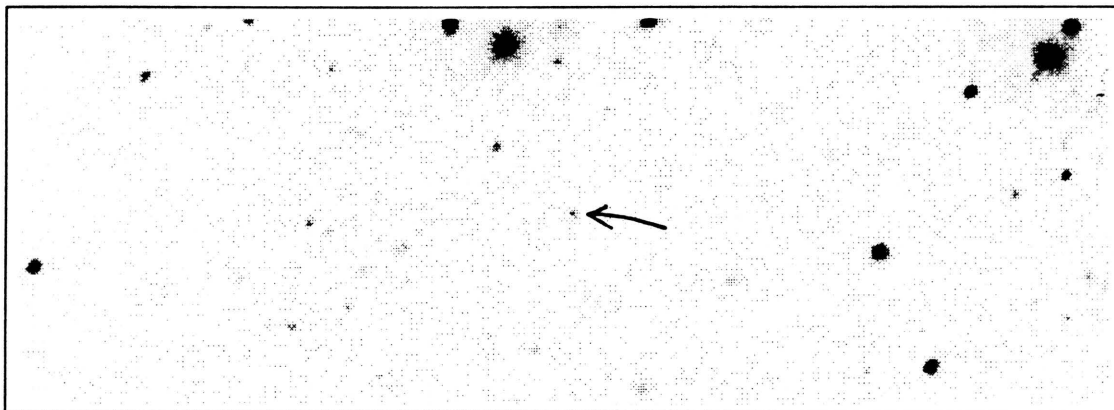
Coordinates: α (1950) = 11:25:50.8 δ (1950) = +28:16:30

Spectral Type: M5.5 V

Photometry: $I_{KC} = 16.91$ $R_{CTI} = 18.47$ $(V-I)_{KC} = 3.61 \pm .24$ $(R-I)_{CTI} = 1.60 \pm .14$ $(V-I)_{CTI} = 3.56 \pm .11$

Notes:

CTI 113104.5+280201



CTI FINDER CHART

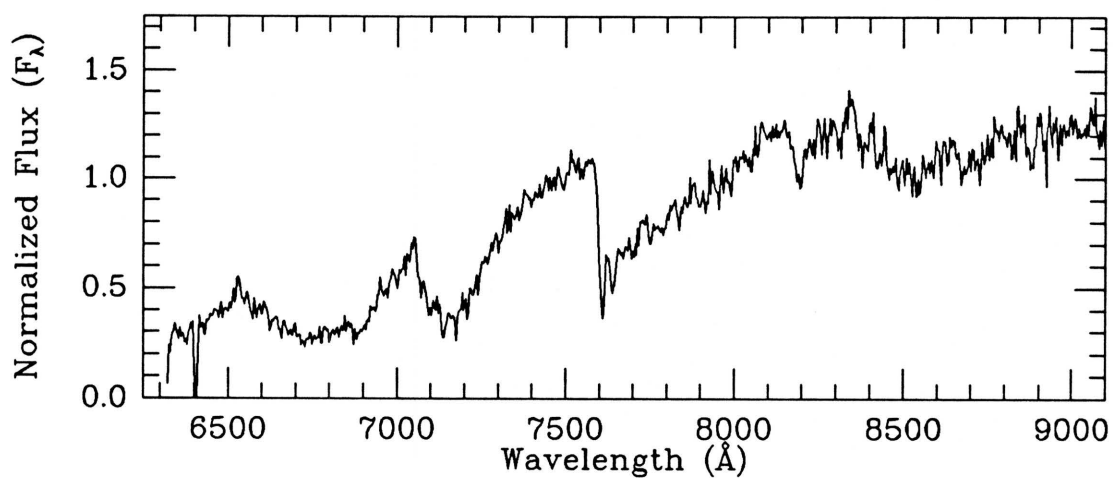
Clear filter

Obs. (UT) 1989 Apr 07

MMT SPECTRUM

Exposure: 2700 sec

Obs. (UT) 1990 Jan 20

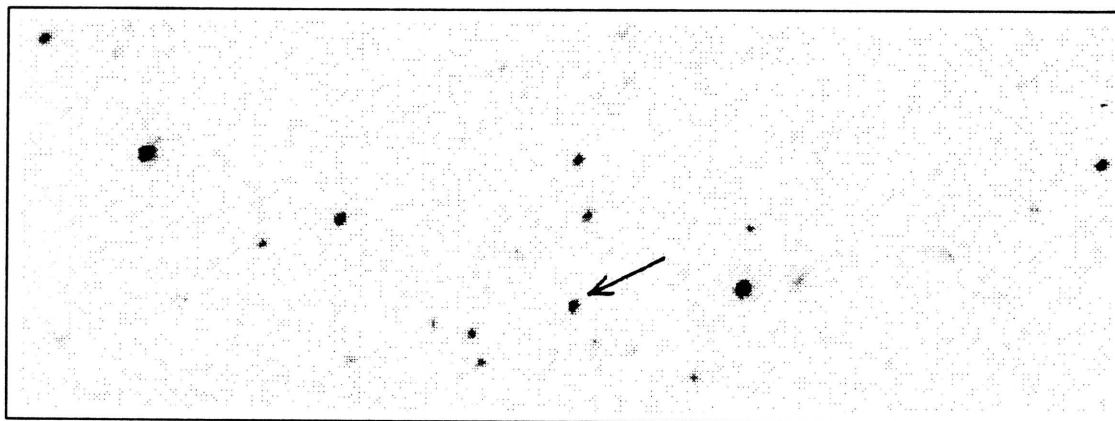
Coordinates: α (1950) = 11:29:05.7 δ (1950) = +28:14:26

Spectral Type: M4 V

Photometry: $I_{KC} = 17.99$ $R_{CTI} = 20.10$ $(V-I)_{KC} = 4.46 \pm .90$ $(R-I)_{CTI} = 2.20 \pm .62$ $(V-I)_{CTI} = 2.42 \pm .12$

Notes:

CTI 115638.5+280002



CTI FINDER CHART

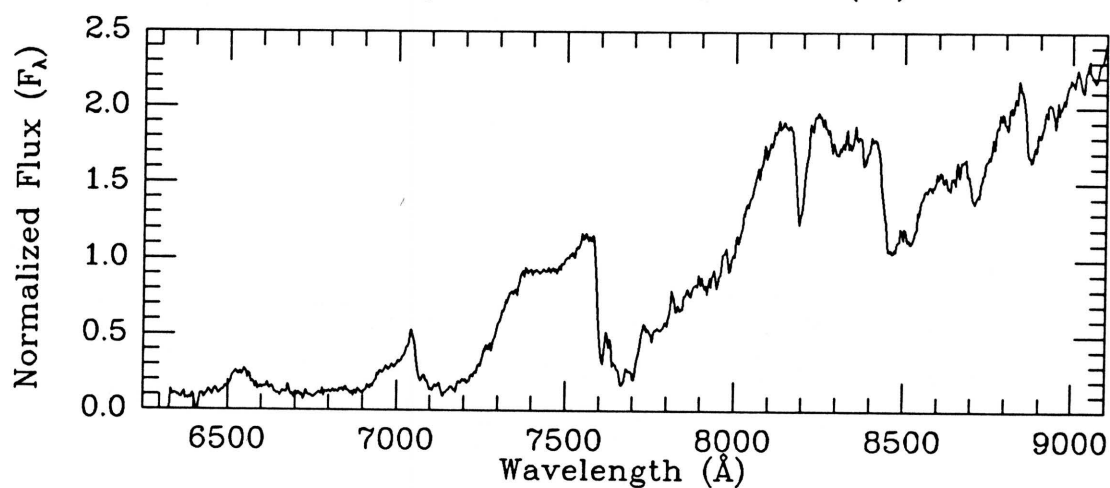
Clear filter

Obs. (UT) 1989 Apr 07

MMT SPECTRUM

Exposure: 2700 sec

Obs. (UT) 1990 Jan 20

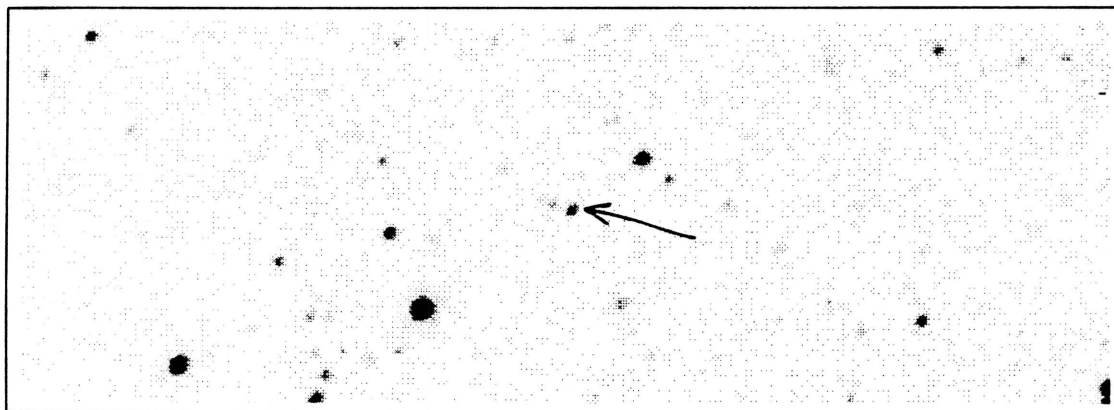
Coordinates: α (1950) = 11:54:42.7 δ (1950) = +28:12:34

Spectral Type: M7 V

Photometry: $I_{KC} = 16.74$ $R_{CTI} = 18.61$ $(V-I)_{KC} = 4.05 \pm .45$ $(R-I)_{CTI} = 1.91 \pm .30$ $(V-I)_{CTI} = 3.76 \pm .19$

Notes: This object is not found on the POSS E plate, probably because of a large proper motion, since the R magnitude is well above the plate limit.

CTI 120144.1+280527



CTI FINDER CHART

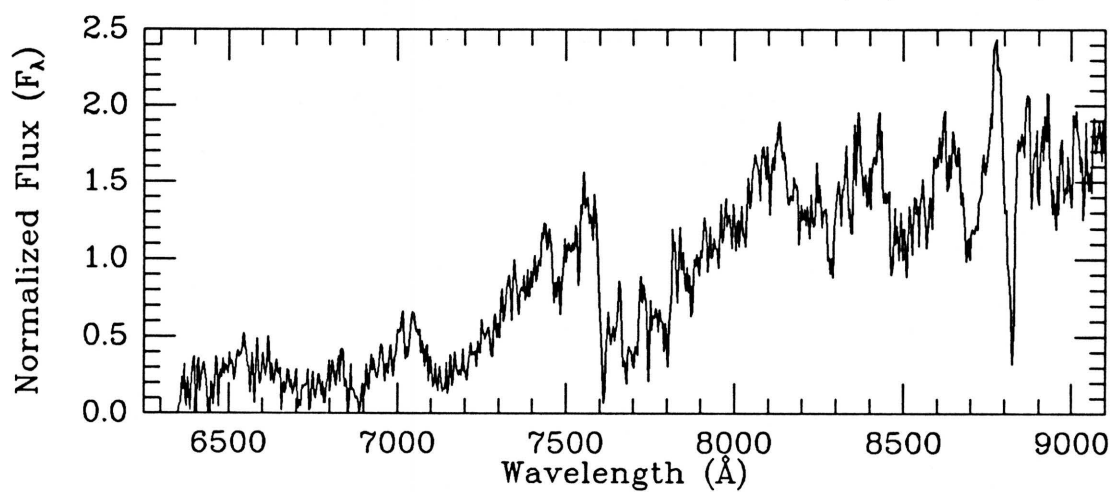
Clear filter

Obs. (UT) 1989 Apr 07

MMT SPECTRUM

Exposure: 3660 sec

Obs. (UT) 1990 May 04

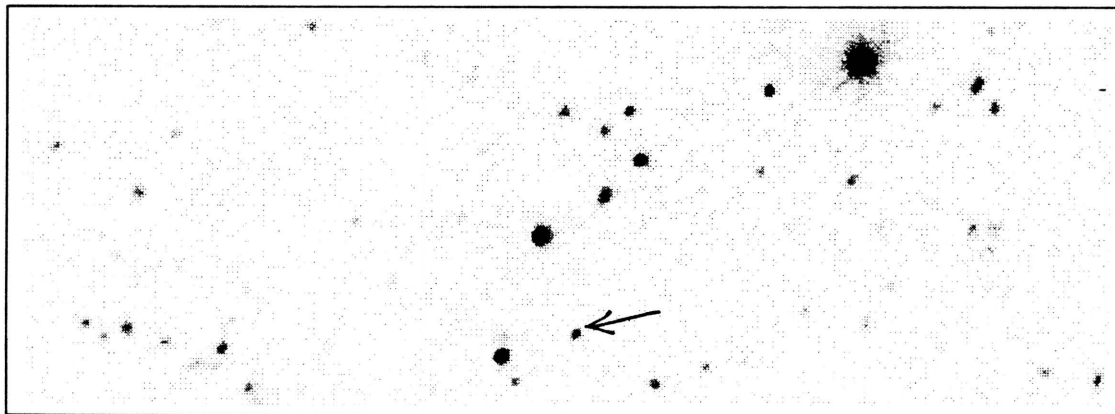
Coordinates: α (1950) = 11:59:48.9 δ (1950) = +28:17:59

Spectral Type: M6: V

Photometry: $I_{KC} = 16.80$ $R_{CTI} = 18.27$ $(V-I)_{KC} = 3.48 \pm 0.18$ $(R-I)_{CTI} = 1.51 \pm 0.09$ $(V-I)_{CTI} = 3.58 \pm 0.13$

Notes:

CTI 120237.0+275949



CTI FINDER CHART

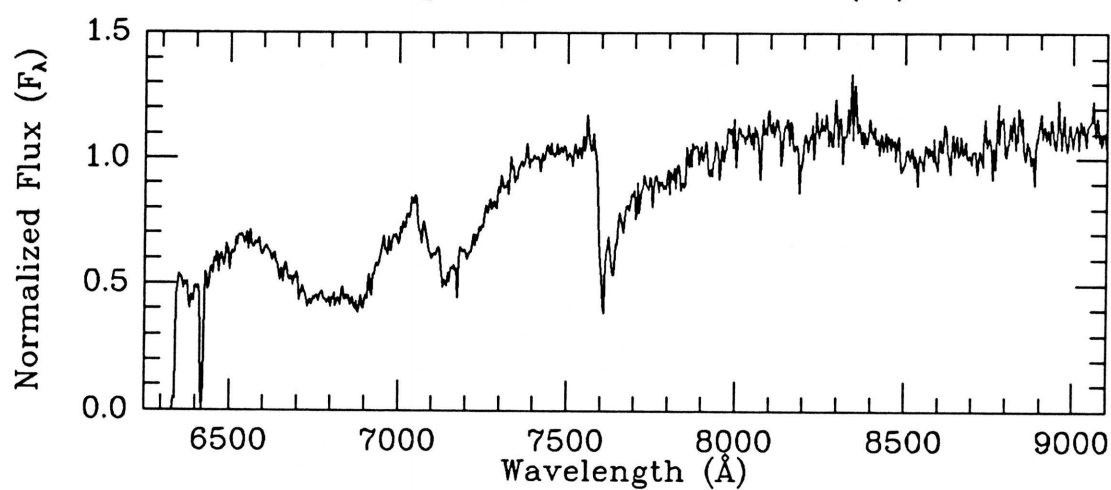
Clear filter

Obs. (UT) 1989 Apr 07

MMT SPECTRUM

Exposure: 2700 sec

Obs. (UT) 1990 Jan 20

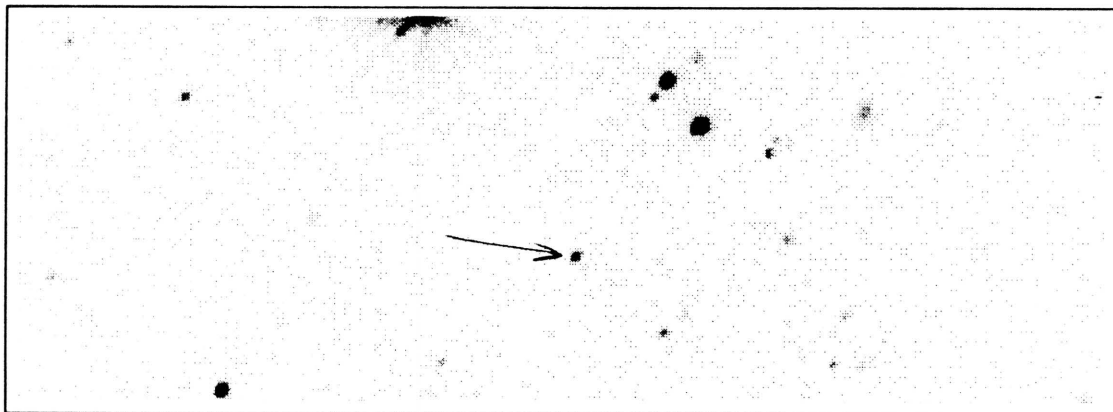
Coordinates: α (1950) = 12:00:41.9 δ (1950) = +28:12:21

Spectral Type: M2.5 V

Photometry: I_{KC} = unknown R_{CTI} = unknown $(V-I)_{KC}$ =unknown $(R-I)_{CTI}>1.94$: $(V-I)_{CTI}=2.76\pm.12$

Notes:

CTI 124450.0+280024



CTI FINDER CHART

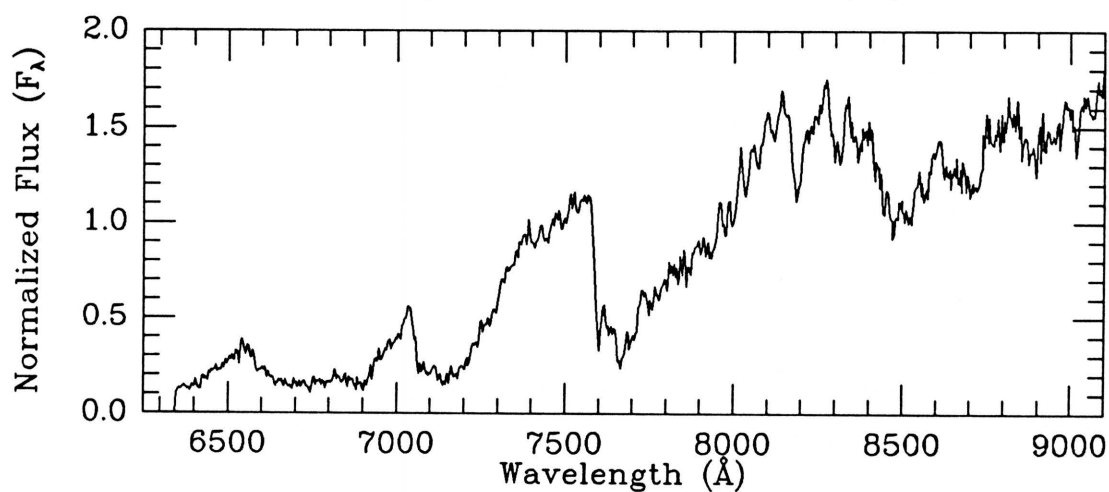
Clear filter

Obs. (UT) 1989 Apr 07

MMT SPECTRUM

Exposure: 3900 sec

Obs. (UT) 1991 Mar 14

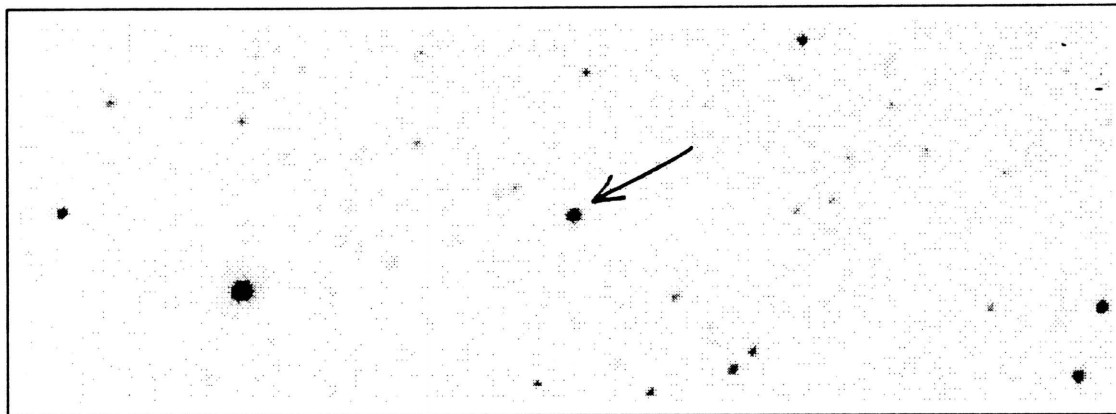
Coordinates: α (1950) = 12:42:59.8 δ (1950) = +28:12:42

Spectral Type: M5.5 V

Photometry: I_{KC} = unknown R_{CTI} = unknown $(V-I)_{\text{KC}}$ =unknown $(R-I)_{\text{CTI}}$ =unknown $(V-I)_{\text{CTI}}=4.10\pm1.00$

Notes:

CTI 124832.6+280502



CTI FINDER CHART

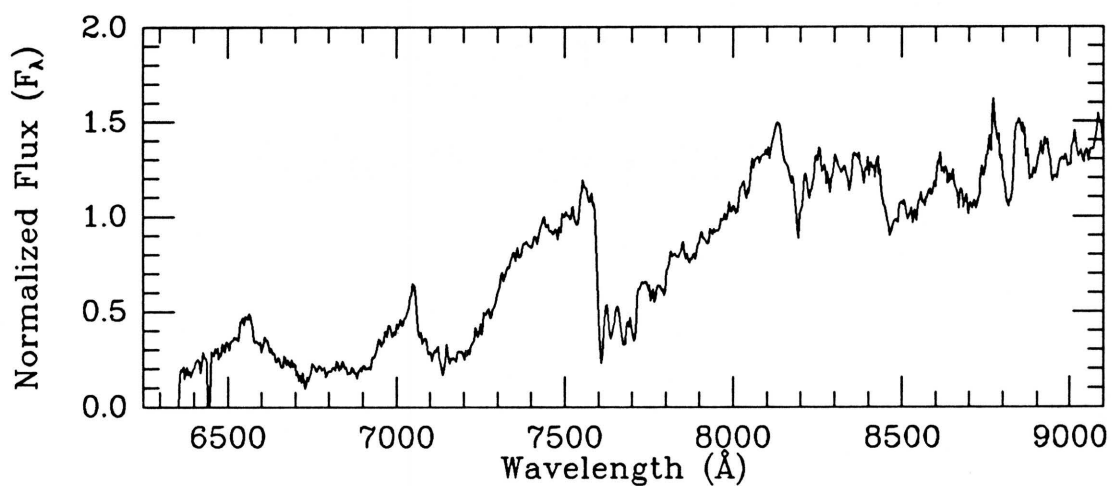
Clear filter

Obs. (UT) 1989 Apr 07

MMT SPECTRUM

Exposure: 2700 sec

Obs. (UT) 1990 May 04

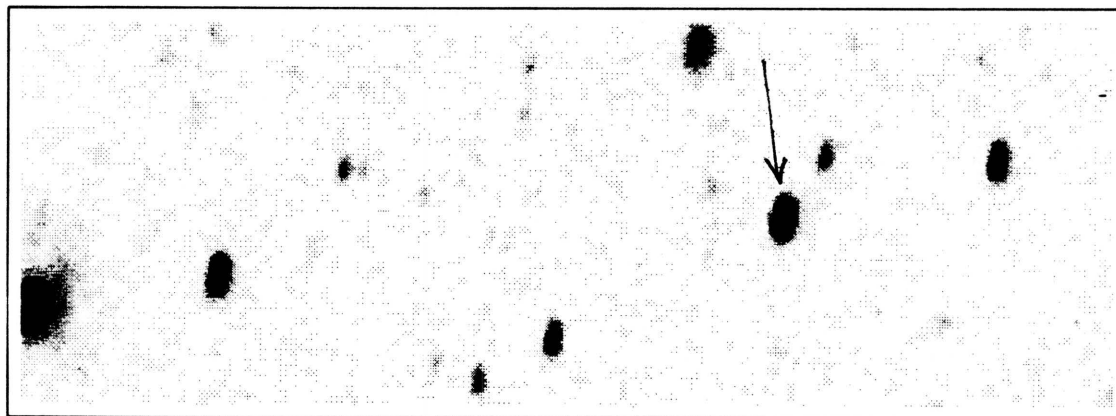
Coordinates: α (1950) = 12:46:42.9 δ (1950) = +28:17:18

Spectral Type: M5.5 V

Photometry: $I_{KC} = 15.36$ $R_{CTI} = 16.92$ $(V-I)_{KC} = 3.51 \pm 0.14$ $(R-I)_{CTI} = 1.53 \pm 0.03$ $(V-I)_{CTI} = 3.50 \pm 0.03$

Notes:

CTI 131541.4+280227



CTI FINDER CHART

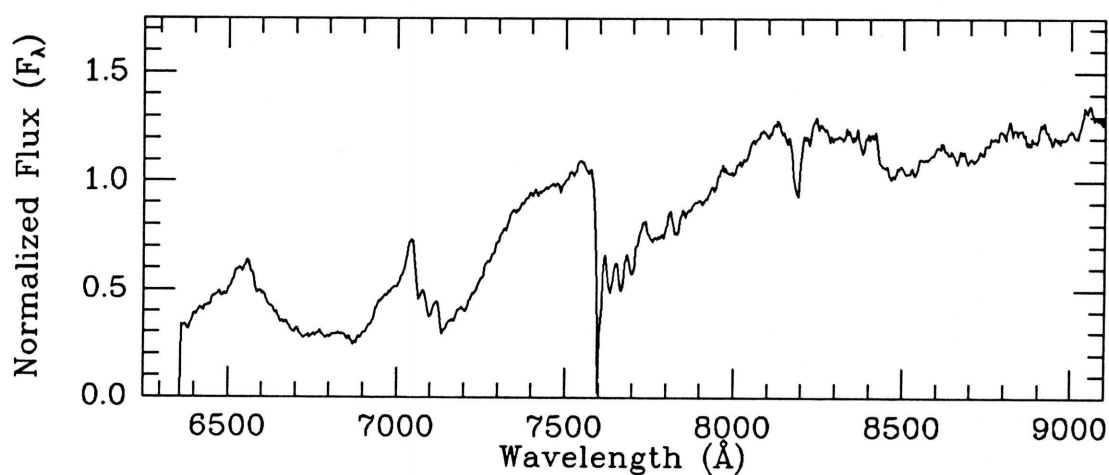
I filter

Coadded frame

MMT SPECTRUM

Exposure: 600 sec

Obs. (UT) 1991 Jun 22

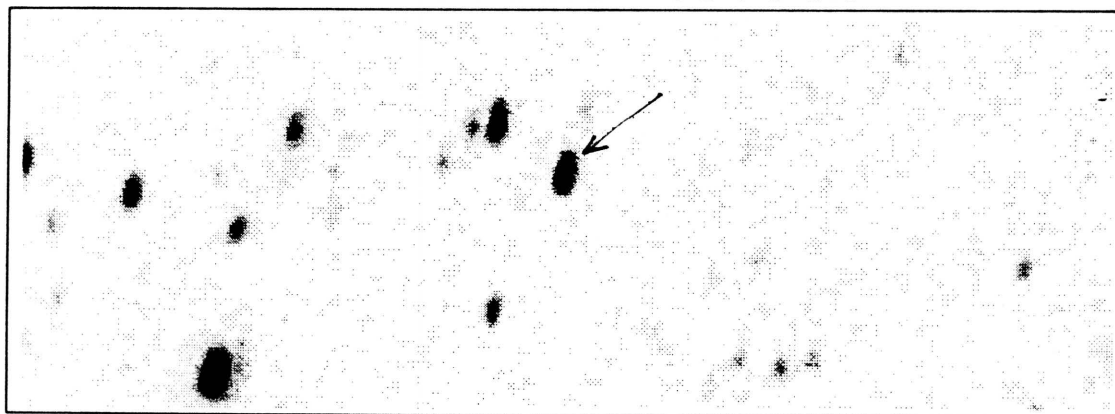
Coordinates: α (1950) = 13:13:54.7 δ (1950) = +28:14:19

Spectral Type: M4 V

Photometry: $I_{KC} = 14.10$ $R_{CTI} = 15.35$ $(V-I)_{KC} = 2.98 \pm 0.04$ $(R-I)_{CTI} = 1.21 \pm 0.01$ $(V-I)_{CTI} = 2.93 \pm 0.01$

Notes: Actual USNO VI photometry.

CTI 131631.5+280542



CTI FINDER CHART

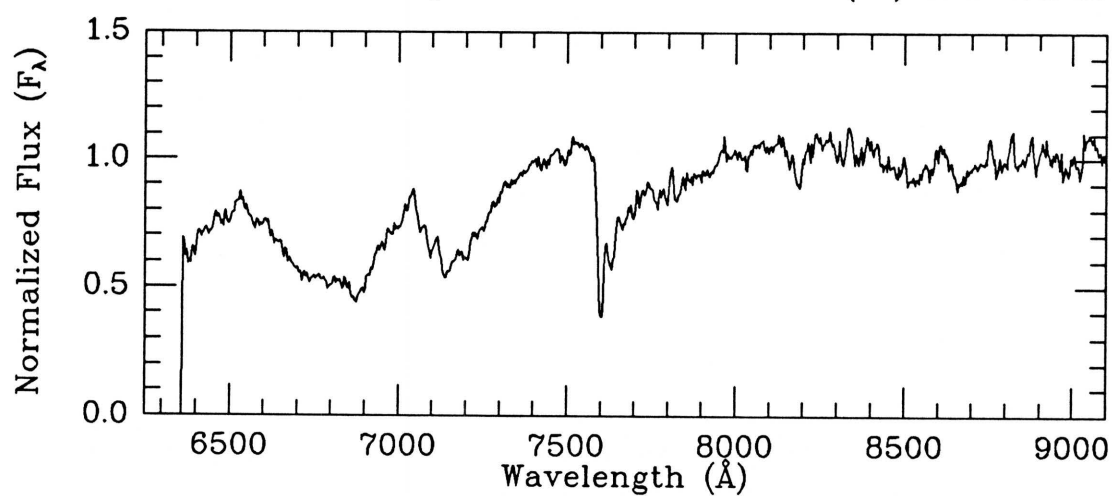
I filter

Coadded frame

MMT SPECTRUM

Exposure: 600 sec

Obs. (UT) 1991 Jun 22

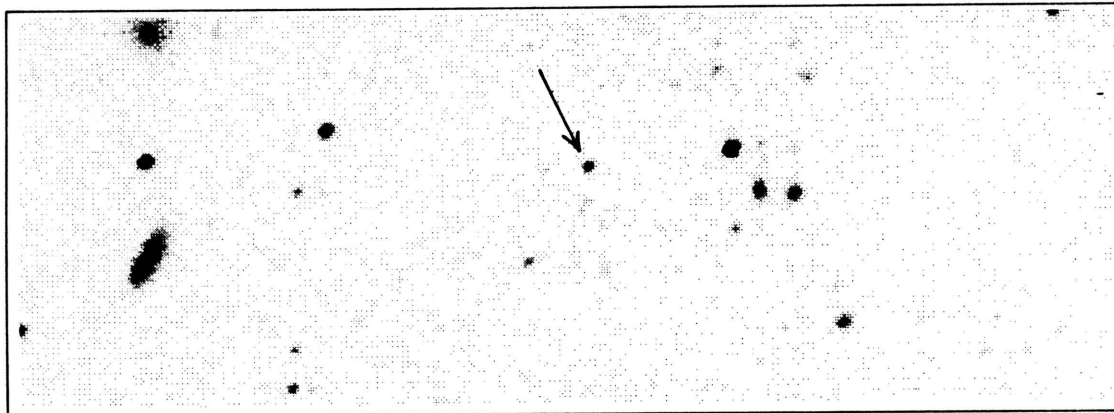
Coordinates: α (1950) = 13:14:44.9 δ (1950) = +28:17:33

Spectral Type: M2 V

Photometry: $I_{KC} = 15.27$ $R_{CTI} = 15.92$ $(V-I)_{KC} = 2.21 \pm 1.1$ $(R-I)_{CTI} = 0.62 \pm 0.03$ $(V-I)_{CTI} = \text{unknown}$

Notes:

CTI 133827.9+280633



CTI FINDER CHART

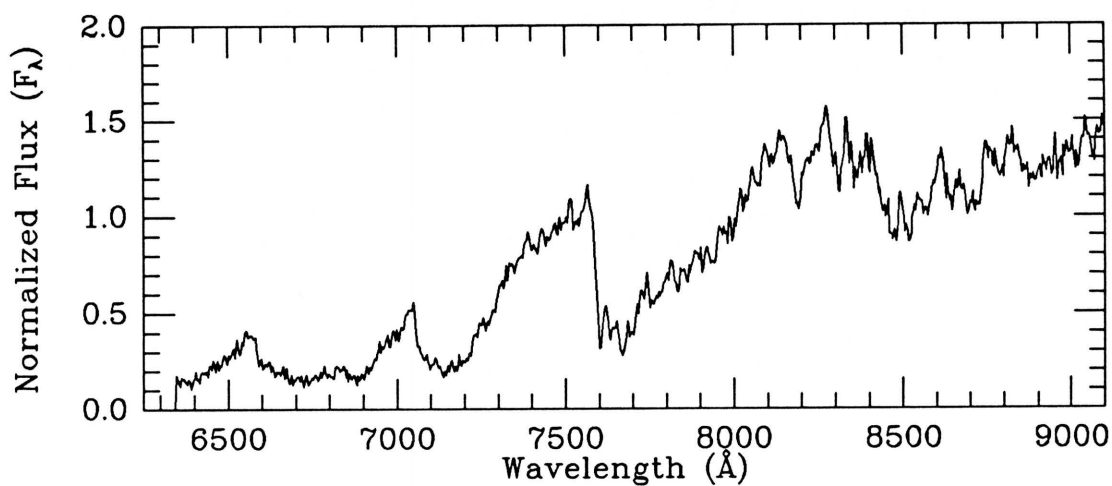
Clear filter

Obs. (UT) 1989 Apr 07

MMT SPECTRUM

Exposure: 2700 sec

Obs. (UT) 1991 Mar 14

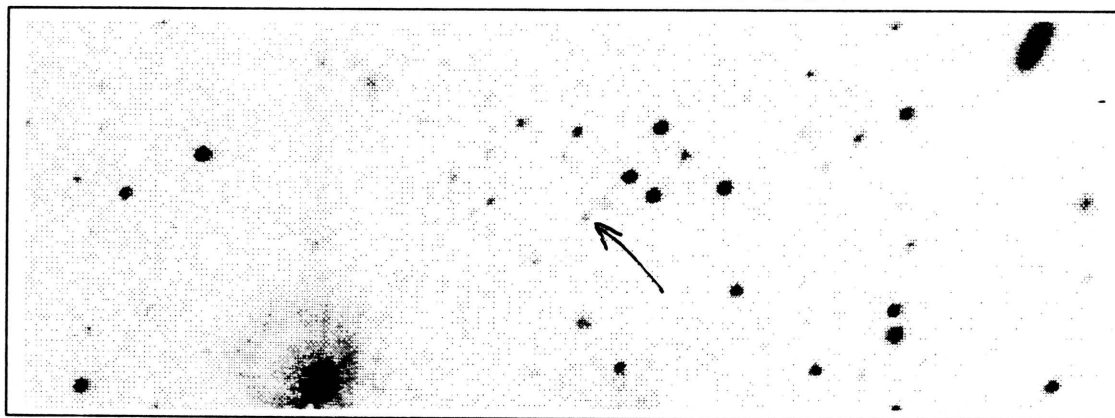
Coordinates: α (1950) = 13:36:43.7 δ (1950) = +28:17:58

Spectral Type: M5.5 V

Photometry: $I_{KC} = 17.21$ $R_{CTI} = 18.96$ $(V-I)_{KC} = 3.91 \pm 0.63$ $(R-I)_{CTI} = 1.81 \pm 0.43$ $(V-I)_{CTI} = 3.23 \pm 0.40$

Notes:

CTI 133857.8+280437



CTI FINDER CHART

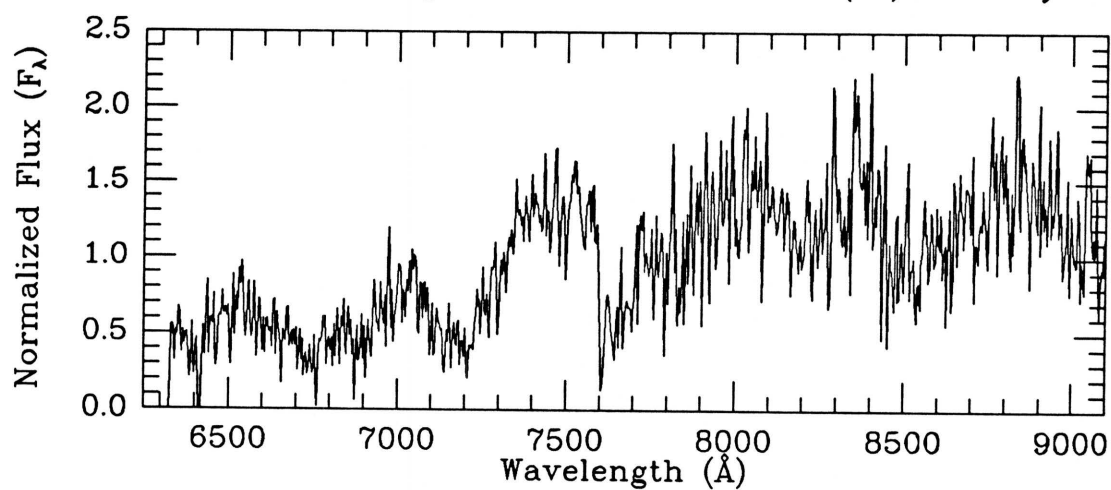
Clear filter

Ob. (UT) 1989 Apr 07

MMT SPECTRUM

Exposure: 1500 sec

Obs. (UT) 1990 May 23

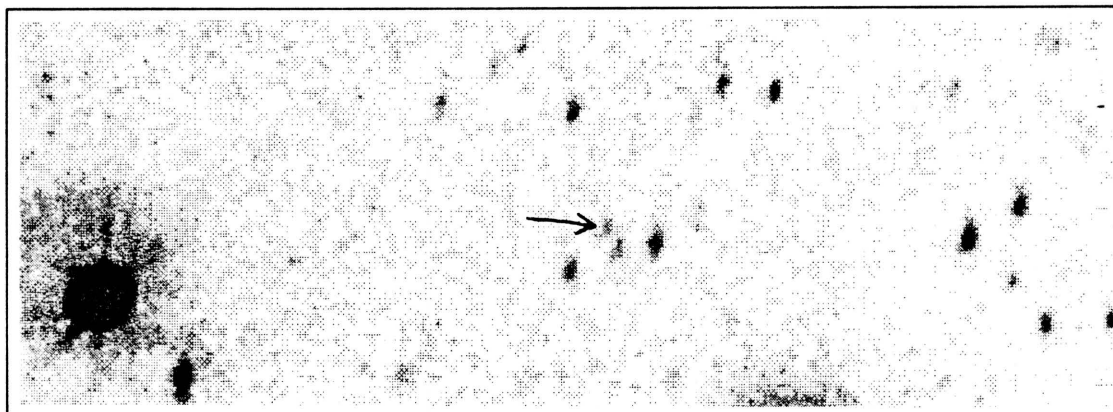
Coordinates: α (1950) = 13:37:13.7 δ (1950) = +28:16:01

Spectral Type: M3.5:V

Photometry: $I_{KC} = 18.41$ $R_{CTI} = 20.32$ $(V-I)_{KC} = 4.21 \pm 1.41$ $(R-I)_{CTI} = 2.02 \pm .98$ $(V-I)_{CTI} = \text{unknown}$

Notes:

CTI 134402.9+280522



CTI FINDER CHART

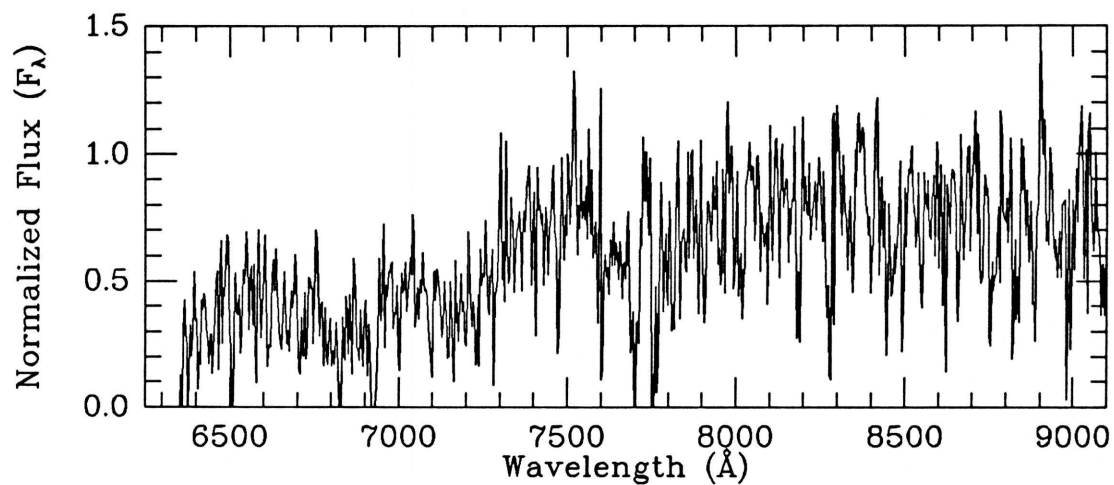
I filter

Coadded frame

MMT SPECTRUM

Exposure: 3900 sec

Obs. (UT) 1991 Jun 24

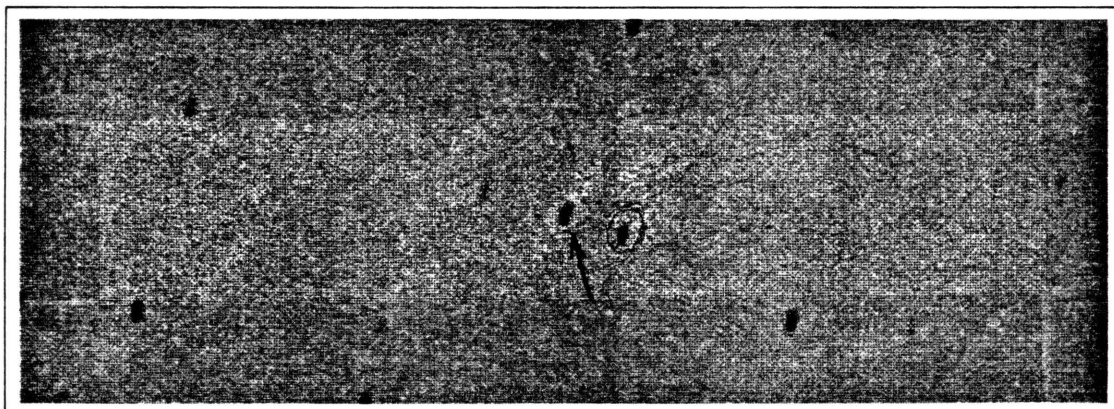
Coordinates: α (1950) = 13:42:19.3 δ (1950) = +28:16:39

Spectral Type: M3: V

Photometry: $I_{KC} = 19.31$ $R_{CTI} = 21.2$ $(V-I)_{KC} = 4.25 \pm 1.45$ $(R-I)_{CTI} = 2.05 \pm 1.01$ $(V-I)_{CTI} = \text{unknown}$

Notes:

CTI 135347.7+280418



CTI FINDER CHART

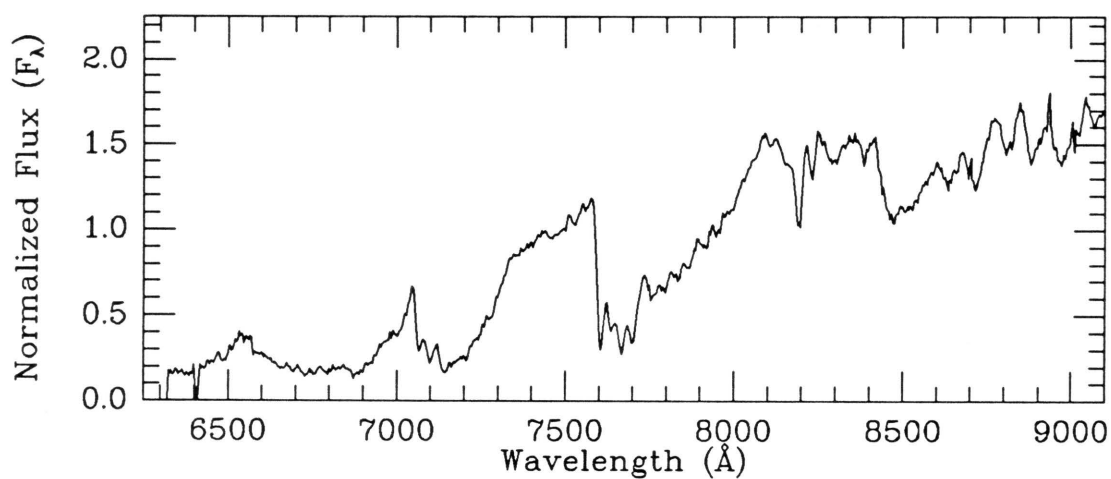
I filter

Obs. (UT) 1988 Mar 18

MMT SPECTRUM

Exposure: 3900 sec

Obs. (UT) 1989 Jul 13

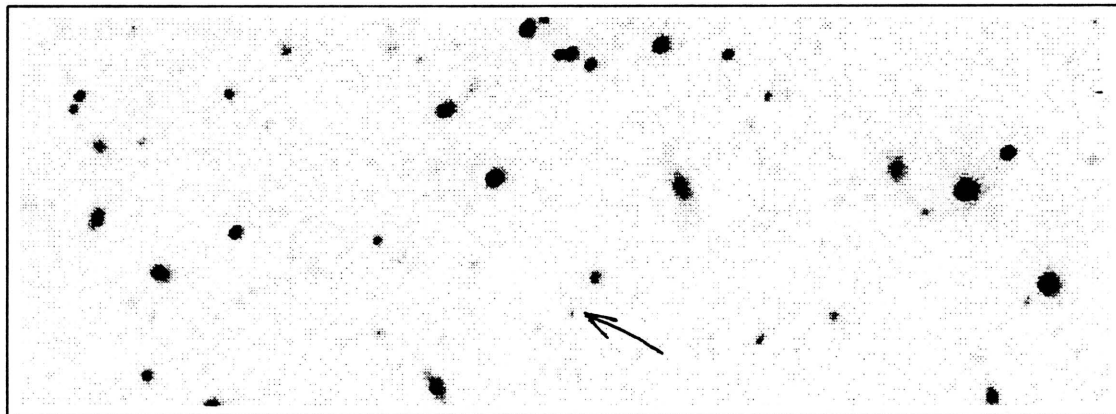
Coordinates: α (1950) = 13:52:05.1 δ (1950) = +28:15:20

Spectral Type: M6 V

Photometry: $I_{KC} = 15.76$ $R_{CTI} = 17.35$ $(V-I)_{KC} = 3.69 \pm 0.05$ $(R-I)_{CTI} = 1.60 \pm 0.06$ $(V-I)_{CTI} = 3.47 \pm 0.06$

Notes: Actual USNO VI photometry. Comparison to POSS E print suggests proper motion of ~ 0.2 arcsec/yr to the north.

CTI 135752.7+275958



CTI FINDER CHART

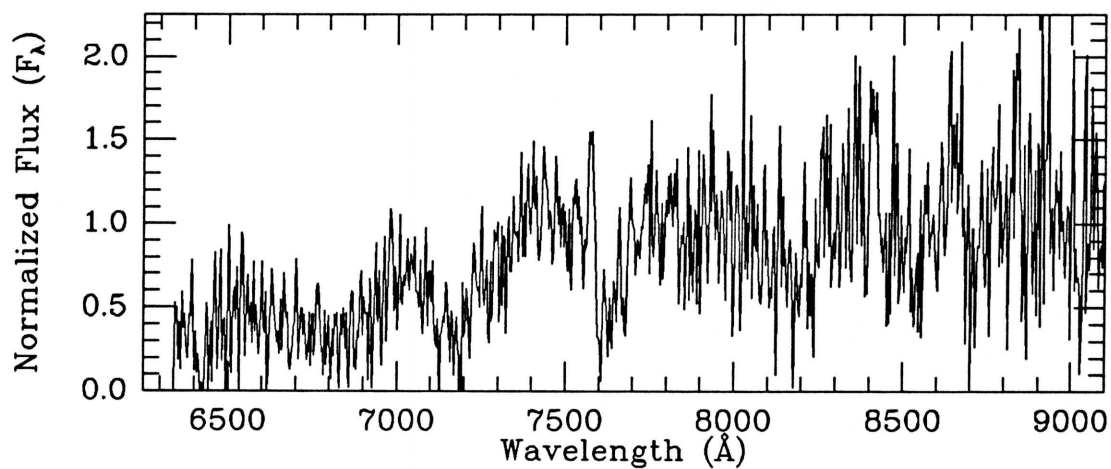
Clear filter

Obs. (UT) 1989 Apr 07

MMT SPECTRUM

Exposure: 1494 sec

Obs. (UT) 1990 May 22

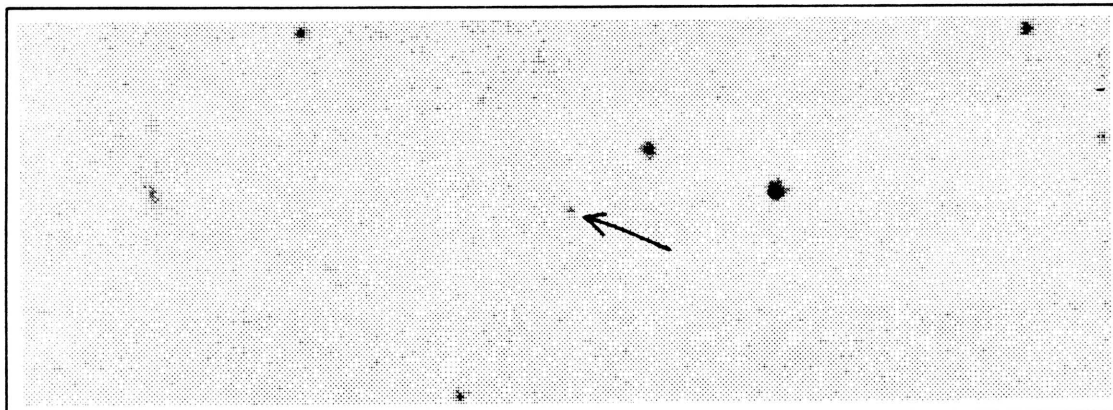
Coordinates: α (1950) = 13:56:10.5 δ (1950) = +28:10:54

Spectral Type: M3: V

Photometry: $I_{KC} = 18.86$ $R_{CTI} = 19.57$ $(V-I)_{KC} = 2.54 \pm .98$ $(R-I)_{CTI} = 0.85 \pm .68$ $(V-I)_{CTI} = 1.63 \pm .71$

Notes:

CTI 141034.3+280158



CTI FINDER CHART

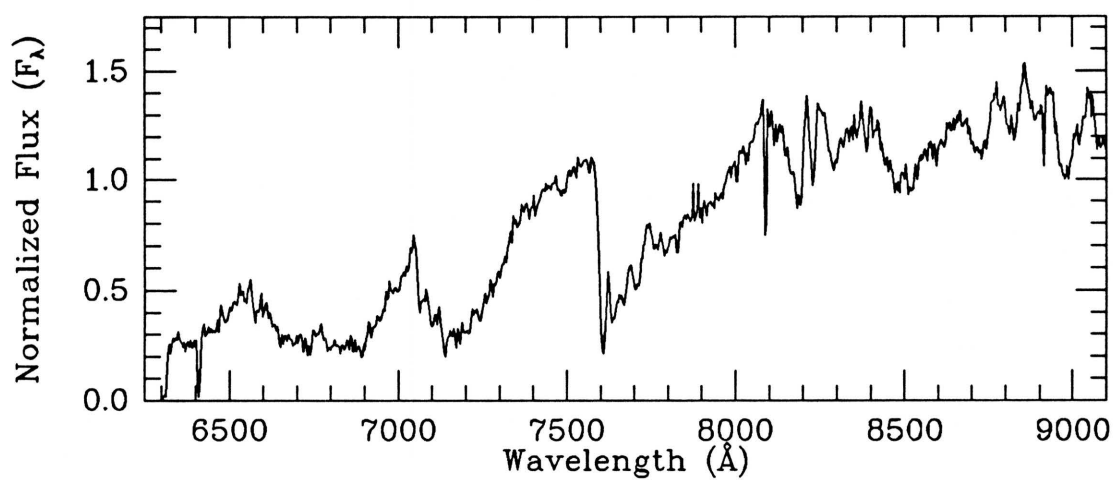
V filter

Obs. (UT) 1986 Apr 04

MMT SPECTRUM

Exposure: 1500 sec

Obs. (UT) 1989 Jul 14

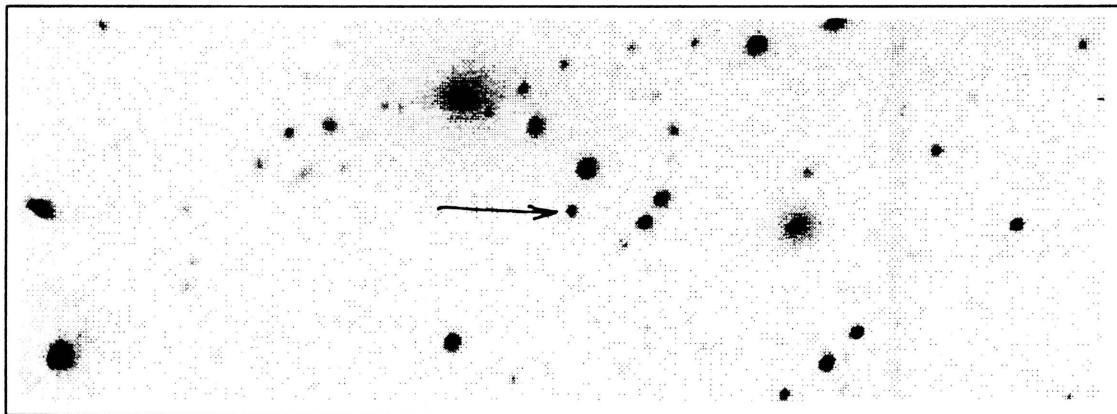
Coordinates: α (1950) = 14:08:53.4 δ (1950) = +28:12:32

Spectral Type: M4.5 V

Photometry: $I_{KC} = 15.01$ $R_{CTI} = 16.39$ $(V-I)_{KC} = 3.23 \pm .13$ $(R-I)_{CTI} = 1.33 \pm .03$ $(V-I)_{CTI} = 3.12 \pm .03$

Notes:

CTI 141111.3+280141



CTI FINDER CHART

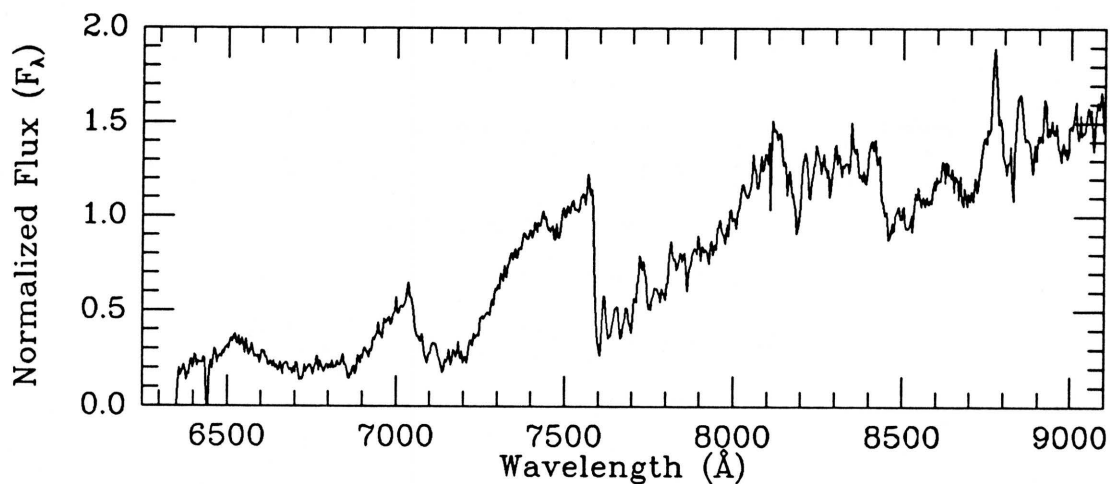
Clear filter

Obs. (UT) 1989 Apr 07

MMT SPECTRUM

Exposure: 2700 sec

Obs. (UT) 1990 May 04

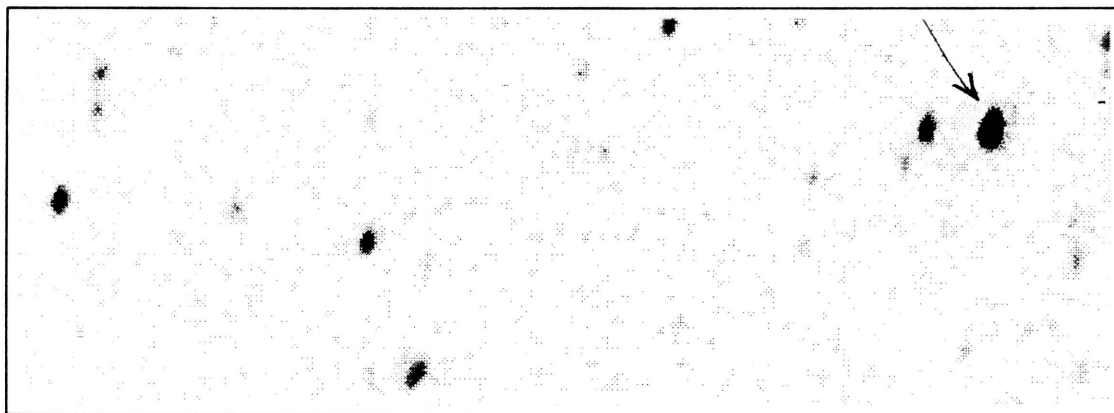
Coordinates: α (1950) = 14:09:30.4 δ (1950) = +28:12:14

Spectral Type: M5.5 V

Photometry: $I_{\text{KC}} = 16.40$ $R_{\text{CTI}} = 17.84$ $(V-I)_{\text{KC}} = 3.54 \pm 0.06$ $(R-I)_{\text{CTI}} = 1.43 \pm 0.09$ $(V-I)_{\text{CTI}} = 3.51 \pm 0.08$

Notes: Actual USNO VI photometry. Comparison to POSS E print suggests proper motion of ~ 0.2 arcsec/yr to the south.

CTI 141237.7+280559



CTI FINDER CHART

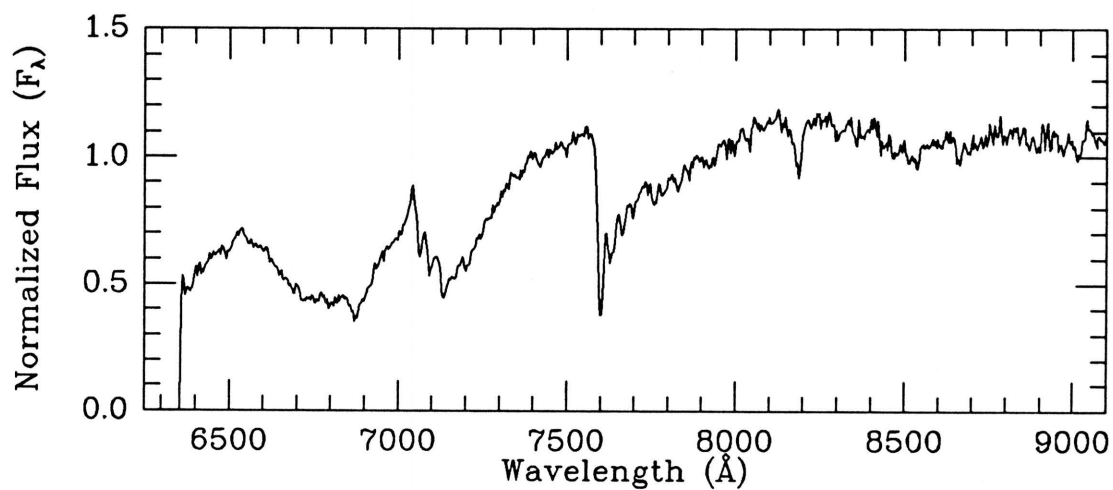
I filter

Coadded frame

MMT SPECTRUM

Exposure: 300 sec

Obs. (UT) 1991 Jun 23

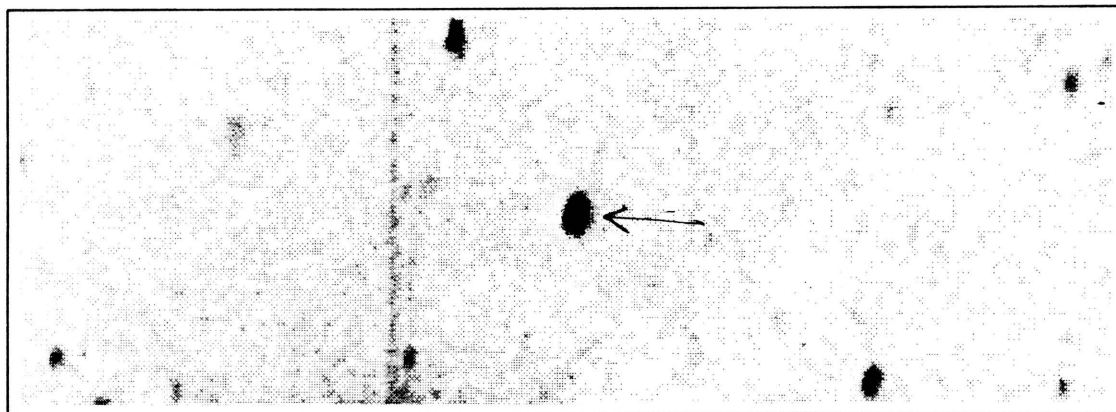
Coordinates: α (1950) = 14:10:57.0 δ (1950) = +28:16:30

Spectral Type: M3 V

Photometry: $I_{KC} = 14.58$ $R_{CTI} = 15.44$ $(V-I)_{KC} = 2.46 \pm 0.04$ $(R-I)_{CTI} = 0.78 \pm 0.02$ $(V-I)_{CTI} = \text{unknown}$

Notes: Actual USNO VI photometry.

CTI 141329.8+280131



CTI FINDER CHART

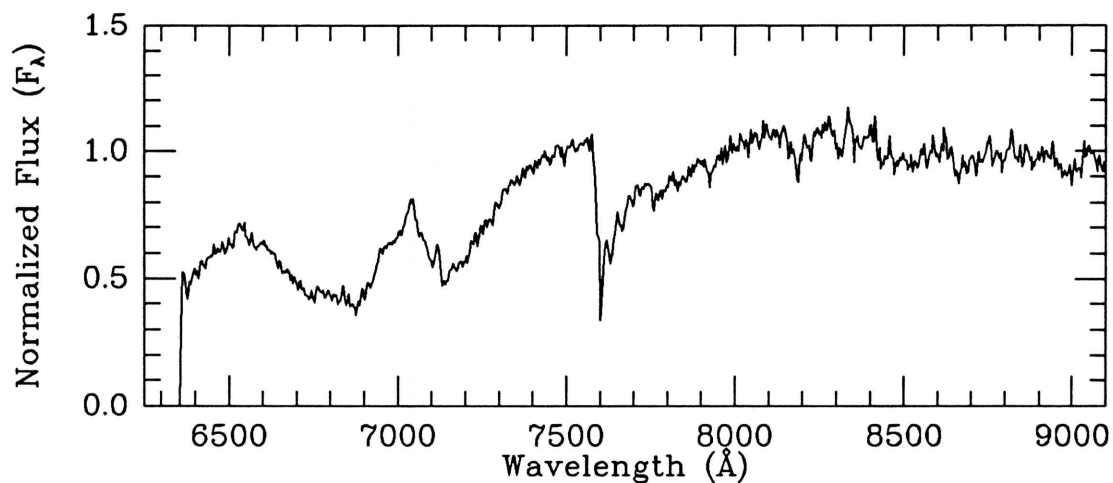
I filter

Coadded frame

MMT SPECTRUM

Exposure: 300 sec

Obs. (UT) 1991 Jun 24

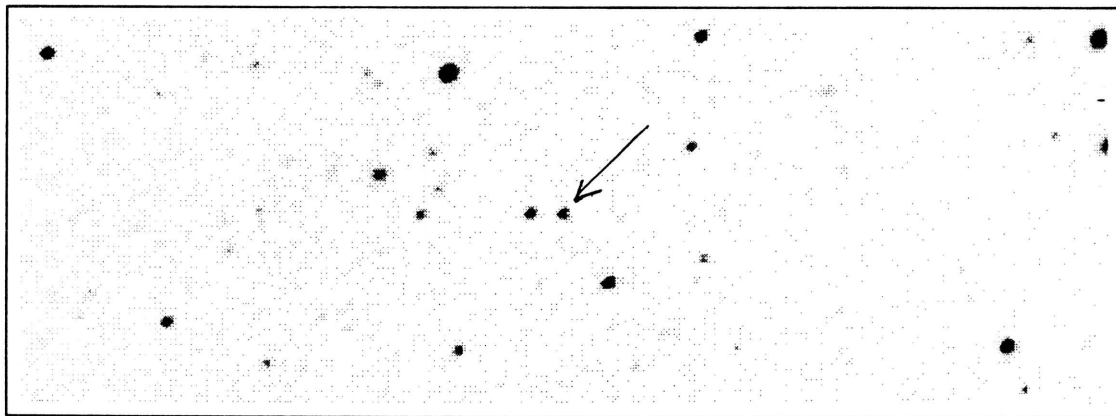
Coordinates: α (1950) = 14:11:49.2 δ (1950) = +28:12:00

Spectral Type: M2.5 V

Photometry: $I_{KC} = 14.58$ $R_{CTI} = 15.37$ $(V-I)_{KC} = 2.36 \pm 0.03$ $(R-I)_{CTI} = 0.73 \pm 0.02$ $(V-I)_{CTI} = \text{unknown}$

Notes: Actual USNO VI photometry.

CTI 150225.7+280231



CTI FINDER CHART

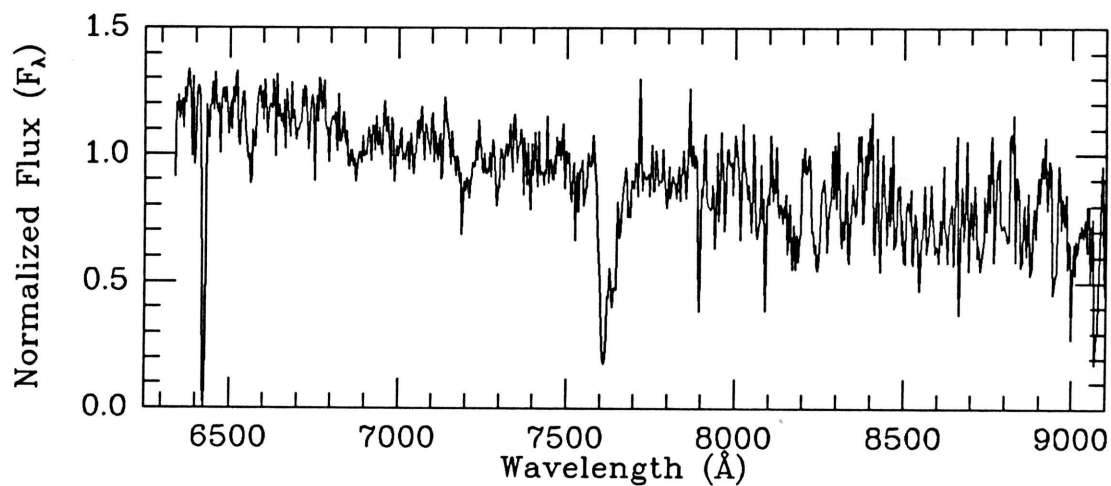
Clear filter

Obs. (UT) 1989 Apr 07

MMT SPECTRUM

Exposure: 1500 sec

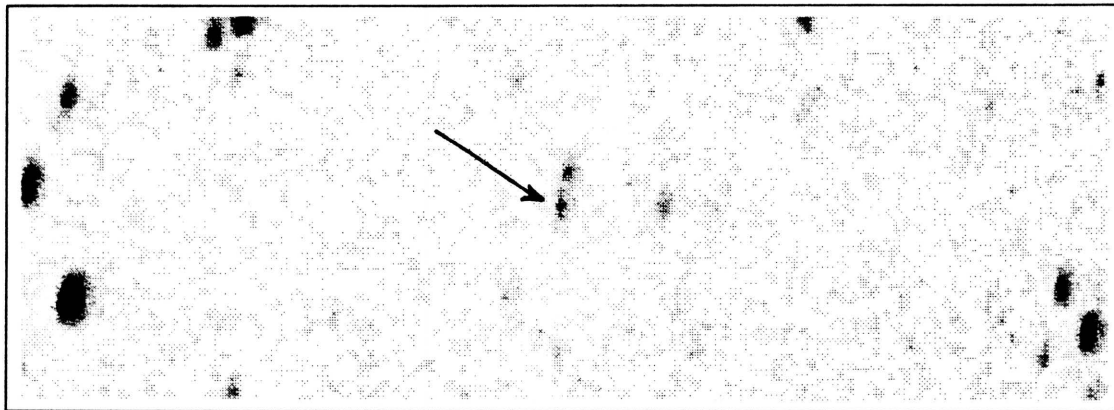
Obs. (UT) 1990 May 22

Coordinates: α (1950) = 15:00:49.5 δ (1950) = +28:11:19

Spectral Type: <K5 V

Photometry: $I_{KC} = 18.01$ $R_{CTI} = 18.74$ $(V-I)_{KC} = 2.51 \pm .23$ $(R-I)_{CTI} = 0.83 \pm .14$ $(V-I)_{CTI} = 0.67 \pm .12$ Notes: Average CTI R magnitude may be incorrect due to the inclusion of an erroneous measurement of $R=20.6$.

CTI 150546.7+280116



CTI FINDER CHART

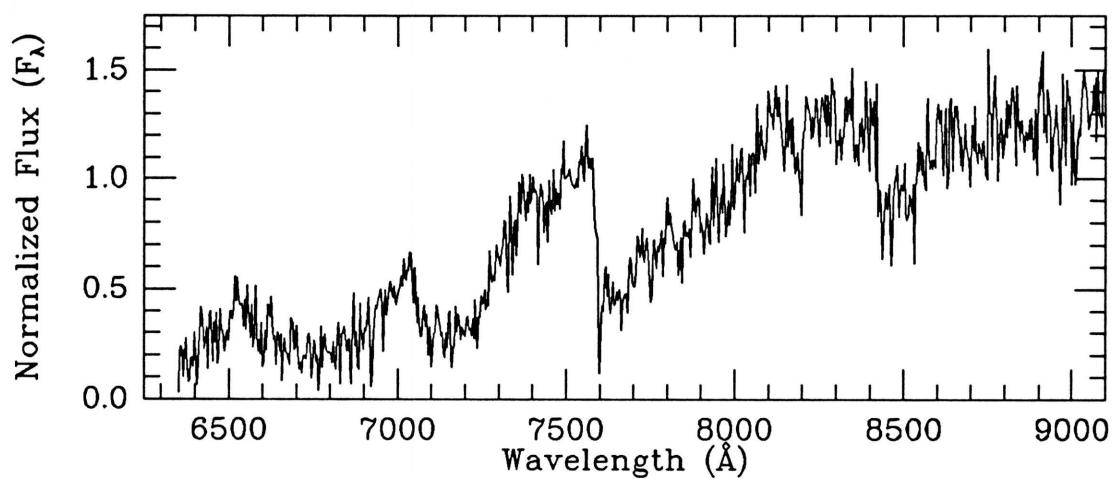
I filter

Coadded frame

MMT SPECTRUM

Exposure: 3900 sec

Obs. (UT) 1991 Jun 23

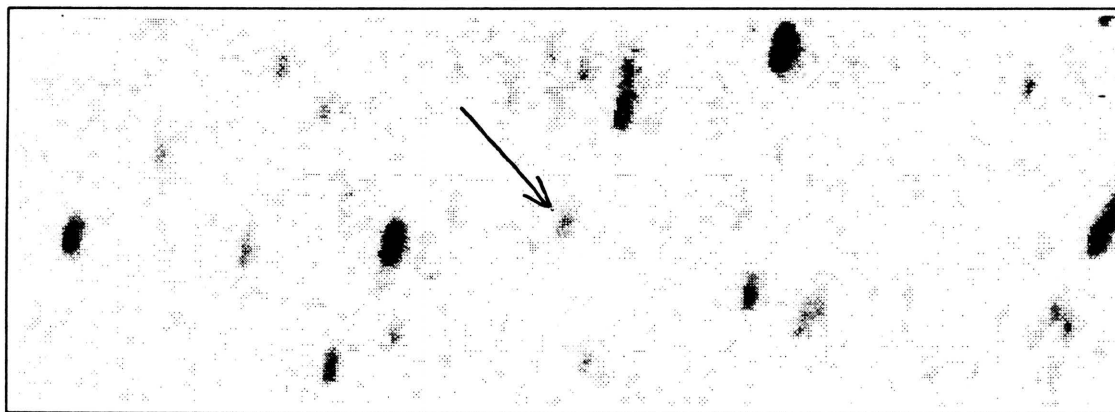
Coordinates: α (1950) = 15:04:10.7 δ (1950) = +28:09:56

Spectral Type: M5.5 V

Photometry: $I_{KC} = 18.55$ $R_{CTI} = \text{unknown}$ $(V-I)_{KC} = \text{unknown}$ $(R-I)_{CTI} = \text{unknown}$ $(V-I)_{CTI} = \text{unknown}$

Notes:

CTI 153729.8+280454



CTI FINDER CHART

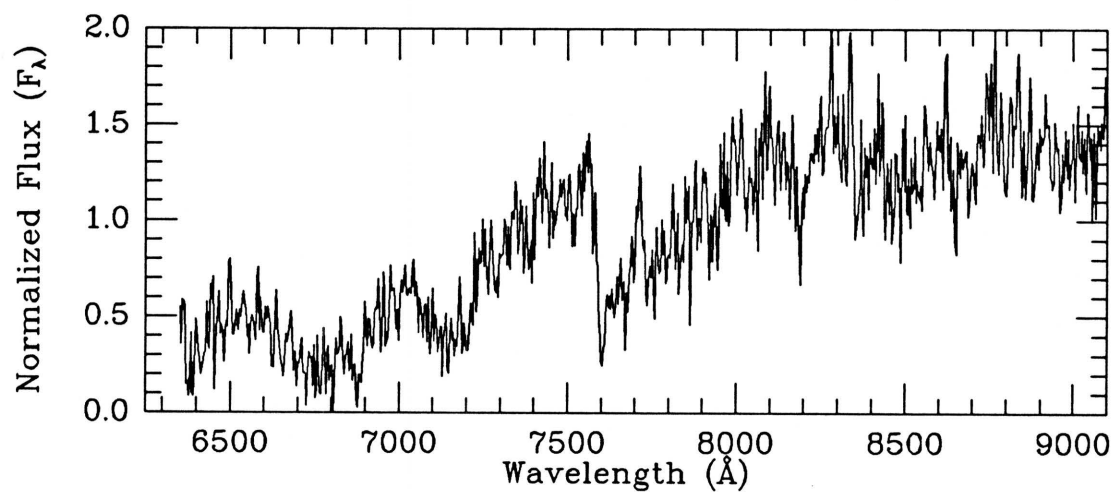
I filter

Coadded frame

MMT SPECTRUM

Exposure: 2700 sec

Obs. (UT) 1991 Jun 23

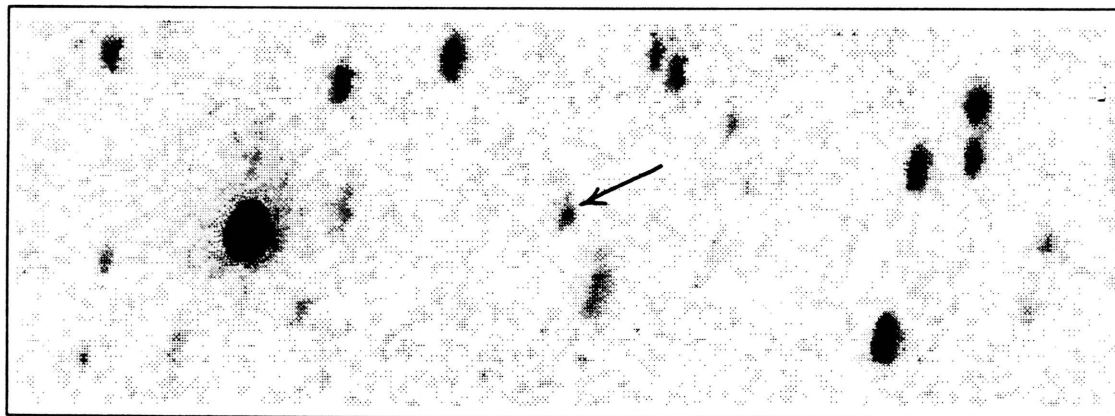
Coordinates: α (1950) = 15:35:56.3 δ (1950) = +28:12:14

Spectral Type: M4.5 V

Photometry: $I_{\text{KC}} = 18.80$ $R_{\text{CTI}} = 21.6$ $(V-I)_{\text{KC}} = 5.51 \pm 1.88$ $(R-I)_{\text{CTI}} = 2.93 \pm 1.31$ $(V-I)_{\text{CTI}} = \text{unknown}$

Notes:

CTI 153915.6+280214



CTI FINDER CHART

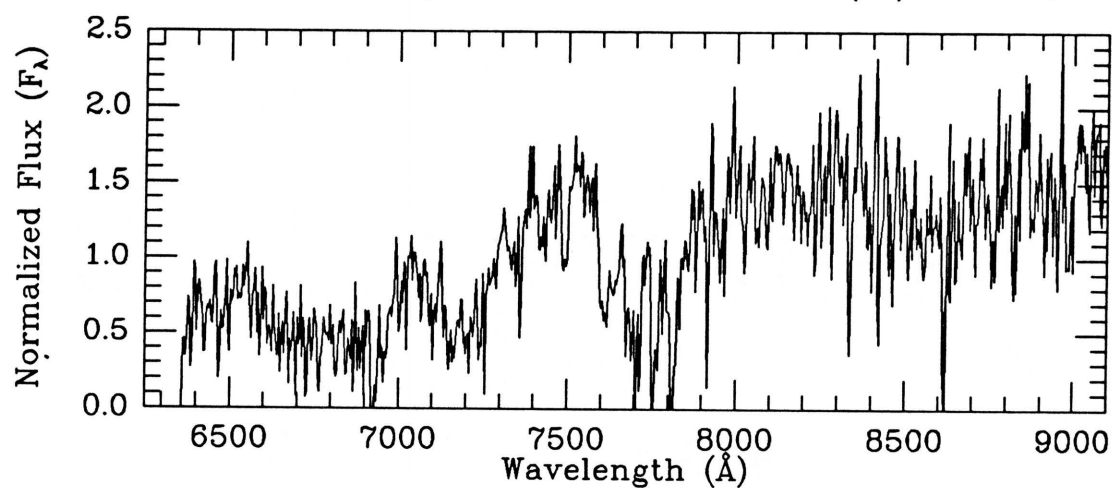
I filter

Coadded frame

MMT SPECTRUM

Exposure: 3000 sec

Obs. (UT) 1991 Jun 22

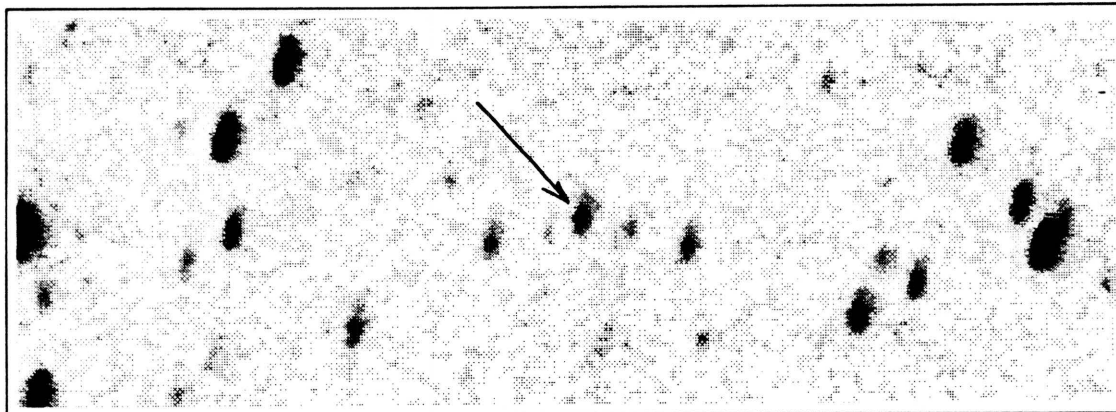
Coordinates: α (1950) = 15:37:42.1 δ (1950) = +28:09:29

Spectral Type: M4: V

Photometry: $I_{KC} = 18.44$ $R_{CTI} = 20.96$ $(V-I)_{KC} = 2.82 \pm 0.06$ $(R-I)_{CTI} = 2.33 \pm 0.79$ $(V-I)_{CTI} = \text{unknown}$

Notes: Actual USNO VI photometry.

CTI 153915.6+280446



CTI FINDER CHART

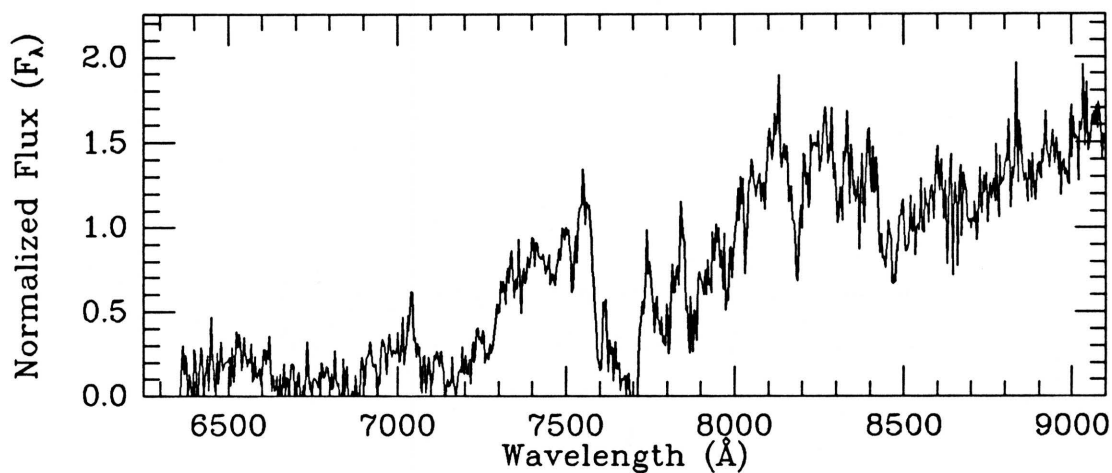
I filter

Coadded frame

MMT SPECTRUM

Exposure: 3900 sec

Obs. (UT) 1991 Jun 22



Coordinates: α (1950) = 15:37:42.2 δ (1950) = +28:12:01

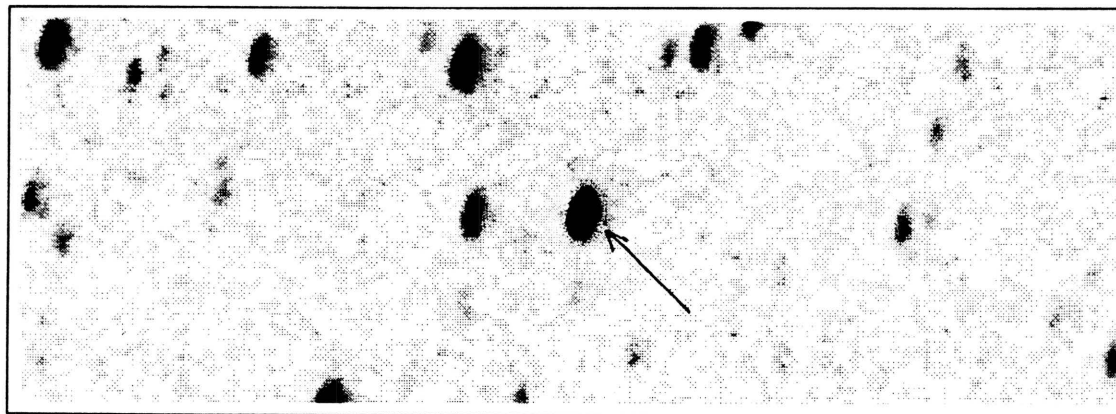
Spectral Type: M6.5 V

Photometry: $I_{KC} = 17.90$ $R_{CTI} = 19.69$

$(V-I)_{KC} = 4.43 \pm 1.12$ $(R-I)_{CTI} = 1.92 \pm 0.49$ $(V-I)_{CTI} = \text{unknown}$

Notes: Actual USNO VI photometry.

CTI 153945.1+280234



CTI FINDER CHART

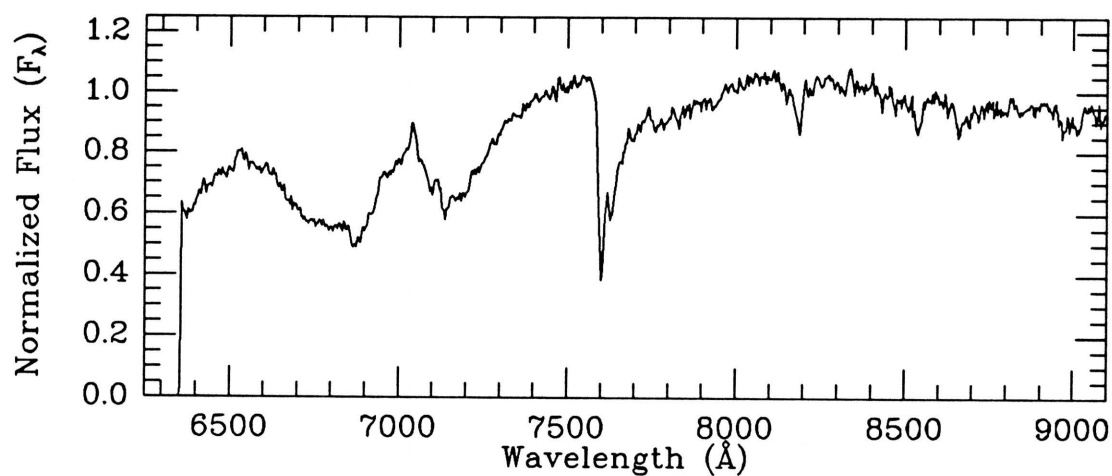
I filter

Coadded frame

MMT SPECTRUM

Exposure: 300 sec

Obs. (UT) 1991 Jun 24

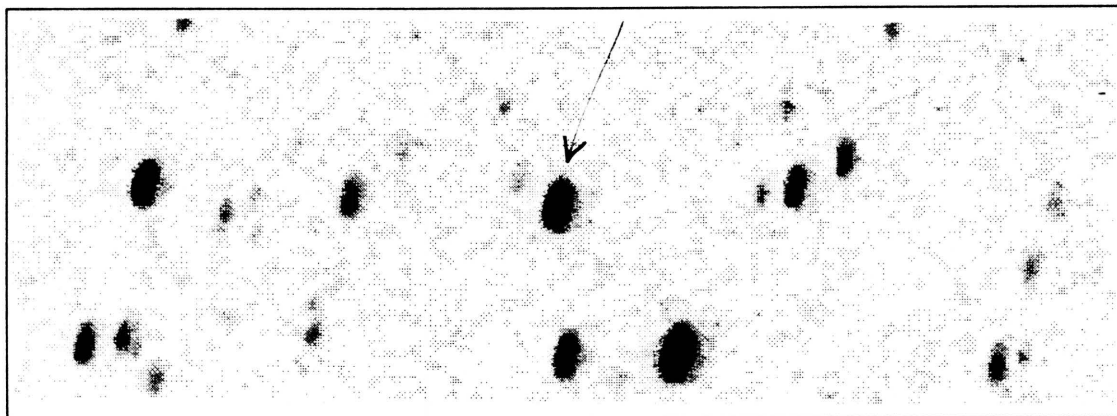
Coordinates: α (1950) = 15:38:11.7 δ (1950) = +28:09:48

Spectral Type: M1.5 V

Photometry: $I_{KC} = 14.04$ $R_{CTI} = 14.70$ $(V-I)_{KC} = 2.12 \pm 0.06$ $(R-I)_{CTI} = 0.56 \pm 0.01$ $(V-I)_{CTI} = \text{unknown}$

Notes: Actual USNO VI photometry.

CTI 153948.1+280322



CTI FINDER CHART

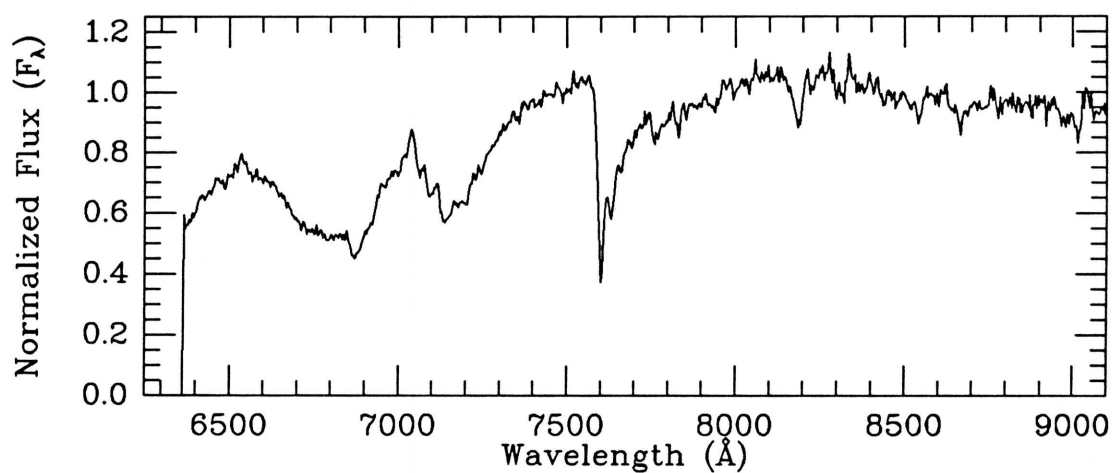
I filter

Coadded frame

MMT SPECTRUM

Exposure: 600 sec

Obs. (UT) 1991 Jun 24

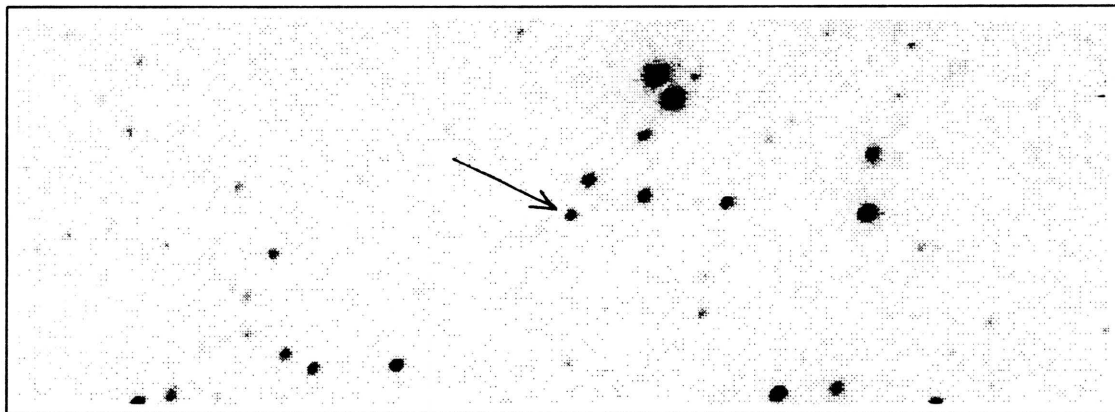
Coordinates: α (1950) = 15:38:14.7 δ (1950) = +28:10:36

Spectral Type: M2 V

Photometry: $I_{KC} = 14.74$ $R_{CTI} = 15.48$ $(V-I)_{KC} = 2.21 \pm 0.03$ $(R-I)_{CTI} = 0.65 \pm 0.02$ $(V-I)_{CTI} = \text{unknown}$

Notes: Actual USNO VI photometry.

CTI 154231.3+280401



CTI FINDER CHART

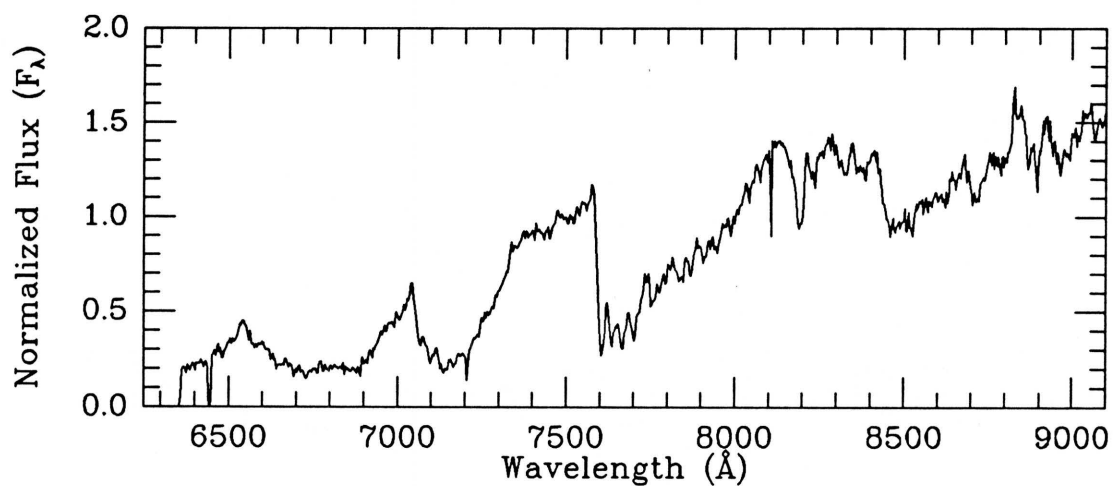
Clear filter

Obs. (UT) 1989 Apr 07

MMT SPECTRUM

Exposure: 2700 sec

Obs. (UT) 1990 May 04

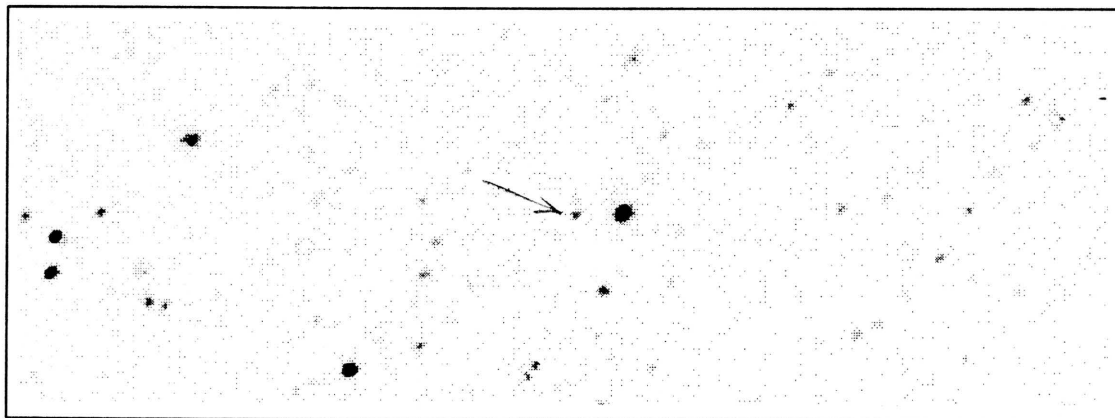
Coordinates: α (1950) = 15:40:58.1 δ (1950) = +28:11:07

Spectral Type: M5.5 V

Photometry: $I_{KC} = 16.71$ $R_{CTI} = 18.31$ $(V-I)_{KC} = 3.62 \pm 0.06$ $(R-I)_{CTI} = 1.57 \pm 0.12$ $(V-I)_{CTI} = 3.44 \pm 0.12$

Notes: Actual USNO VI photometry. Comparison to POSS E print suggests proper motion of ~ 0.2 arcsec/yr to the SW.

CTI 160557.4+280437



CTI FINDER CHART

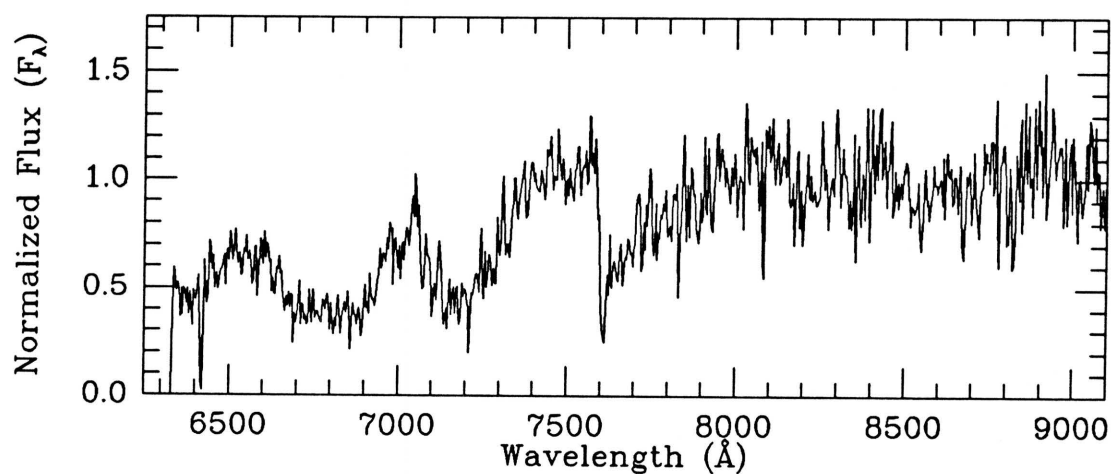
Clear filter

Obs. (UT) 1989 Apr 07

MMT SPECTRUM

Exposure: 3304 sec

Obs. (UT) 1990 May 23

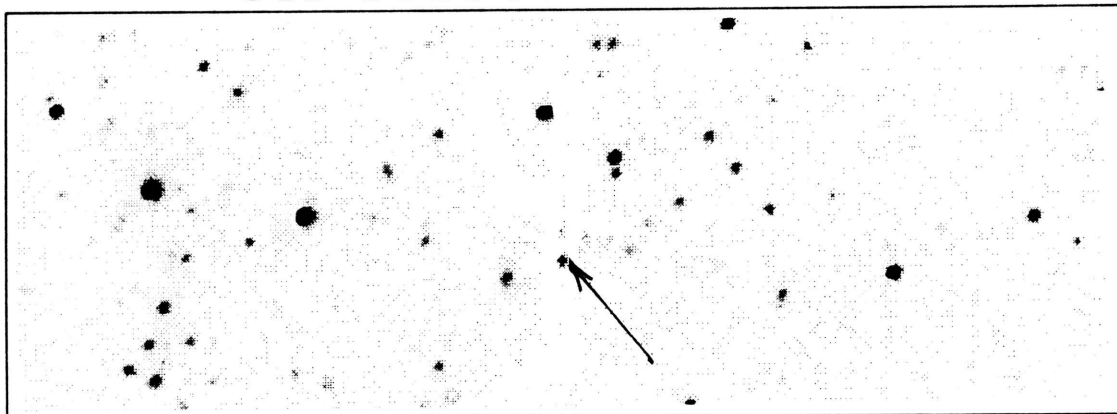
Coordinates: α (1950) = 16:04:25.6 δ (1950) = +28:10:38

Spectral Type: M3 V

Photometry: $I_{KC} = 18.19$ $R_{CTI} = 19.51$ $(V-I)_{KC} = 2.50 \pm 1.0$ $(R-I)_{CTI} = 1.55 \pm 0.28$ $(V-I)_{CTI} = 2.42 \pm 0.28$

Notes: Actual USNO VI photometry.

CTI 161340.2+280011



CTI FINDER CHART

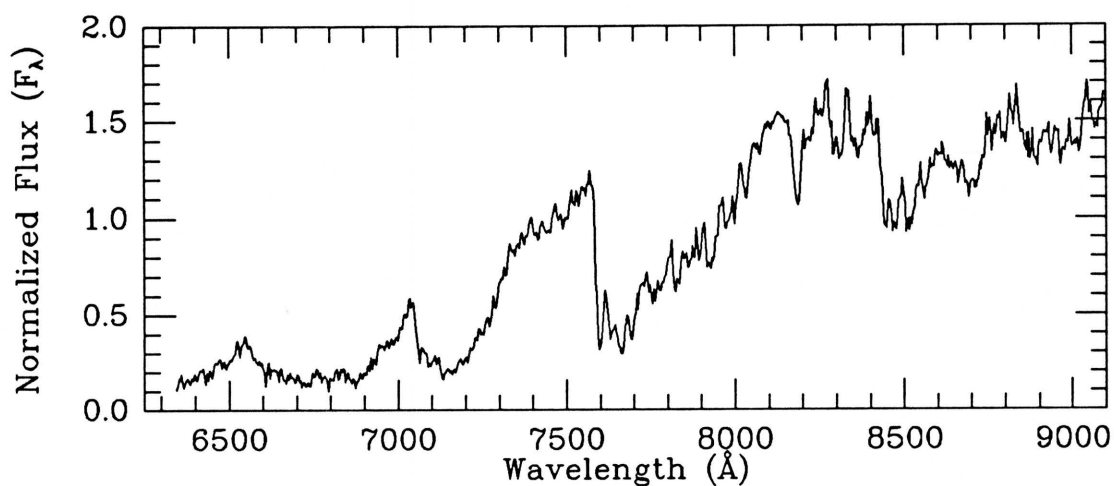
Clear filter

Obs. (UT) 1989 Apr 07

MMT SPECTRUM

Exposure: 3600 sec

Obs. (UT) 1991 May 07

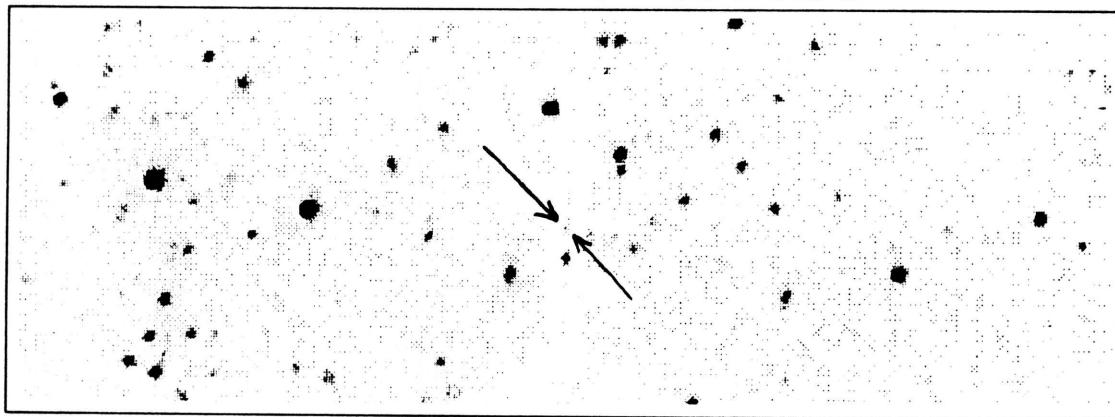
Coordinates: α (1950) = 16:12:08.8 δ (1950) = +28:05:50

Spectral Type: M5.5 V

Photometry: $I_{KC} = 17.31$ $R_{CTI} = 19.09$ $(V-I)_{KC} = 3.92 \pm 0.06$ $(R-I)_{CTI} = 1.77 \pm 0.41$ $(V-I)_{CTI} = 3.02 \pm 0.40$

Notes: Actual USNO VI photometry.

CTI 161340.2+280024



CTI FINDER CHART

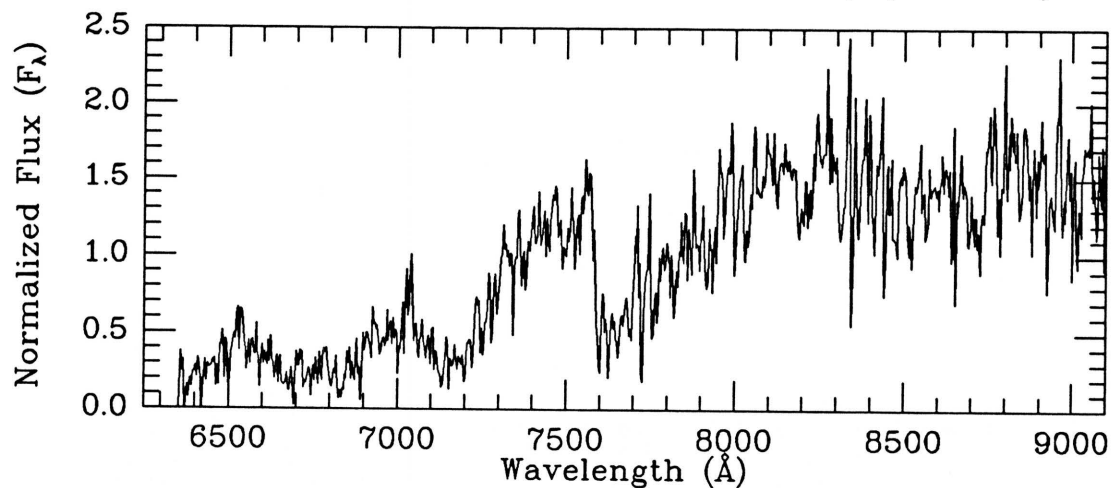
Clear filter

Obs. (UT) 1989 Apr 07

MMT SPECTRUM

Exposure: 3600 sec

Obs. (UT) 1991 May 07

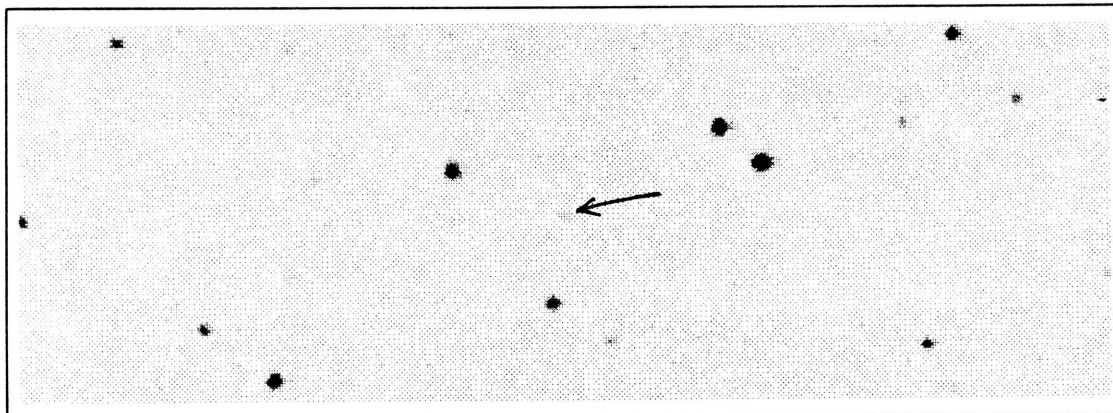
Coordinates: α (1950) = 16:12:08.8 δ (1950) = +28:06:03

Spectral Type: M4.5: V

Photometry: $I_{\text{KC}} = 19.18$ $R_{\text{CTI}} = \text{unknown}$ $(V-I)_{\text{KC}} = 3.55 \pm 0.16$ $(R-I)_{\text{CTI}} = \text{unknown}$ $(V-I)_{\text{CTI}} = \text{unknown}$

Notes: Actual USNO VI photometry. The spectrum of this object was obtained simultaneously with that of the object on the last page.

CTI 162342.9+280305



CTI FINDER CHART

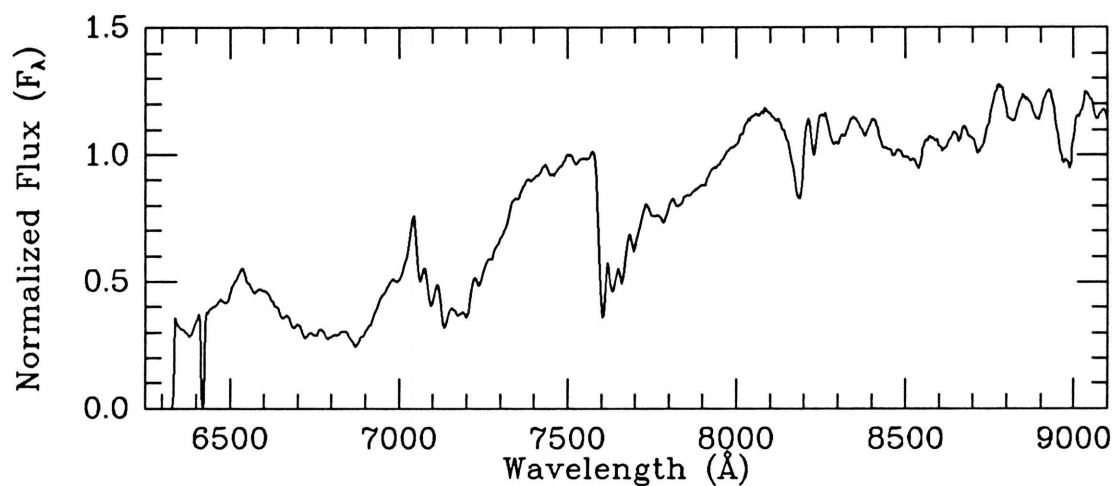
V filter

Obs. (UT) 1986 Apr 04

MMT SPECTRUM

Exposure: 2700 sec

Obs. (UT) 1989 Jul 10

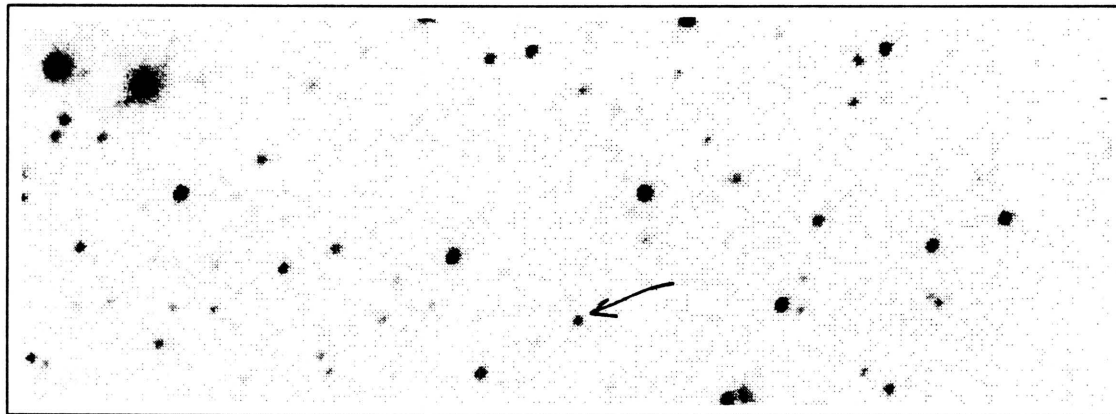
Coordinates: α (1950) = 16:22:12.0 δ (1950) = +28:08:14

Spectral Type: M4 V

Photometry: $I_{KC} = 15.82$ $R_{CTI} = 17.02$ $(V-I)_{KC} = 3.03 \pm 0.14$ $(R-I)_{CTI} = 1.19 \pm 0.05$ $(V-I)_{CTI} = 2.85 \pm 0.04$

Notes:

CTI 162356.1+275942



CTI FINDER CHART

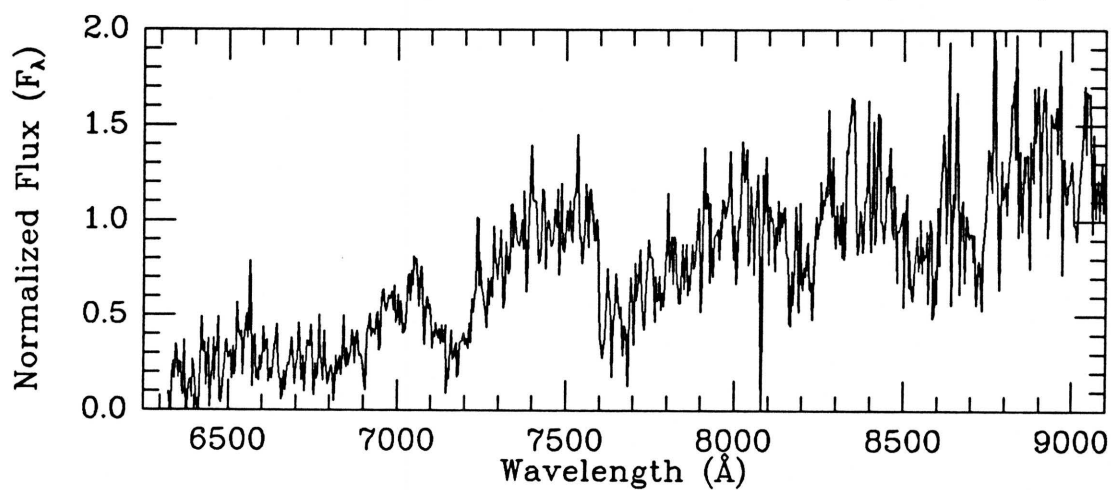
Clear filter

Obs. (UT) 1989 Apr 07

MMT SPECTRUM

Exposure: 1500 sec

Obs. (UT) 1990 May 23

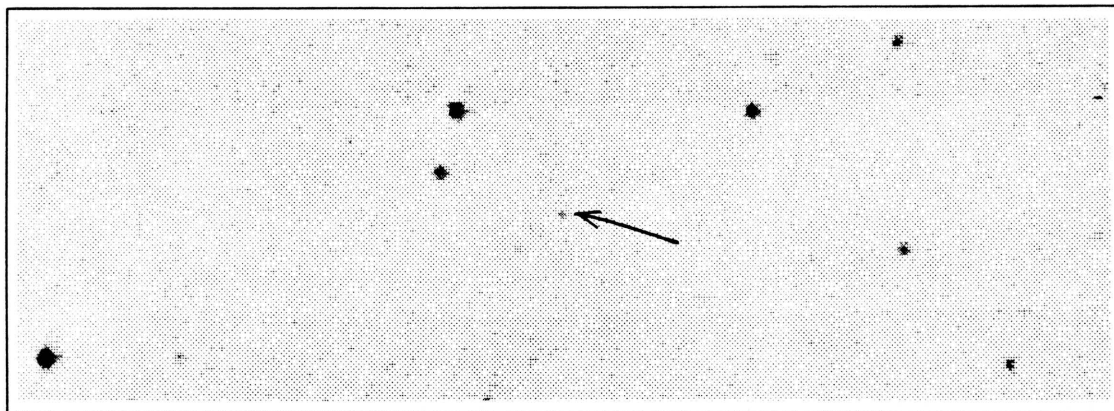
Coordinates: α (1950) = 16:22:25.2 δ (1950) = +28:04:50

Spectral Type: M3 V

Photometry: $I_{KC} = 17.29$ $R_{CTI} = 18.52$ $(V-I)_{KC} = 3.17 \pm .24$ $(R-I)_{CTI} = 1.29 \pm .14$ $(V-I)_{CTI} = 2.98 \pm .14$

Notes:

CTI 162920.4+280238



CTI FINDER CHART

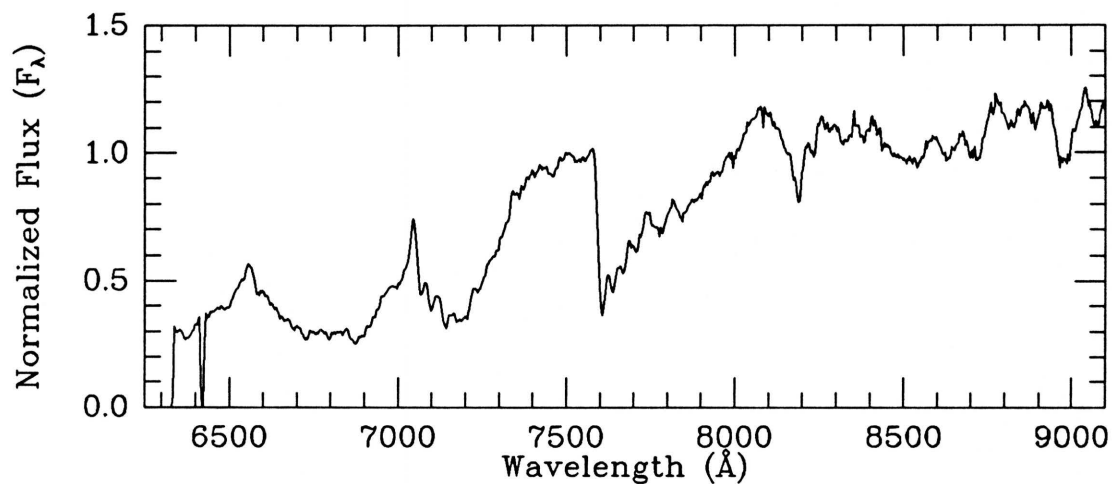
V filter

Obs. (UT) 1986 Apr 04

MMT SPECTRUM

Exposure: 1800 sec

Obs. (UT) 1989 Jul 10

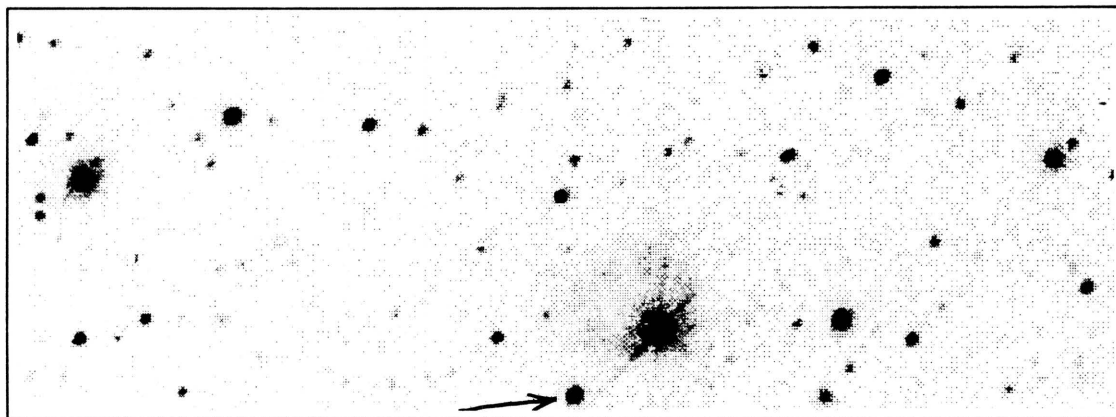
Coordinates: α (1950) = 16:27:49.8 δ (1950) = +28:07:30

Spectral Type: M4 V

Photometry: $I_{\text{KC}} = 15.59$ $R_{\text{CTI}} = 16.55$ $(V-I)_{\text{KC}} = 2.67 \pm 0.15$ $(R-I)_{\text{CTI}} = 0.94 \pm 0.07$ $(V-I)_{\text{CTI}} = 2.63 \pm 0.07$

Notes:

CTI 170958.5+275905



CTI FINDER CHART

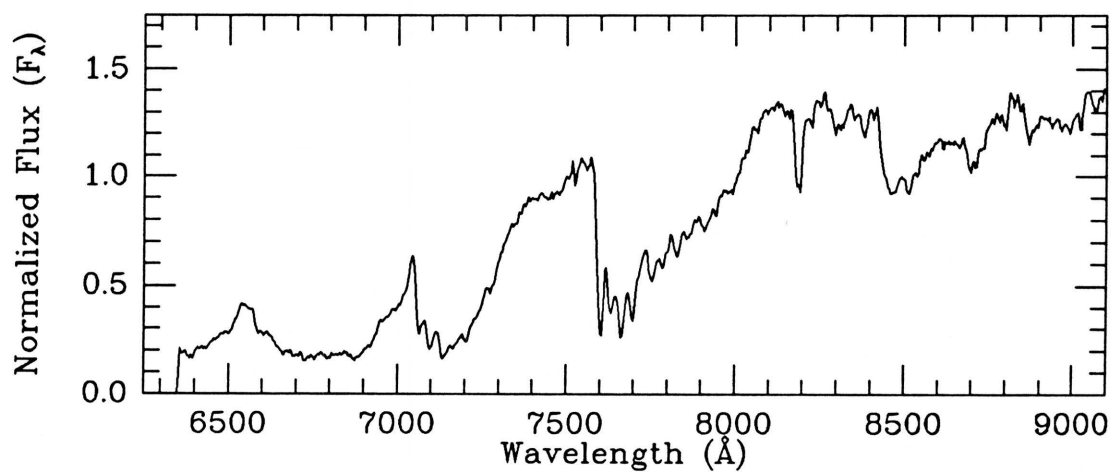
Clear filter

Obs. (UT) 1989 Apr 07

MMT SPECTRUM

Exposure: 300 sec

Obs. (UT) 1991 May 07

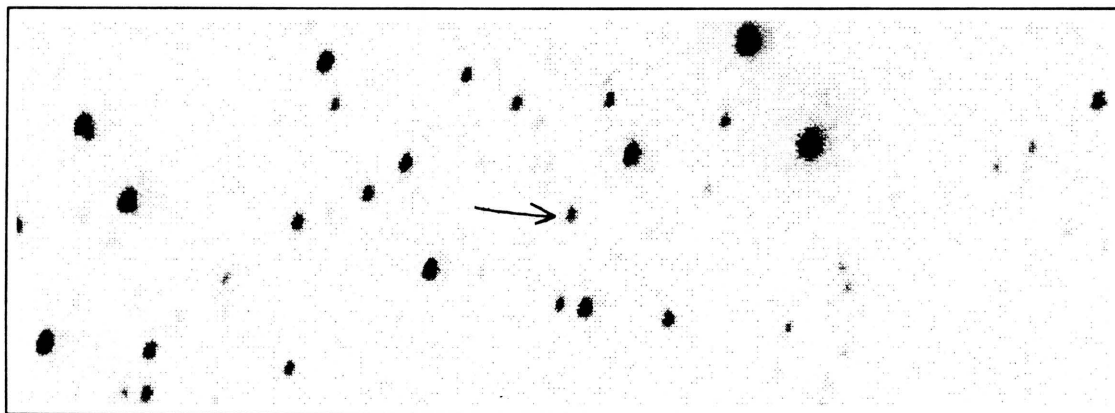
Coordinates: α (1950) = 17:08:29.2 δ (1950) = +28:01:50

Spectral Type: M5.5 V

Photometry: $I_{KC} = 13.90$ $R_{CTI} = 15.46$ $(V-I)_{KC} = 3.67 \pm 0.03$ $(R-I)_{CTI} = 1.58 \pm 0.03$ $(V-I)_{CTI} = 3.65 \pm 0.02$

Notes: Actual USNO VI photometry.

CTI 171818.0+280512



CTI FINDER CHART

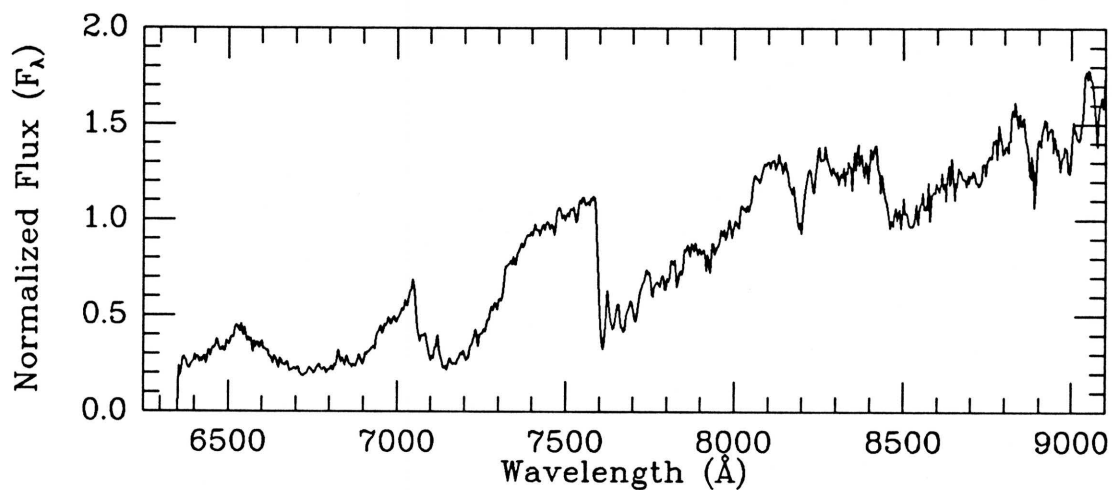
I filter

Obs. (UT) 1990 Jun 20

MMT SPECTRUM

Exposure: 2700 sec

Obs. (UT) 1990 Sep 13

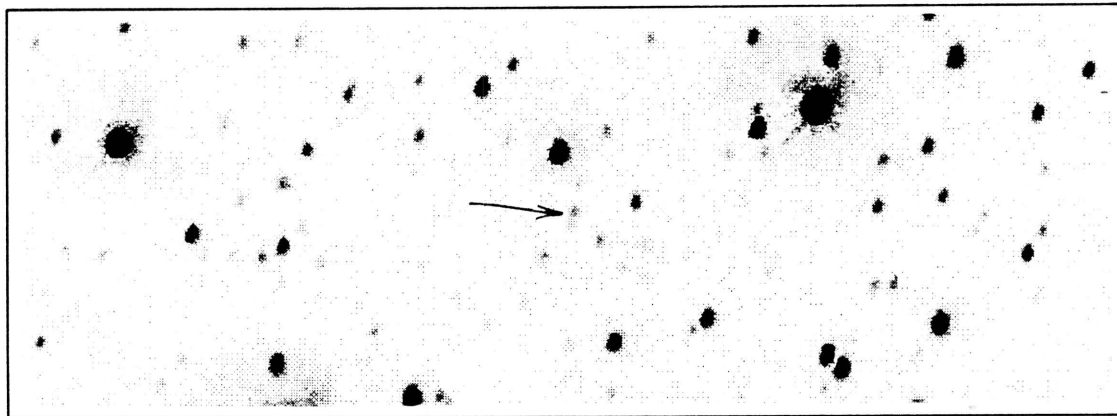
Coordinates: α (1950) = 17:16:49.0 δ (1950) = +28:07:30

Spectral Type: M5 V

Photometry: $I_{\text{KC}} = 16.83$ $R_{\text{CTI}} = 18.50$ $(V-I)_{\text{KC}} = 3.37 \pm 1.12$ $(R-I)_{\text{CTI}} = 1.57 \pm 1.18$ $(V-I)_{\text{CTI}} = 3.57 \pm 1.18$

Notes: Actual USNO VI photometry.

CTI 174729.0+280322



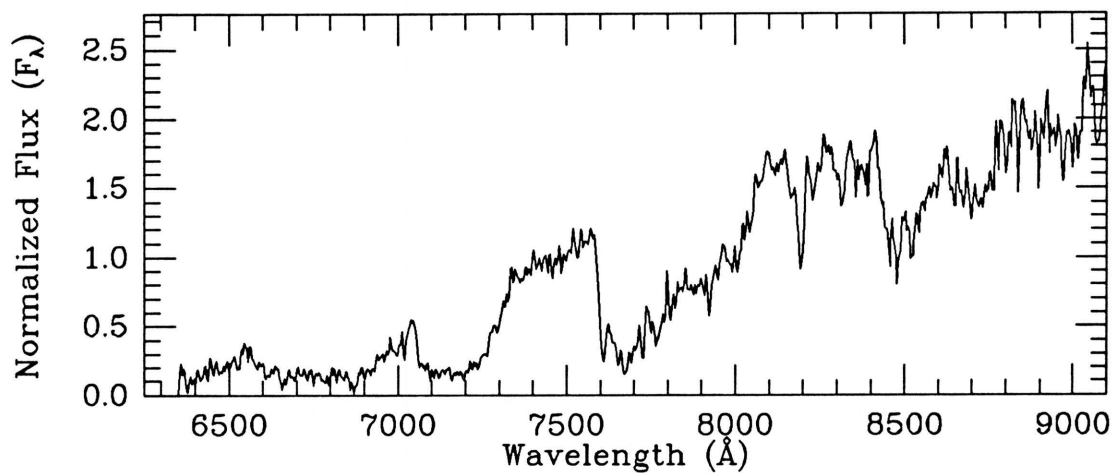
CTI FINDER CHART

I filter

Obs. (UT) 1990 Jun 20

MMT SPECTRUM

Exposure: 5400 sec Obs. (UT) 1990 Sep 13/14

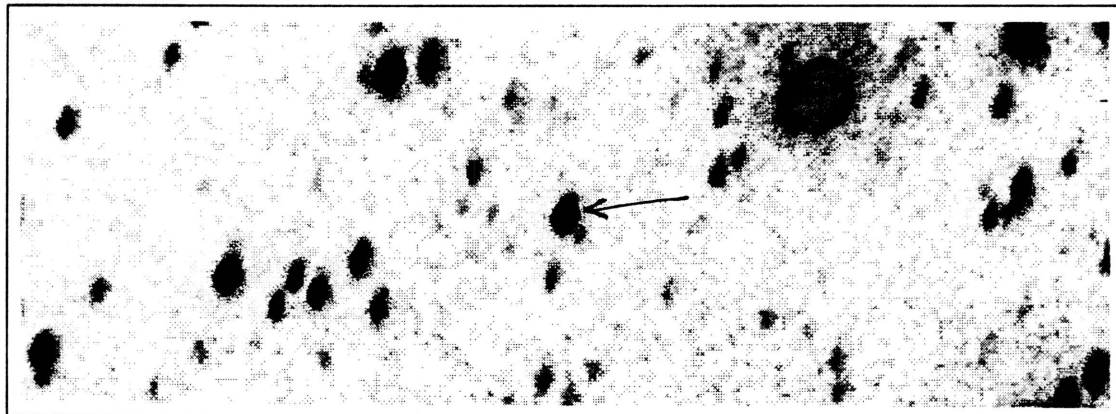
Coordinates: α (1950) = 17:46:00.4 δ (1950) = +28:04:05

Spectral Type: M6.5 V

Photometry: $I_{KC} = 17.87$ $R_{CTI} = 19.78$ $(V-I)_{KC} = 4.27 \pm .20$ $(R-I)_{CTI} = 2.21 \pm .42$ $(V-I)_{CTI} = \text{unknown}$

Notes: Actual USNO VI photometry.

CTI 180120.1+280410



CTI FINDER CHART

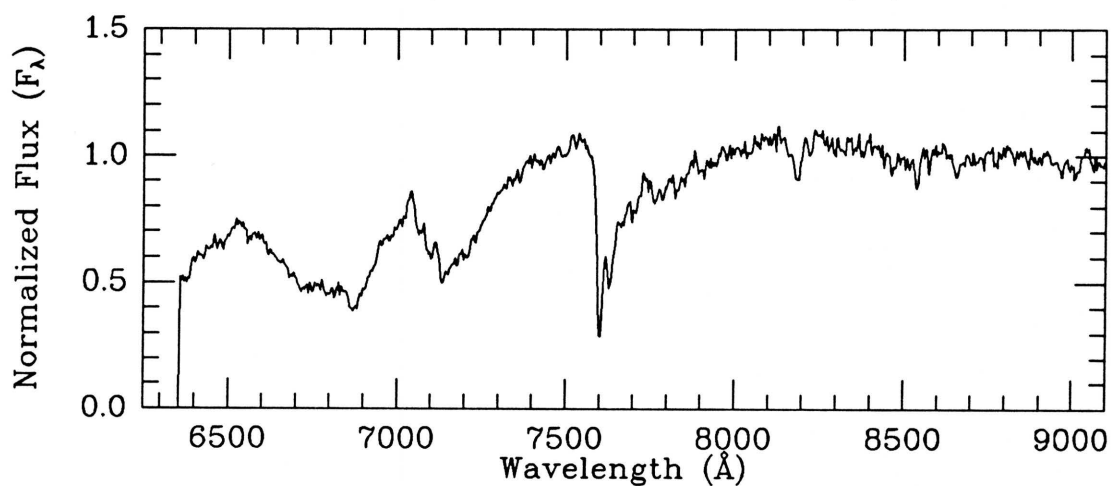
I filter

Coadded frame

MMT SPECTRUM

Exposure: 600 sec

Obs. (UT) 1991 Jun 23

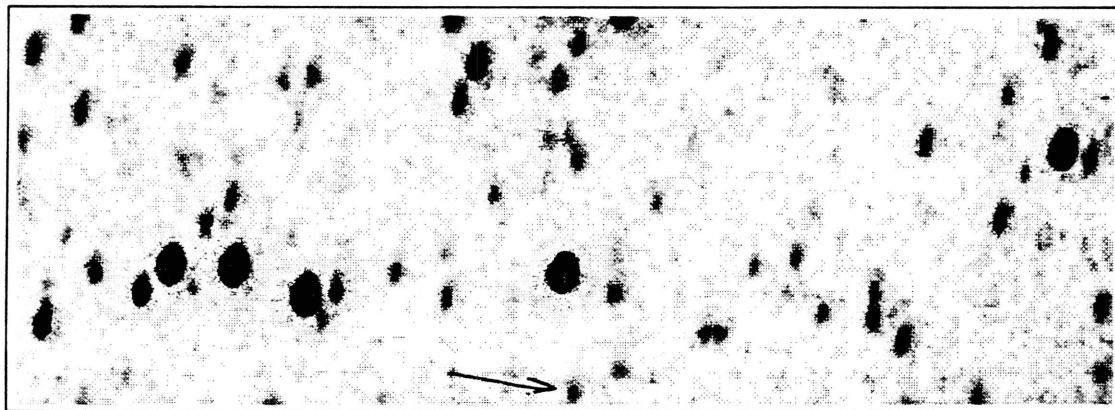
Coordinates: α (1950) = 17:59:51.5 δ (1950) = +28:04:08

Spectral Type: M2.5 V

Photometry: $I_{\text{KC}} = 14.70$ $R_{\text{CTI}} = 15.39$ $(V-I)_{\text{KC}} = 2.27 \pm 0.03$ $(R-I)_{\text{CTI}} = 0.60 \pm 0.02$ $(V-I)_{\text{CTI}} = \text{unknown}$

Notes: Actual USNO VI photometry.

CTI 180142.2+275924



CTI FINDER CHART

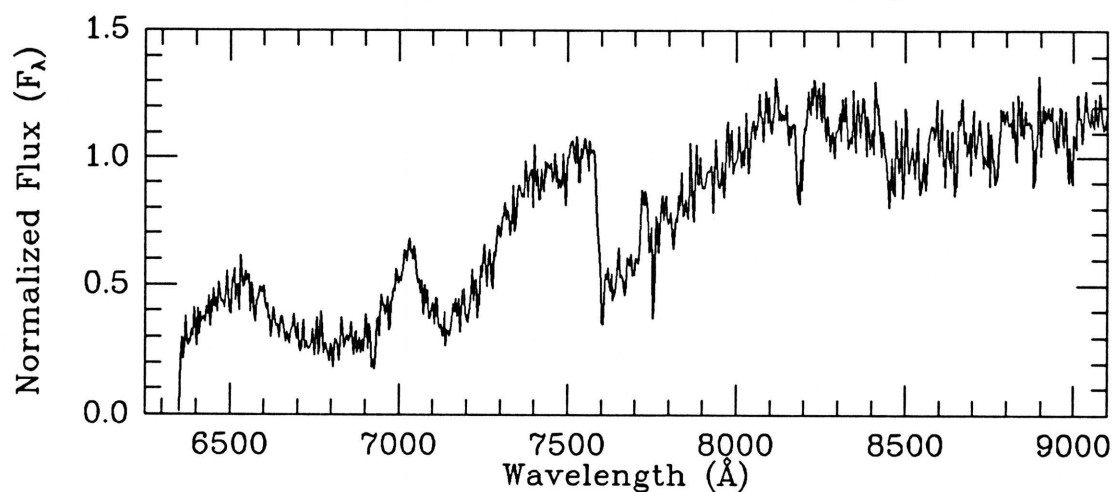
I filter

Coadded frame

MMT SPECTRUM

Exposure: 2700 sec

Obs. (UT) 1991 Jun 24

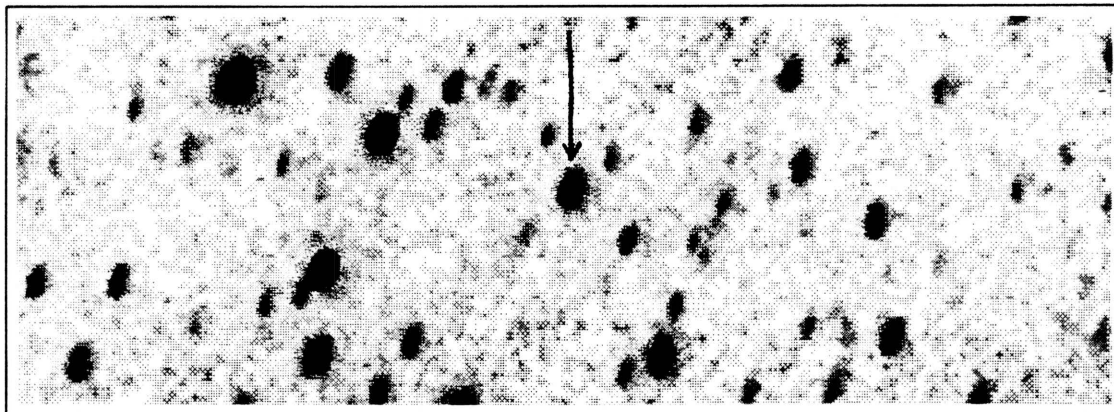
Coordinates: α (1950) = 18:00:13.6 δ (1950) = +27:59:21

Spectral Type: M4 V

Photometry: $I_{KC} = 17.89$ $R_{CTI} = \text{unknown}$ $(V-I)_{KC} = \text{unknown}$ $(R-I)_{CTI} = \text{unknown}$ $(V-I)_{CTI} = \text{unknown}$

Notes:

CTI 180216.7+280458



CTI FINDER CHART

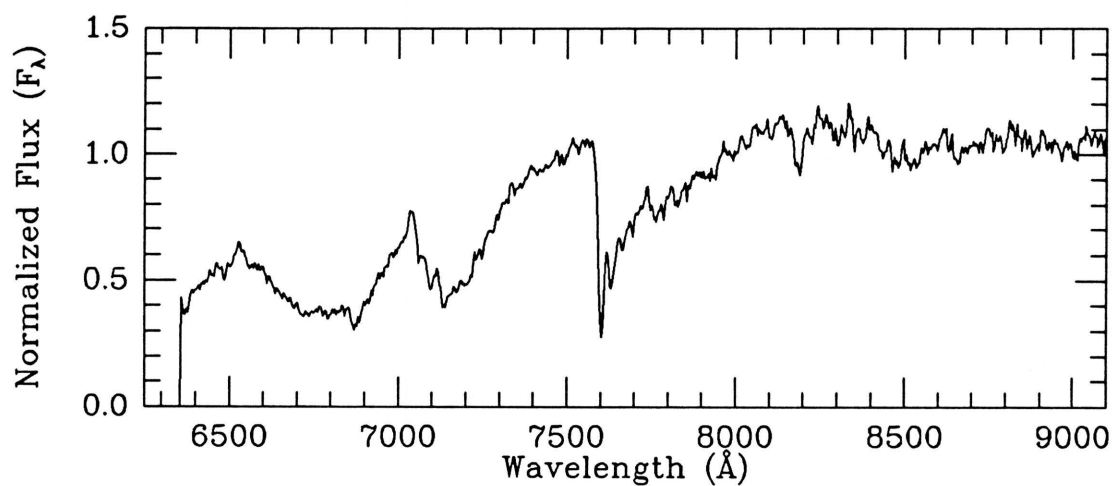
I filter

Coadded frame

MMT SPECTRUM

Exposure: 600 sec

Obs. (UT) 1991 Jun 23

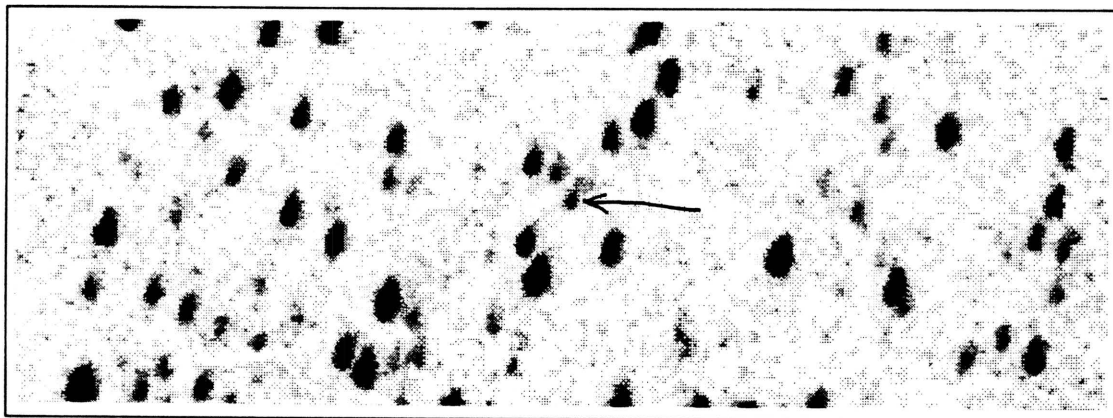
Coordinates: α (1950) = 18:00:48.2 δ (1950) = +28:04:53

Spectral Type: M3 V

Photometry: $I_{KC} = 15.09$ $R_{CTI} = 15.90$ $(V-I)_{KC} = 2.42 \pm 0.12$ $(R-I)_{CTI} = 0.77 \pm 0.03$ $(V-I)_{CTI} = \text{unknown}$

Notes:

CTI 180257.0+280454



CTI FINDER CHART

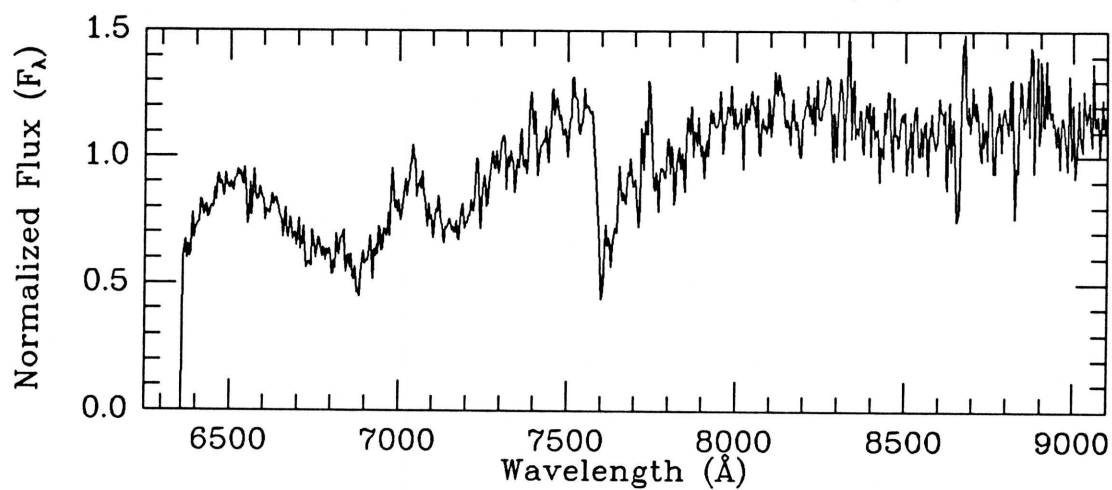
I filter

Coadded frame

MMT SPECTRUM

Exposure: 2700 sec

Obs. (UT) 1991 Jun 22

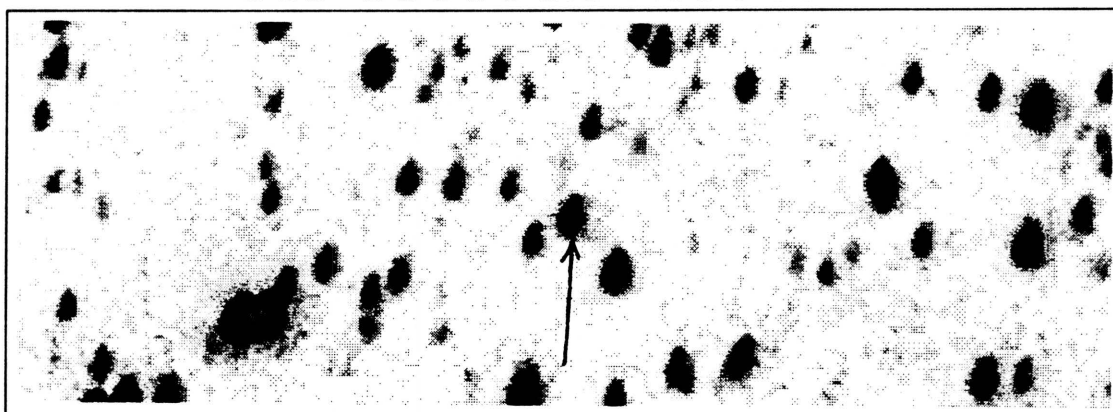
Coordinates: α (1950) = 18:01:28.5 δ (1950) = +28:04:47

Spectral Type: M2: V

Photometry: $I_{KC} = 17.95$ $R_{CTI} = 19.97$ $(V-I)_{KC} = 4.34 \pm 0.63$ $(R-I)_{CTI} = 2.11 \pm 0.43$ $(V-I)_{CTI} = \text{unknown}$

Notes:

CTI 180304.9+280256



CTI FINDER CHART

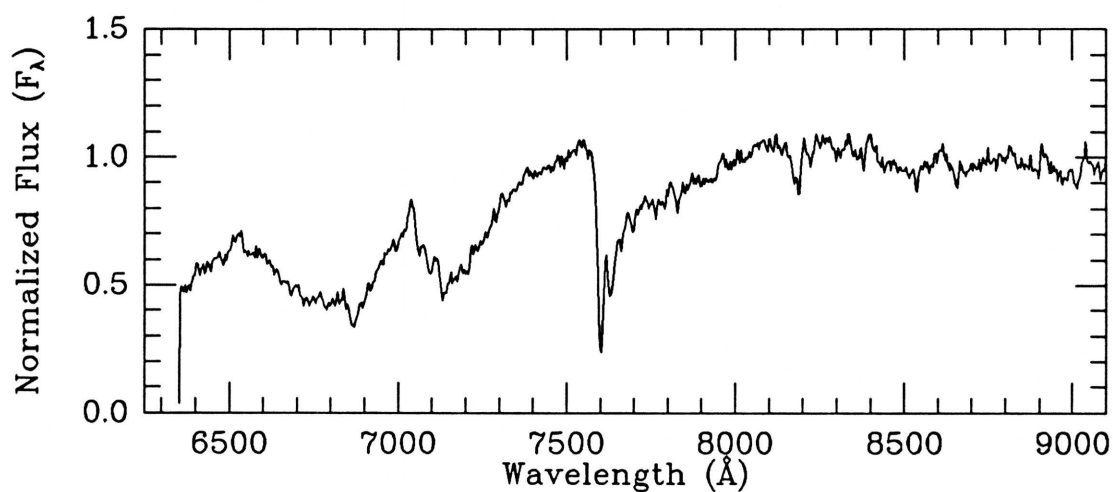
I filter

Coadded frame

MMT SPECTRUM

Exposure: 300 sec

Obs. (UT) 1991 Jun 23

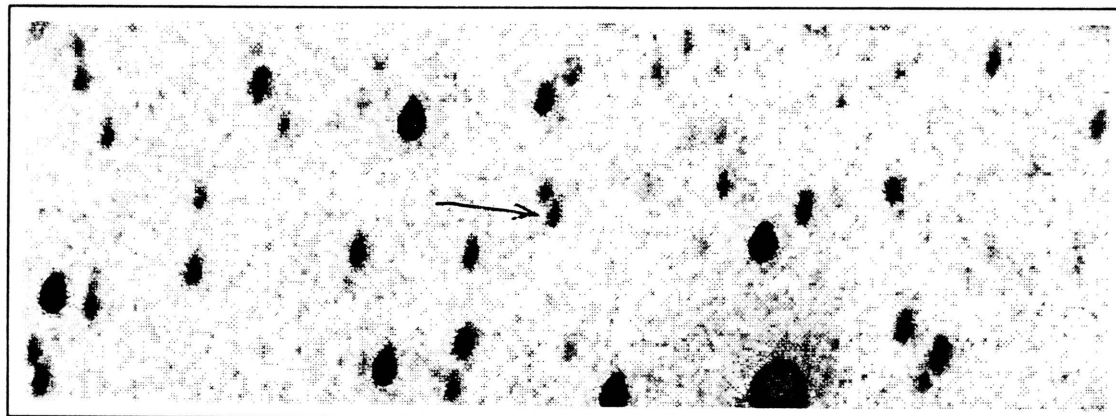
Coordinates: α (1950) = 18:01:36.3 δ (1950) = +28:02:48

Spectral Type: M2.5 V

Photometry: $I_{KC} = 14.88$ $R_{CTI} = 15.77$ $(V-I)_{KC} = 2.37 \pm 0.04$ $(R-I)_{CTI} = 0.76 \pm 0.03$ $(V-I)_{CTI} = \text{unknown}$

Notes: Actual USNO VI photometry.

CTI 180350.7+280133



CTI FINDER CHART

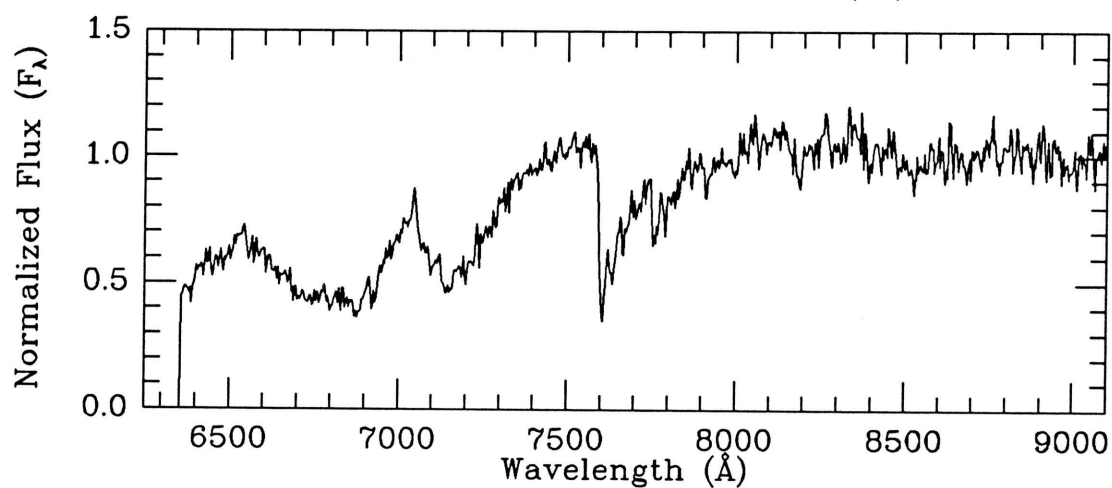
I filter

Coadded frame

MMT SPECTRUM

Exposure: 2700 sec

Obs. (UT) 1991 Jun 23

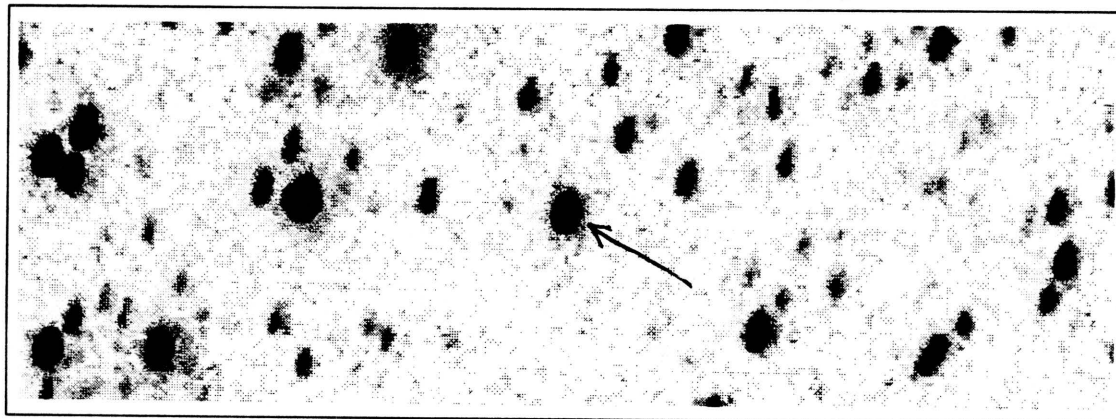
Coordinates: α (1950) = 18:02:22.1 δ (1950) = +28:01:23

Spectral Type: M3 V

Photometry: $I_{KC} = 18.08$ $R_{CTI} = \text{unknown}$ $(V-I)_{KC} = \text{unknown}$ $(R-I)_{CTI} = \text{unknown}$ $(V-I)_{CTI} = \text{unknown}$

Notes:

CTI 180408.2+280353



CTI FINDER CHART

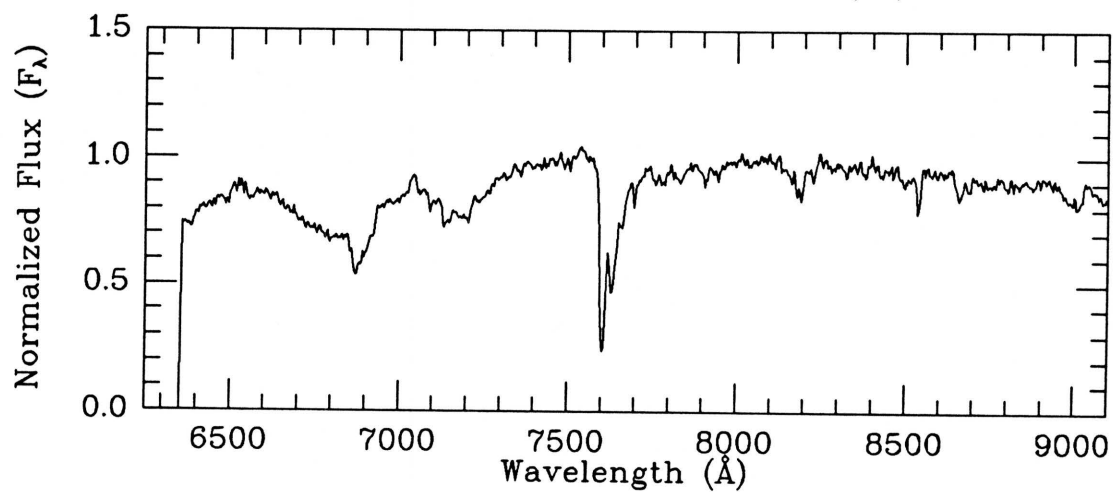
I filter

Coadded frame

MMT SPECTRUM

Exposure: 300 sec

Obs. (UT) 1991 Jun 23

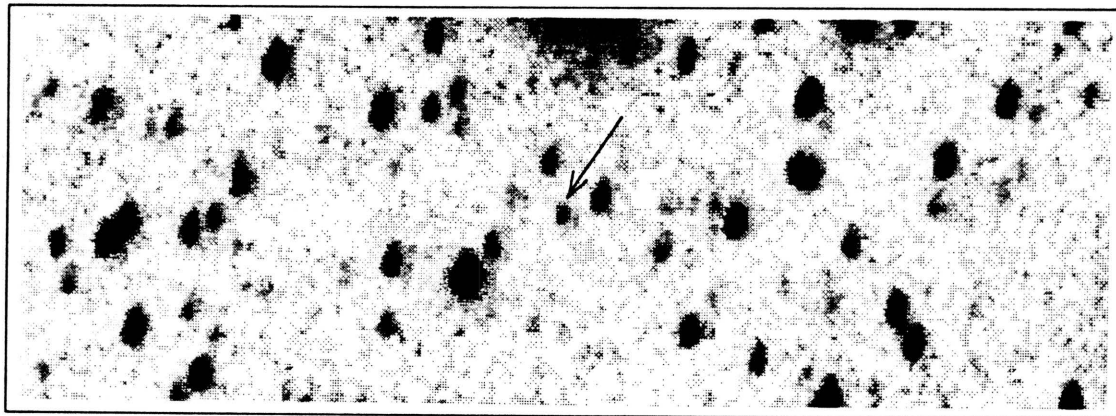
Coordinates: α (1950) = 18:02:39.6 δ (1950) = +28:03:42

Spectral Type: M0 V

Photometry: $I_{KC} = 14.09$ $R_{CTI} = 14.49$ $(V-I)_{KC} = 1.77 \pm 0.10$ $(R-I)_{CTI} = 0.31 \pm 0.01$ $(V-I)_{CTI} = \text{unknown}$

Notes:

CTI 180456.5+280048



CTI FINDER CHART

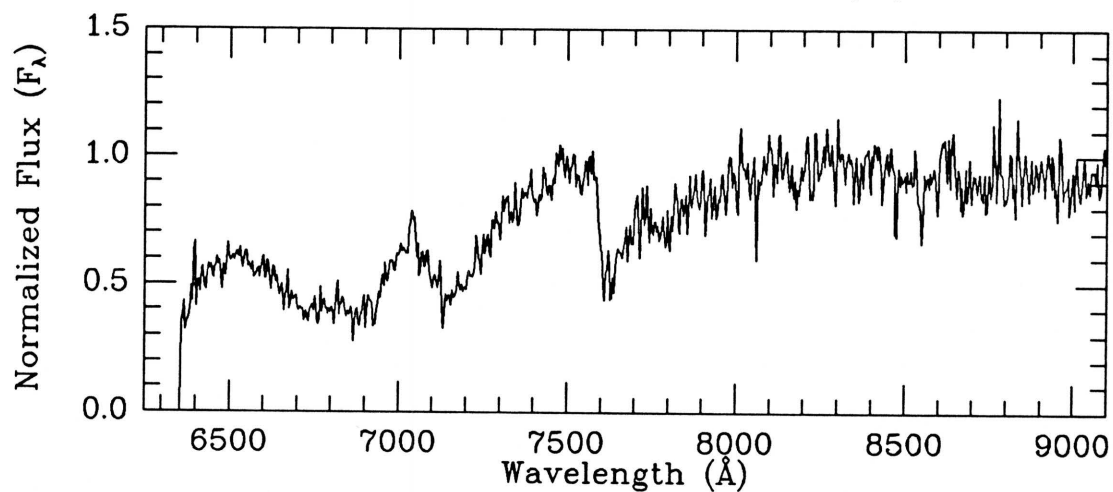
I filter

Coadded frame

MMT SPECTRUM

Exposure: 1500 sec

Obs. (UT) 1991 Jun 23

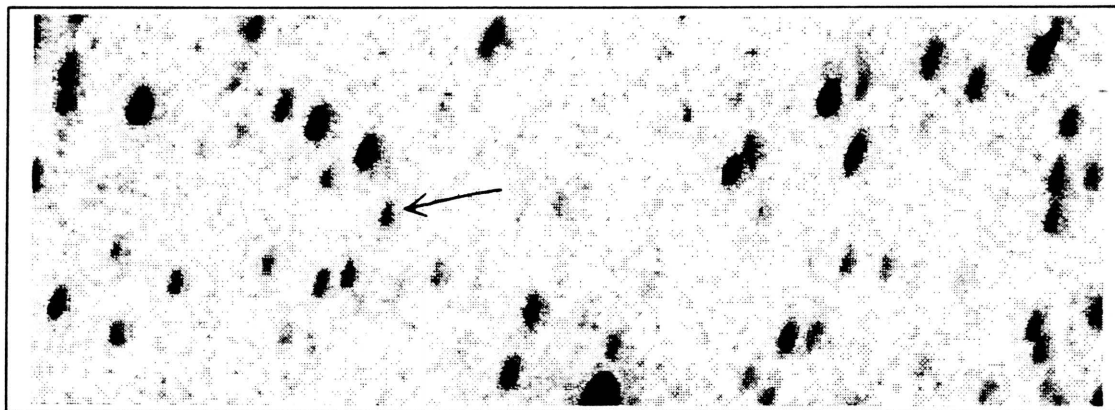
Coordinates: α (1950) = 18:03:28.0 δ (1950) = +28:00:34

Spectral Type: M3 V

Photometry: $I_{KC} = 18.27$ $R_{CTI} = 19.88$ $(V-I)_{KC} = 3.78 \pm .76$ $(R-I)_{CTI} = 1.72 \pm .52$ $(V-I)_{CTI} = \text{unknown}$

Notes:

CTI 180516.3+280447



CTI FINDER CHART

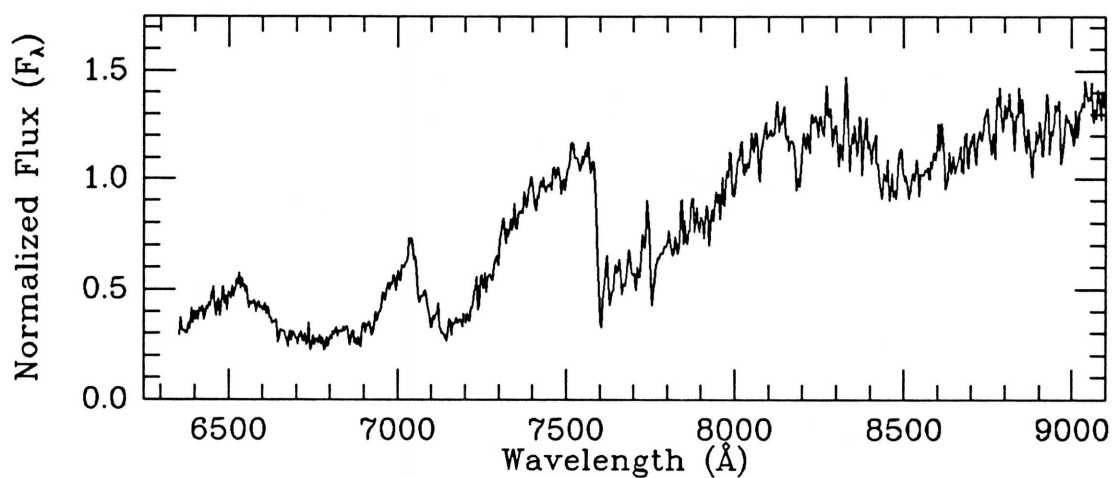
I filter

Coadded frame

MMT SPECTRUM

Exposure: 2700 sec

Obs. (UT) 1991 Jun 22

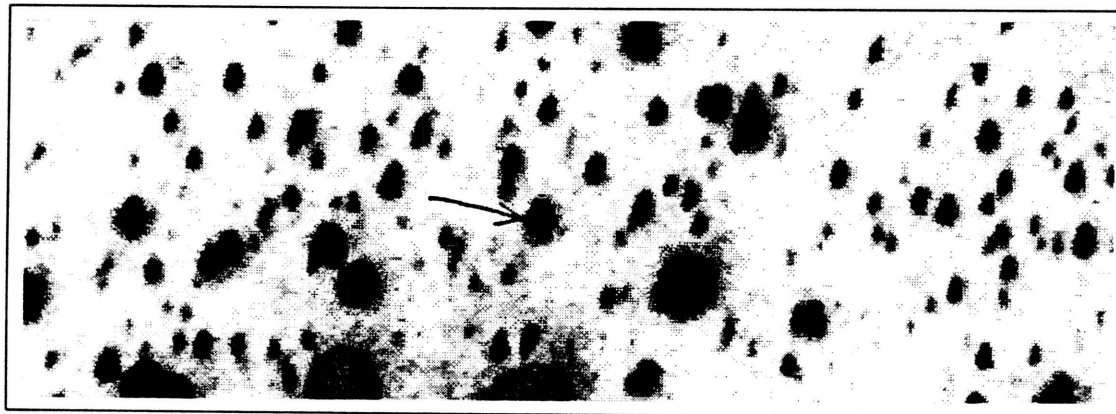
Coordinates: α (1950) = 18:03:47.7 δ (1950) = +28:04:32

Spectral Type: M4.5 V

Photometry: $I_{\text{KC}} = 17.94$ $R_{\text{CTI}} = \text{unknown}$ $(V-I)_{\text{KC}} = \text{unknown}$ $(R-I)_{\text{CTI}} = \text{unknown}$ $(V-I)_{\text{CTI}} = \text{unknown}$

Notes:

CTI 185818.3+280045



CTI FINDER CHART

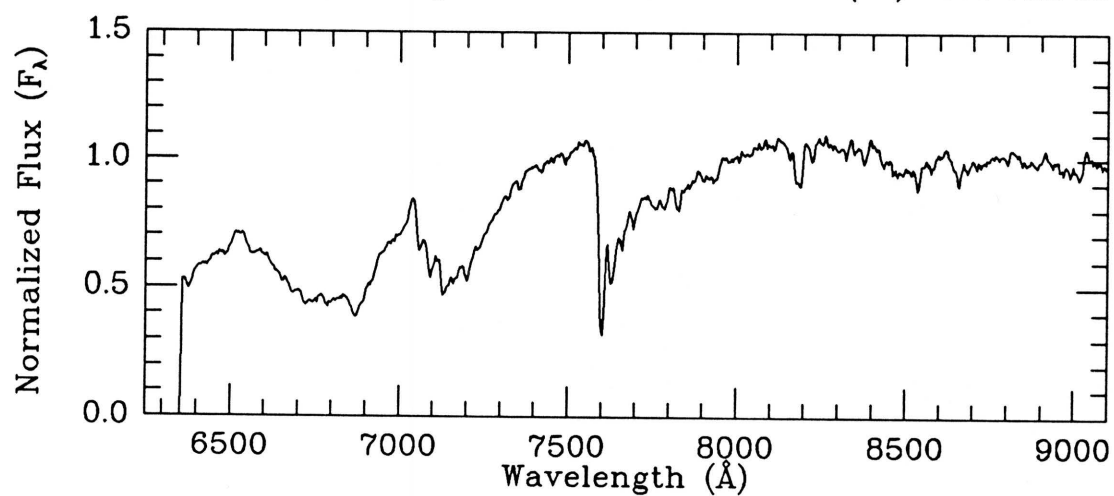
I filter

Coadded frame

MMT SPECTRUM

Exposure: 300 sec

Obs. (UT) 1991 Jun 23

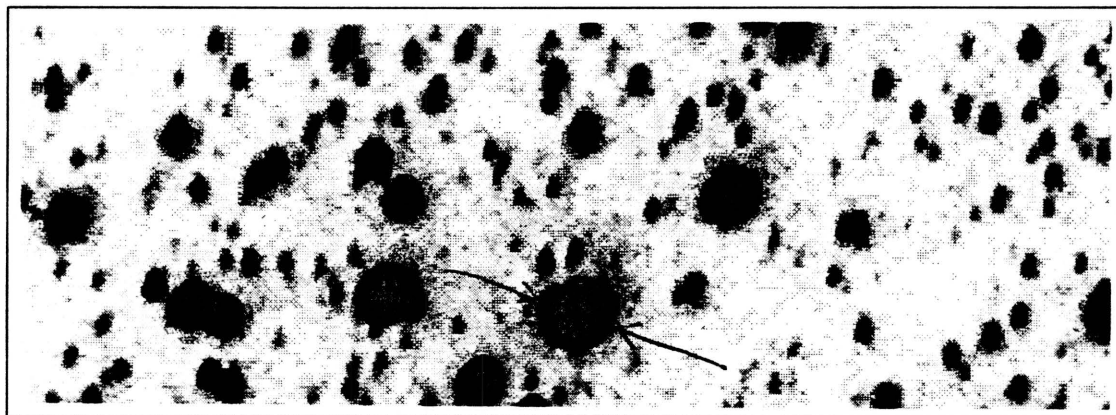
Coordinates: α (1950) = 18:56:48.8 δ (1950) = +27:57:38

Spectral Type: M2.5 V

Photometry: $I_{KC} = 14.06$ $R_{CTI} = 14.82$ $(V-I)_{KC} = 2.28 \pm 0.11$ $(R-I)_{CTI} = 0.67 \pm 0.01$ $(V-I)_{CTI} = \text{unknown}$

Notes:

CTI 185818.4+275940



CTI FINDER CHART

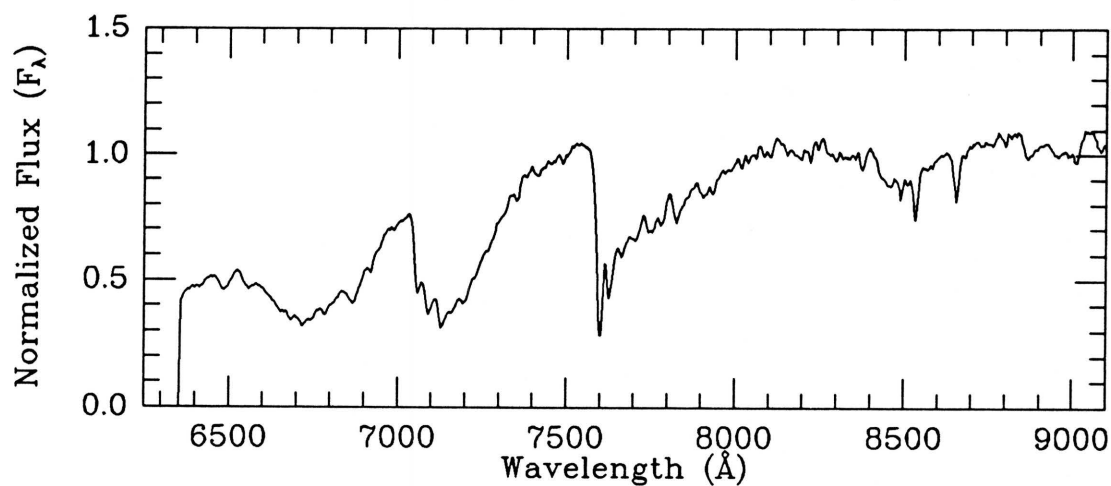
I filter

Coadded frame

MMT SPECTRUM

Exposure: 30 sec

Obs. (UT) 1991 Jun 23

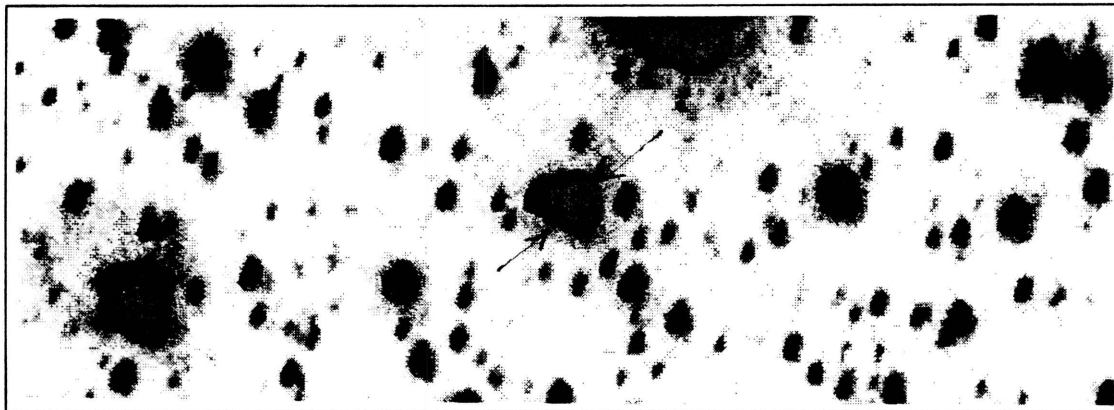
Coordinates: α (1950) = 18:56:48.9 δ (1950) = +27:56:33

Spectral Type: M3 III

Photometry: I_{KC} = unknown R_{CTI} = 11.81 $(V-I)_{KC}$ =unknown $(R-I)_{CTI}$ =0.36 \pm 0.01 $(V-I)_{CTI}$ =1.24 \pm 0.01

Notes: CTI R and I measures probably saturated. A Mira variable whose 14 CTI V measures range from 12.6 to 12.8. Not listed in General Cat. of Variable Stars (Kholopov 1985).

CTI 190006.7+280451



CTI FINDER CHART

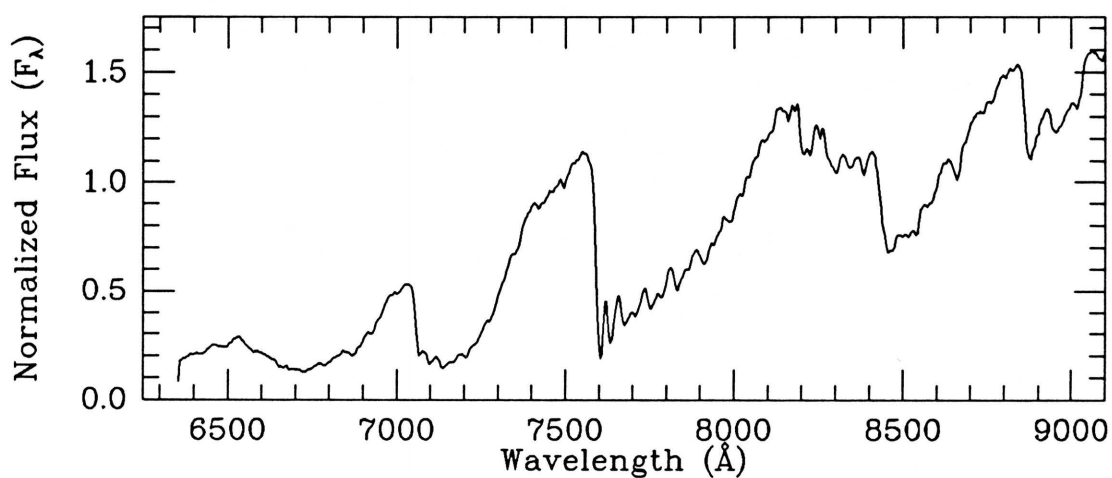
I filter

Coadded frame

MMT SPECTRUM

Exposure: 300 sec

Obs. (UT) 1991 Jun 22

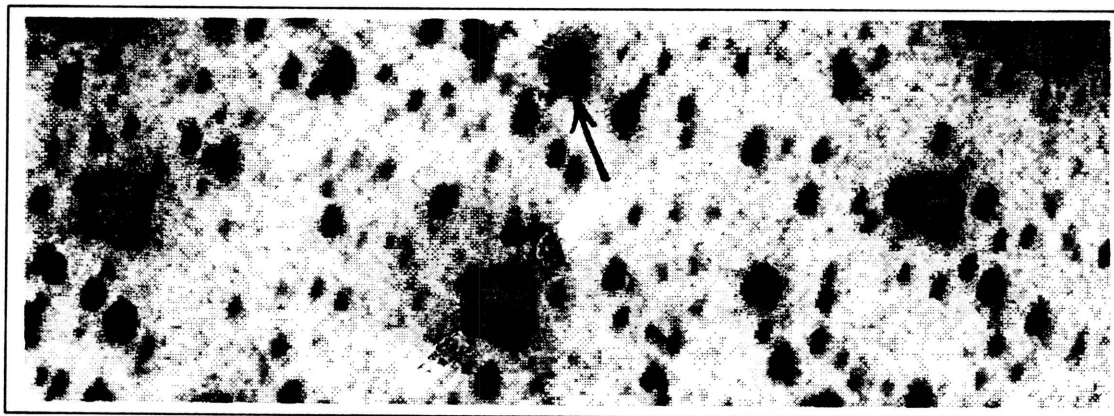
Coordinates: α (1950) = 18:58:37.2 δ (1950) = +28:01:38

Spectral Type: M5.5 III

Photometry: I_{KC} = unknown R_{CTI} = 12.72 $(V-I)_{KC}$ =unknown $(R-I)_{CTI}=1.48\pm.01$ $(V-I)_{CTI}=3.78\pm.01$

Notes: A Mira variable whose 13 CTI V measures range from 14.8 to 15.2. Not listed in General Cat. of Variable Stars (Kholopov 1985).

CTI 190016.9+280539



CTI FINDER CHART

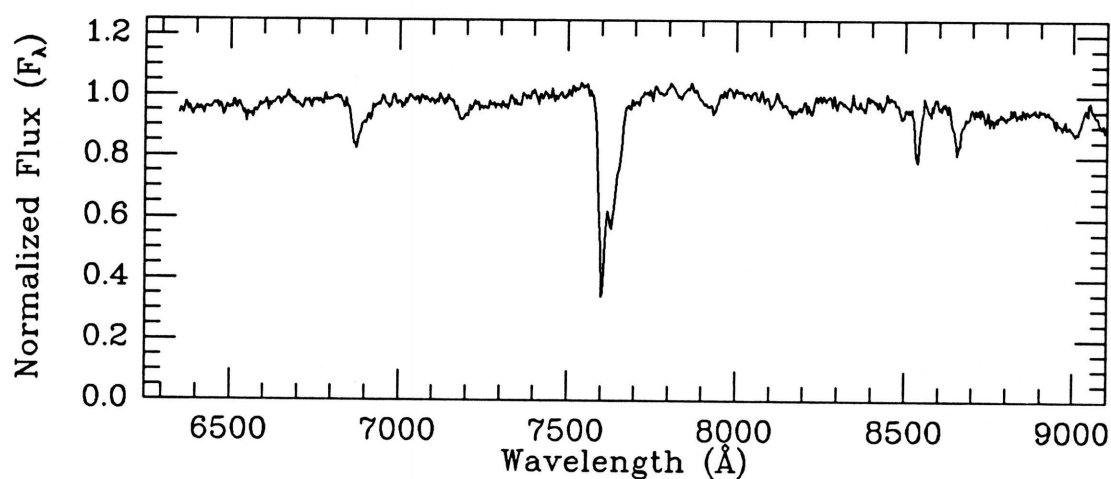
I filter

Coadded frame

MMT SPECTRUM

Exposure: 300 sec

Obs. (UT) 1991 Jun 24

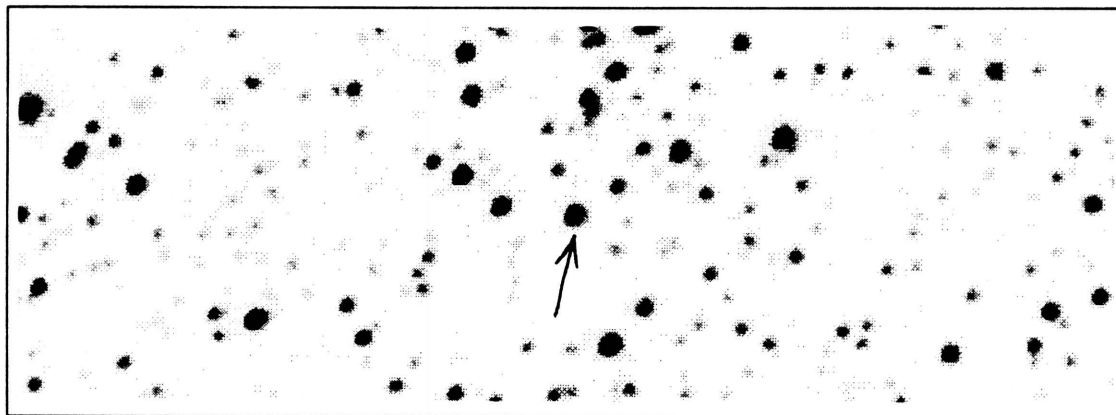
Coordinates: α (1950) = 18:58:47.4 δ (1950) = +28:02:26

Spectral Type: K7 III

Photometry: I_{KC} = unknown R_{CTI} = 13.45 $(V-I)_{KC}$ =unknown $(R-I)_{CTI}=0.34\pm0.01$ $(V-I)_{CTI}=1.24\pm0.01$

Notes: Possible Mira variable whose 12 CTI V measures range from 14.27 to 14.37. Not listed in General Cat. of Variable Stars (Kholopov 1985).

CTI 190917.7+280305



CTI FINDER CHART

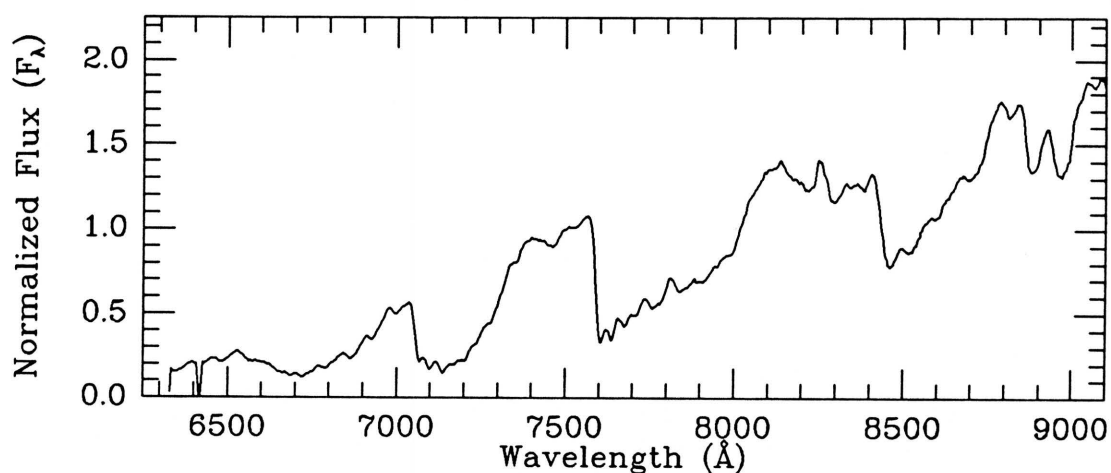
V filter?

Obs. (UT) not known

MMT SPECTRUM

Exposure: 3 sec

Obs. (UT) 1989 Jul 10

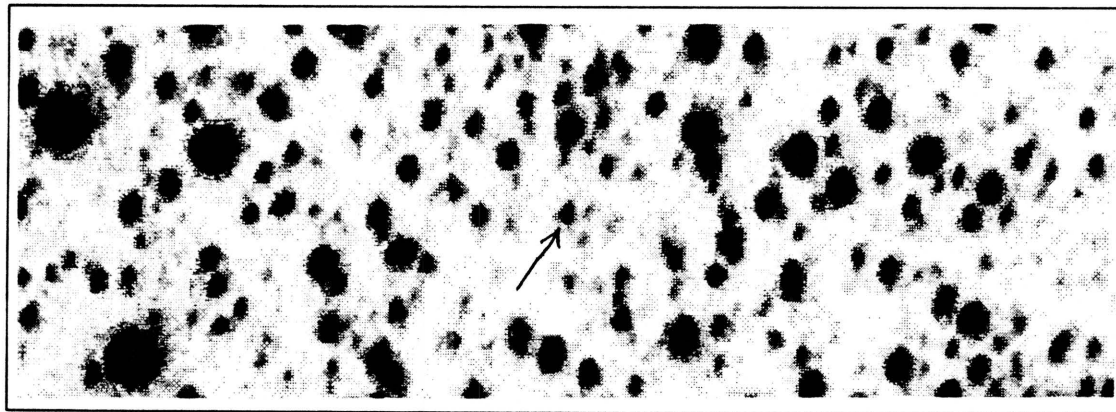
Coordinates: α (1950) = 19:07:47.9 δ (1950) = +27:59:24

Spectral Type: M6 III

Photometry: I_{KC} = unknown R_{CTI} = 9.99 $(V-I)_{KC}$ =unknown $(R-I)_{CTI}$ =2.61: $(V-I)_{CTI}$ =6.00:

Notes: CTI R value is saturated. A Mira variable having 6 CTI V measures ranging from 11.3 to 14.2 over 100 days. Given as TY Lyrae in General Cat. of Variable Stars (Kholopov 1985).

CTI 191216.8+280229



CTI FINDER CHART

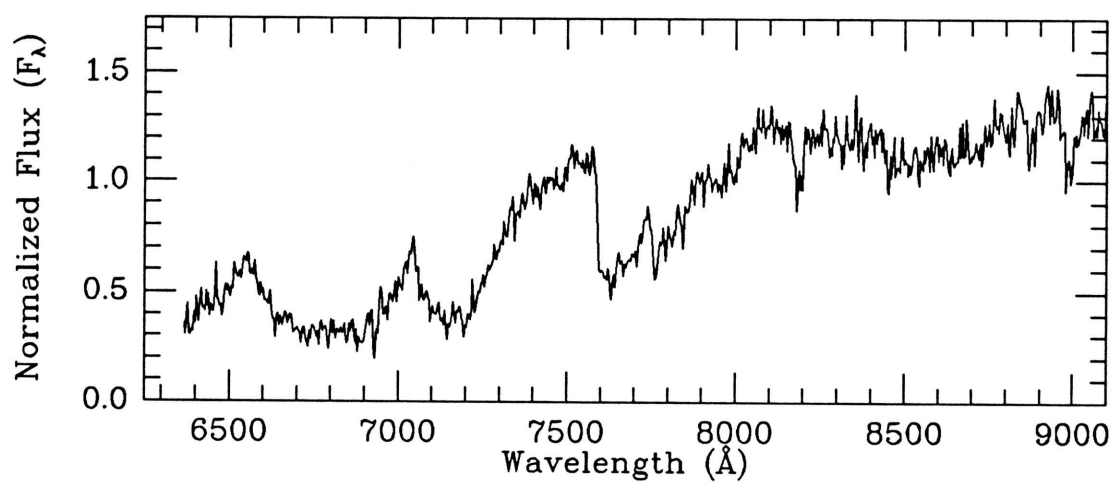
I filter

Coadded frame

MMT SPECTRUM

Exposure: 2700 sec

Obs. (UT) 1991 Oct 17

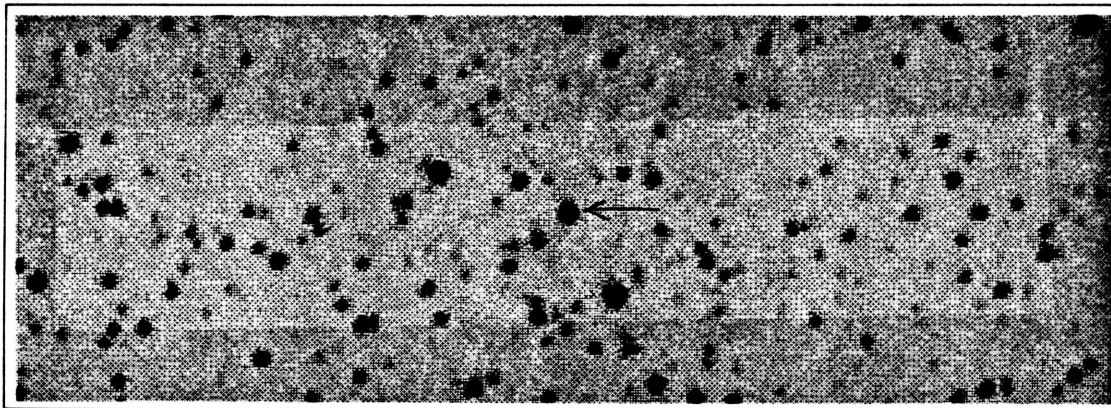
Coordinates: α (1950) = 19:10:46.9 δ (1950) = +27:58:38

Spectral Type: M4 V

Photometry: $I_{KC} = 17.17$ $R_{CTI} = 19.61$ $(V-I)_{KC} = 2.95 \pm 0.06$ $(R-I)_{CTI} = 2.11 \pm 0.4$ $(V-I)_{CTI} = 4.45 \pm 0.4$

Notes: Actual USNO VI photometry.

CTI 191258.9+280352



CTI FINDER CHART

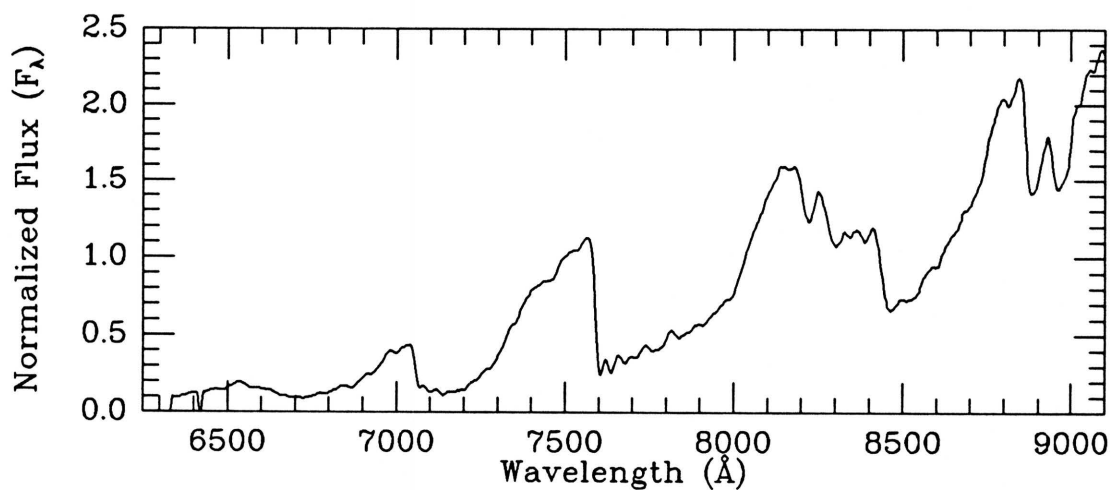
V filter

Obs. (UT) 1988 Jun 08

MMT SPECTRUM

Exposure: 135 sec

Obs. (UT) 1989 Jul 10

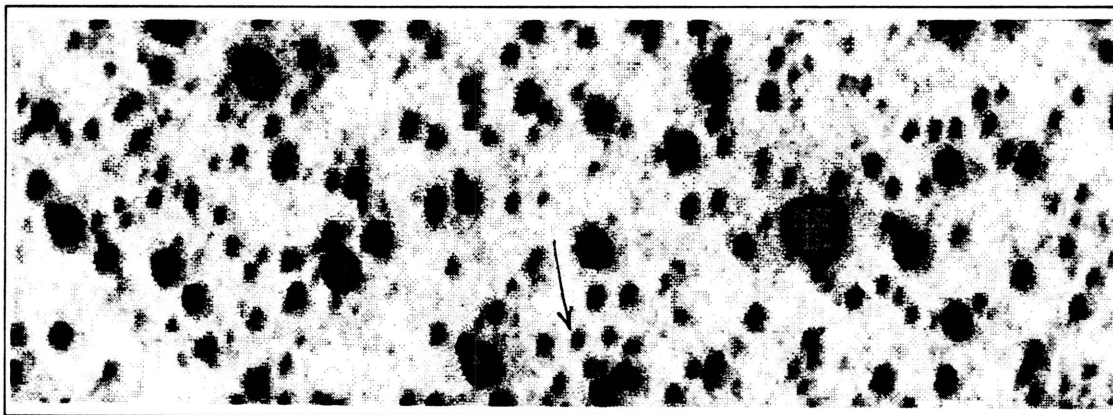
Coordinates: α (1950) = 19:11:29.0 δ (1950) = +27:59:59

Spectral Type: M7 III

Photometry: I_{KC} = unknown R_{CTI} = 11.56 $(V-I)_{KC}$ =unknown $(R-I)_{CTI}=1.46\pm0.01$ $(V-I)_{CTI}=3.75\pm0.01$

Notes: CTI I, and possibly R, saturated. A Mira variable whose 14 CTI V measures range from 13.5 to 14.2. Not listed in the General Catalogue of Variable Stars (Kholopov 1985).

CTI 191326.8+275930



CTI FINDER CHART

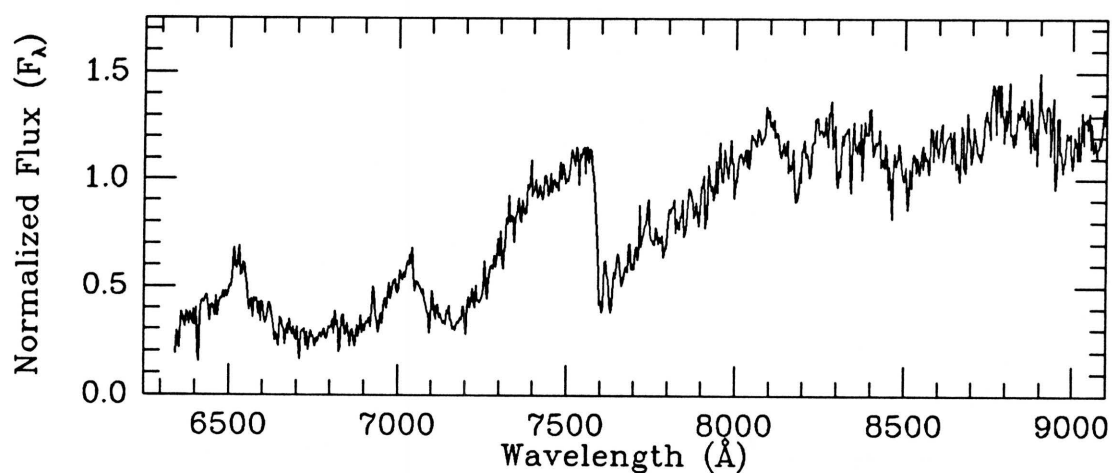
I filter

Coadded frame

MMT SPECTRUM

Exposure: 1500 sec

Obs. (UT) 1991 Sep 15

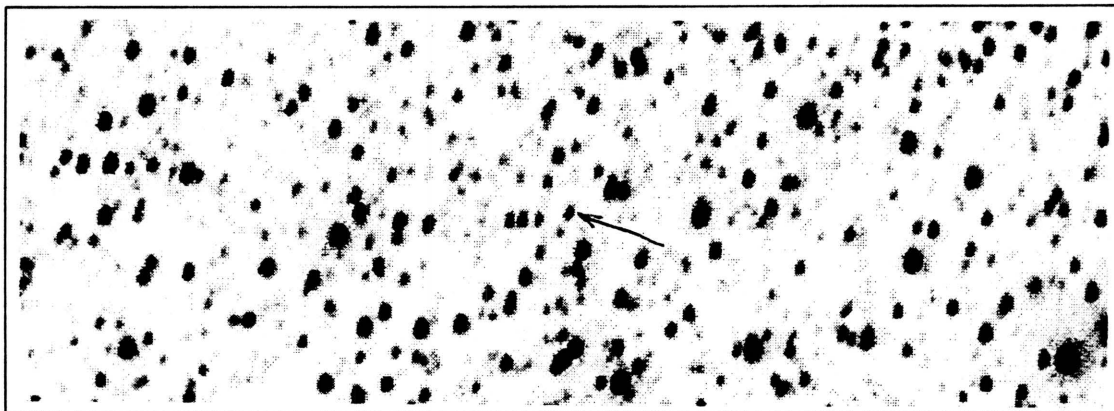
Coordinates: α (1950) = 19:11:56.8 δ (1950) = +27:55:36

Spectral Type: M4.5 V

Photometry: $I_{\text{KC}} = 17.76$ $R_{\text{CTI}} = 20.17$ $(V-I)_{\text{KC}} = 4.88 \pm 1.06$ $(R-I)_{\text{CTI}} = 2.49 \pm 0.73$ $(V-I)_{\text{CTI}} = \text{unknown}$

Notes:

CTI 192121.7+280100



CTI FINDER CHART

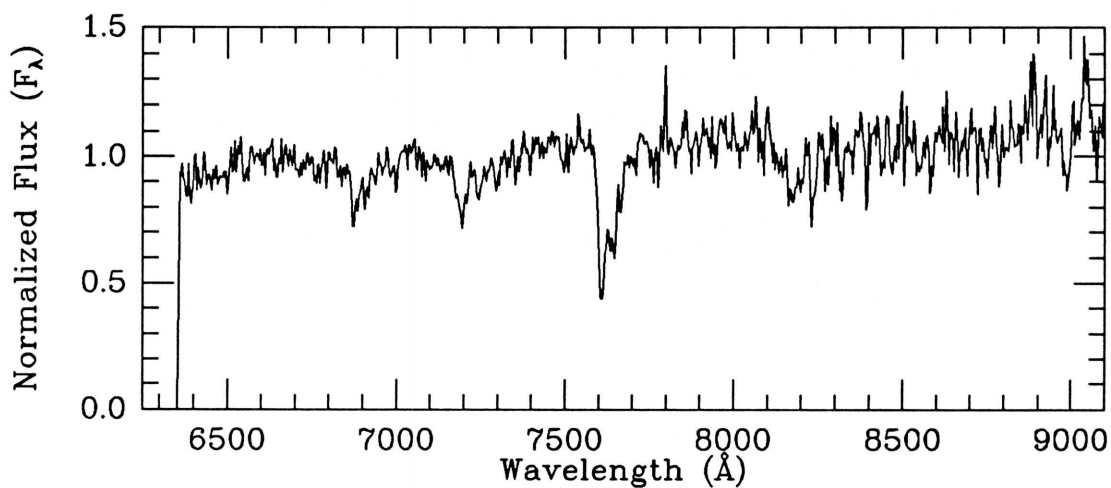
I filter

Obs. (UT) 1990 Jun 20

MMT SPECTRUM

Exposure: 300 sec

Obs. (UT) 1990 Sep 14

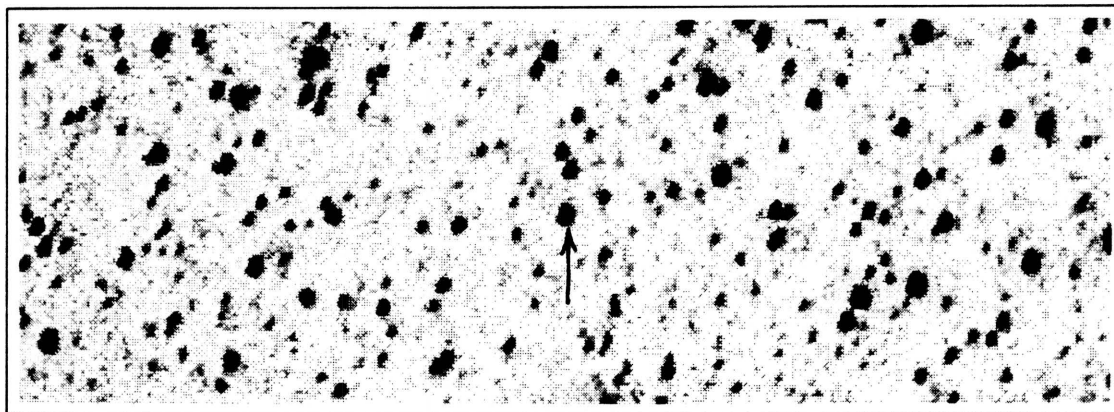
Coordinates: α (1950) = 19:19:51.4 δ (1950) = +27:56:41

Spectral Type: M0 V

Photometry: $I_{KC} = 14.26$ $R_{CTI} = 16.62$ $(V-I)_{KC} = 4.58 \pm 0.18$ $(R-I)_{CTI} = 2.28 \pm 0.06$ $(V-I)_{CTI} = 3.56 \pm 0.06$

Notes:

CTI 192853.3+280415



CTI FINDER CHART

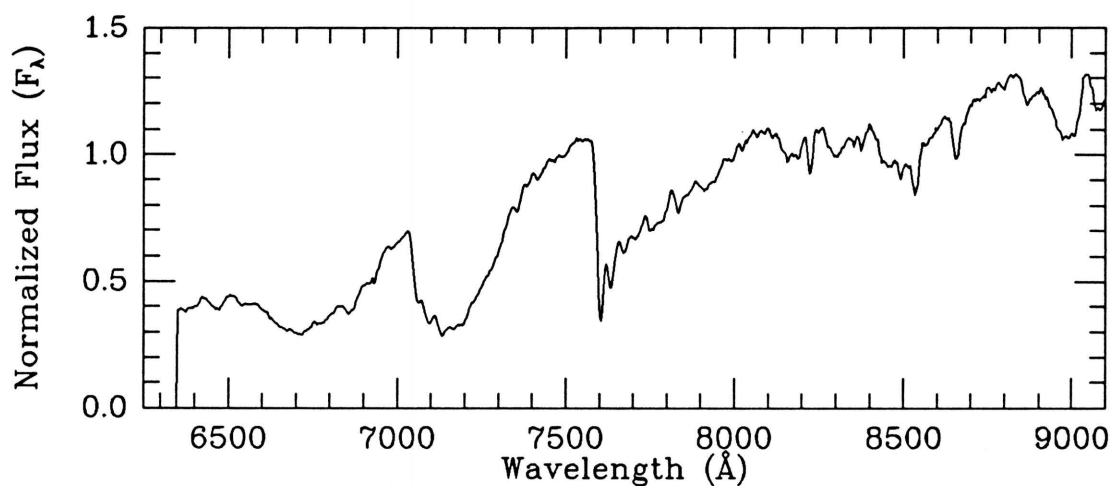
I filter

Obs. (UT) 1990 Aug 24

MMT SPECTRUM

Exposure: 600 sec

Obs. (UT) 1991 Sep 15

Coordinates: α (1950) = 19:27:22.8 δ (1950) = +27:59:33

Spectral Type: M4 III

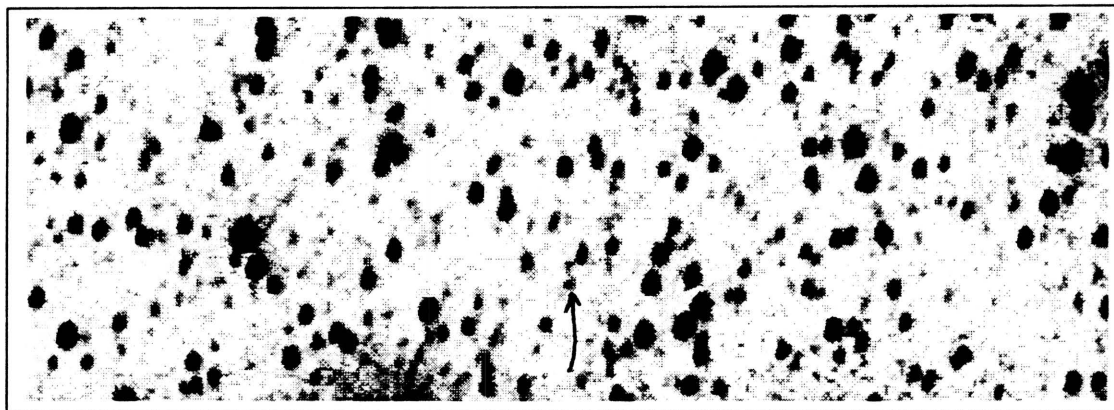
Photometry: $I_{KC} = 12.89$ $R_{CTI} = 14.08$ $(V-I)_{KC} = 2.90 \pm 0.04$ $(R-I)_{CTI} = 1.08 \pm 0.01$ $(V-I)_{CTI} = 2.84 \pm 0.01$

Notes: Actual USNO VI photometry. A possible Mira variable.

Not listed in the General Catalogue of Variable Stars

(Kholopov 1985).

CTI 202636.9+275934



CTI FINDER CHART

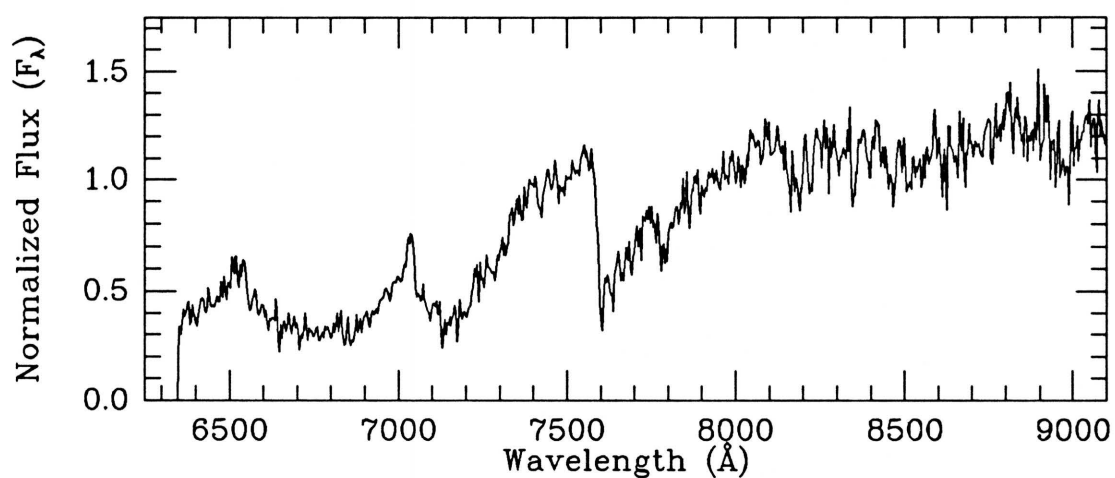
I filter

Coadded image

MMT SPECTRUM

Exposure: 2700 sec

Obs. (UT) 1991 Sep 15

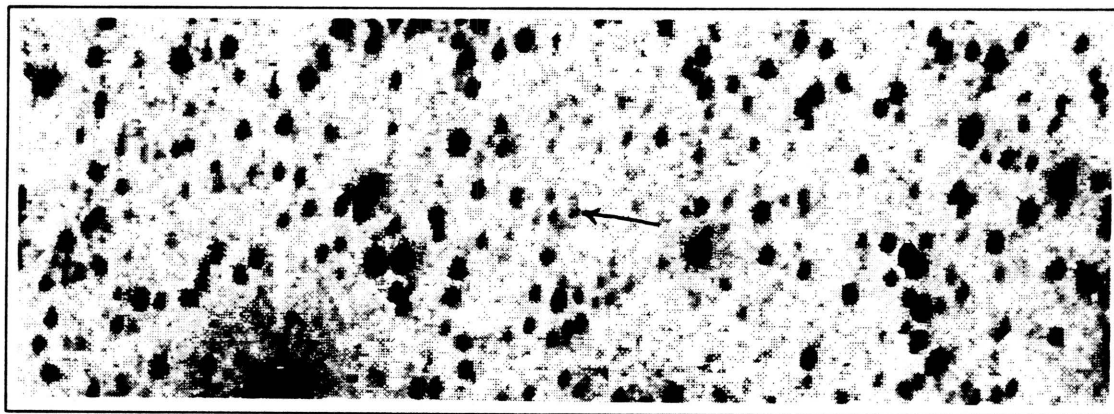
Coordinates: α (1950) = 20:25:03.0 δ (1950) = +27:52:07

Spectral Type: M4 V

Photometry: I_{KC} = unknown R_{CTI} = unknown $(V-I)_{KC}$ =unknown $(R-I)_{CTI}$ =unknown $(V-I)_{CTI}$ =4.44:

Notes:

CTI 202738.5+280227



CTI FINDER CHART

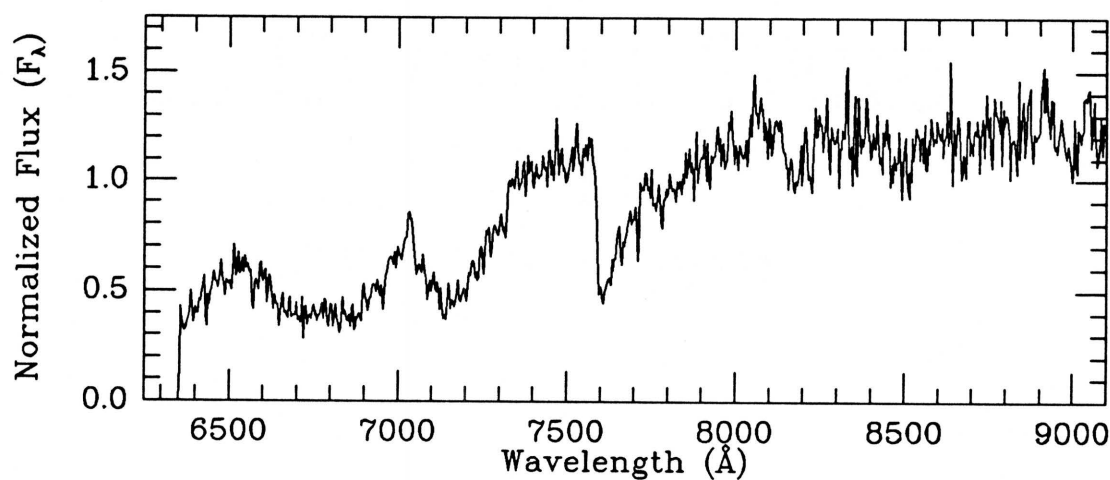
I filter

Coadded image

MMT SPECTRUM

Exposure: 2400 sec

Obs. (UT) 1991 Sep 15

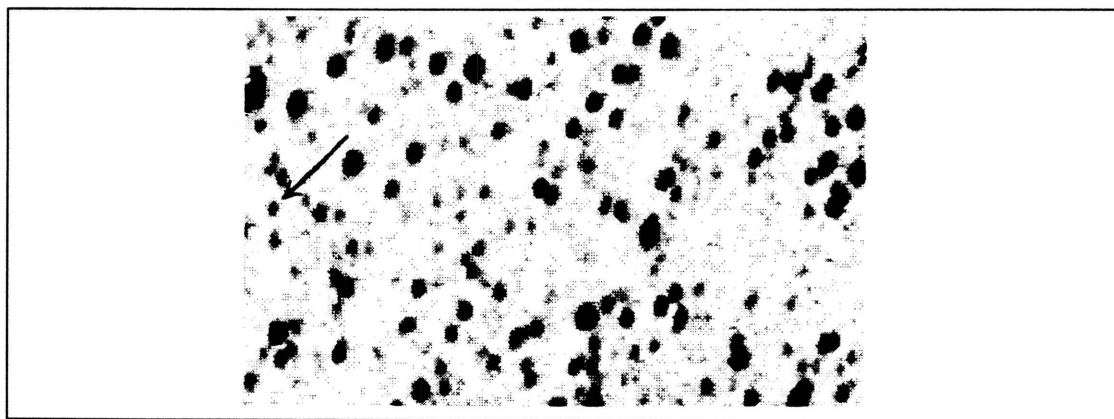
Coordinates: α (1950) = 20:26:04.6 δ (1950) = +27:54:58

Spectral Type: M3 V

Photometry: $I_{KC} = 18.45$ $R_{CTI} = 20.89$ $(V-I)_{KC} = 2.53 \pm 0.13$ $(R-I)_{CTI} = 2.86 \pm 0.5$ $(V-I)_{CTI} = 4.16 \pm 0.5$

Notes: Actual USNO VI photometry. Comparison to POSS E print suggests possible small proper motion (~ 0.3 arcsec/yr) to the NNE.

CTI 202928.1+280152



CTI FINDER CHART

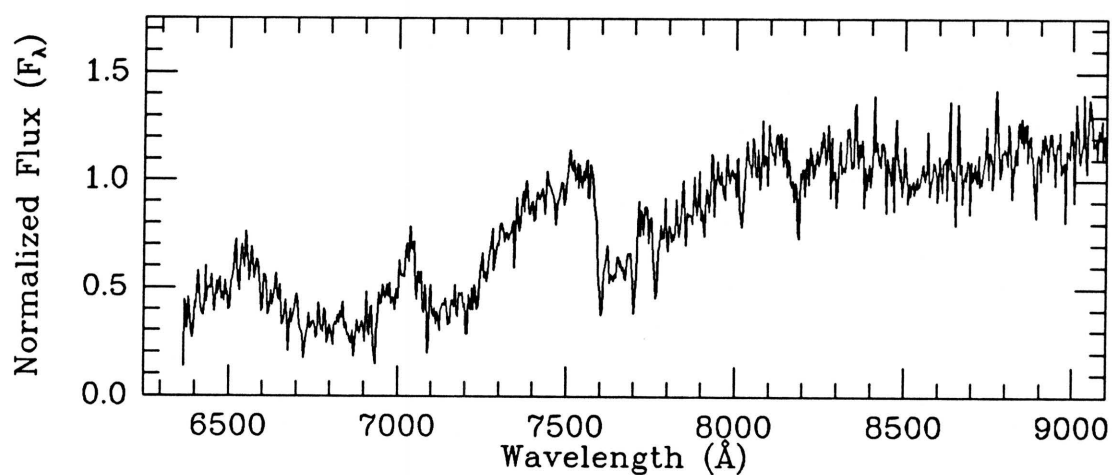
I filter

Coadded image

MMT SPECTRUM

Exposure: 2400 sec

Obs. (UT) 1991 Oct 17

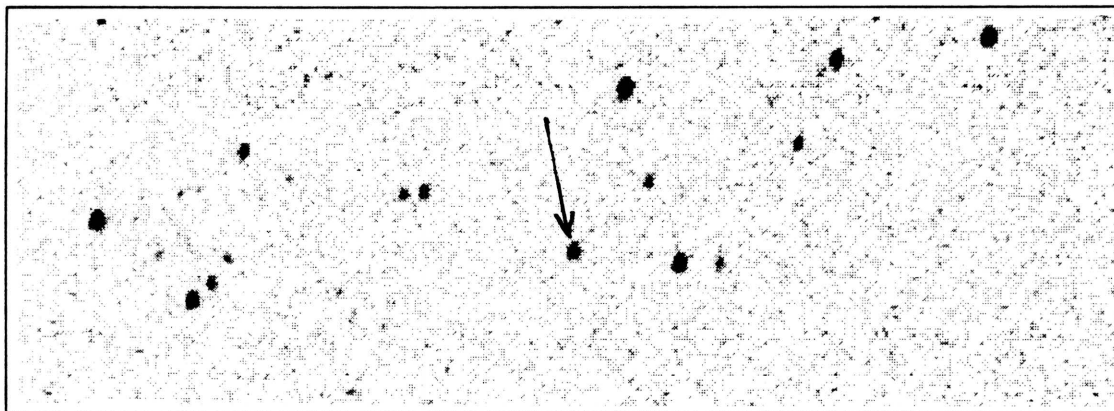
Coordinates: α (1950) = 20:27:54.0 δ (1950) = +27:54:18

Spectral Type: M4 V

Photometry: $I_{KC} = 17.84$ $R_{CTI} = 20.46$ $(V-I)_{KC} = 5.20 \pm 0.74$ $(R-I)_{CTI} = 2.71 \pm .5$ $(V-I)_{CTI} = 3.62 \pm .5$

Notes:

CTI 223752.5+275918



CTI FINDER CHART

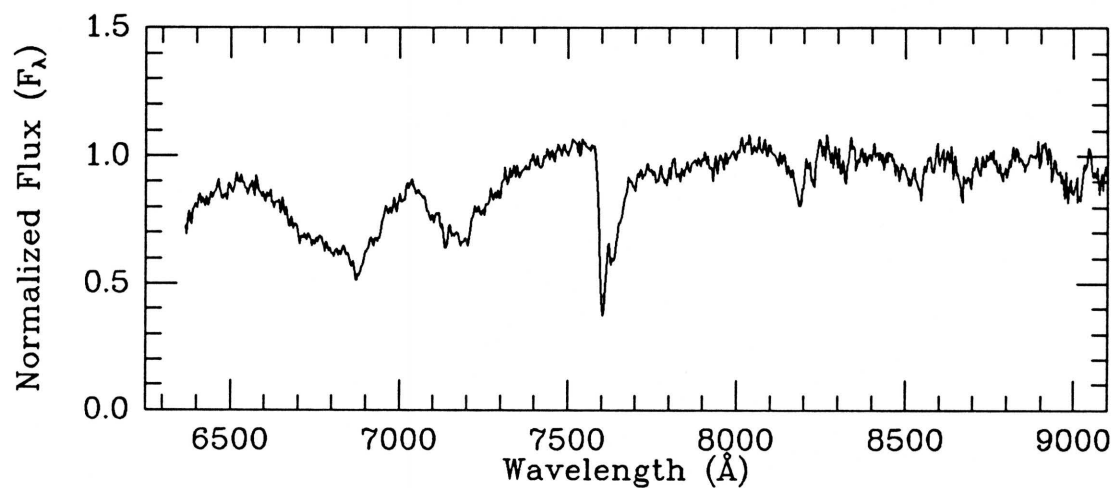
I filter

Obs. (UT) 1990 Aug 24

MMT SPECTRUM

Exposure: 300 sec

Obs. (UT) 1991 Oct 17

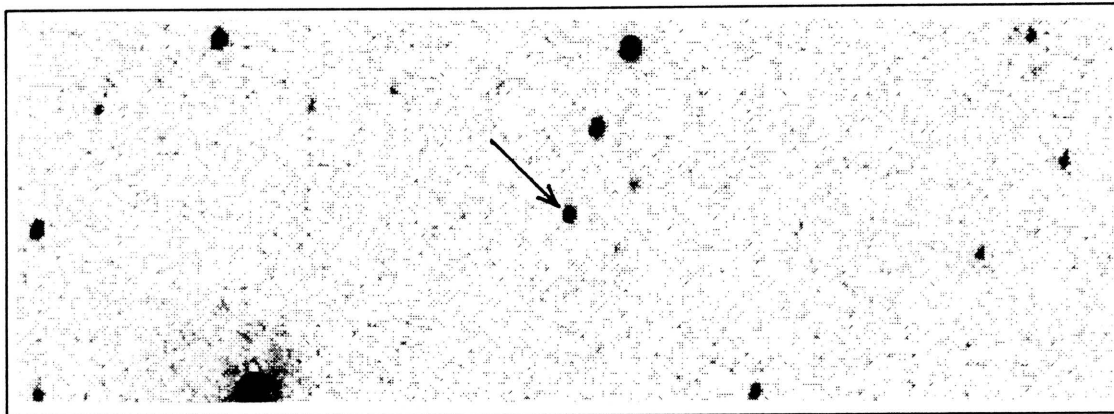
Coordinates: α (1950) = 22:36:06.6 δ (1950) = +27:47:35

Spectral Type: M1 V

Photometry: $I_{KC} = 14.76$ $R_{CTI} = 15.32$ $(V-I)_{KC} = 2.06 \pm 0.06$ $(R-I)_{CTI} = 0.48 \pm 0.03$ $(V-I)_{CTI} = 1.89 \pm 0.01$

Notes: Actual USNO VI photometry.

CTI 224056.1+280052



CTI FINDER CHART

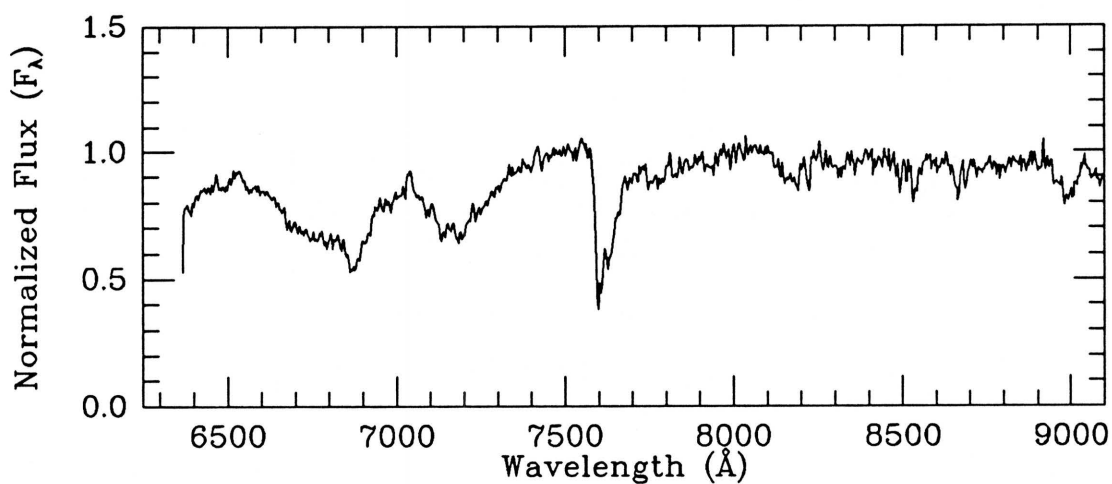
I filter

Obs. (UT) 1990 Aug 24

MMT SPECTRUM

Exposure: 600 sec

Obs. (UT) 1991 Oct 17

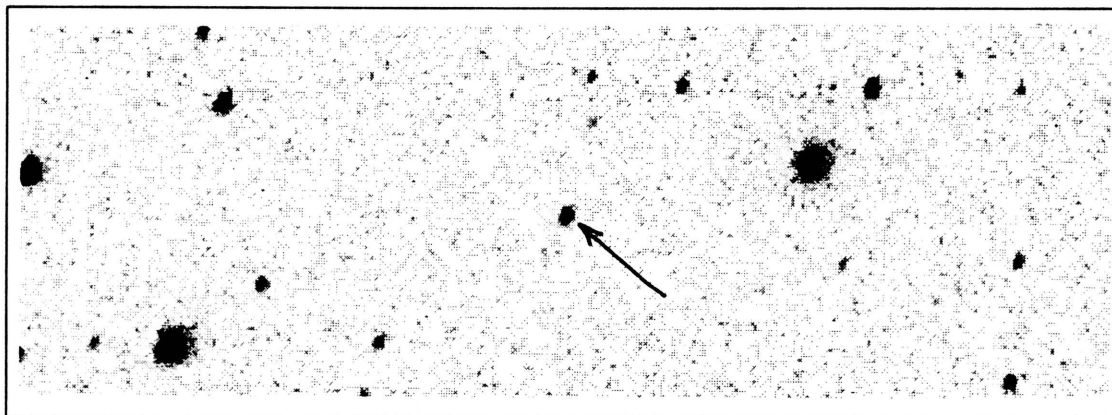
Coordinates: α (1950) = 22:39:09.9 δ (1950) = +27:49:06

Spectral Type: M1 V

Photometry: $I_{KC} = 14.67$ $R_{CTI} = 15.18$ $(V-I)_{KC} = 1.97 \pm .11$ $(R-I)_{CTI} = 0.45 \pm .03$ $(V-I)_{CTI} = 1.82 \pm .01$

Notes:

CTI 225024.0+275956



CTI FINDER CHART

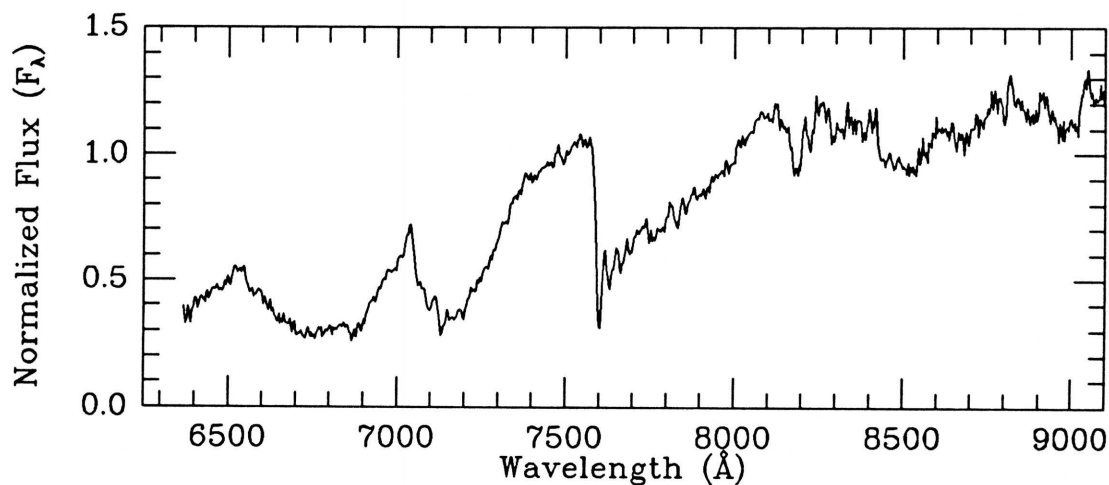
I filter

Obs. (UT) 1990 Aug 24

MMT SPECTRUM

Exposure: 300 sec

Obs. (UT) 1991 Oct 17

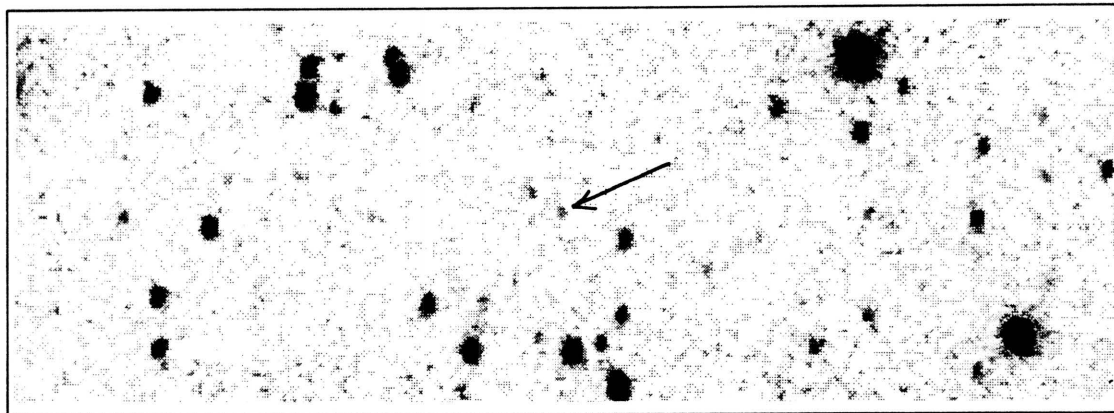
Coordinates: α (1950) = 22:48:36.8 δ (1950) = +27:48:00

Spectral Type: M4 V

Photometry: $I_{KC} = 14.43$ $R_{CTI} = 15.64$ $(V-I)_{KC} = 2.95 \pm 0.13$ $(R-I)_{CTI} = 1.14 \pm 0.03$ $(V-I)_{CTI} = 2.86 \pm 0.01$

Notes:

CTI 225431.2+280046



CTI FINDER CHART

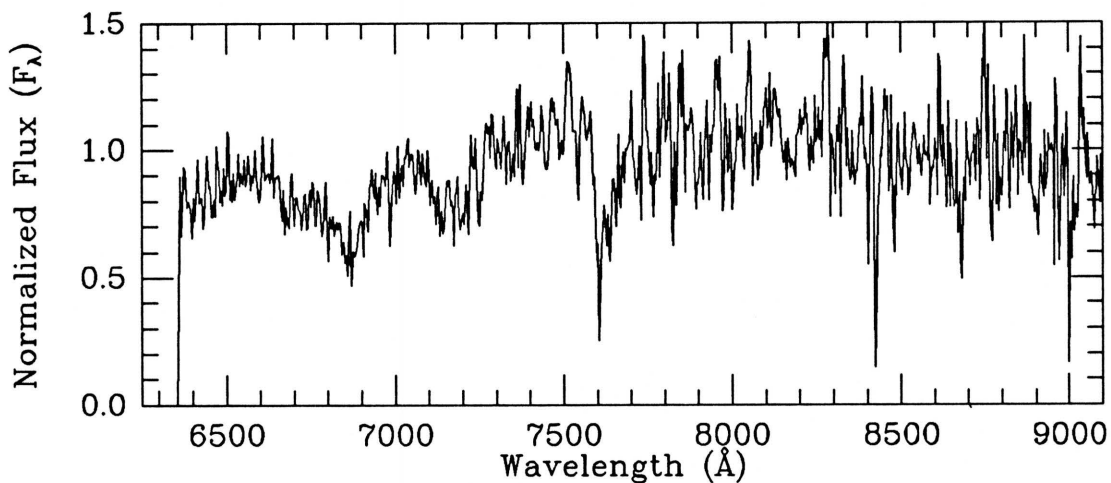
I filter

Coadded frame

MMT SPECTRUM

Exposure: 2400 sec

Obs. (UT) 1991 Jun 24

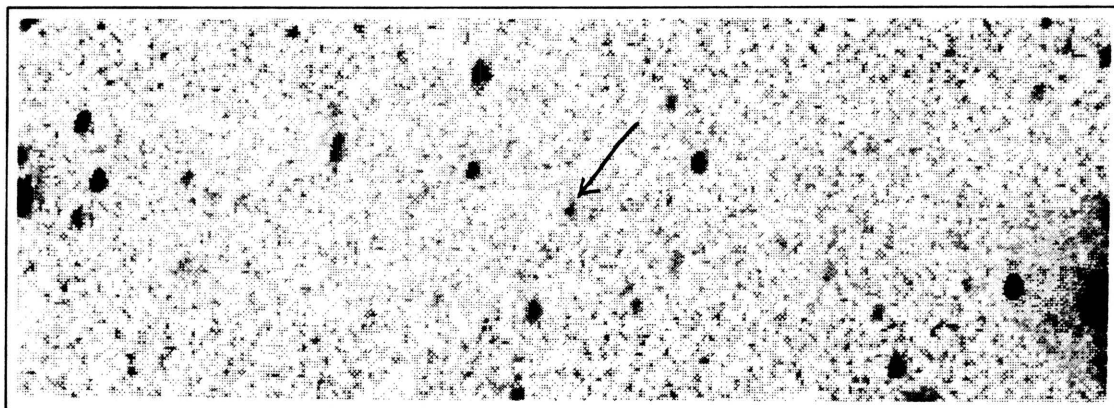
Coordinates: α (1950) = 22:52:43.5 δ (1950) = +27:48:46

Spectral Type: sdM0:

Photometry: I_{KC} = unknown R_{CTI} = 20.59 $(V-I)_{KC}$ =unknown $(R-I)_{CTI}=2.15\pm.60$ $(V-I)_{CTI}$ =unknown

Notes:

CTI 225508.5+280234



CTI FINDER CHART

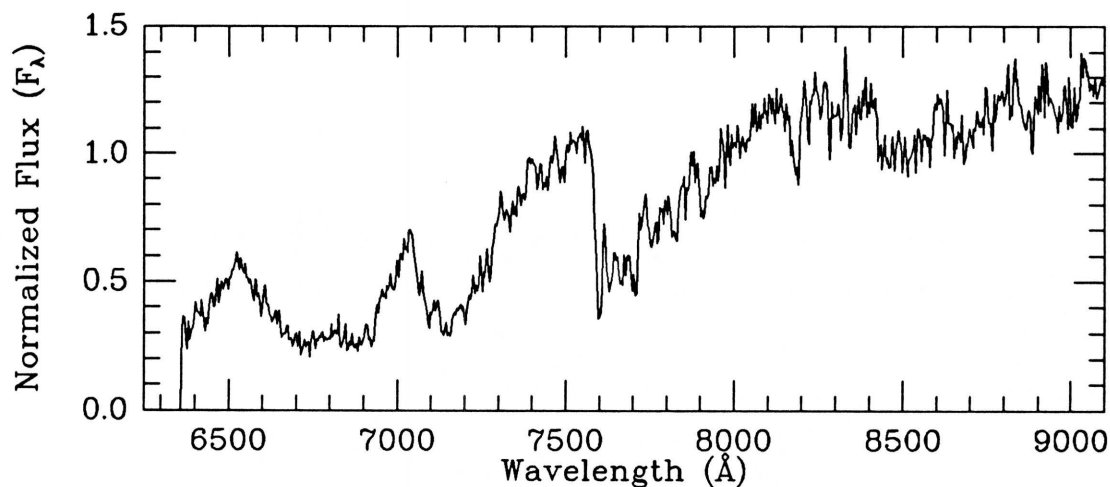
I filter

Coadded frame

MMT SPECTRUM

Exposure: 2400 sec

Obs. (UT) 1991 Jun 22

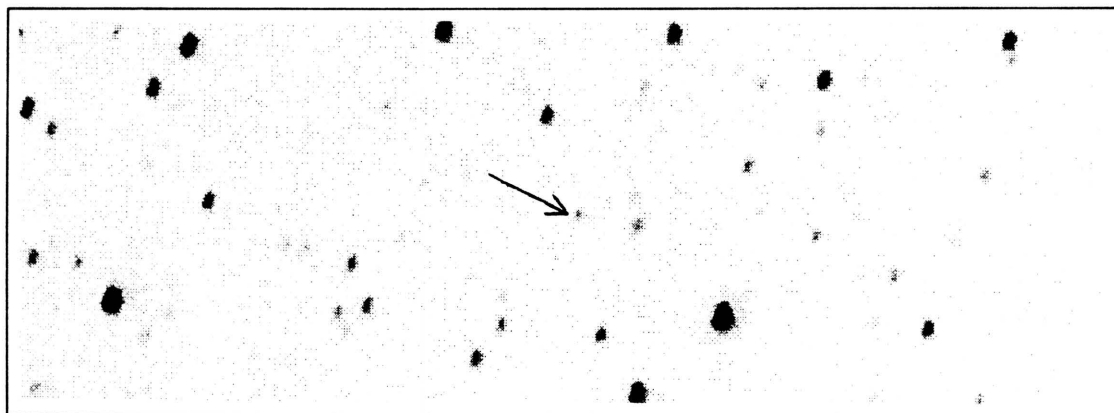
Coordinates: α (1950) = 22:53:20.7 δ (1950) = +27:50:33

Spectral Type: M4 V

Photometry: $I_{KC} = 17.76$ $R_{CTI} = 19.67$ $(V-I)_{KC} = 4.17 \pm .55$ $(R-I)_{CTI} = 1.99 \pm .37$ $(V-I)_{CTI} = \text{unknown}$

Notes:

CTI 230047.6+280216



CTI FINDER CHART

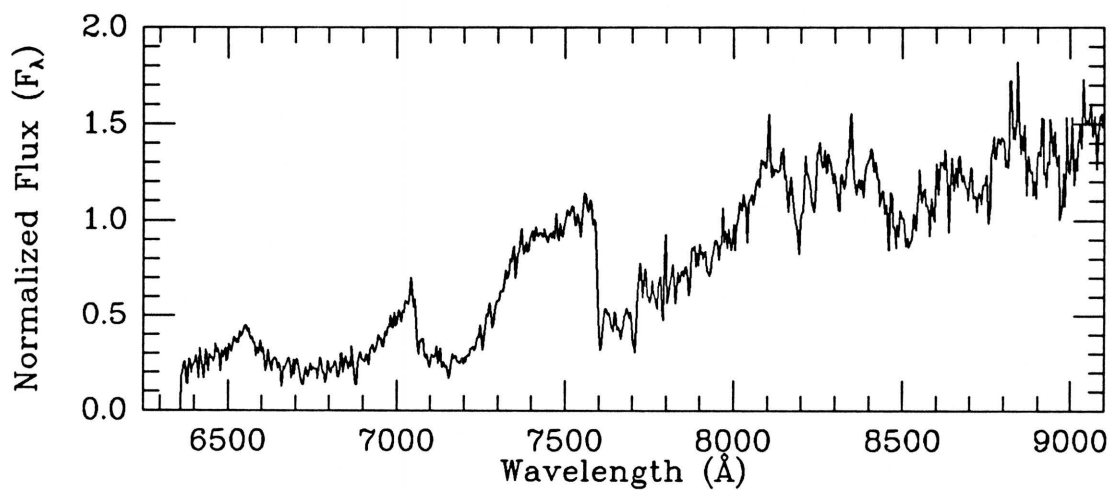
I filter

Obs. (UT) 1988 Nov 01

MMT SPECTRUM

Exposure: 3900 sec

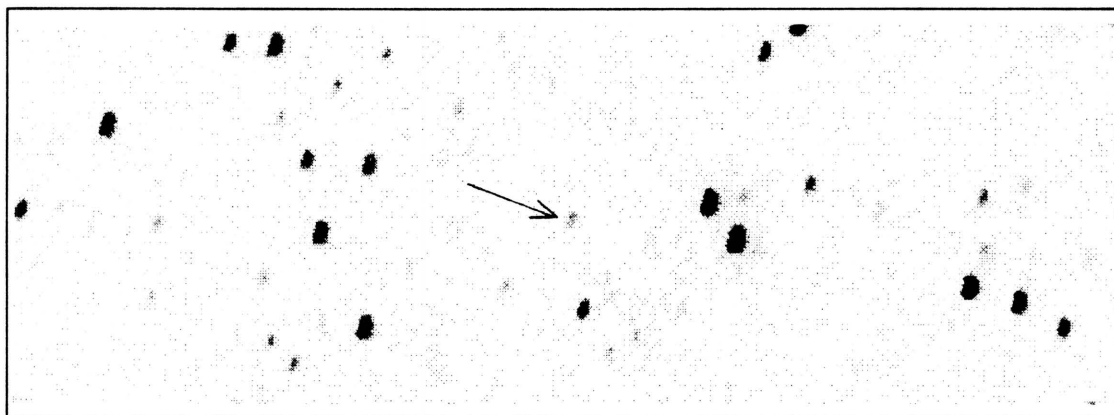
Obs. (UT) 1990 Sep 14

Coordinates: α (1950) = 22:58:59.2 δ (1950) = +27:50:10

Spectral Type: M5 V

Photometry: $I_{\text{KC}} = 17.76$ $R_{\text{CTI}} = 19.50$ $(V-I)_{\text{KC}} = 3.93 \pm .55$ $(R-I)_{\text{CTI}} = 1.82 \pm .37$ $(V-I)_{\text{CTI}} = \text{unknown}$ Notes: Comparison to POSS E print suggests possible small proper motion (~ 0.15 arcsec/yr) to the ESE.

CTI 232425.5+275949



CTI FINDER CHART

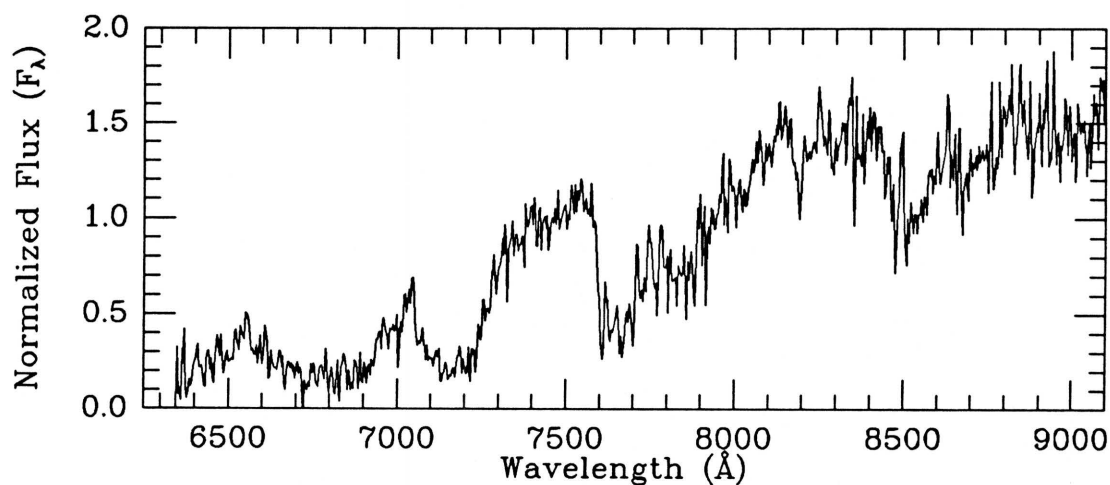
I filter

Obs. (UT) 1988 Nov 01

MMT SPECTRUM

Exposure: 3900 sec

Obs. (UT) 1990 Nov 23

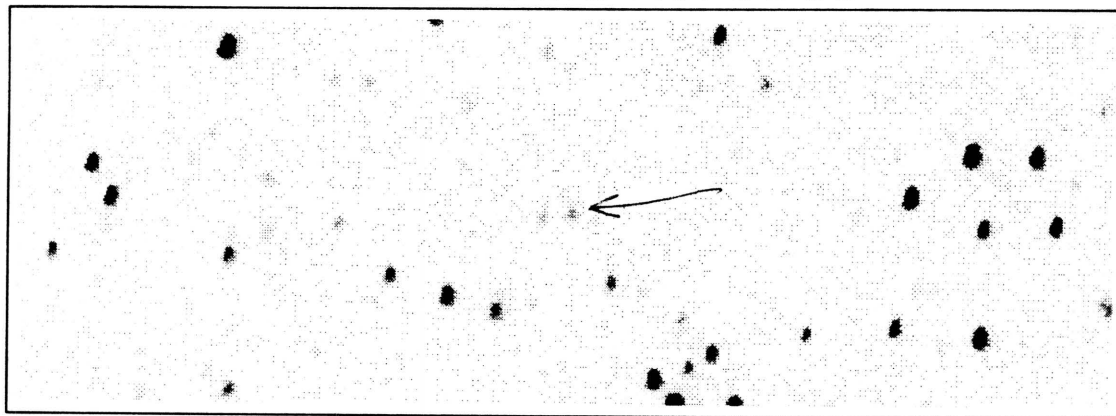
Coordinates: α (1950) = 23:22:34.4 δ (1950) = +27:47:27

Spectral Type: M5.5 V

Photometry: $I_{KC} = 17.94$ $R_{CTI} = 19.79$ $(V-I)_{KC} = 4.10 \pm 0.56$ $(R-I)_{CTI} = 1.94 \pm 0.38$ $(V-I)_{CTI} = \text{unknown}$

Notes:

CTI 233201.1+275943



CTI FINDER CHART

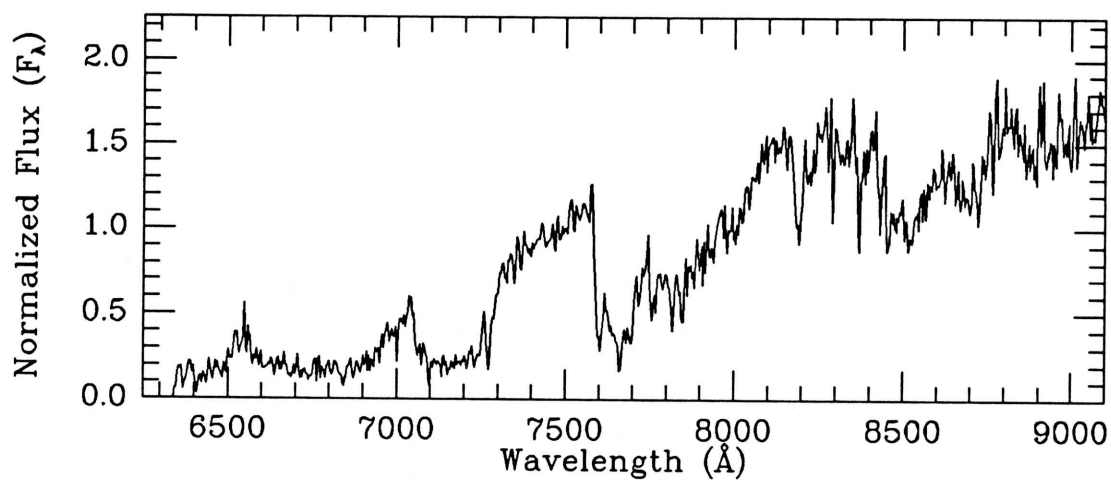
I filter

Obs. (UT) 1988 Nov 01

MMT SPECTRUM

Exposure: 3900 sec

Obs. (UT) 1990 Nov 22

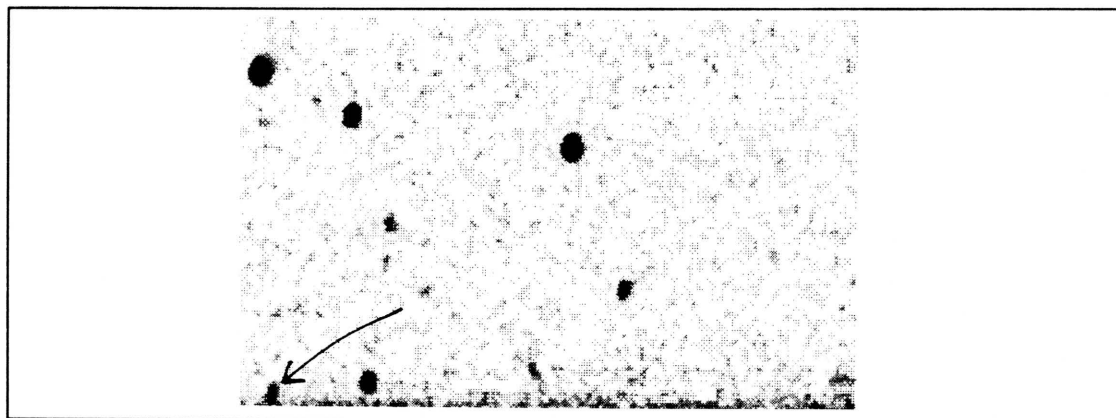
Coordinates: α (1950) = 23:30:09.2 δ (1950) = +27:47:17

Spectral Type: M6 V

Photometry: $I_{KC} = 17.90$ $R_{CTI} = 20.02$ $(V-I)_{KC} = 4.48 \pm 0.62$ $(R-I)_{CTI} = 2.21 \pm 0.42$ $(V-I)_{CTI} = \text{unknown}$

Notes:

CTI 233828.2+275817



CTI FINDER CHART

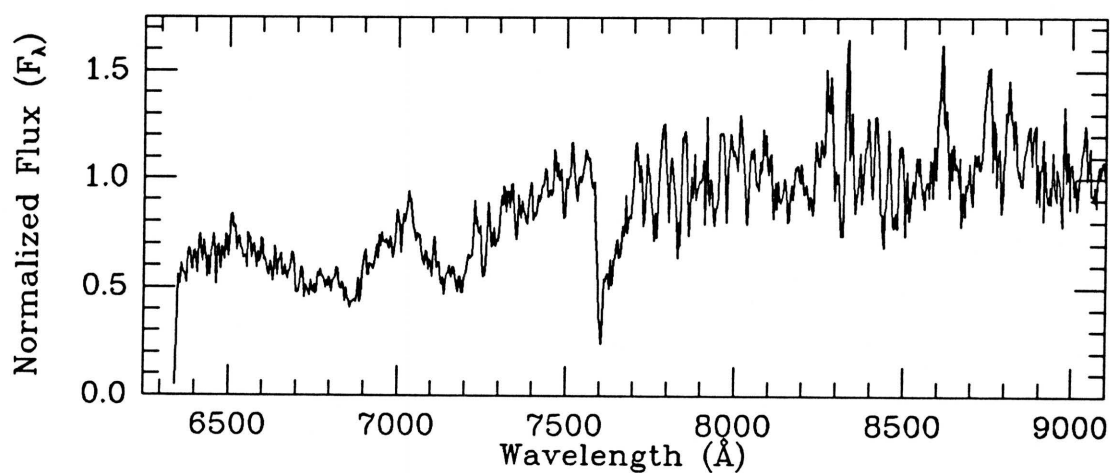
I filter

Coadded frame

MMT SPECTRUM

Exposure: 2700 sec

Obs. (UT) 1991 Sep 15

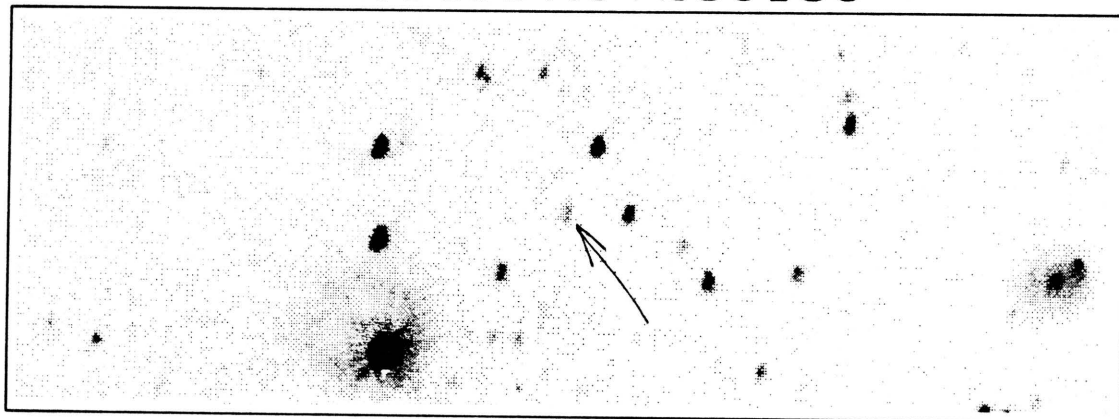
Coordinates: α (1950) = 23:36:35.5 δ (1950) = +27:45:49

Spectral Type: M2.5: V

Photometry: $I_{KC} = 17.22$ $R_{CTI} = 19.14$ $(V-I)_{KC} = 4.15 \pm .45$ $(R-I)_{CTI} = 1.98 \pm .3$ $(V-I)_{CTI} = \text{unknown}$

Notes:

CTI 234957.0+280136



CTI FINDER CHART

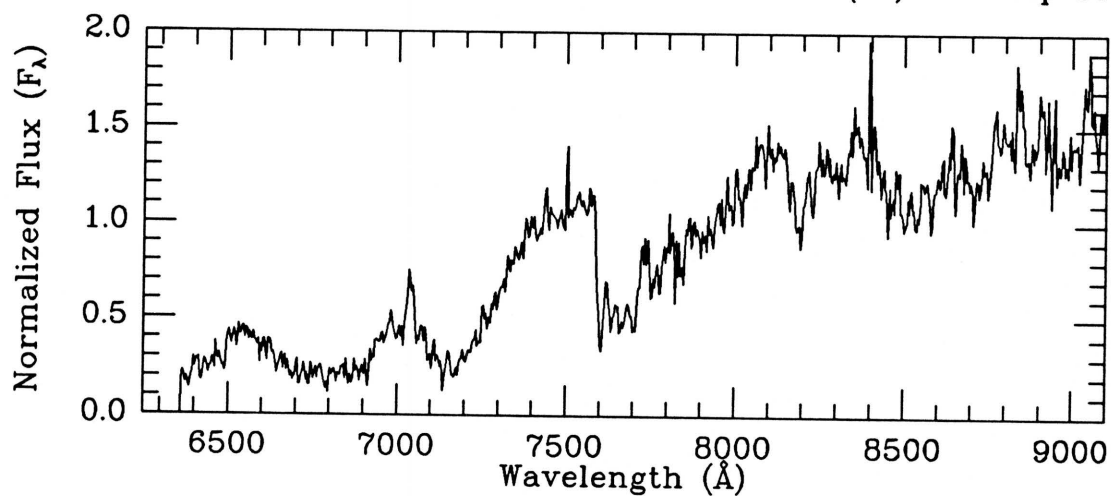
I filter

Obs. (UT) 1988 Nov 01

MMT SPECTRUM

Exposure: 2700 sec

Obs. (UT) 1990 Sep 14

Coordinates: α (1950) = 23:48:03.0 δ (1950) = +27:49:05

Spectral Type: M5 V

Photometry: $I_{KC} = 18.08$ $R_{CTI} = 19.85$ $(V-I)_{KC} = 4.00 \pm .49$ $(R-I)_{CTI} = 1.87 \pm .33$ $(V-I)_{CTI} = \text{unknown}$ Notes: Comparison to the POSS E print suggests a possible proper motion of ~ 0.8 arcsec/yr to the NNW.

REFERENCES

CHAPTER 1

- Bahcall, J. N. 1984, *ApJ*, 276, 169
- Bahcall, J. N. 1987, in *Dark Matter in the Universe*, ed. by J. Kormendy & G. R. Knapp (D. Reidel: Boston), p. 17
- Bahcall, J. N., Flynn, C., & Gould, A. 1992, *ApJ*, 389, 234
- Bailes, M., Lyne, A. G., & Shemar, S. L. 1991, *Nature*, 352, 311
- Becklin, E. E., & Zuckerman, B. 1988, *Nature*, 336, 656
- Bienaymé, O., Robin, A. C., & Crézé, M. 1987, *A&A*, 180, 94
- Boeshaar, P. C., & Tyson, J. A. 1985, *AJ*, 90, 817
- Boeshaar, P. C., Tyson, J. A., & Seitzer, P. 1986, in *Astrophysics of Brown Dwarfs*, ed. M. Kafatos, R. Harrington, & S. P. Maran (Cambridge Univ. Press: Cambridge), p. 76
- Bryja, C., Jones, T. J., Humphreys, R. M., Lawrence, G., Pennington, R. L., & Zumach, W. 1992, *ApJ*, 388, L23
- Campbell, B., Walker, G. A. H., & Yang, S. 1988, *ApJ*, 331, 902
- Chester, T. J., Fullmer, L. D., Beichman, C. A., Gillett, F. C., Low, F. J., & Neugebauer, G. 1986, *BAAS*, 18, 961
- Davis, M., Hut, P., & Muller, R. A. 1984, *Nature*, 308, 715
- Forrest, W., Ninkov, Z., Garnett, J., Skrutskie, M., & Shure, M. 1989, in *Proc. Third Infrared Technology Workshop*, ed. C. McCreight (NASA Tech. Memo. 102209), p. 221
- Fruchter, A. S., Berman, G., Bower, G., Convery, M., Goss, W. M., Hawkins, T. H., Klein, J. R., Nice, D. J., Ryba, M. F., Stinebring, D. R., Taylor, J. H., Thorsett, S. E., & Weisberg, J. M. 1990, *ApJ*, 351, 642
- Gilmore, G., Reid, N., & Hewett, P. 1985, *MNRAS*, 213, 257
- Hambly, N. C., Hawkins, M. R. S., & Jameson, R. F. 1991, *MNRAS*, 253, 1

- Hawkins, M. R. S. 1986, MNRAS, 223, 845
- Hawkins, M. R. S., & Bessell, M. S. 1988, MNRAS, 234, 177
- Henry, T. J. 1991, PhD Thesis, University of Arizona
- Henry, T. J., & McCarthy, D. W., Jr. 1990, ApJ, 350, 334
- Irwin, M., McMahon, R. G., & Reid, N. 1991, MNRAS, 252, 61P
- Irwin, M. J., Webster, R. L., Hewett, P. C., Corrigan, R. T., & Jedrzejewski, R. I. 1989, AJ, 98, 1989
- Jameson, R. F., Sherrington, M. R., & Giles, A. B. 1983, MNRAS, 205, 39P
- Jameson, R. F., & Skillen, I. 1989, MNRAS, 239, 247
- Jarrett, T. H. 1992, PhD Thesis, University of Massachusetts, Amherst
- Kuijken, K. 1991, ApJ, 372, 125
- Kuijken, K., & Gilmore, G. 1989a, MNRAS, 239, 239
- Kuijken, K., & Gilmore, G. 1989b, MNRAS, 239, 651
- Kumar, C. K. 1985, PASP, 97, 294
- Kumar, C. K. 1987, AJ, 94, 158
- Latham, D. W., Stefanik, R. P., Mazeh, T., & Torres, G. 1989, BAAS, 21, 1224
- Leggett, S. K., & Hawkins, M. R. S. 1989, MNRAS, 238, 145
- Lewin, R. 1983, Science, 221, 935
- Liebert, J., Dahn, C. C., & Monet, D. G. 1988, ApJ, 332, 891
- Lippincott, S. L. 1978, Sp. Sci. Rev., 22, 153
- Marcy, G. W., & Benitz, K. J. 1989, ApJ, 344, 441
- Marcy, G. W., & Butler, R. P. 1992, PASP, 104, 270
- Mariotti, J.-M., & Perrier, C. 1991, The Messenger, 64, 29
- Oort, J. H. 1932, Bull. Astr. Inst. Netherlands, 6, 249
- Oort, J. H. 1960, Bull. Astr. Inst. Netherlands, 15, 45
- Perlmutter, S., Burns, M. S., Crawford, F. S., Friedman, P. G., Kare, J. T., Muller, R. A., Pennypacker, C. R., & Williams, R. W. 1986, Astrophysics of Brown Dwarfs, ed. by M. C. Kafatos, R. S. Harrington, & S. P. Maran (Cambridge Univ. Press: New York), p. 87

- Probst, R. G. 1983a, *ApJ*, 274, 237
- Probst, R. G. 1983b, *ApJS*, 53, 335
- Probst, R. G., & O'Connell, R. W. 1982, *ApJ*, 252, L69
- Prosser, C. F. 1992, *AJ*, 103, 488
- Rampino, M. R., & Stothers, R. B. 1984, *Nature*, 308, 709
- Raup, D. M., & Sepkoski, J. J. 1984, *Proc. Natl. Acad. Sci. U.S.A.*, 81, 801
- Rebolo, R., Martín, E. L., & Magazzù, A. 1992, *ApJ*, 389, L83
- Reid, N. & Gilmore, G. 1982, *MNRAS*, 201, 73
- Rieke, G. H., Ashok, N. M., & Boyle, R. P. 1989, *ApJ*, 339, L71
- Rieke, G. H., & Rieke, M. J. 1990, *ApJ*, 362, L21
- Ruiz, M. T., Maza, J., Mendez, R., & Wischnjewsky, M. 1988, *The Messenger*, 53, 36
- Schneider, D. P., Greenstein, J. L., Schmidt, M., & Gunn, J. E. 1991, *AJ*, 102, 1180
- Schwartz, R. D., & James, P. B. 1984, *Nature*, 308, 712
- Shipman, H. L. 1986, in *Astrophysics of Brown Dwarfs*, eds. M. Kafatos, R. Harrington, & S. P. Maran (Cambridge Univ. Press: Cambridge), p. 71
- Simons, D. A., & Becklin, E. E. 1992, *ApJ*, in press
- Skrutskie, M. F., Forrest, W. J., & Shure, M. 1989, *AJ*, 98, 1409
- Stauffer, J., Hamilton, D., Probst, R., Rieke, G., & Mateo, M. 1989, *ApJ*, 344, L21
- Struck-Marcell, C. 1988, *ApJ*, 330, 986
- Tinney, C. G., Mould, J. R., & Reid, I. N. 1992, *ApJ*, in press
- Whitmire, D. P., & Jackson, A. A., IV 1984, *Nature*, 308, 713
- Wolszczan, A., & Frail, D. A. 1992, *Nature*, 355, 145
- Zuckerman, B., & Becklin, E. E. 1987a, *ApJ*, 319, L99
- Zuckerman, B., & Becklin, E. E. 1992, *ApJ*, 386, 260

CHAPTER 2

- Benedict, G. F., McGraw, J. T., Hess, T. R., Cawson, M. G. M., & Keane, M. J. 1991, *AJ*, 101, 279
- Cawson, M. G. M., McGraw, J. T., & Keane, M. J. 1986a, in *SPIE Proceedings* 627, ed. D. L. Crawford (Bellingham, Washington: SPIE), p. 70
- Cawson, M. G. M., McGraw, J. T., & Keane, M. J. 1986b, in *SPIE Proceedings* 627, ed. D. L. Crawford (Bellingham, Washington: SPIE), p. 79
- Hewitt, A. & Burbidge, G. 1980, *ApJS*, 43, 57
- Humphreys, R. M., Pennington, R. L., & Zumach, W. 1989, *BAAS*, 21, 1068
- Kirkpatrick, J. D. & McGraw, J. T. 1988, in *IAU Colloquium* 114, ed. G. Wegner (New York: Springer Verlag), p. 167
- McCook, G. P. & Sion, E. M. 1987, *ApJS*, 65, 603
- McGraw, J. T., Angel, J. R. P., & Sargent, T. A. 1980, in *SPIE Proceedings* 264, ed. D. A. Elliott (Bellingham, Washington: SPIE), p. 20
- McGraw, J. T., Cawson, M. G. M. & Keane, M. J. 1986, in *SPIE Proceedings* 627, ed. D. L. Crawford (Bellingham, Washington: SPIE), p. 60
- McGraw, J. T., Cawson, M. G. M., Kirkpatrick, J. D., & Haemmerle, V. 1988, in *Proceedings of a Workshop on Optical Surveys for Quasars*, ed. P. S. Osmer, A. C. Porter, R. F. Green, and C. B. Foltz (San Francisco: Astronomical Society of the Pacific), p. 163
- Perek, L. & Kohoutek, L. 1967, *Catalogue of Galactic Planetary Nebulae* (Prague: Academia)
- Schmidt, M. & Green, R. F. 1979, in *IAU Symposium* 92, ed. G. O. Abell and P. J. E. Peebles (Dordrecht, Holland: Reidel), p. 73
- Tammann, G. A. 1977, *Supernovae*, ed. D. N. Schramm (Dordrecht, Holland: Reidel), p. 95
- Tyson, J. A. & Jarvis, J. F. 1979, *ApJ*, 230, L153

CHAPTER 3.1

- Abt, H. A. 1963, ApJS, 8, 99.
- Ake, T. B., and Greenstein, J. L. 1980, ApJ, 240, 859.
- Allard, F. 1990, Ph.D. Thesis, University of Heidelberg.
- Berriman, G., and Reid, N. 1987, MNRAS, 227, 315.
- Bessell, M. S. 1991, AJ, 101, 662.
- Bessell, M. S. 1982, Proc. ASA, 4, 417.
- Boeshaar, P. C. 1976, Ph. D. Thesis, Ohio State University.
- Boeshaar, P. C. 1991, private communication.
- Boeshaar, P. C., and Tyson, J. A. 1985, AJ, 90, 817.
- Davis, D. N. 1947, ApJ, 106, 28.
- Eggen, O. J., and Greenstein, J. L. 1965, ApJ, 141, 83.
- Faÿ, T. D., Jr., Stein, W. L., and Warren, W. H., Jr. 1974, PASP, 86, 772.
- Filippenko, A. V. 1982, PASP, 94, 715.
- Filippenko, A. V., and Greenstein, J. L. 1984, PASP, 96, 530.
- Forrest, W. J., Skrutskie, M. F., and Shure, M. 1988, ApJ, 330, L119.
- Geyer, D. W., Harrington, R. S., and Worley, C. E. 1988, AJ, 95, 1841.
- Gahm, G. F. 1970, A&A, 4, 268.
- Giampapa, M. S., and Liebert, J. 1986, ApJ, 305, 784.
- Gliese, W. 1969, Veroff. Astr. Rechen-Inst. Heidelberg, No. 22.
- Gliese, W., and Jahreiss, H. 1979, A&AS, 38, 423.
- Harrington, R. S. 1990, AJ, 100, 559.
- Hawkins, M. R. S., and Bessell, M. S. 1988, MNRAS, 234, 177.
- Heintz, W. D. 1974, AJ, 79, 819.
- Heintz, W. D. 1979, AJ, 84, 1223.
- Heintz, W. D. 1987, PASP, 99, 1084.
- Henry, T. J., and Kirkpatrick, J. D. 1990, ApJ, 354, L29.

- Jacoby, G. H., Hunter, D. A., and Christian, C. A. 1984, *ApJS*, 56, 257.
- Johnson, H. L., and Morgan, W. W. 1953, *ApJ*, 117, 313.
- Joy, A. H. 1947, *ApJ*, 105, 96.
- Joy, A. H., and Abt, H. A. 1974, *ApJS*, 28, 1.
- Keenan, P. C. 1957, *PASP*, 69, 5.
- Keenan, P. C., and McNeil, R. C. 1976, *An Atlas of Spectra of the Cooler Stars: Types G, K, M, S, and C* (Columbus: Ohio State University Press).
- Keenan, P. C., and McNeil, R. C. 1989, *ApJS*, 71, 245.
- Keenan, P. C., and Schroeder, C. W. 1952, *ApJ*, 115, 82.
- Kuiper, G. P. 1938, *ApJ*, 87, 592.
- Kuiper, G. P. 1942, *ApJ*, 95, 201.
- Leggett, S. K., and Hawkins, M. R. S. 1988, *MNRAS*, 234, 1065.
- Liebert, J., Boroson, T. A., and Giampapa, M. S. 1984, *ApJ*, 282, 758.
- Liebert, J., and Ferguson, D. H. 1982, *MNRAS*, 199, 29P.
- Luyten, W. J. 1979, *The LHS Catalogue*, 2nd edition (Minneapolis: Univ. of Minnesota Press).
- Massey, P., Strobel, K., Barnes, J. V., and Anderson, E. 1988, *ApJ*, 328, 315.
- McCarthy, D. W., Jr., Henry, T. J., Fleming, T. A., Saffer, R. A., Liebert, J., and Christou, J. C. 1988, *ApJ*, 333, 943.
- McCarthy, D. W., Jr., Henry, T. J., McLeod, B. A., and Christou, J. C. 1991, *AJ*, 101, 214.
- Merrill, P. W., Deutsch, A. J., and Keenan, P. C. 1962, *ApJ*, 136, 21.
- Morgan, W. W. 1938, *ApJ*, 87, 589.
- Morgan, W. W., and Keenan, P. C. 1973, *ARA&A*, 11, 29.
- Morgan, W. W., Keenan, P. C., and Kellman, E. 1943, *An Atlas of Stellar Spectra*, (Chicago: Univ. of Chicago Press).
- Mould, J. R. 1976, *ApJ*, 207, 535.
- Mould, J. R., and McElroy, D. B. 1978, *ApJ*, 220, 935.
- Öhman, Y. 1934, *ApJ*, 80, 171.

- Öhman, Y. 1936, *Stockholms Obs. Ann.*, 12, No. 3.
- Phillips, J. G. 1950, *ApJ*, 111, 314.
- Probst, R. G., and Liebert, J. 1983, *ApJ*, 274, 245.
- Reid, I. N., and Gilmore, G. 1981, *MNRAS*, 196, 15P.
- Ruiz, M. T., Takamiya, M. Y., and Roth, M. 1991, *ApJ*, 367, L59.
- Sharpless, S. 1956, *ApJ*, 124, 342.
- Solf, J. 1978, *A&AS*, 34, 409.
- Spinrad, H., and Newburn, R. L., Jr. 1965, *ApJ*, 141, 965.
- Spinrad, H., Pyper, D. M., Newburn, R. L., Jr., and Younkin, R. L. 1966, *ApJ*, 143, 291.
- Swensson, J. W., Benedict, W. S., Delbouille, L., and Roland, G. 1970, *The Solar Spectrum from λ 7498 to λ 12016: A Table of Measures and Identifications* (Liège: Institute D'Astrophysique de L'Université de Liège).
- Turnshek, D. E., Turnshek, D. A., Craine, E. R., Boeshaar, P. C. 1985, *An Atlas of Digital Spectra of Cool Stars* (Tucson: Western Research Company).
- Veeder, G. J. 1974, *AJ*, 79, 1056.
- Wilson, O. C. 1967, *AJ*, 72, 905.
- Wing, R. F. 1979, in *IAU Colloquium No. 47*, ed. M. F. McCarthy, A. G. D. Philip, and G. V. Coyne (Vatican City: Vatican Observatory), p. 347.
- Wing, R. F., Spinrad, H., and Kuhi, L. V. 1967, *ApJ*, 147, 117.
- Wing, R. F., and Yorka, S. B. 1979, in *IAU Colloquium No. 47*, ed. M. F. McCarthy, A. G. D. Philip, and G. V. Coyne (Vatican City: Vatican Observatory), p. 519.

CHAPTER 3.2

- Allard, F. 1990, Ph.D. thesis, University of Heidelberg
- Allen, D. A., & Cragg, T. A. 1983, MNRAS, 203, 777
- Berriman, G., & Reid, N. 1987, MNRAS, 227, 315 (BR)
- Berriman, G., Reid, N., & Leggett, S. K. 1992, ApJL, submitted
- Bessell, M. S. 1979, PASP, 91, 589
- Bessell, M. S. 1991, AJ, 101, 662
- Bessell, M. S., & Scholz, M. 1990, in Accuracy of Element Abundances from Stellar Atmospheres (Lecture Notes in Physics 356), ed. R. Wehrse (Springer-Verlag: New York), p. 85
- Burrows, A., Hubbard, W. B., & Lunine J. I. 1989, ApJ, 345, 939 (BHL)
- Caillault, J.-P. & Patterson, J. 1990, AJ, 100, 825
- D'Antona, F., & Mazzitelli, I. 1985, ApJ, 296, 502 (DM)
- Dorman, B., Nelson, L. A., & Chau, W. Y. 1989, ApJ, 342, 1003 (DNC)
- Elias, J. H., Frogel, J. A., Hyland, A. R., & Jones, T. J. 1983, AJ, 88, 1027
- Gliese, W. 1969, Veroff. Astr. Rechen-Inst. Heidelberg, No. 22
- Gliese, W., & Jahreiss, H. 1979, A&AS, 38, 423
- Henry, T. J. & McCarthy, D. W., Jr. 1990, ApJ, 350, 334
- Kirkpatrick, J. D., Henry, T. J., & McCarthy, D. W., Jr. 1991, ApJS, 77, 417 (KHM)
- Lacy, C. H. 1977 ApJS, 34, 479
- Leggett, S. K., & Hawkins, M. R. S. 1988, MNRAS, 234, 1065 (LH)
- Leinert, Ch., Haas, M., Allard, F., Wehrse, R., McCarthy, D. W., Jr., Jahreiss, H., & Perrier, Ch. 1990, A&A, 236, 399.
- Livingston, W., & Wallace, L. 1991, An Atlas of the Solar Spectrum in the Infrared from 1850 to 9000 cm^{-1} (1.1 to 5.4 μm) (NSO and NOAO: Tucson)
- McCarthy, D. W., Jr., Henry, T. J., Fleming, T. A., Saffer, R. A., Liebert, J., & Christou, J. C. 1988, ApJ, 333, 943
- Monet, D. G., Dahn, C. C., Vrba, F. J., Harris, H. C., Pier, J. R., Luginbuhl, C. B., & Ables, H. D. 1992, AJ, 103, 638

- Mould, J. R. 1976, A&A, 48, 443
- Rix, H.-W., Carleton, N. P., Rieke, G., & Rieke, M. 1990, ApJ, 363, 480
- Ruan, K. 1991, Ph.D. thesis, Australian National University
- Scholz, M., & Takeda, Y. 1987, A&A, 186, 200
- Spinrad, H., & Wing, R. F. 1969, ARA&A, 7, 249
- Veeder, G. J. 1974, AJ, 79, 1056

CHAPTER 3.3

- Allard, F. 1990, Ph.D. Thesis, University of Heidelberg
- Bahcall, J. N. 1985, in *Dark Matter in the Universe: Proceedings of the 117th Symposium of the IAU*, eds. J. Kormendy and G. R. Knapp (Boston: D. Reidel), p. 17
- Bahcall, J. N., Flynn, C., & Gould, A. 1992, *ApJ*, 389, 234
- Becklin, E. E., & Zuckerman, B. 1988, *Nature*, 336, 656 (BZ)
- Bessell, M. S. 1979, *PASP*, 91, 589
- Bessell, M. S. 1991, *AJ*, 101, 662
- Boeshaar, P. C. 1976, PhD Thesis, Ohio State University
- Boeshaar, P. C. 1992, private communication
- D'Antona, F., & Mazzitelli, I. 1985, *ApJ*, 296, 502 (DM)
- Davidge, T. J., & Boeshaar, P. C. 1991, *AJ*, 102, 267
- Dick, K. A., & Fink, U. 1977, *J. Quant. Spectrosc. & Radiat. Transfer*, 18, 433
- Dorman, B., Nelson, L. A., & Chau, W. Y. 1989, *ApJ*, 342, 1003 (DNC)
- Gilmore, G., Reid, N., & Hewett, P. 1985, *MNRAS*, 213, 257
- Graham, J. R., Matthews, K., Neugebauer, G., & Soifer, B. T. 1990, *ApJ*, 357, 216
- Greenstein, J. L. 1988, *AJ*, 95, 1494
- Greenstein, J. L. 1990, *PASP*, 101, 787
- Hawkins, M. R. S. 1986, *MNRAS*, 223, 845
- Hawkins, M. R. S., & Bessell, M. S. 1988, *MNRAS*, 234, 177
- Henry, T. J. 1991, Ph.D. Thesis, University of Arizona
- Henry, T. J., Johnson, D. S., McCarthy, D. W., Jr., & Kirkpatrick, J. D. 1992, *A&A*, 254, 116
- Henry, T. J., & Kirkpatrick, J. D. 1990, *ApJ*, 354, L29
- Ianna, P. A., Rohde, J. R., & McCarthy, D. W., Jr. 1988, *AJ*, 95, 1226
- Irwin, M., McMahon, R. G., & Reid, N. 1991, *MNRAS*, 252, 61P
- Kuijken, K., & Gilmore, G. 1989, *MNRAS*, 239, 651

- Kumar, S. S. 1963, *ApJ*, 137, 1121
- Leggett, S. K., & Hawkins, M. R. S. 1989, *MNRAS*, 238, 145
- Liebert, J., Boroson, T. A., & Giampapa, M. S. 1984, *ApJ*, 282, 758
- Lunine, J. I., Hubbard, W. B., & Marley, M. S. 1986, *ApJ*, 310, 238
- Luyten, W. J. 1979, *LHS Catalog*, 2nd Edition (Minneapolis: Univ. of Minnesota)
- Luyten, W. J. 1961, *A Catalogue of 7127 Stars in the Northern Hemisphere with Proper Motions Exceeding 0.2-arcsecond Annually* (Minneapolis: Lund Press)
- Marcy, G. W., & Moore, D. 1989, *ApJ*, 341, 961
- McCook, G. P., & Sion, E. M. 1987, *ApJS*, 65, 603
- Oort, J. H. 1960, *Bull. Ast. Inst. Neth.*, 15, 45
- Owen, T. 1969, *Icarus*, 10, 355
- Probst, R. G., & Liebert, J. 1983, *ApJ*, 274, 245
- Reid, N. 1987, *MNRAS*, 225, 873
- Reid, N., & Gilmore, G. 1981, *MNRAS*, 196, 15P
- Ruiz, M. T., Takamiya, M. Y., & Roth, M. 1991, *ApJ*, 367, L59
- Schneider, D. P., Greenstein, J. L., Schmidt, M., & Gunn, J. E. 1991, *AJ*, 102, 1180
- Taylor, D. J. 1965, *Icarus*, 4, 362
- Tokunaga, A. T., Brooke, T. Y., Becklin, E. E., & Zuckerman, B. 1990, *BAAS*, 22, 1078
- Tokunaga, A. T., Hodapp, K.-W., Becklin, E. E., Cruikshank, D. P., Rigler, M., Toomey, D., Brown, R. H., & Zuckerman, B. 1988, *ApJ*, 332, L71
- van Biesbroeck, G. 1944, *AJ*, 51, 61
- Wolstencroft, R. D., & Smith, R. J. 1979, *Icarus*, 38, 155
- Zuckerman, B. 1992, private communication
- Zuckerman, B., & Becklin, E. E. 1987, *Nature*, 330, 138
- Zuckerman, B., & Becklin, E. E. 1992, *ApJ*, 386, 260 (ZB)

CHAPTER 3.4

- Alden, H. L. 1947, AJ, 52, 137
- Behall, A. L., & Harrington, R. S. 1976, PASP, 88, 204
- Blazit, A., Bonneau, D., & Foy, R. 1987, A&AS, 71, 57
- Davey, B. L. K., Cocke, W. J., Bates, R. H. T., McCarthy, D. W., Jr., Christou, J. C., & Cobb, M. L. 1989, AJ, 98, 1040
- Dawson, P. C., & Forbes, D. 1989, PASP, 101, 614
- Eggen, O. J. 1979, ApJS, 39, 89
- Eggen, O. J. 1987, AJ, 92, 379
- Heintz, W. D. 1973, AJ, 78, 780
- Heintz, W. D. 1986, AJ, 92, 446
- Heintz, W. D. 1987, AJ, 99?, 1084
- Heintz, W. D. 1987, ApJS, 65, 161
- Heintz, W. D. 1988, AJ, 96, 1072
- Heintz, W. D. 1990, AJ, 99, 420
- Henry, T. J. 1991, PhD Thesis, University of Arizona
- Henry, T. J. 1992, private communication
- Henry, T. J., & McCarthy, D. W., Jr. 1990, ApJ, 350, 334
- Hershey, J. L. 1973, AJ, 78, 935
- Ianna, P. A. 1979, BAAS, 11, 688
- Ianna, P. A., Rohde, J. R., & McCarthy, D. W., Jr. 1988, AJ, 95, 1226
- Leggett, S. K. 1992, ApJS, in press
- Lippincott, S. L. 1955, AJ, 60, 379
- Marcy, G. W., & Benitz, K. J. 1989, ApJ, 344, 441
- McCarthy, D. W., Jr. 1986, in *Astrophysics of Brown Dwarfs*, ed. M. C. Kafatos, R. S. Harrington, & S. P. Maran (New York: Cambridge Univ. Press), p. 9
- McCarthy, D. W., Jr. 1992, private communication

- McCarthy, D. W., Jr., Henry, T. J., McLeod, B., & Christou, J. C. 1991, AJ, 101, 214
- Mesrobian, W. S., Griess, T. D., & Titter, J. C. 1972, AJ, 77, 392
- Probst, R. G. 1977, AJ, 82, 656
- Probst, R. G. 1981, PhD Thesis, University of Virginia
- Reuyl, D. 1936, AJ, 45, 133
- Roizman, G. Sh. 1984, Sov. A. Letters, 10, 116
- Routly, P. M. 1972, Publ. USNO, 20, Pt. VI
- van de Kamp, P., & Worth, M. D. 1972, AJ, 77, 762
- Weis, E. W., Nations, H. L., & Upgren, A. R. 1983, AJ, 88, 1515
- Weis, E. W., & Upgren, A. R. 1982, PASP, 94, 821

CHAPTER 4

- Abell, G. O. 1982, *Exploration of the Universe*, 4th ed. (Saunders College Publishing: San Francisco), p. 690
- Benedict, G. F., McGraw, J. T., Hess, T. R., Cawson, M. G. M., & Keane, M. J. 1991, *AJ*, 101, 279
- Burstein, D., & Heiles, C. 1982, *AJ*, 87, 1165
- Conte, S. D., & de Boor, C. 1980, *Elementary Numerical Analysis* (McGraw Hill: San Francisco), pp. 298-9
- Dahn, C. C., Liebert, J., & Harrington, R. S. 1986, *AJ*, 91, 621
- Gilmore, G., & Reid, N. 1983, *MNRAS*, 202, 1025
- Gliese, W., & Jahreiss, H. 1991, *Preliminary Version of the Third Edition of Nearby Stars*
- Henry, T. J., & McCarthy, D. W., Jr. 1990, *ApJ*, 350, 334
- Johnson, H. L. 1965, *ApJ*, 141, 923
- Kholopov, P. N. (editor) 1985, *General Catalogue of Variable Stars* (Nauka Publishing House: Moscow)
- Lang, K. R. 1980, *Astrophysical Formulae: A Compendium for the Physicist and Astrophysicist*, 2nd edition (Springer-Verlag: New York), p. 500
- Leggett, S. K. 1992, *ApJS*, 82, 351
- Leggett, S. K., & Hawkins, M. R. S. 1988, *MNRAS*, 234, 1065
- Lutz, T. E., & Kelker, D. H. 1973, *PASP*, 85, 573
- Luyten, W. J. 1979, *NLTT Catalogue, Vol. II* (University of Minnesota: Minneapolis)
- Mihalas, D., & Binney, J. 1981a, *Galactic Astronomy: Structure and Kinematics*, 2nd ed., (W. H. Freeman & Co.: San Francisco), p. 252
- Mihalas, D., & Binney, J. 1981b, *Galactic Astronomy: Structure and Kinematics*, 2nd ed., (W. H. Freeman & Co.: San Francisco), p. 396
- Monet, D. G., Dahn, C. C., Vrba, F. J., Harris, H. C., Pier, J. R., Luginbuhl, C. B., & Ables, H. D. 1992, *AJ*, 103, 638
- Nelson, L. A., Rappaport, S. A., & Joss, P. C. 1986, *ApJ*, 311, 226
- Reid, N. 1991, *AJ*, 102, 1428

- Reid, N., & Gilmore, G. 1982, MNRAS, 201, 73
- Stobie, R. S., Ishida, K., & Peacock, J. A. 1989, MNRAS, 238, 709
- Wielen, R., Jahreiss, H., & Kruger, R. 1983, in The Nearby Stars and the Luminosity Function, IAU Colloquium 76, ed. A. G. D. Philip & A. R. Upgren (L. Davis Press: Schenectady), p. 163

CHAPTER 5

- Abt, H. A. 1965, ApJS, 11, 429
- Abt, H. A., Sanwal, N. B., & Levy, S. G. 1980, ApJS, 43, 549
- Abt, H. A., & Levy, S. G. 1969, AJ, 74, 908
- Abt, H. A., & Levy, S. G. 1976, ApJS, 301, 273
- Aitken, R. G. 1932, New General Catalogue of Double Stars Within 120° of the North Pole, Vol. 1
- Ake, T. B., & Greenstein, J. L. 1980, ApJ, 240, 859
- Alden, H. L. 1947, AJ, 52, 138
- Alden, H. L. 1951, AJ, 56, 34
- Alden, H. L., et al. 1957, AJ, 62, 276
- Amburster, C. 1978, PASP, 90, 219
- Appelbaum, L. T. 1972, AJ, 77, 518
- Augensen, H. J., & Buscombe, W. 1978, Ap&SpSci, 59, 35
- Baize, P. 1964, J. Obs., 47, 11
- Baize, P. 1976, A&AS, 26, 177
- Baize, P. 1992, A&AS, 92, 31
- Bakos, G. A. 1974, AJ, 79, 866
- Balega, Y., Bonneau, D., & Foy, R. 1984, A&AS, 57, 31
- Bartkevičius, A., 1984, Vilniaus Astronomijos Observatorijos Biuletėnis, 68, 3
- Batten, A. H. 1992, in Observer's Handbook, ed. by R. L. Bishop (Royal Astron. Soc. of Canada: Toronto), p. 196
- Beavers, W. I., & Eitter, J. J. 1986, ApJS, 62, 147
- Beavers, W. I., & Salzer, J. J. 1983, PASP, 95, 79
- Behall, A. L., & Harrington, R. S. 1976, PASP, 88, 204
- Berman, L. 1931, Lick Obs. Bull., 15, 109
- Bessell, M. S. 1982, Proc. Astron. Soc. Australia, 4, 417
- Bessell, M. S. 1991, AJ, 101, 662

- Bessell, M. S., & Wickramasinghe, D. T. 1979, *ApJ*, 227, 232
- Bidelman, W. P. 1985, *ApJS*, 59, 197
- Bidelman, W. P., & Lee, S.-G. 1975, *AJ*, 80, 239
- Bieger, G. S. 1964, *AJ*, 69, 804
- Binnendijk, L. 1950, *AJ*, 55, 38
- Blazit, A., Bonneau, D., Koechlin, L., & Lebeyrie, A. 1977, *ApJ*, 214, L79
- Blazit, A., Bonneau, D., & Foy, R. 1987, *A&AS*, 71, 57
- Boeshaar, P. C. 1976, PhD Thesis, Ohio State University
- Boeshaar, P. C. 1992, private communication
- Bonneau, D., Balega, Y., Blazit, A., Foy, R., Vakili, F., & Vidal, J. L. 1986, *A&AS*, 65, 27
- Bonneau, D., Blazit, A., Foy, R., & Labeyrie, A. 1980, *A&AS*, 42, 185
- Bopp, B. W. 1987, *PASP*, 99, 38
- Breakiron, L. A., Uppgren, A. R., & Weis, E. W. 1982, *AJ*, 87, 141
- Burt, S. E., & Weis, E. W. 1976, *AJ*, 81, 551
- Campbell, B., Walker, G. A. H., & Yang, S. 1988, *APJ*, 331, 902
- Carney, B. W. 1978, *AJ*, 83, 1087
- Carney, B. W. 1979, *ApJ*, 233, 877
- Carney, B. W. 1983a, *AJ*, 88, 610
- Carney, B. W. 1983b, *AJ*, 88, 623
- Carney, B. W., & Latham, D. W. 1987, *AJ*, 93, 116
- Chang, K. 1972, *AJ*, 77, 759
- Christy, J. W. 1978, *AJ*, 83, 1225
- Cochran, W. D., Hatzes, A. P., & Hancock, T. J. 1991, *ApJ*, 380, L35
- Cowley, A. P., & Hartwick, F. D. A. 1982, *ApJ*, 253, 237
- Cowley, A. P., Hiltner, W. A., & Witt, A. N. 1967, *AJ*, 72, 1334
- Dahn, C. C., Harrington, R. S., Kallarakal, V. V., Guetter, H. H., Luginbuhl, C. B., Riepe, B. Y., Walker, R. L., Pier, J. R., Vrba, F. J., Monet, D. G., & Ables, H. D. 1988, *AJ*, 95, 237

- Dahn, C. C., Harrington, R. S., Riepe, B. Y., Christy, J. W., Guetter, H. H., Kallarakal, V. V., Miranian, M., Walker, R. L., Vrba, F. J., Hewitt, A. V., Durham, W. S., & Ables, H. D. 1982, *AJ*, 87, 419
- Dahn, C. C., Liebert, J., & Harrington, R. S. 1986, *AJ*, 91, 621
- Dahn, C. C., Liebert, J., Kron, R. G., Spinrad, H., & Hintzen, P. M. 1977, *ApJ*, 216, 757
- Dawson, P. C., & de Robertis, M. M. 1988a, in *The Mass of the Galaxy: A CITA Workshop*, ed. by M. Fich, p. 21
- Dawson, P. C., & de Robertis, M. M. 1988b, *AJ*, 95, 1251
- Dawson, P. C., & de Robertis, M. M. 1988c, *JRAS (Canada)*, 82, 278
- Dawson, P. C., & de Robertis, M. M. 1989, *AJ*, 98, 1472
- Dearborn, D. S. P., Liebert, J., Aaronson, M., Dahn, C. C., Harrington, R. S., Mould, J. R., & Greenstein, J. L. 1986, *ApJ*, 300, 314
- Deich, A. N. 1978, *Sov. Astr. Letters*, 4, 50
- Deich, A. N., & Orlova, O. N. 1977, *Sov. Astron.*, 21, 182
- Doyle, J. G., & Butler, C. J. 1990, *A&A*, 235, 335
- Duquenois, A. 1987, *A&A*, 178, 114
- Duquenois, A., & Mayor, M. 1988, *A&A*, 200, 135
- Duquenois, A., & Mayor, M. 1991, *A&A*, 248, 485
- Dyer, E. R., Jr. 1954, *AJ*, 59, 218
- Eggen, O. J. 1955, *PASP*, 67, 169
- Eggen, O. J. 1956a, *AJ*, 61, 361
- Eggen, O. J. 1956b, *AJ*, 61, 405
- Eggen, O. J. 1965, *AJ*, 70, 19
- Eggen, O. J. 1971, *PASP*, 83, 271
- Eggen, O. J. 1979a, *ApJS*, 39, 89
- Eggen, O. J. 1979b, *ApJS*, 39, 101
- Eggen, O. J. 1980, *ApJS*, 43, 457
- Eggen, O. J. 1987, *AJ*, 93, 379

- Eggen, O. J., & Sandage, A. 1967, *ApJ*, 148, 911
- Eichhorn, H., & Alden, H. L. 1960, *AJ*, 65, 148
- Evans, D. S., Menzies, A., & Stoy, R. H. 1957, *MNRAS*, 117, 534
- Evans, D. S., Menzies, A., & Stoy, R. H. 1959, *MNRAS*, 119, 638
- Evans, D. W. 1992, *MNRAS*, 255, 521
- Fekel, F. C., Bopp, B. W., & Lacy, C. H. 1978, *AJ*, 83, 1445
- Finsen, W. S. 1941, *Union Obs. Circ.*, 104, 111
- Finsen, W. S. 1959, *MNASSA*, 18, 56
- Finsen, W. S., & Worley, C. E. 1970, *Third Catalogue of Orbits of Visual Binary Stars*, Rep. Obs. Johannesburg Circ., 7, 129
- Flather, E. 1957, *AJ*, 62, 381
- Fleischer, R. 1957, *AJ*, 62, 379
- Fouts, G., & Sandage, A. 1986, *AJ*, 91, 1189
- Giampapa, M. S., & Liebert, J. 1986, *ApJ*, 305, 784
- Giclas, H. L., Burnham, R., Jr., & Thomas, N. G. 1971, *Lowell Proper Motion Survey, Northern Hemisphere — The G Numbered Stars: 8991 Stars Fainter Than Magnitude 8 with Motions $>0.26''/\text{yr}$ (Lowell Obs.: Flagstaff, Arizona)*
- Giclas, H. L., Burnham, R., Jr., & Thomas, N. G. 1978, *Lowell Proper Motion Survey: Southern Hemisphere Catalog 1978*, *Lowell Obs. Bull.* 164, vol. VIII, no. 4, p. 89
- Gliese, W. 1969, *Veröffentlichungen des Astronomischen Rechen-Instituts, Heidelberg*, No. 22
- Gliese, W., & Jahreiss, H. 1979, *A&AS*, 38, 423
- Gliese, W., & Jahreiss, H. 1991, *Preliminary Version of the Third Catalogue of Nearby Stars (available through NASA computer data base)*
- Gómez, A. E., & Abt, H. A. 1982, *PASP*, 94, 650
- Graham, J. R., Matthews, K., Neugebauer, G., & Soifer, B. T. 1990, *ApJ*, 357, 216
- Green, P. J., Margon, B., Anderson, S. F., & MacConnell, D. J. 1992, *ApJ*, 400, in press

- Green, P. J., Margon, B., & MacConnell, D. J. 1991, *ApJ*, 380, L31
- Greenstein, J. L. 1984, *ApJ*, 276, 602
- Greenstein, J. L. 1986, *ApJ*, 304, 334
- Greenstein, J. L., Hack, M., & Struve, O. 1957, *ApJ*, 126, 281
- Greenstein, J. L., & Saha, A. 1986, *ApJ*, 304, 721
- Griffin, R. & R. 1982, *The Observatory*, 102, 217
- Griffin, R. F. 1984, *The Observatory*, 104, 192
- Haas, M., & Leinert, Ch. 1990, *A&A*, 230, 87
- Hall, R. G., Jr. 1948, *AJ*, 54, 106
- Hall, R. G., Jr. 1949, *AJ*, 54, 102
- Harrington, R. S. 1971, *AJ*, 76, 930
- Harrington, R. S. 1977, *PASP*, 89, 214
- Harrington, R. S., Christy, J. W., & Strand, K. Aa. 1981, *AJ*, 86, 909
- Harrington, R. S., & Dahn, C. C. 1980, *AJ*, 85, 454
- Harrington, R. S., & Dahn, C. C. 1988, *AJ*, 96, 718
- Harrington, R. S., Dahn, C. C., Kallarakal, V. V., Riepe, B. Y., Christy, J. W., Guetter, H. H., Ables, H. D., Hewitt, A. V., Vrba, F. J., & Walker, R. L. 1985, *AJ*, 90, 123
- Harrington, R. S., & Kallarakal, V. V. 1982, *BAAS*, 14, 612
- Harrington, R. S., Kallarakal, V. V., & Dahn, C. C. 1983, *AJ*, 88, 1038
- Hartkopf, W. I., & McAlister, H. A. 1984, *PASP*, 96, 105
- Hartwick, F. D. A., Cowley, A. P., & Mould, J. R. 1984, *ApJ*, 286, 269
- Heintz, W. D. 1956, *MNRAS*, 116, 248
- Heintz, W. D. 1967, *Astronomische Nachrichten*, 289, 20
- Heintz, W. D. 1973, *AJ*, 78, 780
- Heintz, W. D. 1974, *AJ*, 79, 819
- Heintz, W. D. 1975, *ApJS*, 29, 315
- Heintz, W. D. 1976, *MNRAS*, 175, 533

- Heintz, W. D. 1978a, *ApJ*, 220, 931
- Heintz, W. D. 1978b, *Double Stars* (D. Reidel: Boston), p. 145
- Heintz, W. D. 1981, *ApJS*, 46, 247
- Heintz, W. D. 1984a, *PASP*, 96, 557
- Heintz, W.D. 1984b, *A&AS*, 56, 5
- Heintz, W. D. 1986, *AJ*, 92, 446
- Heintz, W. D. 1987a, *AJ*, 94, 1077
- Heintz, W. D. 1987b, *ApJS*, 65, 161
- Heintz, W. D. 1988, *AJ*, 96, 1072
- Heintz, W. D. 1989, *A&A*, 211, 156
- Heintz, W. D. 1990a, *A&AS*, 82, 65
- Heintz, W. D. 1990b, *AJ*, 99, 420
- Heintz, W. D. 1991, *AJ*, 101, 1071
- Heintz, W. D., & Borgman, E. R. 1984, *AJ*, 89, 1068
- Henry, T. J. 1991, PhD Thesis, University of Arizona
- Henry, T. J. 1992, private communication
- Henry, T. J., Johnson, D. S., McCarthy, D. W., Jr., & Kirkpatrick, J. D. 1992, *A&A*, 254, 116
- Henry, T. J., & McCarthy, D. W., Jr. 1990, *ApJ*, 350, 334
- Hershey, J. L. 1973, *AJ*, 78, 935
- Hershey, J. L. 1975, *AJ*, 80, 662
- Hershey, J. L. 1978, *AJ*, 83, 308
- Hershey, J. L. 1980, *AJ*, 85, 1399
- Hershey, J. L., & Lippincott, S. L. 1982, *AJ*, 87, 840
- Hill, G. 1989, *A&A*, 218, 141
- Hintzen, P. 1986, *AJ*, 92, 431
- Hintzen, P., & Jensen, E. 1979, *PASP*, 91, 492
- Hirst, W. P. 1950, *MNRAS*, 110, 455

- Hoffleit, D., & Jaschek, C. 1982, *The Bright Star Catalogue, Fourth Revised Edition* (Yale Univ. Obs.: New Haven)
- Hoffleit, D., Saladyga, M., & Wlasuk, P. 1983, *A Supplement to the Bright Star Catalogue* (Yale Univ. Obs.: New Haven)
- Holden, F. 1975, *PASP*, 87, 945
- Holden, F. 1978, *PASP*, 90, 587
- Houk, N. 1978, *Michigan Catalogue of Two-Dimensional Spectral Types for the HD Stars, Vol. 2* (Univ. of Michigan: Ann Arbor)
- Houk, N. 1988, *Michigan Catalogue of Two-Dimensional Spectral Types for the HD Stars, Vol. 3* (Univ. Of Michigan: Ann Arbor)
- Houk, N., & Cowley, A. P. 1975, *Michigan Catalogue of Two-Dimensional Spectral Types for the HD Stars, Vol. 1* (Univ. of Michigan: Ann Arbor)
- Houk, N., & Smith-Moore, M. 1988, *Michigan Catalogue of Two-Dimensional Spectral Types for the HD Stars, Vol. 4* (Univ. of Michigan: Ann Arbor)
- Ianna, P. A. 1979a, *BAAS*, 11, 688
- Ianna, P. A. 1979b, *AJ*, 84, 127
- Ianna, P. A., & Bessell, M. S. 1986, *PASP*, 98, 658
- Ianna, P. A., Rohde, J. R., & McCarthy, D. W., Jr. 1988, *AJ*, 95, 1226
- Jasniewicz, G., & Mayor, M. 1988, *A&A*, 203, 329
- Jeffers, H. M., van den Bos, W. H., & Greeby, F. M. 1963, *Index Catalogue of Visual Double Stars, 1961.0, Part II* (Lick Obs.: Mt. Hamilton, California), p. 66
- Jenkins, L. F. 1952, *General Catalogue of Trigonometric Stellar Parallaxes* (Yale Univ. Obs.: New Haven)
- Jenkins, L. F. 1963, *Supplement to the General Catalogue of Trigonometric Stellar Parallaxes* (Yale Univ. Obs.: New Haven)
- Jensen, O. G., & Ulrych, T. 1973, *AJ*, 78, 1104
- Josties, F. J. 1981, *Lowell Obs. Bull.*, (IAU Colloquium 62), 9, 16
- Joy, A. H. 1947, *ApJ*, 105, 96
- Joy, A. H., & Abt, H. A. 1974, *ApJS*, 28, 1
- Joy, A. H., & Mitchell, S. A. 1948, *ApJ*, 108, 234

- Kamper, C. W. 1966, AJ, 71, 389
- Kamper, K. W. 1985, Van Vleck Obs. Contrib., 1, 357
- Kamper, K. W., & Lyons, R. W. 1981, JRAS (Canada), 75, 56
- Kirkpatrick, J. D., Henry, T. J., & McCarthy, D. W., Jr. 1991, ApJS, 77, 417
- Klemola, A. R., Harlan, E. A., & Wirtanen, C. A. 1981, AJ, 86, 583
- Kuiper, G. P. 1934, PASP, 46, 235
- Kuiper, G. P. 1936, ApJ, 84, 359
- Kuiper, G. P. 1943, APJ, 97, 275
- Kuiper, G. P. 1961, ApJS, 6, 1
- Lacy, C. H. 1977, ApJ, 218, 444
- Lambert, D. L., & McWilliam, A. 1986, ApJ, 304, 436
- Latham, D. W., Mazeh, T., Carney, B. W., McCrosky, R. E., Stefanik, R. P., & Davis, R. J. 1988, AJ, 96, 567.
- Latham, D. W., Mazeh, T., Stefanik, R. P., Mayor, M., & Burki, G. 1989, Nature, 339, 38
- Lee, S.-G. 1984, AJ, 89, 702
- Leinert, C., Jahreiss, H., Haas, M. 1986, A&A, 164, L29
- Liebert, J. 1991, private communication
- Liebert, J., Dahn, C. C., Gresham, M., & Strittmatter, P. A. 1979, ApJ, 233, 226
- Liebert, J., Dahn, C. C., Harris, H. C., Allard, F., & Kirkpatrick, J. D. 1993, in preparation
- Liebert, J., Dahn, C. C., & Monet, D. G. 1988, ApJ, 332, 891
- Liebert, J., & Probst, R. G. 1987, ARA&A, 25, 473
- Liebert, J., & Strittmatter, P. A. 1977, ApJ, 217, L59
- Lippincott, S. L. 1953, AJ, 58, 135
- Lippincott, S. L. 1958, AJ, 63, 230
- Lippincott, S. L. 1969, AJ, 74, 224
- Lippincott, S. L. 1973, AJ, 78, 303

- Lippincott, S. L. 1974, AJ, 79, 974
- Lippincott, S. L. 1975, AJ, 80, 831
- Lippincott, S. L. 1977, AJ, 82, 925
- Lippincott, S. L. 1978, Space Sci. Rev., 22, 153
- Lippincott, S. L. 1979, PASP, 91, 784
- Lippincott, S. L. 1981, PASP, 93, 376
- Lippincott, S. L. 1983, AJ, 88, 542
- Lippincott, S. L., & Borgman, E. R. 1978, PASP, 90, 226
- Lippincott, S. L., & Borgman, E. R. 1979, AJ, 84, 567
- Lippincott, S. L., Braun, D., & McCarthy, D. W., Jr. 1983, PASP, 95, 271
- Lippincott, S. L., & Hershey, J. L. 1983, AJ, 88, 684
- Lippincott, S. L., & Lanning, J. J. 1976, BAAS, 8, 360
- Lippincott, S. L., & Worth, M. D. 1976, AJ, 81, 548
- Lippincott, S. L. & Wyckoff, S. 1964, AJ, 69, 471
- Lu, P. K., Demarque, P., van Altena, W., McAlister, H., & Hartkopf, W. 1987, AJ, 94, 1318
- Luyten, W. J. 1941, Pub. Obs. Univ. Minn., 3, No. 1 & 3
- Luyten, W. J. 1955, A Catalogue of 1849 Stars with Proper Motions Exceeding 0.5" Annually (Lund Press: Minneapolis)
- Luyten, W. J. 1961, A Catalogue of 7127 Stars in the Northern Hemisphere with Proper Motions Exceeding 0.2" Annually (Lund Press: Minneapolis)
- Luyten, W. J. 1963a, Bruce Proper Motion Survey: The General Catalogue, Vol. 1
- Luyten, W. J. 1963b, Proper Motion Survey with the Forty-eight Inch Schmidt Telescope. I. Organization and Purpose (Univ. of Minnesota: Minneapolis)
- Luyten, W. J. 1977, The Stars of Low Luminosity (Univ. of Minnesota: Minneapolis)
- Luyten, W. J. 1979, LHS Catalogue (Univ. of Minnesota: Minneapolis)
- Luyten, W. J., & Albers, H. 1979, LHS Atlas (Univ. of Minn.: Minneapolis)

- Luyten, W. J., & Ebbighausen, E. G. 1935, Harvard College Observatory Announcement Card 336
- Luyten, W. J., & Hughes, H. S. 1982, Proper Motion Survey with the 48-inch Schmidt Telescope, LXII (Univ. of Minnesota: Minneapolis)
- MacConnell, D. J. 1983, in *The Nearby Stars and the Stellar Luminosity Function*, ed. by A. G. D. Philip & A. R. Upgren (L. Davis Press: Schenectady), p. 365
- Marcy, G. W., & Benitz, K. J. 1989, *ApJ*, 344, 441
- Marcy, G. W., Lindsay, A., & Wilson, K. 1987, *PASP*, 99, 490
- Marcy, G. W., & Moore, D. 1989, *ApJ*, 341, 961
- Mariotti, J.-M., Perrier, C., Duquennoy, A., & Duhoux, P. 1990, *A&A*, 230, 77
- Martin, G. E., & Ianna, P. A. 1975, *AJ*, 80, 326
- Mathioudakis, M., & Doyle, J. G. 1991, *A&A*, 244, 409
- Mayor, M., & Mazeh, T. 1987, *A&A*, 171, 157
- Mayor, M., & Turon, C. 1982, *A&A*, 110, 241
- McAlister, H. A. 1978, *PASP*, 90, 288
- McAlister, H. A., Hartkopf, W. I., Hutter, D. J., Shara, M. M., & Franz, O. G. 1987, *AJ*, 93, 183
- McAlister, H. A., Hartkopf, W. I., Sowell, J. R., Dombrowski, E. G., & Franz, O. G. 1989, *AJ*, 97, 510
- McCarthy, D. W., Jr. 1983, in *The Nearby Stars and the Stellar Luminosity Function*, IAU Colloquium 76, ed. by A. G. D. Philip & A. R. Upgren (L. Davis Press: Schenectady), p.107
- McCarthy, D. W., Jr., & Henry, T. J. 1987, *ApJ*, 319, L93
- McCarthy, D. W., Jr., Henry, T. J., Fleming, T. A., Saffer, R. A., Liebert, J., & Christou, J. C. 1988, *ApJ*, 333, 943
- McCarthy, D. W., Jr., Henry, T. J., McLeod, B., & Christou, J. C. 1991, *AJ*, 101, 214
- McCarthy, D. W., Jr., Probst, R. G., & Low, F. J. 1985, *ApJ*, 290, L9
- McCook, G. P., & Sion, E. M. 1987, *ApJS*, 65, 603
- McMillian, R. S., & Smith, P. H. 1987, *PASP*, 99, 849

- McNamara, B. R. 1984, BAAS, 16, 507
- McNamara, B. R., Ianna, P. A., & Fredrick, L. W. 1987, AJ, 93, 1245
- Mellor, L. L. 1917, Pub. Obs. Univ. Mich., 3, 61
- Monet, D. G., Dahn, C. C., Vrba, F. J., Harris, H. C., Pier, J. R., Luginbuhl, C. B., & Ables, H. D. 1992, AJ, 103, 638
- Morbey, C. L., & Griffin, R. F. 1987, ApJ, 317, 243
- Morel, P. J. 1969, AJ, 74, 245
- Morgan, B. L., Beckmann, G. K., & Scaddan, R. J. 1980, MNRAS, 192, 143
- Ohtani, H., & Ichikawa, T. 1977, Contributions from the Dept. of Astron., Univ. of Kyoto, No. 76
- Osvalds, V. 1957, AJ, 62, 274
- Oswalt, T. D., Hintzen, P. M., & Luyten, W. J. 1988, ApJS, 66, 391
- Perlmutter, S., Burns, M. S., Crawford, F. S., Friedman, P. G., Kare, J. T., Muller, R. A., Pennypacker, C. R., & Williams, R. W. 1986, Astrophysics of Brown Dwarfs, ed. by M. C. Kafatos, R. S. Harrington, & S. P. Maran (Cambridge Univ. Press: New York), p. 87
- Perrier, C., & Mariotti, J.-M. 1987, ApJ, 312, L27
- Petit, M. 1979, Inf. Bull. Var. Stars, 1644, 1
- Pettersen, B. R. 1991, Memoire della Societa Astronomica Italiana, 62, 217
- Pettersen, B. R., & Griffin, R. F. 1980, The Observatory, 100, 198
- Pierce, J. A. 1924, Lick Obs. Bull., 2, 131
- Proust, D., Ochsenbein, F., & Pettersen, B. R. 1981, A&AS, 44, 179
- Przybylski, A. 1962, PASP, 74, 230
- Przybylski, A., & Kennedy, P. M. 1965, MNRAS, 129, 63
- Reid, I. N. 1982, MNRAS, 201, 51
- Reid, I. N. 1991, private communication
- Reid, I. N., Brewer, C., Brucato, R. J., McKinley, W. R., Maury, A., Mendenhall, D., Mould, J. R., Mueller, J., Neugebauer, G., Phinney, J., Sargent, W. L. W., Schombert, J., & Thicksten, R. 1991, PASP, 103, 661
- Reuyl, D. 1941, PASP, 53, 337

- Reuyl, D. 1943, ApJ, 97, 186
- Reuyl, D., & Holmberg, E. 1943, ApJ, 97, 41
- Robinson, E. L., Cochran, A. L., Cochran, W. D., Shafter, A. W., & Zhang, E.-H. 1990, AJ, 99, 672
- Robinson, R. D., Slee, O. B., & Little, A. G. 1976, ApJ, 203, L91
- Rodgers, A. W., & Eggen, O. J. 1974, PASP, 86, 742
- Roizman, G. Sh., 1984, Sov. Astr. Letters, 10, 116
- Roman, N. G. 1955, ApJS, 2, 195
- Ruiz, M. T., & Maza, J. 1987, Rev. Mex. Astron. Astrof., 14, 381
- Ruiz, M. T., Maza, J., Mendez, R., & Wischnjewsky, M. 1988, The Messenger, 53, 36
- Ruiz, M. T., Maza, J., Wischnjewsky, M., & González, L. E. 1986, ApJ, 304, L25.
- Ruiz, M. T., Maza, J., Wischnjewsky, M., & González, L. E. 1988, in Progress and Opportunities in Southern Hemisphere Optical Astronomy, ed. by V. M. Blanco, & M. M. Phillips (Brigham Young Univ.: Provo, Utah), p. 342
- Russell, H. N., Dugan, R. S., & Stewart, J. Q. 1927, Astronomy: A Revision of Young's Manual of Astronomy, Vol. II, pp. 640-641
- Russell, J., & Gatewood, G. 1975, AJ, 80, 652
- Russell, J., & Gatewood, G. 1980, AJ, 85, 1270
- Ryan, S. G. 1989 AJ, 198, 1693
- Ryan, S. G., & Norris, J. E. 1991, AJ, 101, 1835
- Sandage, A. 1964, ApJ, 139, 442
- Sandage, A. 1969, ApJ, 158, 1115
- Sandage, A. 1981, AJ, 86, 1643
- Sandage, A., & Fouts, G. 1987, AJ, 93, 74
- Sandage, A., & Kowal, C. 1986, AJ, 91, 1140
- Sanduleak, N., & Pesch, P. 1988, ApJS, 66, 387

- Scarfe, C. D., Funakawa, H., Delaney, P. A., & Barlow, D. J. 1983, *JRAS (Canada)*, 77, 126
- Schaefer, B. E. 1989, *ApJ*, 337, 927
- Sinachopoulos, D. 1988, *A&AS*, 76, 189
- Skrutskie, M. F., Forrest, W. J., & Shure, M. A. 1987, *ApJ*, 312, L55
- Strand, K. 1957, *AJ*, 62, 35
- Strand, K. Aa. 1969, *AJ*, 74, 760
- Strand, K. 1977, *AJ*, 82, 745
- Stryker, L. L., Hesser, J. E., Hill, G., Garlick, G. S., & O'Keefe, L. M. 1985, *PASP*, 97, 247
- Thé, P. S., & Staller, R. F. A. 1974, *A&A*, 36, 155
- Tift, W. G. 1955, *AJ*, 60, 144
- Tinney, C. G., Mould, J. R., & Reid, I. N. 1992, *ApJ*, in press
- Titter, J. C., Mesrobian, W. S., & Upgren, A. R. 1972, *AJ*, 77, 875
- Tokovinin, A. A. 1985, *A&A*, 61, 483
- Tokunaga, A. T., Becklin, E. E., & Zuckerman, B. 1990, *ApJ*, 358, L21
- Tokunaga, A. T., Hodapp, K.-W., Becklin, E. E., Cruikshank, D. R., Rigler, M., Toomey, D., Brown, R. H., & Zuckerman, B. 1988, *ApJ*, 332, L71
- Tomkin, J., McAlister, H. A., Hartkopf, W. I., & Fekel, F. C. 1987, *AJ*, 93, 1236
- Tomkin, J., & Pettersen, B. R. 1986, *AJ*, 92, 1424
- Turnshek, D. E., Turnshek, D. A., Craine, E. R., & Boeshaar, P. C. 1985, *An Atlas of Digital Spectra of Cool Stars* (Western Research Corp.: Tucson)
- Underhill, A. B. 1963, *Pub. Dom. Astroph. Obs.*, 12, 159
- Upgren, A. R., & Kuzma, T. J. 1983, *AJ*, 88, 132
- Upgren, A. R., Weis, E. W., Nations, H. L., & Lee, J. T. 1985, *AJ*, 90, 652
- van Altena, W., & Sawada, K. 1983, *AJ*, 88, 1508
- van Biesbroeck, G. 1961, *AJ*, 66, 528
- van Biesbroeck, G. 1974, *ApJS*, 28, 413
- van de Kamp, P. 1947, *AJ*, 53, 43

- van de Kamp, P. 1950, AJ, 55, 160
- van de Kamp, P. 1969a, AJ, 74, 238
- van de Kamp, P. 1969b, Sky & Telescope, 37, 360
- van de Kamp, P. 1974, AJ, 79, 491
- van de Kamp, P., & Burton, W. B. 1962, AJ, 67, 549
- van de Kamp, P., & Flather, E. 1955, AJ, 60, 448
- van de Kamp, P., Gökkaya, N. G., & Heintz, W. D. 1968, AJ, 73, 361
- van de Kamp, P., & Lippincott, S. L. 1949, AJ, 55, 16
- van de Kamp, P., & Worth, M. D. 1972, AJ, 77, 762
- van den Bos, W. H. 1958, AJ, 63, 63
- van den Bos, W. H. 1963, AJ, 68, 57
- Veeder, G. J. 1974, AJ, 79, 1056
- Vilkki, E. U. 1984, PASP, 96, 161
- Voûte, J. 1946, Riverview Coll. Obs. Pub., 2, 43
- Wagman, N. E. 1951, AJ, 56, 149
- Wagman, N. E. 1961, AJ, 66, 433
- Weis, E. W. 1982, AJ, 87, 152
- Weis, E. W. 1991, AJ, 101, 1882
- Weis, E. W., Nations, H. L., & Upgren, A. R. 1983, AJ, 88, 1515
- Weis, E. W., & Upgren, A. R. 1982, PASP, 94, 821
- Wilson, O. C. 1967, AJ, 72, 905
- Wilson, R. H., Jr. 1982, A&AS, 50, 115
- Worley, C. E. 1956, AJ, 61, 162
- Worley, C. E. 1957, AJ, 62, 153
- Worley, C. E. 1962a, AJ, 67, 403
- Worley, C. E. 1962b, AJ, 67, 396
- Young, A., Sadjadi, S., & Harlan, E. 1987, ApJ, 314, 272
- Zuckerman, B., & Becklin, E. E. 1987, Nature, 330, 138